

AD\_\_\_\_\_

(Leave blank)

Award Number:  
DAMD17-01-1-0744

TITLE:  
Molecular Genetic studies of Bone Mechanical Strain and of  
Pedigrees with Very High Bone Density

PRINCIPAL INVESTIGATOR:  
Subburaman Mohan, Ph.D.

CONTRACTING ORGANIZATION:  
Loma Linda Veterans Association for Research and Education  
Redlands, CA 92374

REPORT DATE:  
November 2010

TYPE OF REPORT:  
FINAL

PREPARED FOR: U.S. Army Medical Research and Materiel Command  
Fort Detrick, Maryland 21702-5012

DISTRIBUTION STATEMENT: (Check one)

- ☒ Approved for public release; distribution unlimited
- ☐ Distribution limited to U.S. Government agencies only;  
report contains proprietary information

The views, opinions and/or findings contained in this report are those of the author(s) and should not be construed as an official Department of the Army position, policy or decision unless so designated by other documentation.

REPORT DOCUMENTATION PAGE				Form Approved OMB No. 0704-0188	
Public reporting burden for this collection of information is estimated to average 1 hour per response, including the time for reviewing instructions, searching existing data sources, gathering and maintaining the data needed, and completing and reviewing this collection of information. Send comments regarding this burden estimate or any other aspect of this collection of information, including suggestions for reducing this burden to Department of Defense, Washington Headquarters Services, Directorate for Information Operations and Reports (0704-0188), 1215 Jefferson Davis Highway, Suite 1204, Arlington, VA 22202-4302. Respondents should be aware that notwithstanding any other provision of law, no person shall be subject to any penalty for failing to comply with a collection of information if it does not display a currently valid OMB control number. <b>PLEASE DO NOT RETURN YOUR FORM TO THE ABOVE ADDRESS.</b>					
1. REPORT DATE (DD-MM-YYYY) 30-nov-2010		2. REPORT TYPE FINAL		3. DATES COVERED (From - To) 15 MAY 2001 - 30 OCT 2010	
4. TITLE AND SUBTITLE Molecular Genetic Studies of Bone Mechanical Strain and of Pedigrees with Very High Bone Density				5a. CONTRACT NUMBER DAMD17-01-1-0744	
				5b. GRANT NUMBER DAMD17-01-1-0744	
				5c. PROGRAM ELEMENT NUMBER	
6. AUTHOR(S) Subburaman Mohan, Ph.D.  E-Mail: subburaman.mohan@va.gov				5d. PROJECT NUMBER	
				5e. TASK NUMBER	
				5f. WORK UNIT NUMBER	
7. PERFORMING ORGANIZATION NAME(S) AND ADDRESS(ES) Loma Linda Veterans Association for Research and Education PO Box 1280 - 710 Brookside Ave Redlands,CA 92373				8. PERFORMING ORGANIZATION REPORT NUMBER	
9. SPONSORING / MONITORING AGENCY NAME(S) AND ADDRESS(ES) U.S. Army Medical Research and Materiel Command Fort Detrick, Maryland 21702				10. SPONSOR/MONITOR'S ACRONYM(S)	
				11. SPONSOR/MONITOR'S REPORT NUMBER(S)	
12. DISTRIBUTION / AVAILABILITY STATEMENT Approved for public release; distribution unlimited					
13. SUPPLEMENTARY NOTES					
14. ABSTRACT: Our studies address the medical problem of stress fractures in the military as stress fractures are one of the most common and potentially debilitating overuse injuries experienced in the military recruit population. The overall hypothesis that we are addressing in this study is that state of the art molecular genetic approaches can identify the genes and their pathways responsible for extreme differences in skeletal anabolic response to mechanical strain. During the funding period, we have used state-of-the-art technologies to identify the genetic components that contribute to the extreme differences in the skeletal anabolic response to mechanical strain in two inbred strains of mice. The candidate genes identified using QTL and whole genome microarray approaches were then validated using siRNA technique <i>in vitro</i> to suppress expression of genes and evaluating biological response to fluid flow shear strain and targeted or conditional disruption of gene of interest <i>in vivo</i> and evaluating skeletal anabolic response to mechanical loading. Our QTL and whole genome microarray studies revealed that several genetic loci in different chromosomes contribute to the variation in skeletal anabolic response to loading in C57BL/6J (B6) and C3H/HeJ strains of mice. <i>In vitro</i> and <i>in vivo</i> approaches utilizing targeted disruption of genes have identified involvement of IGF-I, integrin and BMP signaling pathways in mechanical loading process. Future validation of mechanosensitive genes in genetic association studies will determine their utility to develop genetic screens to identify individuals who are at increased risk of stress fractures.					
15. SUBJECT TERMS Mechanical strain, Quantitative trait loci analysis, microarray analysis, osteoblasts Signaling pathways, bone formation					
16. SECURITY CLASSIFICATION OF: "U"			17. LIMITATION OF ABSTRACT  UU	18. NUMBER OF PAGES  362	19a. NAME OF RESPONSIBLE PERSON USAMRMC
a. REPORT U	b. ABSTRACT U	c. THIS PAGE U			19b. TELEPHONE NUMBER (include area code)

## Table of Contents

### Page

Introduction.....	5
Body.....	6
(Key Research Accomplishments, Reportable outcomes, Conclusion and References are provided by different periods 2001-2010)	
Appendices.....	213

**Final Progress report for DAMD 17-01-1-0744****Title of Project: Molecular Genetic Studies of Bone Mechanical Strain****Principal Investigator: Subburaman Mohan, Ph.D.****Period Covered: May 15, 2001 to November 30, 2010****General Introduction**

Bone has several functions, but its most important function is mechanical performance. In this regard, according to Wolff's Law, mechanical loads determine the amount of bone (bone density) and the architecture of bone. During the past two decades, considerable advances have been made in our understanding of the mechanism whereby mechanical loads regulate bone formation and bone resorption responses in the skeleton. It is now well recognized that mechanical loading leads to an increase in bone density and that immobilization leads to a loss in bone density. *In vivo* studies in turkeys show that mechanical loading results in a several-fold increase in bone formation *in vivo*. In most animal species studied, including humans, there is a marked loss of bone density in response to immobilization. These findings in aggregate emphasize that mechanical stress and strain have important impacts on bone remodeling.

In studies using inbred strains of mice, we found two strains (C3H and B6) that showed very different responses to immobilization and to mechanical loading. Accordingly, the B6 mouse showed a much greater bone loss in response to immobilization, and a much greater bone formation gain in response to mechanical loading, than the C3H mouse. These observations indicate that either the generation of the signals, or the biological bone response to the loading signals, is variable. This implies that some individuals will have a much more robust response than others to mechanical load. These studies also indicate that at least some, if not the majority, of this variation is genetic. Because the differences in response to immobilization and mechanical loading between the B6 and C3H mouse is large, the genetic component of bone response to mechanical load must be biologically significant. Finally, and the most surprising finding was that the animal with the highest peak bone density (i.e. C3H mice) had the most sluggish response to mechanical perturbation. This latter observation contradicted and was exactly opposite to what would have been predicted by Wolff's Law. Such results, which have been obtained in two different types of studies, emphasize our lack of knowledge about the fundamental mechanisms involved in the mechanical regulation of bone structure and function. This line of inquiry is particularly important because the only physiological, negative feedback mechanism that controls bone density and bone architecture is mechanical loading. Consequently, it is critically important to understand the molecular mechanisms involved in mechanical loading and the genetic variations that can occur. Such studies will have an obvious important impact on our understanding of why there is a high frequency of stress fractures in new Army recruits (march fractures). Furthermore, these studies are also relevant to the optimal functioning of a skeleton under combat conditions.

To identify the genetic component, our goal is to apply the QTL technique, a powerful genetic technique, in combination with *in vitro* studies, on the biochemical pathways involved in mechanical strain signaling, in order to determine the genes responsible for the mechanical strain differential responses between these two inbred strains of mice. We believe that the QTL and *in vitro* approaches are complimentary to each other based on the following. By using the QTL approach, we will be able to

identify critical regions in chromosomes that are important in mediating loading response. However, although the QTL approach can locate key regions in chromosomes it cannot identify the genes involved without additional studies. Our *in vitro* approach, which deals with changes in gene and protein expression in osteoblast cell lines derived from C3H and B6 mice, will be able to “rule in” or “rule out” candidate genes that are located within the genetic loci identified by the QTL studies. Further validation of identified genes in mediating mechanical strain response has been carried out using mice with targeted disruption of genes of interest. Thus, we believe that our strategy to combine two approaches, namely *in vivo* QTL and *in vitro* studies on gene and protein expression in response to loading, provide a much better chance of identifying the candidate genes for further functional studies compared to either approach alone.

Our final progress report is divided into two sections. The first part describes the results from *in vivo* studies and second part deals with findings from *in vitro* studies. Our annual progress for the project period of 2001 to 2010 is presented in an ascending manner. We describe the technical objectives followed by progress for each of the technical objectives.

## **Part A – In vivo Studies**

### **Progress for the Period of 2001 to 2003**

**1A. Technical Objective 1:** Our goals are to perform jump training in 10 different mouse strains and to evaluate the bone formation response to jump training in order to identify two mouse strains which show extreme differences in bone formation response to mechanical loading. These two strains will then be used for QTL studies and for *in vitro* studies, which seek to identify candidate genes for mediating the bone formation response to mechanical loading. If, during the course of the jump studies, we find that the jump training technique does not produce a phenotype which is equivalent in magnitude to 4-point bending phenotype (i.e., which causes a large increase in bone formation) we will shift our efforts to the 4-point bending procedure for providing *in vivo* mechanical strain. We chose the jump training regimen as a means to induce mechanical strain mice because it is more physiological.

To accomplish the above technical objective, we performed the following specific objectives during year 1 of this project.

- 1) Develop the conditions for optimal jump training technique, which include:
  - a) determined study duration (i.e., between 7 and 28 days);
  - b) evaluated the most sensitive endpoints, which include histomorphometric measurements of bone formation, pQCT measurements of the bone perimeter, or serum biochemical markers of bone formation;
  - c) determined the optimal sampling site in the skeleton (i.e., the tibia or the femur);
  - d) determined whether the entire bone perimeter should be evaluated or whether only the cortical mid-shaft is required for a sensitive assay.
- 2) Select the optimal mouse pair for our QTL studies. We will also use this mouse pair for our *in vitro* studies designed to discover candidate genes that might mediate the bone formation response to mechanical loading *in vitro*.

*Progress report for technical objective 1*

Five to 6 week old mice, 6-7 per group were evaluated after two, three, and four weeks of jump training. Each mouse jumped ten times per day, five days a week to a height of 25 centimeters. Control mice were placed in the same cage but did not have the electrical stimulation to jump. The end point of this study was pQCT parameters of the femur and serum biochemical markers. The precision of the pQCT was less than 3% and the precision of the biochemical markers (i.e. mouse C-telopeptide, mouse osteocalcin, and mouse skeletal alkaline phosphatase) was 7%, 10%, and 2% for within assay CV, respectively. In the pQCT study, we scanned the bone nine times covering the entire length of the femur. The data are presented as the midshaft slice for all of the density and area calculations. We also examined the entire nine slices to determine if there was any site that was more sensitive to the jump training.

**1A1. Specific Objective 1:** Optimum study duration, no significant changes in pQCT parameters or biochemical markers were seen after two weeks of jumping. At three weeks of jumping, the changes were maximal with significant increases in periosteal parameter, cortical thickness and cortical area (**Tables 1A1, 1A2& 1A3**). However, at four weeks, while significant changes were still seen, these changes, in general, were less than those at three weeks. We also saw at three weeks significant changes in total bone mineral density. In contrast, no significant changes were seen in serum biochemical parameters at any sampling time from 2, 3 and 4 weeks (**Table 1A4**).

**Table 1A1. Cross-sectional parameters and area of mid-shaft femur**

Parameters	2-Week		3-Week		4-Week	
	Control (Mean±SD)	Jump (Mean±SD)	Control (Mean±SD)	Jump (Mean±SD)	Control (Mean±SD)	Jump (Mean±SD)
Periosteal Circumference (mm)	4.23±0.08	4.24±0.052	4.22±0.08	4.35±0.083*	4.19±0.04	4.33±0.11*
Endosteal Circumference (mm)	3.27±0.06	3.23±0.08	3.22±0.06	3.27±0.10	3.17±0.06	3.25±0.103
Cortical thickness (mm)	0.15±0.01	0.16±0.006	0.16±0.003	0.17±0.007**	0.16±0.01	0.17±0.005 <sup>#</sup>
Total Area (mm <sup>2</sup> )	1.43±0.05	1.43±0.033	1.42±0.05	1.50±0.059*	1.40±0.03	1.48±0.075*
Cortical Area (mm <sup>2</sup> )	0.53±0.03	0.60±0.019	0.59±0.013	0.66±0.026**	0.59±0.03	0.64±0.028

p-values, \*p<0.05, \*\*p<0.01

**Table 1A2. Bone mineral content and bone density parameters of mid-shaft femur**

Parameters	<u>2-Week</u>		<u>3-Week</u>		<u>4-Week</u>	
	Control (Mean±SD)	Jump (Mean±SD)	Control (Mean±SD)	Jump (Mean±SD)	Control (Mean±SD)	Jump (Mean±SD)
Cortical content	0.69±0.04	0.72±0.02	0.71±0.03	0.80±0.02**	0.71±0.01	0.78±0.04*
Total content	0.65±0.05	0.69±0.03	0.68±0.04	0.76±0.04**	0.69±0.02	0.76±0.03**
Total bone density (mg/cc)	409±30	434±6	425±19	461±8**	445±13	465±17*

p-values, \*p&lt;0.01, \*\*p&lt;0.001

**Table1A3. P-values for ANOVA**

	ANOVA treatment	ANOVA Weeks	Post Hoc Week 2 vs week 3 or week 4	Post Hoc Week 3 vs week 4
Periosteal Circumference	P=0.046	NS	NS	NS
Total Content	P=0.03	P=0.01	P<0.014	NS
Total Density	P=0.004	P=0.03	P<0.03	NS

**Table 1A4. Biochemical parameters in jump exercise group compared to control group of mice.**

Parameters	<u>2-Week</u>		<u>3-Week</u>		<u>4-Week</u>	
	Control (Mean±SD)	Jump (Mean±SD)	Control (Mean±SD)	Jump (Mean±SD)	Control (Mean±SD)	Jump (Mean±SD)
Skeletal ALP (U/L)	152± 12	141± 34	175 ± 15	191 ± 24	164 ± 23	166 ± 23
Osteocalcin (ng/ml)	166 ± 32	168 ± 46	237 ± 60	200 ± 23	170 ± 58	141 ± 20
C-telopeptide (ng/ml)	4.4 ± 1.4	5.9 ± 1.8	5.2 ± 1.4	6.0 ± 1.7	6.2 ± 1.2	6.1 ± 1.8

Difference between control and jump groups were not statistically significant

The changes in bone size and density parameters measured by pQCT in response to jump training while significant, were rather small. Therefore, histomorphometric studies were not performed because the

precision of these measurements is less than that seen with pQCT. Since the biochemical markers did not show a significant change, the most sensitive test was the pQCT.

With respect to the optimal sampling site in the skeleton, we examined nine different slices throughout the femur and found in essence, no single site which was superior to another and therefore we focused our efforts on the midshaft of the femur, which was slice five (Figure. 1A1).

Sampling with the pQCT was superior for the femur as opposed to the tibia and therefore the tibia was evaluated.

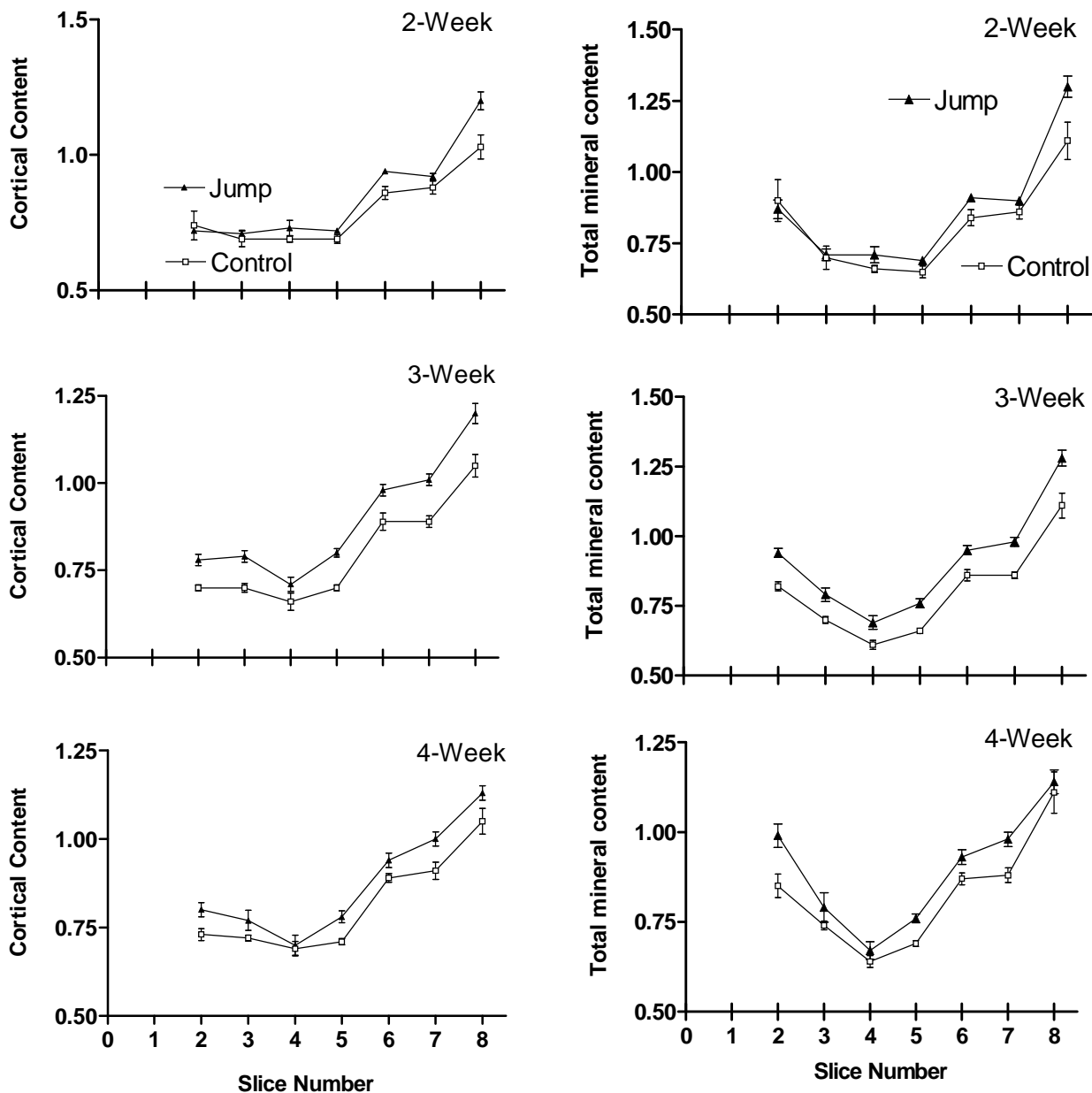


**Figure. 1A1.** Effect of 2, 3 and 4 weeks of jump exercise on cortical and total bone mineral content measured by pQCT at 9 different slices of the femur. Each slice was separated by 11% of the femur length with slice 1 starting at distal end. The data shows (slices 1 & 9 omitted due to large variation) that increase in bone mineral content was throughout the length of the femur. Each data point represents mean  $\pm$  standard error of mean (n=6). P-value for both cortical and total bone mineral content of control vs jump group was  $<0.0001$  by ANOVA for 3-week and 4-week jump exercise groups. P-value for comparison of individual slices in control and jump groups of mice by post hoc tests are  $\#p>0.05$ ,  $*p<0.05$ .

**1A2. Specific Objective 2:** Thus, using *in vitro* strain studies, we find that the most unresponsive mouse strain is the C3H and the most responsive mouse strains are the Balb-C and B6. These mouse strains will be further evaluated for the QTL studies. The corresponding QTL experiments mentioned in specific objective one was carried out using these mouse strains after validating Real time PCR and the four point bending technique mentioned above.

In conclusion, we found that the 14 day time point was the most optimal for jump studies. The most sensitive end point was the pQCT and the optimal sampling site was the femur and within the femur the midshaft site appeared to be most convenient and most optimal site. While the changes with the pQCT were highly significant, they were not large enough to apply to QTL studies, where each individual animal must be assigned a quantitative phenotype. Therefore, we have made two changes in the protocol: 1) we have elected to use 4-point bending as opposed to jumping as our strain stimulus. We indicated that this approach might be necessary in the original grant application; and 2) we elected to explore the possibility of using Microarray to identify genes that were markedly increased or decreased with either jump training or 4-point bending. As shown below, under additional progress, a number of genes were found to express in bone, making them potential candidates for quantitation with real-time PCR. This then led to RT-PCR studies of those genes that showed the largest change with a jump study. These results are also presented below under Additional Progress.

### 1A3. Additional progress report for Technical Objective 1

#### 1). Rationale for our new strategy

We found that neither pQCT nor bone markers showed differences with respect to control in the jump-up and jump-down regimen. Hence, we used microarray and real time PCR methods to analyze the genes that responded to mechanical loading. We evaluated 8,734 genes on the GEM I microarray chips with a threshold of light intensity of 1000 relative units in which 58% of the accessions in the chips was detected at a conservative threshold and on a more liberal threshold of 400 relative units, 88% was detectable in the mouse femur of C57BL/6J strain. Out of the 58%, 93 genes and ESTs had fluorescence signals higher than 10,000 relative units. On Pub-Med search it was found that 31 genes out of 91 are genes expressed in the musculoskeletal system which are shown in **Table 1A5**.

**Table 1A5 List of genes expressed in musculoskeletal system with signals above 10,000 relative units in microarray study**

Signal Level	Genes names	Expression/function
37,831	Procollagen, Type I, alpha	Bone formation
32,419	Lactotransferrin	Bone marrow
29,700	CD24a antigen	Bone marrow and liver

24,486	Hemoglobin alpha, adult chain	Fetal liver, spleen, bone marrow
22,792	Nuclear receptor binding factor 1	Bone
21,503	Glyceraldehyde-3-phosphate dehydrogenase	Bone
19,642	Carbonic anhydrase 2	Osteoclast
19,615	Tubulin alpha 4	Bone marrow stromal cells
19,485	Histocompatibility 2, L region	T cell
19,215	Interferon gamma receptor	Bone marrow
17,889	Histocompatibility 2, L region	Bone marrow
16,708	Secreted phosphoprotein 1	Bone
16,004	ESTs moderately similar to phosphatidylinositol	Osteoclast
15,396	S100 calcium binding protein A8	Bone /teeth
14,295	Interferon-dependent positive-actin transcription factor 3 gamma	Bone resorption
14,264	Hemoglobin alpha, adult chain 1	Bone marrow and fetal liver
12,963	<i>Mus musculus</i> mRNA for Zinc finger protein s11-6, complete cds	Osteoblast
12,861	Lipocalin 2	Bone
12,419	CCAAT/enhancer binding protein (C/EBP), alpha	Osteoblast
12,376	Myeloperoxidase	Hematopoietic cells, bone marrow
12,070	<i>M.musculus</i> endothelial monocyte-activating polypeptide I mRNA, complete cds	Osteoblast
12,044	Beta-2-microglobulin	Bone
11,909	RAB11B, member of RAS oncogene family	Bone
11,356	Calponin 2	Muscle
11,311	Tubulin, beta 5	Bone marrow, spleen developing liver and lung
11,193	Myeloperoxidase	Myeloid cells
11,056	Enolase 3, beta muscle	Muscle
10,991	ATPase-like vacuolar proton channel	Osteoclast
10,942	Cathelin-like protein	Host defense and wound repair
10,451	<i>M.musculus</i> myosin light chain 2mRNA, complete cds	Muscle
10,268	<i>M.musculus</i> Btk locus, alpha -D-galactosidase A (Ags), ribosomal protein (L44L) and Bruton's tyrosine kinase (Btk) genes, complete cds	B-cell

## 2). Isolation of RNA from pooled tibia and femur B6 mice for Microarray analysis

Mechanical training was performed in B6 strain. RNA from tibia and femur was pooled together from these mice to evaluate the greatest gene expression difference between control and jump mice using Microarray. The data were analyzed using Guantarray software. Interestingly we found that Procollagen type 3 and osteocalcin showed high expression with jumping compared to control. As 100µg of RNA was used for each sample, this method was not able to be applied to individual mice. Hence we optimize the conditions for the Microarray method and were able to use 10µg for each sample.

## 3). Development of a real time PCR method for quantification of candidate gene found by Microarray

To quantify and compare the Microarray results of the peak gene expression in response to loading we used a technique called Real time PCR. Reverse transcription followed by RT-polymerase chain reaction (PCR) is the technique of choice for analyzing and quantifying the peak mRNA expression and also for comparing the results with Microarray when RNA in low abundance. We have designed and developed an assay with optimal conditions for obtaining accurate results using smart cycler real time PCR under syber green dye method. The principle of this instrument is similar to an ordinary PCR except a fluorescent dye, which binds to amplified product and emits fluorescence signals that are viewed in terms of cycles and is used for measuring the expression difference between the genes. After optimizing all of the necessary conditions oligonucleotide primers were designed according to target and the PCR reactions were performed in log concentration of a sample RNA. In addition, we also used an internal control b-actin to analyze the results. The syber green dye method showed a high specificity and sensitivity with high test linearity of Pearson correlation coefficient  $r > 0.99$ . This method was used to analyze the results of jumping regimen.

### Comparing the expression of collagen (ColA1) in the Jump-up and Jump down regimens by means of Real time PCR

After optimizing the Microarray conditions, we evaluated the expression of ColA1 gene in response to mechanical stimuli. Six week old mice of B6 strain alone were given mechanical training with different types of jumping as shown in **Table 1A6**. The animals were trained for 4 days and were sacrificed after 24 hours. The RNA isolated from these animals, in terms of quantity and quality, was sufficient for our experiments. In this experiment we used type-I collagen, since it forms 95% of bone matrix and therefore increased expression would be effected in response to loading. For the statistical analysis we have three sub-groups in each jumping regimen. The RNA was reverse transcribed using RT and cDNA was obtained and the real time PCR was performed using 1µg, 0.1µg and 0.01µg concentrations. Each reaction was performed with a positive control b-actin. In neither of the jumping regimens (height and times) were we able to find any significant changes on Type-I collagen gene. The results are tabulated and shown in **Table-III**. These data indicate that the jumping regimens did not produce sufficient mechanical strain to be detected by our RT-PCR technique.

**Table. 1A6. Quantification of Type-I collagen in control vs jumped using real time PCR.**

	Gene	1µg of RNA	0.1µg of RNA	0.01µg of RNA
<i>JUMP DOWN-20cm</i>	Col A1	15.8±0.71	19.56±1.03	24.55±0.55
Control				
Jump-down 20 cm	Col A1	15.68±0.53	24.4±0.97	27.01±1.61

Control	$\beta$ -actin	21.77 $\pm$ 1.7	23.49 $\pm$ 1.07	27.71 $\pm$ 1.44
20cm Jump-down	$\beta$ -actin	21.34 $\pm$ 0.89	22.69 $\pm$ 0.96	27.37 $\pm$ 0.40
<i>JUMP-DOWN-40cm</i>				
Control	Col A1	18.62 $\pm$ 4.03	19.83 $\pm$ 0.72	23.58 $\pm$ 1.11
<u>Jump-down 40cm</u>	Col A1	16.24 $\pm$ 2.24	19.4 $\pm$ 0.7	23.39 $\pm$ 0.87
<u>Control</u>	$\beta$ -actin	19.3 $\pm$ 0.84	21.98 $\pm$ 0.51	26.07 $\pm$ 0.93
<u>40cm Jump-down</u>	$\beta$ -actin	25.66 $\pm$ 10.28	22.75 $\pm$ 1.122	25.41 $\pm$ 1.62
<i>JUMP-UP 20cm</i>				
<u>Control</u>	Col A1	24.4 $\pm$ 3.05	28.32 $\pm$ 2.06	28.82 $\pm$ 0.86
<u>Jump-up 20cm</u>	Col A1	24.25 $\pm$ 2.55	28.65 $\pm$ 1.22	28.82 $\pm$ 0.86
Control	$\beta$ -actin	30.51 $\pm$ 3.51	34.72 $\pm$ 2.56	36.83 $\pm$ 0.43
Jump-up 20cm	$\beta$ -actin	30.84 $\pm$ 1.6	35.51 $\pm$ 1.33	36.91 $\pm$ 1.04

p>.05 for all co-variance

#### 4). Conclusions

1. Microarray studies showed that with over 8,000 genes explored, 93 of these genes showed a more than 10 fold increase in expression above background. 36 of these genes were interpreted on the basis of findings in PUBMED to be associated with the musculoskeletal system. These 36 genes were then used in subsequent studies to further evaluate microarray differences between jump trained animals and controls.
2. We have optimized the conditions for Microarray technique.
3. We have evaluated the gene expression in response to loading using Microarray to look for the candidate genes.
4. To quantify the Microarray results, we have set up a method using Real time PCR.
5. We found that RT-PCR results did not show any significant gene expression changes in jump-up or jump-down training.
6. All of the studies with real time PCR indicate that the method is very reproducible and that the method can be applied using small amounts of RNA, allowing the measurement of candidate gene expression in our sample preparation to be quantitated in each animal. However, the changes were not statistically significant in response to jump training using the collagen (ColA1) gene expression as an end point. We still feel that using the RT-PCR gene expression as an end-point is suitable for our purposes. However, the work shows that we require a greater mechanical strain to illicit sufficient changes to be able to quantitatively phenotype each animal for the QTL analysis. Therefore, in the future, we will continue to evaluate candidate gene expression by Microarray and real-time PCR as our end point but switch to 4-point bending as our means to illicit mechanical strain rather than jump training.

## Progress for the Period of 2003-2004

### Introduction

Physical exercise is believed to increase bone formation and improve bone density in osteoporotic patients and other patients with metabolic disease. However, the mechanisms by which mechanical stress converts mechanical signaling and activates a set of stress-responsive genes leading to bone remodeling, are not fully understood. Our previous studies have shown that two inbred mouse strains, C57BL/6J (B6) and C3H/HeJ (C3H) respond differently to mechanical loading in vivo. B6 mice showed a significant increase in bone density as compared to C3H when subjected to similar loading regimens. These results suggest that mechanical stimulation may induce distinct types of gene expression in B6 mice, which contribute to the subsequent bone formation. Therefore, it is of particular interest to localize chromosomal regions responsible for mechanical stress, and identify osteogenic candidate genes by applying powerful genetic tools, namely quantitative trait loci (QTL).

### Technical Objective: 1

Technical Objective-1 for the past twelve months was revised on 04/15/03. The revised specific objectives for technical objective-1 are provided below. In the original proposal there were two technical objectives for this portion of our work. The second technical objective has now been incorporated into the first technical objective. Therefore, on this progress report we will report on technical objective one, and five specific objectives. We will then skip to technical objective three, which is a progress report on our in vitro work, to evaluate the physical actions of mechanical strain on bone cells in vitro.

Our specific objectives for the revised technical objective are:

- 1) To establish the optimal method for inducing mechanical strain on the tibia.
- 2) To determine the optimal method for quantitating the bone formation response to mechanical strain on the tibia in vivo.
- 3) To determine the number of days required of 4-point bending induced mechanical strain on the tibia in order to elicit an optimal response for quantitative measurements.
- 4) To select the optimal mouse inbred strain pair (i.e. B6 and C3H or some other strain pair) to perform the QTL mapping study.
- 5) To determine the appropriate age of animals to apply the 4-point bending in order to obtain valid quantitative measurements of the bone formation response.

Our goal is to evaluate bone formation in 10 different mouse strains using mechanical loading in order to identify two mouse strains which show extreme differences in the bone formation. These selected strains will then be backcrossed for two more generations (F2) and the F2 mice will be used to identify candidate genes responsible for bone formation by applying a powerful genetic tool, quantitative trait loci (QTL), as described previously. Initially we planned to perform the jump training as a loading model. However, if jump training does not show a significant amount of bone formation, then we will be using four-point bending as alternative loading regimen and real time PCR as the end

point measurement of the bone formation rate in two strains that show extreme difference in bone formation.

### Specific Objective 1: Optimize a method that can induce mechanical strain on bone.

Initially 6-week old B6 mice were given 4-days of jump-up and jump-down training to evaluate the bone formation response. The mice are sacrificed after 24hrs of the last training regimen and bone formation was evaluated in terms of mRNA expression using Real time PCR. In this experiment we used type-I collagen, since it constitutes approximately 95% of bone matrix and therefore will show increased expression in response to loading. However, we found that the jump training did not produce a sufficient amount of stress on bone to see a significant change in the expression of type-I collagen between control and experimental mice (**Table-1**). The values in the table represent the cycles (Ct-values), which corresponds to the amount of amplified product of the target gene.

**Table-1** Quantification of type-1 collagen expression in 6-week old B6 mice in response to jump training using real time PCR. The value represents Mean  $\pm$  SD.

Experiments	Groups	Cycles $\pm$ SD		
		Gene	0.1 $\mu$ g of RNA	Fold Change
<i>JUMP DOWN-20cm</i>				
	<b>Control</b>	Col A1	19.56 $\pm$ 1.03	No change
	<u>Jump-down 20 cm</u>	Col A1	24.40 $\pm$ 0.97	No change
	Control	$\beta$ -actin	23.49 $\pm$ 1.07	No change
	20cm Jump-down	$\beta$ -actin	22.69 $\pm$ 0.96	No change
<i>JUMP-DOWN-40cm</i>				
	<b>Control</b>	Col A1	19.83 $\pm$ 0.72	No change
	<u>Jump-down 40cm</u>	Col A1	19.40 $\pm$ 0.7	No change
	Control	$\beta$ -actin	21.98 $\pm$ 0.51	No change
	40cm Jump-down	$\beta$ -actin	22.75 $\pm$ 1.12	No change
<i>JUMP-UP 20cm</i>				
	<b>Control</b>	Col A1	28.32 $\pm$ 2.06	No change
	<u>Jump-up 20cm</u>	Col A1	28.65 $\pm$ 1.22	No change
	Control	$\beta$ -actin	34.72 $\pm$ 2.56	No change
	Jump-up 20cm	$\beta$ -actin	35.51 $\pm$ 1.33	No change

*N=4, p>.05 for all co-variance*

*ColA1-type-1 collagen,  $\beta$ -actin-beta-actin*

Therefore, we used our next candidate in-vivo-loading regimen, namely four-point bending. The load, cycle and the frequency used for the study were similar to Reckers et al., (1998) except the duration of training was changed from 12 to 4-days of training in order to evaluate the effect of mechanical strain on bone formation in a short time duration. The loading regimen consisted of a 9N load at 2Hz for 36cycles. The training was performed once per day. The right tibia of the mouse was loaded while the left tibia was used as an internal control. The mice were sacrificed 24hrs after the last training regimen

and the mRNA message was quantified using Real time PCR. In this experiment to evaluate bone formation in response to loading we used two major bone markers, namely type-I collagen and osteocalcin. In addition, we also used other bone formation genes, namely bone sialoprotein, alkaline phosphate, osteocalcin and osteopontin.

4-days four-point bending in 16-week old B6 and C3H mice showed a significant ( $p < 0.05$ ) increase in the expression of bone formation genes in loaded bones as compared to unloaded bones. As shown in **Table-2&3** mechanical loading resulted in a 2-fold increase in type-I collagen, bone sialoprotein, alkaline phosphates in both B6 and C3H mice. However B6 mice showed a 1.4-fold increase in Osteocalcin while C3H did not show any change between unloaded and loaded bones.

**Table-2** Quantitative Real time PCR results in response to 4-days training of four-point bending in 16-week old B6 mice using 200 ng RNA concentration.

Genes	Groups	Cycles $\pm$ SD	P-value	Fold Change
Type-I Collagen	Experiment	20.17 $\pm$ 1.37	0.02 <sup>a</sup>	2.2
	Control	18.45 $\pm$ 0.49		
Osteocalcin	Control	24.60 $\pm$ 0.86	0.05 <sup>a</sup>	1.42
	Experiment	23.49 $\pm$ 0.70		
Bone sialoprotein	Control	25.11 $\pm$ 0.97	0.01 <sup>a</sup>	2.2
	Experiment	23.20 $\pm$ 0.59		
Alkaline Phosphatase	Control	29.53 $\pm$ 1.34	0.02 <sup>a</sup>	2.5
	Experiment	27.60 $\pm$ 0.64		
Osteopontin	Control	24.01 $\pm$ 1.38	0.38	No change
	Experiment	23.36 $\pm$ 0.77		
Actin	Control	19.19 $\pm$ 1.04	0.28	
	Experiment	18.60 $\pm$ 0.49		

*N*

= 5<sup>a</sup>  $p < 0.05$

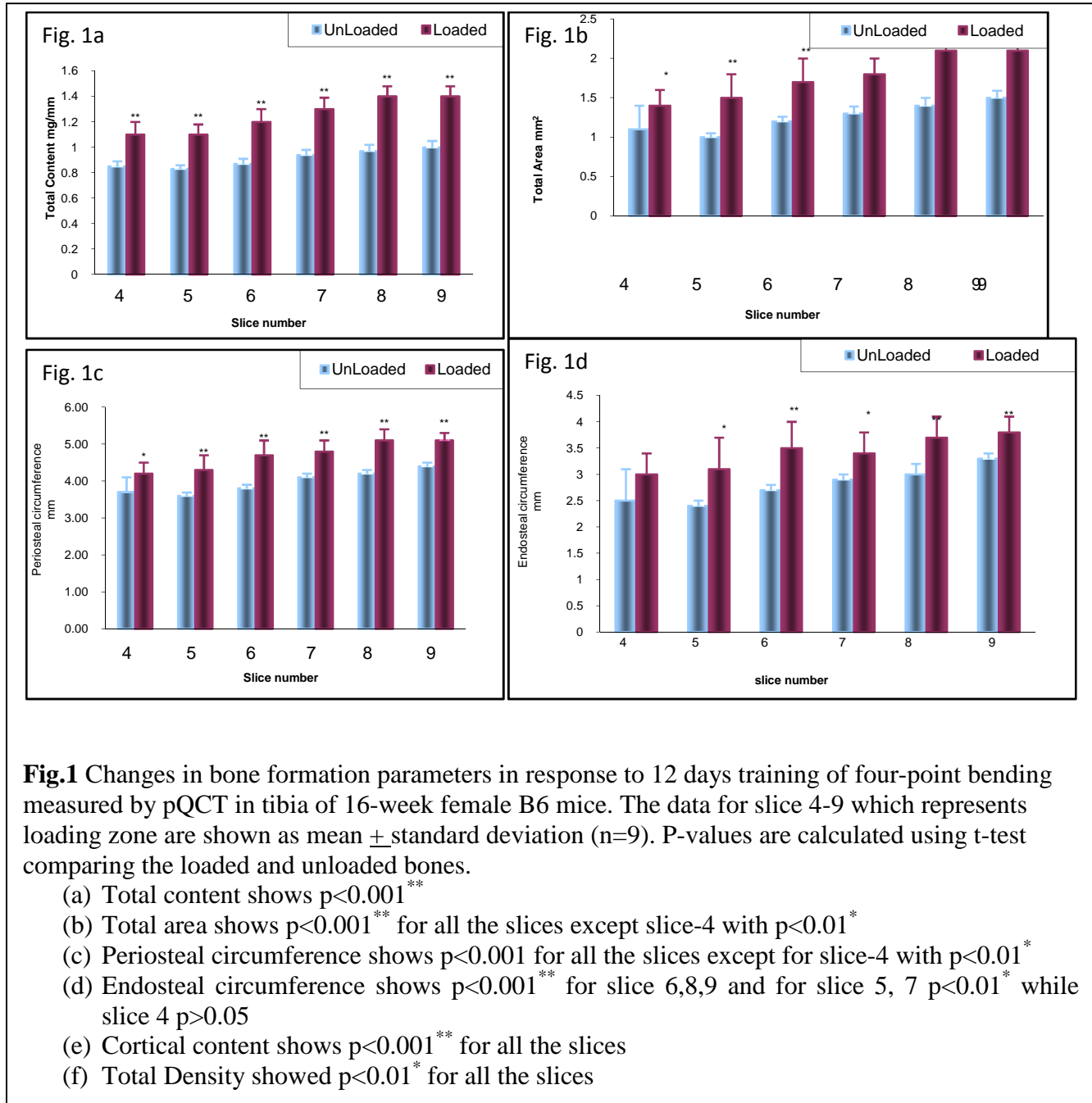
**Table-3** Quantitative Real time PCR results in response to 4-days training of four-point bending in 16-week old C3H mice using 200 ng RNA concentration.

Genes	Groups	Cycles $\pm$ SD	P-value	Fold Change
Type-I collagen	Control	23.77 $\pm$ 1.05	0.0002 <sup>*</sup>	3.0
	Experiment	20.47 $\pm$ 0.58		
Osteocalcin	Control	26.16 $\pm$ 0.86	0.10	No change
	Experiment	25.30 $\pm$ 0.76		
Bone sialoprotein	Control	27.06 $\pm$ 1.85	0.02 <sup>a</sup>	1.52
	Experiment	24.74 $\pm$ 0.57		
Alkaline Phosphatase	Control	31.10 $\pm$ 1.31	0.003 <sup>*</sup>	2.0
	Experiment	28.37 $\pm$ 0.65		
Bone Osteopontin	Control	26.92 $\pm$ 1.62	0.25	No change
	Experiment	25.89 $\pm$ 0.93		
Actin	Control	22.82 $\pm$ 1.68	0.07	
	Experiment	21.11 $\pm$ 0.84		

*N* = 4, <sup>a</sup> $p < 0.05$ , <sup>\*</sup> $p < 0.01$

### Specific Objective 2: Determine an optimal method to evaluate the bone formation

To quantify peak gene expression in response to loading we used a technique called Real time PCR. After the training regimen mice were sacrificed and the total RNA was extracted from the loaded



and unloaded bone by Trizol method. This RNA was used to synthesize single strand cDNA by reverse transcription assay followed by Real time PCR using applied biosystems. The principle of this Real time PCR is similar to an ordinary PCR except a fluorescent dye, which binds to amplified product and emits fluorescence signals that are viewed in terms of cycles or Ct-values. The Ct-values corresponds to the

amount of amplified products and used for calculating the mRNA expression of the target gene. In order to validate these Ct-values we also ran Universal RNA (Stratagene, USA) as a standard during each reaction. We used SYBR Master mix (Fluorescent PCR reagents) kit to perform the above reaction in applied biosystems. In this four-point bending experiment, to evaluate the bone formation response to loading we used two major bone markers, namely type-I collagen and osteocalcin. In addition to this we also used other bone formation genes, bone sialoprotein, alkaline phosphatase and osteopontin, since they play a significant role in mineralization of bone. B-actin was used as an internal control to normalize the data and calculate the exact fold change of genes by applying mathematical formula ( $2^{-\Delta\Delta CT}$ ) of Applied Biosystems.

In order to further validate the four-point bending method and the real time PCR results, we used pQCT and histological methods that are well-established endpoints for measuring the bone formation. We performed 12-day training of four-point bending with similar magnitude of load, frequency and cycle number in 16-week B6 and C3H mice. Since a longer period of time is required to see new bone deposits, we used 12 days of training instead of 4 days. As shown in **Fig.1** 12-days of training in 16-week B6 mice showed maximum change in total area, total content and cortical content in the loaded bones compared to unloaded bones. Significant changes were also observed in periosteal, endosteal circumference and bone density.

Similar to B6, C3H mice also showed maximum change in total area, total content, periosteal and endosteal circumference of bone in response loading. However, in contrast to B6, there was no change in total density in the loaded bones compared to unloaded bone as shown in **Fig.2**

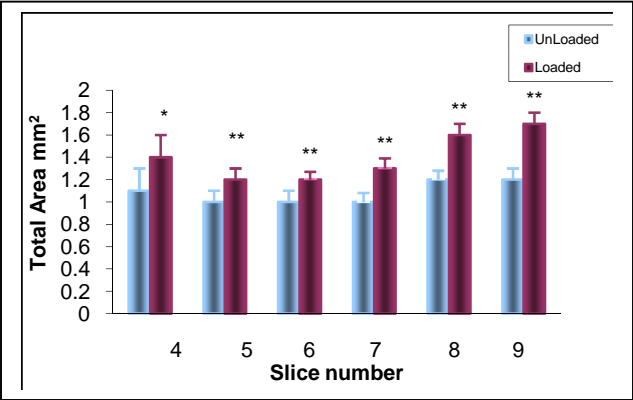


Fig.2 [a]

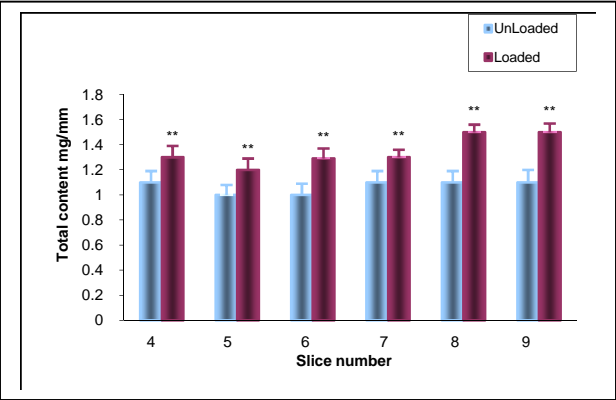


Fig.2 [b]

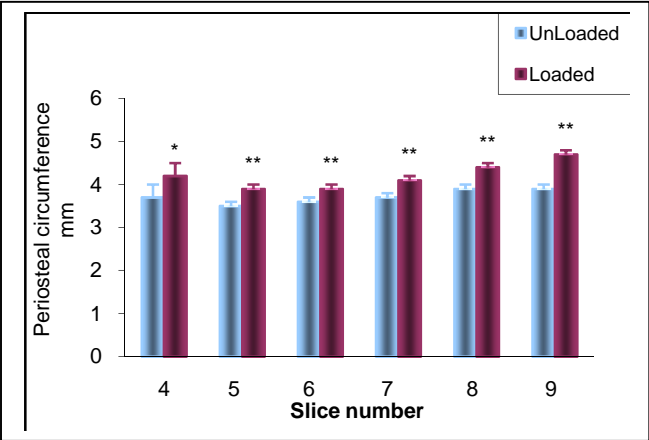


Fig.2 [c]

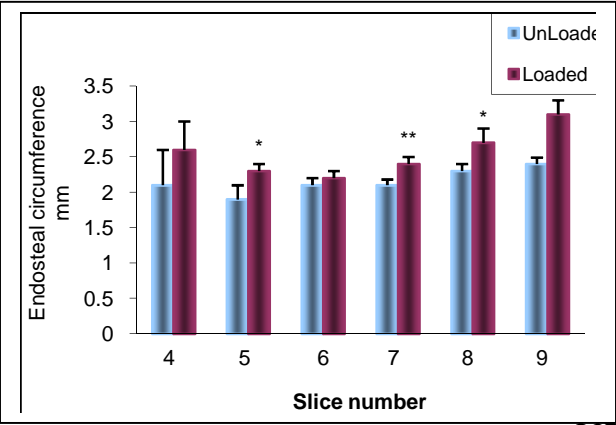


Fig. [2d]

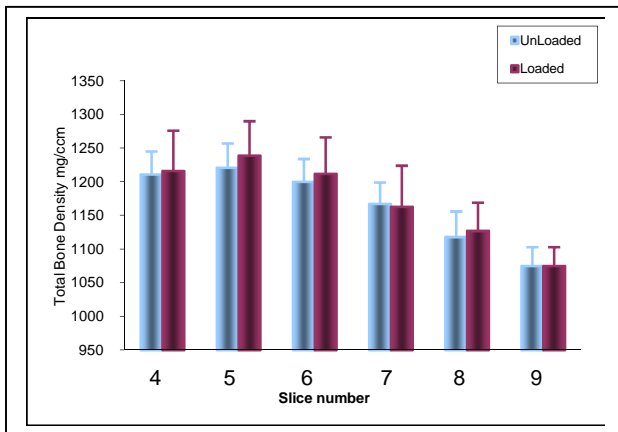


Fig.2 [e]

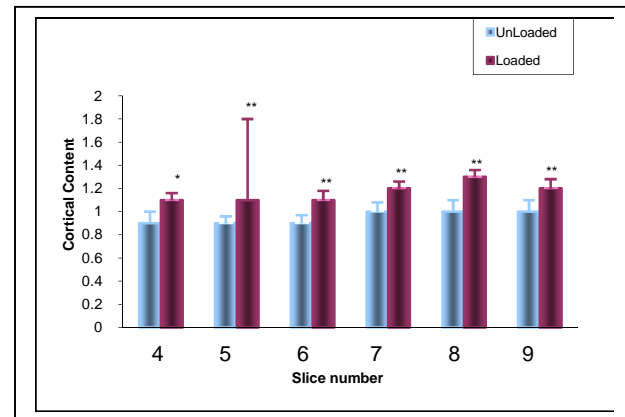
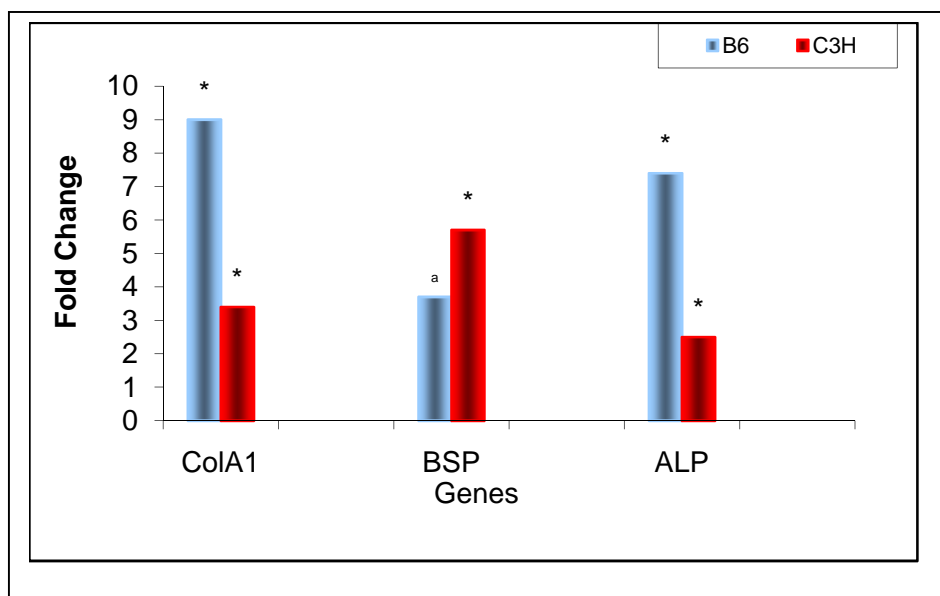


Fig.2 [f]

**Fig.2** Changes in bone formation parameters in response to 12 days of four-point bending measured by pQCT in tibia of 16-week female C3H mice. The data for slice 4-9 which represents mean + standard deviation (n=9). P-values are calculated using t-test comparing the loaded and unloaded bones.

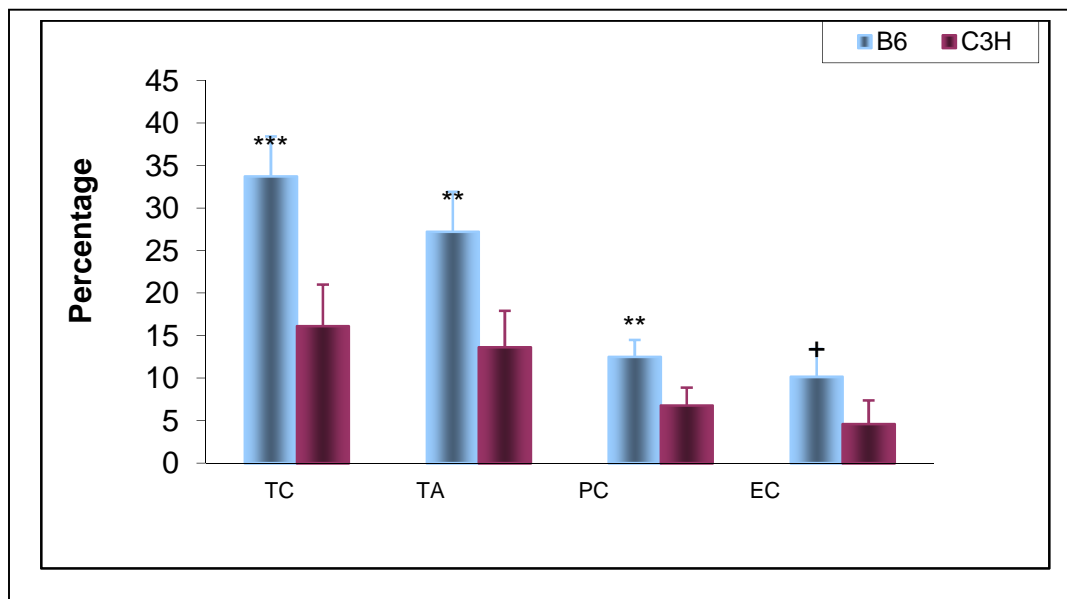
- Total Content shows  $p < 0.001^{**}$
- Total area show  $p < 0.001^{**}$  for all the slices except for slice-4  $p < 0.05^a$
- Periosteal circumference shows  $p < 0.001^{**}$  except for slice-4  $p < 0.01^*$
- Endosteal circumference shows  $p < 0.001^{**}$  for slices 7, 9 while slices 5, 8 showed  $p < 0.01^*$ . Slices 4 & 6 showed  $p > 0.05$
- Total bone density shows  $p > 0.05$  for all the slices
- Cortical Content shows  $p < 0.001^{**}$  for all the slices except slice-4 with  $p < 0.01^*$



$N=5$ , \*  $p<0.01$ , <sup>a</sup>  $p<0.05$

**Fig.3** Fold change in expression of various genes in response to 12 days of four-point bending in B6 and C3H retired breeders.

To correlate the pQCT and gene expression results using real time PCR in response to mechanical loading we performed 12 days of four-point bending in retired breeders of B6 and C3H mice. Twelve-day training of four-point bending in B6 retired breeders showed a 9-fold increase in type-I collagen (ColA1) and a 7-fold increase in alkaline phosphatase (ALP) as compared to C3H retired breeders. However the bone sialoprotein showed a decrease in fold change for B6 compared to C3H. This suggests that long duration of bending treatment decreased the expression of bone sialoprotein in B6 (**Fig.3**). Based on these results, type-I collagen found to be a valuable marker that is increased in all age groups in response to bending. On the other hand, 12 days of four-point bending using pQCT showed increases in total area, total content, periosteal and endosteal circumference of bone for B6 mice compared to C3H mice retired breeders as shown in **Fig.3a**. However, for the total density, B6 showed less change while C3H showed no significant change.



\*\*\*  $p<0.0001$ , \*\*  $p<0.001$ , +  $p<0.05$

**Fig.3a** Increase in bone formation parameters in response to 12 days training of four-point bending measured by pQCT in tibia of B6 and C3H retired breeders. The data shows percentage of increase in TA-Total Content, TA-Total Area, PC-Periosteal circumference, EC-Endosteal circumference as Mean  $\pm$  Standard deviation of loaded zone. P-values are calculated by comparing the percentage of new bone formation between B6 and C3H mice.

We used Real-time PCR and pQCT as two methods for measuring the bone formation rate in response to four-point bending. **Fig.3b** shows the correlation between Bone Mineral Density and Type-I Collagen expression. As shown, there is a significant correlation ( $p<0.05$ ) between the BMD [Measured by

pQCT] and collagen expression [Measured by real time PCR]. Based on these results, we conclude that Real time PCR is the most sensitive and fastest method to evaluate the bone formation in response to four-point bending. Thus, we will be using Real Time PCR as the endpoint in our QTL study.

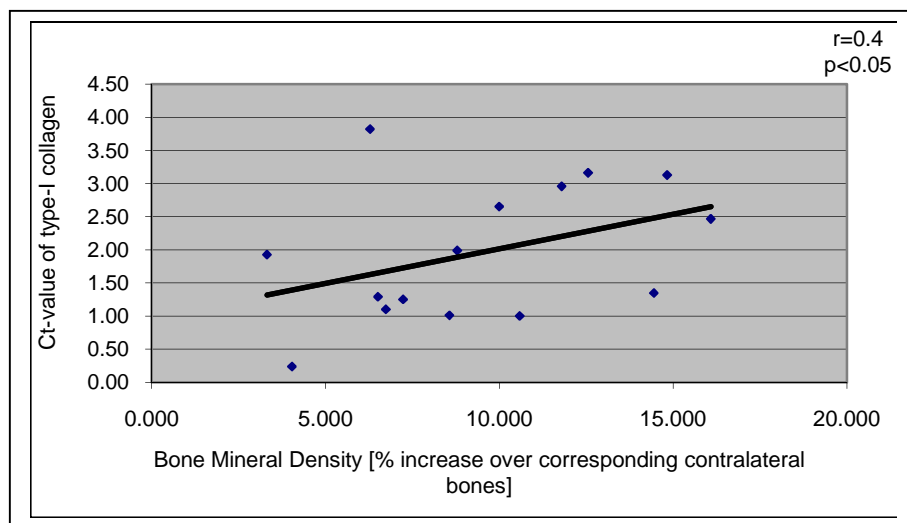


**Fig.3b** Correlation of bone mineral density and type-I collagen expression in response to four-point bending in different age groups of B6 mice. The x-axis represents BMD change measured by percentage increase in loaded bone compared to corresponding contralateral bone. The y-axis shows change in collagen gene expression in response to four-point bending as measured by  $\Delta\Delta$ Ct for loaded bone vs unloaded bone using b-actin as a control gene.

### **Specific Objective 3: Determine an optimal duration of training period**

10-week old B6 mice were subjected to 2 days, 4 days and 8 days training in order to select an optimal duration of training that show maximum effect on bone formation. Two days of four-point bending in B6 mice did not produce any significant effect on bone. The expression of bone formation genes in loaded bones was similar to the control shown in **Table-4**.

**Table 4:** Quantitative Real time PCR results in response to 2 days training of four-point bending in 10-week old B6 mice using 200 ng RNA concentration.

Genes	Groups	Cycles $\pm$ SD	P-value	Fold Change
Type-I collagen	Control	20.61 $\pm$ 1.9	0.97	No change
	Experiment	20.58 $\pm$ 0.4		
Osteocalcin	Control	24.85 $\pm$ 2.2	0.52	No change
	Experiment	24.17 $\pm$ 0.6		
Bone sialoprotein	Control	26.59 $\pm$ 1.4	0.82	No change
	Experiment	26.76 $\pm$ 0.59		
Alkaline Phosphatase	Control	30.70 $\pm$ 1.9	0.86	

	Experiment	30.86 ± 0.5		No change
Actin	Control	22.40 ± 2.4	0.48	Internal control
	Experiment	21.60 ± 0.49		

$N=5$ ,  $p>0.05$

Four -days four-point bending in 10-week old B6 mice resulted in 2.9 and 4.5 fold increase in type-1-collagen and bone sialoprotein respectively. On the other hand, no change was observed in alkaline phosphates, osteocalcin and osteopontin (**Table-5**). B-actin was used as internal control to normalize the data in order to obtain the fold change of the target gene.

**Table-5** Quantitative Real time PCR results in response to 4 days four-point bending in 10-week old B6 mice using 200 ng RNA concentration.

Genes	Groups	Cycles ± SD	P-value	Fold Change
Type-I Collagen	Experiment	21.75 ± 1.8	0.06	2.9
	Control	19.45 ± 1.5		
Bone sialoprotein	Control	27.21 ± 1.4	0.02 <sup>a</sup>	4.5
	Experiment	24.22 ± 1.9		
Osteocalcin	Control	25.28 ± 1.1	0.49	No change
	Experiment	24.76 ± 1.06		
Alkaline phosphatase	Control	31.88 ± 2.4	0.14	No change
	Experiment	29.55 ± 2.1		
Osteopontin	Control	24.36 ± 1.3	0.34	No change
	Experiment	23.57 ± 1.1		
Actin	Control	22.56 ± 1.6	0.47	Internal Control
	Experiment	21.84 ± 1.3		

$N=5$ , <sup>a</sup>  $p<0.05$

Eight - days of four-point bending in tibia of 10-week old B6 mice showed a significant change in expression of bone formation genes compared to 2-days and 4-days of training. As shown in **Table-6**, 8-days of training showed a 4-fold increase in type-I collagen, 2.7-fold in osteocalcin, 3.6 fold in Bone sialoprotein and 2.8 fold in alkaline phosphatase.

**Table-6** Quantitative Real time PCR results in response to 8 days four-point bending in 10-week old B6 mice using 200 ng RNA concentration.

Genes	Groups	Cycles ± SD	P-value	Fold Change
Type-I collagen	Control	22.02 ± 0.4	0.00001 <sup>**</sup>	3.8
	Experiment	19.35 ± 0.4		
Osteocalcin	Control	24.94 ± 1.1	0.01 <sup>a</sup>	2.7
	Experiment	22.76 ± 0.9		
Bone sialoprotein	Control	26.79 ± 0.8	0.003 <sup>*</sup>	3.7
	Experiment	24.16 ± 1.1		
Alkaline Phosphatase	Control	29.78 ± 0.9	0.001 <sup>*</sup>	2.9
	Experiment	27.53 ± 0.5		
	Control	22.56 ± 1.1	0.24	Internal control

Actin	Experiment	21.83 ± 0.6		
-------	------------	-------------	--	--

$N=5$ , \* $p<0.01$ , \*\* $p<0.001$ , <sup>a</sup> $p<0.05$

**Specific Objective 4: Determine optimal mouse strain pair that show extreme difference in bone formation.**

With the optimized loading regimen, four-point bending was carried out in 10-week-old B6, Balbc, AKR/J, 129J, NZB mice and the bone formation was evaluated using Real time PCR. AKR/J showed 1-fold change in type-I collagen, alkaline phosphatase and 2-fold change in Bone sialoprotein while no change in osteocalcin was seen (**Table-7**). 129J showed 3 fold change in type-I collagen and bone sialoprotein. However, no change in alkaline phosphatase, osteocalcin and osteopontin was observed (**Table-8**). NZB showed no change in any of the bone markers in response to four-point bending (**Table-9**). In the case of Balbc the bone (tibia) broke at 9N load, therefore 6N load was applied. There was no change in expression of bone formation genes between control and experiment in Balb/c mice (**Table-10**). The B6 mice showed a 3-4 fold increase in type-I collagen and bone sialoprotein. However, there was no change in alkaline phosphatase and osteocalcin (**Table-11**). Overall, AKR, 129J and B6 mice showed similar gene expression in response to four-point bending while Balb/c and NZB showed no significant change in expression of bone formation genes shown in **Table-12**

**Table-7** Quantitative Real time PCR results in response to 4-days four-point bending in 10-week old AKR/J using 200 ng RNA concentration.

Genes	Groups	Cycles ± SD	P-value	Fold Change
Type-I Collagen	Experiment	18.16 ± 0.9	0.01 <sup>a</sup>	1.0
	Control	19.35 ± 0.4		
Bone sialoprotein	Control	25.27 ± 1.7	0.01 <sup>a</sup>	2.7
	Experiment	22.76 ± 1.1		
Alkaline Phosphatase	Control	24.23 ± 0.8	0.02 <sup>a</sup>	1.3
	Experiment	22.87 ± 0.9		
Osteocalcin	Control	22.11 ± 0.4	0.44	No change
	Experiment	21.74 ± 1.0		
Actin	Control	20.73 ± 1.5	0.1	Internal control
	Experiment	19.65 ± 0.9		

$N=5$ , <sup>a</sup> $p<0.05$

**Table-8** Quantitative Real time PCR results in response to 4-days four-point bending in 10-week old 129J using 200 ng RNA concentration.

Genes	Groups	Cycles ± SD	P-value	Fold Change
Type-I Collagen	Experiment	20.87 ± 0.7	0.06	2.6
	Control	19.66 ± 0.9		
Bone sialoprotein	Control	23.48 ± 0.3	0.05 <sup>a</sup>	2.8
	Experiment	22.14 ± 1.3		
Alkaline Phosphatase	Control	27.33 ± 1.3	0.57	No change
	Experiment	26.80 ± 1.5		

Osteopontin	Control	29.33 ± 0.4	0.37	No change
	Experiment	29.93 ± 1.3		
Osteocalcin	Control	26.49 ± 0.6	0.53	No change
	Experiment	26.26 ± 0.4		
Actin	Control	19.62 ± 1.1	0.53	Internal Control
	Experiment	20.07 ± 1.0		

$N=5$ ,  $^a p < 0.05$

**Table-9** Quantitative Real time PCR results in response to 4-days four-point bending in 10-week old NZB using 200 ng RNA concentration.

Genes	Groups	Cycles ± SD	P-value	Fold Change
Type-I Collagen	Experiment	19.50 ± 2.4	0.63	No change
	Control	18.94 ± 1.3		
Bone sialoprotein	Control	23.89 ± 1.6	0.12	No change
	Experiment	24.77 ± 2.6		
Osteocalcin	Control	22.16 ± 1.7	0.50	No change
	Experiment	24.13 ± 2.3		
Actin	Control	20.86 ± 1.4	0.31	Internal control
	Experiment	21.92 ± 1.9		

$N=5$ ,  $p > 0.05$

**Table-10** Quantitative Real time PCR results in response to 4-days four-point bending in Balbc10-week old mice using 200 ng RNA concentration.

Genes	Groups	Cycles ± SD	P-value	Fold change
Type-I Collagen	Experiment	17.80 ± 1.4	0.98	No change
	Control	17.78 ± 1.7		
Bone sialoprotein	Control	23.32 ± 1.5	0.49	No change
	Experiment	22.59 ± 1.5		
Alkaline Phosphatase	Control	25.32 ± 2.1	0.81	No change
	Experiment	25.00 ± 1.4		
Osteopontin	Control	28.51 ± 2.0	0.88	No change
	Experiment	28.35 ± 1.1		
Actin	Control	17.86 ± 1.0	0.33	Internal control
	Experiment	17.21 ± 0.9		

$N=5$   $p > 0.05$

**Table-11** Quantitative Real time PCR results in response to 4 days training of four-point bending in 10-week old B6 mice using 200ng RNA concentration

Genes	Groups	Cycles ± SD	P-value	Fold Change
-------	--------	-------------	---------	-------------

Type-I Collagen	Experiment	21.75 ± 1.8	0.06	2.9
	Control	19.45 ± 1.5		
Bone sialoprotein	Control	27.21 ± 1.4	0.02 <sup>a</sup>	4.5
	Experiment	24.22 ± 1.9		
Osteocalcin	Control	25.28 ± 1.1	0.49	No change
	Experiment	24.76 ± 1.0		
Alkaline phosphatase	Control	31.88 ± 2.4	0.14	No change
	Experiment	29.55 ± 2.1		
Osteopontin	Control	24.36 ± 1.3	0.34	No change
	Experiment	23.57 ± 1.1		
Actin	Control	22.56 ± 1.6	0.47	Internal control
	Experiment	21.84 ± 1.3		

$N=5$ , <sup>a</sup> $p<0.05$

**Table-12** Ranking of mouse strain [Good and Poor responder] based upon the expression of bone formation genes in response to 4 days of four-point bending.

Bone Formation Markers	Fold change in response to 4-days training of four-point bending in different inbred strains of mice [10-week old]					
	Good Responder			Poor Responder		
Genes	B6	129J	AKR/J	NZB	Balbc	
Type-I collagen	2.9	2.6	1.0	-	-	
Bone sialoprotein	4.5	2.8	2.7	-	-	
Alkaline phosphatase	-	-	1.3	-	-	
Osteocalcin	-	-	-	-	-	

- No change

**Specific Objective 5: Determine appropriate age of mice that show significant affect on bone formation through optimized protocol.**

With the optimized loading regimen [9N load at 2Hz –36cycles], four-point bending was applied to 10-week old B6 mice, , 16-week old and Retired Breeders and bone formation was evaluated using real time PCR. As shown in **Table-13**, 10-week old mice in response to 4-days training showed increased expression of type-I collagen and bone sialoprotein ( $p<0.05$ ) while no change in osteocalcin and alkaline phosphatase. While 16-week old mice showed a 2-fold change in type-I collagen, bone sialoprotein, alkaline phosphatase and 1.4 fold change in osteocalcin shown in **Table-14**. Interestingly, in the retired breeders, we found a better bone formation response with 4-days training of 9N load. The

type-I collagen and bone sialoprotein showed a significant fold change with  $p < 0.01$  while alkaline phosphatase and osteocalcin showed  $p < 0.05$  (**Table-15**).

**Table-13** Quantitative Real time PCR results in response to 4-days four-point bending in 10-week old female B6 mice using 200 ng RNA concentration

Genes	Groups	Cycles $\pm$ SD	P-value	Fold Change
Type-I Collagen	Experiment	21.75 $\pm$ 1.8	0.06	2.9
	Control	19.45 $\pm$ 1.5		
Bone sialoprotein	Control	27.21 $\pm$ 1.4	0.02 <sup>a</sup>	4.5
	Experiment	24.22 $\pm$ 1.9		
Osteocalcin	Control	25.28 $\pm$ 1.1	0.49	No change
	Experiment	24.76 $\pm$ 1.06		
Alkaline phosphatase	Control	31.88 $\pm$ 2.4	0.14	No change
	Experiment	29.55 $\pm$ 2.1		
Osteopontin	Control	24.36 $\pm$ 1.3	0.34	No change
	Experiment	23.57 $\pm$ 1.1		
Actin	Control	22.56 $\pm$ 1.6	0.47	Internal control
	Experiment	21.84 $\pm$ 1.3		

$N=5$ , <sup>a</sup> $p < 0.05$

**Table-14** Quantitative Real time PCR results in response to 4-days four-point bending in 16-week old Male B6 mice using 200 ng RNA concentration.

Genes	Groups	Cycles $\pm$ SD	P-value	Fold Change
Type-I Collagen	Experiment	20.17 $\pm$ 1.37	0.02 <sup>a</sup>	2.2
	Control	18.45 $\pm$ 0.49		
Osteocalcin	Control	24.60 $\pm$ 0.86	0.05 <sup>a</sup>	1.42
	Experiment	23.49 $\pm$ 0.70		
Bone sialoprotein	Control	25.11 $\pm$ 0.97	0.01 <sup>a</sup>	2.2
	Experiment	23.20 $\pm$ 0.59		
Alkaline Phosphatase	Control	29.53 $\pm$ 1.34	0.02 <sup>a</sup>	2.5
	Experiment	27.60 $\pm$ 0.64		
Osteopontin	Control	24.01 $\pm$ 1.38	0.38	No change
	Experiment	23.36 $\pm$ 0.77		
Actin	Control	19.19 $\pm$ 1.04	0.28	Internal control
	Experiment	18.60 $\pm$ 0.49		

$N = 5$ , <sup>a</sup> $p < 0.5$

**Table-15** Quantitative Real time PCR results in response to 4 days four-point bending in B6 Retired breeders using 200 ng RNA concentration

Genes	Groups	Cycles $\pm$ SD	P-value	Fold Change
Type-I collagen	Control	22.26 $\pm$ 1.0	0.0007 <sup>*</sup>	6.5
	Experiment	18.61 $\pm$ 0.54		
Bone sialoprotein	Control	25.58 $\pm$ 1.1	0.002 <sup>*</sup>	6.5
	Experiment	21.93 $\pm$ 0.98		

Alkaline phosphatase	Control	30.16 $\pm$ 1.5	0.02 <sup>a</sup>	4
	Experiment	27.14 $\pm$ 1.2		
Osteocalcin	Control	27.28 $\pm$ 1.0	0.04 <sup>a</sup>	2
	Experiment	25.33 $\pm$ 1.1		
Actin	Control	20.82 $\pm$ 0.64	0.12	Internal control
	Experiment	19.88 $\pm$ 0.82		

$N = 4$ , <sup>a</sup> $p < 0.05$ , \* $p < 0.01$

## Conclusions:

1. Determination of an appropriate response parameter. Because pQCT is a time-consuming labor-intensive method, we sought a more rapid, but yet sufficiently sensitive method for measuring bone formation and response to mechanical loading. Measurement of bone marker expression by real time PCR has not been previously used to evaluate bone formation in a quantitative manner. Therefore, it was important for us to correlate the changes within an acceptable bone formation measurement, namely pQCT, with our data obtained from real time PCR on gene expression. In this study, we found a good correlation between the real time PCR changes and the pQCT changes. [pQCT is a measure of bone density whereas we have interpreted this to indicate bone formation because the amount of change in bone density is a reflection of bone formation.] In conclusion, we found that real time PCR evaluation of specific bone marker genes fulfilled our criteria for a rapid, sensitive and reliable method of skeletal anabolic response to four-point bending.
2. Duration of application of mechanical strain. Our studies indicate that four days of four-point bending in our femoral *in vivo* loading regimen is adequate for a measurable response in our proposed QTL studies.
3. Identification of bone response. We found that alkaline phosphatase, osteocalcin, bone sialoprotein, and type-1 collagen genes showed statistically significant increases in RNA harvested from bone tissue following four days of four-point bending. These are genes that can be assayed as a group in real time PCR for assessment of the bone formation response to four-point bending. Consequently, these genes were selected for further application.
4. Determination of the animal chronological age for application of four-point bending. We found that retired breeder mice and 16-week old mice showed the greatest increase in our bone formation parameters in response to four-point bending. However, we would prefer to use mice at 10 weeks of age since we could progress in our QTL studies much more rapidly by using the younger mice. We are now in the process of settling whether we can use the 10-week old mice for our four-point bending QTL study.
5. The two strains of mice most appropriate for the four-point bending QTL study. In addition to C3 and B6 animals we have studied four additional strains; AKR, 129J, NZB, and the Balb/c mice. The AKR and the 129J showed a good response whereas the NZB and the Balb/c showed no response. We are now in the process in determining whether some combination of these latter four strains would be superior to the C3 and B6 for the high and low response pair.

**Reportable Outcomes:**

None

**Key Accomplishments::**

1. Methodologic criteria to accomplish correct methodologic goals to accomplish before beginning the QTL studies. We have now completed all of the goals required for QTL studies except one, which we did not include in our technical objective, namely a dose response. Apart from that, we are ready to begin the QTL study. We are now in the process of doing a dose response to determine the optimal response range which best distinguishes the two different strains of mice, the C3H mice and B6 mice.
2. Selection of the optimal strains of mice. Based on the data so far, the C3H and B6 mice are the best strain pair and as mentioned above the final decision on this issue will be based on the dose response.
3. Real time PCR measurements of bone markers as a surrogate for pQCT measurement. When we plotted type-I collagen as our real time PCR measurement and the increment in pQCT bone density over the unloaded bone control bone, we found a significant correlation, which supports the view that we can use real time PCR as a much faster means to obtain our phenotype after four-point bending.
4. Additional phenotypes. Not only can we use these measurements of message level of bone proteins as indices of the bone formation response, we can also use them separately to evaluate their level of expression as separate phenotypes to determine the QTLs responsible for quantitative levels of expression of each real time PCR mRNAs.

**References:**

- 1) Akhter MP, Cullen DM, Pedersen EA, Kimmel DB, Recker RR. Bone response to in vivo mechanical loading in two inbreeds of mice. *Calcif Tissue Int* 1998 Nov; 63(5):442-9.
- 2) Kodama Y, Uemura Y, Nagasawa S, Beamer WG, Donahue LR, Rosen CR, Baylink DJ, Farley JR. Exercise and mechanical loading increase periosteal bone formation and whole bone strength in C57BL/6J mice but not in C3H/HeJ mice. *Calcif Tissue Int* 2000 Apr; 66(4):298-306.

## Progress for the Period of 2004-2006

### Introduction

It is well established that maintenance of bone mass and the development of skeletal architecture are dependent on mechanical stimulation. A number of studies have shown that mechanical loading promotes bone formation in the modeling skeleton and that removal of this stimulus results in a reduction in bone mass (1). In addition, recent studies have also shown that the increase in bone mass was variable in different subjects given the same amount of mechanical stress, with some exhibiting a robust osteogenic response and others responding more modestly (2,3). We and others have found evidence that this variation in response to mechanical loading is, in large part, genetically determined. Accordingly, we have identified two inbred mouse strains that differ in peak bone density and exhibit considerable differences in their bone response to immobilization (4) and mechanical loading (5). In our studies, we found that the C57Bl/6J mouse strain showed a greater loss of bone and immobilization by sciatic neurectomy compared to the C3H/HeJ strain. Furthermore, studies by Umemura et al. and Kodama et al. (4,5) as well as four-point bending studies by Akhter et al. (6) have revealed that an identical amount of mechanical strain applied to both mouse models produces a greater increase in the bone formation [periosteal and endosteal formation] parameters using histology in the C57B/6J mice compared to the C3H/HeJ mice.

A number of *in vitro* studies have employed mechanical stimulation using various models in human and mouse cells (7,8) and have found that several signaling pathways, including MAPK (9), FAK (10) and nitric oxide (11), mediate the effects of mechanical loading in bone. However, the genetic mechanisms that contribute to any variations in anabolic response to loading remain unclear. One approach often used to identify the genetic factors or genes that contribute to differences in phenotypic variation is the QTL technique. In the QTL approach, two inbred mouse strains exhibiting a phenotypic difference of interest are crossed and any genetic loci that co-segregate with the phenotype are identified. A successful QTL requires the following components: a) optimal inbred mouse strains; b) an optimized *in vivo* loading model; c) valid endpoints to measure the difference in bone anabolic response; and d) an optimal age that shows the greatest difference in the phenotype in response to mechanical loading. Our goals for the last twelve months of the funding period for the revised technical objectives-I, as well as our progress for each of the specific objectives in technical objective-I, are described below.

### III. Revised Technical Objective 1: Molecular Genetic Studies of Bone Mechanical Strain

Our Specific Objectives during the remainder of this continuation proposal are:

- 1) To establish the optimal method for inducing mechanical strain on the tibia.
- 2) To determine the optimal method for quantitating the bone formation response to mechanical strain on the tibia *in vivo*.
- 3) To determine the number of days required of 4-point bending induced mechanical strain on the tibia in order to elicit an optimal response for quantitative measurements.
- 4) To select the optimal mouse inbred strain pair (i.e. B6 and C3 or some other strain pair) to perform the QTL mapping study.
- 5) To determine the appropriate age of animals to apply the 4-point bending in order to obtain valid quantitative measurements of the bone formation response.
- 6) To test 4-point bending responses in CAST and HS stock mice. These two strains of mice exhibit more polymorphisms with the traditional inbred strains of mice than any other strains. Therefore, such strains of mice would be excellent mating partners in our genetic studies. Accordingly, the greater the genetic polymorphism between the two strains of mice used for

QTL mapping studies, the greater the opportunity to fine-map the QTL down to an operational size.

**Specific Objective 1:** To establish the optimal method for inducing mechanical strain on the tibia.

Previously we used jump training as a method to induce bone response in mice. Since the amount of response produced by jump training was not sufficient to quantitate, we therefore choose our next alternative-loading model, “four-point bending”, for the following reasons: 1) Studies using this model on rats and mice have shown greater increase in the periosteal bone formation using histology, 2) In this method the amount of load, cycles and frequency applied on tibia of mice is controlled by an external device and the loading area is specific, 3) also the right tibia is used for loading and the left tibia as internal control, thus avoiding the need of extra mice for control groups. We therefore chose this model as a method to induce bone formation in our study.

Recent studies on rats have shown that the magnitude of load applied by four-point bending is important in increasing the anabolic response of bone. Histomorphometric studies on mice have shown increased bone formation using a fixed load, cycle and frequency. All these observations led us to hypothesize that the magnitude of load applied by four-point bending is very important in determining the anabolic response within and between the strains of mice. To test this hypothesis we evaluated anabolic response of bone as function of different loads (6-9N) on 10-wk female B6 and C3H mice for 12 days using four-point bending device. The rationale for selecting this range of loads is as follows: 1) The four-point bending device is not sensitive below a 5N load; 2) load above 12 N results in fracture in some mice and 3) higher loads produce greater mechanical strain on bone that might be more than from physiological range. Based on these observations we selected the above dose of loads for our study

Mouse right tibia is used for the loading test while the left tibia is used as an internal control. Prior to loading, and while the mice are anesthetized, we use the ankle of the tibia that sits on the lower secondary immobile point as a reference allowing us to position the loading region of the tibia similarly for each mouse. To anesthetize the mice we use halothane [95% Oxygen and 5% Halothane] for 2-3 minutes and perform mechanical loading while the mice are anesthetized. The mice are trained for 6 days/week with 1 day of rest for 2-weeks. Two days after the last loading, mice were sacrificed, tibias collected and changes in the bone parameters (loaded vs unloaded) were measured using the pQCT system from Stratec XCT Research. Scanning was performed using the manufacturer supplied software program, designed to analyze the data and generate the values for the change in bone parameters. The X-ray attenuation data are based upon the software-defined threshold. We set up two thresholds for our analysis. A 180-730 mg/cm<sup>3</sup> threshold was used to measure total area, total mineral content, periosteal circumference, and endosteal circumference in the loaded vs. unloaded bones. A 730-730-mg/cm<sup>3</sup> threshold was used to measure cortical thickness, total volumetric density, and material bone mineral density. In order to minimize the measurement errors caused by positioning of tibia for pQCT, we used tibia-fibular junction as the reference line. We selected four-slices that start 3 mm proximal from tibia-fibular junction for pQCT measurement. This region corresponds to the loading zone. Each slice is at 1mm intervals and the values presented in the results are an average of these four slices. After successfully troubleshooting these difficulties in the four-point bending method we evaluated bone response from 6 to 9N load for 12 days in 10-week old B6 and C3H. The results are as follow:

*Total bone mineral content:* Four-point bending caused an increase in total bone mineral content in both the B6 and C3H mouse strains. The magnitude of increase varied depending on the amount of load between the B6 and C3H (Table-1). At 9N, the percentage increase in total bone mineral content in response to four-point bending was significantly greater in the B6 (48%) mice than in the C3H (19%) mice (Fig.1).

*Area:* Total area increased in response to four-point bending in both the B6 and C3H strains of mice. A dramatic increase of 44% and 26% in total area was seen after 12 days of four-point bending in the B6 and C3H mice, respectively (Table-1). The B6 mice ( $p<0.05$ ) showed a greater increase in total area than in the C3H mice at a 9N load in contrast to other loads (Table-1 & Fig.1).

*Periosteal circumference:* The periosteal circumference increased by 20% and 12% in the B6 and C3H mice, respectively, in response to four-point bending (Table-1). The B6 mice showed a greater increase in periosteal circumference than the C3H mice ( $p<0.05$ ) mice at 9N compared to other loads (Table-1 & Fig.1).

*Total volumetric density:* Four-point bending caused a dose-dependent increase in the total bone density seen in the B6 mice (regression analysis  $p<0.01$ ), but not in the C3H mice (Table-1). The B6 mice showed 5% and 15% greater density at loads of 8 and 9N after 12 days of loading, while the C3H mice exhibited no change (Table-1, Fig.1&2).

*Cortical density:* Cortical density increased by 4% in the B6 mice, but not in the C3H mice, at a load of 9N after 12 days of four-point bending (Fig.1).

*Cortical thickness:* Four-point bending increased cortical thickness in both the B6 and C3H mouse strains after two-weeks of mechanical loading at a load of 9N. The magnitude of increase was much greater in the B6 mice (27%) compared to that seen in the C3H mice (7%) (Fig.1).

*Endosteal circumference:* Endosteal circumference in response to four-point bending increased by 23% and 18% in both the B6 and C3H mouse strains, respectively (Table-1). The C3H mice showed a greater increase in the endosteal circumference compared to the B6 mice at a load of 8N ( $p<0.05$ ).

**Table-1** Changes in bone parameters in response to varying magnitude of loads applied by four-point bending in 10-week old female B6 and C3H inbred strains of mice in vitro.

Bone parameters	C57BL/6J							
	6N		7N		8N		9N	
	Un loaded	Loaded	Un loaded	Loaded	Un loaded	Loaded	Un loaded	Loaded
Total Area, mm <sup>2</sup>	1.42±0.06	1.52±0.06 <sup>a</sup>	1.40±0.07	1.60±0.10 <sup>b</sup>	1.47±0.04	1.74±0.04 <sup>c</sup>	1.50±0.10	2.13±0.10 <sup>d</sup>
Total Mineral Content, mg/mm	0.89±0.03	0.96±0.06 <sup>a</sup>	0.83±0.07	0.96±0.07 <sup>a</sup>	0.89±0.03	1.08±0.02 <sup>c</sup>	0.87±0.02	1.29±0.06 <sup>d</sup>
Periosteal circumference, mm	4.21±0.09	4.36±0.09 <sup>a</sup>	4.18±0.10	4.47±0.13 <sup>b</sup>	4.30±0.06	4.67±0.05 <sup>c</sup>	4.33±0.14	5.17±0.12 <sup>d</sup>
Endosteal circumference, mm	3.12±0.12	3.21±0.05	3.15±0.04	3.35±0.12 <sup>b</sup>	3.25±0.07	3.46±0.07 <sup>c</sup>	3.29±0.16	4.02±0.13 <sup>d</sup>
Total Density, mg/ccm	678±31.59	680±18.63	637±29.8	655±27.9	646±24.0	675±15.4 <sup>a</sup>	626±41.5	721±29.2 <sup>c</sup>
Cortical Density mg/ccm	1110.0±17	1114.8±15	1090±21	1095±18	1095±14	1110±6.63 <sup>a</sup>	1078±40	1115±35 <sup>b</sup>

Bone parameters	C3H/HeJ							
	6N		7N		8N		9N	
	Un loaded	Loaded	Un loaded	Loaded	Un loaded	Loaded	Un loaded	Loaded
Total Area, mm <sup>2</sup>	1.15±0.04	1.2±0.07	1.16±0.03	1.30±0.10 <sup>b</sup>	1.15±0.04	1.41±0.08 <sup>b</sup>	1.13±0.08	1.42±0.05 <sup>d</sup>
Total Mineral Content, mg/mm	1.03±0.03	1.07±0.03 <sup>a</sup>	1.04±0.04	1.16±0.07 <sup>b</sup>	1.04±0.05	1.24±0.05 <sup>b</sup>	1.04±0.07	1.24±0.03 <sup>c</sup>
Periosteal circumference, mm	3.79±0.06	3.88±0.11	3.81±0.05	4.04±0.16 <sup>b</sup>	3.79±0.07	4.20±0.12 <sup>b</sup>	3.76±0.1	4.22±0.08 <sup>d</sup>
Endosteal circumference, mm	2.31±0.04	2.38±0.16	2.32±0.04	2.49±0.11 <sup>b</sup>	2.30±0.07	2.62±0.15 <sup>b</sup>	2.26±0.10	2.70±0.17 <sup>c</sup>
Total Density, mg/ccm	1001±11.7	1017±25.7	1013±16.6	1019±24.8	1021±12.1	1029±11.9	1047±9.7	1042±19.7
Cortical Density mg/ccm	1267±8.7	1264±17	1272±14	1258±8.0	1267±13	1256±3.66	1269±36	1250±34

The values shown are mean ± standard deviation of loaded zone compared to unloaded bones from the same mice.

<sup>a</sup>  $p<0.05$ , <sup>b</sup>  $p<0.01$ , <sup>c</sup>  $p<0.001$ , <sup>d</sup>  $P<0.0001$  vs corresponding unloaded bones

N=6 for each load in both strains

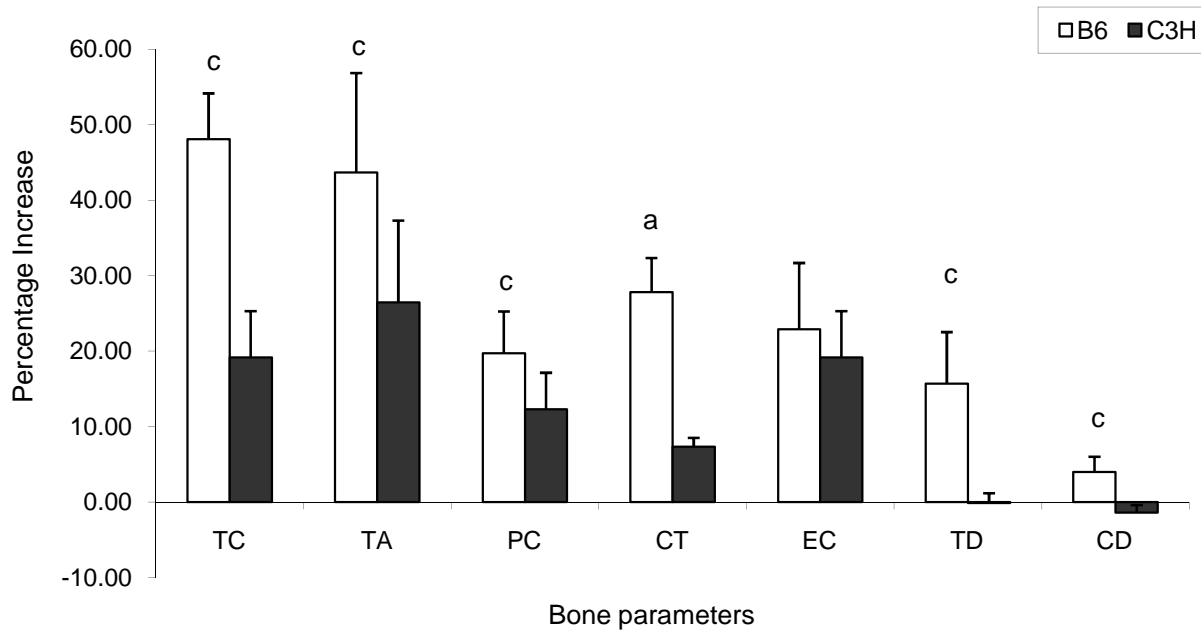


**Figure 1:** Changes in bone geometrical parameters after 12 days of four-point bending at 9N load in 10-week old B6 and C3H inbred strains of mice in vitro.

The data shows percentage change in Total content-TC, Total area-TA, Periosteal circumference-PC, Cortical thickness-CT, Endosteal circumference-EC, Total density-TD and Cortical density-CD. The values shown are as Mean  $\pm$  standard deviation of loaded zone from compared to corresponding unloaded contralateral bones. The y-axis represents the percentage change and x-axis represents various bone phenotypes as measured by pQCT.

$N=6$ , <sup>a</sup>  $p<0.05$ , <sup>c</sup>  $p<0.001$  between the strains

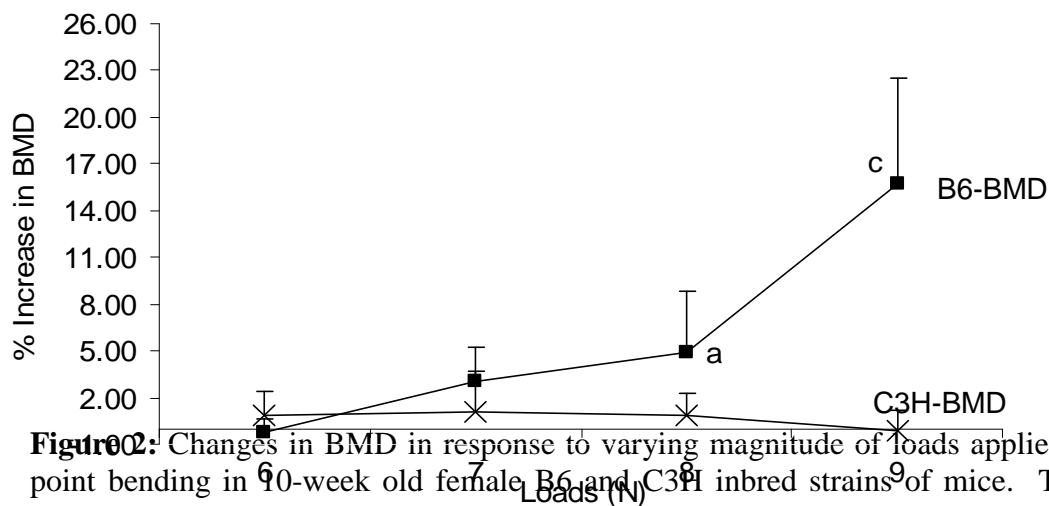


**Figure 2:** Changes in BMD in response to varying magnitude of loads applied by four-point bending in 10-week old female B6 and C3H inbred strains of mice. The values shown are mean  $\pm$  standard deviation of loaded bone compared to unloaded bones from

the same mice. The y-axis represents the percentage increase and x-axis represents varying magnitude of load.

$N=6$  for each load in both strains, <sup>a</sup> $p<0.05$ , <sup>c</sup> $p<0.001$  vs corresponding unloaded bones

In our dose response study, we found four-point bending caused a significant increase of 15% and 4.5% in total vBMD and cortical vBMD in B6 mice at 9N load. In contrast to the response observed in the B6 mice, none of the four loading regimens applied (i.e. 6, 7, 8, and 9N) produced any significant increase in total vBMD or cortical vBMD in the tibia of the C3H mice. The increased BMD response in B6 and not in C3H mice led us to hypothesize that the amount of mechanical strain produced by loads on the tibia of B6 mice is higher compared to C3H mice due to difference in bone geometrical properties. To test this hypothesis we measured the amount of mechanical strain produced by loads in the loaded area of both B6 and C3H inbred strains of mice using the strain gauge technique. We used a single gauge to measure the strain on this loaded area since our 4mm vertically movable points touch this area, which is 3mm away from the tibia-fibular junction.

In brief, a P-3500 portable strain indicator and strain gauge of specific range (EP-XX-015DJ-120, used to measure strain up to 5000  $\mu\epsilon$  according to manufacturer instruction) were used to measure the amount of strain produced by different loads. Initially, the ends of the strain-gauge circuits were soldered to copper wire and glued on the medial side of tibia, 2.09 mm away from the tibia-fibular junction to provide a consistent position on the 4mm loading zone. These copper wires were connected to the indicator and the amounts of strain produced by the loads were recorded. The strain-gage data from four individual mice were averaged for each load. The results from our study as shown in table-2 revealed an increase in mechanical strain with an increase in mechanical load in both B6 and C3H mice. The C3H mice showed slightly higher mechanical strain compared to B6 mice in all the loads and the difference was statistically significant ( $p<0.01$ , ANOVA) (**Table-2**). Therefore the lack of significant change in total vBMD cannot be explained on by inadequate mechanical strain, since a load of 9N produced 3865  $\mu\epsilon$  in the tibia of the C3H mice, which is notably, higher than the mechanical strain produced in the tibia of the B6 mice. Furthermore, a mechanical load of 9N caused a significant increase in both total area and periosteal circumference in the C3H mice, suggesting that the observed increase in vBMD response in the tibia of this strain is not caused by a lack of reduced mechanical strain.

In terms of the rapid increase in total vBMD in B6 mice in response to four-point bending, cortical thickness is increased by 27% in B6 mice. Consistent with this increase in cortical thickness, bone area increased significantly as well in the B6 response to mechanical loads of 9N. The increase in bone area and cortical thickness can be explained by the observed increase of nearly 20% in periosteal circumference, which results in a 50% increase in total area in the loaded tibia compared to unloaded tibia after 12 days of four-point bending. In contrast to the increases observed in the B6 mice, the magnitude of increase in periosteal circumference, total area, and cortical thickness were substantially less in the C3H mice by histomorphometric analysis. Consistent with these data, Recker et al., (6) have found a greater increase in the periosteal bone formation

response in B6 mice compared to C3H mice after four-point bending. Similarly, we found a significantly greater increase in the expression of bone formation marker genes in the loaded tibia of tested B6 mice compared to C3H mice. Based on these data, we have concluded that a greater increase in periosteal bone response in the B6 mouse contributes, in part, to the observed increase in total vBMD.

Our findings demonstrate for the first time that mechanical loading results in a significant increase in material BMD, which also contributes to an increase in total vBMD. In this regard, we consider the increase in cortical density to represent changes in mBMD since the vascular canal volume as determined by histological analysis was too low in the loaded bones to account for the increase in cortical BMD. Therefore, we believe that a mechanical load of 9N caused a maximum mineralization an increase in bone age in the tibia of the B6 mice. Consistent with this interpretation, we found that four-point bending caused an acute down regulation of expression of bone resorption marker genes at two and four days of four-point bending. Thus, the loading-induced decrease in remodeling could contribute to an increase in the rate of mineralization, and thereby contribute to the observed increase in mBMD and total vBMD in the tibia of the B6 mice.

As we mentioned earlier, in our pQCT analysis, we used two thresholds to measure changes in bone parameters. A threshold of 180-730 mg/cm<sup>3</sup> for evaluation of loading induced changes in total area, total mineral content, periosteal and endosteal circumference. A threshold of 730-730 mg/cm<sup>3</sup> for evaluating total vBMD and mBMD. These two thresholds were selected to include the newly formed bone, which may not have been fully mineralized. Thus, it is possible that the dramatic changes in mineral content and bone size after two weeks of loading may represent woven bone in addition to mature lamellar bone. Further studies are needed to evaluate the relative contribution of woven and lamellar bone to loading induced increase in bone size and total mineral content.

**Table-2** Mechanical strain produced by varying magnitude of loads applied by four-point bending in tibia of 10-week old B6 and C3H mice measured by strain gauge.

Load	$\mu\epsilon$ (Mean $\pm$ SD)	
	B6	C3H *
6N	2610 $\pm$ 219	2763 $\pm$ 64
7N	3020 $\pm$ 173	3188 $\pm$ 116
8N	3371 $\pm$ 143	3545 $\pm$ 157
9N	3682 $\pm$ 181	3865 $\pm$ 182

*N=4 in each load*

\* $p < 0.01$  is significantly higher compared to B6 by ANOVA)

Specific Objective 2: To determine the optimal method for quantitating the bone formation response to mechanical strain on the tibia *in vivo*.

To date, changes in the bone parameters have been largely measured by pQCT and histology. These two methods are well established but are time consuming and require long-term loading. In the present study, we evaluated if changes in the mRNA of bone

formation/resorption genes measured by Real time PCR could be used as surrogates for pQCT measurement of bone loading response. To test this, we performed mechanical loading using the four-point bending device on 10-week female B6 mice for 12 days at 9N load. Two days after the last loading, *in vivo* pQCT was performed to measure changes in bone parameters (loaded vs unloaded) (**Fig.3**). Later the same mice were sacrificed and the tibias were collected for gene expression study using Real time PCR. The results from our study are shown in **Table-3**. In this study, we compared gene expression changes with changes in skeletal parameters measured by pQCT to determine the usefulness of gene expression data as a surrogate marker for the bone anabolic response to mechanical loading. We therefore hypothesized that expression levels of one or more genes in bone formation would reflect BMD changes, and therefore could be used as phenotypes for our QTL studies. Accordingly, in our correlation study we found that bone sialoprotein (BSP), MMP-9, and TRAP showed the strongest correlation with bone parameters measured by pQCT, suggesting that expression phenotypes of these genes may be used as surrogates for pQCT measurement of bone's response to mechanical loading. It remains to be determined why the correlation between gene expression changes and cortical BMD was higher compared to the correlation between real time PCR data and total vBMD.

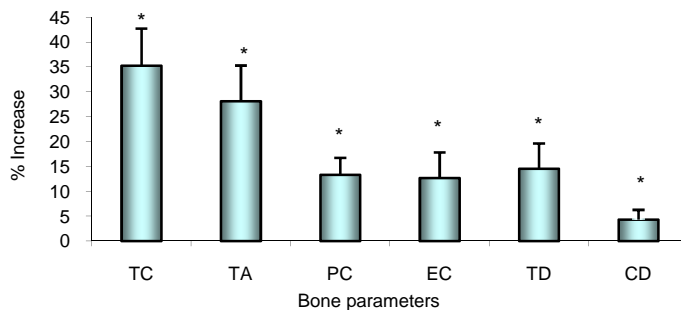


**Figure 3.** Changes in bone parameters in response to 12 days of four-point bending measured by *in vivo* pQCT in the tibia of 10-week old female B6 mice. The data shown here is the percentage that corresponds to the loading zone of tibia compared to unloaded tibia and are mean  $\pm$  standard deviation. P-values are calculated using t-test by comparing the loaded and unloaded bones. The y-axis represents percentage and x-axis represent bone parameters TC; Total content, TA; Total area, PC; periosteal circumference, EC; endosteal circumference; TD; total density and CD; cortical density. N=9, \* $p < 0.0001$  vs corresponding unloaded bones

**Table-3** Correlation between pQCT and Real time PCR data from tibia [same mouse tibia was used for pQCT and mRNA quantitation] measurement obtained from 12 days of four-point bending in 10-week old female B6 mice.

Bone markers	Total Density	Cortical Density
Type-I collagen	-0.08	0.05
Bone sialoprotein	0.60	0.68 <sup>a</sup>
Alkaline phosphatase	0.25	0.22
Osteocalcin	0.28	0.36
MMP-9	0.11	0.70 <sup>a</sup>
TRAP	0.39	0.67 <sup>a</sup>
COX-2	0.47	0.57

For pQCT measurement N=9

For Real time PCR N=9

<sup>a</sup> $p < 0.05$

**Specific Objective 3:** To determine the number of days required of 4-point bending induced mechanical strain on the tibia in order to elicit an optimal response for quantitative measurements.

The increase in bone mass in response to skeletal loading is an important adaptive response. It is likely that regulation of both osteoblast and osteoclast cell functions are involved in producing an optimal response to a given mechanical load. In order to evaluate the osteoblast and osteoclast cell response to mechanical input, we carried out a time course of mechanical loading using four-point bending device on 10-week female B6 mice. A 9N load at 2Hz for 36cycles was applied on right tibia by four-point bending and the left tibia was used as an internal control. Two days after the last loading mice were sacrificed, 4mm-tibias are collected and RNA is extracted using a Qiagen Kit. The quality and quantity of RNA was evaluated using Bioanalyzer and Nano-Drop. Expression changes were measured using real time PCR in 12 genes that related to bone formation and resorption at 2, 4, 8 and 12 days of training. The data were normalized using b-actin and the exact fold changes of genes were calculated by applying mathematical formula ( $2^{-\Delta\Delta CT}$ ) from Applied Biosystems. Primers for the bone markers genes were designed using Vector NTI and purchased from IDT-DNA.

As shown in **Table-4**, **Fig.4**, 2 days of four-point bending performed on the B6 mice caused significant decreases in the expression of bone resorption genes, but had no significant effect on the expression levels of bone formation genes in loaded tibia compared to unloaded tibia of B6 mice. In addition, 4 days of loading induced expression of both type-I collagen and bone sialoprotein by 2-fold and down regulated MMP-9, TRAP, Sodium-potassium pump, and Cathepsin K by 3-, 5- and 2-fold, respectively in B6 mice. No change was found in the expression of osteocalcin and alkaline phosphatase (**Table-4**). Eight days of loading caused an increase in the expression of type-I collagen, bone sialoprotein, alkaline phosphatase, and osteocalcin by 3-fold, and down regulation of TRAP by 3-fold. No change in expression was found between loaded and unloaded bones for MMP-9 and Na-K pump genes after 8 days of loading (**Table-4**). Prolongation of loading of up to 12 days showed significant changes in expression for both bone formation (type-I collagen, bone sialoprotein, alkaline phosphatase and osteocalcin with

4.2-, 8-, 6-, and, 4-fold) and resorption marker genes (RANKL, MMP-9, TRAP with 5-, 12-, and 7.5-fold, respectively) (**Table-4**). It is interesting to note that mechanical load caused an acute inhibition of bone resorption, as evidenced by down regulation of MMP-9 and TRAP. This finding is consistent with the previous *in vitro* study in which mechanical stress reduced the expression of RANKL, inhibiting both osteoclast formation and activation (12). However, 12 days of prolonged loading induced expression of bone resorption marker genes as shown in Table-4. This increased bone resorption that occurs at 12 days after loading may be the consequence of remodeling in response to increased bone formation. Accordingly, in our pQCT analysis we found endosteal circumference is increased after 12 days loading. Furthermore, the expression of RANKL, a key regulator of bone resorption, was increased by 5-fold after 12 days of loading, suggesting that any loading-induced increase in bone resorption at the endosteum may be mediated via an increase in the production of RANKL. These findings suggest that 12 days of loading involves both osteoblast and osteoclast cell functions.

**Table-4** Fold change in the mRNA levels of bone formation and resorption genes in response to 2, 4, 8, and 12 days of four-point bending in 10-week old female B6 mice.

(a) Bone Formation genes

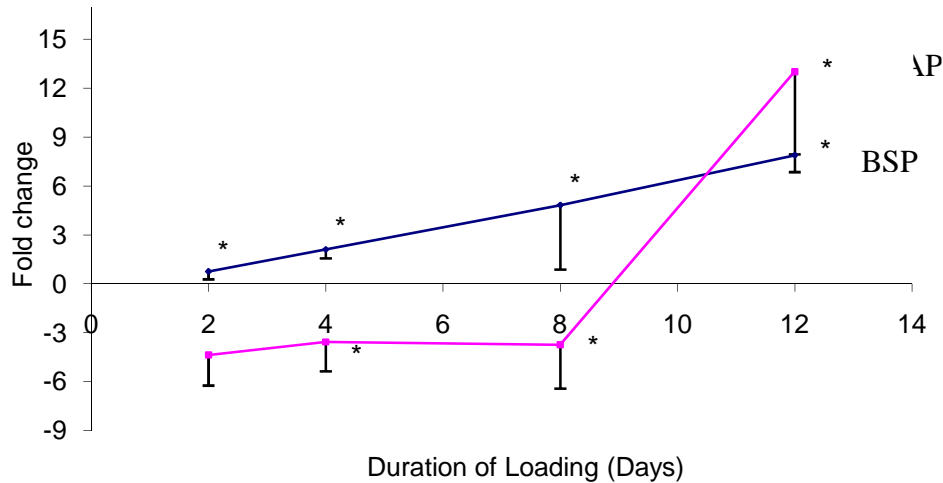
Duration of loading	Genes	$2^{-\Delta\Delta Ct}$	Fold Change	P-value
2-days	Type-I Collagen	$-0.27 \pm 0.43$	1.21	0.45
	Bone sialoprotein	$-0.05 \pm 1.09$	1.03	0.29
	Alkaline Phosphatase	$-0.41 \pm 0.37$	1.3	0.66
	Osteocalcin	$-1.20 \pm 1.24$	-2.3	0.08
4-days	Type-I Collagen	$-1.02 \pm 0.29$	2.04	0.03
	Bone sialoprotein	$-1.03 \pm 0.37$	2.04	0.006
	Alkaline Phosphatase	$-0.53 \pm 0.39$	1.45	0.18
	Osteocalcin	$-0.12 \pm 1.02$	1.0	0.73
8-days	Type-I Collagen	$-1.93 \pm 0.25$	3.84	0.00001
	Bone sialoprotein	$-1.89 \pm 1.15$	3.71	0.003
	Alkaline Phosphatase	$-1.53 \pm 0.73$	2.88	0.001
	Osteocalcin	$-1.45 \pm 0.97$	2.72	0.01
12-days	Type-I Collagen	$-2.06 \pm 0.25$	4.18	0.000001
	Bone sialoprotein	$-3.01 \pm 0.19$	7.82	0.00000002
	Alkaline Phosphatase	$-2.55 \pm 0.43$	5.86	0.0000005
	Osteocalcin	$-2.01 \pm 0.34$	4.03	0.0005

(b) Bone Resorption genes

Duration of loading	Genes	$2^{-\Delta\Delta Ct}$	Fold Change	P-value
2-days	TRAP	$-1.88 \pm 0.79$	-3.70	0.005

	MMP-9	$-1.61 \pm 0.89$	-3.06	0.002
4-days	TRAP	$-1.68 \pm 0.76$	-3.20	0.004
	MMP-9	$-1.98 \pm 0.53$	-3.95	0.002
	Na-K pump	$-2.47 \pm 0.39$	-5.56	0.0008
	Cathepsin K	$-0.93 \pm 0.87$	-1.90	0.07
8-days	MMP-9	$-0.28 \pm 0.47$	1.21	0.2
	TRAP	$-1.61 \pm 1.0$	-3.06	0.007
	Na-K pump	$0.10 \pm 1.12$	0.92	0.12
	Cathepsin K	$1.14 \pm 0.84$	0.45	0.34
12-days	TRAP	$-3.61 \pm 0.53$	12.25	0.00000003
	MMP-9	$-2.91 \pm 0.35$	7.54	0.000000008
	RANKL	$-2.65 \pm 0.37$	5.17	0.00001
	OPG	$0.47 \pm 0.33$	1	0.81

N=5-7



N=5-7, \*p&lt;0.01 vs corresponding unloaded bones

**Figure 4:** Changes in the expression of bone sialoprotein and TRAP in response to a time course of mechanical loading. The x-axis corresponds to varying time points and the y-axis represents fold change measured by real time PCR.

**Specific Objective 4:** To select the optimal mouse inbred strain pair (i.e. B6 and C3 or some other strain pair) to perform the QTL mapping study.

One of our main objectives in this study was to select two mouse strains that show extreme differences in their bone response to mechanical loading. To achieve this, we compared the bone anabolic response to four-point bending using pQCT in four different inbred mouse strains that differ in the genetic background, namely B6, DBA, Balb/c, and C3H mice. A 9N load was applied to the tibia of these inbred strains (except Balb/c, in which 8N was used since 9N caused fractures) for 12 days and changes in the bone parameters were measured using pQCT in the loaded vs. unloaded bone. We used total

vBMD and bone size as endpoint to compare the bone response between four inbred strains because they are major determinants of bone strength. The results from this study are shown in table-5. A dramatic 15% and 10% increase in the total vBMD was observed in the B6 and DBA mice after 12 days of loading (**Table-5**). However, there was no significant change in the BMD of the Balb/c and C3H mice after the same duration of loading. Mechanical loading increased bone size, as measured by total area or periosteal circumference, in all four strains tested. However, the increase in bone size was greatest in the B6 mice. Based on these data, we chose the B6 as the good responder for further studies. Although neither the C3H nor Balb/c mice showed any increase in BMD in response to four-point bending, we chose C3H as a poor responder for further studies for two main reasons. First, both the C3H and B6 mice exhibited similar body and bone size while Balb/c mice were smaller both in body size and bone size. Second, 9N load could not be applied to Balb/c as repeated application of 9N load led to fracture in some mice. In conclusion, our pQCT data demonstrate that the skeletal response to mechanical loading is variable among inbred strains of mice, as it has been reported in other studies using histology (13). Furthermore, these data suggest that the effects of mechanical loading on bone size and BMD are influenced by distinct genetic mechanisms.

**Table-5.** Changes in bone parameters [measured by pQCT] in response to 12 days of 4-point bending at 9N load in 10-week old female Balb/c, B6, DBA/J, and C3H mice.

Bone parameters	Balb/c <sup>#</sup>	C3H	DBA/J	B6
Total Content	14.03 ± 4.7 <sup>a</sup>	19.17 ± 6.14 <sup>a</sup>	48.37 ± 2.85 <sup>a b</sup>	47.83 ± 6.0 <sup>a c</sup>
Total area	13.04 ± 1.89 <sup>a</sup>	26.45 ± 10.85 <sup>a</sup>	33.56 ± 6.00 <sup>a</sup>	43.5 ± 13 <sup>a</sup>
Periosteal circumference	6.22 ± 0.92 <sup>a</sup>	12.3 ± 4.8 <sup>a</sup>	18.50 ± 7.15 <sup>a b</sup>	19.5 ± 5.6 <sup>a c</sup>
Endosteal circumference	5.75 ± 2.33 <sup>a</sup>	20.35 ± 9.9 <sup>a</sup>	16.81 ± 12.85 <sup>a</sup>	23.0 ± 8.8 <sup>a</sup>
Total density	2.97 ± 1.8	-0.45 ± 1.75	10.82 ± 5.50 <sup>a b</sup>	15.67 ± 6.7 <sup>a c</sup>
Cortical density	0.80 ± 1.35	-1.45 ± 1.08	2.72 ± 2.12 <sup>a</sup>	4.00 ± 2.0 <sup>a d</sup>

The values represent % increase in the loaded bone compared to unloaded bone and are mean ± standard deviation of 6 animals for each strain. <sup>#</sup>8N was applied on Balb/c since some of the tibias fractured at 9N.

<sup>a</sup>*p* < 0.05 vs. unloaded bones.

<sup>b</sup>*p* < 0.05 between Balb/c and C3H

<sup>c</sup>*p* < 0.05 between Balb/c and C3H

<sup>d</sup>*p* < 0.05 between Balb/c, DBA/J, and C3H

Using the above loading regimen we compared gene expression changes between B6 (good responder) and C3H (poor responder) mice to test the hypothesis that the difference in the bone response between these strains in pQCT can be observed in the expression levels of bone formation and resorption genes. As anticipated, we found B6 and C3H mice showed increased expression of both bone formation and resorption marker genes after 12 days loading. However, the magnitude of increases in the

expression phenotypes was found to be significantly greater in B6 compared to C3H mice (Table-6). This is consistent with our pQCT data that showed greater change in the bone parameters in B6 compared to C3H mice after 12 days of 9N load. Thus, we show the influence of genetic in determining the bone anabolic response to mechanical load using expression changes of genes as well as change in bone parameters. Our ongoing QTL studies will examine the genetic traits that contribute to variation in bone anabolic response using BMD and gene expression changes as end points.

**Table-6** Fold change in the mRNA expression of bone formation and resorption markers genes in response to 12 days four-point bending in 10-week old female B6 and C3H mice.

Genes	B6*	C3H	p-value
	Mean $\pm$ SD	Mean $\pm$ SD	
Type-I collagen	4.23 $\pm$ 0.74	3.19 $\pm$ 0.77	0.02
Bone sialoprotein	7.88 $\pm$ 1.03	2.90 $\pm$ 0.54	0.0000
Alkaline phosphatase	6.08 $\pm$ 4.64	3.83 $\pm$ 1.12	0.01
Osteocalcin	4.13 $\pm$ 1.0	2.93 $\pm$ 0.77	0.02
TRAP	13.02 $\pm$ 5.06	7.66 $\pm$ 2.30	0.02
MMP-9	7.75 $\pm$ 2.02	4.20 $\pm$ 1.25	0.001
RANKL	5.38 $\pm$ 1.68	3.36 $\pm$ 1.41	0.04

N=7 in both B6 and C3H mice

\*B6 is significant over C3H in the expression of bone markers genes.

**Specific Objective 5:** To determine the appropriate age of animals to apply the 4-point bending in order to obtain valid quantitative measurements of the bone formation response.

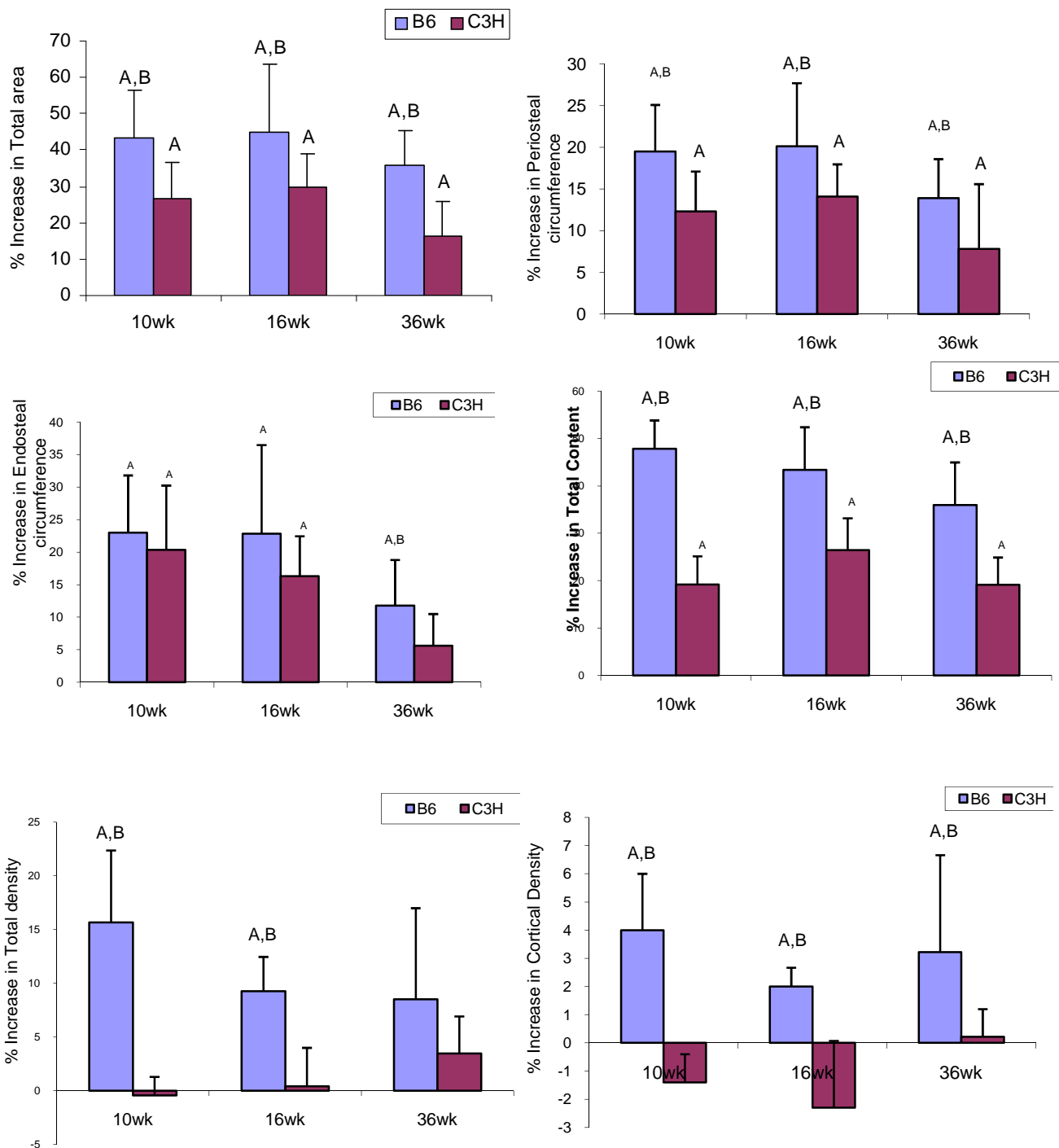


**Figure 5.** Changes in the bone parameters in response to 12 days four-point bending in different age groups of B6 and C3H mice. The y-axis represents percentage increase and the anabolic response of bone between the strains. To perform this we carried out four- x-axis represents varying ages. The blue color histogram corresponds to B6 mice and brown color represents C3H mice.

A=  $p < 0.05$  vs unloaded control bones

B=  $p < 0.05$  v C3H mice

Another goal in the study was to select an optimal age that shows significant difference in the anabolic response of bone between the strains. To perform this, we carried out four-point bending with a similar loading regimen in varying age groups [10-week, 16-week, and retired breeders] of the B6 and C3H mice to study the anabolic response of bone to a load of 9N as a function of age. The results from our experiment indicated that four-point bending caused significant changes in the bone parameters of both strains of mice in all three age groups tested (**Fig.5**). B6 mice showed greater changes than C3H mice in the total mineral content, total area, periosteal circumference, and total volumetric density and cortical density in all 3 age groups studied. Most surprising was mechanical strain-induced bone response showed no difference regardless of age in three age groups tested [10, 16, and 36 weeks] in either the B6 or the C3H mouse strains. This was determined using the Bonferroni Post Hoc test. In contrast to our report, other studies on mice, rats, turkeys, and humans have shown that bone response induced by mechanical stimuli declines with age. There are a number of potential explanations for the discrepancy between our data and previous studies, which include: 1) Age-related impairment in bone anabolic response may be seen in mice older than 36-weeks of age; 2) Aging may have a greater effect on bone's response to loading in some inbred strains of mice than in others; and 3) Bone's response to mechanical load may vary with age at lower loads but not at higher loads.

**Specific Objective 6:** To test 4-point bending responses in CAST and HS stock mice. These two strains of mice exhibit more polymorphisms with the traditional inbred strains of mice than any other strains. Therefore, such strains of mice would be excellent mating partners in our genetic studies. Accordingly, the greater the genetic polymorphism between the two strains of mice used for QTL mapping studies, the greater the opportunity to fine-map the QTL down to an operational size.

Our final goal in the study was to use CAST or HS stock mice to perform the QTL study if we do not get a bigger difference in the anabolic response of bone between the inbred strains of mice. Since B6 and C3H mice showed a greater difference in the bone adaptation to mechanical loading, we have selected these two inbred strains as optimal mouse pair for our QTL study and therefore we did not proceed further with CAST and HS stock mice.

### Conclusions:

- Jump training produced a significant difference in the osteogenic response between B6 and C3H mice but the response was too small to measure in the individual F2 mice.
- Four-point bending technique was established and validated.
- Four-point bending increased material BMD and volumetric BMD significantly in B6 but not in C3H mice.
- 9N load showed peak differences in the bone anabolic responses between B6 and C3H mice.
- 12 days of loading induced caused 40% increase in bone area and 15% increase in vBMD in B6 mice.

- Gene expression changes showed difference in the bone anabolic response to a given load between B6 and C3H mice.
- PQCT and Real time PCR were used as endpoints in the measurement of bone phenotypes in response to mechanical loading.
- Chronological age (10-wk to 36 wk) had no effect on bone response to mechanical loading.
- B6 and C3H mice were selected as the optimal mouse pair for the QTL study out of four strains tested.

### **Publications/Posters**

- 1) Chandrasekhar K, Mohan S, Susanna O and Baylink DJ., Evidence that BMD response to mechanical loading (ML) in vivo is caused by acute up-regulation of both bone formation (BF) genes and down regulation of bone resorption (BR) genes. ASBMR 26th Annual Meeting, October 1-5, 2004, Washington State Convention & Trade Center, Seattle, WA, USA. 1 October 2004.
- 2) Chandrasekhar K, Baylink DJ, Wergedal J E and Mohan S., Inbred mouse strain development variations in the skeletal adaptive response to 4-point bending evidence for involvement of different genetic mechanisms. ASBMR 26th Annual Meeting, October 1-5, 2004, Washington State Convention & Trade Center, Seattle, WA, USA. 1 October 2004.
- 3) Chandrasekhar K, Mohan S, Wergedal J E and Baylink DJ., Bone anabolic response to a mechanical load is a complex trait and involves bone size, material bone density (mBMD) and volumetric bone density (vBMD) phenotypes. ASBMR 26th Annual Meeting, October 1-5, 2004, Washington State Convention & Trade Center, Seattle, WA, USA., 1 October 2004.

### **References:**

- 1) Umemura Y, Baylink DJ, Wergedal JE, Mohan S, Srivastava AK. A time course of bone response to jump exercise in C57BL/6J mice. *J Bone Miner Metab* 2002;20(4):209-15.
- 2) Dalsky GP, Stocke KS, Ehsani AA, Slatopolsky E, Lee WC, Birge SJ. Weight bearing exercise training and lumbar bone mineral content in postmenopausal women. *Ann Intern Med* 108:824-828, 1988.
- 3) Snow-Harter C, Bouxsein ML, Lewis Bt, Carter DR, Marcus R. Effects of resistance and endurance exercise on bone mineral status of young women: a randomized exercise intervention trial. *J Bone Miner Res* 7:761-769, 1992.
- 4) Kodama Y, Dimai HP, Wergedal J, Sheng M, Malpe R, Kutilek S, Beamer W, Donahue LR, Rosen C, Baylink DJ and others. Cortical tibial bone volume in two strains of mice: effects of sciatic neurectomy and genetic regulation of bone response to mechanical loading. *Bone* 1999;25(2):183-90.
- 5) Kodama Y, Umemura Y, Nagasawa S, Beamer WG, Donahue LR, Rosen CR, Baylink DJ, Farley JR. Exercise and mechanical loading increase periosteal bone

- formation and whole bone strength in C57BL/6J mice but not in C3H/HeJ mice. *Calcif Tissue Int*. 2000 Apr;66(4):298-306
- 6) Akhter MP, Cullen DM, Pedersen EA, Kimmel DB, Recker RR. Bone response to in vivo mechanical loading in two breeds of mice. *Calcif Tissue Int* 1998;63(5):442-9.
  - 7) Boutahar N, Guignandon A, Vico L, Lafage-Proust MH. Mechanical strain on osteoblasts activates autophosphorylation of focal adhesion kinase and proline-rich tyrosine kinase 2 tyrosine sites involved in ERK activation. *J Biol Chem* 2004;279(29):30588-99.
  - 8) Kapur S, Baylink DJ, Lau KH. Fluid flow shear stress stimulates human osteoblast proliferation and differentiation through multiple interacting and competing signal transduction pathways. *Bone* 2003;32(3):241-51.
  - 9) Peverali FA, Basdra EK, Papavassiliou AG. Stretch-mediated activation of selective MAPK subtypes and potentiation of AP-1 binding in human osteoblastic cells. *Mol Med* 2001;7(1):68-78.
  - 10) Mechanical strain on osteoblasts activates autophosphorylation of focal adhesion kinase and proline-rich tyrosine kinase 2 tyrosine sites involved in ERK activation. *J Biol Chem*. 2004 Jul 16;279(29):30588-99. Epub 2004 Apr 19.
  - 11) Kunnel JG, Igarashi K, Gilbert JL, Stern PH. Bone anabolic responses to mechanical load in vitro involve COX-2 and constitutive NOS. *Connect Tissue Res* 2004;45(1):40-9.
  - 12) Rubin J, Murphy TC, Fan X, Goldschmidt M, Taylor WR. Activation of extracellular signal-regulated kinase is involved in mechanical strain inhibition of RANKL expression in bone stromal cells. *J Bone Miner Res* 2002;17(8):1452-60.
  - 13) Robling AG and Turner CH. Mechanotransduction in bone: genetic effects on mechanosensitivity in mice. *Bone*. 2002 Nov;31(5):562-9.

## Progress for the period of 2006-2007

### Introduction:

Mechanical stimulation is one of the important factors in the development and maintenance of skeletal tissues [1, 2]. Several *in-vivo* studies have shown that increased mechanical stress on bone tissue changes bone density and morphology, resulting in an increased bone mass and biomechanical strength, whereas lack of mechanical stress leads to rapid bone loss as evidenced by immobilization and bed rest studies [3-7]. Thus, physical exercise has been perceived as an important therapeutic strategy in humans to maintain bone mass and prevent osteoporosis. Recent studies in humans have also shown that bone anabolic response to a given mechanical load is highly variable, with some individuals exhibiting robust bone anabolic response with others responding modestly [8-10]. A similar variation has been observed among inbred strains of mice. We [11, 12] and others have shown that mouse strains such as C57BL/6J (B6) respond with a much higher increase in bone density (BMD) and bone cross-sectional area as compared to the C3H/HeJ (C3H) strain of mouse in response to a similar amount of *in-vivo* loading. These data suggest that variations in skeletal response to mechanical loading (ML) in humans and mice are largely determined by genetic factors. However, very little is known about the genetic regulation of mechanical loading and, so far, not a single gene has been identified that influences the skeletal response to mechanical loading.

Quantitative trait loci (QTL) analyses in inbred strains of mice provide a powerful and practical approach to perform a genome-wide search for genetic loci that contribute to variation in a quantitative phenotype. This approach has been used extensively to study genetic regulation of bone density and other related traits, such as bone metabolism, strength, quality, and size, using an intercross of two inbred strains of mice that exhibit extreme differences in the phenotype of interest [13-15]. In this study, we used two inbred strains, C57BL/6J and C3H/HeJ, good and poor responder strains respectively, to perform a genome-wide search for loci regulating bone adaptive response to exercise.

Our goals for the first year of this continuation proposal for the *in-vivo* studies for the revised Technical Objective-I, as well as our progress for each of the specific objectives in Technical Objective-I, are described below.

Our specific objectives for the first 12 months of the funding period for the *in vivo* studies are as follows:

- 1) To cross two strains of mice (a poor responder strain and a good responder strain) to produce F1 mice.
- 2) To intercross F1 mice from these two strains to produce about 300 F2 mice.
- 3) To begin phenotyping the 300 F2 mice with our newly validated phenotype (i.e. realtime PCR of bone marker genes)
- 4) To begin genotyping the 300 F2 mice.
- 5) To determine the fate of new bone gained during 2 weeks of mechanical loading (i.e. to determine how long the bone density and/or bone strength gained during 2 weeks of mechanical loading is maintained after termination of 4-point bending).
- 6) To determine if the load applied to increase optimal anabolic response causes micro cracks in loaded bone.

**Specific objective 1: To cross two strains of mice (a poor responder strain and a good responder strain) to produce F1 mice.**

In the previous report, we demonstrated that the B6 mouse is a good responder to mechanical loading and C3H is a poor responder in terms of BMD response. We therefore selected these two inbred strains of mice for our QTL study to localize the genetic regions responsible for increasing bone's anabolic response to mechanical stress. We crossed female B6 with male C3H mice and generated 100F1s (a mix of male & female).

**Specific objective 2: To intercross F1 mice from these two strains to produce about 300 F2 mice.**

A population of 329 F2 female mice was generated from 100 F1s (brother-sister mating). We used female mice for our study in the F2 population for three reasons: 1) There was no difference in the bone response to mechanical loading between the sexes in the parental strains (B6 and C3H mice); 2) The males are aggressive and territorial compared to females; and 3) All of our previous experiments to establish the phenotypic difference between the B6 and C3H mice to mechanical load were carried out in females.

**Specific objective 3: To continue the phenotyping of about 300 F2 mice**

The F2 animals, after reaching 10-weeks, were mechanically loaded for 12 days using four-point bending according to our optimized regimen (9N load at 2Hz, 36 cycles). We used halothane [95% Oxygen and 5% Halothane] for 2-3 minutes to anesthetize the mice and performed mechanical loading while the mice were anesthetized. Prior to loading and while the mice were anesthetized, we used the ankle of the tibia that sits on the lower secondary immobile point as a reference which allowed us to position the loading region of the tibia similarly for each mouse. The right tibia was used for loading and the left tibia was used as an internal control. Two days after the last loading regimen, changes in the bone parameters were measured *in vivo* in the loaded vs. unloaded tibia using the pQCT system from Stratec XCT Research. The mice were anesthetized using a solution of sterile water, ketamine (16.6 mg/mL), and xylazine (3.3 mg/mL). The mice were weighed and the ketamine/xylazine solution was injected in cubic centimeters (ccs) based on the gram weight of the mice [gram weight multiplied by 0.0036 (0.06 mg ketamine/g mouse, 0.012 mg xylazine/g mouse)]. The bone measurements were then taken using pQCT while the mice were anesthetized and afterwards the mice recovered from the anesthesia near a heat source.

To minimize the measurement errors caused by positioning of the tibia for pQCT, we used the tibia-fibular junction as the reference line in all F2 mice. We selected two-slices (1mm intervals) that were 4 mm proximal from the tibia-fibular junction for pQCT measurement. The reasons for selecting the two slices were as follows: 1) this region corresponds to the loading zone based on our preliminary study; 2) To complete pQCT scanning of more than two slices would take 25 minutes and longer for one mouse; 3) Since we are performing *in vivo* pQCT, straight positioning (90° angle) of the tibia in our scout view was very important for measuring the transverse-cross section accurately, which also consumes time; and 4) Long duration of ketamine/xylazine anesthesia can

lead to death in the mice, which would have reduced the number of mice in our F2s. We next analyzed the pQCT data for the changes in the bone parameters such as vBMD, cortical vBMD, bone size and cortical thickness in the non-loaded and loaded bones of F1 and F2 animals. We used two thresholds that have been selected based on preliminary studies. A 180-730 mg/cm<sup>3</sup> threshold was used to measure total area, total mineral content, periosteal circumference, and endosteal circumference in the loaded vs. non-loaded bones. A 730-730-mg/cm<sup>3</sup> threshold was used to measure cortical thickness, total volumetric density, and material bone mineral density.

We now, have completed the pQCT measurement of bone parameters, followed by the data analysis and organization. The mean percent increase in response to loading in the female F1 mice (n=100) was 2.8% for total vBMD, 0.8% for cortical vBMD, 8.0% for PC and 11.7% for CTh. These loading-induced increases in various skeletal parameters in F1 mice were intermediate between parent strains based on results published previously [11]. In the F2 mice (n=329), the mean increase in total vBMD was 5%, and that of cortical vBMD, PC, CTh, were 1.5%, 9%, and 14%, respectively.

#### **Specific objective 4: To continue the genotyping of the F2 mice**

Two-days after the last loading, we sacrificed the mice and collected tissues such as liver, tibia, and muscle and stored at -80°C for later use. Genomic DNA was extracted from liver tissue of 329 F2 mice using a Qiagen DNA extraction kit. The quality and quantity of the DNA was analyzed using bio-analyzer and Nana-Drop respectively. We selected 111 markers, which were chosen depending upon the position on the chromosome, in an effort to distribute them at <15cM to generate a complete genome wide scan. Polymerase Chain Reaction (PCR) primers were purchased from Applied Biosystems (ABIPRISM, Foster City, CA) to perform the genome-wide genotyping scan of the F2 population. PCR reaction conditions allowed 3-4 microsatellite markers to be multiplexed in a single electrophoretic lane. The pooled products were analyzed for fragments size on the ABI 3100 Sequence Detection System and Gene Scan software was used to detect size of the alleles. Allele calls and edits were performed using Genotyper software and in house software, and exported as text files for downstream analysis. We have completed genotyping for all the F2 mice.

Before proceeding with the QTL study, previously, we have reported that mechanical loading by four-point bending caused greater changes in the BMD and bone size in B6 mice after 12 days of 9N load. In order to determine if the increase in bone anabolic response induced by bending is not due to periosteal pad pressure, we performed sham-bending in 10-week old female B6 mice for 12 days using 9N load at 2Hz for 36 cycles. The results from our pQCT analysis revealed no significant changes in the BMD, periosteal circumference and other bone parameters (**Table-1**). This finding implies that changes in bone parameters induced by bending are not due to periosteal pad pressure as evidenced from sham-loading study. We have therefore used four-point bending as a loading model in our QTL study.

**Table-1** Changes in the bone parameters in response to 12 days of sham-bending at 9N load in 10-week female B6 mice.

	Mean ± SD
--	-----------

Bone parameters	Non-loaded	Loaded	p-value
Total Area, mm <sup>2</sup>	2.01 ± 0.11	2.07 ± 0.10	0.30
Total Mineral content, mg/mm	1.08 ± 0.04	1.10 ± 0.04	0.46
Periosteal. Circum, mm	5.02 ± 0.14	5.10 ± 0.12	0.29
Endosteal. Circum, mm	4.09 ± 0.15	4.17 ± 0.12	0.31
Total vBMD, mg/cm <sup>3</sup>	649 ± 14.64	663.7 ± 19.7	0.15
Cortical vBMD, mg/cm <sup>3</sup>	1031 ± 9.8	1038 ± 13.5	0.26

N=7

Using the above phenotype (bone parameters) and genotype data, we next performed classical QTL analysis to identify the loci regulating the bone anabolic response to loading. The bone anabolic response to mechanical loading in the F2 mice was calculated from measurements of well-established parameters, such as total vBMD, cortical vBMD, PC and CTh, in loaded tibia. Results for each parameter were expressed as percent change from identical measurements performed on non-loaded left tibia in each F2 mouse. Analysis of percent change from non-loaded bone was based on the rationale that variable genetic background in each F2 mouse would affect the bone morphology (such as cross sectional area) and influence the skeletal response independently of genetic regulation of loading. In addition, there are naturally segregating allelic variations between C3H and B6 mice that could affect BMD and bone size traits. Therefore, the use of absolute changes in BMD or periosteal circumference phenotype to study linkage would identify common, rather than specific, genetic components relevant for response to loading. Subsequently, genotyping for 329 F2 mice was completed. Alleles were called, edited using in house and ABI genotyper software.

We then used parametric mapping (a mapping strategy that requires the assumption of normal distribution for the quantitative trait investigation) for total vBMD, Cortical vBMD, PC and CTh in our QTL analysis. Because the distribution of the PC showed some significant skewing, analysis was also performed on log transformed PC data. The log transformation normalized the distribution but did not alter the identification of QTL and produced only slight changes in LOD scores. The interval mapping was performed by using a MapQTL software program (Verison 5.0; Wageningen, The Netherlands). The threshold values for significance of association were determined by a 1000 permutation test. QTLs with a genome wide error of 1%, 5% and 32% were classified as highly significant, significant and suggestive, respectively.

The linkage map, constructed using 111 markers (average marker density: 15 cM) and loading-induced changes in total vBMD, cortical vBMD, PC, and CTh phenotypes in 329 female F2 mice, revealed evidence for the presence of several significant and suggestive loci as shown in **Table-2 and Figure 1**. Loci regulating total vBMD (and cortical vBMD) were located on Chromosomes (Chr) 1, 3, 8, and 9, whereas loci regulating bone size, which includes periosteal circumference and cortical thickness were located on Chrs 8, 9, 11, 17, and 18. The strongest linkage was observed on chromosome 8 for total vBMD (LOD score 4.2, 60 cM) (**Figure 1**). **Figure 2** shows posterior probability density plots for QTLs located on Chrs 1, 3, and 8. The posterior probability density plot is a likelihood statistic that gives rise to the 95% confidence intervals for QTL peak indicated by a horizontal bar in the plot. The four BMD QTLs (includes total

vBMD and cortical vBMD) on Chrs 1, 3, 8, and 9 accounted for 19% of the variance in response to ML. Loci on Chrs 8, 9, 11, 17, and 18 regulating bone size (includes PC and CTh) accounted for the 16% variance in the F2 mice (**Table-2**). Chrs 8 and 9 QTL for BMD, PC and CTh were colocalized, whereas loci on Chrs 1 and 3 were specific for BMD, and Chrs 11, 17 and 18 loci were specific for bone size. Because there was a slight negative correlation between % changes in BMD response in loaded bones versus body weight, we performed QTL analysis after adjusting for body weight in the F2 mice. We found that body weight adjustment yielded an additional locus (Chr17) in addition to loci on Chr 1, 8 and 9.

**Table-2** Significant and suggestive QTLs for the mechanical load-induced phenotypes in the B6xC3H F2 female mice.

Phenotype	Chromosome	Locus	cM	LOD score	% Variation
Total vBMD	1	D1Mit113	91.8	3.4 <sup>a</sup>	5.5
	8	D8Mit88	60.1	4.2 <sup>a</sup>	8.5
	9	D9Mit336	33.9	2.5 <sup>c</sup>	4.8
Cortical vBMD	1	D1Mit113	91.8	2.3 <sup>c</sup>	3.6
	3	D3Mit320	50.3	3.6 <sup>a</sup>	7.3
	9	D9Mit355	49.2	2.5 <sup>c</sup>	3.4
Periosteal circumference	8	D8Mit49	68.9	3.0 <sup>b</sup>	4.3
	9	D9Mit97	24	2.2 <sup>c</sup>	3.3
	11	D11Mit333	69.9	2.1 <sup>c</sup>	3.3
	18	D18Mit64	0	3.0 <sup>b</sup>	4.4
Cortical thickness	8	D8Mit88	60.1	3.6 <sup>a</sup>	5.7
	9	D9Mit2	13.1	3.0 <sup>b</sup>	3.2
	11	D11Mit333	69.9	2.5 <sup>c</sup>	4.2
	17	D17Mit93	39.3	3.0 <sup>b</sup>	4.2

<sup>a</sup>The threshold for the highly significant LOD score is  $p < 0.01$

<sup>b</sup>The threshold for the significant LOD score is  $p < 0.05$

<sup>c</sup>The threshold for the suggestive LOD score is  $p < 0.1$

Variances explained are from the peak LOD score in each phenotype

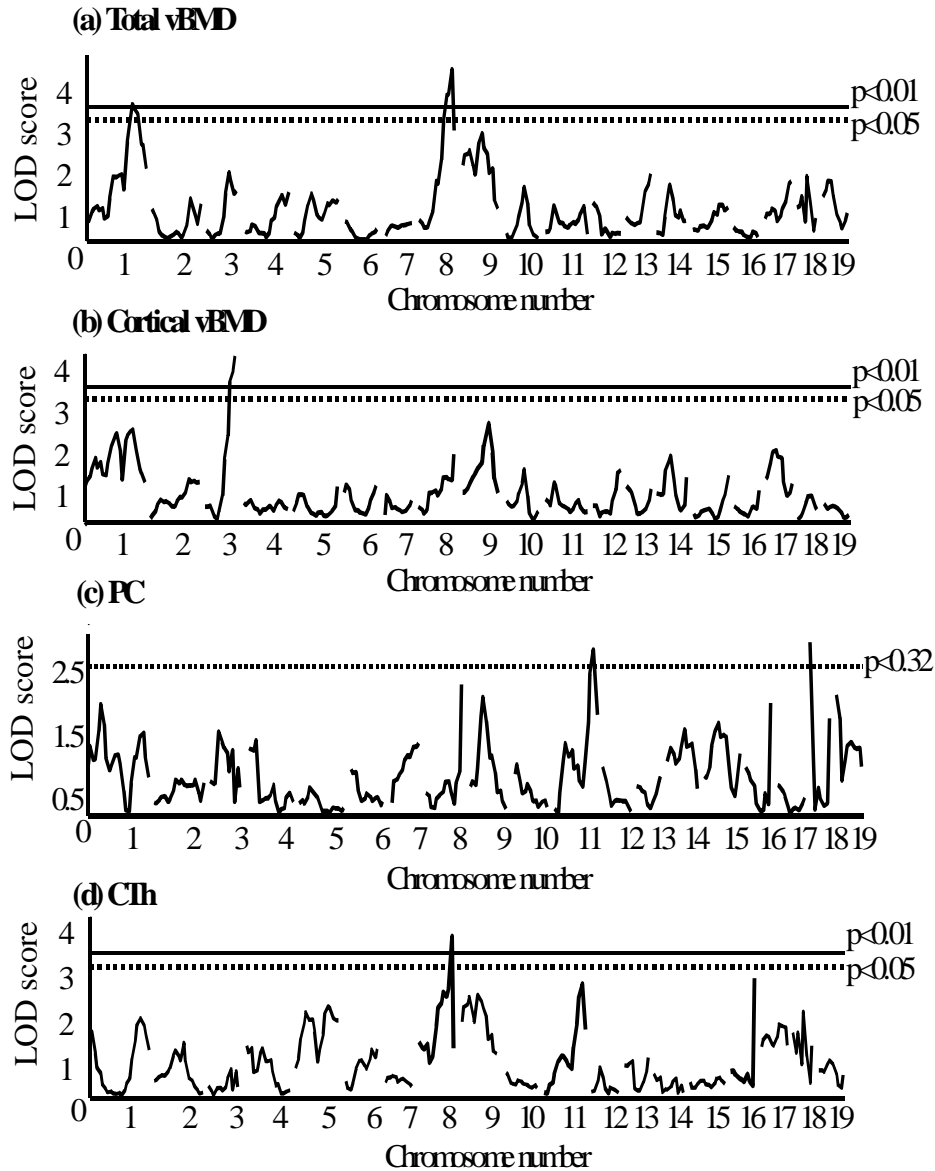


**Figure 1:** Genome-wide scan for percent change in (a) Total vBMD, (b) Cortical vBMD and (c) PC and (d) CTh induced by mechanical loading in the F2 population of B6xC3H intercross. The y-axis indicates LOD score and x-axis represent chromosomes. The solid line indicates genome-wide thresholds for significant QTL and broken links indicate thresholds for suggestive QTL.

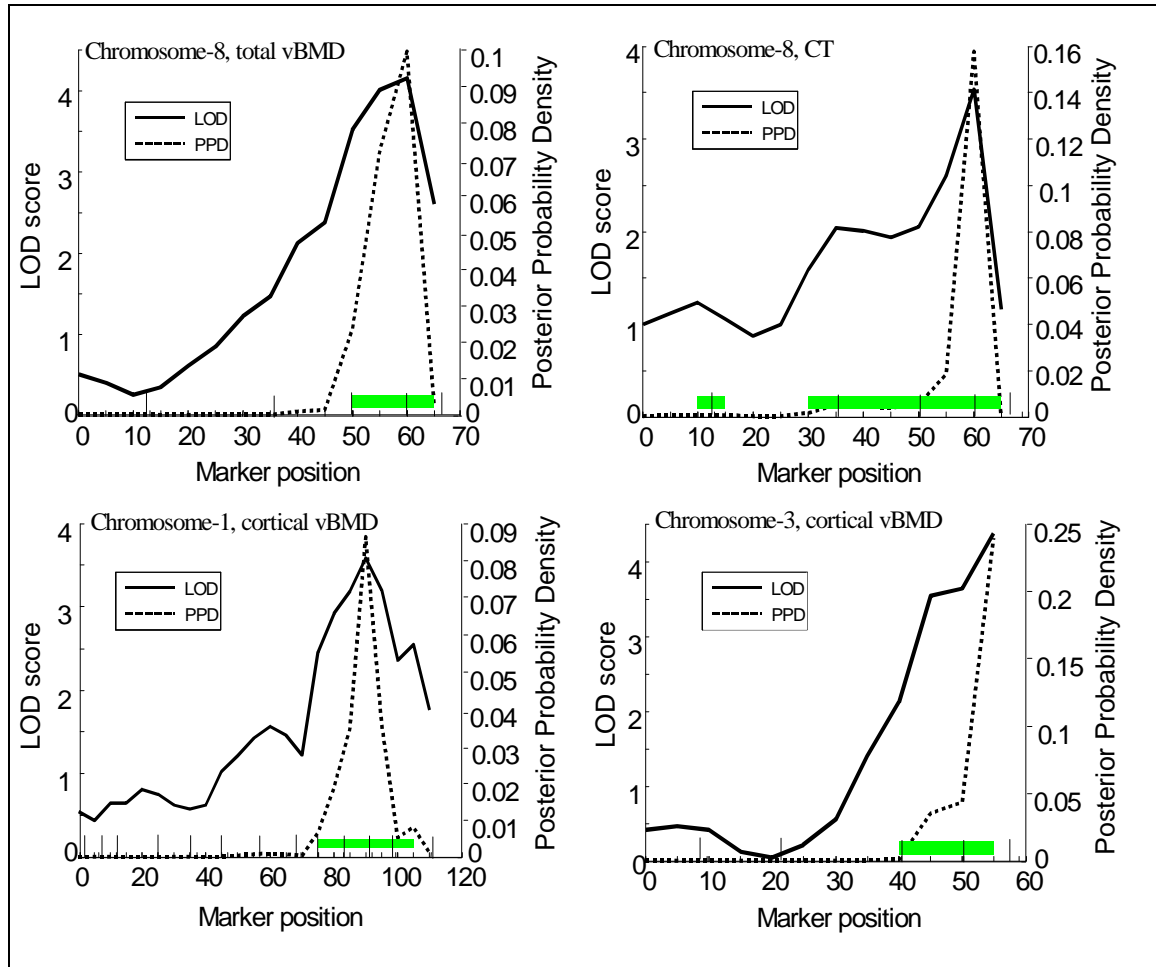


**Figure 2:** Detailed map for chromosomes 8, 1 and 3 showing significant QTLs for total vBMD, cortical thickness and cortical vBMD. LOD scores between markers were determined using Pseudomarker MAINSCAN program with a default setting of 2.5cM between steps. The markers' positions are highlighted as vertical lines in the x-axis. Posterior probability density (shown on right y-axis) plots allow best estimate of putative QTL position on the marker map.

In addition to loci regulating response to loading, we used data from non-loaded tibia to identify linkage to BMD and bone size parameters. All four traits (total vBMD, cortical vBMD, PC, and CTh) showed normal distribution. Since there was a significant positive correlation ( $r$ -value range from 0.13 to 0.55,  $p < 0.05$ ) between the body weight and PC, and body weight and BMD, we performed QTL analyses after adjustment for body weight. We identified 13 chromosomes that regulate changes in BMD and bone size including Chrs 1, 2, 3, 4, 6, 10, 11, 12, 15, 16, 17, 18, and 19 (**Table-3, Figure 3**). Table-3 provides a list of QTLs that showed significant and suggestive linkages, the closest markers on peak QTL, and the percent variance explained by each QTL for different phenotypes. Some of the QTLs observed for the non-loaded phenotypes that include BMD and bone size, are similar to the previously published QTLs [16-19]. In addition, we identified novel QTL for BMD on Chr 3 (LOD score 2.8, 59.0cM), 10 (LOD score 3.8, 63.4cM) and 17 (LOD score 5.4, 39.0cM), and PC QTL on Chrs 3 (LOD score 4.0, 46.4 cM), 10 (LOD score 2.4, 57.3 cM), 11 (LOD score 4.3, 49.2 cM), 15 (LOD score

3.1, 41.5 cM), 16 (LOD score 3.1, 24.0 cM), 17 (LOD score 5.1, 39.3 cM), and CTh QTL on Chrs 1, 3, 10, 16, 17, 18, and 19 (Table-3). Together, data from the loaded and non-loaded tibia, we found that ML BMD QTL for Chr. 8 and 9 and bone size QTL for Chr. 8 and 18 could not be detected using phenotype data from non-loaded bones, suggesting that these QTLs are unique to ML phenotypes.

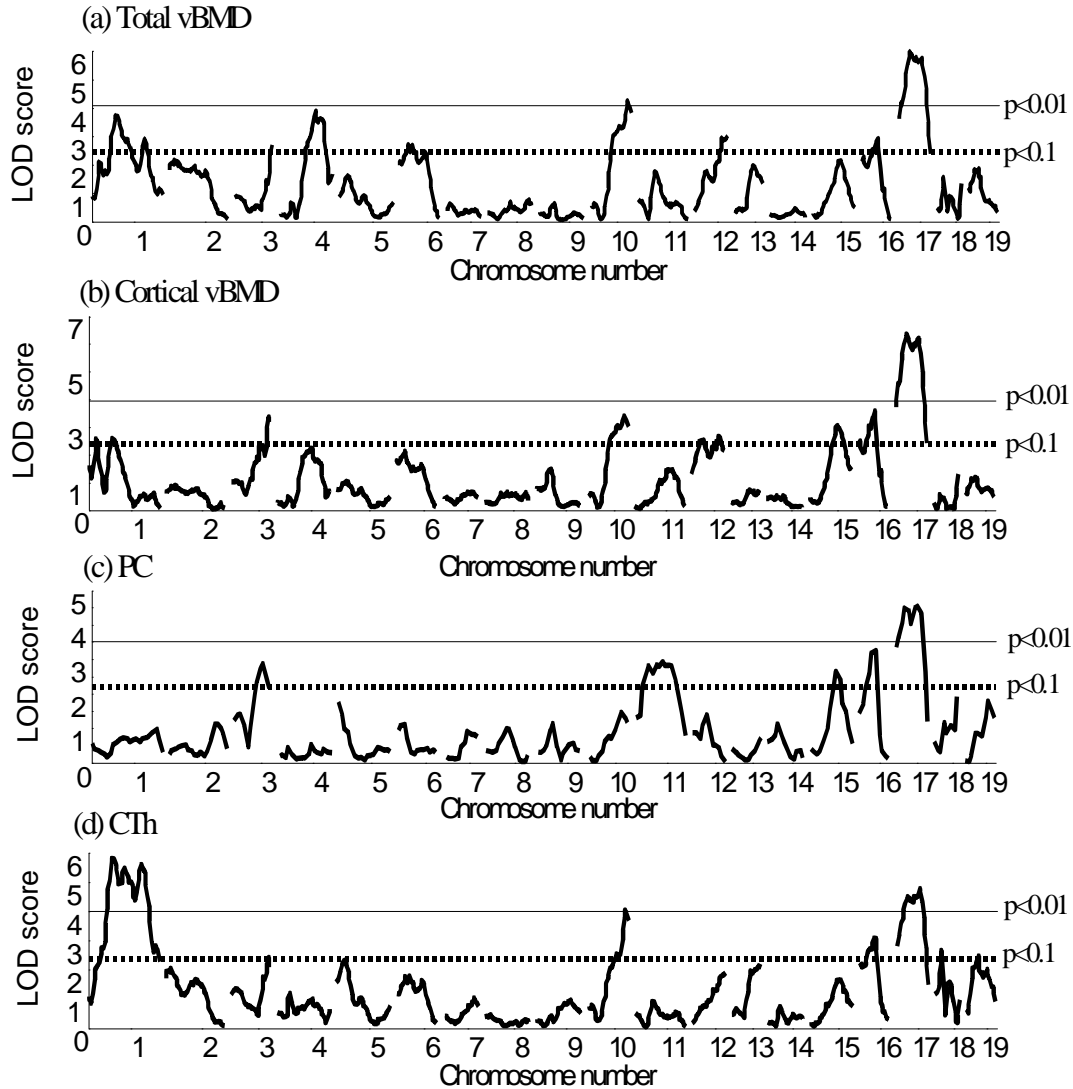


**Figure 3:** Genome-wide scan associated with non-loaded (a) Total vBMD, (b) Cortical vBMD, (c) PC and (d) CTh in the F2 population of B6-C3H intercross. The y-axis indicates LOD score and x-axis represents chromosomes. The solid line indicates genome-wide threshold for significant QTL and broken lines indicate thresholds for suggestive QTL.

**Table-3** Significant and suggestive QTLs for the non-loaded phenotypes in the B6xC3H F2 female mice.

Phenotypes	Chromosome	Locus	cM	LOD score	% Variation
Total vBMD	1	D1Mit380	37.1	3.8 <sup>a</sup>	5.3
		D1Mit106	83.1	2.8 <sup>c</sup>	3.9
	2	D2Mit1*	14.2	2.3 <sup>c</sup>	4.6
	<b>3</b>	<b>D3Mit147</b>	<b>59.0</b>	<b>2.8<sup>c</sup></b>	<b>3.9</b>
	4	D4Mit251	66.7	3.6 <sup>a</sup>	5.4
	6	D6Mit209*	16.9	2.9 <sup>c</sup>	4.8
	<b>10</b>	<b>D10Mit233</b>	<b>63.4</b>	<b>3.8<sup>a</sup></b>	<b>5.3</b>
	12	D12Mit16*	44.5	3.3 <sup>a</sup>	5.9
	16	D16Mit60	24.0	2.9 <sup>c</sup>	4.0
	<b>17</b>	<b>D17Mit93</b>	<b>39.0</b>	<b>5.4<sup>a</sup></b>	<b>7.4</b>
Cortical vBMD	1	D1Mit380	37.2	2.7 <sup>c</sup>	3.8
	<b>3</b>	<b>D3Mit147</b>	<b>59.1</b>	<b>3.2<sup>a</sup></b>	<b>4.6</b>
	<b>10</b>	<b>D10Mit95</b>	<b>50.3</b>	<b>3.0<sup>b</sup></b>	<b>4.2</b>
	12	D12Mit16*	40.5	2.9 <sup>c</sup>	5.7
	15	D15Mit107	41.5	3.0 <sup>b</sup>	4.5
	16	D16Mit60	24.0	3.6 <sup>a</sup>	4.9
	<b>17</b>	<b>D17Mit93</b>	<b>39.3</b>	<b>5.9<sup>a</sup></b>	<b>8.0</b>
	<b>3</b>	<b>D3Mit320*</b>	<b>46.4</b>	<b>4.0<sup>a</sup></b>	<b>7.2</b>
	<b>10</b>	<b>D10Mit233*</b>	<b>57.3</b>	<b>2.4<sup>c</sup></b>	<b>3.9</b>
	<b>11</b>	<b>D11Mit285</b>	<b>49.2</b>	<b>4.3<sup>a</sup></b>	<b>6</b>
Periosteal circumference	<b>15</b>	<b>D15Mit107</b>	<b>41.5</b>	<b>3.1<sup>b</sup></b>	<b>4.7</b>
	<b>16</b>	<b>D16Mit60</b>	<b>24.0</b>	<b>3.1<sup>b</sup></b>	<b>4.3</b>
	<b>17</b>	<b>D17Mit93</b>	<b>39.3</b>	<b>5.1<sup>a</sup></b>	<b>7</b>
	<b>1</b>	<b>D1Mit380</b>	<b>37.2</b>	<b>5.9<sup>a</sup></b>	<b>8</b>
	<b>3</b>	<b>D1Mit106</b>	<b>83.1</b>	<b>5.4<sup>a</sup></b>	<b>7.3</b>
		<b>D3Mit147*</b>	<b>55.3</b>	<b>2.5<sup>c</sup></b>	<b>4.2</b>
Cortical thickness	<b>10</b>	<b>D10Mit233</b>	<b>63.4</b>	<b>3.7<sup>a</sup></b>	<b>5.1</b>
	<b>16</b>	<b>D16Mit60</b>	<b>24.0</b>	<b>3.1<sup>b</sup></b>	<b>4.2</b>
	<b>17</b>	<b>D17Mit93</b>	<b>39.3</b>	<b>4.7<sup>a</sup></b>	<b>6.5</b>
	<b>18</b>	<b>D18Mit12</b>	<b>9.8</b>	<b>2.7<sup>c</sup></b>	<b>3.8</b>
	<b>19</b>	<b>D19Mit28*</b>	<b>9.8</b>	<b>2.8<sup>c</sup></b>	<b>6</b>

<sup>a</sup>The threshold for the highly significant LOD score is  $p < 0.01$ <sup>b</sup>The threshold for the significant LOD score is  $p < 0.05$ <sup>c</sup>The threshold for the suggestive LOD score is  $p < 0.1$ **Novel QTLs are highlighted in bold**

\* Corresponds to marker closer to the peak LOD score

The genome-wide search for associations between marker genotypes and the quantitative phenotypes of bone anabolic response to loading resulted in the localization of several QTLs in C3HxB6 F2 mice. The primary mechanism by which mechanical

loading induces increases in BMD is believed to involve Periosteal modeling [11], leading to increased cortical thickness and an eventual increase in volumetric BMD. Based on this hypothesis, the QTLs identified in this study can be grouped into three categories: 1) QTLs that affect both BMD and bone size response to ML; 2) QTLs that affect only BMD response to ML; and 3) QTLs that only influence bone size response to ML.

Our findings that genetic loci in Chrs 8 and 9 show significant linkage with multiple measures of skeletal response to loading (total vBMD, PC and CTh), even though our analysis eliminated effects of confounding factors, such as bone size, suggest that these loci may contain genes that play a key role in mediating bone cell response to loading by regulating both BMD and bone size. Consistent with this idea, previous studies have shown that Chrs 8 and 9 contain genetic loci that regulate biomechanical and femur breaking strength in the multiple inbred mouse strain crosses including B6xC3H (Chr 8, 30-90 cM) [20], B6XD2 F2 mice (Chr 8, 30-57 cM) [21, 22] and MRLXSLJL (30-60cM) [13, 23]. Taken together, these data may suggest genes in these regions regulate biomechanical strength possibly with consequence of superior (or more favorable) response to exercise.

In addition to the ML QTL that regulated both BMD and bone size, Chr 1 (91.8 cM) and Chr 3 (50.3 cM) QTL specifically affected BMD but not bone size. ML QTL in Chr 1 (91.8 cM) colocalizes with a major QTL identified earlier for total vBMD and other structural properties in the congenic and B6xC3H F2 mice [20, 24]. Accordingly, QTL analysis of the BMD phenotype for non-loaded bones in the present study revealed a major QTL on Chr 1 at 83.1 cM, which is closer to the previous published BMD QTL. While the B6 alleles in Chr 1 contributed to higher BMD response to four-point bending (Figure 5), C3H alleles contributed to higher BMD in non-loaded bone (data not shown). Thus, Chr 1 QTL may contain genes: 1) that contribute to natural variation in BMD between B6 and C3H strains; and 2) that respond to mechanical loading by increasing the vBMD. Our linkage analysis also identified loci on Chr 11 (69.9 cM), Chr 17 (39.3 cM), and Chr 18 (0 cM) that only influence bone size in response to mechanical loading. Furthermore, several novel loci regulating bone size on Chrs 3, 10, 11, 15, 16, 17, 18, and 19 were discovered using data from non-loaded bones. Based on these findings, it can be concluded that complex genetic mechanisms regulate variations in BMD and bone size in non-loaded and loaded bones. Another finding that provides substantial support for this concept of complex regulation of BMD and bone size is appearance of novel QTLs (Chr 5 and Chr 13) in the interaction study mentioned below but not in the mainscan.

We next determined the contribution of alleles from B6 and C3H mice for the major QTL affecting BMD and PC. As shown in Figure 5, for Chr 1 BMD QTL, homozygous B6 alleles at marker *D1Mit113* showed dominant effect over C3H homozygous mice and were 5.6% (Figure 5) higher than the homozygotes for C3H alleles. Although the response to mechanical loading was higher in the B6 strain, it is noteworthy that C3H alleles at Chr 8 increased BMD in response to mechanical loading (**Figure 4**). Thus, homozygous C3H alleles at marker *D8Mit88* had 5.8% higher BMD than the homozygous B6 alleles. For this QTL, the C3H alleles best fit a recessive mode of inheritance. For PC QTL, homozygous alleles from B6 mice at marker *D8Mit49* showed 10% higher PC values than the mice with homozygous C3H alleles. The Chr 8 loci regulating PC inherited in dominant mode. It is noteworthy that a previous study

reported that a congenic strain in which a small fragment of C3H Chr 4 (40-80 cM) was introgressed in a B6 background showed increased mechanosensitivity to loading [25]. Our study, however, did not identify any QTL on Chr 4. There are several possible explanations for why we did not find a QTL in chromosome 4: 1) the two models of loading used to study the bone anabolic responses are different. 2) The number of F2 mice used may not be adequate to identify all of the mechanical loading QTL and 3) While many of the mechanical loading QTL may regulate anabolic response to four-point bending at multiple skeletal sites, there may be some QTL that are site specific i.e. regulate anabolic response in some but not other skeletal sites. In this regard, it is known that there are common BMD QTL that regulate BMD at multiple skeletal sites and site specific BMD QTL that regulate BMD at some, but not other, sites. Consistent with the previous study, we did observe that the BMD response to mechanical loading was higher for C3H alleles on Chr 8 QTL as compared to B6 alleles. Since C3H mice demonstrate poor adaptation to mechanical loading as compared to the B6 mice, these findings of high response alleles in C3H were unexpected. It is possible that C3H alleles at these loci are phenotypically silent in the context of the C3H genome but increase BMD in response to four-point bending in the presence of one or more B6 alleles.

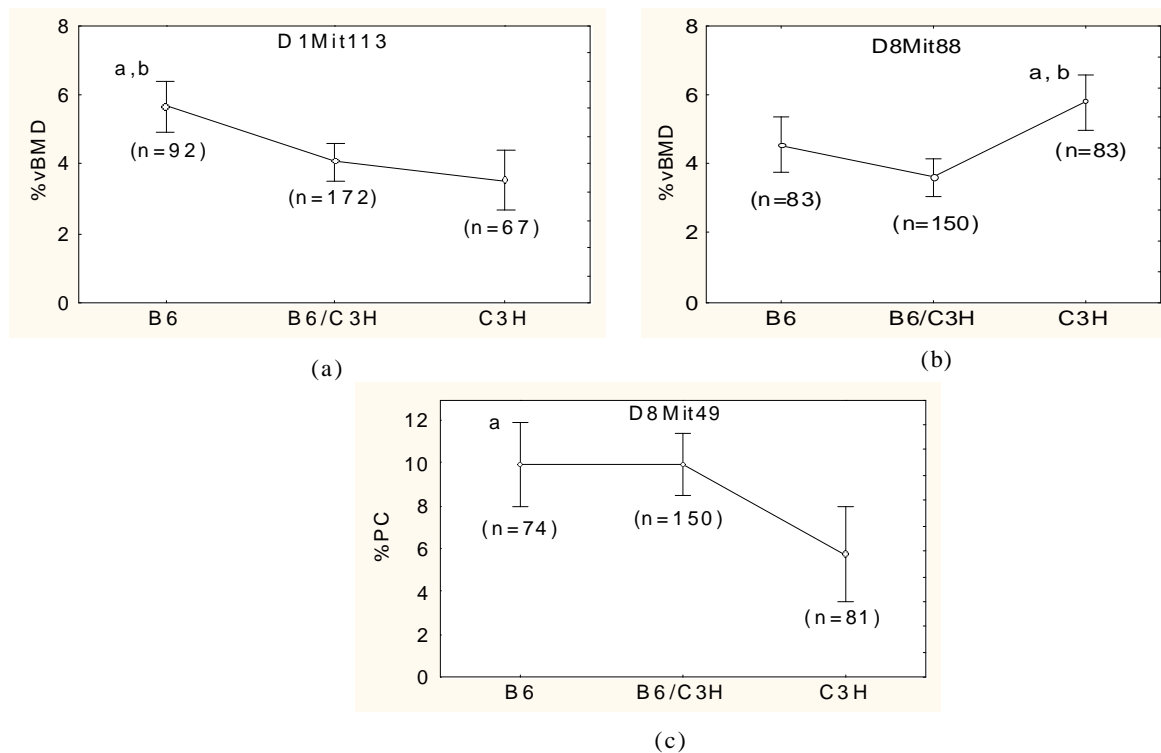


**Figure 4:** Effect of B6 vs. C3H alleles at the major QTLs affecting total vBMD and bone size phenotypes on chromosome 1 and 8. Significant differences ( $p < 0.01$ ) are indicated by the lowercase letters, where “a” indicates the B6 or C3H allele is significantly different than mice with C3H or B6 allele and “b” indicates that the B6 or C3H allele differs from mice with B6C3H allele. The values shown here are mean  $\pm$  SD. The y-axis represents percent change of vBMD and PC in the F2 population and x-axis represents mouse genotypes. The total number of mice was 329 but due to missing data the number of genotype marker data varied.

To determine the genetic variance that remains unaccounted for in our study we performed PAIRSCAN analysis in search of loci-loci interaction. Interaction was observed between loci on Chr 8 with other loci on Chr 13 and 5 for total vBMD and cortical thickness (**Table-4**). Similarly, Chr 1 locus interacted with loci on Chr 3 and 13 for vBMD and cortical vBMD (**Table-4**). These four interactions combined together accounted for approximately 11% of the variance in loading induced changes in BMD (includes total vBMD and cortical vBMD) and CTh (calculated by Pseudomarker FITQTL algorithm). It was interesting to note that Chr 13 and 5 loci did not show significant main effects for BMD and cortical thickness, but showed significant interaction of LOD score with Chr 8 and 1 that showed significant QTL for BMD and cortical thickness in the main effect. We believe that the two novel loci may contain genes that are closely associated with the candidate genes, but not genetically inherited, within the other locus identified in the main scan. These associated genes can be in the same signaling pathways, either upstream or downstream. The expression of the associated genes can be regulated or modified by the candidate genes responsible for the mechanical loading. Further functional screening of candidate genes from the QTL regions may provide more substantive data to answer the mechanisms of gene-gene interactions.

**Table-4** List of significant marker pairs showing interaction from genome-wide analysis of multiple phenotypes in B6xC3H F2 female mice.

Phenotype	Chr pairs	cM1	cM2	LOD Full	LOD Int	p-value (interaction)
Total vBMD	8 × 13	60	45	9.10	2.96	0.008
	1 × 13	90	45	7.57	2.65	0.01
Cortical vBMD	1 × 3	75	55	8.72	2.17	0.04
CT	5 × 8	80	10	7.41	4.50	0.004

For vBMD full LOD score threshold (effect of both markers in effecting the bone phenotype) significance was 7.68 ( $p < 0.05$ ) and for cortical vBMD full LOD score threshold significant was 7.95 ( $p < 0.05$ ). Suggestive threshold was 7.32 ( $p < 0.1$ ) for vBMD and 6.83 ( $p < 0.6$ ) for CT Full LOD score effect.

While QTL analysis leads to precise mapping of the genetic loci that contribute to a phenotype of interest, the next phase lies in identifying the potential candidate genes within the region of a QTL, which is the first step in understanding the underlying molecular mechanisms responsible for increasing the bone adaptive response to ML. Each of the QTL regions identified in this study is more than 15 cM in length and contains hundreds of genes. To identify potential candidate genes for the ML QTL, we used several criteria including findings from clinical association studies, gene knockout studies and *in-vitro* studies on the effects of mechanical strain on bone cells [26-29].

Candidate genes for locus on Chr 8 (38–68.9 cM) include carboxypeptidase E (cpe), annexin A10 (Anxa10), SH3 multiple domains 2 (Sh3md2), chloride channel 3 (Clcn3), ATPase, H<sup>+</sup> transporting, V1 subunit B, isoform 2 (Atp6v1b2), high mobility group box 2 (Hmgb2), vascular endothelial growth factor C (Vegfc), ectonucleotide pyrophosphatase/phosphodiesterase 6 (Enpp6) and Lrp2 binding protein. Candidate genes for the Chr 9 locus include calponin 1 (Cnn1), and 5-hydroxytryptamine (serotonin) receptor 3A&B (Htr3a&b). The Chr 3 (41-59 cM) contains possible candidate genes protocadherin (Pcdh) 10, 18, OSF (postn), transient receptor potential cation channel, subfamily C, member 4 (Trpc4), Smad8 and Vpurinergic receptor P2Y, G-protein coupled 12, 13 and 14 (P2ry). Possible candidate genes on Chr 11 (64-71cM) include mitogen activated protein kinase kinase 4 (Map2k4), fibroblast growth factor 11 (fgf11), and synaptotagmin (Stx8). The loci on Chr 17 include FK506 binding protein 5 (Fkbp5), opsin 5 (opn5), and runt related transcription factor 2 (Runx2), and Chr 18 include mitogen activated protein kinase kinase kinase 8 (Map3K8) and BMP and activin membrane-bound inhibitor (Bambi). Further studies are needed to determine if any of the above candidate genes is, in fact, a ML QTL gene.

Although this first genome-wide research for mechanical loading QTL using C3H and B6 strains of mice has revealed evidence for the presence of multiple genetic loci regulating the skeletal response to loading, our findings should be viewed in the context of the following limitations. The use of growing mice rather than mature mice may have confounded the response. In this regard, we have recently found that four-point bending significantly increased bone density in B6 mice compared to C3H mice at 10-, 16- and 36-week (11), regardless of age. In addition, the non-loaded contralateral bone was used to control for growth effects. Second, in our recent study, we observed that the amount of strain in C3H and B6 mice was similar at 9N force. However, the variable genetic background in each F2 mouse resulted in mice with variable cross-sectional area of tibia. With a fixed amount of force (9N), the amount of strain experienced by each mouse will depend on cross-sectional area (moment of inertia), suggesting that a mouse with a large cross-sectional area will experience lower strain and vice versa. This would generate a variable response to loading independent of genetic response to loading. The results from our study showed a weak correlation between bone size and loading response and our quartile analysis showed that the increase in bone size response to loading in the F2 mice varied somewhat depending on the size of bone (**Figure 5**). We therefore performed QTL analysis after adjustment with non-loaded PC bone which produced the same QTL as unadjusted data suggesting that loading response in F2 mice is largely genetically determined. Third, in the phenotype distribution, we found some of the F2 mice showed negative BMD response to mechanical loading. Whether the negative BMD response is due to loading induced changes in architecture/shape or due to rapid increase in poorly mineralized bone at the periosteum, remains unknown. Fourth, our study used a relatively low number of F2 mice (n=329) to perform the QTL analysis. This was mainly due to practical difficulties in performing four-point bending-based loading in a large number of mice. Therefore, the power to detect QTL was less than studies with 600-1000 animals. Thus, there are likely additional chromosomal regions that affect the bone response to loading which were undetected in this study. This was further evident by the loci interactions that showed only 11% variance. Finally, hormonal status is shown to

significantly influence the response to loading, therefore the QTLs identified in this study could be specific to female mice. In this regard, mapping of each locus in the male mice will provide more definitive proof as to whether the same loci or closely linked loci underlie the QTLs mapped to overlapping chromosomal regions using only females.

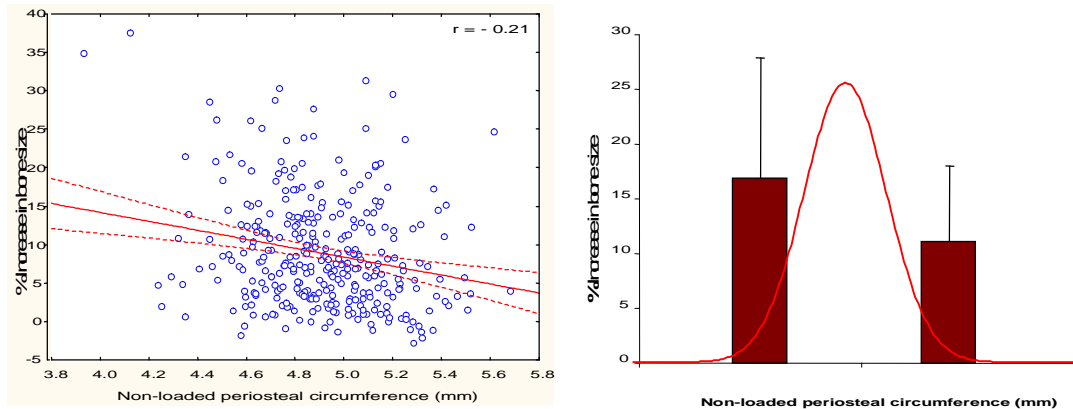


**Figure 5:** Periosteal bone response to mechanical loading is dependent on bone size. Correlation of non-loaded PC values (mm) vs. percent change in bone size in response to loading (A) and quartile analysis of the bone size response to mechanical loading in the B6XC3H F2 population (B).

**Specific objective 5:** To determine the fate of new bone gained during 2 weeks of mechanical loading (i.e. to determine how long the bone density and/or bone strength gained during 2 weeks of mechanical loading is maintained after termination of 4-point bending).

At present, we are carrying out this experiment. We will include the data of this proposed specific objective in our next annual progress report.

**Specific objective 6:** To determine if the load applied to increase optimal anabolic response causes micro cracks in loaded bone

We performed four-point bending for 12 days at 9N load in 10-week old female B6 and C3H mice and 2 days after last loading tibias were collected and stored at 10% formalin. One thick cross-section was obtained on the loaded and unloaded bones, and both sides were measured for micro-cracks (Bone area  $\text{mm}^2$ ). In order to rule out the possibility that the changes on bone parameters induced by a load of 9N are due to micro-crack induced healing, we measured micro-cracks by histological analysis. The micro-cracks area ( $\text{mm}^2$ ) was not significantly different between the loaded vs unloaded bones ( $n=5$ ) for either B6 ( $0.82 \pm 0.05$  vs.  $0.60 \pm 0.04$ ) or C3H ( $0.87 \pm 0.07$  vs.  $0.95 \pm 0.02$ ) mice. Furthermore, the micro-crack area was not significantly different between the two strains in either the loaded or unloaded bone suggesting that the bone anabolic response produced by 9N was not due to micro-cracks.

**Successes to Date**

- 1) We provide evidence from the sham-bending study that four-point bending induced changes in bone parameters were due to bending and not due to periosteal pad pressure.
- 2) We provide evidence from our micro-crack experiment that bone anabolic response induced by 9N load on tibia of B6 mice was not due to pathological changes.
- 3) We determined that although bone response to mechanical loading is dependent on the size of the bone, it is largely determined by genetic factors.
- 4) We identified six loci that regulate the bone adaptive response to loading using classical QTL approach.
- 5) We found that ML BMD QTL for Chrs. 8 and 9, and bone size QTL for Chrs. 8 and 18, could not be detected using phenotype data from unloaded bones, suggesting that these QTLs are unique to ML phenotypes.
- 6) Our study has identified known (Chrs 10, 11, 15, 16, and 17) and novel QTL on Chr 3 for the periosteal circumference (PC) or bone size trait in the B6XC3H F2 mice. Chrs 10 and 11 have been identified in multiple strain crosses, suggesting the importance of this QTL in PC regulation.
- 7) QTL identified for non-loaded tibia PC are the same as QTL previously identified for femur, suggesting that the same mechanisms are involved in the regulation of bone size in both femur and tibia.

**Conclusions**

Our results confirm that response to mechanical loading has a strong genetic component with several loci regulating loading induced bone modeling. The future discovery of genes at these loci could provide a basis for the observed variability in bone mass accretion and maintenance due to exercise in normal healthy individuals.

**Reportable Outcomes**

1. Chandrasekhar K, Baylink DJ, Apurva K. Srivastava, Susanna O, Hongrun Yu, Jon E. Wergedal and Mohan S. Identification of genetic loci that regulate bone adaptive response to loading in C57BL/6J and C3H/HeJ intercross. Bone 39: 634-643, 2006 Chandrasekhar K, S Mohan, H Yu, S Oberholtzer, J.E Wergedal, D.J.Baylink. Novel Mechanoresponsive BMD and Bone Size QTL Identified In A Genome Wide Linkage Study Involving C57BL/6J-C3H/HeJ Intercross. ASBMR 27<sup>th</sup> Annual Meeting, 2005.
2. Chandrasekhar K, D. J Baylink, K. Susanna, J. E. Wergedal, H. Yu, and S. Mohan. Quantitative Trait loci for Tibia Periosteal Circumference in the C57BL/6J-C3H/HeJ mice intercross. ASBMR 28<sup>th</sup> Annual Meeting, 2005.

**References:**

1. Borer, K.T., *Physical activity in the prevention and amelioration of osteoporosis in women : interaction of mechanical, hormonal and dietary factors*. Sports Med, 2005. **35**(9): p. 779-830.
2. Bailey, D.A. and R.G. McCulloch, *Bone tissue and physical activity*. Can J Sport Sci, 1990. **15**(4): p. 229-39.
3. Bikle, D.D., T. Sakata, and B.P. Halloran, *The impact of skeletal unloading on bone formation*. Gravit Space Biol Bull, 2003. **16**(2): p. 45-54.
4. Bikle, D.D. and B.P. Halloran, *The response of bone to unloading*. J Bone Miner Metab, 1999. **17**(4): p. 233-44.
5. Umemura, Y., et al., *A time course of bone response to jump exercise in C57BL/6J mice*. J Bone Miner Metab, 2002. **20**(4): p. 209-15.
6. Kodama, Y., et al., *Exercise and mechanical loading increase periosteal bone formation and whole bone strength in C57BL/6J mice but not in C3H/HeJ mice*. Calcif Tissue Int, 2000. **66**(4): p. 298-306.
7. Kodama, Y., et al., *Cortical tibial bone volume in two strains of mice: effects of sciatic neurectomy and genetic regulation of bone response to mechanical loading*. Bone, 1999. **25**(2): p. 183-90.
8. Dhamrait, S.S., et al., *Cortical bone resorption during exercise is interleukin-6 genotype-dependent*. Eur J Appl Physiol, 2003. **89**(1): p. 21-5.
9. Dalsky, G.P., et al., *Weight-bearing exercise training and lumbar bone mineral content in postmenopausal women*. Ann Intern Med, 1988. **108**(6): p. 824-8.
10. Snow-Harter, C., et al., *Effects of resistance and endurance exercise on bone mineral status of young women: a randomized exercise intervention trial*. J Bone Miner Res, 1992. **7**(7): p. 761-9.
11. Kesavan, C., et al., *Mechanical loading induced gene expression and BMD changes are different in two inbred mouse strains*. J Appl Physiol, 2005.
12. Akhter, M.P., et al., *Bone response to in vivo mechanical loading in two breeds of mice*. Calcif Tissue Int, 1998. **63**(5): p. 442-9.
13. Li, X., et al., *Chromosomal regions harboring genes for the work to femur failure in mice*. Funct Integr Genomics, 2002. **1**(6): p. 367-74.
14. Masinde, G.L., et al., *Quantitative trait loci for periosteal circumference (PC): identification of single loci and epistatic effects in F2 MRL/SJL mice*. Bone, 2003. **32**(5): p. 554-60.
15. Srivastava, A.K., et al., *Mapping quantitative trait loci that influence blood levels of alkaline phosphatase in MRL/MpJ and SJL/J mice*. Bone, 2004. **35**(5): p. 1086-94.
16. Beamer, W.G., et al., *Quantitative trait loci for femoral and lumbar vertebral bone mineral density in C57BL/6J and C3H/HeJ inbred strains of mice*. J Bone Miner Res, 2001. **16**(7): p. 1195-206.
17. Turner, C.H., et al., *Congenic mice reveal sex-specific genetic regulation of femoral structure and strength*. Calcif Tissue Int, 2003. **73**(3): p. 297-303.
18. Shultz, K.L., et al., *Congenic strains of mice for verification and genetic decomposition of quantitative trait loci for femoral bone mineral density*. J Bone Miner Res, 2003. **18**(2): p. 175-85.

19. Bouxsein, M.L., et al., *Mapping quantitative trait loci for vertebral trabecular bone volume fraction and microarchitecture in mice*. J Bone Miner Res, 2004. **19**(4): p. 587-99.
20. Koller, D.L., et al., *Genetic effects for femoral biomechanics, structure, and density in C57BL/6J and C3H/HeJ inbred mouse strains*. J Bone Miner Res, 2003. **18**(10): p. 1758-65.
21. Lang, D.H., et al., *Quantitative trait loci analysis of structural and material skeletal phenotypes in C57BL/6J and DBA/2 second-generation and recombinant inbred mice*. J Bone Miner Res, 2005. **20**(1): p. 88-99.
22. Volkman, S.K., et al., *Quantitative trait loci that modulate femoral mechanical properties in a genetically heterogeneous mouse population*. J Bone Miner Res, 2004. **19**(9): p. 1497-505.
23. Li, X., et al., *Genetic dissection of femur breaking strength in a large population (MRL/MpJ x SJL/J) of F2 Mice: single QTL effects, epistasis, and pleiotropy*. Genomics, 2002. **79**(5): p. 734-40.
24. Yershov, Y., et al., *Bone strength and related traits in HcB/Dem recombinant congenic mice*. J Bone Miner Res, 2001. **16**(6): p. 992-1003.
25. Robling, A.G., et al., *Evidence for a skeletal mechanosensitivity gene on mouse chromosome 4*. Faseb J, 2003. **17**(2): p. 324-6.
26. Riechman, S.E., et al., *Association of interleukin-15 protein and interleukin-15 receptor genetic variation with resistance exercise training responses*. J Appl Physiol, 2004. **97**(6): p. 2214-9.
27. McCole, S.D., et al., *Angiotensinogen M235T polymorphism associates with exercise hemodynamics in postmenopausal women*. Physiol Genomics, 2002. **10**(2): p. 63-9.
28. Kapur, S., et al., *Fluid shear stress synergizes with insulin-like growth factor-I (IGF-I) on osteoblast proliferation through integrin-dependent activation of IGF-I mitogenic signaling pathway*. J Biol Chem, 2005. **280**(20): p. 20163-70.
29. Hens, J.R., et al., *TOPGAL mice show that the canonical Wnt signaling pathway is active during bone development and growth and is activated by mechanical loading in vitro*. J Bone Miner Res, 2005. **20**(7): p. 1103-13.
30. Kesavan et al., *Identification of genetic loci that regulate bone adaptive response to mechanical loading in C57BL/6J and C3H/HeJ mice intercross*. Bone 39(3): 634-643, 2006

## **Progress Report for the period of 2007-2008**

### **Introduction:**

Mechanical loading (ML) plays an important role in the maintenance of bone mass and strength. Several reports have provided evidence that mechanical loading stimulates bone formation and that immobilization, or a loss of mechanical stimulation, such as bed rest or space flight, leads to a decrease in bone formation and an increase in bone loss (1, 10, 13, 14, 18, 24, 30, 31) (3, 4, 11, 17, 26, 36). Recent studies in humans have demonstrated that bone anabolic response varies widely among individuals when subjected to the same degree of mechanical load ranging from good to moderate response (7, 9, 27, 29). Analogously, experimental animals, particularly inbred strains of mice, have also shown variability with respect to mechanical loading. Studies have shown that there are greater fold changes in bone marker genes in C57BL/6J (B6) mice as compared with C3H/HeJ (C3H) mice when subjected to a same loading regimen (11). It is likely that these variations in the bone anabolic response, in both human and mouse models, are due to differences in the transcription levels of genes, i.e., they are genetically controlled.

One of the approaches often used to study the genetic regulation of an observed phenotype is QTL mapping. This approach has been well-established in both human and mouse models and has revealed hundreds of chromosomal regions containing genes affecting bone phenotypes such as BMD, bone size and bone strength (2, 15, 22, 23). Previously, using this traditional or “classical” quantitative trait loci analysis (cQTL), we have identified several loci that regulate BMD and bone size in response to mechanical loading in the B6XC3H cross (12). In order to validate these findings and to discover additional QTLs, we have used expression QTL mapping (eQTL) in the same inbred strain cross.

Recently, a number of studies in human and animal models have provided evidence that expression levels of genes are amenable for genetic analysis in search of loci for the phenotypic variation (8, 20, 25, 28, 32, 34, 35). This eQTL approach has several advantages: 1) it can map a QTL to the gene itself, indicating whether cis changes or trans factors are responsible for the different expression levels, 2) it allows one to identify genetic regions that directly control the expression levels of genes and 3) it validates the chromosomal region identified from cQTL analysis and determines whether these regions are responsible for the difference in transcription levels of genes responsible for the difference in bone response to loading between the two strains of mice. In the present study, we have treated expression levels of bone markers genes as quantitative traits for two inbred strains, C57BL/6J and C3H/HeJ, a good and poor responder, respectively, in order to perform a genome-wide search of loci regulating bone anabolic response to mechanical loading.

Our goals for the last ten months of the funding period for the revised Technical Objective-I, as well as our progress for each of the specific objectives in Technical Objective-I, are described below.

Our specific objectives during the **final 10 months** of the continuation grant for the *in vivo* studies are as follows.

- 1) To begin phenotyping the 300 F2 mice with our newly validated phenotype (i.e. realtime PCR of bone marker genes).
- 2) To continue the genotyping of the F2 mice.
- 3) To apply MAP QTL Pseudomarker or other programs to identify genetic loci that are involved in mediating anabolic response to loading.
- 4) To obtain congenic strains of mice, which contain bone density and/or bone size QTL and evaluate if identified QTL region for bone density/bone size contain gene/s that contribute to bone anabolic response to mechanical loading.

**Specific objective 1: To begin phenotyping the 300 F2 mice with our newly validated phenotype (i.e. realtime PCR of bone marker genes)**

After the last loading regimen, followed by *in vivo* pQCT measurement, mice were sacrificed, tibias were collected and store in RNA later for later RNA extraction. We used Qiagen lipid RNA extraction kit [Qiagen, Valencia, CA] to extract RNA from bones with the following modification. After euthanization, tissues were removed from test mice and stored with RNA later (a chemical that prevents degradation of RNA) at -80°C. The autoclaved mortar and pestle were washed twice prior to our extraction, using DEPC water and cooled with liquid nitrogen (This kept the bone RNA from degrading while in the mortar). At this point, 5-7 mm bone was added and liquid nitrogen was added three times until it froze. This caused the bone to become brittle and therefore, easier to achieve a fine powder. Approximately 1ml of Trizol was added to each sample and ground until it became a finer powder. This fine bone powder were removed from the cold mortar using a sterile razor blade and transferred quickly to a fresh 1.5 ml RNase free tube. Chloroform (200 µl) was added to each sample, and each sample was shaken (up & down) for 15 seconds and incubated at room temperature for 3 minutes (This step is highly important because long duration of incubation and forceful shaking degrade the RNA). The samples were then centrifuged at 12,000 g for 15 minutes and the aqueous layer was removed carefully to a fresh tube after centrifugation. Approximately 700 µl of ethanol was added to the fresh samples and shaken gently (up & down) for 15 seconds. The samples were then transferred to a spin column and the RNA was purified according to the manufacturer's instructions. Quality and quantity of RNA were analyzed using Bio-analyzer and Nano-drop instrumentation [Agilent]. We have completed total RNA extraction from 329 F2 mice. An excel chart has been made that contains information about the quantity, quality and mice ID for each total RNA extracted from mice [not included].

Based on our previous studies, we selected two bone genes to evaluate the bone anabolic response to mechanical loading in F2 mice. These two genes, as evidenced from our study as well as from other studies, have been used to define increase or decrease in bone formation response. These genes are: 1) Bone sialoprotein and 2) alkaline phosphatase. Quantitation of messenger Ribonucleic acid (mRNA) expression was carried out according to the manufacturer's instructions (ABIPRISM, Foster City, CA.) using the SYBR Green method on 7900 Sequence Detection systems from Applied

Biosystems. Briefly, purified total RNA [200µg/µl] was used to synthesize the first strand cDNA by reverse transcription according to the manufacturer's instructions [Bio-Rad, CA]. One µl of this first strand cDNA reaction was subjected to real time PCR amplification using gene specific primers. The primers were designed using Vector NTI software and were purchased from IDT-DNA. Approximately 25µl of reaction volume was used for the real time PCR assay that consisted of 1X [12.5µl] Universal SYBR green PCR master mix [Master mix consists of SYBR Green dye, reaction buffers, dNTPs mix, and Hot Start Taq polymerase] [Applied Biosystems, Foster City, CA], 50nM of primers, 24µl of water, and 1ul of template. The thermal conditions consisted of an initial denaturation at 95°C for 10 minutes followed by 40 cycles of denaturation at 95°C for 15 seconds (sec), annealing and extension at 60°C for 1 minute, and a final step melting curve of 95°C for 15 sec, 60°C for 15 sec, and 95°C for 15 sec. All reactions were carried out in duplicate to reduce variation. The data were analyzed using SDS software, version 2.0, and the results were exported to Microsoft Excel for further analysis.

Expression levels from each of the bone formation markers were measured as fold change by comparing the difference between loaded tibiae versus non-loaded tibiae. For gene expression studies, we used 241 samples since they represented RNA of high quality and sufficient yield. The mean fold increases in BSP and ALP, in the parents, female F1 and F2 mice, normalized by  $\beta$ -actin and by PPIA are shown in Table-1. The fold change data for the BSP and ALP marker genes in the female F2 mice, obtained after normalizing with  $\beta$ -actin and PPIA, show skewed distribution (Figure 1). The skewed distribution appears to be due to the fold change calculation which amplifies the difference geometrically ( $2^{-\Delta\Delta CT}$ ). Thus, by adjusting the data with natural log, the distribution became normal. The broad sense of heritability, calculated as described previously, for the loading-induced fold changes in the BSP and ALP, after normalizing with  $\beta$ -actin was 87% and 91% respectively, and after normalizing with PPIA was 88%, and 91%, respectively in the F2 population.

**Table-1: Fold changes in the expression levels of bone marker genes in response to 12 days four-point bending on 10-week female mice.**

Groups	BSP	ALP	N=
B6 Parents	8.41 $\pm$ 0.76	6.29 $\pm$ 0.71	5
C3H Parents	2.93 $\pm$ 0.62	3.38 $\pm$ 0.69	5
F1 $\beta$ -actin normalized	1.87 $\pm$ 2.36	2.09 $\pm$ 2.03	16
PPIA normalized	1.44 $\pm$ 1.82	1.82 $\pm$ 1.89	
F2 $\beta$ -actin normalized	3.0 $\pm$ 2.59	2.82 $\pm$ 2.52	241
PPIA normalized	2.83 $\pm$ 2.31	2.70 $\pm$ 2.31	

Values mentioned above are Mean  $\pm$  SD of the fold change

We next determined whether the mRNA levels of bone formation marker genes (fold change), measured by real time PCR, correlate with the changes in BMD and log PC measured by pQCT. The results show a significant positive correlation between fold changes and BMD ( $r = 0.25$  to  $0.30$ ), and bone size ( $r = 0.27$  to  $0.36$ ). These findings suggest that these two bone formation markers are responsible, in part, for the increase in BMD and PC in response to loading in the F2 mice.

Since B6 and C3H mice exhibit differences in bone size due to their genetic background, we expected a variation in the cross-sectional area among F2 mice. Due to this variation, mice with smaller cross-sectional areas are predicted to receive a higher mechanical strain, while mice with larger cross-sectional areas to receive less mechanical strain to the same load. In order to determine if this variation in strain affected the expression levels of these markers, we performed a correlation analysis between the fold changes in BSP and ALP, normalized with  $\beta$ -actin and PPIA, and non-loaded PC measurements of each F2 mouse. These results showed no correlation ( $r = -0.003$  to  $0.03$ ). Similarly, we found no correlation between body-weight and fold change data for BSP and ALP. These data suggest that variation in the increase in mRNA levels of BSP and ALP genes induced by mechanical loading is largely independent of bone size and body weight in the B6XC3H intercross.

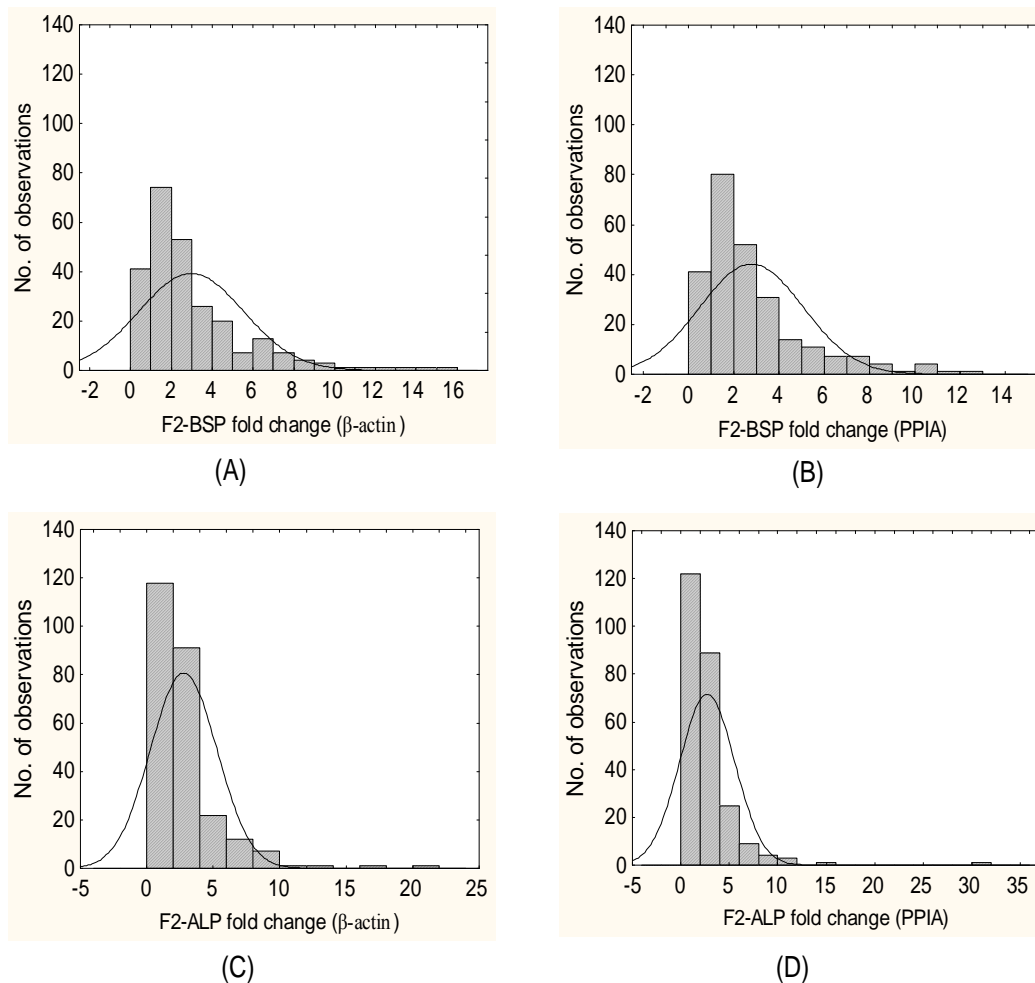


**Fig 1:** Distribution of fold changes for (A) BSP normalized with  $\beta$ -actin, (B) BSP normalized with PPIA, (C) ALP normalized with  $\beta$ -actin, and (D) ALP normalized with PPIA in the F2 population after two weeks of four-point bending. The x-axis represents the fold change and y-axis represents the number of observations (mice). BSP; Bone sialoprotein, ALP; Alkaline phosphatase,  $\beta$ -actin; Beta actin and PPIA; Peptidyl-prolyl cis-trans isomerase A. The solid line represents theoretical skewed **distribution. Based**

on kolmogorov-smirnov test, both BSP and ALP fold change data show skewed distribution (n=241).

**Specific objective 2: To continue the genotyping of the F2 mice.**

We have now extracted DNA from the liver of each F2 mouse using a Qiagen DNA extraction kit. The quality and quantity of the extracted DNA was measured by nano-drop and bio-analyzer. One hundred twenty Polymerase chain reaction primers were purchased from Applied Biosystems to perform the genotyping on the F2 population (n=329). All of these markers were chosen depending upon the position on the chromosome in an effort to distribute them at <15cM to generate a complete genome wide scan. To proceed faster and restrict the usage of more chemicals in our genotyping reaction, we have optimized the PCR reactions (Eppendorf reagents were used) and running conditions to perform multiplexed (3-4 micro satellite markers) in a single electrophoretic lane. The pooled products were analyzed for fragments size on the ABI 3100 Sequence Detection System and Gene Scan software was used to detect size of the alleles. Allele calls and edits were performed using Genotyper software and in house software, and exported as text files for downstream analysis.

**Specific objective 3: To apply MAP QTL pseudomarker or other programs to identify genetic loci that are involved in mediating anabolic response to loading.**

We used non-parametric mapping due to skewed distribution of BSP and ALP fold change data in the F2 population. The mapping was performed by using a MapQTL software program (Verison 5.0; Wageningen, The Netherlands). The significance of the QTL were derived based on the Map QTL program as described earlier (12). Using 111 micro-satellite markers and loading induced fold change data of BSP and ALP marker genes of F2 female mice (n=241), a genome-wide analysis revealed the presence of significant and suggestive genetic loci affecting bone anabolic response (Table-2). Loci regulating both the expression of BSP and ALP, normalized with  $\beta$ -actin and PPIA, were located on Chromosomes 8, 9, 16, 17, 18 and 19. Loci regulating only BSP were located on Chrs 1, 5 and 9, whereas loci regulating only ALP were located on Chrs 1, 3 and 4. For BSP, highly significant LOD scores were observed on Chr 1 [LOD score 10.4 @ 91.8], Chr 17 [LOD score 11.2 @ 14.2cM], and Chr 19 [LOD score 10.2 @ 3.3cM]. For ALP, highly significant LOD scores were observed on Chr 8 [LOD score 12.8, @ 60cM], Chr 17 [LOD score 9.3, @ 14.2] and Chr 18 [LOD score 12.6 @38cM].

**Table-2: Significant and suggestive QTL identified using fold change data for the mechanical loading induced phenotypes in the B6XC3H F2 mice.**

Phenotypes	Chr	Locus	cM	Actin Normalization	PPIA Normalization
				LOD score	LOD score
Bone sialoprotein	1	D1Mit113	91.8	-	10.4 <sup>a</sup>
	5	D5Mit143	73.2	-	5.2 <sup>c</sup>
	8	D8Mit88	60.1	7.5 <sup>b</sup>	8.8 <sup>b</sup>
	9	D9Mit2	13.1	7.0 <sup>b</sup>	4.8 <sup>c</sup>
	9	D9Mit151	69.9	7.1 <sup>b</sup>	5.0 <sup>c</sup>
	16	D16Mit153	45.9	6.7 <sup>b</sup>	7.0 <sup>b</sup>

	17	D17Mit51	14.2	9.2 <sup>a</sup>	12.3 <sup>a</sup>
	18	D18Mit144	38	8.0 <sup>b</sup>	-
	19	D19Mit68	3.3	7.2 <sup>b</sup>	10.7 <sup>a</sup>
Alkaline phosphatase	1	D1Mit215	47	5.0 <sup>c</sup>	7.5 <sup>b</sup>
		D1Mit102	75.4	6.3 <sup>b</sup>	7.6 <sup>b</sup>
	3	D2Mit147	59	7.7 <sup>b</sup>	8.3 <sup>b</sup>
	4	D4Mit308	54.6	5.5 <sup>c</sup>	5.6 <sup>b</sup>
		D4Mit256	82	5.6 <sup>c</sup>	5.0 <sup>c</sup>
	8	D8Mit88	60.1	10.5 <sup>a</sup>	12.3 <sup>a</sup>
	9	D9Mit151	69.9	7.4 <sup>b</sup>	-
	16	D16Mit153	45.9	5.1 <sup>c</sup>	5.9 <sup>c</sup>
	17	D17Mit51	14.2	9.3 <sup>a</sup>	9.0 <sup>b</sup>
	18	D18Mit144	38	12.6 <sup>a</sup>	5.8 <sup>c</sup>
	19	D19Mit68	3.3	-	6.9 <sup>b</sup>

<sup>a</sup>The threshold for the highly significant LOD score is  $p < 0.01$ .

<sup>b</sup>The threshold for the significant LOD score is  $p < 0.05$ .

<sup>c</sup>The threshold for the suggestive LOD score is  $p < 0.1$ .

- Corresponds to no QTL.

We undertook a number of precautions to ensure that the QTLs we identified are real and not due to technical or design artifacts: 1) We chose two markers, BSP and ALP, that showed significant positive correlation in bone anabolic response to loading in a previous study (11). 2) We used fold changes rather than Ct-values to study linkages so that we would identify specific genetic changes rather than general changes. 3) We used two housekeeping genes, rather than one, to normalize the expression data in order to avoid identification of QTLs stemming from variations in RNA quality among samples.

Our linkage analysis revealed several QTLs that are responsible for the increased expression levels of BSP and ALP, induced by mechanical loading in the F2 mice. If changes in BSP and ALP markers reflect skeletal changes to mechanical loading, one would expect QTLs which are common to both markers. Accordingly, we found co-localized loci on Chrs 8, 16, 17, 18 and 19 for both BSP and ALP, suggesting that both markers are responding to the same upstream signaling.

Our findings also revealed four loci on Chrs 3, 8, 17 and 18 which are identical to QTLs we previously found for BMD and/or bone size parameters (12). This is consistent with other studies which have shown that Chrs 8 (30-90cM), 17 (6.6cM) and 18 (32-46cM) contain a loci which regulate biomechanical properties in several inbred mouse strain crosses (15, 16, 21, 22). The fact that we found QTLs at the same loci using both bone parameters and bone formation markers, indicate that these loci do, in fact, contain genes that are not only involved in increasing bone formation in response to loading, but also involved in regulating mechanical properties of the bone, in part, through ALP and BSP expression. While the expression QTLs found on Chr 17 and 18 were contained within the region identified for the BMD and bone size, the broad QTL regions in these chromosomes raise the possibility that more than one gene could be responsible for the

phenotypic changes. Fine mapping will narrow down the size of the QTL and allow us to identify is as the same QTL as identified for BMD or as a different QTL. Surprisingly, we identified additional QTLs for BSP and/or ALP which do not correspond with any QTLs reported for bone parameters. This could be explained by: 1) changes in gene expression might be more sensitive to external loading than net change in the bone parameters (measured by pQCT) and 2) these regions may be involved in regulating the expression of BSP or ALP, but have no measured effect on bone formation.

To assure that the QTLs identified for BSP and ALP fold change in response to mechanical loading are not due to changes in the housekeeping genes, we calculated fold change of  $\beta$ -actin normalized by PPIA and PPIA fold change normalized by  $\beta$ -actin. We found that the mean fold difference in  $\beta$ -actin was  $0.99 \pm 0.30$  and in PPIA was  $1.05 \pm 0.33$  in the F2 mice. Interval mapping using F2 mice (n = 241) revealed four suggestive QTL on chromosomes 1, 9 and X and one significant QTL on Chr 2 (Table-3). We found that one of the loci on Chr 9 (69.9cM) identified for the  $\beta$ -actin fold change data corresponds to one of the loci identified for both BSP and ALP fold change data. This finding leads us to suspect that the QTL identified for ALP and BSP on Chr 9 could be due to expression changes in the house keeping gene rather than due solely to expression changes in the marker genes. Thus, the validity of Chr 9 QTL remain to be established.

**Table-3: Interval mapping for the fold change in  $\beta$ -actin (normalized by PPIA) and PPIA (normalized by  $\beta$ -actin) in response to mechanical loading in the B6XC3H F2 mice.**

Phenotypes	Chr	Locus	cM	LOD Score	Variance
$\beta$ -actin	1	D1Mit430	6.6	2.0 <sup>c</sup>	3.6
	2	D2Mit66	48.1	2.8 <sup>b</sup>	5.4
	9	D9Mit151	69.9	1.9	3.6
PPIA	2	D2Mit285	72.1	*	3.3
	X	DXMit172	40.4	2.1 <sup>c</sup>	4.7

<sup>b</sup>The threshold for the significant LOD score is  $p < 0.05$

<sup>c</sup>The threshold for the suggestive LOD score is  $p < 0.1$

\* QTL with very low LOD score

Variance are explained from peak LOD Score

In addition to the mechanical loading QTL, we identified QTLs that regulate the basal expression of BSP and ALP in the non-loaded tibiae, by using Ct-values from Real time PCR, after normalization with  $\beta$ -actin and PPIA. Both BSP and ALP showed normal distribution in the F2 population (Figure 2). We found that the BSP and ALP data showed no correlation with body weight suggesting that the basal expression of these two bone formation marker genes are independent of the body weight. Interval mapping was then performed using F2 female mice (n=241), which revealed four chromosomes, Chrs 4, 10, 16, & 18 that regulate the basal expression of BSP and ALP in the non-loaded tibiae (Table-4).

**Table-4: Significant and suggestive QTL identified using CT values for the non-externally loaded phenotypes in the B6XC3H F2 female mice.**

Phenotype	Ch	Locus	cM	LOD	Varianc	LOD	Varianc
s	r			Actin Normalizatio n	e	PPIA Normalizatio n	e
BSP	4	D4Mit42	76.5	2.7 <sup>b</sup>	5.2	2.4 <sup>c</sup>	4.5
	18	D18Mit64	0	2.4 <sup>c</sup>	4.6	*	2.3
ALP	4	D4Mit42	76.5	2.8 <sup>b</sup>	5.2	*	3.3
	10	D10Mit213	6.6	2.3 <sup>c</sup>	4.3		
	16	D16Mit153	45.9	1.9	3.6	2.3 <sup>c</sup>	4.2
	18	D18Mit144	38.3	2.4 <sup>c</sup>	6.7	*	2.3

<sup>b</sup>The threshold for the significant LOD score is  $p < 0.05$ <sup>c</sup>The threshold for the suggestive LOD score is  $p < 0.1$ 

\* QTL with very low LOD score

Variance are explained from peak LOD Score

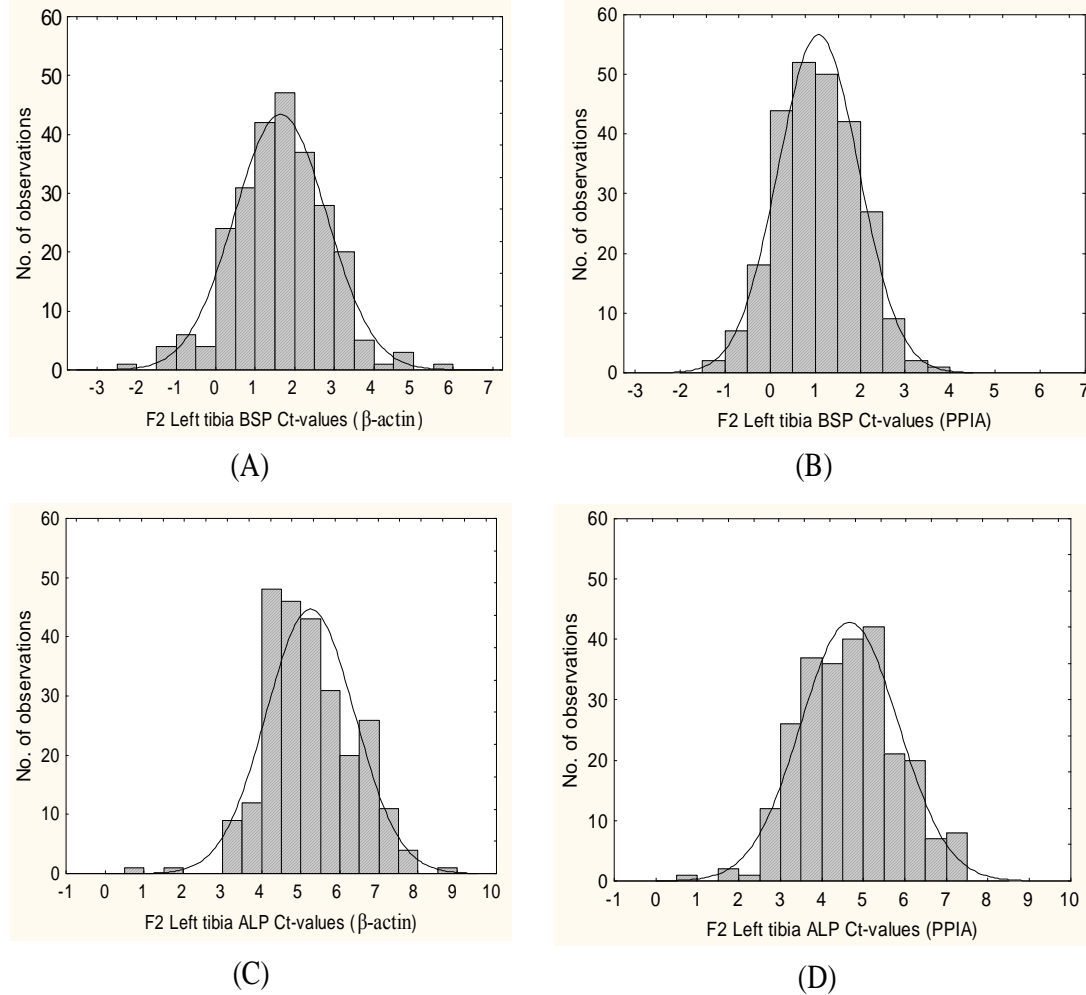


**Fig 2:** Distribution of Ct-values of non-external loaded tibia for (A) BSP normalized with  $\beta$ -actin, (B) BSP normalized with PPIA, (C) ALP normalized with  $\beta$ -actin and (D) ALP normalized with PPIA in the F2 population after two weeks of four-point bending. The x-axis represents the fold change and y-axis represents the number of observations (mice). BSP; Bone sialoprotein, ALP; Alkaline phosphatase,  $\beta$ -actin; Beta actin and PPIA; Peptidyl-prolyl cis-trans isomerase A. The solid line represents theoretical normal distribution. Based on kolmogorov-smirnov test, both BSP and ALP show normal distribution (n=241).

The QTLs identified in this study common to both BSP and ALP are more than 10cM in length, and thus, contain hundreds of genes and EST's. Some of the known candidate genes located in these QTL regions are shown in table-5. We have previously reported that the expression of some of these genes increase with mechanical loading using a genome-wide microarray analysis (33). Others using various approaches have shown that many of these genes are involved in skeletal development. This confirms our present QTL findings. Although QTL analysis leads to a precise mapping of the genetic loci which contribute to our phenotype of interest, these regions are broad and contain many possible significant genes. The next phase of our study, therefore, lies in

identifying which specific genes within our identified QTL regions are associated with mechanical loading.

**Table-5: List of potential candidate genes located in the QTL region identified for skeletal anabolic response to mechanical loading.**

Chrs	cM	Genes	Predicted functions in bone
8	38-69	Ptger1 Junb Mt1, 2  Cdh11 Hsd11b2 Cdh1 Cbfb  Hsd17b2 Il17c	Prostaglandin E2 stimulates fibronectin through ptger1. Involved in osteoblast cell proliferation. Regulate early stage of mesenchymal stem cells differentiation. Knock out (KO) mice show reduced bone density. Regulate glucocorticoid signaling. Important in embryonic limb buds development. Required for the function of Runx1 and Runx2 in skeletal development. Involved in regulation of estrogen action. Involved in osteoclastogenesis.
16	30-46	Col8a1 EphA3 Pit1	Increased in bone in response to mechanical loading. Involved in tooth development. Mediates bone formation by regulating the expression of BSP.
17	0-25	Map3k4 Clcn7 Thbs2 Traf7 Tnf Notch3 Vegfa Runx2	Involved in normal skeletal patterning. Critical for osteoclast resorption. KO mice show increased bone density and cortical thickness. Involved in MEKK3 signaling and apoptosis. Important in osteoclastogenesis. Involved in tooth development. Involved in angiogenesis of bone. Involved in skeletal development.
18	15-40	Lox Pdgfrb Adrb2 Mc4r Mapk4 Nfatc1 Galr1	Play a key role in the collagen deposition by osteoblast. Involved in bone remodeling phase. Produces anabolic effects on bone. KO mice show decreased bone resorption and high bone mass. Intracellular mediator of growth factor. Important in osteoclastogenesis. Important for bone healing.
19	0-24	Gal Lrp5 Esrra Lpxn Ostf1 Jak2	Involved in bone healing. Regulates osteoblast function. Important in bone metabolism. Involved in podosomal signaling complex in osteoclast. Stimulate osteoclast formation. Involved in osteoblast signaling.

Some of the limitations of this study are: 1) we used a relatively small number of F2 mice to perform the eQTL analysis (n=241) relative to the cQTL analysis (n=329). This is due to fact that we encountered problems with quality and quantity in the RNA extracted

from 6 mm, marrow-flushed tibiae. This relatively small sample size may account for the reduced LOD score for some of the QTLs identified in our study. 2) The QTLs identified in this study for bone formation response induced by mechanical loading were obtained from female mice. To date, studies have shown that hormones enhance the effects of mechanically induced bone formation (5, 6, 19). Further studies with male mice may not only reveal whether any of the QTLs we found are female specific but may also lead to the identification of male specific QTLs involved in bone response to mechanical loading. 4) It has been predicted that some of the skeletal changes in the F2 mice could be due to periosteal pressure caused by four-point bending. Our previous findings that sham loading neither increased periosteal bone formation nor caused changes in expression levels of bone formation marker genes (data not shown) argue against this possibility (12).

**Specific Objective 4: To obtain congenic strains of mice, which contain bone density and/or bone size QTL and evaluate if identified QTL region for bone density/bone size contain gene/s that contribute to bone anabolic response to mechanical loading.**

In Previous studies we have collaborated with scientists to identify genetic loci that contribute to variation in BMD using B6-CAST and B6-C3H inbred strain crosses. In subsequent studies, we have generated B6 congenic lines of mice that carry small fragments of Chr 1 from CAST mice and Chr 4 from C3H mice that contain BMD QTL gene. In order determine if the BMD QTL gene in CAST Chr 1 and/or C3H Chr 4 could also contribute to mediating response to mechanical strain. We undertook studies to generate adequate number of congenic mice to evaluate bone anabolic response to mechanical loading. If we find evidence that one or both of these congenic lines exhibit greater bone anabolic response to mechanical loading, this would help to narrow down the location of candidate gene for mechanical loading.

Presently, we have completed four-point bending on 10-week female B6 WT and B6-CAST 1-6 congenic mice. The changes in bone parameters measured by in-vivo pQCT are shown in Table-6. The results from our study indicate that changes in bone parameters were increased significantly after 12 days of four-point bending in both female B6: CAST 1-6 congenic mice and WT B6 mice. There was no significant difference in the increase in bone size and total vBMD and/cortical vBMD between both sets of mice. Based on this finding, we conclude that CAST Chr 1 (89Mb) fragment is not critical for mechanical loading induced changes in bone parameters.

**Table-6:** Changes in the bone parameters measured by in-vivo pQCT after 12 days of four-point bending in 10-week female littermate mice and B6: CAST 1-6 congenic mice.

A) WT B6 mice

Bone parameters	Mean $\pm$ SD			
	Non-loaded	Loaded	p-value	% change
Total Area mm <sup>2</sup>	2.12 $\pm$ 0.82	2.64 $\pm$ 1.04	0.01	26.0 $\pm$ 5.9
Total Mineral content	1.20 $\pm$ 0.13	1.55 $\pm$ 0.17	0.003	30.0 $\pm$ 4.25
Periosteal. Circum mm	5.13 $\pm$ 0.29	5.73 $\pm$ 0.38	0.01	12.0 $\pm$ 2.63
Total vBMD mg/ccm	696 $\pm$ 22	770 $\pm$ 22	0.0001	11 $\pm$ 4.28

Cortical vBMD mg/ccm	1072 $\pm$ 18	1110 $\pm$ 12	0.001	4.0 $\pm$ 1.96
Cortical thickness mm	0.22 $\pm$ 0.01	0.27 $\pm$ 0.01	0.0002	24 $\pm$ 5.85

N=6

## B) Female B6: CAST 1-6

Bone parameters	Mean $\pm$ SD			
	Non-loaded	Loaded	p-value	% change
Total Area mm <sup>2</sup>	2.06 $\pm$ 0.14	2.49 $\pm$ 0.22	0.004	24.2 $\pm$ 16
Total Mineral content mg/mm	1.15 $\pm$ 0.06	1.51 $\pm$ 0.14	0.0002	31.76 $\pm$ 11.5
Periosteal. Circum mm	4.98 $\pm$ 0.11	5.53 $\pm$ 0.29	0.001	12.0 $\pm$ 6.2
Total vBMD mg/ccm	723 $\pm$ 35	806 $\pm$ 37	0.006	11.27 $\pm$ 2.3
Cortical vBMD mg/ccm	1076 $\pm$ 22	1116 $\pm$ 14	0.006	3.73 $\pm$ 1.54
Cortical thickness mm	0.22 $\pm$ 0.01	0.27 $\pm$ 0.02	0.0001	25.65 $\pm$ 5.48

N=6

**Successes To Date:**

1. Identification of several common QTL for BMD, BSP and ALP phenotypes suggests that the skeletal response to ML is largely mediated by increased BF.
2. We show, from both our QTL study as well as from other QTL studies, that Chr 8 contains genes involved in increasing bone formation induced by mechanical loading and for biomechanical properties of the bone.
3. We identified two new ML QTLs on Chrs 16 and 19 using gene expression data.
4. We show that the QTL identified on Chr 4, 16 and 18 for non-loaded BSP and ALP basal expression were identical to ML QTL suggesting that these chromosomes are responsible for both the natural variation in ALP and BSP and the increase in ALP and BSP in response to loading.
5. Using a congenic approach, we show Chr 1 fragment (D1Mit216-D1Mit112, 89Mb) from CAST is not involved in regulating the bone anabolic response to loading.

**Conclusions**

Bone formation response varies among individuals and is strongly regulated by genetic factors, as is evident from both our previous cQTL and our present eQTL analyses. Further study, with congenic and gene KO mice may help to understand the role of specific genes at the loci we have found and could provide a basis for understanding the observed variability in bone mass accretion and maintenance, resulting from exercise, in normal healthy individuals.

**Reportable Outcomes:**

- Kesavan C, David J Baylink, Susanna Kapoor, and Subburaman Mohan. Novel Loci Regulating Bone Anabolic Response to Loading: Expression QTL Analysis in C57BL/6JXC3H/HeJ Mice Cross, *Bone*, 41: 223-230, 2007.
- Kesavan C, D J Baylink, S Kapoor and S Mohan Identifying Mechanical Loading QTL by Gene Expression Changes for Alkaline Phosphatase and Bone

Sialoprotein in C57BL/6J (B6) X C3H/HeJ (C3H) Intercross. ASBMR 29<sup>th</sup> Annual Meeting 2007 Hawaii, USA.

### References:

1. Akhter, M. P., Cullen, D. M., Pedersen, E. A., Kimmel, D. B., and Recker, R. R. Bone response to in vivo mechanical loading in two breeds of mice. *Calcif Tissue Int* 63:442-9; 1998.
2. Beamer, W. G., Shultz, K. L., Donahue, L. R., Churchill, G. A., Sen, S., Wergedal, J. R., Baylink, D. J., and Rosen, C. J. Quantitative trait loci for femoral and lumbar vertebral bone mineral density in C57BL/6J and C3H/HeJ inbred strains of mice. *J Bone Miner Res* 16:1195-206; 2001.
3. Bikle, D. D., and Halloran, B. P. The response of bone to unloading. *J Bone Miner Metab* 17:233-44; 1999.
4. Bikle, D. D., Sakata, T., and Halloran, B. P. The impact of skeletal unloading on bone formation. *Gravit Space Biol Bull* 16:45-54; 2003.
5. Borer, K. T. Physical activity in the prevention and amelioration of osteoporosis in women : interaction of mechanical, hormonal and dietary factors. *Sports Med* 35:779-830; 2005.
6. Caiozzo, V. J., and Haddad, F. Thyroid hormone: modulation of muscle structure, function, and adaptive responses to mechanical loading. *Exerc Sport Sci Rev* 24:321-61; 1996.
7. Dalsky, G. P., Stocke, K. S., Ehsani, A. A., Slatopolsky, E., Lee, W. C., and Birge, S. J., Jr. Weight-bearing exercise training and lumbar bone mineral content in postmenopausal women. *Ann Intern Med* 108:824-8; 1988.
8. Deutsch, S., Lyle, R., Dermitzakis, E. T., Attar, H., Subrahmanyam, L., Gehrig, C., Parand, L., Gagnebin, M., Rougemont, J., Jongeneel, C. V., and Antonarakis, S. E. Gene expression variation and expression quantitative trait mapping of human chromosome 21 genes. *Hum Mol Genet* 14:3741-9; 2005.
9. Dhamrait, S. S., James, L., Brull, D. J., Myerson, S., Hawe, E., Pennell, D. J., World, M., Humphries, S. E., Haddad, F., and Montgomery, H. E. Cortical bone resorption during exercise is interleukin-6 genotype-dependent. *Eur J Appl Physiol* 89:21-5; 2003.
10. Gross, T. S., Srinivasan, S., Liu, C. C., Clemens, T. L., and Bain, S. D. Noninvasive loading of the murine tibia: an in vivo model for the study of mechanotransduction. *J Bone Miner Res* 17:493-501; 2002.
11. Kesavan, C., Mohan, S., Oberholtzer, S., Wergedal, J. E., and Baylink, D. J. Mechanical loading-induced gene expression and BMD changes are different in two inbred mouse strains. *J Appl Physiol* 99:1951-7; 2005.
12. Kesavan, C., Mohan, S., Srivastava, A. K., Kapoor, S., Wergedal, J. E., Yu, H., and Baylink, D. J. Identification of genetic loci that regulate bone adaptive response to mechanical loading in C57BL/6J and C3H/HeJ mice intercross. *Bone* 39:634-43; 2006.
13. Kodama, Y., Dimai, H. P., Wergedal, J., Sheng, M., Malpe, R., Kutilek, S., Beamer, W., Donahue, L. R., Rosen, C., Baylink, D. J., and Farley, J. Cortical tibial bone volume in two strains of mice: effects of sciatic neurectomy and

- genetic regulation of bone response to mechanical loading. *Bone* 25:183-90; 1999.
14. Kodama, Y., Umemura, Y., Nagasawa, S., Beamer, W. G., Donahue, L. R., Rosen, C. R., Baylink, D. J., and Farley, J. R. Exercise and mechanical loading increase periosteal bone formation and whole bone strength in C57BL/6J mice but not in C3H/HeJ mice. *Calcif Tissue Int* 66:298-306; 2000.
  15. Koller, D. L., Schriefer, J., Sun, Q., Shultz, K. L., Donahue, L. R., Rosen, C. J., Foroud, T., Beamer, W. G., and Turner, C. H. Genetic effects for femoral biomechanics, structure, and density in C57BL/6J and C3H/HeJ inbred mouse strains. *J Bone Miner Res* 18:1758-65; 2003.
  16. Lang, D. H., Sharkey, N. A., Mack, H. A., Vogler, G. P., Vandenberg, D. J., Blizard, D. A., Stout, J. T., and McClearn, G. E. Quantitative trait loci analysis of structural and material skeletal phenotypes in C57BL/6J and DBA/2 second-generation and recombinant inbred mice. *J Bone Miner Res* 20:88-99; 2005.
  17. Lang, T. F., Leblanc, A. D., Evans, H. J., and Lu, Y. Adaptation of the proximal femur to skeletal reloading after long-duration spaceflight. *J Bone Miner Res* 21:1224-30; 2006.
  18. Lanyon, L. E. Using functional loading to influence bone mass and architecture: objectives, mechanisms, and relationship with estrogen of the mechanically adaptive process in bone. *Bone* 18:37S-43S; 1996.
  19. Lee, K. C., Jessop, H., Suswillo, R., Zaman, G., and Lanyon, L. E. The adaptive response of bone to mechanical loading in female transgenic mice is deficient in the absence of oestrogen receptor-alpha and -beta. *J Endocrinol* 182:193-201; 2004.
  20. Li, J., and Burmeister, M. Genetical genomics: combining genetics with gene expression analysis. *Hum Mol Genet* 14 Spec No. 2:R163-9; 2005.
  21. Li, X., Masinde, G., Gu, W., Wergedal, J., Hamilton-Ulland, M., Xu, S., Mohan, S., and Baylink, D. J. Chromosomal regions harboring genes for the work to femur failure in mice. *Funct Integr Genomics* 1:367-74; 2002.
  22. Li, X., Masinde, G., Gu, W., Wergedal, J., Mohan, S., and Baylink, D. J. Genetic dissection of femur breaking strength in a large population (MRL/MpJ x SJL/J) of F2 Mice: single QTL effects, epistasis, and pleiotropy. *Genomics* 79:734-40; 2002.
  23. Masinde, G. L., Wergedal, J., Davidson, H., Mohan, S., Li, R., Li, X., and Baylink, D. J. Quantitative trait loci for periosteal circumference (PC): identification of single loci and epistatic effects in F2 MRL/SJL mice. *Bone* 32:554-60; 2003.
  24. Mori, T., Okimoto, N., Sakai, A., Okazaki, Y., Nakura, N., Notomi, T., and Nakamura, T. Climbing exercise increases bone mass and trabecular bone turnover through transient regulation of marrow osteogenic and osteoclastogenic potentials in mice. *J Bone Miner Res* 18:2002-9; 2003.
  25. Nettleton, D., and Wang, D. Selective transcriptional profiling for trait-based eQTL mapping. *Anim Genet* 37 Suppl 1:13-7; 2006.
  26. Notomi, T., Okazaki, Y., Okimoto, N., Tanaka, Y., Nakamura, T., and Suzuki, M. Effects of tower climbing exercise on bone mass, strength, and turnover in orchidectomized growing rats. *J Appl Physiol* 93:1152-8; 2002.

27. Snow-Harter, C., Bouxsein, M. L., Lewis, B. T., Carter, D. R., and Marcus, R. Effects of resistance and endurance exercise on bone mineral status of young women: a randomized exercise intervention trial. *J Bone Miner Res* 7:761-9; 1992.
28. Spence, J., Liang, T., Foroud, T., Lo, D., and Carr, L. Expression profiling and QTL analysis: a powerful complementary strategy in drug abuse research. *Addict Biol* 10:47-51; 2005.
29. Tajima, O., Ashizawa, N., Ishii, T., Amagai, H., Mashimo, T., Liu, L. J., Saitoh, S., Tokuyama, K., and Suzuki, M. Interaction of the effects between vitamin D receptor polymorphism and exercise training on bone metabolism. *J Appl Physiol* 88:1271-6; 2000.
30. Turner, C. H. Bone strength: current concepts. *Ann N Y Acad Sci* 1068:429-46; 2006.
31. Umemura, Y., Baylink, D. J., Wergedal, J. E., Mohan, S., and Srivastava, A. K. A time course of bone response to jump exercise in C57BL/6J mice. *J Bone Miner Metab* 20:209-15; 2002.
32. Wang, D., and Nettleton, D. Identifying genes associated with a quantitative trait or quantitative trait locus via selective transcriptional profiling. *Biometrics* 62:504-14; 2006.
33. Xing, W., Baylink, D., Kesavan, C., Hu, Y., Kapoor, S., Chadwick, R. B., and Mohan, S. Global gene expression analysis in the bones reveals involvement of several novel genes and pathways in mediating an anabolic response of mechanical loading in mice. *J Cell Biochem* 96:1049-60; 2005.
34. Yaguchi, H., Togawa, K., Moritani, M., and Itakura, M. Identification of candidate genes in the type 2 diabetes modifier locus using expression QTL. *Genomics* 85:591-9; 2005.
35. Yamashita, S., Wakazono, K., Nomoto, T., Tsujino, Y., Kuramoto, T., and Ushijima, T. Expression quantitative trait loci analysis of 13 genes in the rat prostate. *Genetics* 171:1231-8; 2005.
36. Ziambaras, K., Civitelli, R., and Papavasiliou, S. S. Weightlessness and skeleton homeostasis. *Hormones (Athens)* 4:18-27; 2005.

## **Progress Report for the Period of 2008- 2009**

### **[A] Introduction:**

Mechanical loading plays an important role in the maintenance of bone mass and strength [1-4]. Several reports have provided evidence that mechanical loading stimulates bone formation and that immobilization or a loss of mechanical stimulation, such as bed rest or space flight, leads to a decrease in bone formation and an increase in bone loss [5-7]. Recent studies in humans have demonstrated that bone anabolic response varies widely among individuals when subjected to the same degree of mechanical load ranging from good to moderate response [8-11]. Analogously, experimental animals, particularly inbred strains of mice, have also shown variability with respect to mechanical loading. Studies have shown that there are greater fold changes in bone marker genes as well as increase in the changes in bone parameters in C57BL/6J (B6) mice as compared with C3H/HeJ (C3H) mice when subjected to a same loading regimen [1, 12]. It is likely that these variations in the bone anabolic response, in both human and mouse models are largely, in part, regulated by genetic factors.

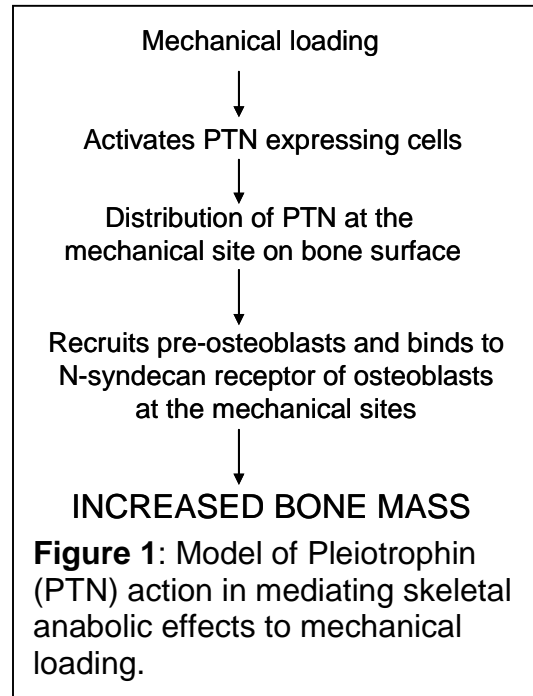
One of the approaches often used to study the genetic regulation of an observed phenotype is quantitative trait loci mapping. Using this approach, we have discovered several genetic loci that regulate bone adaptive response to loading [13, 14]. Thus, the finding of our studies provided evidence that bone formation response varies among individuals and is strongly regulated by genetic factors. Although quantitative trait loci analysis leads to a precise mapping of the genetic loci which contribute to our phenotype of interest, these regions are broad and contain many possible significant genes. The next phase of our study, therefore, lies in identifying which specific genes within our identified quantitative trait loci regions are associated with mechanical loading. In addition to this, we also performed genome-wide microarray analysis in a good responder C57BL/6J mouse, to identify possible candidate genes responsible for bone adaptive response to loading [15]. The results of this study have led to identification of thousands of genes that are differentially expressed in response to loading. Our next goal is to select potential candidates based on the microarray and quantitative trait loci findings, to study their role in anabolic effects of mechanical on bone formation.

### **[B] Technical Objectives**

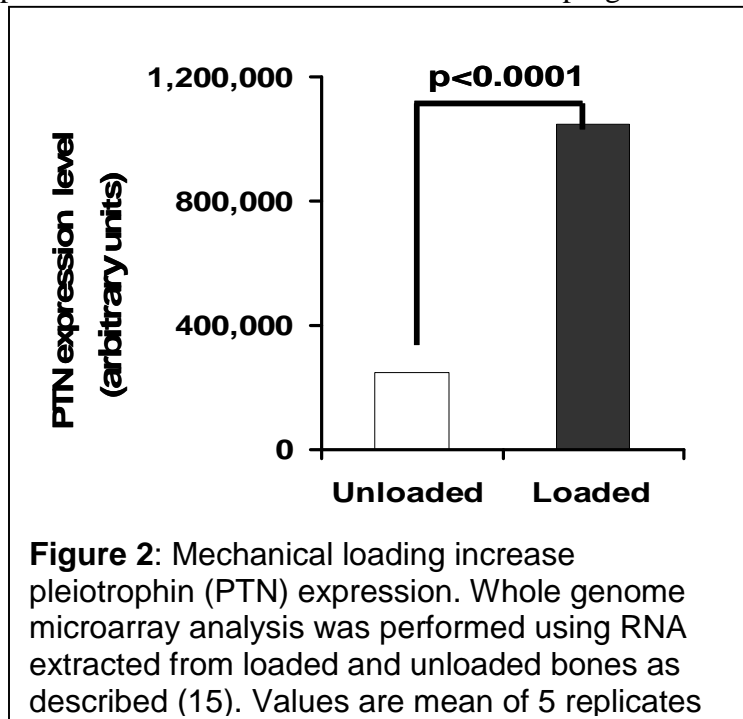
- 1) Evaluate the role of pleiotrophin in mediating skeletal anabolic response to loading
- 2) Evaluate the role of Ras association domain family 1 isoform C (RassF1C) in mediating skeletal anabolic response to loading
- 3) Fate of newly formed bone in response to mechanical strain after cessation of loading
- 4) Generate Insulin like growth factor-I (IGF-I) conditional knockout mice for testing the role of locally produced IGF-I in mediating skeletal anabolic response to loading
- 5) Prepare annual progress report for submission to TATRC.

### [C] **Body1. Heparin binding growth factor/Pleiotrophin**

Bone is a dynamic tissue that undergoes constant remodeling and turnover. These processes are mediated by two types of cells: osteoblasts, involved in bone formation, and osteoclasts, involved in bone resorption. The process of new bone formation can be classified into several stages. The pioneer stage refers to the recruitment of osteoblast precursor cells to a site for osteoid deposition. Upon arrival to the site, these precursor cells are then differentiated into fully functional osteoblasts. Bone formation has a high degree of specificity and must be precisely regulated, in terms of both the amount of formation and the site of formation which depends on the recruitment of bone forming cells. This process, therefore, is regulated by several osteoinductive factors, many of which are present within the bone matrix and have the potential to stimulate bone growth as well [16, 17]. One seemingly important factor among these is Pleiotrophin (PTN).



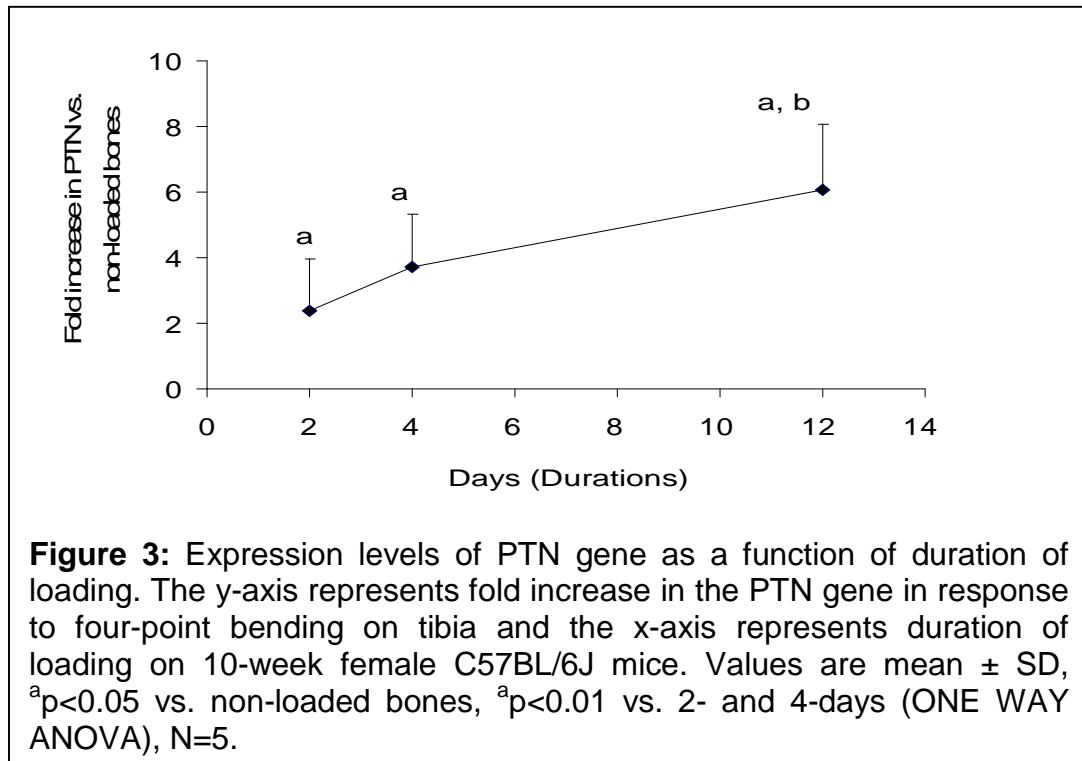
PTN, a 36 amino acid bone growth factor rich in lysine and cysteine residues, is also known as Osteoblast Specific Factor 1. PTN is involved in diverse functions, which include: cell recruitment, cell attachment and proliferation, differentiation, angiogenesis, and neurogenesis [18-20]. *In vitro* studies have demonstrated that PTN has the ability to promote adhesion, migration, expansion and differentiation of human osteoprogenitor and MC3T3-E1 cells [21-23]. *In vivo* studies using transgenic approach have shown that mice with ovariectomy induced bone loss, due to estrogen deficiency, were protected by an increase in the expression of the PTN gene [24]. A transgenic study, with over expression of the human PTN gene, showed an increase in cortical thickness, bone volume and cancellous bone volume [21]. In addition, immunocytochemistry studies have provided visual evidence for PTN at the site of new bone formation [21, 22]. Few other studies have shown that the cell



surface receptor for PTN, syndecan and receptor protein tyrosine phosphatase  $\zeta$ , are known to be expressed in osteoblasts and are known to regulate skeletal development. Furthermore, the downstream molecules of syndecan and receptor protein tyrosine phosphatase, namely PI3K and beta catenin are known to exert significant biological effects on osteoblasts.

If PTN is indeed responsible for recruitment of osteoblasts to specific sites of bone formation, then one would expect PTN to play a significant role in bone formation. Based on the current literature, we propose a model of PTN action in mediating mechanical loading induced bone formation as shown in Figure 1. To date, bone formation response induced by mechanical loading is well-established [3]. The molecular components that are responsible for increasing bone's in vivo adaptive response to loading, however, are not well understood. Recently, using microarray, we have shown that the PTN gene was increased 4-fold in C57BL/6J mice in response to mechanical loading (Figure 2). [15]. Based on the above findings and our data that PTN expression is increased in response to mechanical loading, we hypothesize that PTN play a role in mediating anabolic effects of mechanical loading on bone formation.

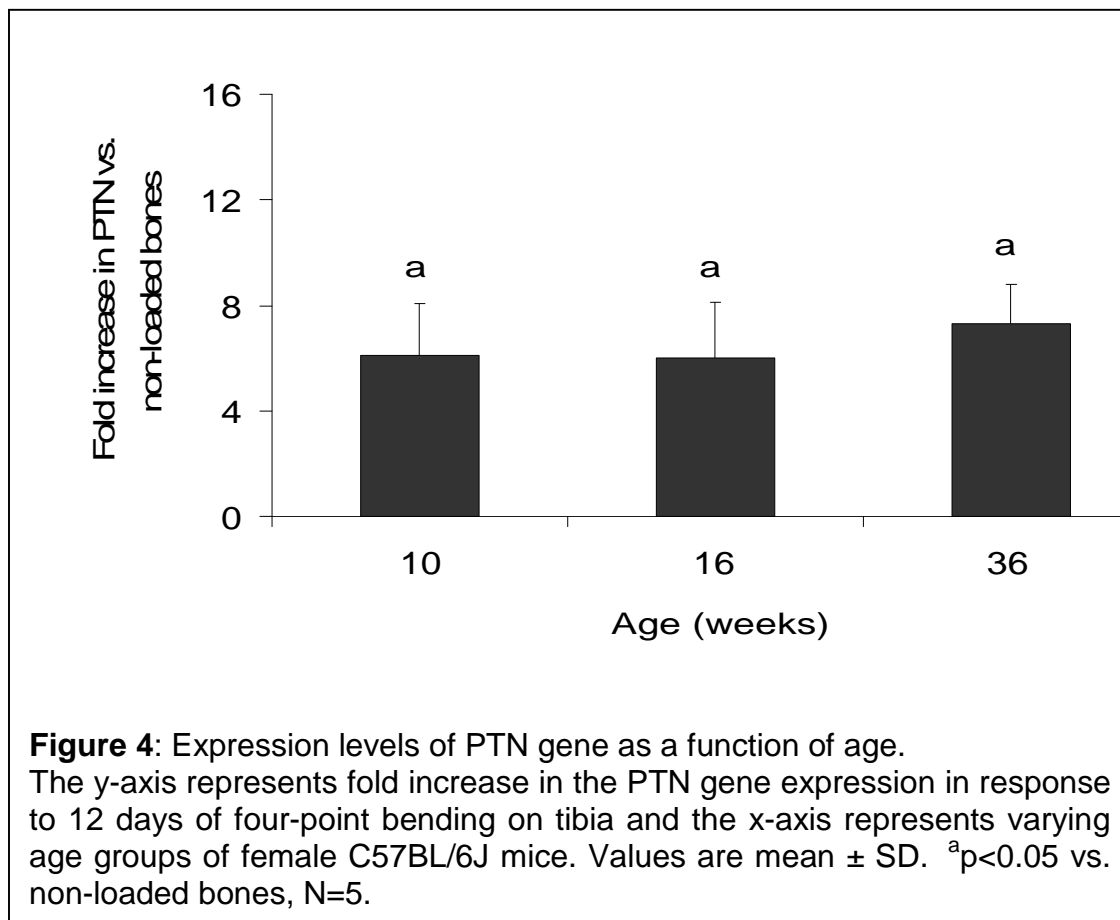
To confirm the microarray data we evaluated the expression levels of PTN by real time RT-PCR in 2 different experiments as described below. In the past, we have reported that the bone formation response to mechanical loading increases with a time-course of loading as evidenced from the expression levels of bone formation marker genes [1]. If the PTN gene is associated with bone formation response, one would



anticipate PTN expression to increase with an increase in the duration of loading. We performed four-point bending as a time-course (2, 4-, and 12-days) on 10-week female C57BL/6J mice. Expressions levels of PTN were measured by real time PCR using gene specific primers. The expression levels were calculated as fold change by comparing the

difference between loaded and non-loaded tibiae. Furthermore, the expression data are normalized with the housekeeping gene (b-actin and PPIA) to assure that the effect is not due to change in RNA quality or quantity. The results from this study show PTN gene expression was, in fact, increased by 2-, 3- and 6-fold at 2-, 4- and 12-days of loading (**Figure 3**). Our results support the finding that PTN is associated with an early response to mechanical loading, presumably with recruitment of osteoblast. In addition to duration of loading, we also performed 12 days four-point bending as a function of age (10-, 16- and 36 wk) in female C57BL/6J mice to determine their expression levels. The results from our study show PTN gene expression was in fact increased by 6-, 7- and 10-fold in 10-, 16- and 36-wk female C57BL/6J mice, respectively. Mechanical loading induced PTN expression was increased in all three age groups of mice (Figure-4).

Overall, these data demonstrate that PTN is a mechanoresponsive gene in the bones of mice. In contrast to this *in vivo* finding, an *in vitro* study using cultured human osteoblast cells have shown that PTN expression decreases in response to mechanical stimulation [25]. Although we cannot fully explain this discrepancy between our data and the *in vitro* study, possible explanations include: 1) osteoblast responsiveness to mechanical loading may differ *in vivo* vs. *in vitro*. 2) the type of mechanical loading and the amount of strain utilized were different between the two studies.



In the past, we have reported that four-point bending caused a 15% increase in bone mineral density (BMD) in B6 female mice. This increase in BMD in the C56BL/6J

mice is the result of an increased periosteal circumference (PC), which in turn leads to an increased cortical thickness (CTh). In the C3H/HeJ mice, in contrast to the B6 mice, there was no observed change in the BMD. However, there were changes in the PC and CTh although the magnitude of these changes was much less than those of C57BL/6J mice. Both B6 and C3H/HeJ mice showed similar changes in resorption at the endosteal circumference, while the magnitude of the periosteal response in the C3H/HeJ mice was much less, thus explaining the reason for no change in BMD in C3H/HeJ mice. This, then, raises a question of whether the greater magnitude of bone response to loading in C57BL/6J mice may be related to the expression levels of PTN. We therefore, using real time PCR, evaluated the expression levels PTN using a good responder (B6) and a poor responder (C3H) mouse strains. We found increases in PTN expression in response to four-point bending from 12 days loading. We found that the expression of PTN gene was greater in C57BL/6J (6-fold) mice than C3H/HeJ mice (2.95 fold). The fact that PTN was expressed to a greater extent in the good responder (B6) than in the poor responder (C3H) provides additional strong evidence that PTN is associated with the skeletal anabolic response to mechanical loading. Together, this finding and data from the above experiments, show that PTN mediates skeletal anabolic response to loading, though direct evidence is lacking.

To test the hypothesis that PTN is a mediator of skeletal anabolic response, we used targeted PTN knockout mice to evaluate PTN role in mechanical loading. PTN gene knock out (KO) mice (PTN-129 in B6 background) were generated by Dr. Thomas F. Vogt and the breeding pairs were kindly provided by Princeton University, NJ, USA, for our studies. PTN KO mice were crossed with wild type C57BL/6J mice (Jackson laboratory, Bar Harbor, ME) to generate the heterozygotes. These were crossed with each other to generate 25% homozygous PTN KO mice, 50% heterozygous and 25% littermate wild type mice. The body weights of PTN KO and control mice used for this study were  $18.18 \pm 0.97$  g and  $19.0 \pm 1.39$  g, respectively. The body weights of PTN KO and control mice were not statically different. All mice were housed under standard conditions of 14-hour light and 10-hour darkness, and had free access to food and water. The experimental protocols were in compliance with animal welfare regulations and approved by local IACUC.

At 3-weeks (wks) of age, DNA was extracted from tail of female mice, using a PUREGENE DNA purification kit (Gentra System, Inc., Minneapolis, MN) according to the manufacturer's protocol. Polymerase chain reaction (PCR) was performed to identify PTN KO mice from wild type or heterozygous mice. Primers specific for neomycin gene (forward 5' CTT GCT CCT GCC GAG AAA GTA T 3' and reverse 5' AGC AAT ATC ACG GGT AGC CAA C 3' with a PCR product of 369 bp), and primers specific for PTN gene (forward 5' TCT GAC TGT GGQA GAA TGG CAG T 3' and reverse 5' CTT CTT CCA GTT GCA AGG GAT C 3' with a PCR product of 147 bp) were used for genotyping. The following conditions were used to perform the PCR reaction: 95°C for 2 minutes; 35 cycles at 95°C for 40 sec, 57°C for 40 sec, 72°C for 40 sec; 70°C for 40 sec. The PCR products were run on a 1.5% agarose gel and the image taken with a ChemiImager 4400 (Alpha Innotech Corp., San Leandro, CA).

It is well established that the amount of mechanical strain exerted by a given load is largely dependent on the cross sectional area (moment of inertia) such that a mouse with a large cross-sectional area will experience lower mechanical strain and vice versa

for a small circumference. In order to assure that the difference in the bone responsiveness to loading between PTN KO mice and controls is not due to difference in the mechanical strain, we measured the bone size by pQCT at tibia mid diaphysis and calculated the mechanical strain using a mathematical model (Stephen C. Cowin: Bone Mechanics Handbook, 2nd edition, 2001, Chapter: Techniques from mechanics and imaging) for both sets of mice before the loading. We found that there was no significant difference in the bone size (4.55 mm vs. 4.69 mm,  $p=0.50$ ) as well as in the mechanical strain for 9N (6310 $\mu\epsilon$  vs. 6351  $\mu\epsilon$ ,  $p=0.91$ ) between the PTN KO mice and controls. Therefore, we chose the same mechanical load to induce bone formation in both sets of mice.

To determine if mechanical loading induced increase in PTN expression contributes to anabolic effects of mechanical loading, we performed four-point bending using a load (9N) at 2 Hz frequency for 36 cycles, once a day, for 12 days under inhalable anesthesia (5% Isoflurane and 95% oxygen). The right tibia was used for loading and the left tibia as internal non-loaded control. If PTN is an important mediator of skeletal anabolic response to loading, we anticipated PTN KO mice to show reduced anabolic effects of mechanical loading on bone. We found that there was, indeed, a small reduction in mechanical loaded response, measured by pQCT, in the PTN KO mice (**Figure 5, Table-1**); however, these changes were not statistically significant.

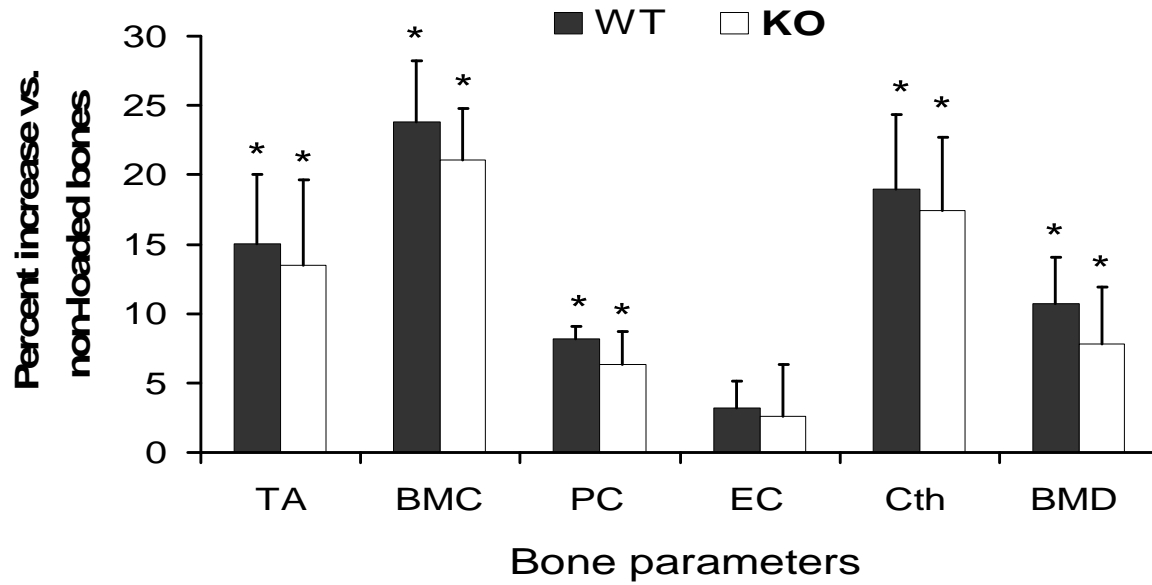


**Figure 5:** Changes in bone parameters in response to ML on 10-wk female PTN KO and control mice. Values are mean  $\pm$  SD. The y-axis represents percent increase in bone parameters in response to four-point bending on tibia and x-axis represent skeletal parameters. TA, Total area; BMC, bone mineral content; PC, periosteal circumference; EC, endosteal circumference; Cth, cortical thickness and BMD, bone mineral density. \* $p < 0.05$  vs. corresponding non-externally loaded tibiae,  $N=7$ .

**Table 1:** Changes in bone parameters in response to loading between PTN KO and control mice

Bone parameters	PTN KO		WT	
	Mean $\pm$ SD		Mean $\pm$ SD	
	Non-Loaded	Loaded	Non-Loaded	Loaded
Bone mineral content (mg/mm <sup>3</sup> )	1.16 $\pm$ 0.10	1.40 $\pm$ 0.07*	1.17 $\pm$ 0.14	1.44 $\pm$ 0.13*
Periosteal circumference (mm)	4.55 $\pm$ 0.23	4.83 $\pm$ 0.23*	4.69 $\pm$ 0.21	5.03 $\pm$ 0.26*
Endosteal circumference (mm)	3.36 $\pm$ 0.18	3.44 $\pm$ 0.20	3.53 $\pm$ 0.17	3.69 $\pm$ 0.24
Total vBMD (mg/cm <sup>3</sup> )	881 $\pm$ 52	949 $\pm$ 55*	839 $\pm$ 40	926 $\pm$ 27*
Cortical thickness (mm)	0.27 $\pm$ 0.01	0.31 $\pm$ 0.01*	0.25 $\pm$ 0.01	0.29 $\pm$ 0.01*

\* $p < 0.05$  vs. corresponding non-externally loaded tibiae,  $N=7$

We further extended our study to determine whether PTN has any influence on the cancellous or woven bone formation induced by mechanical loading between the two sets of mice. Of several conventional methods, though routinely used, none can analyze the architecture of the newly formed bone in response to loading to the extent that Micro-CT, a high resolution tomography image system (Scanco In vivo CT40, Switzerland). Routine calibration was performed once a week using a three-point calibration phantom corresponding to the density from air to cortical bone. Bones (PTN KO and controls) were immersed in 1X PBS to prevent them from drying and scanning was performed using 75Kv X-ray. A scout view was performed and 400 slices with a slice increment of 10.5 $\mu$ m were taken starting 3 mm away from the tibia-fibular junction and progressing towards proximal. After acquiring the radiographic data, images were reconstructed by using 2-D image software (as described by manufacturers). The areas of the loaded region of bone were outlined within the mid-shaft compartment. Every 10 sections were outlined, and the intermediate sections were interpolated with the contouring algorithm to create a volume of interest, followed by three dimensional analyses using Scanco in vivo software. Parameters such as bone volume/total volume (BV/TV %), trabecular number (Tb.N, mm<sup>-1</sup>), trabecular thickness (Tb.Th,  $\mu$ m), trabecular space (Tb.Sp,  $\mu$ m), were evaluated in the loaded and unloaded bones of both sets of mice. In Figure 6, we show the newly formed bone on the tibia lateral side of the loaded bones of both PTN KO and control mice. However, we did not observe any difference in the amount of newly formed bone in response to loading as measured from the above parameters. This finding suggests that the microarchitecture of newly formed bone is not influenced by the lack of PTN.

A potential explanation for the lack of significant differences between the control and KO mice is that PTN disruption could lead to increased expression of other molecules which share similar functional properties to compensate for the loss of PTN. For example, midkine belongs to the same family of HB-GAM as PTN that has been shown to have similar functional properties. Accordingly, we evaluated the expression levels of midkine between PTN KO and control mice. The result of this study showed significantly increase in the PTN KO mice when compared control mice in response to

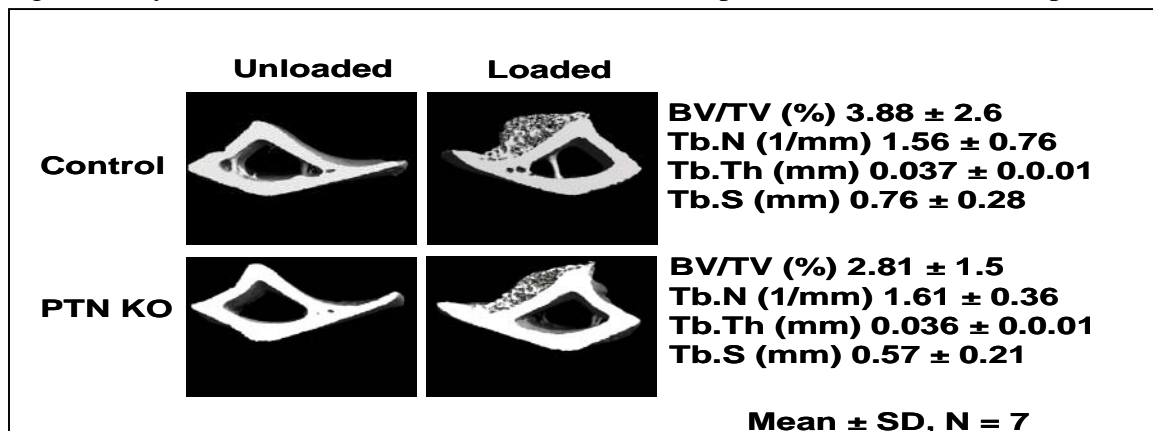


**Figure 6:** Micro-CT analysis of skeletal response to loading between PTN KO and control mice. Values are mean of 7 replicates per group. BV/TV, bone volume/total volume; Tb. N, trabecular number; Tb.Th, trabecular thickness and Tb.S, trabecular space.

loading (Figure 7). Similar to our findings, other studies have shown that mice with midkine or PTN deficiency have normal auditory response while mice with both gene deficits showed impaired auditory response [26]. A similar observation has been also reported with regard to fertility. Mice with disruption of both genes were infertile while mice with deficiency in either midkine or PTN gene were able to produce similar number of offspring [27]. Another study has shown that mice with absence of PTN gene resulted in normal skeletal growth and this is likely due to an increase in midkine expression as evident from their microarray data [28]. Overall, these findings suggest that factors of the same family are exhibiting overlapping function and thus, interfering with the activity of one factor may not necessarily lead to disruption of physiological activities such as bone formation response to loading. The issue of whether disruption of both PTN and midkine will exert a significant deficit in the skeletal anabolic response to mechanical loading compared to individual knockout requires further study.

## 2. Ras association domain family 1 isoform C (RASSF1C) and skeletal anabolic response to loading

In the background, we mentioned that using the QTL approach, we have identified several chromosomal regions that regulate bone adaptive response to loading in the B6XC3H intercross [13, 14]. Among these QTL regions, we have identified several receptor coupled G-protein as potential candidate genes. Previous studies have shown that activation of G-protein coupled receptor leads to the stimulation of Ras signaling, which then activates multiple downstream signaling pathways. These pathways, MAPK, PI3K and RAF, regulate diverse cellular function and, according to recent studies, also regulate the bone adaptive response to mechanical loading [29-32] [15]. Studies have also shown that these downstream signaling pathways, mediated by Ras, require the binding of a cytoplasmic protein called Ras associated protein (RASS) for activation. Several of these proteins have been identified. Among these, our group has shown that RASSF1C is

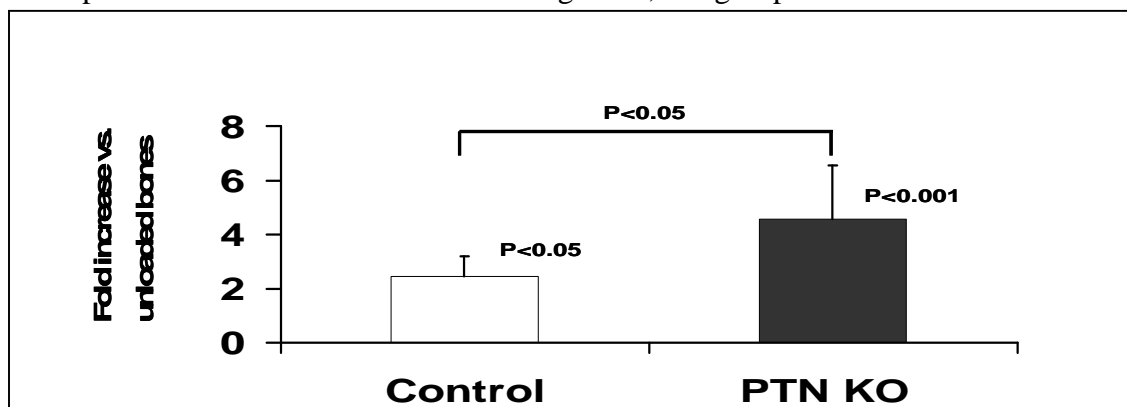
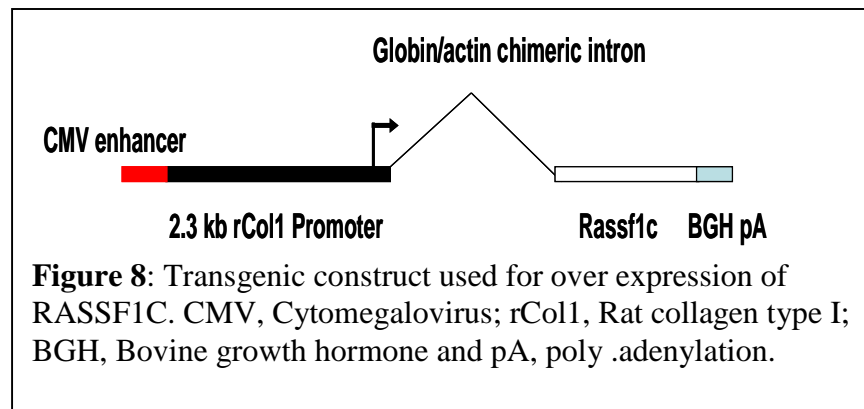


**Figure 7:** Increase in midkine expression in response to mechanical loading. RNA from unloaded and loaded bones of PTN KO and control mice were subjected to real time RT-PCR using midkine specific primers. Values are fold changes compared to corresponding unloaded bones, N=6.

expressed in many types of osteoblast cells and it regulates osteoblast cell proliferation [33]. Bone formation induced by mechanical loading results from an increase in osteoblast number which has been shown to involve the Ras-Raf-MAPK signaling pathways. We, therefore, predicted that RASSF1C could be involved in the molecular pathway for bone anabolic response to loading.

To test this prediction, we generated a transgenic mouse in which RASSF1C expression is driven by type-I collagen promoter. To generate this transgenic mouse line to over-express RASSF1C specifically in osteoblast cells, we amplified the complete coding

sequences of RASSF1C from our cDNA clone by PCR, tagged with a Flag synthetic epitope at its amino terminus, and cloned the Flag/RASSF1C fusion gene



into the place of LacZ in pWHERE expression vector (Invitrogen, San Diego, CA). We then inserted a heterozygous promoter containing CMV enhancer and the actin/globin intron. The entire transgene (9.3kb) in pWHERE/2.3 Col1A1/Flag/RASSF1C also contains two mH19 insulators derived from mouse Igf2 gene on either side of the Flag/RASSF1C transcription unit (Figure 8). Both insulators are expected to protect the integrated transcriptional Flag/RASSF1C unit from negative as well as positive influences from neighboring sequences. We expect that the transgene would be expressed in a position-independent manner in vivo.

To test the transgene expression in vitro, we transfected the pwhere/2.3Col1A1/Flag/RASSF1C plasmid into pre-osteoblast cells (MC3T3-E1) and African green monkey kidney cells (Vero 2-2) and measured the expression levels by western immunoblotting with antibody against Flag (Sigma). We found that the transgene was expressed as a 32-33 kDa protein by Western immunoblot analysis in both MC3T2-E1 and Vero 2-2 cells. After confirming the transgene expression in osteoblast cells, we sent out the DNA to the transgenic Core Facility at the University of Southern California (USC) for microinjection. DNA was microinjected into the pronuclei of fertilized zygotes from C57BL X CBA/CA mice. F1 generation mice were produced by breeding the transgenic founders with C57BL/6J mice. F2 and subsequent generations of transgenic mice were generated by breeding. All mice were housed under the standard conditions of 14-hour light and 10-hour darkness, and had free access to food and water. The experimental protocols were in compliance with animal welfare regulations and approved by local IACUC. At 3-weeks of age mice were genotyped to differentiate transgenic from wild type. The genotyping protocol are described earlier. Since the amount of strain produced by same load on bone is related to bone size, for example, mice with small circumference tend to receive higher mechanical strains and vice versa in the large circumference, we measured periosteal circumference (bone size) in both sets of mice.

This is to assure that the difference in the mechanical strain due variation in bone size is not be responsible for the difference in the skeletal anabolic response to loading between mice. But, we found no differences in the bone size between both groups and therefore, we applied the same mechanical load on both set of mice. A 9 N load was applied on the right tibia at 2Hz for 36 cycles, once per day for 12 days. The left tibia was used as internal control. After 48 hrs of last loading *in vivo* pQCT was performed and tibias were collected and frozen at -80°C for further study. The result from our study indicate that loading has caused a significant increase in the bone parameters in both control and RASSF1C mice. We also found that the changes in bone parameters induced by mechanical loading were higher ( $p<0.05$ ) in the RASSF1C transgenic mice when compared to control mice (Figure 9). These findings suggest involvement of Ras-Raf-MAPK signaling pathway in mechanical loading induced bone formation.

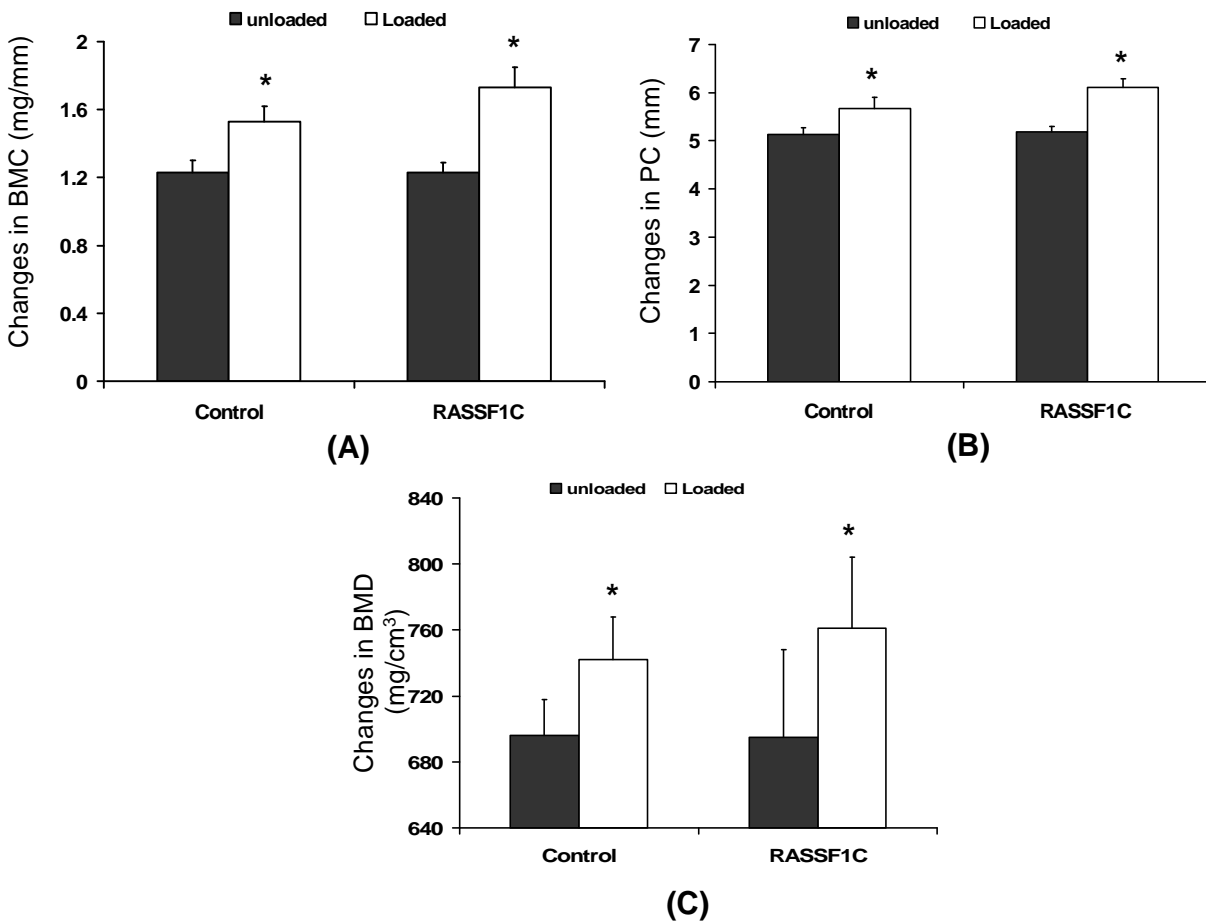


**Figure 9:** Changes in (A) BMC, (B) PC and (C) BMD in response to 12 days four-point bending between control and RASSF1C mice. The y-axis represents absolute change in bone parameters and x-axis represent mice group,  $N=5$ ,  $p<0.05$  vs. non-loaded bones.

### 3. Skeletal Anabolic response after cessation of loading

It is now well established that mechanical loading is an effective stimulator of bone formation. Thus, physical exercise has been used as a strategy to maintain BMD and prevent osteoporosis and fractures in men and women. Recent clinical studies in young and postmenopausal women who were subjected to treadmill exercise have shown that exercise induced benefits, such as increases in BMD and bone mineral content (BMC), are eventually lost if exercise is ceased completely [8]. Similar data was presented by Vuori et al. when reporting that unilateral leg presses done four times a week for 12 months increased bone mass (BMD) but returned to pre-training levels with only 3 months of retirement from exercise [34] [35]. Data from various independent studies in humans suggest that exercise induced bone mass benefits seem to be eroded by time. Animal studies using a rat model have shown that increased femoral BMD, gained through treadmill exercise, resulted in decreased bone formation rate after deconditioning [36] [37]. We, and others, have previously shown that C57BL/6J (B6), a low bone density mouse, responds well to mechanical loading. We have reported that mechanical loading by four-point bending causes a 10-15% increase in the tibia BMD in 10-week female B6 mice with compared to C3H/HeJ mice, after 2 weeks of loading [1]. We have extended this study, further, to examine how long this newly formed bone induced by four-point bending is maintained and their fate, after cessation of loading using the good responder, B6 mouse.

To investigate this, female B6 were purchased from the Jackson Laboratory (Bar Harbor, Me). All mice were housed under the standard conditions of 14-hour light and 10-hour darkness, and had free access to food and water. The experimental protocols were in compliance with animal welfare regulations and approved by local IACUC.

At 10 weeks of age the mice were subjected to mechanical loading using the four-point bending device as described previously [1]. The loading protocol consists of a  $9.0 \pm 0.2$  Newton (N) force at a frequency of 2 Hz for 36 cycles performed daily under inhaleable anesthesia (5% Halothane and 95% oxygen). The loading procedure was repeated for 6 days/week with 1 day of rest for 2 weeks. Mice were euthanized 48 hours after the last loading and tissue samples were collected and stored at  $-20^{\circ}\text{C}$  for further study.

After 12 days of loading, we used pQCT (Stratec XCT 960M, Norland Medical System, Ft. Atkinson, WI) to measure loading-induced changes in the bone parameters in loaded and non-loaded tibiae, as described previously [1]. *In-vivo* pQCT measurements were performed at immediately, 2, 4, 6, 8, and 12 weeks after the last loading regimen. Data are presented as Mean  $\pm$  Standard error (SE). Regression analysis, and standard t-test were used to compare differences from loading between the time points using the percentage obtained from loaded vs. non-loaded bones. We used STATISTICA software (StatSoft, Inc version 7.1, 2005) for our analysis and the results were considered significantly different at  $p < 0.05$ .

Two weeks of four-point bending on the right tibiae when compared to left tibiae resulted in a significant increase in bone parameters, such as BMC, periosteal circumference (PC) and BMD, as shown in Figure 10. The mechanism through which bending induces an increase in BMD is by increasing PC and cortical thickness (Cth). Our present findings are consistent with our previous study [1]. However, we also found, that this increase in bone size and BMD did not continue over time after termination of

loading. This is because BMD increased with age in non-loaded but not in the loaded tibia and as such the difference in BMD between loaded and non-loaded tibia was lost 4-wks after cessation of loading (Figure 10). This suggests that bone anabolic response does not continue once loading is terminated.

In this study, we found that the loading induced a 15% and 40% increase in BMD and bone size (total area), respectively, immediately after 2 weeks four-point bending (**Figure 11**). However, cessation of loading resulted in a continuous loss of both BMD and bone size (Total area). We found that the loading induced changes in volumetric BMD returned to normal at 12 weeks with a half life of 6-weeks. The change in total area (bone size) declined with a half life of 8.5 weeks and was still significantly elevated at 12 weeks. Thus, the decline in elevated TA proceeded at a much slower pace than the loading induced increase in vBMD.

In our pQCT analysis of bone parameters, using the lower threshold (180-730) we found that the magnitude of increase in PC was  $18\% \pm 7.0$  after the last loading and was very significant when compared with  $7.2\% \pm 1.7$  using the higher threshold (730-730). This is due to an increase in the low density bone mineralized at the periosteal surface. This is most prevalent at 0-time point, as seen by the red color using the pQCT threshold indicator (Figure 12). Consequently, we found a significant increase in bone size at 0-time point, accompanied by an increase in BMD. Over time, we found that PC increased with age in the non-loaded but not loaded tibia. As a result, the magnitude of difference between loaded and non-loaded tibia decreased with time after cessation of loading and subsequently we found no difference in the periosteal circumference of loaded tibiae between lower (PC,  $9.13\% \pm 3.9$ ) and higher threshold (PC,  $9.8 \pm 1.2$ ). These data suggest that the newly formed bone undergoes remodeling at the periosteal site over time which leads to a reduction in bone size in order to accommodate the loading induced changes in bone shape. During this remodeling process, we found that the rate of loss in gained bone size (total area) after cessation of loading was 10% every 2 weeks for 8 weeks. These data, together, suggest that the positive effects of mechanical loading on bone size were maintained for several weeks after cessation of loading.

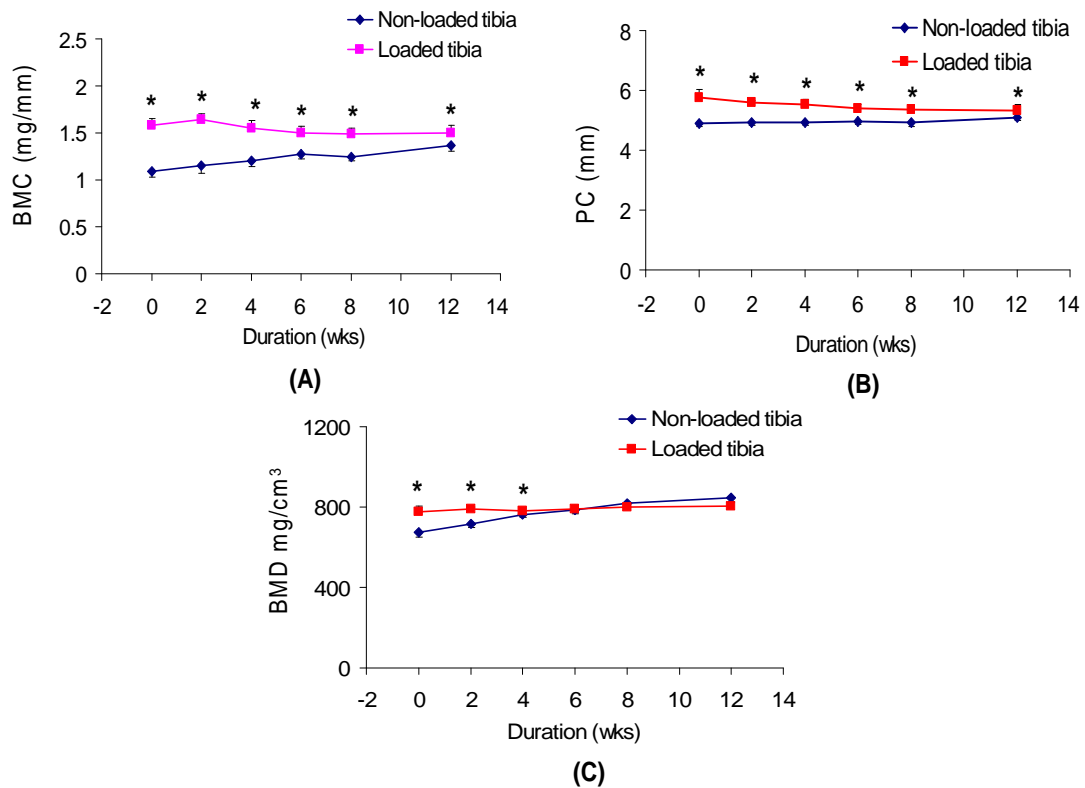


**Figure 10:** Changes in the bone parameters measured by *in vivo* pQCT at different time points after 12 days of four-point bending on 10 week female B6 mice. (A) Bone mineral content (BMC), (B) Periosteal circumference (PC) and (C) Bone mineral density (BMD). Values are mean  $\pm$  SD, \* $p < 0.05$  vs. non-loaded tibiae, N=5

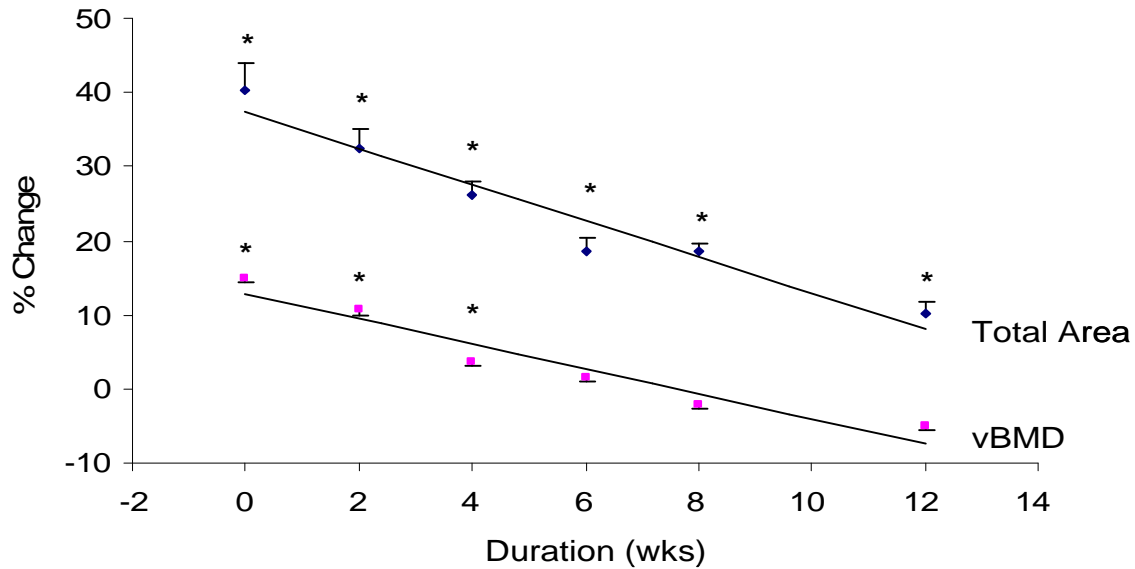


**Figure 11:** Percent changes in the total Area and BMD after termination of loading at different time points in 10 week female B6 mice. The y-axis represents percent change and the x-axis corresponds to duration (weeks). TA, Total area and vBMD, total volumetric bone mineral density, values are given as mean  $\pm$  SE, \* $p < 0.05$  vs. non-loaded tibiae, N=5.

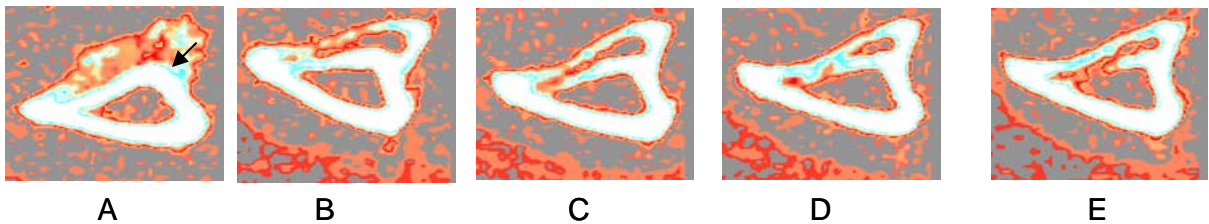
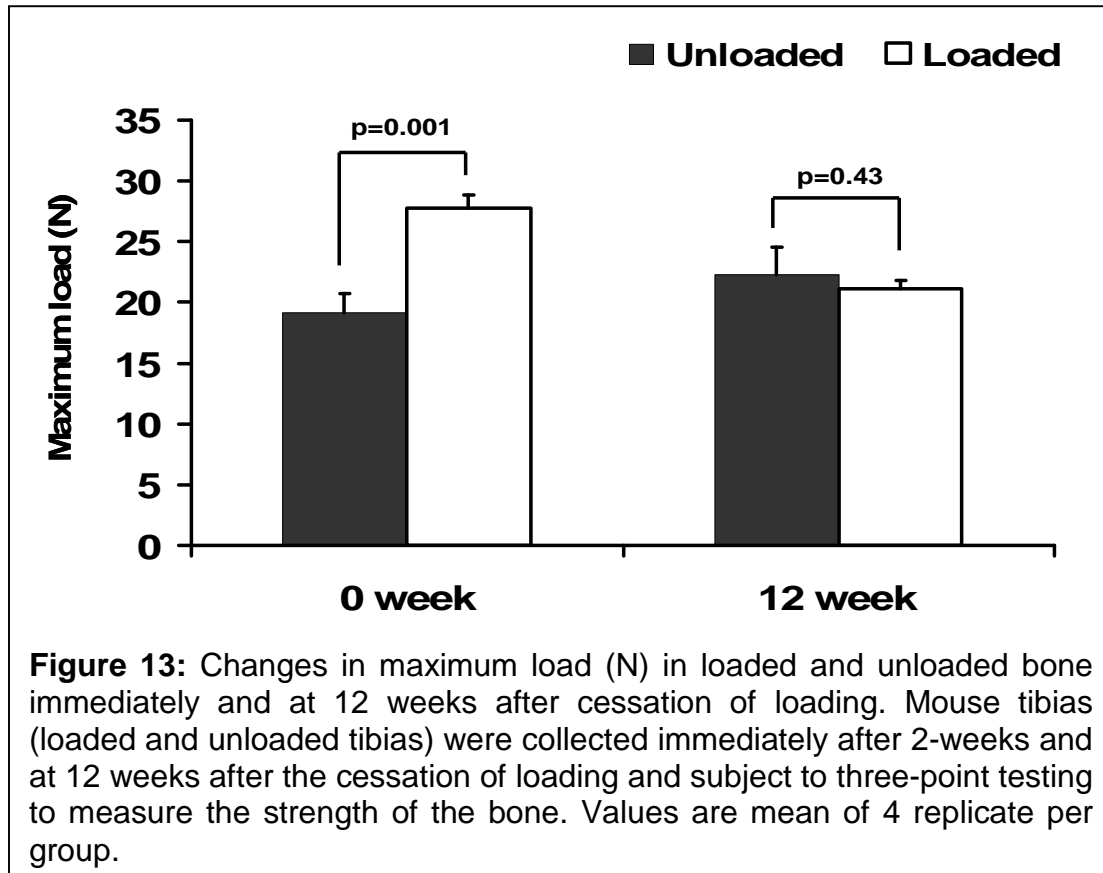


**Figure 12:** Cross sectional area of the loaded tibia. This figure shows the newly formed bone at the periosteal site in response to 2-weeks loading and their fate over time after cessation of loading. A, 0- week; B, 2-weeks; C, 4-weeks; D, 6-weeks and E, 8-weeks. The arrow corresponds to newly formed bone and the white color represents cortical bone.

In this study, we observed that the accommodation of this newly formed bone, gained through loading over time altered the shape of bone compared with non-loaded tibiae as seen from our pQCT cross-sectional slice. Since studies have shown that changes in bone size and BMD parameters lead to an increase in bone mechanical properties, one would expect a difference in these properties of bone immediately and 12 weeks, after termination of loading. To test this difference we used a three-point bending device (Model 8840; Instron, Canton, MA, USA). The frozen tibiae were thawed at 4°C. The tibiae were placed on two immovable supports which were 12 mm apart. An initial 1.0N was applied on the tibiae to prevent rotation of the bone and they were centrally loaded at a constant rate (10mm/minute) until fracture. Load displacement curves were

used to calculate maximum load phenotype. The result from our study show a significant increase in the bone strength immediately after 2- weeks of loading in the loaded bones compared to non-loaded bones, as evident from maximum load data ( $-19.14 \text{ N} \pm 1.57$  vs.  $-24.74 \text{ N} \pm 1.14$ ,  $p < 0.001$ ,  $n=4$ ). However, this increase in bone strength was lost at 12 weeks. We found that there was no difference in the maximum load phenotype between the loaded and non-loaded bones ( $-22.26 \pm 2.28$  vs.  $21.07 \pm 0.70$ ,  $p=0.43$ ,  $n=4$ ) at 12 weeks after cessation of loading (Figure 13). This is consistent with the changes in bone parameters. Together, the findings of our study indicate that the external loading-induced



increases in bone are lost over a period of time but at a much slower pace than the induction of the increases; 2) While a single burst of external loading provides increased bone mass temporarily, periodic loading may be necessary to maintain long term bone strength.

#### 4. Generation of IGF-I conditional Knock out mice

It is now well known from several studies that IGF-I produced by osteoblast cells is an important regulator of both prenatal and postnatal skeletal growth [38-40]. Since local IGF-I is an important regulator of bone formation and mechanical loading is a key regulator of bone formation, we and others predict that local IGF-I is essential for bone formation response to loading. To date there is abundant evidence that demonstrates IGF-I as a potential mediator of the anabolic effects of mechanical loading on bone formation. These include: 1) Rapid induction of IGF-I mRNA levels have been shown to occur in response to mechanical stimulation in bone cells *in vitro* and bones *in vivo* [31, 41, 42].

2) IGF-I treatment induced bone formation in GH-deficient normally loaded rats but not in unloaded rats, thus suggesting that skeletal unloading induces resistance to IGF-I [43, 44]. 3) Transgenic mice with elevated IGF-I expression in osteoblast exhibit increased bone formation when compared to control mice [45]. In addition to these studies, our genome-wide microarray data also revealed that IGF-I expression was increased by 2-fold ( $p < 0.003$ ) after the mechanical loading in a good

responder C57BL/6J mouse. Furthermore, we also found an increase in the expression levels of several other genes that are directly or indirectly, associated and regulated by IGF-I [15]. If IGF-I gene is associated with bone formation response induced by mechanical loading, one might expect IGF-I expression to also be increased across the various ages as we previously reported that skeletal anabolic response to loading increased across these ages. Accordingly, we performed 12 days loading using four-point bending device as a function of age (16- and 36-wk) in female C57BL/6J mice. The results from our study show IGF-I gene expression was in fact increased by 1.6 to 2.1-fold ( $N=5$ ,  $p < 0.05$ ) in 16- and 36-week female C57BL/6J mice, respectively in the loaded bone when compared to non-loaded bones (Figure 14). These findings suggest that 1) anabolic effects of mechanical loading on bone formation are mediated by IGF-I and 2) IGF-I is inducible to mechanical loading. Although, these findings provide indirect evidence for the role of IGF-I in mediating the bone anabolic response to loading, *the cause and effect relationship between loading-induced increases in IGF-I expression and*

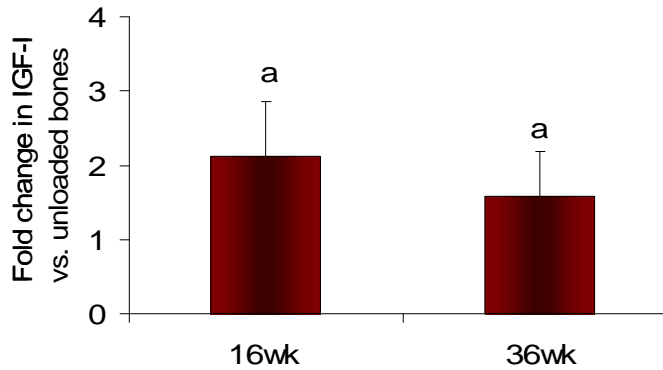
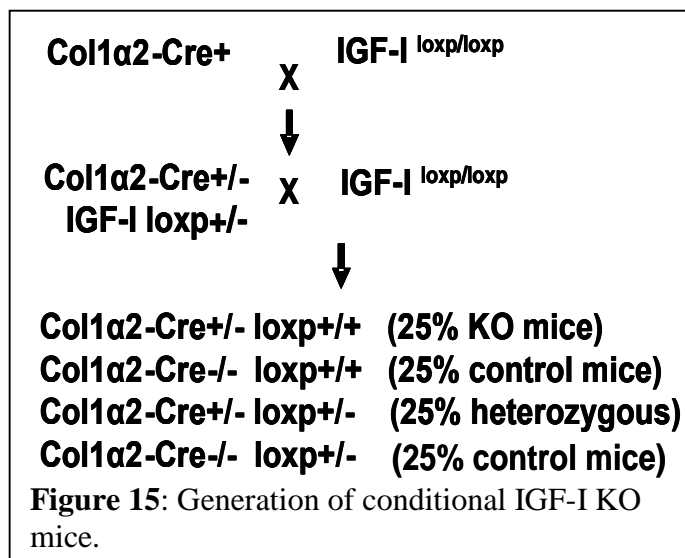


**Figure 14:** Increase in the mRNA levels of IGF-I gene after 12 days of four-point bending as a function of age in female B6 mice. <sup>a</sup> $p < 0.05$  vs. unloaded bones.



*skeletal anabolic changes is lacking.* To test for a role for locally produced IGF-I in mediating the effects of mechanical strain, we propose to generate IGF-I conditional KO mice. Our group recently developed a loxP IGF-I mouse in which exon 4 of the IGF-I gene is flanked by the loxP gene (IGF-I<sup>lox/lox</sup>). Breeding pairs of transgenic mice in which Cre recombinase driven by the procollagen, type-I  $\alpha$ II gene (Col1a2-Cre) are available in our laboratory. At present,

we are crossing this loxp IGF-I mice with Cre mice to generate conditional IGF-I KO mice and littermate controls. A schematic representation of the breeding is shown in Figure 15.

### Conclusions

1. Disruption of PTN gene alone is not sufficient to impair skeletal anabolic response to loading in mice.
2. Disruption of both PTN and midkine may be necessary to fully evaluate the role of heparin binding growth associated molecules in mediating anabolic effects of mechanical loading in bone.
3. Rass1FC, an upstream signaling molecule, is associated in mediating skeletal anabolic response to loading.
4. Our study shows that the external loading induced changes in bone are lost over a period of time and not rapidly after cessation of loading.
5. A single burst of external loading provides increased bone mass temporarily, periodic loading may be necessary to maintain long term bone strength.

### Reported outcomes

1. Poster presentation at 29<sup>th</sup> meeting of ASBMR for the paper entitled “The Increased vBMD and Bone Area due to Mechanical Loading Gradually Decreased Following Cessation of Loading 2007.
2. Oral presentation at 30<sup>th</sup> meeting of ASBMR for the paper entitled “Anabolic Response to Skeletal Loading in Mice with Targeted Disruption of Pleiotrophin Gene, 2008.
3. Kesavan C and Subburaman Mohan. Anabolic Response to Skeletal Loading in Mice with Targeted Disruption of the Pleiotrophin gene, *BMC Research Notes*, Dec1;1:124, 2008. Kesavan C and Subburaman Mohan. Increased vBMD and Bone Area due to Mechanical Loading Gradually Decreased Following Cessation of Loading on 10 week C57BL/6J Mice. Manuscript writing is in progress



**References:**

1. Kesavan C, Mohan S, Oberholtzer S, Wergedal JE, Baylink DJ: **Mechanical loading-induced gene expression and BMD changes are different in two inbred mouse strains.** *J Appl Physiol* 2005, **99**(5):1951-1957.
2. Kodama Y, Umemura Y, Nagasawa S, Beamer WG, Donahue LR, Rosen CR, Baylink DJ, Farley JR: **Exercise and mechanical loading increase periosteal bone formation and whole bone strength in C57BL/6J mice but not in C3H/HeJ mice.** *Calcif Tissue Int* 2000, **66**(4):298-306.
3. Bailey DA, McCulloch RG: **Bone tissue and physical activity.** *Can J Sport Sci* 1990, **15**(4):229-239.
4. Turner CH, Akhter MP, Raab DM, Kimmel DB, Recker RR: **A noninvasive, in vivo model for studying strain adaptive bone modeling.** *Bone* 1991, **12**(2):73-79.
5. Bikle DD, Halloran BP, Morey-Holton E: **Impact of skeletal unloading on bone formation: role of systemic and local factors.** *Acta Astronaut* 1994, **33**:119-129.
6. Bikle DD, Sakata T, Halloran BP: **The impact of skeletal unloading on bone formation.** *Gravit Space Biol Bull* 2003, **16**(2):45-54.
7. Kodama Y, Dimai HP, Wergedal J, Sheng M, Malpe R, Kutilek S, Beamer W, Donahue LR, Rosen C, Baylink DJ *et al*: **Cortical tibial bone volume in two strains of mice: effects of sciatic neurectomy and genetic regulation of bone response to mechanical loading.** *Bone* 1999, **25**(2):183-190.
8. Dalsky GP, Stocke KS, Ehsani AA, Slatopolsky E, Lee WC, Birge SJ, Jr.: **Weight-bearing exercise training and lumbar bone mineral content in postmenopausal women.** *Ann Intern Med* 1988, **108**(6):824-828.
9. Dhamrait SS, James L, Brull DJ, Myerson S, Hawe E, Pennell DJ, World M, Humphries SE, Haddad F, Montgomery HE: **Cortical bone resorption during exercise is interleukin-6 genotype-dependent.** *Eur J Appl Physiol* 2003, **89**(1):21-25.
10. Snow-Harter C, Bouxsein ML, Lewis BT, Carter DR, Marcus R: **Effects of resistance and endurance exercise on bone mineral status of young women: a randomized exercise intervention trial.** *J Bone Miner Res* 1992, **7**(7):761-769.
11. Tajima O, Ashizawa N, Ishii T, Amagai H, Mashimo T, Liu LJ, Saitoh S, Tokuyama K, Suzuki M: **Interaction of the effects between vitamin D receptor polymorphism and exercise training on bone metabolism.** *J Appl Physiol* 2000, **88**(4):1271-1276.
12. Akhter MP, Cullen DM, Pedersen EA, Kimmel DB, Recker RR: **Bone response to in vivo mechanical loading in two breeds of mice.** *Calcif Tissue Int* 1998, **63**(5):442-449.
13. Kesavan C, Mohan S, Srivastava AK, Kapoor S, Wergedal JE, Yu H, Baylink DJ: **Identification of genetic loci that regulate bone adaptive response to mechanical loading in C57BL/6J and C3H/HeJ mice intercross.** *Bone* 2006, **39**(3):634-643.
14. Kesavan C, Baylink DJ, Kapoor S, Mohan S: **Novel loci regulating bone anabolic response to loading: expression QTL analysis in C57BL/6JXC3H/HeJ mice cross.** *Bone* 2007, **41**(2):223-230.

15. Xing W, Baylink D, Kesavan C, Hu Y, Kapoor S, Chadwick RB, Mohan S: **Global gene expression analysis in the bones reveals involvement of several novel genes and pathways in mediating an anabolic response of mechanical loading in mice.** *J Cell Biochem* 2005, **96**(5):1049-1060.
16. Kale AA, Di Cesare PE: **Osteoinductive agents. Basic science and clinical applications.** *Am J Orthop* 1995, **24**(10):752-761.
17. Elima K: **Osteoinductive proteins.** *Ann Med* 1993, **25**(4):395-402.
18. Gieffers C, Engelhardt W, Brenzel G, Matsuishi T, Frey J: **Receptor binding of osteoblast-specific factor 1 (OSF-1/HB-GAM) to human osteosarcoma cells promotes cell attachment.** *Eur J Cell Biol* 1993, **62**(2):352-361.
19. Petersen W, Rafii M: **Immunolocalization of the angiogenetic factor pleiotrophin (PTN) in the growth plate of mice.** *Arch Orthop Trauma Surg* 2001, **121**(7):414-416.
20. Amet LE, Lauri SE, Hienola A, Croll SD, Lu Y, Levorse JM, Prabhakaran B, Taira T, Rauvala H, Vogt TF: **Enhanced hippocampal long-term potentiation in mice lacking heparin-binding growth-associated molecule.** *Mol Cell Neurosci* 2001, **17**(6):1014-1024.
21. Imai S, Kaksonen M, Raulo E, Kinnunen T, Fages C, Meng X, Lakso M, Rauvala H: **Osteoblast recruitment and bone formation enhanced by cell matrix-associated heparin-binding growth-associated molecule (HB-GAM).** *J Cell Biol* 1998, **143**(4):1113-1128.
22. Yang X, Tare RS, Partridge KA, Roach HI, Clarke NM, Howdle SM, Shakesheff KM, Oreffo RO: **Induction of human osteoprogenitor chemotaxis, proliferation, differentiation, and bone formation by osteoblast stimulating factor-1/pleiotrophin: osteoconductive biomimetic scaffolds for tissue engineering.** *J Bone Miner Res* 2003, **18**(1):47-57.
23. Tare RS, Oreffo RO, Clarke NM, Roach HI: **Pleiotrophin/Osteoblast-stimulating factor 1: dissecting its diverse functions in bone formation.** *J Bone Miner Res* 2002, **17**(11):2009-2020.
24. Masuda H, Tsujimura A, Yoshioka M, Arai Y, Kuboki Y, Mukai T, Nakamura T, Tsuji H, Nakagawa M, Hashimoto-Gotoh T: **Bone mass loss due to estrogen deficiency is compensated in transgenic mice overexpressing human osteoblast stimulating factor-1.** *Biochem Biophys Res Commun* 1997, **238**(2):528-533.
25. Liedert A, Augat P, Ignatius A, Hausser HJ, Claes L: **Mechanical regulation of HB-GAM expression in bone cells.** *Biochem Biophys Res Commun* 2004, **319**(3):951-958.
26. Zou P, Muramatsu H, Sone M, Hayashi H, Nakashima T, Muramatsu T: **Mice doubly deficient in the midkine and pleiotrophin genes exhibit deficits in the expression of beta-tectorin gene and in auditory response.** *Lab Invest* 2006, **86**(7):645-653.
27. Muramatsu H, Zou P, Kurosawa N, Ichihara-Tanaka K, Maruyama K, Inoh K, Sakai T, Chen L, Sato M, Muramatsu T: **Female infertility in mice deficient in midkine and pleiotrophin, which form a distinct family of growth factors.** *Genes Cells* 2006, **11**(12):1405-1417.

28. Lehmann W, Schinke T, Schilling AF, Catala-Lehnen P, Gebauer M, Pogoda P, Gerstenfeld LC, Rueger JM, Einhorn TA, Amling M: **Absence of mouse pleiotrophin does not affect bone formation in vivo.** *Bone* 2004, **35**(6):1247-1255.
29. Matsuda N, Morita N, Matsuda K, Watanabe M: **Proliferation and differentiation of human osteoblastic cells associated with differential activation of MAP kinases in response to epidermal growth factor, hypoxia, and mechanical stress in vitro.** *Biochem Biophys Res Commun* 1998, **249**(2):350-354.
30. Peverali FA, Basdra EK, Papavassiliou AG: **Stretch-mediated activation of selective MAPK subtypes and potentiation of AP-1 binding in human osteoblastic cells.** *Mol Med* 2001, **7**(1):68-78.
31. Lau KH, Kapur S, Kesavan C, Baylink DJ: **Up-regulation of the Wnt, estrogen receptor, insulin-like growth factor-I, and bone morphogenetic protein pathways in C57BL/6J osteoblasts as opposed to C3H/HeJ osteoblasts in part contributes to the differential anabolic response to fluid shear.** *J Biol Chem* 2006, **281**(14):9576-9588.
32. Danciu TE, Adam RM, Naruse K, Freeman MR, Hauschka PV: **Calcium regulates the PI3K-Akt pathway in stretched osteoblasts.** *FEBS Lett* 2003, **536**(1-3):193-197.
33. Amaar YG, Baylink DJ, Mohan S: **Ras-association domain family 1 protein, RASSF1C, is an IGFBP-5 binding partner and a potential regulator of osteoblast cell proliferation.** *J Bone Miner Res* 2005, **20**(8):1430-1439.
34. Vuori I, Heinonen A, Sievanen H, Kannus P, Pasanen M, Oja P: **Effects of unilateral strength training and detraining on bone mineral density and content in young women: a study of mechanical loading and unloading on human bones.** *Calcif Tissue Int* 1994, **55**(1):59-67.
35. Karlsson MK: **The skeleton in a long-term perspective--are exercise induced benefits eroded by time?** *J Musculoskelet Neuronal Interact* 2003, **3**(4):348-351; discussion 356.
36. Iwamoto J, Yeh JK, Aloia JF: **Effect of deconditioning on cortical and cancellous bone growth in the exercise trained young rats.** *J Bone Miner Res* 2000, **15**(9):1842-1849.
37. Pajamaki I, Kannus P, Vuohelainen T, Sievanen H, Tuukkanen J, Jarvinen M, Jarvinen TL: **The bone gain induced by exercise in puberty is not preserved through a virtually life-long deconditioning: a randomized controlled experimental study in male rats.** *J Bone Miner Res* 2003, **18**(3):544-552.
38. Baylink DJ, Finkelman RD, Mohan S: **Growth factors to stimulate bone formation.** *J Bone Miner Res* 1993, **8 Suppl 2**:S565-572.
39. Mohan S, Richman C, Guo R, Amaar Y, Donahue LR, Wergedal J, Baylink DJ: **Insulin-like growth factor regulates peak bone mineral density in mice by both growth hormone-dependent and -independent mechanisms.** *Endocrinology* 2003, **144**(3):929-936.
40. Govoni KE, Wergedal JE, Florin L, Angel P, Baylink DJ, Mohan S: **Conditional deletion of insulin-like growth factor-I in collagen type 1alpha2-expressing**

- cells results in postnatal lethality and a dramatic reduction in bone accretion.** *Endocrinology* 2007, **148**(12):5706-5715.
41. Reijnders CM, Bravenboer N, Tromp AM, Blankenstein MA, Lips P: **Effect of mechanical loading on insulin-like growth factor-I gene expression in rat tibia.** *J Endocrinol* 2007, **192**(1):131-140.
  42. Triplett JW, O'Riley R, Tekulve K, Norvell SM, Pavalko FM: **Mechanical loading by fluid shear stress enhances IGF-1 receptor signaling in osteoblasts in a PKCzeta-dependent manner.** *Mol Cell Biomech* 2007, **4**(1):13-25.
  43. Sakata T, Halloran BP, Elalieh HZ, Munson SJ, Rudner L, Venton L, Ginzinger D, Rosen CJ, Bikle DD: **Skeletal unloading induces resistance to insulin-like growth factor I on bone formation.** *Bone* 2003, **32**(6):669-680.
  44. Sakata T, Wang Y, Halloran BP, Elalieh HZ, Cao J, Bikle DD: **Skeletal unloading induces resistance to insulin-like growth factor-I (IGF-I) by inhibiting activation of the IGF-I signaling pathways.** *J Bone Miner Res* 2004, **19**(3):436-446.
  45. Zhao G, Monier-Faugere MC, Langub MC, Geng Z, Nakayama T, Pike JW, Chernausek SD, Rosen CJ, Donahue LR, Malluche HH *et al*: **Targeted overexpression of insulin-like growth factor I to osteoblasts of transgenic mice: increased trabecular bone volume without increased osteoblast proliferation.** *Endocrinology* 2000, **141**(7):2674-2682.

## Progress Report for the Period of 2009- 2010

### Introduction:

Osteoporosis is a disease that is characterized by low bone density and poor bone quality: bone becomes more fragile and the risk of fracture is greatly increased, especially in hip, spine and wrists. To date, the annual economic burden of osteoporosis is \$20 billion and is expected to reach \$62 billion by the year 2020 (1). These numbers exceed the cost of congestive heart failure, asthma and breast cancer combined. Thus, one of the major goals of our current research is to reduce the incidence of osteoporosis.

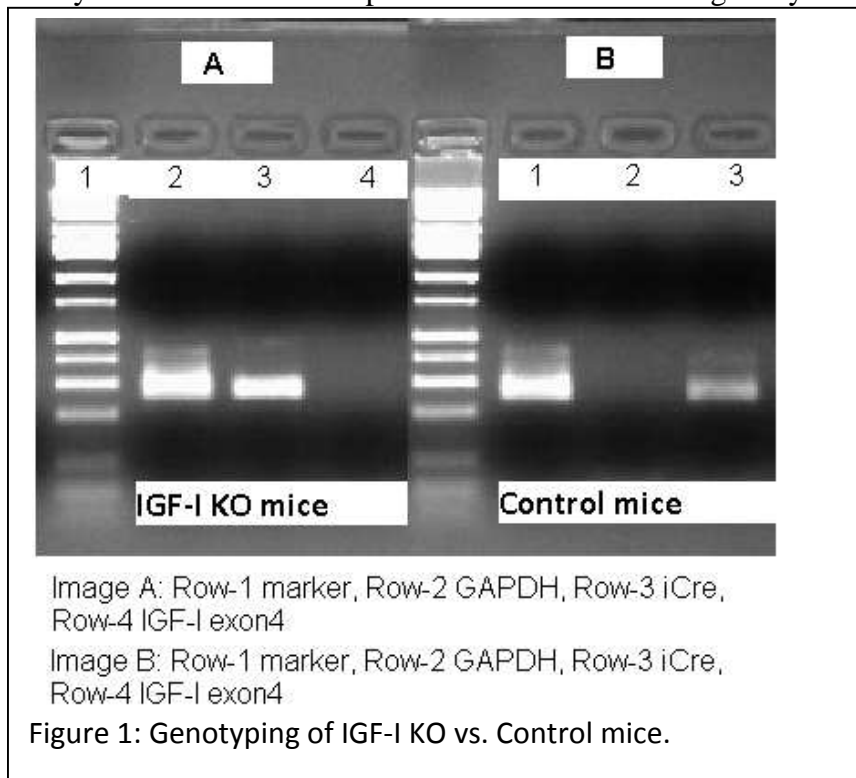
One approach to prevent osteoporosis is to increase new bone formation. At present, physical exercise has been used as one of the strategies to maintain bone mass and prevent bone loss in humans. Numerous studies using different loading models in humans and animals have demonstrated that loading stimulates bone formation while unloading decreases bone formation (2-5). The mechanism through which mechanical loading increases bone formation is mechanical stimulation which activates signaling receptors, which in turn activates a cascade of intra-cellular signaling pathways. This, in turn, activates several cellular processes leading to an increase in bone formation. To date, a series of cellular and molecular events, particularly the intra- and intercellular signaling pathways, and the molecular components that regulate this pathway by responding to mechanical stimulation, have been investigated using *in vitro* models (6-12). The data generated from *in vitro* models, although informative, is limited by the fact that most of the data were obtained from homogenous osteoblast cells in cell cultures. These models lack the vital communication between various types of cells, such as osteocytes, osteoblast and osteoprogenitors cells, which have been shown to respond to ML. Thus, the molecular components that respond to ML *in vivo* have not been fully understood. Once these components have been identified, their role in regulating bone formation will become more clear. This, in turn, leads to a better understanding of the complex series of cellular and molecular events involved in bone formation, thus providing strategic pharmacological intervention to enhance or maximize the osteogenic effects of exercise. Our technical objectives for the past one year are as follows:

#### Technical objectives

- 1) Continue to generate IGF-I Knockout and control mice and evaluate skeletal anabolic response to four-point bending.
- 2) Continue the ongoing studies on the role of leptin receptor signaling pathway in mechanical strain response in osteoblasts.
- 3) Evaluation of the role of formin-2 in mediating mechanical loading response on the skeleton.
- 4) Evaluate if 14104M gene is a mechanosensitive gene.
- 5) Evaluate the influence of mechanical strain on bone regeneration.
- 6) Continue *in vitro* phosphorylation studies to identify signaling proteins that are activated by mechanical strain in KO and control mice.
- 7) Continue data analysis and prepare manuscripts for submission to peer review journals for publication.
- 8) Prepare final progress report for submission to TATRC.

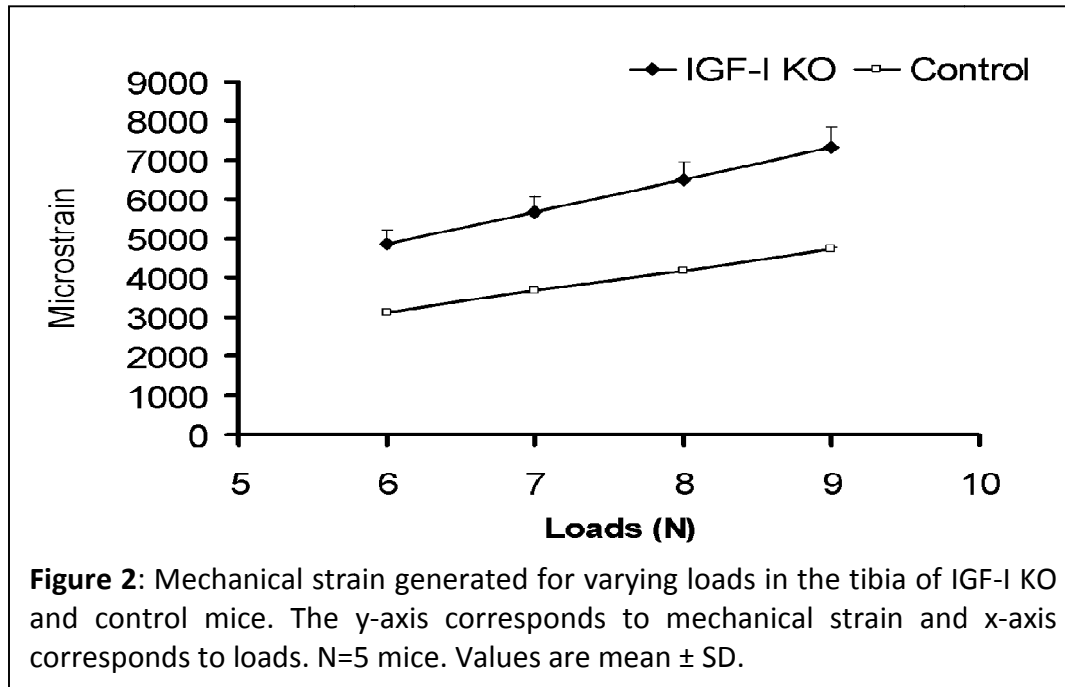
**Technical objective 1: Continue to generate IGF-I Knock out and control mice and evaluate skeletal anabolic response to four-point bending.**

During the past one year, we crossed Cre- recombinase transgenic mice [Cre gene was driven by the procollagen, type IaII gene (Col1a2-Cre)] with loxp mice in which exon 4 of the IGF-I gene is flanked by the *loxP* gene to generate Cre<sup>+</sup> loxp<sup>+/+</sup> (homozygous conditional IGF-I KO), and Cre negative loxp (control) mice for our studies proposed in technical objective 1. At three weeks of age, tail snips were collected from mice and DNA was extracted using a PUREGENE DNA Purification Kit (Gentra Systems, Inc., Minneapolis, MN) according to the manufacturer's protocol. Polymerase chain reaction (PCR) was performed to identify the different genotypes (homozygous IGF-I KO, heterozygous IGF-I KO and control mice). We used Cre-recombinase primer (F- TTA GCA CCA CGG CAG CAG GAG GTT and R-CAG GCC AGA TCT CCT GTG CAG CAT) and loxp primer (Primer 1, AGT GAT AGG TCA CAA AGT TCC; Primer 2, AAA CCA CAC TGC TCG ACA TTG and Primer 3, CAC TAA GGA GTC TGT ATT TGG ACC) for the genotyping. The following optimized conditions were used to perform the PCR reaction: 95°C for 2 minutes; 35 cycles at 95°C for 40 sec, 57°C for 40 sec, 72°C for 40 sec; 70°C for 40 sec. The PCR products were run on a 1.5% agarose gel and the image was taken with a chemilmager 4400 (Alpha Innotech Corp., San Leandro, CA). **Figure 1** shows an example of how the different genotypes can be identified. After weaning, the mice were segregated according to the genotype and maintained on standard laboratory chow until they become 10 weeks to perform mechanical loading study.



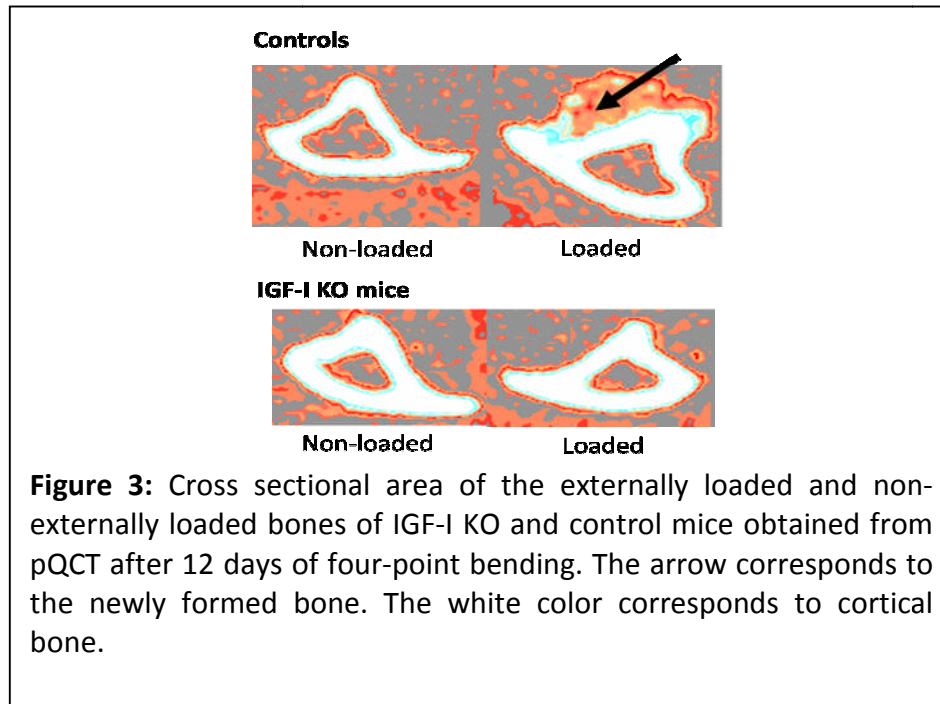
It is well established that the amount of mechanical strain exerted by a given load is largely dependent on the cross sectional area (moment of inertia) such that a mouse with a large cross sectional area will experience lower mechanical strain and vice versa

for a mouse with small circumference. Since bones of IGF-I KO mice have smaller circumference than the age- and sex-matched control mice, we calculated the amount of mechanical strain produced by varying loads using mathematical approach (Stephen C. Cowin: Bone Mechanics Hand book, 2nd edition, 2001, Chapter: Techniques from mechanics and imaging) on both IGF-I KO and control mice. Our goal is to apply loads that produced equivalent amounts of strain in the KO and control mice such that the difference in bone anabolic response induced by mechanical load is due to lack of osteoblast derived IGF-I and not due to difference in mechanical strain caused by varying bone size (periosteal circumference). As shown in Figure 2, 6N load in IGF-I KO mouse produces mechanical strain equivalent to 9N load in the control mice. Based on this data, adjusted loads were applied on both sets of mice using the four-point bending device (4). The loading was performed under Isoflurane anesthesia at 2Hz frequency, 36 cycles, once per day for 12 days. The right tibia was used for loading and the left tibia as internal contralateral control. After 48 hours of the

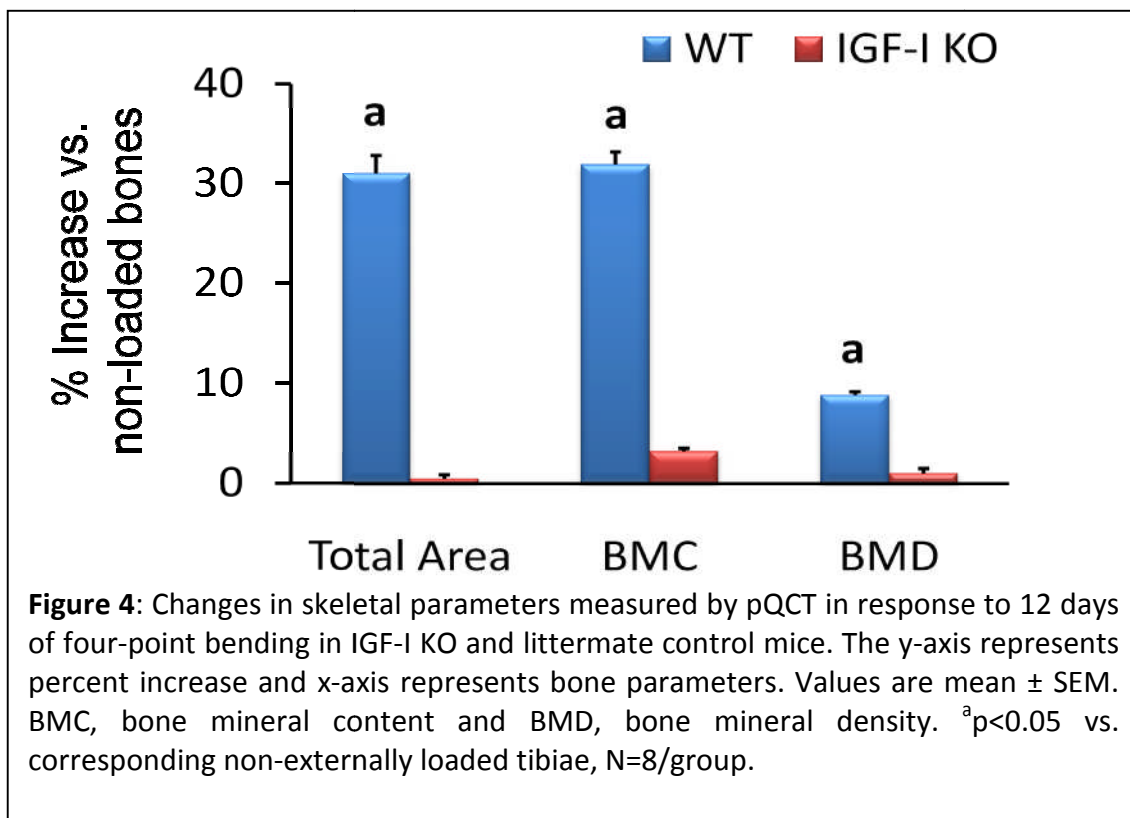


last loading, skeletal changes were measured in the loaded and non-externally loaded tibia of both sets of mice by *in vivo* pQCT (4). The mice were then euthanized and tibias were collected for further experiments.

Figure 3, shows that, in response to 12 days of four-point bending, the loaded bones of control mice showed significant increase in the newly formed bone while no such new bone formation was seen in the loaded bones of IGF-I KO mice (Figure 3). Accordingly, skeletal parameters, such as total area, bone mineral content and bone mineral density, measured by pQCT, were significantly increased in the externally loaded bones when compared to non-externally loaded bones of control mice (Figure 4). In contrast, in the IGF-I KO, many of these parameters showed little or no change in response to loading when compared to non-externally loaded bones of KO mice (Figure 4).



It is known that application of load by four-point bending technique produces pressure on the periosteal bone. Since there is a considerable amount of new bone formation on the periosteal surface of loaded bone, it is of concern whether the new bone formation response to loading by four-point bending is due to mechanical strain on the bone or due to periosteal pressure. To rule out the possibility that the skeletal anabolic



response induced by bending is not due to periosteal pressure, we performed a sham bending experiment in which the load was applied for the same period of time but not cyclically. In this study, we found that sham-loading neither increased periosteal bone formation nor caused changes in expression levels of bone marker genes, demonstrating that the skeletal changes induced by bending are not due to periosteal pressure (13). This finding also applies to the present study since we used the same loading model as well as regimen.

To further validate the pQCT measurements, we measured expression levels of bone marker genes and transcription factors induced by four-point bending in both control and IGF-I KO mice. The rationales for selecting these genes were based on previous studies (4, 14). We found that bone sialoprotein (BSP) and osteoblast specific factor 2 (OSF2) were increased by 2-2.5 fold in the loaded bones of IGF-I control mice while in the IGF-I KO mice, OSF2 decreased by 2.80 fold and no significant change was observed in BSP of the loaded bones (Table-1). These findings, together, reveal that osteoblast derived IGF-I is critically important in mediating skeletal anabolic response to mechanical loading. Our findings also suggest that Runx2 is downstream of IGF-I signaling pathway in the loaded bones. Additional studies are required to further validate the gene expression results.

Table 1: Quantitation of mRNA levels of bone genes in response to 12 days of four-point bending on 10 week female control and IGF-I KO mouse.

A) Control

Genes	Non-Loaded	Loaded	P-value	Fold Change
Bone sialoprotein	23.07 $\pm$ 0.14	21.77 $\pm$ 0.11	0.01	2.40 $\pm$ 0.17
Osteoblast specific factor 2	31.75 $\pm$ 0.22	30.37 $\pm$ 0.19	0.04	2.1 $\pm$ 0.09

B) IGF-I KO mice

Genes	Non-Loaded	Loaded	P-value	Fold Change
Bone sialoprotein	23.6 $\pm$ 0.15	23.99 $\pm$ 0.16	0.62	1.3 $\pm$ 0.2
Osteoblast specific factor 2	30.7 $\pm$ 0.2	32.3 $\pm$ 0.18	0.01	$\downarrow$ 2.80 $\pm$ 0.2

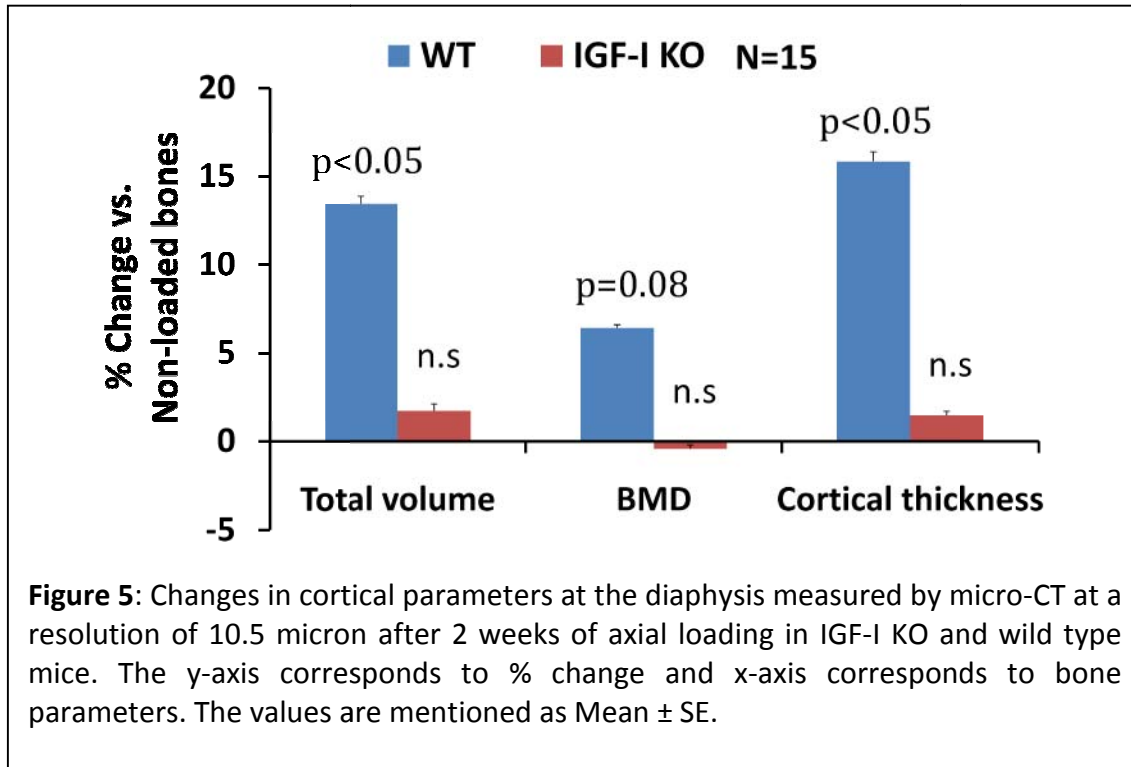
N=5, the values mentioned above corresponds to Ct (cycles) obtained from real time PCR and are represented as mean  $\pm$  SE.

One of the issues that is repeatedly raised against the four-point bending method of loading is that this model induces mainly periosteal bone formation since the mid diaphysis site at which loading is applied contains little or no trabecular bone. In terms of the pathogenesis of osteoporosis, it is known that loss of trabecular bone is a major contributor. Therefore, the next goal of our study was to select an in vivo loading model that can stimulate both trabecular and periosteal bone formation. To date, a number of loading models including jump exercise, wheel running and axial loading have been used to evaluate trabecular bone formation response. We chose the axial loading model because this model mimics exercise patterns of walking in humans and this model has been shown to induce both cortical as well as trabecular bone formation response to mechanical loading. Furthermore, studies have shown that axial loading on ulna or tibia results in a robust increase in both cortical and trabecular bone formation after two weeks of mechanical loading (15-20). Based on these rationales, we next evaluated the trabecular anabolic response to axial loading in both IGF-I KO and wild type mice.

To determine the effects of axial loading on the bone formation response, we generated both male and female IGF-I KO mice and control mice as described above. Again, due to difference in bone size between KO and wild type mice, we measured mechanical strain produced by loads using strain-gauge technique at the metaphysis region of tibia. The strain data shows that female wild type and KO mice produced 825  $\mu\epsilon$  and 780  $\mu\epsilon$ , respectively. Similarly, the male wild type and KO mice produced 773  $\mu\epsilon$  and 745  $\mu\epsilon$ , respectively. Based on these data, adjusted loads were applied to both male and female IGF-I KO and wild type mice such that both sets of mice receive same amount of mechanical strain. The loading was performed 40 cycles with 10 seconds rest between each cycle once per day for 3 alternative days for 2 weeks (15, 16).

In order to measure microarchitectural changes of trabecular bone and cortical bone changes in response to two weeks of axial loading we used Micro-CT, a high resolution tomography image system (Scanco In vivo CT40, Switzerland). Routine calibration was performed once a week using a three-point calibration phantom corresponding to the density from air to cortical bone. After the last day of loading, mice were euthanized and tibias were collected and stored in 1X PBS to prevent them from drying. Scanning was performed using 75Kv X-ray at resolution of 10.5  $\mu\text{m}$ . To minimize the position error (slice positioning) and to be consistent in our sampling site from mouse to mouse, we undertook several precautionary steps, which include: 1) A scout view of the whole tibia was taken first in the micro-CT to determine landmarks and precise selections of measurement sites. 2) We used the growth plate of the tibia as the reference point. 3) To measure trabecular parameters, we started our scan 30 slices away from the growth plate, which was 0.315 mm and progressing towards distal up to 0.840 mm providing a total of 50 slices (525  $\mu\text{m}$ ) and 3) Similarly, to measure cortical parameters, scanning was performed at 5.5 mm away from the growth plate and progressing distally up to 6.55 mm, providing a total of 100 slices (1050  $\mu\text{m}$ ). This area of scanning represents 37% positioning of the whole bone. After acquiring the radiographic data, images were reconstructed by using 2-D image software (as described by the manufacturer). The area of the trabecular bone was outlined within the trabecular compartment and a similar analysis was done for the cortical bone. Every 10 sections were outlined, and the intermediate sections were interpolated with the contouring algorithm to create a volume of interest, followed by a three dimensional analysis using

Scanco software. Parameters such as bone volume fraction (BV/TV, %), apparent density (mg HA/ccm), trabecular number (Tb.N,  $\text{mm}^{-1}$ ), trabecular thickness (Tb.Th,  $\mu\text{m}$ ) and trabecular space (Tb.Sp,  $\mu\text{m}$ ) were evaluated in the loaded and non-externally loaded bones of both sets of mice. The values shown in Figure 5 are average of the above slices for each parameter. Since IGF-I KO mice are smaller in bone length compared to wild type littermate; we adjusted for this difference in length using standard calculation such that the sampling site is same for both sets of mice.



Consistent with the data, we obtained from four-point bending, we found axial loading increased the amount of cortical bone in the wild type but not in the IGF-I knockout mice. Axial loading increased total volume, BMD and cortical thickness by 7 to 13% in the wild type (Figure 5). While in the IGF-I KO mice, little or no change was seen in these parameters in response to loading (Figure 5).

In addition to cortical bone, we next measured loading induced changes in trabecular parameters. Figure 6 shows micro-CT images of the loaded vs. non-loaded bones of both sets of mice. As you can see from figure 6, the loaded tibia of control mice show significant increase in the new bone compared to non-loaded tibia. While in the IGF-I KO mice, there is no difference between loaded and non-loaded tibia. Quantitative analysis shown in Figure 7 revealed that, in response to 2 weeks of axial loading, wild type mice show 18-20% increase in BV/TV, trabecular thickness and BMD with 5% increase in trabecular number. Thus, the mechanism through which axial loading increases trabecular bone in the wild type mice is largely by increasing the thickness of existing trabeculae rather than generating new trabeculae. This finding is consistent with previous published reports. Surprisingly, in the IGF-I KO mice, not only was trabecular volume not increased but we also observed a small decrease in the trabecular thickness in

response to loading (Figure 7). Together, findings from both loading models demonstrate that loading increases cortical and trabecular bone response in the IGF-I control mice but not in the mice that are deficient in osteoblast-derived IGF-I.

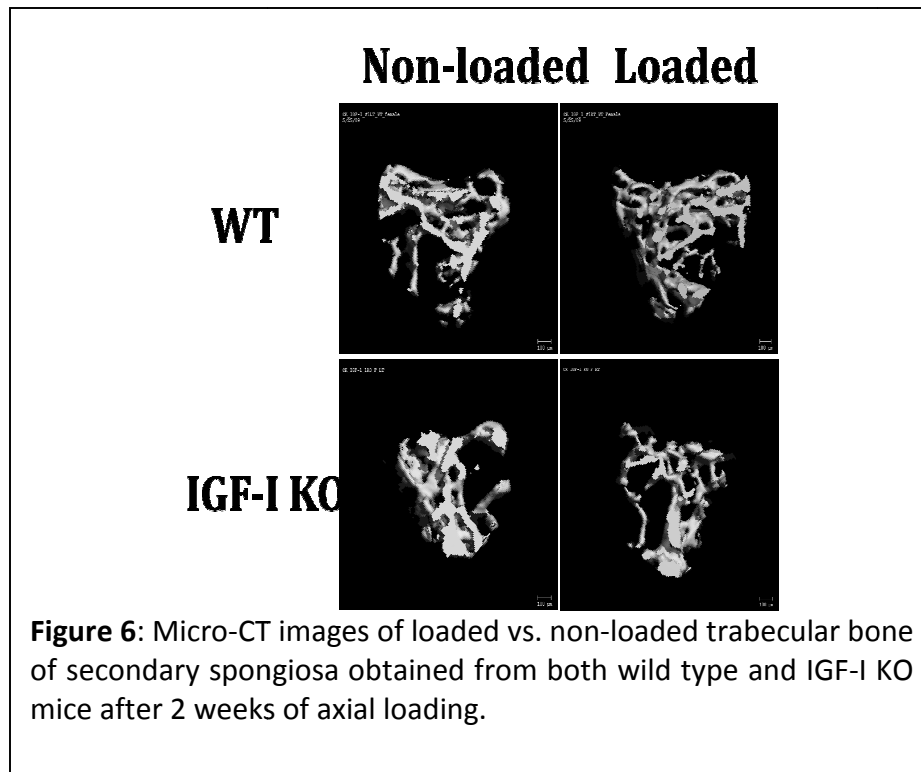


**Figure 6:** Micro-CT images of loaded vs. non-loaded trabecular bone of secondary spongiosa obtained from both wild type and IGF-I KO mice after 2 weeks of axial loading.

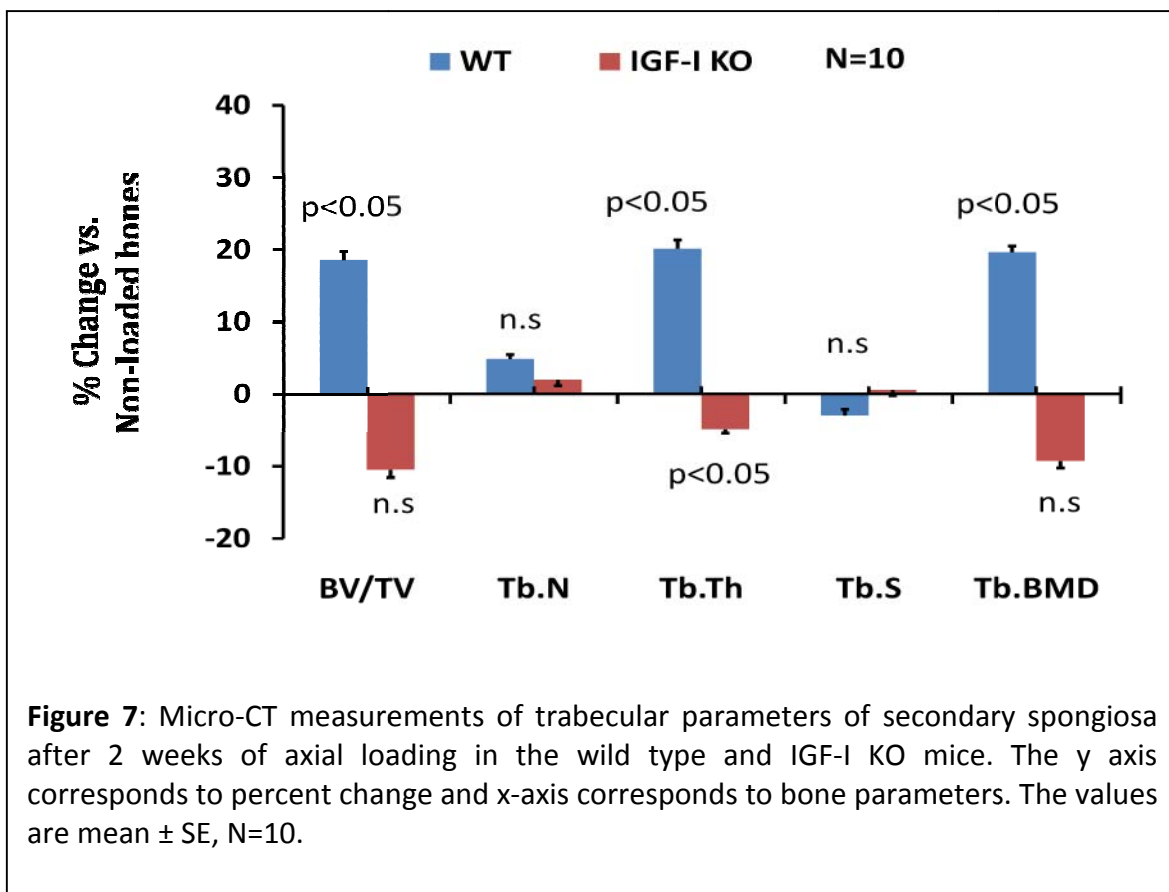
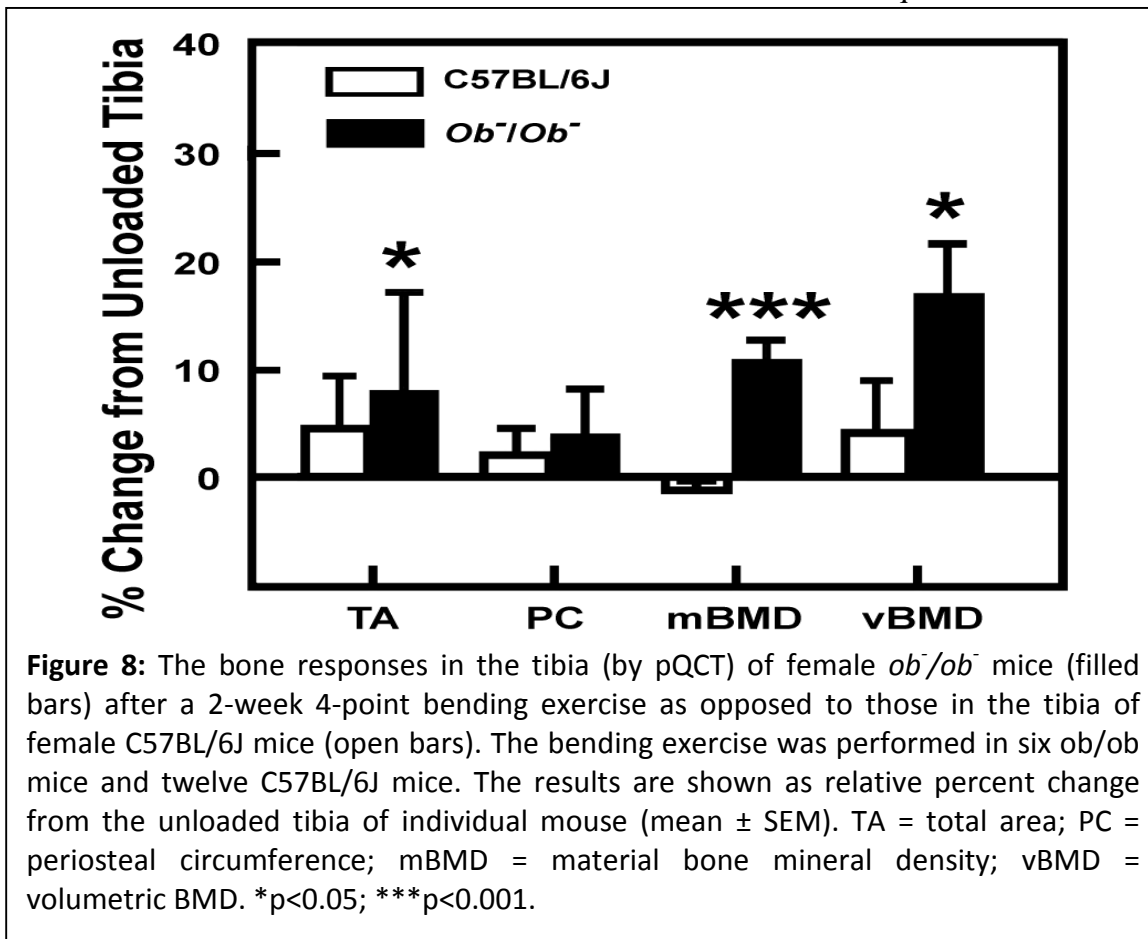


**Figure 7:** Micro-CT measurements of trabecular parameters of secondary spongiosa after 2 weeks of axial loading in the wild type and IGF-I KO mice. The y axis corresponds to percent change and x-axis corresponds to bone parameters. The values are mean  $\pm$  SE, N=10.

In our data analyses, we combined data from both male and female mice of each group since in our past studies we did not find appreciable difference in skeletal anabolic response to mechanical loading between male and female mice. The increased cortical and trabecular bone volume in the loaded bones of control mice could be due to increased bone formation and/or decreased bone resorption. To evaluate the target cell types affected by mechanical loading, we are in the process of performing histology on the bones used for micro-CT analysis. In addition, we are also generating more IGF-I KO and wild type mice to perform gene expression study to identify the signaling pathways impacted by the lack of IGF-I in the loaded bones. The outcome of this work will be reported in our next progress report.

**Technical Objective 2: Continue the ongoing studies on the role of leptin receptor signaling pathway in mechanical strain response in osteoblasts.**

In previous reports, we have presented compelling evidence that the leptin receptor (Lepr) signaling pathway is a negative mechanosensitivity modulating gene or pathway. Briefly, heterozygous male and female leptin-deficient *ob<sup>-</sup>/ob<sup>-</sup>* breeder mice (B6.v-Lep<sup>ob</sup>/J) [in C57BL/6J genetic background] were obtained from the Jackson Laboratories (Bar Harbor, ME) to generate the *ob/ob* colony in our laboratory. The size (i.e., periosteal circumference, measured by pQCT) of tibia of *ob<sup>-</sup>/ob<sup>-</sup>* mice was significantly bigger (by ~14%) than that of age-matched female C57BL/6J tibia (shown in previous report). Because the tibia of C57BL/6J mice with a smaller bone size had experienced a much higher strain at any given load than tibias of *ob<sup>-</sup>/ob<sup>-</sup>* mice, a significant larger load is needed for C57BL/6J tibia than for *ob<sup>-</sup>/ob<sup>-</sup>* mice to achieve an equivalent mechanical



strain (shown in previous report). By applying a similar mechanical strain to female *ob<sup>-</sup>/ob<sup>-</sup>* mice (~2,100  $\mu\epsilon$  or a 9-N load) and to adult female age-matched C57BL6/J mice (~2,500  $\mu\epsilon$  or a 6-N load) in the form of 2-week four-point bending exercise, we found that this strain increased significantly total bone mineral content, cortical area, cortical content, cortical thickness, and material and volumetric bone mineral densities at the site of loading in *ob<sup>-</sup>/ob<sup>-</sup>* mice but not in WT control mice (Figure 8), indicating that female *ob<sup>-</sup>/ob<sup>-</sup>* mice exhibited an enhanced bone formation response to mechanical loading.

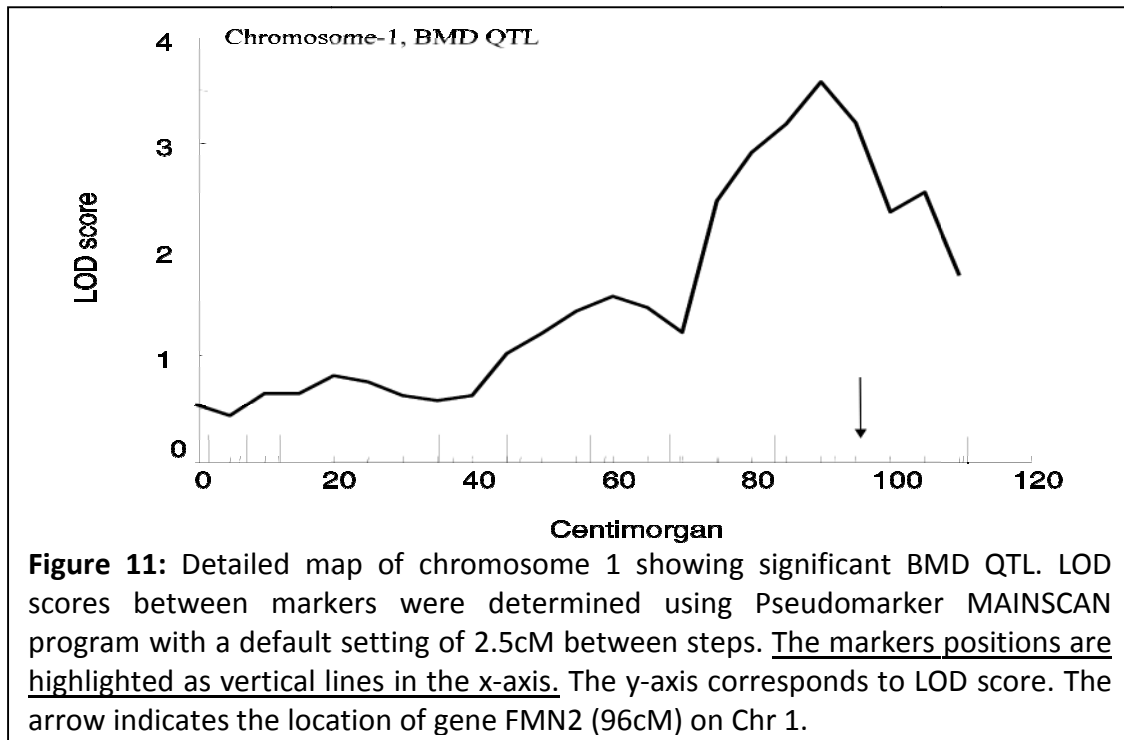
Our previous *in vivo* experiments utilized Leptin deficient rather than Leptin receptor (Lepr) deficient mice. In order to ensure that the observation seen with leptin-deficient mice was due to the lack of Lepr signaling and not indirectly through leptin deficiency, we sought to confirm that Lepr deficient mice also exhibited an enhanced osteogenic response to mechanical loading on periosteal bone formation in Lepr-deficient mice. For this work, we have established a Lepr KO mouse colony in our laboratory for investigation. Accordingly, we have purchased a breeding pair of heterozygous Lepr KO mice (B6.Cg-mLpr<sup>db/+</sup>+/J) from the Jackson Laboratories. Homozygous Lepr KO mice are infertile and cannot be used for breeding purposes. Because *Lepr<sup>db</sup>* homozygotes are functionally sterile, the coat color marker misty (*m*) has been incorporated into stocks for maintenance of the diabetes (*db*) mutation. This repulsion double heterozygote (*m*+/+ *Lepr<sup>db</sup>*) would facilitate identification of heterozygotes for breeding, while the coupling double heterozygote, (*m Lepr<sup>db</sup>*/+ +, this strain), allows identification of homozygotes before the onset of clinical symptoms. The recessive misty mutation causes a mild dilution of coat color.

We have now obtained a colony of Lepr deficient mice. As was seen in leptin deficient mice, the size (periosteal perimeter) of tibia of 10-weeks-old female *Lepr<sup>-</sup>/Lepr<sup>-</sup>* mice was also significantly smaller than that of tibia of age-matched female WT littermates (data not shown). Therefore, the load applied to the tibia has to be adjusted for each mouse strain, such that a similar mechanical strain is applied to the two mouse strains. Accordingly, a 9-N load was applied to the WT tibia, which yielded a strain of  $4603 \pm 256\mu$  strain; while a 7-N load was applied to the *Lepr<sup>-</sup>/Lepr<sup>-</sup>* tibia, which produced a strain of  $4549 \pm 52\mu$  strain. The loading was applied at 2 Hz for 36 cycles, once a day for 12 days. The animals were then sacrificed one day after the last loading, and *de novo* bone formation at the loaded site and at the contralateral unloaded site of each animal was determined by pQCT.

Figure 9 shows that at the test mechanical strain (4,500-4,600  $\mu$ strain), the adult female WT littermates (in C57BL/6J genetic background) responded to the 12 days of daily mechanical loading with significant increases in total bone area, periosteal circumference, material bone mineral density, and volumetric bone mineral density by 5 to 10%. However, these bone responses of the age-matched female *Lepr<sup>-</sup>/Lepr<sup>-</sup>* KO mice, which are in the range of 10-30%, were significantly much greater ( $p < 0.05$ ) than the bone responses in WT littermates. These results are consistent with the contention that Lepr and its signaling mechanism have negative regulatory actions on the mechanosensitivity of bone. These results also confirm that the enhancing effects of leptin deficient in *Ob<sup>-</sup>/Ob<sup>-</sup>* mice were due to Lepr signaling and not other effects of leptin.

### **Technical Objective 3: Evaluation of the role of formin-2 (FMN2) in mediating mechanical loading response on the skeleton.**

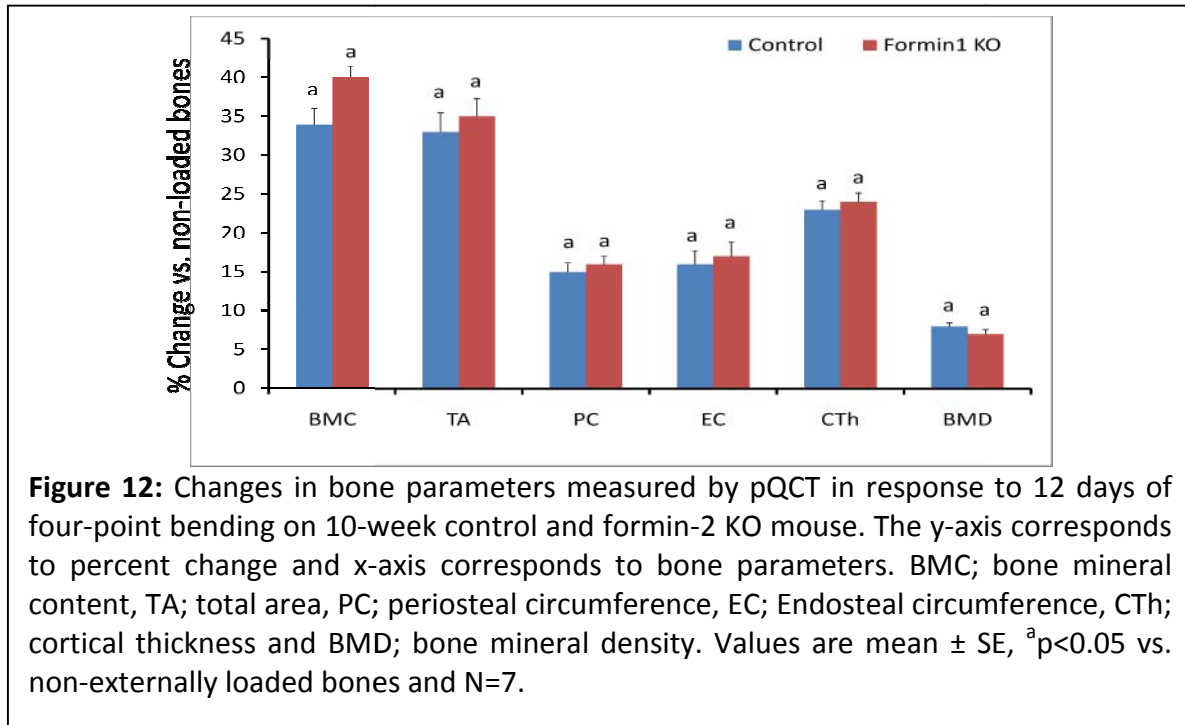
It is well known that exercise increases bone formation but the molecular components responsible for increased bone formation resulting from exercise are not well known. Identifying these molecules and their pathways may lead to a better understanding of how exercise maintains bone health and could lead to the development of a novel therapeutic strategy. To date, a number of signaling pathways activated by mechanical strain have been investigated using *in vitro* cell culture models. While the data generated from these models have identified new signaling pathways that are activated by mechanical strain, there are certain deficiencies with these models. For example, many of the *in vitro* models utilize homogeneous population of cells and lack vital communication between various types of cells and cell-matrix interactions that occur *in vivo* at the three dimensional level. Since little is known on the molecular components that are activated in the skeletal tissue in response to mechanical loading *in vivo*, we performed a genome wide microarray analysis using RNA extracted from a good responder C57BL/6J (B6) mouse to identify the mechanoresponsive genes. Of the 346 genes that were differentially expressed in the loaded bones compared to externally non-loaded control bones, we found formin-2 mRNA levels were increased significantly (21). Furthermore, we also found this gene to reside within the region of mechanical loading QTL, one of the major QTL (Chr 1, 96cM) that we identified in our study for bone response to mechanical loading (Figure 11) and by others for mechanical properties (13,



14). These findings led us to speculate that FMN2 may be involved in mediating the anabolic effects of ML on bone formation. Based on the above rationale and our preliminary data, we next tested the hypothesis that bone anabolic response is mediated by FMN2.

To test the above hypothesis, we obtained FMN2 knockout mice from Dr. Philip Leder (Department of Human Genetics, Harvard Medical School, Howard Hughes Medical Institute, Boston, MA). These mice were originally generated in inbred 129Sv by homologous recombination of a targeting vector with 1300 bp of the FH1 domain of FMN2 deleted and replaced by 1257 bp containing the PGK-Neo gene followed by stop codons in all three reading frames. Two heterozygote FMN2 (+/-) male/female pairs were bred to generate wild type (+/+), and knock out (-/-) pups to perform the above study.

Before proceeding into the loading experiment, we measured bone size (periosteal circumference) of both KO and wild type mice by using pQCT. This is because the amount of mechanical strain exerted by a given load is largely dependent on bone size (moment of inertia) such that a mouse with a larger circumference will experience lower mechanical strain and vice versa for a mouse with a small circumference. In order to assure that the difference in skeletal anabolic response to loading is due to lack of FMN2 gene and not due to difference in bone size, we measured bone size by pQCT in both control and FMN2 KO mice before initiation of loading experiment. We found that there was no difference in bone size between the two sets of mice and therefore we chose to apply the same mechanical load for both FMN2 KO and control mice. At 10 weeks, mechanical loading was performed using four-point bending device. A 9N load was applied on both control and FMN2 KO mice. The loading was performed at 2Hz Frequency, for 36 cycles, once per day. The loading was carried out for 2 weeks (6 day/week, 1 day rest) under Isoflurane anesthesia. The left tibia was used for loading and the right tibia was used as the contralateral control. After 48 hours of the last loading, mice were anesthetized with Isoflurane and skeletal changes were measured by pQCT in the loaded and non-externally loaded bones of both sets of mice. The results from our study show that skeletal parameters were increased significantly in the loaded bones compared to unloaded bones in both formin-2 KO and control mice, but no differences were observed between the two genotypes (Figure 12). The lack of difference in the anabolic response to mechanical loading between the FMN2 KO and control mice was surprising which could be due to compensation by other members of the formin family in the knockout mice.



#### **Technical Objective 4: Evaluate if 14104M gene is a mechanosensitive gene.**

As a part of the army funded study, we have used ENU (N-ethyl-N-nitrosourea) mutagenesis in the mouse model to identify genes that regulate bone density and bone size, two important determinants of bone strength. ENU is a powerful mutagen that causes base transverse and point mutation in the genome with which one can identify and study a phenotype of interest (22). Using this approach, our group has established several lines of mutant mice that exhibit differences in bone size or bone density (23, 24). One such a mutant line, termed 14104M, exhibited large differences in bone size compared to corresponding control mice. Because we found large increases in periosteal bone formation in response to mechanical strain, we considered the possibility that 14104M gene is a mechanoresponsive gene. In order to identify the candidate gene responsible for the 14104 mutant phenotype, we used 2 approaches, single nucleotide polymorphism (SNP) analyses and gene expression changes. These 2 strategies have been successfully used by us as well as others in the identification of QTL gene for a variety of complex phenotypes including bone density (25-29). The SNPs can change the encoded amino acids (nonsynonymous) or can be silent (synonymous) or simply occur in the noncoding regions. They may influence promoter activity (gene expression), messenger RNA (mRNA) conformation (stability), and subcellular localization of mRNAs and/or proteins and thereby influence gene function. To identify the mutant gene, we are using a functional positional candidate gene approach in which candidate genes are identified within the mutant locus based on their known functions for subsequent sequencing the coding regions of selected candidate genes. Table 2 represents the candidate genes selected for sequence analyses. For gene expression profiling, we have used microarray techniques to compare gene expression between RNA isolated from the mutant's bones

and the wild type B6 bones. Identification of differentially expressed genes that are located within the mutant locus or signaling pathway affected in the mutant mice will lead to the identification of candidate genes.

### **Sequencing candidate genes**

*(1) Designed oligos to amplify the appropriate regulatory regions.*

Using NCBI database, we have designed primers that over-lap with each other in order to cover the whole coding region of each gene; the primers used are described in Table 3.

*(2) Prepare cDNA and PCR amplify the cDNA fragments from the mutant and B6 mice.*

RNA was isolated from tissues isolated from B6 and from the 14104 mutant mice. cDNA was generated using M-MLV reverse transcription enzyme (Promega, Madison, WI, USA). Then, after optimizing the PCR conditions for every pair of primers, we prepared 5 x 100 µl PCR product from every segment and every strain (we used B6 and mutant DNA). Then the PCR products were purified using QIAquick PCR purification kit from Qiagen.

*(3) Sequence the DNA fragments of regulatory regions.* 5-20 ng from purified PCR products were sequenced using the ABI machine.

*(4) Compare the sequence between congenic and B6 mice.*

Table 4 represents a summary of the results of the sequencing. We have sequenced the coding regions of 5 candidate genes but no SNP was found between the 14104 mut. and the WT mice, only a small region at the 5'-end of the Cbx2 gene remains to be sequenced.

### **Expression profiling**

For expression profiling, we used cDNA chips from Illumina that carry 27 000 mouse genes and 37 000 probes, with 8 control genes spotted in 40-20 replicates. Among the 175 genes and EST in the region 109-119 Mb of chr 11, 10 showed a significant difference ( $P < 0.05$ ) in the expression between the mutant (mut) and the wild type B6 (Table 5). The genes that showed more than 1.9-fold change between the mutant and the wild type (WT) mice will be rechecked with real Time PCR. Then, the gene(s) differentially expressed between the mutant and the WT will be sequenced to identify the mutation that caused the difference in the expression.

**Table 2: Selected candidate genes from the 14104 mutant locus.**

Symbol, Name	Known Molecular or Cellular Function related to bone	Skeletal Phenotype of Targeted Disruption
Axin2, Axin 2	Negatively regulates expansion of osteoprogenitors and maturation of osteoblasts	Skeletal defects, craniosynostosis
Slc9a3r1, solute carrier family 9 (sodium/hydrogen exchanger), isoform 3	osteoblast differentiation	Hypophosphatemia and premature death

regulator 1		
Sox9, SRY-box containing gene 9	Transcriptional regulation of osteoblast	Skeletal dysplasias
Grb2, growth factor receptor bound protein 2	Intracellular signaling cascade, Negative regulator of osteoclastogenesis and osteoblast differentiation	Enhanced Bone Volume, Craniofacial
Cbx2, chromobox homolog 2 (Drosophila Pc class)	chromatin assembly or disassembly	Mutations cause malformations of the axial skeletal
Socs3, Suppressor of cytokine signaling	Involved in GH signaling (JAK2)(STA5) in osteoblasts and regulates CD11c+ dendritic cell-derived osteoclastogenesis	Decreased embryo size, increased resistance to induced-obesity diet, weigh loss

**Table 3: The sequences of the primers used for sequencing.**

Symbol	Name	Sequence
Axin2	Axin2	5'-AGCCCCTGCTGACTTAAGAG 5'-GTTTCATCTGCCTGAACCCAT 5'-TAGGCGGAATGAAGATGGAC 5'-TGGGGAGGTAGCCACATAAG 5'- GGCAGTGATGGAGGAAAATG 5'-CACGTAGGTTCCGGCTATGT 5'-AGAGGTGGTCGTCCAAAATG 5'- AGAAAAGGAGGGGTCTGAGC 5'-ACCTCTGCTGCCACAAACT 5'- CAAGACCAAGGAGGAGATCG 5'-CAGGCTTCCTCTAGCTGTGC 5'-AGCTACCCATTGGAGTCTGC 5'-GCTGAGCTGCTCCTTGAAGT 5'- AAGAGCCAAAGAACTGGCA 5'-GTCCCTCCCTAGGCTTTGTC 5'-CTGCGATGCATCTCTCTCTG
Slc9a3r1	solute carrier family 9 (sodium/hydrogen exchanger), isoform 3 regulator 1	5'-GAGAAAGGTCGTGAGTCCCC

		5'-GCTTGTTTCGGACTTCTCCTG 5'- CGGTGAGAATGTGGAGAAGG 5'-CCTTGTCTACCACCAGCAGC 5'-TTGTGGAGGTCAATGGTGTC 5'- AAGGGGAGCTAGGTAGGGTG
Sox9	SRY-box containing gene 9	5'- GGCAGCTGAGGGAAGAGGAG 5'-TCCAGAGCTTGCCCAGAGTC 5'-CAGGAAGCTGGCAGACCAGT 5'-TGTTGGAGATGACGTCGCTG 5'-TTGATCTGAAGCGAGAGGGG 5'-TAGGAGATCTGTTGCGGGGA 5'-CTGAGCCCCAGCCACTACAG 5'-CTGGAATCCCAGCAATCGTT
Grb2	growth factor receptor bound protein 2	5'-CATTGTGTGTCCCAGTGTGC 5'-CTTACCACCCACAGGAAAT 5'- GAGCCAAGGCAGAAGAAATG 5'-AGTTGCAACCCAATGAGAGG
Cbx2	chromobox homolog 2 (Drosophila Pc class)	5'-CTTTGTGTGCAGCAGTGAGC 5'-TTTTTCTGAGGCACTGGATG 5'-ATCCAAATCCAGCAGTTCGT 5'-AACCTGACTCTGGCTCATGC 5'-GCCAGTCTGATGAAAGGCAT 5'-TCAGCTTTTCCCCTTTGTTG 5'-GGCTATTCCTGCTACCAACC 5'-TCTCAGGACAGGGCAGAGTT
Socs3	Suppressor of cytokine signaling	5'-TAGACTTCACGGCTGCCAAC 5'-CCCTCACACTGGATGCGTAG 5'-GTTGAGCGTCAAGACCCAGT 5'-GGCTGGATTTTTGTGCTTGT

**Table 4: Summary of the sequencing progress**

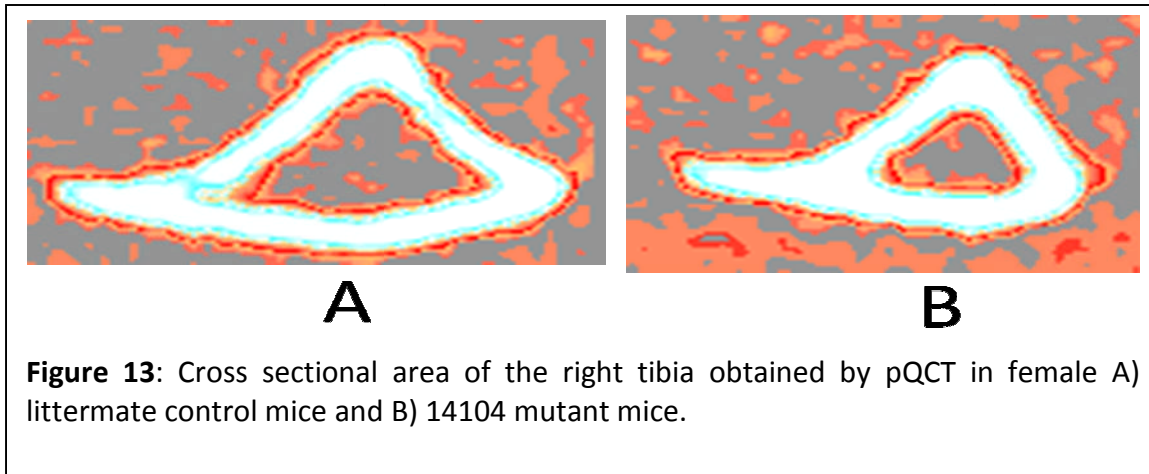
Symbol, Name	Coding sequence (bp)	Region already sequenced (bp)	SNPs found (region remained to be sequenced bp)
Axin2, Axin 2	350-2872	230-3024	none
Slc9a3r1, solute carrier family 9 (sodium/hydrogen exchanger), isoform 3 regulator 1	186-1253	126-1315	none
Sox9, SRY-box containing gene 9	353-1876	273-2064	none
Grb2, growth factor receptor bound protein 2	332-985	210-1128	none
Cbx2, chromobox homolog 2 (Drosophila Pc class)	81-1640	423-1726	None (81-422 bp)
Socs3, Suppressor of cytokine signaling	377-1054	264-1136	none

**Table 5: Genes at 109-119 Mb in chr 11 that showed significant difference between the 14104 mutant and the wild type B6 mice.**

Symbol, Name	Description	ttest (P value)	Fold-change1*	Fold-change2#
2600014M03Rik	EST	0.007815	2.22757103	1.326567
Slc39a11	Solute carrier family 39 (metal ion transporter), member 11	0.008198	0.811734	1.36306375
2310075G12Rik	EST	0.013453	0.814241	1.36727384
Rhbd16	Rhomoid 5 homolog 2 (Drosophila)	0.019647	1.349861	2.26668677
Sdk2	Sidekick homolog 2 (chicken)	0.026345	1.222787	2.05330424
Kctd2	Potassium channel tetramerisation domain containing 2	0.026628	0.861888	1.44728288
1700012B07Rik	EST	0.031338	1.262735	2.12038517
Recql5	RecQ protein-like 5	0.041487	1.157285	1.94331246
BC034097	EST	0.045313	1.302127	2.18653082
Evpl	Envoplakin	0.046496	1.23859	2.07984009

\*Fold-change before normalization and # after normalization with all control genes in the chip

To determine whether the genomic region responsible for the 14104M phenotype is also responsible for mediating or regulating anabolic effects of mechanical loading on bone formation, we propose to evaluate the bone anabolic response to mechanical loading in 14104 mutant and corresponding control mice.



To obtain mutant and control mice for mechanical loading studies we have crossed 14104 female mutant mice with C57BL/6J male mutant mice to generate pups. At 9 weeks, we performed in vivo pQCT on the tibia of these mice to screen for mutant and littermate control. We choose periosteal circumference as an endpoint to differentiate the mouse lines. Quantitative analysis revealed a group of mice with reduced periosteal circumference (4.42 mm) compared to another group of mice whose periosteal circumference (5.01 mm) was very similar to the control C57BL/6J mice. Figure 13 shows cross sectional area of the female mutant mice versus littermate control mice. Based on this phenotypic difference, we segregated the mice into two groups: mutant and wild type. Once these mice reach 10 weeks they will be subjected to mechanical loading to evaluate the skeletal anabolic response. The rationale for selecting 10 week age for the mechanical loading study is based on our findings from our previous age-related study.

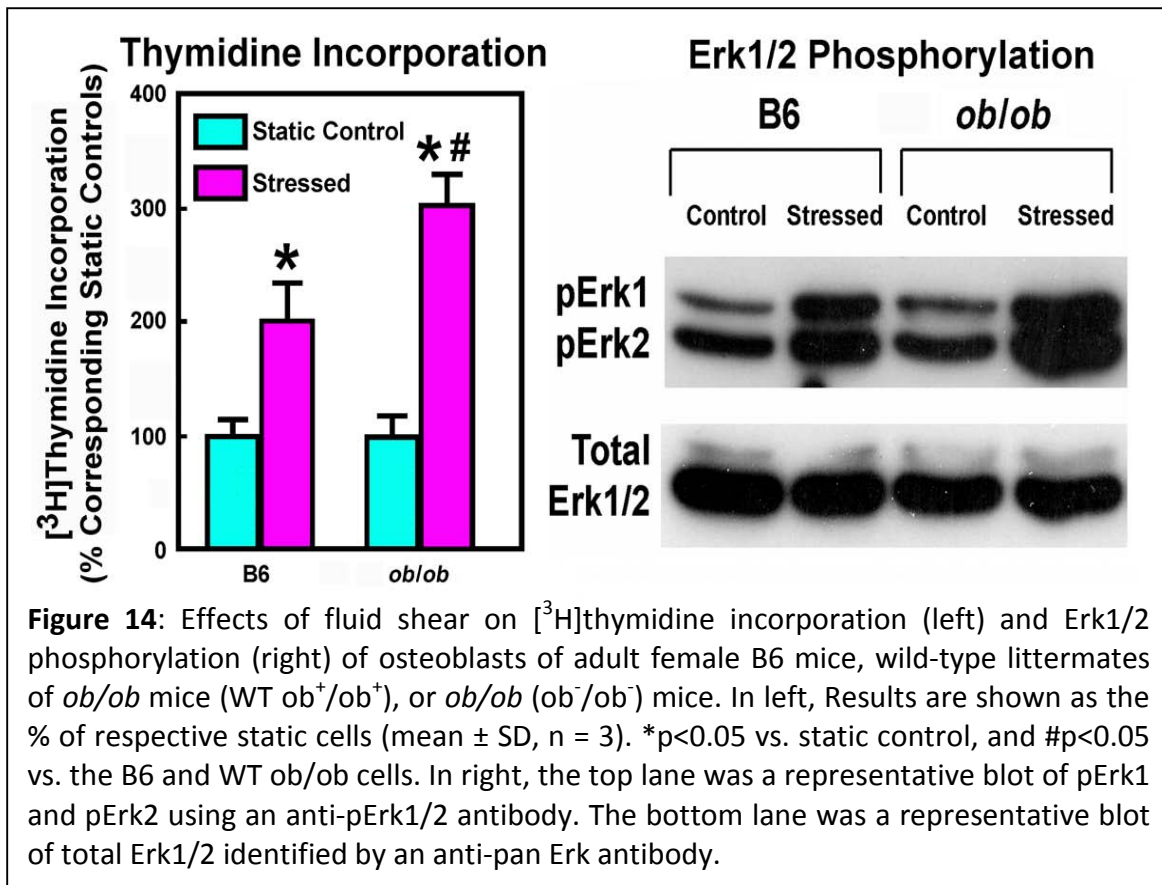
Before proceeding into the loading experiment, we measured mechanical strain on tibia of both mutant and wild type mice. This is because, the mechanical strain generated by a given load depends largely on bone size, and therefore, we predict that mice with smaller circumference tend to produce more mechanical strain than mice with larger circumference. In order to assure that the difference in bone anabolic response to mechanical loading between 14104 mutant and wild type mice is not due to difference in mechanical strain produced due to bone size differences, we measured mechanical strain by using strain gauge technique on tibia of 10 week ENU mutant mice and wild type mice. The results from our study shows that female mutant mice produced 600  $\mu\epsilon$  (N=4) and wild type female mice produced 370  $\mu\epsilon$  (N=4) for a 6N load. Based on these data, we propose to apply 6N load to female mutant mice and 10N load to female wild type mice such that both mice receive the same amount of mechanical strain. Currently, we are in process of measuring the strain rate for loads on male mice. We are also crossing 14104M female mutant with 14104 male mutant mice to generate more pups. We intend to use some of these pups for the strain gauge experiment since we need more data points

to validate above strain data and the rest will be used for axial loading once the appropriate load is selected which is based on the strain-gauge data.

**Technical Objective 5: Evaluate the influence of mechanical strain on bone regeneration.** A model using tail vertebra healing is being developed to study the influence of mechanical strain on bone regeneration. Please see the report on the final six months of the project period for the progress on this objective.

**Technical Objective 6: Continue in vitro phosphorylation studies to identify signaling proteins that are activated by mechanical strain in KO and control mice.**

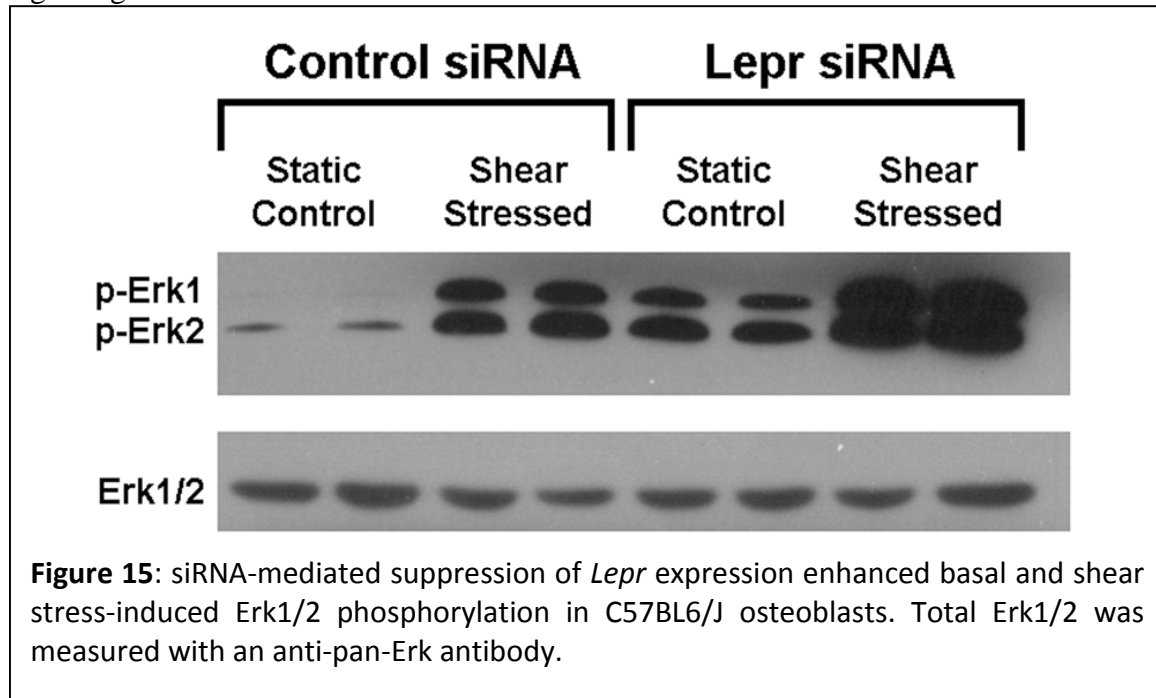
Our previous studies have shown that mechanical transduction in osteoblasts involves protein-tyrosine phosphorylation of key signaling proteins, including Erk1/2 (shown in previous report), that is known to mediate various anabolic signaling pathways (6,7). Accordingly, to further test if deficiency of leptin or *Lepr* signaling would lead to an enhanced osteogenic response to mechanical stimuli, we also examined the effects of a steady fluid shear on Erk1/2 phosphorylation in osteoblasts isolated from adult female *ob/ob* mice as opposed to those in adult female B6 osteoblasts *in vitro*. For comparison, osteoblasts of the WT littermates of *ob/ob* mice (*ob<sup>+</sup>/ob<sup>+</sup>*) were included. In addition, to evaluate whether the increase in Erk1/2 phosphorylation was associated with an osteogenic effects, we also measured [<sup>3</sup>H]thymidine incorporation in this experiment. Figure 14 confirms that a 30-min steady fluid shear of 20 dynes/cm<sup>2</sup> significantly

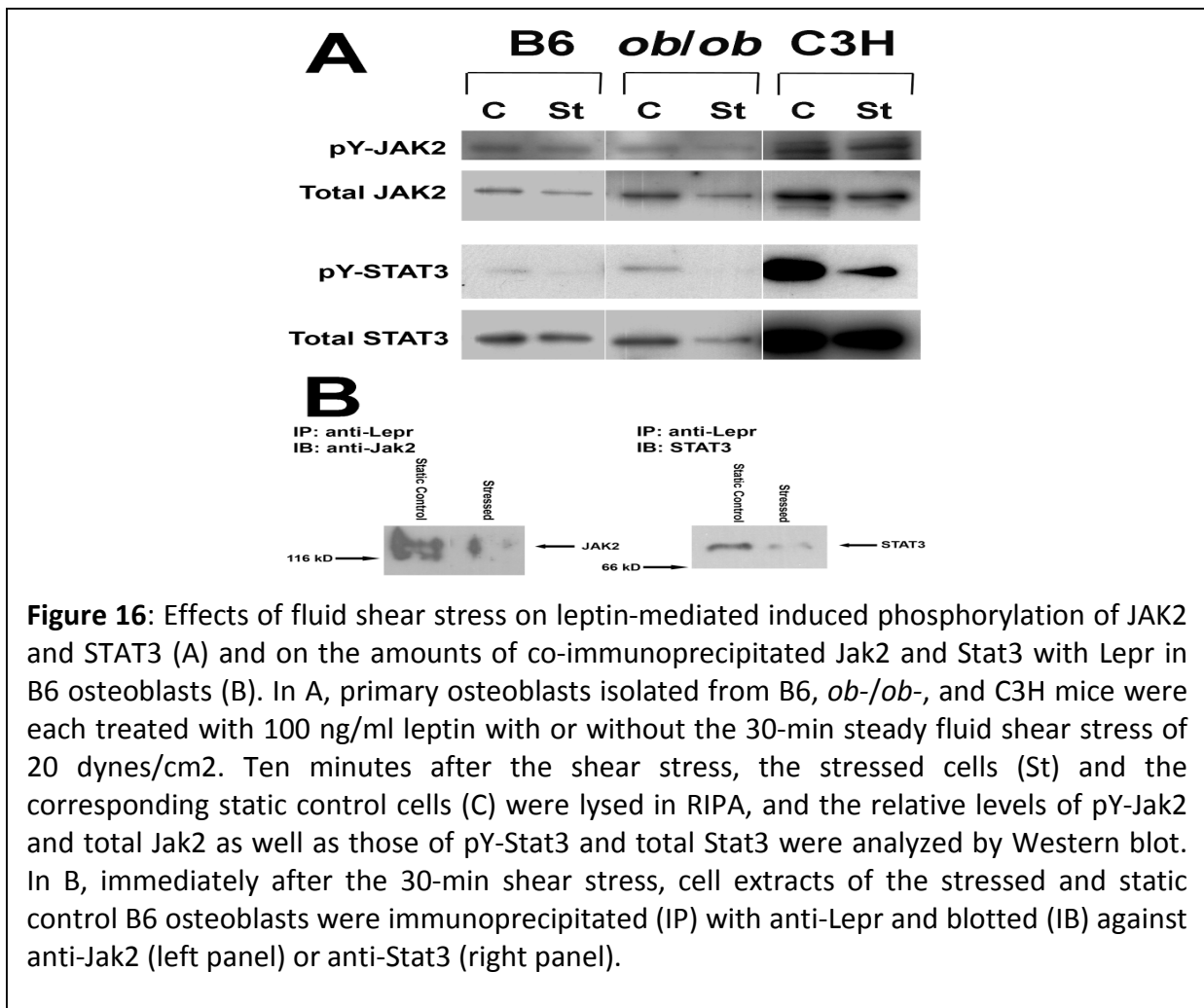


stimulated [<sup>3</sup>H] thymidine incorporation and Erk1/2 phosphorylation in female B6

osteoblasts. The same shear stress produced significantly greater increases in [ $^3$ H]thymidine incorporation and Erk1/2 phosphorylation in *ob<sup>-</sup>/ob<sup>-</sup>* osteoblasts than those in B6 osteoblasts and osteoblasts of WT *ob<sup>+</sup>/ob<sup>+</sup>* littermates. The shear stress-induced [ $^3$ H]thymidine incorporation and Erk1/2 phosphorylation in WT *ob<sup>+</sup>/ob<sup>+</sup>* osteoblasts were not different from those in B6 osteoblasts. These results are highly reproducible and were seen in every repeat experiment. Figure 15 shows that down-regulation of *Lepr* expression in C57BL/6J osteoblasts by *Lepr* siRNA2 enhanced both basal (i.e., static control) and fluid shear-induced Erk1/2 phosphorylation much further in C57BL/6J osteoblasts, indicating that regulation of mechanosensitivity by leptin and/or *Lepr* signaling also involves mediation of protein-tyrosine phosphorylation of Erk1/2 in osteoblasts.

*Lepr* is a member of the class I cytokine receptor family and uses the Jak2/Stat 3 pathway as its primary signaling pathway. Thus, we measured the relative levels of protein-tyrosine phosphorylated (pY-)Jak2/Jak2 and pY-Stat3/Stat3 as an index of activation of the *Lepr* signaling, in C3H/HeJ and C57BL/6J osteoblasts without (basal) or with the fluid shear. Osteoblasts of *ob<sup>-</sup>/ob<sup>-</sup>* mice were included in this experiment for comparison. To ensure full activation of the *Lepr* signaling, the cells were pre-treated with 100 ng/ml leptin for 24 hrs prior to the shear stress. Figure 16A shows that the basal leptin-dependent increases in pY-Jak2 and pY-Stat3 levels were much higher in the C3H/HeJ osteoblasts than those in C57BL/6J and *ob<sup>-</sup>/ob<sup>-</sup>* osteoblasts, suggesting that C3H/HeJ osteoblasts have a functionally more active *Lepr* signaling. Figure 16B also shows that shear stress reduced the relative amounts of pY-Jak2 and pY-Stat3 in all three osteoblasts, suggesting that fluid shear stress may have suppressive effects on the *Lepr* signaling in mouse osteoblasts.





It is interesting that the total Jak2 and Stat3 levels were several folds higher in C3H osteoblasts than in C57BL/6J and *ob/ob* osteoblasts. Thus, in as much as the fluid shear suppressed the leptin-mediated pY-Jak2 and pY-Stat3 levels in C3H/HeJ osteoblasts, the remaining pY-Jak2 and pY-Stat3 levels in C3H/HeJ osteoblasts were still several folds higher than basal pY-Jak2 and pY-Stat3 levels in B6 and *ob/ob* osteoblasts.

Other members of the class I cytokine receptor family could also activate the Jak2/Stat3 signaling. To ensure that the fluid shear-mediated reduction in the Jak2/Stat3 activation was related to the *Lepr* signaling, we performed a co-immunoprecipitation experiment to assess the relative amounts of Lepr-associated Jak2/Stat3 in B6 osteoblasts (Fig. 16B). The fluid shear reduced markedly the amounts of Lepr-bound Jak2 and Stat3; a finding consistent with the contention that the reduced Jak2/Stat3 activation was related to the shear stress-mediated reduction in the *Lepr* signaling.

In studies with respect to the role of IGF-I signaling in mechanotransduction involving protein-tyrosine phosphorylation, we are now using knock out approach, which has demonstrated that osteoblast derived IGF-I is critical in mediating skeletal anabolic response to mechanical loading. The next phase of our study is to identify the genes and

the signaling pathways that are downstream of IGF-I involved in increasing the bone formation in response to mechanical loading. To do so, we generated IGF-I KO and littermate wild type mice. At 5 weeks of age, these mice were euthanized and tibias were collected, marrow flushed and stored in DMEM+ antibiotic tube. Later, to harvest primary osteoblast cells, these bones were chopped and incubated at 37°C for 2 hour with 0.1% collagenase. After the incubation, the supernatant was discarded and cells were collected and transferred to a culture plate that contains 10% FBS, antibiotics and DMEM. Currently we are setting up the fluid flow stress to perform in vitro mechanical stimulation on the collected primary osteoblast cells from both KO and wild type mice. Once mechanical stimulation is completed, protein will be extracted from the mechanical stimulated vs. non-stimulated cell and western blot approach will be used to evaluate signaling proteins that are increased in response to mechanical loading. The finding of this study will be reported in our next progress report.

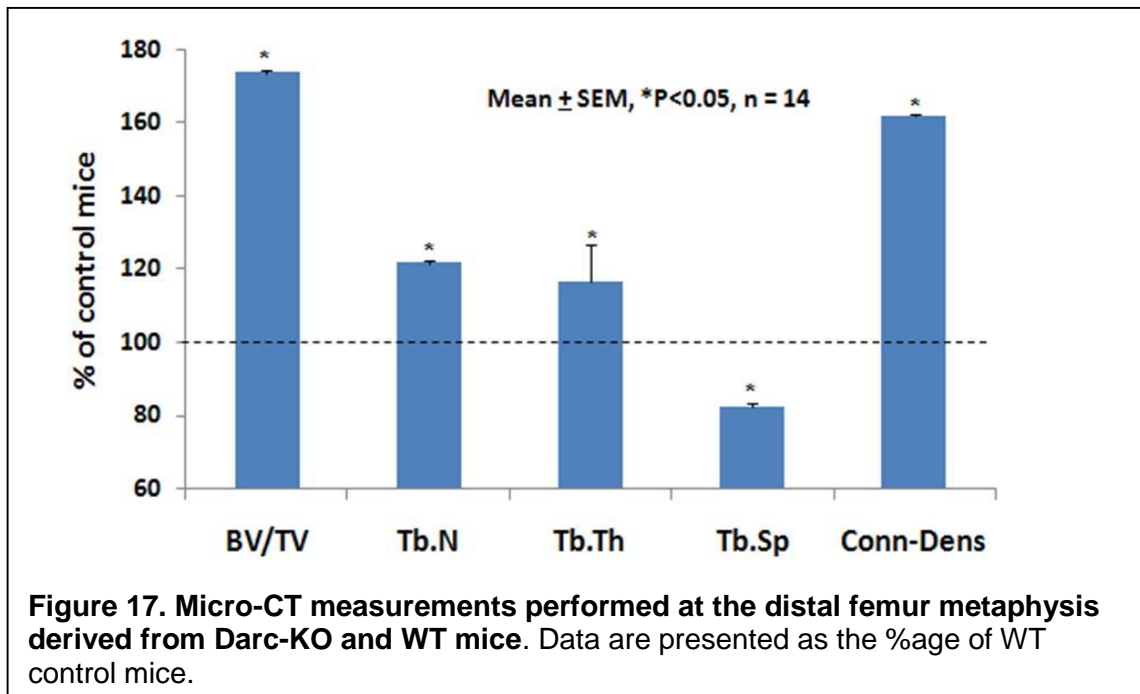
**Technical Objective 7: Continue data analysis and prepare manuscripts for submission to peer review journals for publication**

We have submitted a manuscript on our results of the potential role of leptin receptor as a negative regulator of mechanosensitivity (The leptin receptor signaling functions as a negative modulator of bone mechanosensitivity in mice) has been submitted for publication in the Journal of Biological Chemistry.

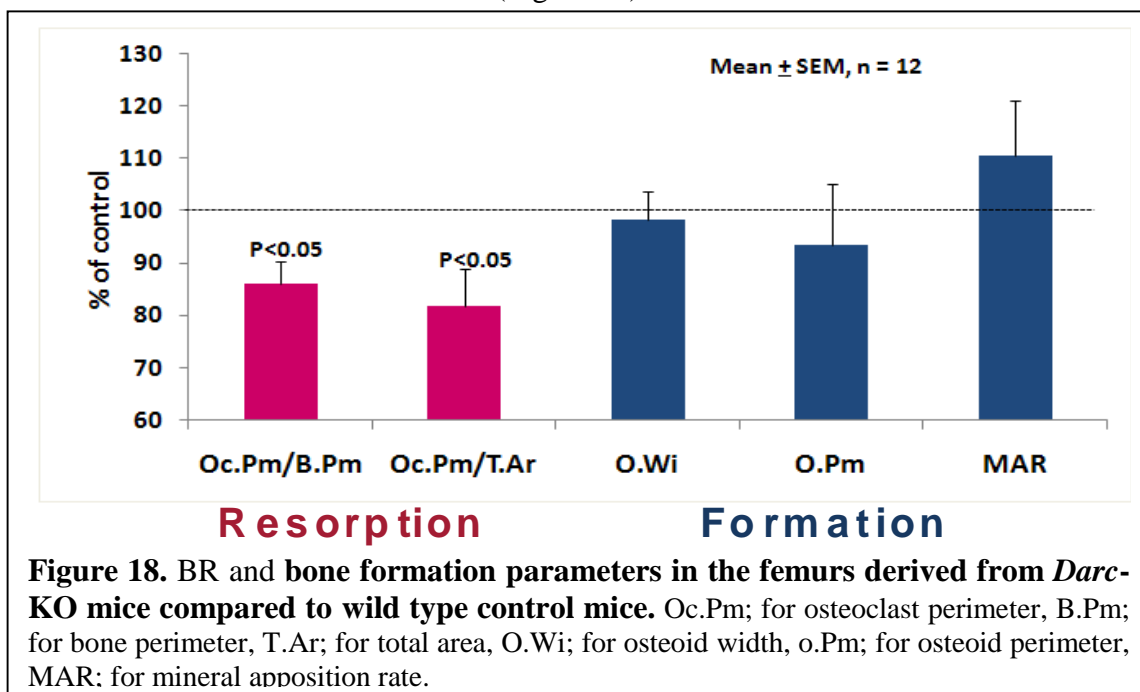
We have completed the data analysis for the previous bone termination study and this manuscript has recently been submitted.

**Additional Progress – Studies on the role of *Duffy Antigen Receptor for Chemokines (Darc)* in bone.**

We previously demonstrated evidence that genetic variation in DARC sequence contributes to peak bone density differences (31). To determine if the increased BMD in the DARC-KO mice is caused by changes in cortical and/or trabecular bone parameters, we used a micro-CT analysis at a resolution of 10 microns to measure cortical (at mid-diaphysis) and trabecular (at metaphysis) bone parameters (n=14-16). At the mid-diaphysis, total vBMD was not significantly different between DARC- KO and WT mice at 16 weeks of age ( $606 \pm 9$  vs  $620 \pm 9$  mg/cm<sup>3</sup>, P=0.26). Accordingly, no significant difference was found in cortical thickness between the KO and WT mice (data not shown). In contrast, at the metaphysis, trabecular bone volume/tissue volume was increased by 62% in the KO mice (P<0.001) which was consistent with the 45% increase in trabecular vBMD in the KO mice (n=14-16, P<0.001) compared to WT mice as measured by pQCT (data not shown). To determine the cause for increased trabecular bone volume and BMD, we measured trabecular bone microarchitecture (Micro-Ct measurements. Figure 17) and found increases in trabecular number (22%, P<0.01) and thickness (16%, P<0.01) and decreases (17.6%, P<0.01) in trabecular separation. The gain in trabecular elements increased the number of interconnections as reflected by 62% increase in connectivity density in the KO mice. These data together with the 20% decrease (P<0.001) in SMI, an estimate of prevalence of rods vs plates, suggest a decrease in bone resorption as the cause for the observed trabecular changes in the KO mice.

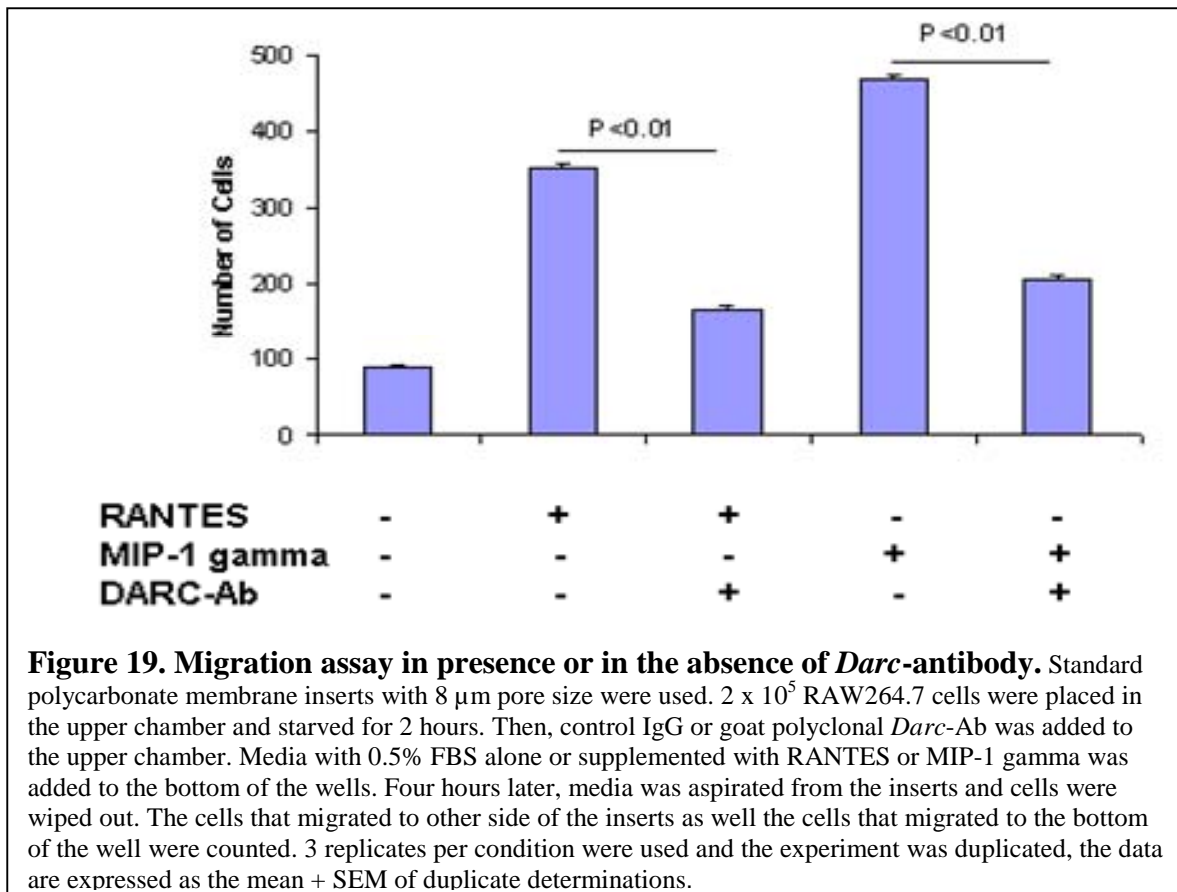


To determine if the increased femur vBMD in *Darc*-KO mice is due to an increase in bone formation or due to a reduction in BR, we have performed histomorphometry measurements at the metaphysis of femurs isolated from *Darc*-KO mice and from control *Darc*<sup>+/+</sup> mice (Figure 18).



We found TRAP positive bone resorbing surface was significantly reduced in the femurs isolated from the *Darc*-KO mice compared to control mice. In contrast, bone formation parameters were similar in both lines of mice.

To get more insight on the mechanism by which *DARC* could regulate bone resorption, we considered the possibility of the involvement of *DARC* in osteoclast fusion based on the finding that *DARC* protein is involved in the pro-migratory activities of chemokines on the endothelium-blood interface. Thus, to test the role of *DARC* in regulating chemotaxis in osteoclast precursors, we used a mouse monocyte cell line Raw264.7 as a model since it has been reported that RANKL increased the production of chemokines that bind to *DARC* in both Raw264.7 and bone marrow cells. To evaluate the prediction that *DARC* is involved in regulating mobility of osteoclast precursors towards chemokines, we determined the consequence of neutralizing *DARC* action on the migration of RAW264.7 cells towards chemokines (RANTES and MIP-1-gamma). The number of cells that migrated to bottom of the wells containing RANTES or MIP-1 gamma was significantly greater than the control. Furthermore, treatment of cells with *DARC*-antibody led to a significant reduction in the number of cells that migrated towards the bottom of the wells containing the chemokines. These data demonstrate that RAW264.7 cells migrate towards chemokines in the absence of RANKL and that chemotaxis of RAW264.7 cells towards chemokines is dependent on functional *DARC*. We continue to obtain additional preliminary data on the mechanism of *DARC* action that can be used as a supporting data for an extramural grant application to NIH.



## Key Findings

1. Mechanical loading by four-point bending in the mid-diaphysis produced osteogenic response in the wild type mice but not in the conditional IGF-I KO mice.
2. Axial loading of tibia increased both cortical and trabecular BMD in the wild type mice but not in the conditional IGF-I KO mice.
3. Mechanical loading-induced increase in Runx2 expression failed to occur in the IGF-I KO mice, thus suggesting IGF-I is essential for mechanical loading-induced increase in Runx2 expression. Mechanical loading-induced increases in bone density and bone size were not different between the Formin-2 KO and wild type mice. Our *in vitro* data together with the *in vivo* loading data demonstrate that deficiency of leptin expression or *Lepr* signaling enhanced the osteogenic response to mechanical stimulation
4. Several potential functional candidates in the mutant locus of 14104M did not show mutation in the coding region.
5. Trabecular BMD was significantly reduced in femur bones derived from *Darc*-KO mice compared to wild type control mice.
6. Bone resorption but not bone formation was reduced in *Darc*-KO compared wild type control.
7. Blocking *Darc* function with specific antibodies alters RAW264.7 cell migration towards chemokines.

## Conclusions

- 1) Osteoblast produced IGF-I is essential for the mechanical loading-induced increase in new bone formation, thus suggesting that other growth factors cannot compensate for the lack of local IGF-I to produce skeletal anabolic response to mechanical loading.
- 2) Formin-2 KO study proves that this gene is not a major mediator of skeletal anabolic response to loading.
- 3) Our sequencing studies of functional positional candidates in the 14104M mutant locus reveal that 14104M gene is a novel gene that regulates bone size.
- 4) Our *in vivo* and *in vitro* findings demonstrate that leptin signaling is an important negative regulator of mechanical loading response.
- 5) *Darc* affects trabecular BMD but regulating bone resorption.
- 6) The data from our *in vitro* assays demonstrated that RAW264.7 cells migrate towards chemokines in the absence of RANKL and that chemotaxis of RAW264.7 cells towards chemokines is dependent on functional *DARC*

## Reportable Outcomes

1. Oral presentation at the 31<sup>st</sup> Annual meeting of ASBMR for the paper entitled “Conditional Disruption of IGF-I Gene in Osteoblasts Demonstrates Obligatory and Non-Redundant Role of IGF-I in Skeletal Anabolic Response to Mechanical Loading”. 2009 - Denver, Colorado, USA
2. Kesavan C and Subburaman Mohan. Bone mass gained in response to external loading is lost following cessation of loading in 10 week C57BL/6J mice. Manuscript communicated to *Biomechanics and Modeling in Mechanobiology*, In Press.
3. Oral presentation at the 31<sup>st</sup> Annual meeting of ASBMR for the paper entitled “Lack of DARC, a BMD QTL Gene, Primarily Affects Trabecular but not Cortical Bone via inhibiting Bone Resorption”. 2009 - Denver, Colorado, USA

### References:

4. Gullberg B, Johnell O, Kanis JA 1997 World-wide projections for hip fracture. *Osteoporos Int* 7(5):407-13.
5. Akhter MP, Cullen DM, Pedersen EA, Kimmel DB, Recker RR 1998 Bone response to in vivo mechanical loading in two breeds of mice. *Calcif Tissue Int* 63(5):442-9.
6. Umemura Y, Baylink DJ, Wergedal JE, Mohan S, Srivastava AK 2002 A time course of bone response to jump exercise in C57BL/6J mice. *J Bone Miner Metab* 20(4):209-15.
7. Kesavan C, Mohan S, Oberholtzer S, Wergedal JE, Baylink DJ 2005 Mechanical loading-induced gene expression and BMD changes are different in two inbred mouse strains. *J Appl Physiol* 99(5):1951-7.
8. Bikle DD, Sakata T, Halloran BP 2003 The impact of skeletal unloading on bone formation. *Gravit Space Biol Bull* 16(2):45-54.
9. Lau KH, Kapur S, Kesavan C, Baylink DJ 2006 Up-regulation of the Wnt, estrogen receptor, insulin-like growth factor-I, and bone morphogenetic protein pathways in C57BL/6J osteoblasts as opposed to C3H/HeJ osteoblasts in part contributes to the differential anabolic response to fluid shear. *J Biol Chem* 281(14):9576-88.
10. Kapur S, Mohan S, Baylink DJ, Lau KH 2005 Fluid shear stress synergizes with insulin-like growth factor-I (IGF-I) on osteoblast proliferation through integrin-dependent activation of IGF-I mitogenic signaling pathway. *J Biol Chem* 280(20):20163-70.
11. Kapur S, Chen ST, Baylink DJ, Lau KH 2004 Extracellular signal-regulated kinase-1 and -2 are both essential for the shear stress-induced human osteoblast proliferation. *Bone* 35(2):525-34.
12. Boutahar N, Guignandon A, Vico L, Lafage-Proust MH 2004 Mechanical strain on osteoblasts activates autophosphorylation of focal adhesion kinase and proline-rich tyrosine kinase 2 tyrosine sites involved in ERK activation. *J Biol Chem* 279(29):30588-99.

13. Liedert A, Kaspar D, Blakytyn R, Claes L, Ignatius A 2006 Signal transduction pathways involved in mechanotransduction in bone cells. *Biochem Biophys Res Commun* 349(1):1-5.
14. Kunnel JG, Igarashi K, Gilbert JL, Stern PH 2004 Bone anabolic responses to mechanical load in vitro involve COX-2 and constitutive NOS. *Connect Tissue Res* 45(1):40-9.
15. Danciu TE, Adam RM, Naruse K, Freeman MR, Hauschka PV 2003 Calcium regulates the PI3K-Akt pathway in stretched osteoblasts. *FEBS Lett* 536(1-3):193-7.
16. Kesavan C, Mohan S, Srivastava AK, Kapoor S, Wergedal JE, Yu H, Baylink DJ 2006 Identification of genetic loci that regulate bone adaptive response to mechanical loading in C57BL/6J and C3H/HeJ mice intercross. *Bone* Sep;39(3):634-43.
17. Kesavan C, Baylink DJ, Kapoor S, Mohan S 2007 Novel loci regulating bone anabolic response to loading: expression QTL analysis in C57BL/6JXC3H/HeJ mice cross *Bone* Aug;41(2):223-30.
18. De Souza RL, Matsuura M, Eckstein F, Rawlinson SC, Lanyon LE, Pitsillides AA 2005 Non-invasive axial loading of mouse tibiae increases cortical bone formation and modifies trabecular organization: a new model to study cortical and cancellous compartments in a single loaded element. *Bone* 37(6):810-8.
19. Sugiyama T, Saxon LK, Zaman G, Moustafa A, Sunter A, Price JS, Lanyon LE 2008 Mechanical loading enhances the anabolic effects of intermittent parathyroid hormone (1-34) on trabecular and cortical bone in mice. *Bone* 43(2):238-48.
20. Ohashi N, Robling AG, Burr DB, Turner CH 2002 The effects of dynamic axial loading on the rat growth plate. *J Bone Miner Res* 17(2):284-92.
21. Alam I, Warden SJ, Robling AG, Turner CH 2005 Mechanotransduction in bone does not require a functional cyclooxygenase-2 (COX-2) gene. *J Bone Miner Res* 20(3):438-46.
22. Warden SJ, Turner CH 2004 Mechanotransduction in the cortical bone is most efficient at loading frequencies of 5-10 Hz. *Bone* 34(2):261-70.
23. Srinivasan S, Weimer DA, Agans SC, Bain SD, Gross TS 2002 Low-magnitude mechanical loading becomes osteogenic when rest is inserted between each load cycle. *J Bone Miner Res* 17(9):1613-20.
24. Xing W, Baylink D, Kesavan C, Hu Y, Kapoor S, Chadwick RB, Mohan S 2005 Global gene expression analysis in the bones reveals involvement of several novel genes and pathways in mediating an anabolic response of mechanical loading in mice. *J Cell Biochem* 96(5):1049-60.
25. Mohan S, Baylink DJ, Srivastava AK. 2007 A chemical mutagenesis screen to identify modifier genes that interact with growth hormone and TGF-beta signaling pathways. *Bone*. 2008 Feb;42(2):388-95.
26. Srivastava AK, Kapur S, Mohan S, Yu H, Kapur S, Wergedal J, Baylink DJ. 2005 Identification of novel genetic loci for bone size and mechanosensitivity in an ENU mutant exhibiting decreased bone size. *J Bone Miner Res* Jun; 20(6):1041-50.
27. Mohan S, Chest V, Chadwick RB, Wergedal JE, Srivastava AK. 2007 Chemical mutagenesis induced two high bone density mouse mutants map to a concordant distal chromosome 4 locus. *Bone* Nov; 41(5):860-8.

28. Wheeler HE, Metter EJ, Tanaka T, Absher D, Higgins J, Zahn JM, Wilhelmy J, Davis RW, Singleton A, Myers RM, Ferrucci L, Kim SK 2009 Sequential use of transcriptional profiling, expression quantitative trait mapping, and gene association implicates MMP20 in human kidney aging. *PLoS Genet.* 2009 Oct; 5(10):e1000685.
29. Umeno J, Matsumoto T, Esaki M, Kukita Y, Tahira T, Yanaru-Fujisawa R, Nakamura S, Arima H, Hirahashi M, Hayashi K, Iida M. 2009 Impact of group IVA cytosolic phospholipase A ( 2 ) gene polymorphisms on phenotypic features of patients with familial adenomatous polyposis. *Int J Colorectal Dis.* Oct 1.
30. Edvardson S, Hama H, Shaag A, Gomori JM, Berger I, Soffer D, Korman SH, Taustein I, Saada A, Elpeleg O 2008 Mutations in the fatty acid 2-hydroxylase gene are associated with leukodystrophy with spastic paraparesis and dystonia. *Am J Hum Genet* Nov;83(5):643-8.
31. Edderkaoui B, Baylink DJ, Beamer WG, Wergedal JE, Porte R, Chaudhuri A, Mohan S 2007 Identification of mouse Duffy antigen receptor for chemokines (Darc) as a BMD QTL gene. *Genome Res* May; 17(5):577-85.
32. Meyer-Lindenberg A, Nichols T, Callicott JH, Ding J, Kolachana B, Buckholtz J, Mattay VS, Egan M, Weinberger DR 2006 Impact of complex genetic variation in COMT on human brain function. *Mol Psychiatry* Sep; 11(9):867-77, 797.

## **Progress Report for the final 6 months of the Project Period**

**Technical Objective: Evaluate the influence of mechanical strain on bone regeneration.**

Bone injury is a serious health problem. There are a variety of causes for bone injury. However, the most common underlying cause is a medical condition called osteoporosis. Osteoporosis is a disease characterized by loss of bone tissue and low bone mass that lead to weak and fragile bones. In the United States, osteoporosis affects over 25 million people. Individuals that suffer osteoporosis are at increased risk for bone injury. It is predicted that about 50% of women and 12% of men older than 50 years will have an osteoporosis-related bone injury in their lifetime. The most common bone injury is fractures, which can occur at many sites of the body including radius, humerus, femur, ankle and spine [1]. Fall and hip fractures are the leading cause of often fatal injury to older people. More than one-third of adults ages 65 years and older fall each year in the United States. Fracture of the spine, i.e. vertebra fracture, is the most frequent fracture. Approximately 30-50% of women and 20-30% of men develop vertebra fractures [2]. Vertebra fractures are associated with reduced pulmonary functions, chronic back pain and loss of height among other symptoms [3]. Despite these serious effect, only 30% of the vertebra fractures and the most severe patients receive clinical attention [1]. Patients with one fracture often develop multiple fractures including those at other parts of the body during their life time [2]. Most of the fractures heal naturally within a reasonable time. However, normal healing of fractures is sometimes impaired by seriously delayed union or non-union of fractured bones [4]. The impaired healing occurs in 5-10% of the fractures [4-6], causing disability and pain to the patients, and requiring clinical interventions.

Clinical interventions of the impaired fracture healing involve surgical, biological, mechanical and biophysical enhancement [5]. In biological enhancement, therapeutic interventions using osteogenic and angiogenic factors have emerged as potential solutions to promote bone regeneration and to facilitate bone healing [5, 7-17]. The osteogenic and angiogenic factors that are currently used in therapeutics are transforming growth factors, bone morphogenetic proteins, and prostaglandins [5, 8, 9, 16, 18], which have not been shown to be very effective in promoting the healing of delayed union and non-union of the fractured bone. Identifying novel therapeutic molecules that enhance bone regeneration would greatly improve clinical treatment of osteoporosis and bone injury. The goal of this technical objective is to develop a new bone regeneration model in mice and to evaluate different strains of mice for their bone regenerative ability.

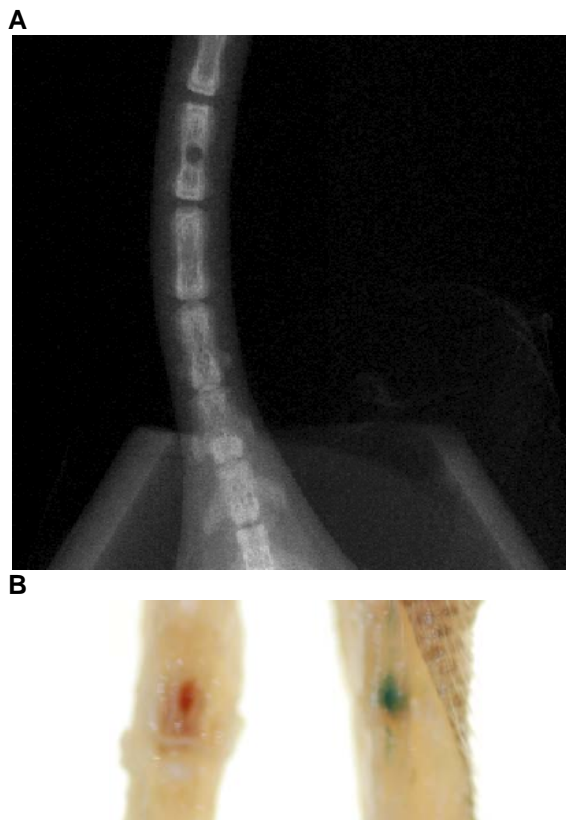


**Figure 1.** The drill holes in the tail vertebrae of mice. **(A)** The  $\mu$ CT image of a drill hole in the tail vertebrae of a MRL/MpJ mouse. The 0.71 mm hole is drilled with a Dremel dental tool using size 70 drill bit in the third vertebra. **(B)** Viral vectors transfected vertebrae stained in beta-galactosidase substrate a week after the tail drill and viral injection. **R:** MLV vector containing beta-galactosidase gene; **L:** MLV vector containing GFP gene.

ANOVA  $F = 8.69$   $P < 0.0001$

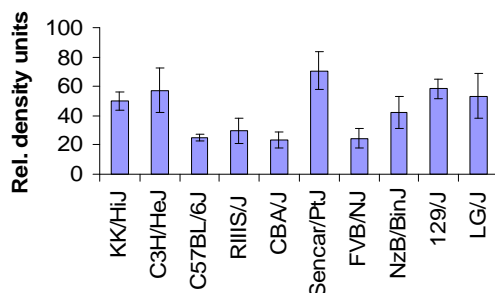


**Figure 2.** Bone generative capacity among inbred strains of mice as measured by relative density units. Values are mean of 3-10 mice plus and minus standard deviation.

#### Animal model for bone regeneration.

The ability to regenerate tissues is limited in mammals [19]. Bone is one of the very few mammalian adult tissues capable of healing without a scar, a process that is a truly regenerative process [20]. A common bone regeneration model is the fracture model. However, the fracture model is mainly associated with endochondral bone formation [21]. As an alternative, our group developed the “drill hole” model in mice [22], where the third vertebra from the base of the tail is used, and a through-through hole of less than 1 mm in diameter is drilled through. In the current project, we have improved this model by coupling with the state-of-the-art MicroCT technology in the quantification of bone formation (Figure 1A). We discovered that while a standard fracture leads to callus formation outside of the injury site with little bony union in the initial response, our data using this model indicated that nascent bone was formed directly within the drill hole. Observations from this as well as others show that in drill hole models bone is regenerated through intramembranous bone formation [23]. Because the strength of fractured bone is largely dependent on the extent of bony union at the fracture site [15], the “drill hole” model with intramembranous bone formation will be important for studies on bone regeneration.

In terms of the use of the drill hole model for in vivo functional testing, there are two advantages. First, this model is more effective. No surgery is needed for the animals. The therapeutic protein or viral particle solutions for interested genes can be easily injected subcutaneously into the

drill hole region of the tail. Because the injected therapeutic agent is localized around the drill hole, the therapeutic effect may be maximized. Second, compared with the femur fracture model, MicroCT to determine bone parameters can easily be done on live animals since the tail is naturally protruding out. We have conducted a study using this model for in vivo fractional testing. A MLV (murine leukemia virus) vector containing cDNA for the  $\beta$ -gal (beta-galactosidase) gene or GFP (green fluorescent protein) gene was injected. At day 7, the mice were euthanized, and the tails were excised. Then, skin was removed from the region of the third vertebra containing the drill hole. The tail vertebra bones were stained in an x-gal solution. It can be seen from Figure 1B that the drill hole at the center of the vertebra on the right, which was injected with a MLV vector containing the  $\beta$ -gal gene, stained blue as expected, while the one on the left, which was injected with a MLV vector containing the control GFP gene, showed a red blood clog, but no blue staining. This illustrates that the drill hole model can be used effectively for in vivo functional testing.

Because we experienced technical difficulties in using the tail vertebra healing model for mechanical strain studies, we focused on identifying genes and their pathways that contribute to bone regeneration as discussed below.

**Genetic variation in bone regeneration.** Our previous study using the drill hole model demonstrated that bone regenerative healing capacity differed significantly among major

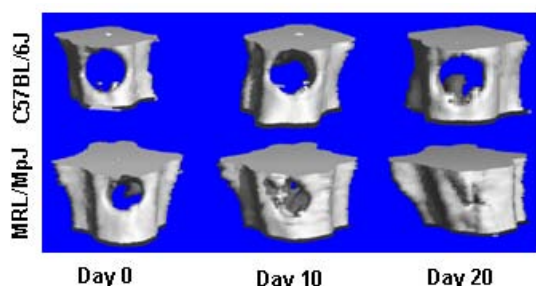


**Figure 3.** Reconstructed  $\mu$ CT images of drill holes in the tail vertebrae of mice showing the healing progression of the drill hole region in both MRL/MpJ and C57BL/6J mice.

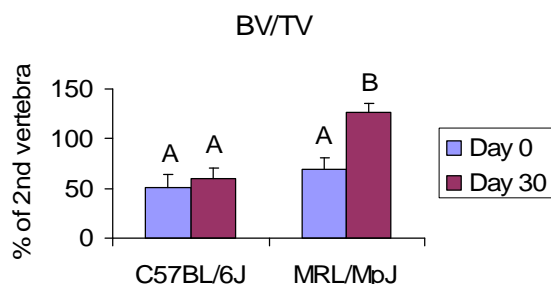


**Figure 4.** Changes of BV/TV between day 0 and day 30 after the tail drill. Values are mean of 3 C57BL/6J or 4 MRL/MpJ mice plus standard deviation. Values with the same letter are not significant from each other at  $P < 0.05$

**Table 1.** Histomorphometric and histological bone formation parameters of MRL/MpJ and C57BL/6J mice.

inbred strains of mice (Figure 2), and these differences were largely genetically determined with an estimated heritability of 72% [22]. While C57BL, a commonly used inbred strain in skeletal research, and many other strains were poor healers, there were good healers including Sencar/PtJ mice. C57BL was also shown to be a poor healer in the healing of ear soft tissues [24].

We also used MRL. We chose MRL based on the following two reasons. First, recent findings show that both cortical and trabecular bone mineral bone density (BMD) of distal femur and lumbar vertebrae is higher for MRL than for 12 other evaluated inbred strains [25], suggesting that MRL may be capable of fast bone regeneration. Second, we and others have shown that MRL mice have the unique ability to heal both soft and hard tissues. They can close ear punch holes quickly with features of regeneration [26, 27]. They also

exhibit superior ability of regenerating damaged cornea, heart tissues and amputated digit tips [28-32]. Thus, MRL may also be a good bone healer.

As shown in the  $\mu$ CT images derived from analyses of the preliminary data (Figure 3), MRL exhibited superior healing of the tail vertebra. Starting at day 10, it healed significantly better than C57BL. We used bone volume (BV/TV) as a measure of bone healing to compare the injured third vertebra with the control second vertebra. After 30 days of healing, bone volume of the injured third vertebra in C57BL was increased little when compared to day 0 (Figure 4). However, bone volume in the injured vertebra of MRL was increased to 127.0% of the control vertebra, which was significant from both the day 0 value of MRL and the day 30 value of C57BL. Thus, we conclude that the drill hole injury induced significantly more regeneration of trabecular bone in MRL than in C57BL, and MRL is a better healer.

**Table 2. Microarray based expression analysis of Rap1 during bone regeneration.**

	Day 5		Day 10	
	Fold Change <sup>a</sup>	p value	Fold Change <sup>a</sup>	p value
Rap1a	2.10	0.016	2.16	0.018
Rap1b	1.69	0.002	1.51	0.008

<sup>a</sup> Compared to day 0.

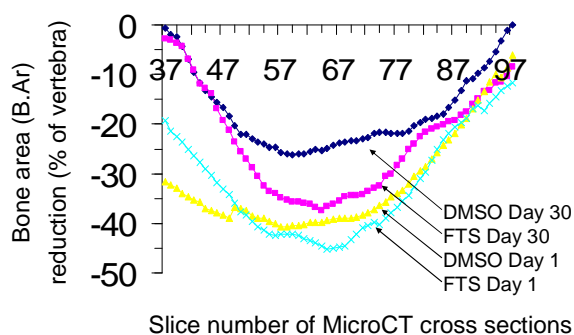


**Figure 5.** 2D  $\mu$ CT analysis of bone regeneration in the drill hole region. Values shown are bone area (B.Ar) reduction expressed as the percentage of the injured vertebra with the un-injured control vertebra as 100%. The number of mice is 4 and 6 for the FTS and DMSO group, respectively.

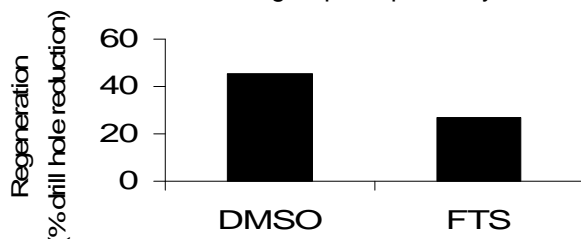


**Figure 6.** Effect of FTS injection on new bone regeneration expressed as the percentage of the drill hole filled averaged across the entire drill hole region as shown in Figure 5.

### Histological analysis of bone regeneration.

In addition to the  $\mu$ CT experiments, we have also conducted histology related experiments as part of our studies. The purpose is twofold: (1) to further quantify the healing difference between good healer MRL/MpJ and poor healer C57BL/6J, and (2) to determine what cell types are involved in this difference. By examining the cell types, we would be able to determine whether bone regeneration in the drill hole model is through intramembranous bone formation. To be specific, if we can determine that a newly formed mineralized bone is derived from osteoblasts rather than chondrocytes, then we can conclude that this model is an intramembranous bone formation event.

There are two observations from the obtained histology related data. First, the fluorescent calcein labeling experiment showed that the mineral apposition rate (MAR), which is a histomorphometric measure of bone formation, in the healing vertebra of MRL was 50% more than that in C57BL (3.30  $\mu$ m/day vs. 2.18  $\mu$ m/day), although

this difference has not reached statistical significance (Table 1). Goldner's trichrome staining of the injured vertebra cross sections revealed extensive osteoid areas, which are a histological measure of new bone formation. The osteoid width (O.Wi) in MRL was twice much as that in C57BL (27.6  $\mu\text{m}$  versus 11.03  $\mu\text{m}$ ), which was significant at  $P < 0.05$ . Therefore, MRL had more new bone formation than C57BL in the healing vertebra. Second, we noticed extensive staining for cartilage at other regions such as epiphyseal plates, but not at the drill hole region. The lack of cartilage suggests that bone regeneration in the drill hole model had mainly gone through intramembranous bone formation. Since the samples were collected at day 30, a late time for bone formation and it can be argued that some chondrocytes might have been converted to bone. However, based on our gene expression analysis, this is not the case. The gene expression analysis showed a strong up-regulation of the osteoblast specific genes at day 10, an early time point at the beginning of the rapid healing period.

*Ras genes in bone regeneration.* In order to identify genes that influence bone regeneration, especially those early expressing genes, we used the drill hole model to create an injury in MRL mice. We then conducted a microarray study using the vertebra bone tissues. Based on the analysis of the microarray data, we identified a list of genes that were up-regulated from day 0 at both day 5 and day 10. We screened this list of genes based on their functions by excluding structural genes and emphasizing transcriptional factors, growth factors and signal peptides. We further evaluated the selected genes for the presence of function domains in the peptides. In the end, we obtained about a dozen genes, among which there were several Ras oncogenes including Rap1 and Ran. There are two closely related forms of Rap1 [33], Rap1a and Rap1b, which share 95% amino acid identity. Both Rap1a and Rap1b were up-regulated significantly at both day 5 and day 10 time points during bone regeneration (fold change varies from 1.51 to 2.16) (Table 2). This result clearly shows the importance of the Ras oncogenes during the early phase of bone regeneration.

A Ras protein is located within the inner surface of cell membrane. Its association with membrane is promoted by farnesylation with the addition of a COOH-terminal farnesylcysteine carboxymethyl ester. If the farnesylation is blocked, the protein will remain in cytosol and lose its transforming activity that takes place in the nucleus. Therefore, Ras function can be inhibited by compounds that resemble farnesylcysteine of Ras that will affect interaction of Ras with cell membrane. One such compound is S-trans, trans-farnesylthiosalicylic acid (FTS). FTS competes with Ras for binding to Ras-escort proteins, which possess putative farnesyl-binding domains. Thus, FTS can dislodge oncogenic Ras proteins from the membrane anchorage sites and inhibits Ras transformation [34]. Also called salirasib as a cancer drug, FTS exhibits profound anti-oncogenic effect in many cancer cell lines [35, 36]. For example, Blum et al. [35] found that in human cells treated with FTS, growth was arrested and the cells died. To test any effect Ras has on bone regeneration in vivo, we carried out an experiment by injecting the Ras inhibitor FTS subcutaneously into the drill hole region of eight weeks old MRL mice. Bone regeneration was then quantified by the healing of the drill hole using MicroCT. We calculated the bone area (B.Ar) reduction in the percentage of the injured vertebra using the intact vertebra as 100%. First, we found that at the center of drill hole, bone area (B.Ar) in the DMSO treated mice at day 1 was -41% of the vertebra (Figure 5).

After a 30 day healing, this was increased to -26% (DMSO day 30), which represents an increase of 15% of the vertebra. These numbers can also be put in terms of drill hole reduction: the drill hole was  $15/41=37\%$  reduced or filled by new bone regeneration during the 30 day healing period. Similarly, at the center of the drill hole, bone area reduction in the FTS treated mice was -45% and -37% of the vertebra at day 1 and day 30, respectively. These numbers represent a bone area increase of 8% of the vertebra and a new bone regeneration of 18% of the drill hole. It can be seen that much less new bone was regenerated in the FTS treated mice than in the DMSO ones (18% vs. 37%), and FTS caused a reduction of nearly one-half of the new bone regeneration. Second, averaged across the entire drill hole region as shown in Figure 5, 45% of the drill hole was filled by new bone regeneration in the DMSO treated mice, while only 27% of the drill hole was regenerated in the FTS treated mice (Figure 6). This again shows that FTS caused a reduction of nearly one-half of the new bone regeneration compared to the DMSO control. Third, a factorial ANOVA analysis of the center region of the drill hole indicated that healing duration was a significant factor ( $p = 0.024$ ), and the injection treatment was close-to-significant ( $p = 0.08$ ).

To summarize, based on the microarray analysis we have identified a new class of factors, the Ras oncogenes for bone regeneration. The in vivo experiment using a Ras inhibitor showed an important role of Ras in bone regeneration. Chief among the Ras oncogenes was Rap1. Both Rap1a and Rap1b were significantly up-regulated during the early period of bone regeneration. Thus, Rap1 may have contributed to the observed Ras in vivo effect. Rap1 belongs to the Ras subfamily of Ras oncogenes. Members of this subfamily are involved in the regulation of cell proliferation, differentiation and survival [37-40]. The decreased bone regeneration in the healing tissue using the Ras inhibitor seems to suggest the positive role of Ras in cell proliferation and survival.

#### **Technical Objective: Continue evaluation of skeletal anabolic response to axial loading in IGF-I KO mouse versus littermate control**

In our 2009 progress report, we mentioned that we will be evaluating the bone formation response to loading using histology and gene expression analysis for the IGF-I project. In order to perform these two sets of experiment we generated conditional IGF-I KO and littermate controls during 2010. In our last loading experiment, in one group, mice were injected with calcein according to their body weight on the 1<sup>st</sup> and 10<sup>th</sup> days before the last day of loading. After the last day of loading, mice were euthanized; tibias were collected and fixed overnight with 10% cold neutral buffered formalin. Twenty four hours later, bones were rinsed with 1XPBS to be free of formalin and embedded in methyl methacrylate. Thick cross-sections (0.5 mm in thickness) were cut from the mid-diaphysis of the bones with a wire saw (Delaware Diamond Kives) and this cross-section was then ground lightly. For metaphyseal sections thin longitudinal section (5 microns) were cut, stained with Goldners trichrome stain, mounted in Fluoromount-G (Fisher Scientific, Pittsburgh, PA), or left unstained and examined under a Olympus BH-2 fluorescence/bright field microscope. Histomorphometric analysis was performed on these bones as described earlier.

To determine the impact of osteoblast derived IGF-I deficiency on bone formation response to mechanical loading, we performed histomorphometric measurements at the secondary spongiosa of trabecular bone on both loaded and non-externally loaded bones of IGF-I KO and WT mice. We found that osteoid perimeter, a measure of length of formation and trabecular thicknesses were increased by 60% approximately in the loaded bones of WT mice (Figure 7). In the IGF-I KO mice, no such increase was seen in any of these parameters in the loaded bones.

In our previous report, we mentioned that there was a small decrease in trabecular response to mechanical loading in the IGF-I KO mice in our micro-CT analysis which was an unexpected finding and thus, it also raises a question whether this is due to an increase in bone resorption. To address this, we measured TRAP labeled surface on the bones (loaded and non-externally loaded tibia) of both sets of mice to determine whether axial loading induced increase in bone resorption is the causes for the trabecular bone loss in the loaded bones of IGF-I knockout mice. However, the results from our study revealed no such increase in TRAP+ positive OC cells in the loaded bones of IGF-I KO mice. In contrast, in the loaded bones of WT mice, we found a significant decrease in TRAP+ OC cells suggesting that axial loading blocks bone resorption. These findings, together demonstrate that loss of trabecular bone in the loaded bones of IGF-I KO mice is not due to increase in bone resorption. However, further study is require to provide an

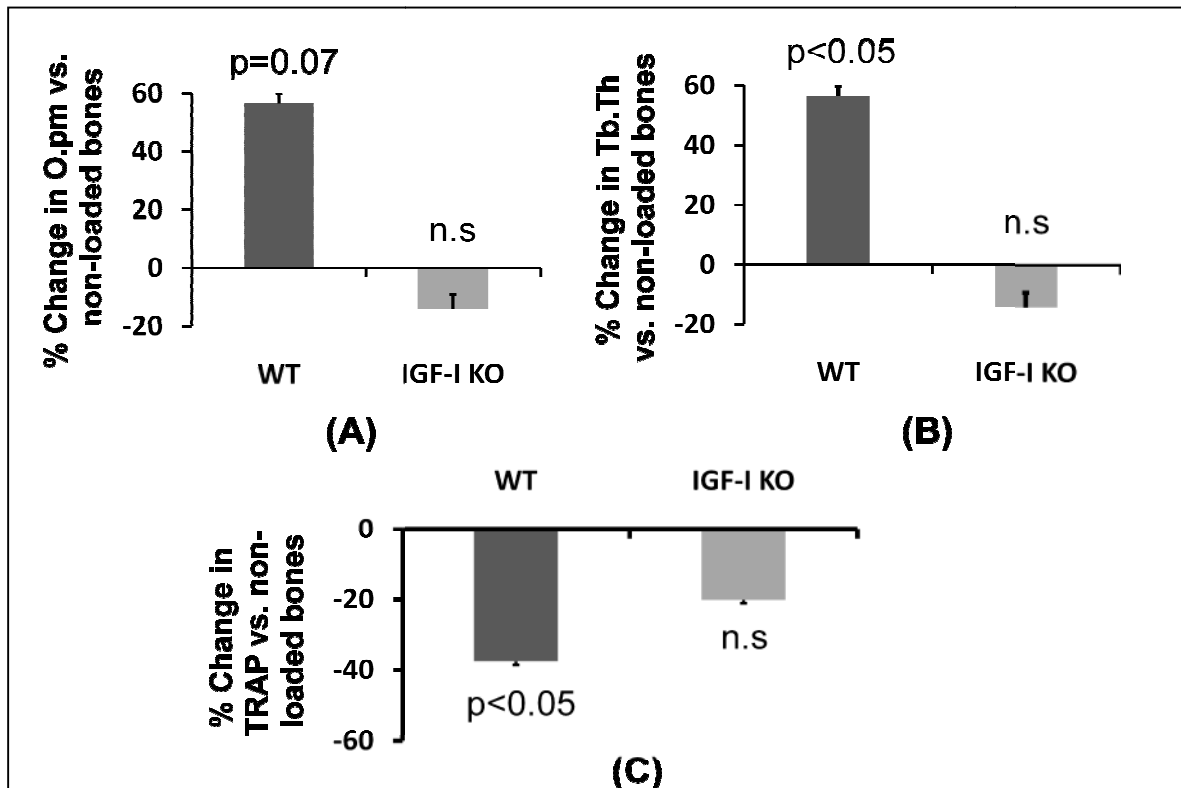


**Figure 7:** Histomorphometric analyses of bone formation response to axial loading in IGF-I KO and wild type mice. Values are mentioned as mean  $\pm$  SE. The O.pm, osteoid perimeter; Tb.Th, trabecular thickness and TRAP, tartrate-resistance acidic phosphatase, N=9.

explanation for the small loss of trabecular bone volume in the IGF-I KO mice in response to loading.

Now, using both tomography and loading models, we have shown that osteoblast derived IGF-I are involved in mediating bone anabolic response to mechanical loading, the next phase of our study is to identify the molecular components that are down stream of IGF-I contributing for the increased bone anabolic response to loading using mRNA from osteoblast derived IGF-I mice. After the last day of mechanical loading, we extracted RNA from the loaded and non-externally loaded bones using qiagen lipid extraction kit [Qiagen, Valencia, CA], as previously described. Quality and quantity of RNA were analyzed using the 2100 Bio-analyzer (Agilent, Palo Alto, CA, USA) and Nano-drop (Wilmington, DE). We used a Real time RT-PCR approach to measure mRNA levels of various genes in the loaded and non-externally loaded bones of both IGF-I KO and WT mice. These includes dentin matrix sialoprotein, IGF-I, Tnnt2, ephrin B2, ephrin A2, ephrin A4, b-catenin, EphB2, EphB4, Nr4a3, SOST, Osterix and SDF1. The rationale for selecting these genes was based on our earlier findings in microarray and QTL study, and their relevance in bone [41-45]. Real time RT-PCR was carried out according to the manufacturer's instructions (ABI PRISM, Foster City, CA.) using the SYBR Green method on 7900 Sequence Detection systems from Applied Biosystems. Briefly, purified total RNA [200µg/µl] was used to synthesize the first strand cDNA by reverse transcription according to the manufacturer's instructions [Bio-Rad, CA]. 5µl of the five times diluted first strand cDNA reaction, was subjected to real time PCR amplification using gene specific primers as described earlier. The data were analyzed using SDS software, version 2.0, and the results were exported to Microsoft Excel for further analysis. Data normalization was accomplished using the endogenous control ( $\beta$ -actin, PPIA) to correct for variation in the RNA quality among samples. The normalized Ct values were subjected to a  $2^{-\Delta\Delta Ct}$  formula to calculate the fold change between the non-externally loaded and loaded groups. The formula and its derivations were obtained from the instrument user guide. The results from our study show that IGF-I, ephrin B1, B2, A2, EphB2, Nr4a3 and Tnnt2 expression were different in the loaded bones of WT mice (1.5 to 3-fold,  $p < 0.05$ ) when compared to non-externally loaded bones. In contrast, in the IGF-I KO mice, there was no change in any of these genes in the loaded bones compared to non-externally loaded bones (Table-3).

Our results revealed several genes that differentially expressed in loaded and unloaded bones. Among these, increase in IGF-I gene expression in response to loading in the WT mice provides substantial evidence for the proposed hypothesis in this study. In addition to this, increase in other genes such as ephrin A2, B1, B2, EphB2, Nr4a3 and Tnnt2 in response to loading in the WT but not in the IGF-I KO mice suggests that these genes, to some extent, in part are, responsible for the IGF-I mediated bone anabolic response to loading. Reports in the past have shown that ephrin B1, B2, EphB2 and Nr4a3 are involved in osteoblast differentiation, however, our study shows that they are also involved in bone response to mechanical loading [41-43, 45] Increase in ephrin A2, EphB2 and Tnnt2 are new and their relevance to bone is yet to be determined. Presently, we are evaluating the expression levels of more possible candidates and our future goal is to utilize various molecular approaches to determine the functional role of these genes in relation to bone adaptive response to mechanical loading.

**Table -3** Quantitative analysis of mRNA levels of genes measured by real time RT-PCR after two weeks of axial loading on 10 week IGF-I KO and wild type mice.

Genes	Fold Change	
	WT	IGF-I KO
Insulin like growth factor-1	2.34 ± 0.28 *	1.0 ± 0.16
Ephrin B2	2.06 ± 0.1 *	0.51 ± 0.07
Ephrin A2	1.7 ± 0.04 *	0.59 ± 0.06
EphB2	3.94 ± 2.5*	1.3 ± 1.1
EphB4	1.3 ± 0.81	0.77 ± 0.68
Tnnt2	4.5± 2.0*	1.5 ±1.0
Ephrin B1	2.3±1.3*	0.97±1.0

\*p<0.05 vs. non-externally loaded bones, Values are Mean ± SE, N=5-6

**Technical Objective: Continue to evaluate if 14104M gene is a mechanosensitive gene.**

The bone size of 14104M mutant is smaller compared to corresponding control mice. Because the amount of mechanical strain that a bone receives for a given load is largely determined by the size of the bone, we measured mechanical strains of bones derived from mutant and control mice to determine loads that produce similar amounts of strain in the two strains of mice. Accordingly, we measured mechanical strain by using a strain gauge technique on the tibia of 10 week ENU mutant mice and WT male mice. We found 9N load produced 477 µε (N=3) which is equal to 6N load in the ENU mutant male mice that produced 411 µε (N=5). Based on this data, we propose to apply adjusted load on tibia of mutant and WT mice such that both sets of mice receive same amount of mechanical strain.

During the year 2010, we have generated enough female mutant and littermate controls to perform mechanical loading and evaluate bone anabolic response to loading. PIXIMUS was performed at age 4 and 8 weeks to differentiate the mutant mice from littermate controls. At 10 weeks of age, we applied mechanical load on tibia of these mice using axial method [46, 47]. We chose this model for the following reasons: 1) Axial loading model induces stress on the whole bone and the loading pattern mimics the

exercise pattern in humans; 2) This model induces both cortical and trabecular response, a site more relevant to osteoporosis; 3) the load frequency and cycles applied to the mouse tibia are controlled by an external device; 4) It avoids the need for external controls because the right tibia is used for loading and the left tibia as contralateral controls and 5) We have reported from past studies that axial loading has caused a 8 to 25% increase in both cortical and trabecular BMD and total volume, respectively in C57BL/6J mice, which is caused by greater increase in bone formation. Adjusted axial load (Trapezoidal-shaped pulse period=0.1s [loading 0.025s, hold 0.05s and unloading 0.025s]; rest time between pulse=10 s; cycles/day=40) were applied on the right tibia of female 14104 mutant and WT mice such that both sets of mice receive the same amount of mechanical strain. The left tibia was used as a contralateral internal control. The loading was performed on 3 alternate days/ week for 2 weeks. After the last day of loading mice were euthanized, bones were collected and immersed in PBS for further analysis.

Micro-Ct measurements revealed that two weeks of adjusted axial load caused an 8% change in the total area followed by a 5% change in the BV/TV of cortical bone in the control mice while in the 14104 mutant mice little or no change was seen. In addition to cortical bone, we also analyzed the effect of loading on the trabecular bone of 14104 mutant and WT mice. We found that the trabecular response was increased in the WT mice but not in the 14104 mutant mice in response to loading. The results from our study show that BV/TV and trabecular thickness were increased by 40 and 20% respectively in the WT mice while in the 14104 mutant mice little or no change was seen. Our findings that the skeletal anabolic response to mechanical strain is impaired in the 14104M mutant mice are consistent with our hypothesis that the 14104M gene is likely to be a mechanosensitive gene. Future elucidation of the signaling pathway by which 14104M mediates its effects in bone should lead to increased understanding of the mechanism for mechanical loading effects on skeleton and identification of gene variants that contribute to variation in skeletal anabolic response to loading in different army recruits.

#### **Additional Progress – Studies on the role of Duffy Antigen Receptor for Chemokines (Darc) in bone.**

*DARC* is also known to regulate cells transendothelial migration of certain cell types. it has been recently demonstrated that osteoclast precursors have to transmigrate through vascular endothelial cells to reach bone sites. Thus, we proposed the hypothesis that *Darc* functions to regulate chemokine mediated-transendothelial migration of osteoclast precursors (OCP). To test this hypothesis, we performed transendothelial migration assay using mouse brain endothelial cell line to form monolayer at the bottom of the inserts. RANTES was added at the bottom of the wells as a chemoattractant, and mouse monocyte cell line RAW264.7 were added to the transwells, Then, the cells that migrated to the other side of the transwell as well as the cells that migrated to the bottom of the wells were collected and counted. To evaluate the role of *DARC* in transmigration of osteoclast precursors, we compared the transmigration of transgenic RAW264.6 cells that overexpress *Darc* with Raw cells transfected with empty vector. We found transmigration of cells towards chemokine, RANTES, was increased several fold in control RAW cells

which is not surprising since these cells express *Darc* endogenously. Furthermore, a significant increase in cell transmigration towards RANTES was observed in Raw cells expressing *Darc* compared to control RAW cells (Figure 8). These data demonstrate that osteoclast transmigration towards chemokine is in part regulated by *Darc*.

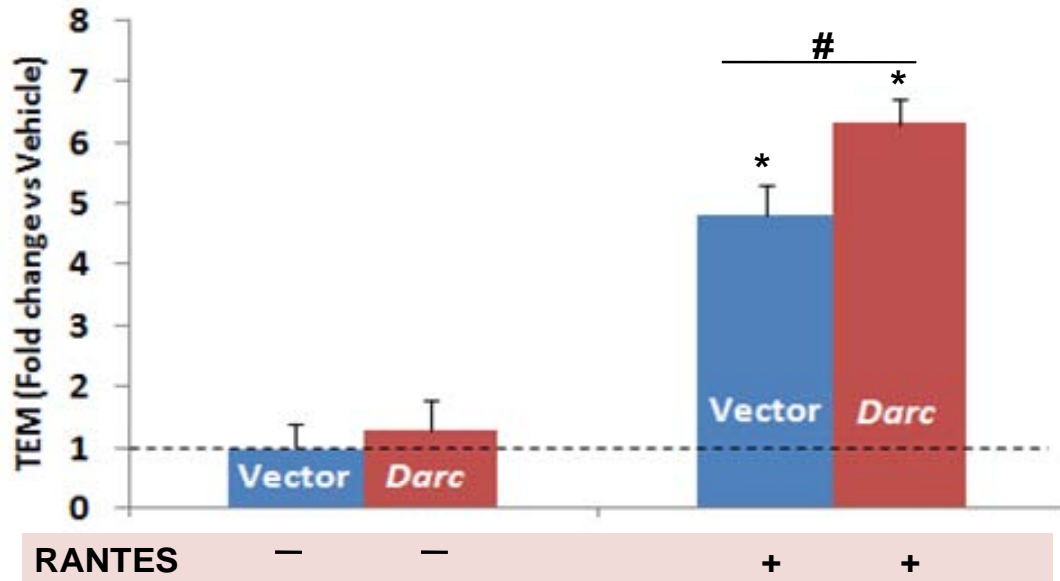


**Figure 8. Over-expression of *Darc* gene in RAW264.7 cells enhances transendothelial migration (TEM).** n = 6, \*P<0.05 vs vehicle treated, #P<0.05 Darc vs vector control.

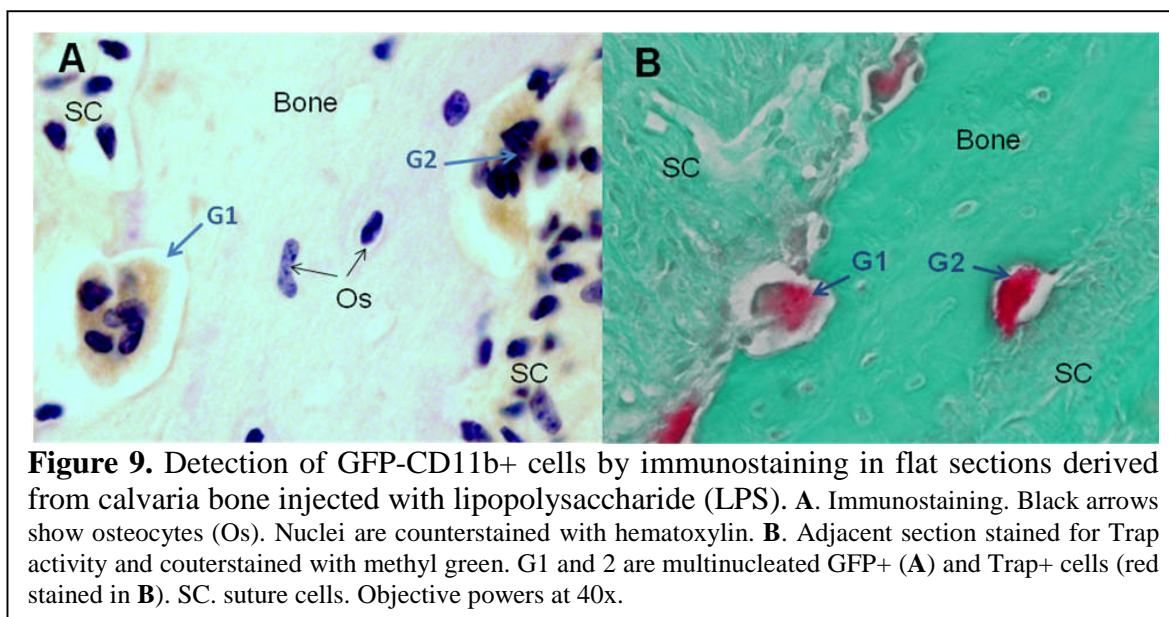
To assess the transendothelial migration (TEM) of osteoclast precursors (OCP) from blood circulation to inflammation sites, we have used CD11b as a marker to isolate OCP cells. This gene is only expressed in hematopoietic cells and is up-regulated during myeloid differentiation, with the highest levels in mature monocytes, macrophages and neutrophils (48, 49). CD11b gene is also expressed along osteoclast differentiation pathway from mononucleated early osteoclast progenitor cells to mature polynucleated osteoclast (50, 51). Bone marrow cells (BMCs) were flushed out from femurs and tibia bones collected from two female C57BL/6-Tg-GFP (GFP) mice. Erythrocytes were lysed using ammonium chloride solution. Table 4 shows the number of BMCs collected before and after lysis and the percentage of CD11b positive cells was evaluated by FACSDiva software (version 6.1). We recovered approximately 4 million CD11b+ cells from 2 mice, which represent ~ 18% of total BMCs after lysis. Thus, we don't anticipate any problem in isolating adequate numbers of CD11b+ cells from the donor mice for the proposed work.

**Table.4. Number of BM cells used and the percentage of CD11b+ before and after sorting.**

Number of cells	Whole BMCs	CD11b +	GFP/CD11b+
Before lysis	245.3 .10 <sup>6</sup>	19.9%	14.4%
After lysis	24.7 .10 <sup>6</sup>	55.1%	34.3
After sorting	4.38 . 10 <sup>6</sup>	91.6%	48.2%

Local injection of 20 µl bacterial LPS (100 µg) was performed subcutaneously on

the top of the parietal bone of WT C57BL/6 (B6) mice. Six hours later, mice received retro-orbital injection of the collected  $10^6$  CD11b<sup>+</sup> cells. Mice were, then, sacrificed 2 days-post injection. Calvaria bone was collected and fixed in 10% buffered formalin. Then, bones were partially decalcified in EDTA for 4 days. Paraffin-embedded sections (serial sections of 5  $\mu$ m) were processed for immunostaining using a primary goat anti-GFP antibody (Rockland, PA, USA) and a horse anti-goat antibody conjugated to avidin-biotin and developed with peroxidase using the manufacturer's protocols (Vector Laboratories, CA, USA). Images were acquired using light microscope (model BX60; Olympus) equipped with a digital camera (model DP72; Olympus). The adjacent section of each immunostained section was used for TRAP-staining. Figure 9 shows the GFP cells that show Trap-activity from calvaria bone injected with LPS. Thus, our preliminary data showed that systemically administered OCP reach inflammation site and form Trap<sup>+</sup> osteoclasts in two days-post injection. These data will form preliminary data for an RO1 grant to investigate the molecular pathway involved in OCP recruitment. The establishment of the molecular mechanism by which *Darc* regulates recruitment of OCPs to inflammatory sites could provide novel pathway targets for the development of therapies for osteoporosis, osteoarthritis and other bone diseases.



## Conclusions

- 1) Our group previously developed the “drill hole” model in mice. In the current project, we have improved the plausibility and accuracy of this model by coupling with the state-of-the-art MicroCT technology in the quantification of bone formation. Transfection studies with MLV vector cDNA containing the  $\beta$ -galactosidase gene or the GFP gene indicated

- that the drill hole model can be used effectively for in vivo functional testing.
- 2) Using the drill hole model, we have demonstrated that there was a wide range of genetic variation among major inbred strains of mice, the drill hole injury induced significantly more regeneration of trabecular bone in MRL/MpJ mice than in other mice, and MRL is a better bone healer.
  - 3) Evidence from histological analysis shows that bone regeneration in the drill-hole model is through intramembranous bone formation, and supports the conclusion that MRL is a good bone healer.
  - 4) Based on the microarray analysis of the drill hole model, we have identified a new class of factors, the Ras oncogenes, for bone regeneration. The decreased bone regeneration in the healing tissue treated with a Ras inhibitor seemed to suggest a positive role of Ras in cell proliferation and survival. Therefore, Ras is important in bone regeneration.
  - 5) Our study demonstrates that osteoblast derived IGF-I are critical in mediating mechanical signal into anabolic signal in bone and other growth factors cannot compensate for the loss of osteoblast derived IGF-I.
  - 6) Real time RT-PCR led to identify several genes downstream of IGF-I in mediating bone anabolic response to loading.
  - 7) Micro-CT findings revealed that 14104 mutant mice are less sensitive to mechanical loading.
  - 8) Transendothelial migration assay showed that osteoclast transmigration towards chemokine is in part regulated by *Darc*.
  - 9) We have showed that osteoclast precursors have to transmigrate through blood vessels to reach bone inflamed site for subsequent resorption.

## References

1. Gallacher, S.J., et al., *The prevalence of vertebral fracture amongst patients presenting with non-vertebral fractures*. Osteoporos Int, 2007. **18**(2): p. 185-92.
2. Suzuki, N., O. Ogikubo, and T. Hansson, *The course of the acute vertebral body fragility fracture: its effect on pain, disability and quality of life during 12 months*. Eur Spine J, 2008. **17**(10): p. 1380-90.
3. Lewiecki, E.M. and A.J. Laster, *Clinical review: Clinical applications of vertebral fracture assessment by dual-energy x-ray absorptiometry*. J Clin Endocrinol Metab, 2006. **91**(11): p. 4215-22.
4. Megaw, P., *Classification of non-union*. Injury, 2005. **36 Suppl 4**: p. S30-7.
5. Einhorn, T.A., *Enhancement of fracture-healing*. J Bone Joint Surg Am, 1995. **77**(6): p. 940-56.
6. Hannouche, D., H. Petite, and L. Sedel, *Current trends in the enhancement of fracture healing*. J Bone Joint Surg Br, 2001. **83**(2): p. 157-64.
7. Eckardt, H., et al., *Recombinant human vascular endothelial growth factor enhances bone healing in an experimental nonunion model*. J Bone Joint Surg Br, 2005. **87**(10): p. 1434-8.

8. Egermann, M., et al., *Direct adenoviral transfer of bone morphogenetic protein-2 cDNA enhances fracture healing in osteoporotic sheep*. Hum Gene Ther, 2006. **17**(5): p. 507-17.
9. Egermann, M., et al., *Effect of BMP-2 gene transfer on bone healing in sheep*. Gene Ther, 2006. **13**(17): p. 1290-9.
10. Einhorn, T.A., et al., *A single percutaneous injection of recombinant human bone morphogenetic protein-2 accelerates fracture repair*. J Bone Joint Surg Am, 2003. **85-A**(8): p. 1425-35.
11. Jingushi, S., et al., *Acidic fibroblast growth factor (aFGF) injection stimulates cartilage enlargement and inhibits cartilage gene expression in rat fracture healing*. J Orthop Res, 1990. **8**(3): p. 364-71.
12. Joyce, M.E., S. Jingushi, and M.E. Bolander, *Transforming growth factor-beta in the regulation of fracture repair*. Orthop Clin North Am, 1990. **21**(1): p. 199-209.
13. Kawaguchi, H., et al., *Acceleration of fracture healing in nonhuman primates by fibroblast growth factor-2*. J Clin Endocrinol Metab, 2001. **86**(2): p. 875-80.
14. Pelled, G., et al., *Direct Gene Therapy for Bone Regeneration: Gene Delivery, Animal Models and Outcome Measures*. Tissue Eng Part A, 2009.
15. Rundle, C.H., et al., *Retroviral-based gene therapy with cyclooxygenase-2 promotes the union of bony callus tissues and accelerates fracture healing in the rat*. J Gene Med, 2008. **10**(3): p. 229-41.
16. Tarkka, T., et al., *Adenoviral VEGF-A gene transfer induces angiogenesis and promotes bone formation in healing osseous tissues*. J Gene Med, 2003. **5**(7): p. 560-6.
17. Yasko, A.W., et al., *The healing of segmental bone defects, induced by recombinant human bone morphogenetic protein (rhBMP-2). A radiographic, histological, and biomechanical study in rats*. J Bone Joint Surg Am, 1992. **74**(5): p. 659-70.
18. Keila, S., A. Kelner, and M. Weinreb, *Systemic prostaglandin E2 increases cancellous bone formation and mass in aging rats and stimulates their bone marrow osteogenic capacity in vivo and in vitro*. J Endocrinol, 2001. **168**(1): p. 131-9.
19. Heber-Katz, E., et al., *Spallanzani's mouse: a model of restoration and regeneration*. Curr Top Microbiol Immunol, 2004. **280**: p. 165-89.
20. Rundle, C.H., et al., *Microarray analysis of gene expression during the inflammation and endochondral bone formation stages of rat femur fracture repair*. Bone, 2006. **38**(4): p. 521-9.
21. Adams, S.L., A.J. Cohen, and L. Lassoova, *Integration of signaling pathways regulating chondrocyte differentiation during endochondral bone formation*. J Cell Physiol, 2007. **213**(3): p. 635-41.
22. Li, X., et al., *Genetic variation in bone-regenerative capacity among inbred strains of mice*. Bone, 2001. **29**(2): p. 134-40.
23. Monfoulet, L., et al., *Bone sialoprotein, but not osteopontin, deficiency impairs the mineralization of regenerating bone during cortical defect healing*. Bone. **46**(2): p. 447-52.
24. Li, X., et al., *Analysis of gene expression in the wound repair/regeneration process*. Mamm Genome, 2001. **12**(1): p. 52-9.

25. Sabsovich, I., et al., *Bone microstructure and its associated genetic variability in 12 inbred mouse strains: microCT study and in silico genome scan*. Bone, 2008. **42**(2): p. 439-51.
26. Clark, L.D., R.K. Clark, and E. Heber-Katz, *A new murine model for mammalian wound repair and regeneration*. Clin Immunol Immunopathol, 1998. **88**(1): p. 35-45.
27. Heber-Katz, E., *The regenerating mouse ear*. Semin Cell Dev Biol, 1999. **10**(4): p. 415-9.
28. Chadwick, R.B., et al., *Digit tip regrowth and differential gene expression in MRL/Mpj, DBA/2, and C57BL/6 mice*. Wound Repair Regen, 2007. **15**(2): p. 275-84.
29. Haris Naseem, R., et al., *Reparative myocardial mechanisms in adult C57BL/6 and MRL mice following injury*. Physiol Genomics, 2007. **30**(1): p. 44-52.
30. Heber-Katz, E., et al., *The scarless heart and the MRL mouse*. Philos Trans R Soc Lond B Biol Sci, 2004. **359**(1445): p. 785-93.
31. Leferovich, J.M., et al., *Heart regeneration in adult MRL mice*. Proc Natl Acad Sci U S A, 2001. **98**(17): p. 9830-5.
32. Ueno, M., et al., *Accelerated wound healing of alkali-burned corneas in MRL mice is associated with a reduced inflammatory signature*. Invest Ophthalmol Vis Sci, 2005. **46**(11): p. 4097-106.
33. Yan, J., et al., *Rap1a is a key regulator of fibroblast growth factor 2-induced angiogenesis and together with Rap1b controls human endothelial cell functions*. Mol Cell Biol, 2008. **28**(18): p. 5803-10.
34. Gana-Weisz, M., et al., *The Ras inhibitor S-trans,trans-farnesylthiosalicylic acid chemosensitizes human tumor cells without causing resistance*. Clin Cancer Res, 2002. **8**(2): p. 555-65.
35. Blum, R., et al., *Ras inhibition in glioblastoma down-regulates hypoxia-inducible factor-1alpha, causing glycolysis shutdown and cell death*. Cancer Res, 2005. **65**(3): p. 999-1006.
36. Rotblat, B., et al., *The Ras inhibitor farnesylthiosalicylic acid (Salirasib) disrupts the spatiotemporal localization of active Ras: a potential treatment for cancer*. Methods Enzymol, 2008. **439**: p. 467-89.
37. Gao, L., et al., *Ras-associated protein-1 regulates extracellular signal-regulated kinase activation and migration in melanoma cells: two processes important to melanoma tumorigenesis and metastasis*. Cancer Res, 2006. **66**(16): p. 7880-8.
38. Ishida, D., et al., *Myeloproliferative stem cell disorders by deregulated Rap1 activation in SPA-1-deficient mice*. Cancer Cell, 2003. **4**(1): p. 55-65.
39. Munemitsu, S., et al., *Molecular cloning and expression of a G25K cDNA, the human homolog of the yeast cell cycle gene CDC42*. Mol Cell Biol, 1990. **10**(11): p. 5977-82.
40. Wennerberg, K., K.L. Rossman, and C.J. Der, *The Ras superfamily at a glance*. J Cell Sci, 2005. **118**(Pt 5): p. 843-6.
41. Allan, E.H., et al., *EphrinB2 regulation by PTH and PTHrP revealed by molecular profiling in differentiating osteoblasts*. J Bone Miner Res, 2008. **23**(8): p. 1170-81.

42. Pirih, F.Q., et al., *Parathyroid hormone induces the nuclear orphan receptor NOR-1 in osteoblasts*. Biochem Biophys Res Commun, 2003. **306**(1): p. 144-50.
43. Raab-Cullen, D.M., et al., *Mechanical loading stimulates rapid changes in periosteal gene expression*. Calcif Tissue Int, 1994. **55**(6): p. 473-8.
44. Xing, W., et al., *Global gene expression analysis in the bones reveals involvement of several novel genes and pathways in mediating an anabolic response of mechanical loading in mice*. J Cell Biochem, 2005. **96**(5): p. 1049-60.
45. Xing, W., et al., *Ephrin B1 regulates bone marrow stromal cell differentiation and bone formation by influencing TAZ transactivation via complex formation with NHERF1*. Mol Cell Biol. **30**(3): p. 711-21.
46. Alam, I., et al., *Mechanotransduction in bone does not require a functional cyclooxygenase-2 (COX-2) gene*. J Bone Miner Res, 2005. **20**(3): p. 438-46.
47. De Souza, R.L., et al., *Non-invasive axial loading of mouse tibiae increases cortical bone formation and modifies trabecular organization: a new model to study cortical and cancellous compartments in a single loaded element*. Bone, 2005. **37**(6): p. 810-8.
48. Beller DI, Springer TA, Schreiber RD. *Anti-Mac-1 selectively inhibits the mouse and human type three complement receptor*. J Exp Med. 1982;156(4):1000-9.
49. Rosmarin AG, Weil SC, Rosner GL, Griffin JD, Arnaout MA, Tenen DG. *Differential expression of CD11b/CD18 (Mo1) and myeloperoxidase genes during myeloid differentiation*. Blood. 1989;73(1):131-6.
50. Fujikawa Y, Quinn JM, Sabokbar A, McGee JO, Athanasou NA. *The human osteoclast precursor circulates in the monocyte fraction*. Endocrinology. 1996;137(9):4058-60.
51. Shalhoub V, Elliott G, Chiu L, Manoukian R, Kelley M, Hawkins N, Davy E, Shimamoto G, Beck J, Kaufman SA, Van G, Scully S, Qi M, Grisanti M, Dunstan C, Boyle WJ, Lacey DL. *Characterization of osteoclast precursors in human blood*. Br J Haematol. 2000;111(2):501-12.

## Part B – In vitro studies

### Progress for the Period of 2001 to 2003

Our goal is to evaluate the effects of mechanical signaling using a physiologically relevant CytoDyne flow chamber in order to produce a fluid flow shear strain for evaluation of proliferation and differentiation and also for studies of gene expression and signal transduction pathways in cultures of C3H and B6 mouse osteoblasts.

This report includes our progress for the first twelve months of our proposed work. The specific objectives for Technical Objective 3 as described in our proposal are:

- 1) Apply the CytoDyne flow chamber to evaluate mechanical signaling of osteoblast cells *in vitro*. This will first involve the development of the optimal flow- conditions to obtain measurable responses to two *in vitro* parameters, namely bone cell proliferation and differentiation. Differentiation will be assessed initially by alkaline phosphatase activity and, subsequently, will be confirmed by other differentiation markers, such as N-terminal procollagen peptide production for example.
- 2) Evaluate dose-response in terms of levels of strain and continuous vs. pulsated flow.
- 3) Determine the bone cells' time response to optimal flow conditions. The doses of fluid flow shear strain will range from 0.5 to 10 dynes/cm<sup>2</sup>.
- 4) Phenotypic analysis will be made in 8-week old mice, whereas it is easier to culture osteoblasts from newborn mice. Therefore, we will compare the phenotypic differences between the C3H and the B6 mice in response to fluid flow shear strain to determine if these are evident in bone cells derived from newborn mice; in which case, we would use newborn mice as a surrogate for our 8-week old mice.
- 5) Once the optimal conditions for fluid flow shear strain have been established, we will begin to evaluate strain-induced tyrosine phosphorylation levels of key signaling proteins by immunoprecipitation-immunoblotting approach using available antibodies.
- 6) Once we have established the optimal fluid flow shear strain conditions, we will begin to apply microarray technology to evaluate gene expression in osteoblasts exposed to fluid flow shear strain.

We have accomplished most of the above specific objectives; our progress in each of these specific objectives is given below.

### Progress on Technical Objective 3

Several *in vitro* models have been developed to evaluate mechanical signaling in the past. Application of mechanical force to bone can produce two different localized mechanical strains on bone cells: 1) deformation of extracellular matrix (physical strain); and 2) increased extracellular fluid flow (shear strain). Accordingly, there are at least two forms of mechanical strain that can be applied to cultured bone cells: physical strain that is created by physical deformation of the cell by application of mechanical stress on the bone matrix and fluid flow strain that is caused by the changes in blood flow and interstitial fluid flow due to loading induced intraosseous pressure changes.

Several reports in the literature have indicated that fluid flow shear strain would be more relevant to bone cell metabolism than the physical strain. In this regard, Dr. Frangos of the

University of California at San Diego has developed a Cytodyne Flow Chamber that could generate a defined fluid flow shear strain on cultured cells, including osteoblasts. Consequently, we decided to set up the Cytodyne Flow Chamber in our laboratory for our investigation of fluid flow shear on cultured bone cells.

We elected to determine the optimal conditions for application of the CytoDyne flow chamber using human osteosarcoma cells for Specific Objectives 1, 2 and 3. These conditions were then used to make specific evaluations of the differential response of C3H and B6 mice in Specific Objectives 4, 5 and 6.

**Specific Objective 1: Development of an *in vitro* system to apply defined mechanical strains to cultured bone cells.** We used physiologically relevant flow shear strains of 20 dynes/cm<sup>2</sup> and measured the effect on [<sup>3</sup>H] thymidine incorporation (an index of cell proliferation) and the specific activity of alkaline phosphatase (a marker of osteoblast differentiation) in normal human mandible-derived osteoblasts. We found that application of steady fluid flow shear strain of 20 dynes/cm<sup>2</sup> for 30 minutes on normal human osteoblasts caused a significant ( $p < 0.001$ ) increase (50-100%) in the [<sup>3</sup>H] thymidine incorporation 24 hours later compared to control cells without the shear strain. The same shear strain also induced a significant ( $p < 0.001$ ) increase (25-75% compared to unstrained controls) in the specific activity of alkaline phosphatase assayed at 24 hours (Figure 2).

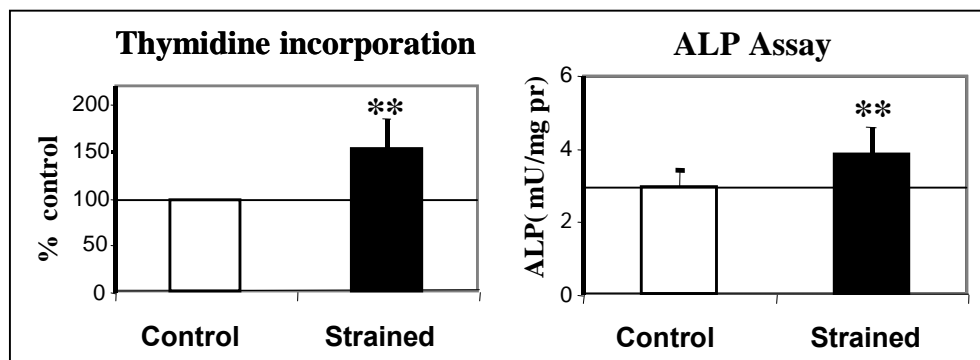


**Figure 2.** [<sup>3</sup>H]thymidine incorporation (left) and ALP specific activity (right) in human osteoblasts subjected to 30 minute steady fluid flow shear strain. Cells were subject to fluid flow of 20 dynes/cm<sup>2</sup> for 30min. [<sup>3</sup>H]thymidine incorporation and ALP specific activity were measured after 24hours. \*\* $p < 0.001$ .

**Specific Objective 2: Evaluate dose response in terms of levels of strain and continuous vs. pulsated flow.** In order to study the effect of levels of shear strain, we used two different magnitudes of shear strain (i.e. 20dynes/cm<sup>2</sup> and 50 dynes /cm<sup>2</sup>). As shown in Figure 3, [<sup>3</sup>H] thymidine incorporation was significantly ( $p < 0.001$ ) increased in response to shear strain of 20 dynes/cm<sup>2</sup> as well as 50 dynes /cm<sup>2</sup> in human osteosarcoma TE85 cells *in vitro*. However, there was no significant difference in the [<sup>3</sup>H] thymidine incorporation induction between the two levels of shear strain. These results indicate that higher levels of shear strain might be needed to induce bigger response in cell proliferation. Since fluid flow higher than 50 dynes /cm<sup>2</sup> would be beyond the physiological level of stress, we focused our studies at 20dynes/cm<sup>2</sup>.

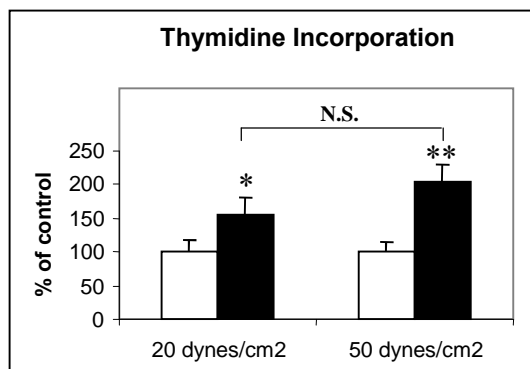


**Figure 3** Dose response of [ $^3\text{H}$ ] thymidine incorporation to shear strain. Cells were subjected to fluid flow of 20-50 dynes/cm<sup>2</sup> for 30min. [ $^3\text{H}$ ]thymidine incorporation was measured after 24 hours. \* $p < 0.01$ , \*\* $p < 0.001$ . Empty bars represent control cells while filled bars represent strained cells.

To study the effect of continuous vs. pulsatile fluid flow on the bone cell proliferation, normal human osteoblasts were subjected to a fluid flow shear strain of 20 dynes/cm<sup>2</sup> for 30 minutes continuously or pulsatile flow (10 minute flow and 10 minute rest period with a total of 30 minute flow). The control cells were not subjected to any fluid flow. Figure 4 shows that, as compared to the control cells, there was a significant ( $p < 0.001$ ) induction in cell proliferation in response to steady, (~50%) as well as pulsatile (~80%), fluid flow shear strain.

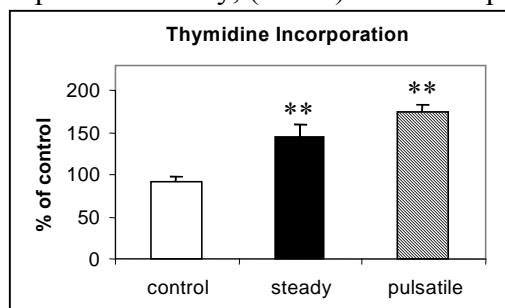


**Figure 4.** Effect of steady or pusatile fluid flow on [ $^3\text{H}$ ] thymidine incorporation. Normal human osteoblasts were subjected to steady or pusatile fluid flow of 20 dynes/cm<sup>2</sup> for 30 min. [ $^3\text{H}$ ]thymidine incorporation was measured after 24 hours. \*\* $p < 0.001$ .

**Specific Objective 3: Determine a time response of the bone cells to optimal flow conditions.** Based on the studies above, we chose to use continuous fluid flow shear strain of 20 dynes /cm<sup>2</sup> as the optimal flow. To further determine the optimal time to obtain a measurable response in the cell proliferation, human osteosarcoma TE85 cells were subjected to steady flow of 20 dynes /cm<sup>2</sup> for different time points (30 minutes to 10 hours). As seen in Figure 5, there was a time-dependent significant increase in [ $^3\text{H}$ ] thymidine incorporation for up to 4 hours as compared to the control cells not subjected to any flow. After that time point, cell proliferation induced by fluid flow starts to decrease with no significant induction at 10 hours. Based on these results, we decided to use steady fluid flow of 20 dynes/cm<sup>2</sup> for 30 minutes as the optimal conditions to get a response in cell proliferation as well differentiation.

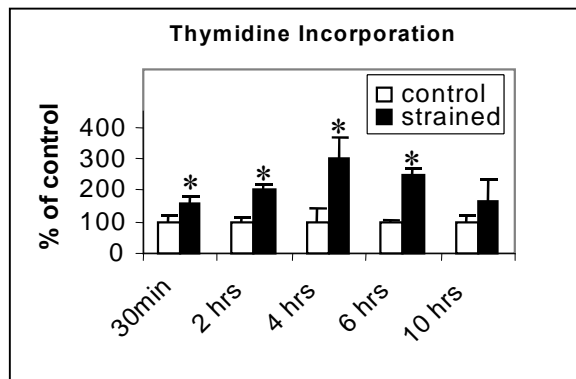


**Figure 5.** Time course response of [ $^3\text{H}$ ] thymidine incorporation to shear strain. Cells were subjected to fluid flow of 20 dynes/cm<sup>2</sup> for 30min to 10 hours. [ $^3\text{H}$ ]thymidine incorporation was measured after 24 hours. \* $p < 0.01$ .

**Specific Objective 4: Compare the phenotypic differences between the C3H and B6 mice in response to fluid flow shear strain.** Adult C3H mice have shown a 50% greater peak bone density compared to B6 mice. In addition, recent phenotypic studies comparing the skeletal response to mechanical loading and unloading *in vivo* between C3H and B6 mice revealed that C3H mice were relatively unresponsive to both mechanical loading and unloading as compared to B6 mice (1,2). This led us to postulate that the mechanical signaling mechanism in C3H bone cells is probably defective. To test this hypothesis, osteoblasts were isolated from six-week old C3H and B6 mice by sequential collagenase digestion and subjected to a fluid flow shear strain of 20 dynes/cm<sup>2</sup> for 30 minutes. Our data shows that there was a significant ( $P < 0.001$ ) increase in [<sup>3</sup>H] thymidine incorporation to the shear strain in B6 osteoblasts whereas no such increase was noted in C3H osteoblasts (**Figure 6**). A similar difference on ALP specific activity in response to fluid flow shear strain was observed between bone cells derived from C3H mice and on those derived from B6 mice.

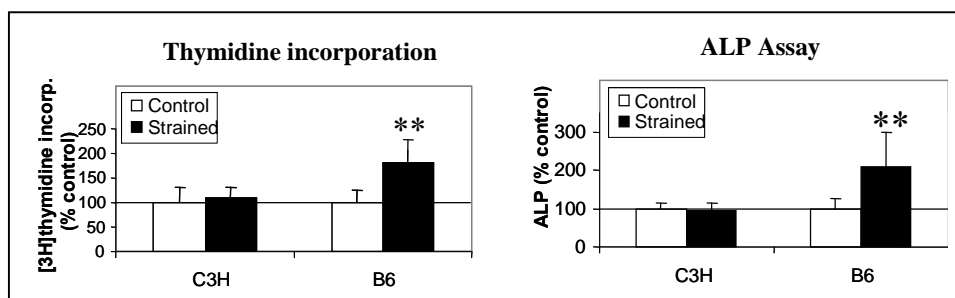


**Figure 6.** [<sup>3</sup>H]thymidine incorporation (left) and ALP specific activity (right) in osteoblasts from C3H and B6 mice subjected to 30 minute steady fluid flow shear strain. Cells were subject to fluid flow of 20 dynes/cm<sup>2</sup> for 30min. [<sup>3</sup>H]thymidine incorporation and ALP specific activity was measured after 24hours. \*\* $p < 0.001$ .

**Specific Objective 5: Evaluate strain-induced tyrosine phosphorylation levels of key signaling proteins in C3H and B6 mice.** In order to clarify the signaling pathways that could possibly lead to the changes in fluid flow induced cell proliferation and differentiation in B6 bone cells and not in the bone cells isolated from C3H mice, we studied the fluid flow induced phosphorylation of MAPK and integrin expression in these cells. As shown in Figure 7, fluid flow did not have any significant effect on the integrin  $\beta 1$  expression in the C3H bone cells. Interestingly, B6 bone cells showed a significant increase in the integrin  $\beta 1$  expression when subjected to fluid flow.

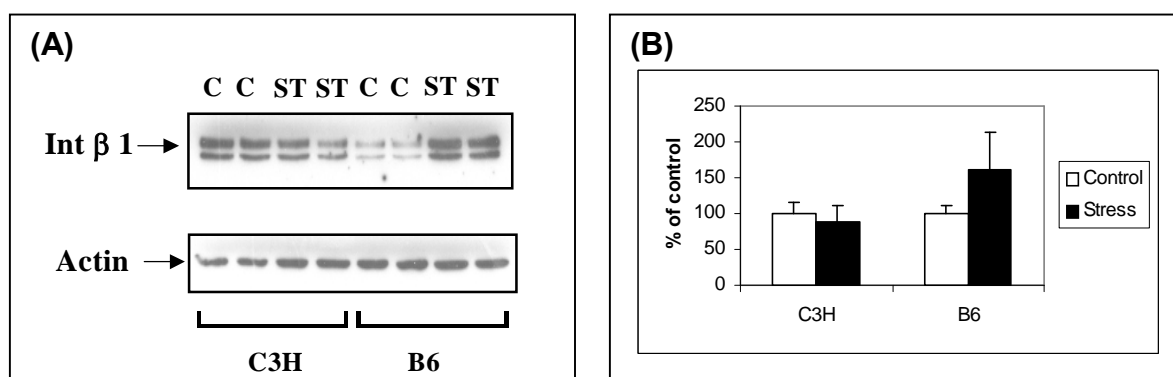


**Figure 7.** Effect of shear stress on integrin  $\beta 1$  in osteoblasts isolated from C3H and B6 mice. Cells were subjected to fluid flow of 20 dynes/cm<sup>2</sup> for 30 minutes. **(A).** Cell lysates were immunoblotted with anti-integrin  $\beta 1$  and anti-actin antibodies. **(B).** The graph represents the densitometric measurements of integrin  $\beta 1$  levels from western blots normalized by actin. "C" represents control; "ST" represents strained.

Similarly, when the effect of fluid flow on MAPK phosphorylation was studied, it was observed that there was a significant increase in the phosphorylation levels of both the p44 and p42 in B6 bone cells when subjected to fluid flow. However, in C3H bone cells, no change was noted in response to fluid flow in either p44 or p42 phosphorylation levels (Figure 8).

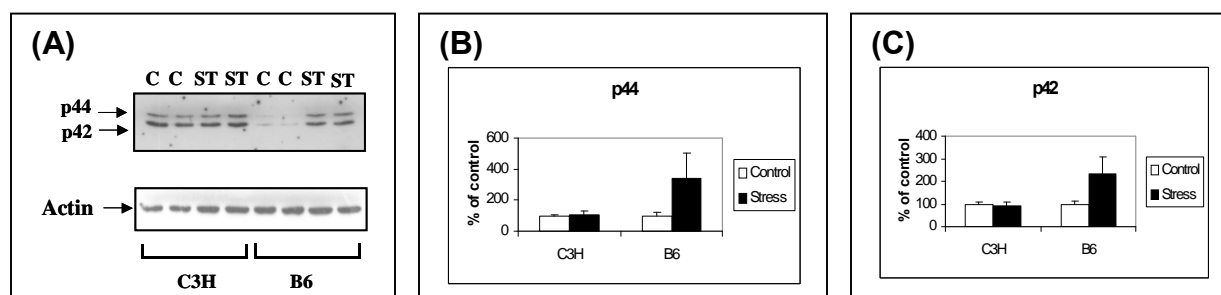


**Figure 8.** Effect of shear stress on phosphorylation levels of MAPK in osteoblasts isolated from C3H and B6 mice. Cells were subjected to fluid flow of 20 dynes/cm<sup>2</sup> for 30 minutes. **(A):** Cell lysates were immunoblotted with anti-phospho-ERK and anti-actin antibodies. **(B&C):** The graph represents the densitometric measurements of p44 and p42 phosphorylation levels from western blots normalized by actin. "C" represents control; "ST" represents strained.

### Specific Objective 6: Determine the optimal concentration of RNA for microarray technology to evaluate gene expression in C3H and B6 bone cells in response to fluid flow.

In order to apply fluid flow shear strain to the bone cells using the CytoDyne flow chamber, cells are plated on glass slides (75x38mm) at  $5 \times 10^4$  cells/slide. Thus, the total amount of RNA extracted from a single slide is very low (2-3 $\mu$ g). Previous kits (Cyscribe) required at least 100 $\mu$ g of RNA for labeling procedure in order to analyze gene expression. In order to optimize for the smaller amount of RNA, we used recently developed Micromax TSA labeling and detection kit from PerkinElmer, as the supplier's recommendation was to use 1 $\mu$ g of RNA. To optimize the amount of RNA needed to do the microarray analysis, we used different concentrations of RNA (2 $\mu$ g-0.125 $\mu$ g). Total RNA was extracted from MRL mouse liver and gene expression was analyzed using in-house microarray slides containing ~6000 genes. Figure 9 shows the expression levels of number of genes expressing low (0-1000), intermediate (1000-10000) and high (10000-70000) Cy3 signal values. As shown in the figure, there was no difference in number of genes between 1 $\mu$ g and 2 $\mu$ g of total RNA. At 0.5 $\mu$ g of RNA, more genes were expressed at lower intensity and a fewer number of genes were expressed at a higher intensity. At 0.125 $\mu$ g of RNA, the amount of RNA was too low, as most of the genes were expressed at low level of Cy3 signal value. Therefore, we decided to use 1-2 $\mu$ g of RNA for the future evaluation of gene expression in C3H and B6 bone cells in response to shear strain.

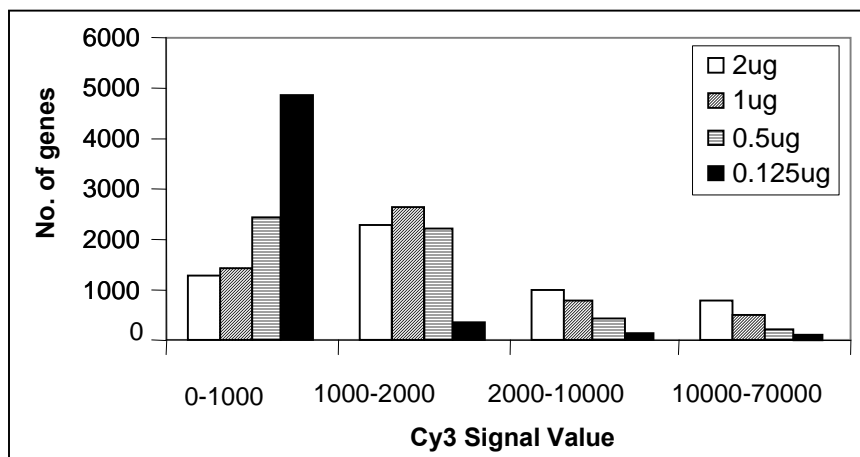


**Figure 9.** Number of genes expressing low (0-1000), intermediate (1000-10000) and high (10000-70000) Cy3 signal values.

### Conclusions - Molecular Genetics Studies on Bone Mechanical Strain

- 1) We developed an *in vitro* system to apply defined mechanical strain to cultured bone cells.
- 2) We evaluated dose response in terms of levels of strain and continuous vs. pulsated flow.
- 3) We also determined a time response of the bone cells to optimal flow conditions.
- 4) We compared the phenotypic differences between the C3H and B6 mice in response to fluid flow shear strain and found that osteoblasts isolated from B6 mice were significantly responsive to shear strain in terms of cell proliferation and differentiation. On the other hand, osteoblasts isolated from C3H mice were unresponsive to the same shear stress.
- 5) We determined the optimal concentration of RNA for microarray technology to evaluate gene expression in C3H and B6 bone cells in response to fluid flow.
- 6) We have optimized conditions for Microarray Technique.

## Progress for the Period of 2003 to 2004

### Introduction

It is well established that mechanical loading leads to an increase in bone density and that immobilization leads to a loss in bone density. Although the response of bone cells to mechanical stimuli is relatively well understood, the knowledge about the signaling mechanisms and the genes involved in the mechanical regulation of bone structure and function are less understood or limited. In our recent study we have shown that two inbred strains of mice (C3H and B6) showed differing responses in bone turnover to mechanical loading, suggesting that the genetic component of bone response to mechanical loading must be biologically significant. To identify the genetic component involved, our goal is to apply a powerful genetic approach known as quantitative trait loci (QTL) in combination with *in vitro* studies on the biochemical pathways involved in mechanical stress signaling in order to determine the genes responsible for the mechanical stress differential responses between the two inbred strains of mice that show good and poor response of bone formation.

### Technical Objectives:

To evaluate the effects of mechanical signaling using a physiologically relevant CytoDyne flow chamber to produce a fluid flow shear strain for evaluation of proliferation and differentiation and also for studies of gene expression and signal transduction pathways in cultures of C3H and B6 mouse osteoblasts. We will have the following specific objectives during the second year of this grant period:

- 7) We will complete our initial evaluation of strain-induced tyrosine phosphorylation levels of key signaling proteins by immunoprecipitation-immunoblotting approach using available antibodies. This technology will be applied to compare the responses of C3H vs. B6 mice.
- 8) Apply in-house microarrays to evaluate changes in gene expression of those genes known to be involved in mediating loading signal.
- 9) The genes that we identified by the above technique (i.e., the microarray technique) will be further compared with real time PCR.

In our previous report, we optimized the conditions to develop an *in vitro* system to apply defined mechanical strain to cultured bone cells and compared the phenotypic differences between the C3H and B6 mice in response to fluid flow shear stress. We found that osteoblasts isolated from B6 mice were highly responsive to shear stress in terms of cell proliferation and differentiation. On the other hand, osteoblasts isolated from C3H mice were unresponsive to the same shear stress. The following is our progress toward each of our objectives during Year 2 of this period (i.e., the last 12 months).

### **Specific Objective 7: Evaluate strain-induced tyrosine phosphorylation levels of key signaling proteins in C3H and B6 mice.**

In order to clarify the signaling pathways which could lead to the changes in the fluid flow induced cell proliferation and differentiation in B6 bone cells and not in the bone cells isolated from C3H mice, we studied the fluid flow induced phosphorylation of MAPK and integrin expression in these cells, since the MAPK pathway and the integrin pathway have each been implicated in the mechanical signaling mechanism. As shown in Figure 1, fluid flow did

not have any significant effect on the integrin  $\beta 1$  expression in the C3H bone cells. Interestingly, B6 bone cells showed a significant increase in the integrin  $\beta 1$  expression when subjected to fluid flow. These findings suggest that shear stress-induced osteoblast proliferation and differentiation in B6 mice may be associated with the shear stress-dependent upregulation of integrin  $\beta 1$  expression.

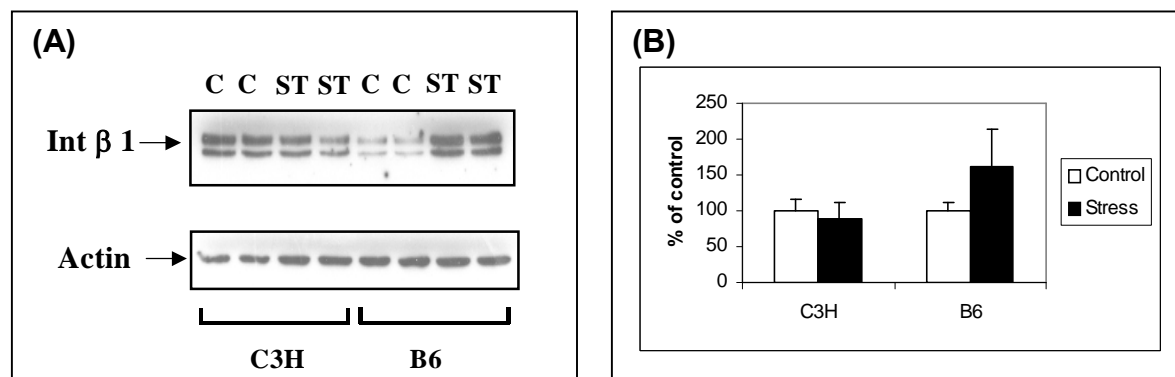


**Figure 1. Effect of shear stress on integrin  $\beta 1$  in osteoblasts isolated from C3H and B6 mice.** Cells were subjected to fluid flow of 20 dynes/cm<sup>2</sup> for 30 minutes. (A). Cell lysates were immunoblotted with anti-integrin  $\beta 1$  and anti-actin antibodies. (B). The graph represents the densitometric measurements of integrin  $\beta 1$  levels from western blots normalized by actin.

Further, when the effect of fluid flow on MAPK phosphorylation was studied, it was observed that there was a significant increase in the phosphorylation levels of both the ERK1 and ERK2 in B6 bone cells when subjected to fluid flow. However, in C3H bone cells, no change was noted either in ERK1 or ERK2 phosphorylation levels in response to fluid flow (Figure 2). These findings suggest that the ERK signaling pathway is essential in the osteogenic response to mechanical stimuli in B6 bone cells. However, a remaining key question is whether activation of either ERK1 or ERK2 or both is required.

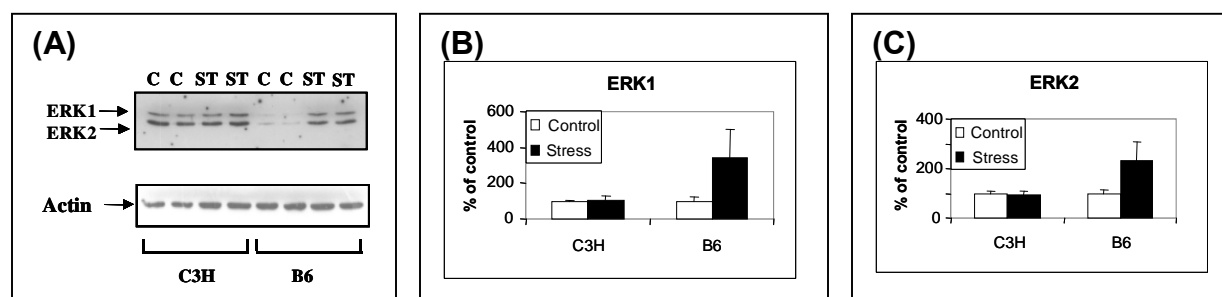


**Figure 2. Effect of shear stress on phosphorylation levels of MAPK in osteoblasts isolated from C3H and B6 mice.** Cells were subjected to fluid flow of 20 dynes/cm<sup>2</sup> for 30 minutes. (A): Cell lysates were immunoblotted with anti-phospho-ERK and anti-actin antibodies. (B&C): The graph represents the densitometric measurements of ERK1 and ERK2 phosphorylation levels from western blots normalized by actin.

To further evaluate the involvement of the ERK-signaling pathway as to whether the protein kinase activity of ERK1 and/or 2 is essential for the fluid flow shear stress-induced osteoblast proliferation, we overexpressed dominant-negative constructs of ERK1 and ERK2 in bone cells, and determined whether blocking the activation of the ERK1 and/or ERK2 would prevent the mechanical stress-induced bone cell proliferation.

Shear stress-induced cell proliferation was studied in human TE85 osteosarcoma cells that were transduced with MLV retroviral-based vectors expressing either the wild type (wt) or dominant negative, kinase-dead (kd) ERK1 and 2. Due to very low transduction efficiency in osteoblasts isolated from B6 mice, we used human TE85 cells in this part of the study as the transduction efficiency of TE85 cells is very high (79-90%). A HA tag was added to the N-terminus of each construct to help to distinguish the overexpressed enzyme from the endogenous enzyme. In order to distinguish the overexpressed ERK2 from the endogenous protein, a tag of 35 amino acids in size was introduced to the C-terminus of the protein. An MLV-red fluorescent protein (RFP) vector was also included as a control for comparison.

To ascertain that the wild-type ERK expression vectors expressed functionally active ERK1 and ERK2, and that the kinase-dead mutants of ERK vectors expressed inactive ERK1 and ERK2, protein kinase activity was assayed. As shown in Figure 3, ERK1 and ERK2 expressed by each corresponding wild-type expression vector (E1 and E2) were active as a MAPK whereas ERK1 and ERK2 expressed by each corresponding kinase-dead expression vector (e1 and e2) were completely inactive as a MAPK. Furthermore, the results here also suggest that the addition of a 35 amino acid tag at the C-terminus did not appear to have any effect on the protein kinase activity of ERK2.

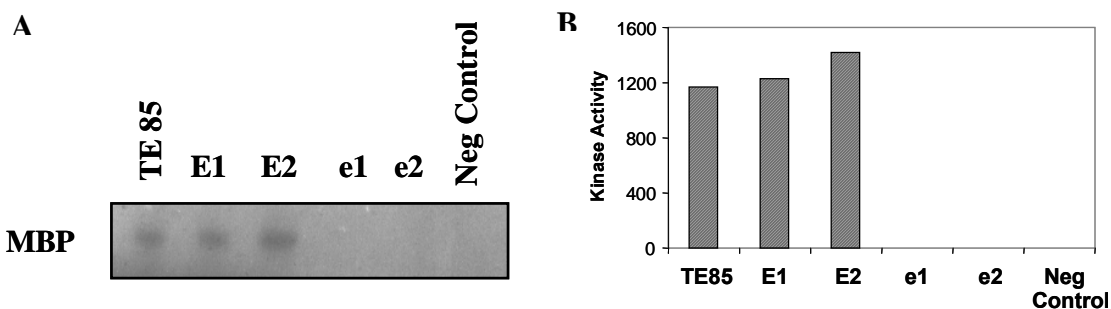


**Figure 3. The Protein kinase activity of protein products expressed by each ERK expression vector.**

**(A):** To ascertain that the wild-type ERK expression vectors expressed functionally active ERK1 and ERK2, respectively, and that the kinase-dead mutants of ERK vectors expressed inactive ERK1 and ERK2, respectively, the corresponding ERK in lysates of *E. coli* expressing wild type GST-ERK1 and GST-ERK2 vectors (E1 and E2, respectively) or that of *E. coli* expressing kinase-dead GST-ERK1 and ERK2 vectors (e1 and e2, respectively) were isolated with glutathione-conjugated beads. The protein kinase assay was then assayed with MBP as the substrate. A negative control (lysates of *E. coli* without the ERK construct) and TE85 cell lysate (positive control) were included for comparison. **(B):** The graph represents the densitometric measurements of kinase activity.

Human TE85 osteosarcoma cells were transduced three times with each of the test retroviral vectors with a total MOI of 30. To ensure that human TE85 cells transduced with ERK expressing MLV vectors indeed overexpress corresponding ERKs, we measured the protein level of overexpressed (oERK1 and oERK2, respectively) and endogenous (eERK1 and eERK2) ERK1 and 2 in cell lysates of transduced TE85 cells. As shown in Figure 4, TE85 cells transduced with MLV vectors expressing either wild type or kinase-dead mutants of ERK1 or 2 led to overexpression of ERK1 and ERK2 protein, respectively.

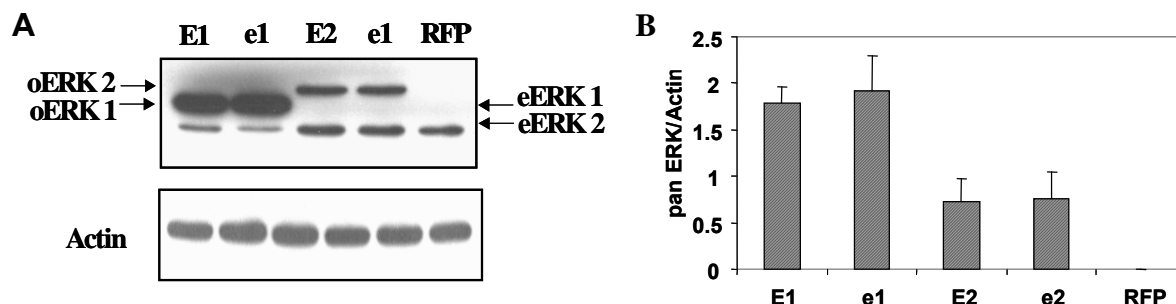


**Figure 4. Overexpression of ERK proteins in human TE85 cells transduced with MLV vectors expressing wild-type (E1 and E2) or kinase-dead mutants (e1 and e2) of ERK. (A):** To ensure that human TE85 cells transduced with ERK expressing MLV vectors indeed overexpress corresponding ERKs, the protein level of overexpressed (oERK1 and oERK2, respectively) and endogenous (eERK1 and eERK2) ERK1 and 2 was measured in cell lysates of TE85 cells transduced with respective MLV vectors by western blot analysis. The oERK2 has an extra 35 aa at the C-terminus compared to eERK2. Cells transfected with MLV-RFP vector were included as a negative control. The blot was stripped and reblotted with anti-actin antibody to assess the protein loading. **(B):** The graph represents the densitometric measurements of ERK1 and ERK2 expression levels from western blots normalized by actin.

To test whether the protein kinase activity of ERK1 and/or ERK2 is essential for the fluid flow shear stress-induced proliferation of osteoblasts, we determined the effect of overexpression of kinase-dead ERK1 (e1) or ERK2 (e2) on [ $^3$ H]thymidine incorporation in response to shear stress. Figure 5 shows that TE85 cells exhibited a significant (~2-fold) increase in cell proliferation in response to a 30-min steady 20 dynes/cm<sup>2</sup> shear stress. Furthermore, overexpression of either wild type ERK1 or ERK2 resulted in a similar increase in cell proliferation in response to shear stress as compared to the controls. On the other hand, either a dominant-negative, kinase-dead ERK1 (e1) or ERK2 (e2) mutant completely blocked the mitogenic response of TE85 cells to the shear stress, suggesting that ERK1 and ERK2 each have an important role in mediating the shear stress-induced bone cell proliferation. Figure 5 also shows that MLV-RFP showed a similar response to shear stress as normal TE85 cells thus indicating that transfection of TE85 cells with the MLV vector did not affect the bone cell mitogenic response of these cells to the 30-min shear stress.

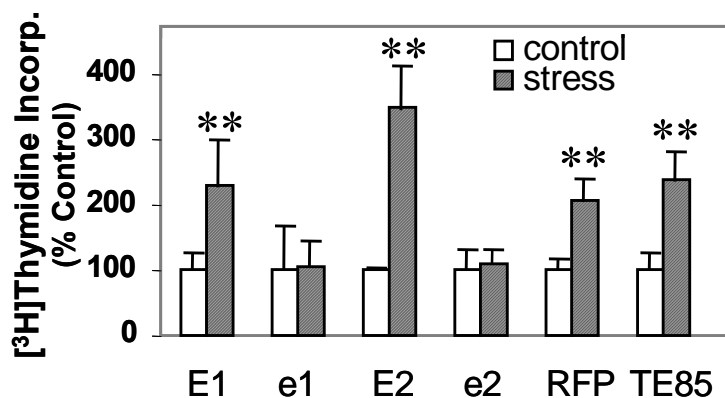


**Figure 5: Effect of overexpression of ERK1 (E1 and e1) or ERK2 (E2 and e2) on the shear stress-induced increase in [<sup>3</sup>H]thymidine incorporation.** To test whether the protein kinase activity of ERK1 and/or ERK2 is essential for the fluid flow shear stress-induced proliferation of osteoblasts, we determined the effect of overexpression of kinase-dead ERK1 (e1) or ERK2 (e2) on [<sup>3</sup>H]thymidine incorporation in response to shear stress. \* \*p<0.01.

These results clearly show that the protein kinase activity of both ERK1 and ERK2 is essential for the fluid flow shear stress-induced osteoblast proliferation. The most intriguing finding of this study is that overexpressing of an inactive form of ERK1 or ERK2 alone is sufficient to block the actions of endogenous ERKs in response to flow shear stress in bone cell proliferation.

#### **Specific Objective 8: Evaluate changes in gene expression of those genes known to be involved in mediating loading signal using in-house microarray.**

In order to study the genes involved in the mechanical signaling pathway, we applied the microarray technique. Our hypothesis is that the expression level of the genes involved in the mechanical signaling would be higher in the B6 mice as compared to C3H mice since B6 mice are responsive to mechanical stress whereas C3H mice do not respond to mechanical loading. Thus, to study the genetic basis for difference in loading signal in response to shear stress between C3H and B6 mice strains, we identified the genes in which the expression level increased more than two-fold when subjected to shear stress as compared to no stress in these two strains. The bone cells isolated from B6 and C3H mice were subjected to fluid flow shear stress of 20 dynes/cm<sup>2</sup> for 30 minutes. After 4 hours, RNA was extracted and microarray was performed.

#### **Significantly Increased or Decreased Gene Expression from B6 Osteoblasts After Sheer Stress (Tables 1 & 2)**

**Table 1.** List of genes in which expression level increased more than two-fold after application of shear stress as compared to control cells isolated from B6 mice. The ratios for the microarray were determined by using Genespring software.

Accession #	Fold Change	Gene Name
C81354	6.021867	
X15848	3.62071	Retinoic acid receptor gamma
J04113	3.536071	Mouse thyroid hormone receptor (NUR/77)
AF013170	3.508688	TNF related ligand TRANCE
TC159688	3.315779	Mus musculus IGFBP5 mRNA, complete cds
X05010	3.117075	Colony stimulating factor alpha (TNFa) gene
AU024669	3.105589	
M69293	3.028576	Mouse Id2 protein (Id-2)
E04743	2.992537	Mouse IL-1 alpha
X57796	2.960955	Mouse 55-kda tumor necrosis factor receptor
J00370	2.927765	Mouse c-fos gene; cellular homolog to viral oncogene
J05265	2.894687	Interferon gamma receptor
U64331	2.887784	Mouse Osteoprotegerin (OPG)
AF009011	2.781368	axin
AB015978	2.778422	Mouse Oncostatin M receptor beta
U81451	2.773452	Estrogen receptor beta (ESTRB)
M28021	2.752648	Mouse Homeo domain protein (HOX 1.3)
C78332	2.727276	
M59929	2.726371	Signal-trans. guanine nucleotide-binding protein (GNA01)
U58503	2.682652	Keratinocyte growth factor/fibroblast growth factor-7
E01057	2.672017	Mouse interleukin-1(IL-1) precursor
D49438	2.64229	Mouse 25-hydroxyvitamin D3 24-hydroxylase
X56848	2.610531	Bone morphogenetic protein 4 (BMP-4)
AF053713	2.600324	Mouse Osteoprotegerin ligand
AJ009862	2.584103	Transforming growth factor-beta 1
L35303	2.571284	TNF receptor associated factor 2 (TRAF2)
L0253F11-3	2.566142	Mus musculus orphan nuclear hormone receptor (CAR) gene, complete sequence
L28108	2.553446	Mouse PTH/PTHrP
L0065H09-3	2.529236	Homo sapiens ribosomal protein S21 (RPS21), mRNA
TC201479	2.526702	Homo sapiens MEBP-1 mRNA for MAPK-ERK binding protein-1, complete cds
TC175431	2.519852	
D89628.1	2.506003	Vascular endothelial growth factor D (VEGF-D)
BB500047	2.498375	beta-catenin
U39060	2.49294	Glucocorticoid receptor interacting protein 1 (GRIP1)
U36384	2.488445	Mouse twist-related bHLH protein Dermo-1
TC157862	2.438857	Homo sapiens mRNA; cDNA DKFZp586C1620); partial cds
U85259	2.437383	Estrogen related receptor alpha (ESTRRA)
X15202	2.428389	Fibronectin Receptor beta-chain (VLA5-homolog.)
M89798	2.414296	Mouse WNT-5a
U51001	2.398422	DLX-1 gene
SU78076	2.394921	Mouse sepiaterin reductase gene
SJ00357	2.394785	Mouse alpha amylase-2 gene
U78048	2.38784	Bone morphogenetic protein type II receptor BRK-3

D16250.1	2.37863	Mouse BMP receptor
AF019048	2.370698	Mouse RANKL
TC200632	2.360679	Homo sapiens CCR4-NOT transcription complex, subunit 8 (CNOT8), mRNA
AF068615	2.358135	Ciliary neutotrophic factor receptor alpha precursor
NM_010703	2.355529	Lef 1
X76401	2.340111	Tumor necrosis factor receptor 2
J04069	2.338559	Insulin-like growth factor II (IGF-II)
SU96809	2.333815	Mouse chromatin structural protein homolog gene
TC177706	2.332596	
C78942	2.326618	
C80859	2.321968	
V00727	2.315034	c-fos oncogene
D17630	2.31364	Mouse mRNA for interleukin-8 receptor
TC187351	2.313193	Homo sapiens actin related protein 2/3 complex, subunit 4 (20 kD) (ARPC4), mRNA
D31942	2.295312	Mouse Oncostatin M
AF179369	2.28034	Insuline-like growth factor binding protein 5 protease
C85074	2.27293	
TC202099	2.258783	
E03515	2.257122	Mouse interleukin 6 receptor protein
J04766.1	2.254782	Plasminogen
L0029F01-3	2.248046	
Y15800	2.242617	Mouse mRNA for G-protein coupled receptor kinase 6-D
L0051E10-3	2.22982	Mus musculus fibrillarin (Fbl), mRNA
C76615	2.224257	
TC188980	2.223752	
TC186487	2.210573	Mus musculus (clone Clebp-1) high mobility group 1 protein (HMG-1)mRNA,complete cds
TC161819	2.210151	
L12447	2.194287	Insuline-like growth factor binding protein 5 (IGFBP5)
TC186750	2.191918	Mus musculus protein tyrosine phosphatase 4a1 (Ptp4a1), mRNA
M92416	2.191191	Fibroblast growth factor (FGF6)
TC166114	2.186043	Mouse mRNA for ELP3, complete cds
M29464	2.179255	Mouse platelet-derived growth factor a chain (PDGA)
TC160957	2.176756	
TC162199	2.171346	Mus musculus PL-6 (Pl6), mRNA
TC186822	2.155771	Homo sapiens splicing factor (CC1.3) (CC1.3), mRNA
C81425	2.154317	
X53802	2.150552	Mouse mRNA for interleukin-6 receptor
TC176196	2.149525	
SM95800	2.14905	Mouse Myogenin gene
TC160277	2.138307	Mus musculus 15 kDa selenoprotein (Sep15) mRNA, complete cds
TC201280	2.131578	Mus musculus D-dopachrome tautomerase gene, complete cds
J04953	2.129044	Gelsolin gene
TC186937	2.125651	Mus musculus DBA/2J delta proteasome subunit gene, complete cds
AF067191	2.124936	Fibroblast growth factor 1.a gene, exon 1
TC188018	2.116157	
TC174028	2.107252	Mus musculus spermidine/spermine N1-acetyl transferase (Sat), mRNA
TC160410	2.089787	Mus musculus serum and glucocorticoid-dependent protein kinase (Sgk)mRNA
TC175783	2.08736	Mus musculus hyaluronidase 2 (Hyal2), mRNA

H3147A10	2.081017	
TC187978	2.074785	Mus musculus recombining binding protein suppressor of hairless(Drosophila)(Rbpsuh)
AF120489	2.073418	Growth hormone receptor/growth hormone-binding protein
M63650	2.071397	Mouse M-twist gene
TC174003	2.070687	Mus musculus kidney predominant protein NCU-G1 (NCU-G1), mRNA
TC174701	2.069076	Homo sapiens JTV1 gene (JTV1), mRNA
TC200417	2.060727	Human gene for dihydrolipoamide succinyltransferase, complete cds (exon 1-15)
TC173360	2.057717	Homo sapiens actin related protein 2/3 complex, subunit 5 (16 kD) (ARPC5), mRNA
AF075717	2.044671	Transforming growth factor beta 1-induced factor 2
TC199965	2.043639	Homo sapiens cDNA FLJ14219 fis, clone NT2RP3003800, highly similar to Rattus norvegicus tyro
TC162168	2.041731	Homo sapiens CGI-147 protein (LOC51651), mRNA
C80763	2.038737	
AU022524	2.028801	
X58636.1	2.025792	(LEF1) lymphoid enhancer binding factor 1
H3120A04	2.021601	
C86855	2.018469	Mus musculus scmh1 mRNA for sex comb on midleg homolog protein, complete cds
L32751	2.013074	Mouse (Clone M1) GTPase (RAN)
AA119293	2.012701	small inducible cytokine A6
TC186472	2.00335	Mouse t-complex protein (Tcp-1x) mRNA, 3' end
TC201234	2.000614	Rattus norvegicus lamina associated polypeptide 1C (LAP1C) mRNA, complete cds

**Table 2. List of genes in which expression level decreased more than two-fold after application of shear stress as compared to control cells isolated from B6 mice. The ratios for the microarray were determined by using Genespring software.**

Accession #	Fold Change	Gene Name
TC163213	6.323833	
TC186806	4.749427	Homo sapiens apoptosis-related protein PNAS-3 (PNAS-3) mRNA, partial cds
C79115	4.397889	
C87796	4.207526	
TC177345	4.145114	Homo sapiens hypothetical protein FLJ10761 (FLJ10761), mRNA
TC193180	3.797844	Mus musculus tyrosine hydroxylase (Th), mRNA
TC167104	3.656022	
C80790	3.562263	
C79008	3.479888	
TC160201	3.372998	Homo sapiens mRNA; cDNA DKFZp586A0722 (from clone DKFZp586A0722)
TC176539	3.316524	Mus musculus small GTP-binding protein RAB25 (Rab25) gene, complete cds
TC190432	3.315813	
TC173689	3.286380	Mus musculus putative CCAAT binding factor 1 (mCBF) mRNA, mCBF1, complete cds
TC176094	3.229843	Homo sapiens KIAA0205 gene product (KIAA0205), mRNA
TC159792	3.224493	Homo sapiens ribosomal protein S9 (RPS9), mRNA
L0298F03-3	3.224286	
AU019373	3.178850	
C86899	3.094014	

TC202698	3.087886	Homo sapiens zinc finger protein 198 (ZNF198), mRNA
TC158511	3.063481	Homo sapiens mRNA;cDNA DKFZp586P0123 (from clone DKFZp586P0123);partial cds
L0069G07-3	3.044982	Homo sapiens hypothetical protein FLJ10579 (FLJ10579), mRNA
TC174040	3.028745	
TC188831	3.027351	Homo sapiens small nuclear ribonucleoprotein polypeptide F (SNRPF), mRNA
TC178609	3.017881	Mus musculus nuclear RNA export factor 1 homolog (S. cerevisiae) (Nxf1), mRNA
TC204210	3.013675	Homo sapiens B-cell CLL/lymphoma 9 (BCL9), mRNA
TC208948	3.009861	Mus musculus Janus kinase 2 (Jak2), mRNA
AU024699	2.999606	
C81530	2.965025	
AU022331	2.935256	
TC204243	2.907804	Homo sapiens mRNA for KIAA1524 protein, partial cds
TC175962	2.872361	Homo sapiens clone CTB-10G5, complete sequence
TC189875	2.871053	Homo sapiens hypothetical protein FLJ11110 (FLJ11110), mRNA
TC162398	2.857831	Homo sapiens insulin receptor tyrosine kinase substrate (LOC55971), mRNA
L0223G04-3	2.835623	
TC161135	2.828019	Homo sapiens cDNA FLJ14228 fis, clone NT2RP3004148
TC163534	2.797985	
TC190975	2.791493	Homo sapiens centrosomal P4.1-associated protein (CPAP) mRNA, complete cds
AU020234	2.767904	Homo sapiens TRPM-2, cytosolic epoxide hydrolase, nicotinic acetylcholine receptor alpha2 subu
C87530	2.755052	
L0226E04-3	2.734502	Homo sapiens LIM domain only 7 (LMO7), mRNA
TC202077	2.674004	
TC191546	2.673286	Homo sapiens cDNA FLJ12145 fis, clone MAMMA1000395
C80806	2.666355	
TC178272	2.665531	Homo sapiens cDNA FLJ13303 fis, clone OVARC1001372, highly similar to Homo sapiens liprin-
C81384	2.663685	Homo sapiens KIAA0042 gene product (KIAA0042), mRNA
L0051A02-3	2.622076	Homo sapiens heterogeneous nuclear ribonucleoprotein A0 (HNRPA0), mRNA
H3129D12	2.609591	
TC163806	2.601031	Homo sapiens heat shock transcription factor 2 binding protein (HSF2BP), mRNA
TC157219	2.574551	Homo sapiens eukaryotic protein synthesis initiation factor mRNA, complete cds
C81435	2.564388	
TC187187	2.547066	Homo sapiens mRNA; cDNA DKFZp761M2324 (from clone DKFZp761M2324)
TC189163	2.544920	Homo sapiens cDNA: FLJ23321 fis, clone HEP12396
C78157	2.535713	
L0290G10-3	2.516292	Homo sapiens KIAA0738 gene product (KIAA0738), mRNA
TC157805	2.512923	Homo sapiens GTP-binding protein (NGB), mRNA
TC173604	2.511347	Homo sapiens loss of heterozygosity, 11, chromosomal region 2, gene A (LOH11CR2A).
TC210779	2.507478	Homo sapiens KIAA0513 gene product (KIAA0513), mRNA
TC159887	2.492242	Homo sapiens KIAA0005 gene product (KIAA0005), mRNA
TC188500	2.489737	Homo sapiens mRNA for repressor protein, partial cds
TC160230	2.480316	Homo sapiens mRNA; cDNA DKFZp566J151 (from clone DKFZp566J151); complete cds
TC174370	2.479888	Mus musculus solute carrier family 34 (sodium phosphate), member 2 (Slc34a2), mRNA
NM-008513	2.473082	LRP5 #6
TC178738	2.470564	
TC176946	2.458136	Homo sapiens hypothetical protein FLJ20241 (FLJ20241), mRNA
TC189678	2.452885	Homo sapiens mRNA for KIAA0693 protein, partial cds
TC161711	2.422831	Homo sapiens nesca protein (NESCA), mRNA

TC186798	2.416530	Homo sapiens hypothetical protein FLJ10488 (FLJ10488), mRNA
TC188265	2.399167	Homo sapiens Sec31 protein mRNA, complete cds
TC206463	2.385723	
C86942	2.350195	
TC204786	2.340445	Homo sapiens SWI/SNFrelated,matrix associated,actin dependent regulator of chromatin a, men
TC174182	2.333507	Mus musculus platelet-activating factor acetylhydrolase, isoform 1b,(Pafah1b3), mRNA
S67455	2.324881	Osteocalcin
TC163121	2.321306	Homo sapiens cDNA FLJ12969 fis, clone NT2RP2005841
TC176186	2.298626	Homo sapiens LIM and cysteine-rich domains 1 (LMCD1), mRNA
L0291D11-3	2.279614	
L0013H08-3	2.278326	Homo sapiens eukaryotic translation elongation factor 1 gamma (EEF1G), mRNA
TC190732	2.274502	Homo sapiens cDNA: FLJ21020 fis, clone CAE06067
TC192702	2.261900	
EST03087	2.260475	
TC177370	2.242102	Human Tcr-C-delta gene,exons 1-4; Tcr-V-delta gene,exons 1-2 Tcr-C-alpha gene, exons 1-4
TC176521	2.238748	Homo sapiens KIAA0615 gene product (KIAA0615), mRNA
TC159038	2.221344	Homo sapiens mRNA; cDNA DKFZp761E212 (from clone DKFZp761E212)
TC201917	2.219296	Homo sapiens cDNA FLJ12783 fis, clone NT2RP2001876
TC191320	2.217481	Rattus norvegicus gene for T cell receptor eta chain, partial cds
AU022414	2.214434	Homo sapiens KIAA0940 protein (KIAA0940), mRNA
TC160509	2.214421	Homo sapiens diaphorase (NADH) (cytochrome b-5 reductase) (DIA1), mRNA
C85917	2.205803	Homo sapiens spinocerebellar ataxia 1
TC190467	2.199626	Homo sapiens cDNA FLJ13645 fis, clone PLACE1011310
TC203547	2.198232	Homo sapiens cDNA FLJ12642 fis, clone NT2RM4001965
TC160176	2.198150	Homo sapiens mRNA for KIAA1470 protein, partial cds
TC161597	2.194239	
TC202599	2.181680	Homo sapiens KIAA0244 protein (KIAA0244), mRNA
TC190059	2.174398	Homo sapiens transmembrane 4 superfamily member(tetraspan NET-7) (NET-7),mRNA
TC157266	2.169345	Mus musculus macrophage galactose N-acetyl-galactosamine specific lectin(Mgl),mRNA
TC199932	2.167705	Homo sapiens MADS box transcription enhancer factor2, polypeptide B (MEF2B),mRNA
TC161470	2.163998	Homo sapiens mRNA; cDNA DKFZp434E0121 (from clone DKFZp434E0121)
TC163446	2.158835	Mus musculus murinoglobulin 1 (Mug1), mRNA
TC178608	2.158464	Homo sapiens 8q22.1 region and MTG8 (CBFA2T1) gene, partial cds
L0261D05-3	2.158177	Homo sapiens similar to phosphorylase kinase, alpha 2 (liver) (H. sapiens) (LOC63600),
TC190403	2.152387	Homo sapiens G-protein-coupled receptor induced protein GIG2 (GIG2) mRNA
TC167570	2.146512	Mus musculus citrin (Slc25a13) mRNA, complete cds
TC157243	2.139440	Homo sapiens myosin IC (MYO1C), mRNA
TC158841	2.133129	Homo sapiens cDNA FLJ13924 fis, clone Y79AA1000540
TC160307	2.131873	Homo sapiens isocitrate dehydrogenase 3 (NAD+) alpha (IDH3A), mRNA
TC176029	2.128533	Homo sapiens mRNA; cDNA DKFZp434L1850(from clone DKFZp434L1850);partial cds
L0221A07-3	2.125280	
C81146	2.119302	
TC160464	2.116825	Homo sapiens mRNA-associated protein mrnp41 mRNA, complete cds
TC202524	2.112259	Human TFIID subunits TAF20 and TAF15 mRNA, complete cds
TC189397	2.096525	Homo sapiens hypothetical protein (FLJ20323), mRNA
TC189007	2.094517	Mus musculus RAD50 homolog (S. cerevisiae) (Rad50), mRNA
TC188371	2.094454	Human clone 23721 mRNA sequence
TC188050	2.093248	Homo sapiens MDS017 (MDS017) mRNA, complete cds

C78068	2.078961	
TC163941	2.074859	
TC204346	2.066088	Homo sapiens cDNA: FLJ22573 fis, clone HSI02387
AU019250	2.063553	Homo sapiens T-box 19 (TBX19), mRNA
L0215A02-3	2.058678	
TC200441	2.047412	Homo sapiens guanine nucleotide binding protein (G protein), (GNAI3), mRNA
TC191257	2.044590	Human IGF-I mRNA for insulin-like growth factor I
TC187210	2.040991	Homo sapiens cDNA FLJ13872 fis, clone THYRO1001322
TC173819	2.035938	Homo sapiens thyroid receptor interactor (TRIP3) mRNA, 3' end of cds
C76739	2.032122	Mus musculus macrophage C-type lectin (Mpci), mRNA
AU019952	2.032041	Homo sapiens mRNA for KIAA0597 protein, partial cds
AU041136	2.027832	Bacteriophage lambda, complete genome
TC188786	2.026039	Rattus norvegicus NADH/NADPH mitogenic oxidase subunit p65-mox mRNA
AU024767	2.024597	Mus musculus mRNA for PC3B protein
L0290B05-3	2.023050	
TC160773	2.020360	M.musculus DNA 3'flanking minisatellite transgene 110C
AU019202	2.015859	Homo sapiens MSTP046 mRNA, complete cds
TC204088	2.015016	Homo sapiens HYA22 protein (HYA22), mRNA
AU022194	2.010488	
TC163812	2.010332	Homo sapiens cDNA FLJ10366 fis, clone NT2RM2001420
TC164591	2.009105	M.musculus mRNA for intestinal tyrosine kinase
TC176191	2.008425	Homo sapiens BM022 protein (BM022), mRNA
AU024701	2.008356	
TC203734	2.000904	Homo sapiens mRNA for KIAA1302 protein, partial cds
C78087	2.000170	

As shown in Table 1, there are 109 genes that show more than two-fold increase in expression in cells subjected to fluid flow shear stress as compared to the non-stressed cells in B6 mice. Table 2 shows that there are 139 genes that show more than two-fold decrease in expression in stressed cells as compared to the non-stressed cells in B6 mice.

### Significantly Increased or Decreased Gene Expression in C3 Osteoblasts After Sheer Stress (Tables 3 & 4)

**Table 3. List of genes in which expression level increased more than two-fold after application of shear stress as compared to control cells isolated from C3H mice. The ratios for the microarray were determined by using Genespring software.**

Accession #	Fold Change	Gene Name
M69293	5.342443	Mouse Id2 protein (Id-2)
AF179369	4.480995	Insuline-like growth factor binding protein 5 protease
M63650	4.314368	Mouse M-twist gene
D16250.1	4.153827	Mouse BMP receptor
M89798	3.86404	Mouse WNT-5a

U85259	3.828085	Estrogen related receptor alpha (ESTRRA)
AF056187	3.623736	Insulin-like growth factor I receptor
AF126159	3.500622	Mouse big MAP kinase 1a (BMK1), mRNA
X57413	3.49456	Transforming growth factor-beta 2
L27424	3.46014	Mouse metalloproteinase inhibitor TIMP-3)
U39060	3.454962	Glucocorticoid receptor interacting protein 1 (GRIP1)
U58503	3.376605	Keratinocyte growth factor/fibroblast growth factor-7
AJ009862	3.354771	Transforming growth factor-beta 1
D17630	3.210925	Mouse mRNA for interleukin-8 receptor
U67610	3.206105	Fibroblast growth factor 1 (FGF-1)
X05010	3.13227	Colony stimulating factor alpha (TNFa) gene
AB015978	3.128478	Mouse Oncostatin M receptor beta
M92416	3.113992	Fibroblast growth factor (FGF6)
AB009993	3.08771	Collagen A1(V)
M97017	3.059502	Osteogenic protein-2 (OP-2)
L25602.1	3.019166	Mouse morphogenetic protein 2 (BMP-2) gene
X67348	3.012249	COL10A1 gene for alpha - collagen type x
X15202	2.947969	Fibronectin Receptor beta-chain (VLA5-homolog.)
J00370	2.937989	Mouse c-fos gene; cellular homolog to viral oncogene
TC177706	2.931965	
U39545	2.926427	Bone morphogenetic protein 8b (BMP8b)
M59929	2.915431	Signal-trans. guanine nucleotide-binding protein (GNA01)
U70429	2.847221	Interleukin-4 induced gene-1 (FIG1)
U81451	2.841179	Estrogen receptor beta (ESTRB)
J04953	2.811038	Gelsolin gene
AB006034	2.796519	Mouse 25-hydroxyvitamin D3 1 alpha-hydroxylase
L32751	2.788244	Mouse (Clone M1) GTPase (RAN)
M29464	2.778772	Mouse platelet-derived growth factor a chain (PDGA)
L35303	2.759914	TNF receptor associated factor 2 (TRAF2)
AF020681	2.758174	Mouse core binding factor alpha1 sub unit isoform (Cbfa-1)
TC175431	2.745054	
D89628.1	2.738802	Vascular endothelial growth factor D (VEGF-D)
X14759	2.72283	Mouse Homeo box (HOX-7.1)
U64331	2.718682	Mouse Osteoprotegerin (OPG)
X57796	2.678408	Mouse 55-kda tumor necrosis factor receptor
D63644	2.6558	ARNT2 (F2#335)
E04743	2.655764	Mouse IL-1 alpha
TC200162	2.654953	Homo sapiens ribosomal protein L39 (RPL39), mRNA
X15848	2.650977	Retinoic acid receptor gamma
M28021	2.638262	Mouse Homeo domain protein (HOX 1.3)
TC173131	2.605621	Homo sapiens eukaryotic translation initiation factor 2,subunit 2(beta, 38kD )(EIF2S2)
AB021228.1	2.602641	Membrane-type 3 matrix metalloproteinase
TC173318	2.540124	Homo sapiens transmembrane trafficking protein (TMP21), mRNA
NM_010703	2.507729	Lef 1
J04113	2.482183	Mouse thyroid hormone receptor (NUR/77)
TC188890	2.457797	Mus musculus calponin 1 (Cnn1), mRNA
TC187062	2.448608	Homo sapiens 6.2 kd protein (LOC54543), mRNA
Perkin Elmer	2.425088	EST 91 from A.Thaliana

C86855	2.401036	Mus musculus scmh1 mRNA for sex comb on midleg homolog protein, complete cds
SU78076	2.395678	Mouse sepiaterin reductase gene
J05265	2.391902	Interferon gamma receptor
U36384	2.39182	Mouse twist-related bHLH protein Dermo-1
SM95800	2.381928	Mouse Myogenin gene
X62622	2.374983	(TIMP-2) Tissue inhibitor of metalloproteinases
TC158549	2.365563	
TC161819	2.363219	
TC190585	2.352407	
J04069	2.350386	Insulin-like growth factor II (IGF-II)
L0227G08-3	2.347008	Homo sapiens clone 82F9, complete sequence
L15436	2.336559	Isoform of TGF-b type II receptor
TC160410	2.316149	Mus musculus serum and glucocorticoid-dependent protein kinase (Sgk) mRNA
TC186487	2.30955	Mus musculus (clone Clebp-1) high mobility group 1 protein (HMG-1) mRNA
H3120A04	2.303708	
AF067191	2.290257	Fibroblast growth factor 1.a gene, exon 1
L28108	2.288727	Mouse PTH/PTHrP
TC187351	2.267528	Homo sapiens actin related protein 2/3 complex, subunit 4 (20 kD) (ARPC4), mRNA
L0011C07-3	2.266767	
TC201280	2.252388	Mus musculus D-dopachrome tautomerase gene, complete cds
AA253928	2.252074	endothelial monocyte
TC160692	2.249222	Homo sapiens myeloid leukemia factor 2 (MLF2), mRNA
H3124G02	2.242975	
C78676	2.236116	
AF026305	2.230761	Mouse Zinc finger transcription factor GLI
Y15800	2.227902	Mouse mRNA for G-protein coupled receptor kinase 6-D
TC160740	2.21674	Homo sapiens translocation protein 1 (TLOC1), mRNA
C78942	2.21332	
C87911	2.21322	Mus musculus SIL, MAP_17, CYP_a, SCL & CYP_b genes
X81582	2.210164	Insulin-like growth factor binding protein-4
TC191001	2.210023	Mus musculus transcription factor LRG-21 mRNA, complete cds
AF126063	2.209931	Connective tissue growth factor-like protein precursor
C81495	2.208941	
AA119293	2.203506	small inducible cytokine A6
TC159712	2.199665	Mus musculus RNA polymerase 1-1 (40 kDa subunit) (Rpo1-1), mRNA
TC159899	2.198992	
D31942	2.197945	Mouse Oncostatin M
TC173358	2.197787	Homosapienssignal sequence receptor,beta(translocon-associated protein beta)(SSR2)
C81364	2.179308	
TC160481	2.174184	Mus musculus calcium-binding protein Cab45a mRNA, complete cds
TC159868	2.173848	Mus musculus necdin (Ndn), mRNA
TC186472	2.169085	Mouse t-complex protein (Tcp-1x) mRNA, 3' end
TC186937	2.168598	Mus musculus DBA/2J delta proteasome subunit gene, complete cds
AU022429	2.168419	
C81299	2.167638	
TC161269	2.166696	Homo sapiens hypothetical protein FLJ20272 (FLJ20272), mRNA
C76825	2.154873	Mus musculus transient receptor potential-related protein (ChaK), mRNA
TC190469	2.149796	

TC201640	2.149553	Mus musculus arginine methyltransferase (Prmt2) mRNA, complete cds
AU024669	2.149365	
L0253F11-3	2.146557	Mus musculus orphan nuclear hormone receptor (CAR) gene, complete sequence
L0065E08-3	2.146445	
C78257	2.145905	Human mRNA for NADP dependent leukotriene b4 12-hydroxydehydrogenase,partial cds
AF009011	2.145423	axin
C87927	2.139591	
TC174006	2.135762	Homo sapiens asparaginyl-tRNA synthetase (NARS), mRNA
AF013170	2.135479	TNF related ligand TRANCE
X56848	2.13524	Bone morphogenetic protein 4 (BMP-4)
AA067193	2.131849	UDP-glucose dehydrogenase
TC174140	2.128732	Mus musculus Cdc42 GTPase-inhibiting protein (Cdgip-pending), mRNA
TC160359	2.125901	Homo sapiens clone RP11-486I22, complete sequence
D49438	2.125615	Mouse 25-hydroxyvitamin D3 24-hydroxylase
TC200023	2.119359	Mus musculus ribosomal protein L27 (Rpl27), mRNA
TC174370	2.117575	Mus musculus solute carrier family 34 (sodium phosphate), member 2 (Slc34a2), mRNA
C86037	2.107628	
BB500047	2.099311	beta-catenin
L0041A01-3	2.090664	
C78966	2.077118	
L0065H09-3	2.074872	Homo sapiens ribosomal protein S21 (RPS21), mRNA
C78958	2.068447	
TC189109	2.065315	Mus musculus transcription elongation factor B (SIII), polypeptide 3 (110kD) (Tceb3)
TC181404	2.061944	
TC160525	2.06007	Homo sapiens cDNA: FLJ21894 fis, clone HEP03434
L0029F01-3	2.059959	
L0008A03-3	2.048002	
TC201527	2.047403	Homo sapiens from HeLa cyclin-dependent kinase 2 interacting protein (CINP), mRNA
TC187519	2.047178	
TC157688	2.046966	Mus musculus hematological and neurological expressed sequence 1 (Hn1), mRNA
TC173042	2.03422	Homo sapiens NADH-ubiquinone dehydrogenase 1 beta subcomplex mRNA, complete cds
U78048	2.028893	Bone morphogenetic protein type II receptor BRK-3
AU040912	2.02622	
TC157249	2.020829	Homo sapiens mRNA for KIAA0622 protein, partial cds
TC160904	2.015319	
C76812	2.013664	
TC160230	2.011371	Homo sapiens mRNA; cDNA DKFZp566J151 (from clone DKFZp566J151); complete cds
SJ00357	2.00887	Mouse alpha amylase-2 gene
TC159122	2.007755	Homo sapiens clone RP11-359J14, complete sequence
C81549	2.005677	
TC157612	2.002072	Mus musculus thioredoxin reductase 1 (Txnrd1), mRNA
X76401	2.001228	Tumor necrosis factor receptor 2

**Table 4. List of genes in which expression level decreased more than two-fold after application of shear stress as compared to control cells isolated from C3H mice. The ratios for the microarray were determined by using Genespring software.**

<b>Accession #</b>	<b>Fold Change</b>	<b>Gene Name</b>
L0003B11-3	7.251633	Homosapiens FRA3B common fragile region, diadenosine triphosphate hydrolase (FHIT)
C81354	5.150292	
AU024549	4.566669	
C86942	4.135808	
TC161706	3.814792	
AU023208	3.674891	Mus musculus guanine nucleotide binding protein, alpha 14 (Gna14), mRNA
TC203078	3.630153	
TC169364	3.333058	
AU019631	3.262583	
TC158443	3.253914	
AU040173	3.189639	
TC173754	3.153296	Mus musculus DAZ-like putative RNA binding protein mRNA, complete cds
TC187226	3.104026	Mus musculus EST from clone 1498755, 3' end
AU040981	2.964905	
TC171051	2.935193	
C78087	2.929459	
EST03087	2.875889	
TC162350	2.870055	Mus musculus UDP-N-acetyl-alpha-D-galactosamine:polypeptideN- 3 (Galnt3), mRNA
TC160175	2.781838	Mus musculus serine/threonine kinase receptor associated protein (Strap), mRNA
TC208960	2.779201	
TC174179	2.777212	Mus musculus nuclear transcription factor RelA (Rela) gene, complete cds
TC188305	2.769935	
TC178738	2.715629	
C78068	2.696100	
C87638	2.679857	
TC157385	2.675020	Mus musculus Ena-VASP-like isoform (Evl1)mRNA, complete cds, alternatively spliced
AU041329	2.651487	
L0208A04-3	2.645424	
AU021860	2.603490	
AU022194	2.598836	
NM_007561	2.594891	Human BMP2/4
TC173759	2.577267	
AU022374	2.566131	
TC174791	2.531756	Mus musculus X transporter protein 3 (Xtrp3), mRNA
C80763	2.498239	
TC173399	2.490726	Mus musculus signal sequence receptor, delta (Ssr4), mRNA
H3126E09	2.477740	
AU021733	2.463330	
TC162016	2.459140	Mus musculus X-linked lymphocyte-regulated 3b (Xlr3b), mRNA
C78061	2.443694	
C86825	2.440315	

C78093	2.437616	
AU022156	2.435370	
TC162632	2.404160	Rattus norvegicus bHLH transcription factor Mist1 (Mist1) gene, complete cds
AU022430	2.385197	
C78157	2.374702	
EST03029	2.366326	
TC189251	2.343817	Homo sapiens KIAA0553 protein gene, complete cds;and alphaIIb protein gene
C86821	2.323865	
TC173324	2.310638	Psammomys obesus beacon mRNA, complete cds
TC205126	2.306227	
AU022065	2.303341	
AU021745	2.299328	
AU023256	2.296894	
TC192702	2.288848	
C79008	2.271746	
AU022321	2.270753	
EST03446	2.263182	Rattus norvegicus mRNA for dihydrolipoamide acetyltransferase
C76575	2.262311	
AU022331	2.262090	
AU024767	2.257646	Mus musculus mRNA for PC3B protein
TC198946	2.241669	
TC187710	2.233919	Mus musculus mRNA for hypothetical protein expressed in thymocytes), partial
TC172405	2.224768	
TC188356	2.222745	
TC186921	2.220592	Mus musculus U22 snoRNA host gene (UHG) gene, complete sequence
EST03496	2.214832	
TC174040	2.198529	
TC203464	2.194281	Mus musculus caspase 12 (Casp12), mRNA
L0219C11-3	2.191261	
TC163941	2.189350	
TC165384	2.187309	Homo sapiens sciellin (SCEL), mRNA
AU022363	2.185691	
C87602	2.178928	
AU024748	2.175758	
AU021952	2.163344	
C80899	2.161401	
TC200616	2.160273	Mus musculus gene rich cluster, C8 gene (Grcc8), mRNA
NM_019305	2.156498	Human FGF2
AU024596	2.154303	
TC163888	2.146388	Mouse integrin beta 4 subunit mRNA
AU023218	2.144509	
EST02095	2.142997	
AU023189	2.140748	
NM_013414	2.139277	Rat OSTEOCALCIN
AU024605	2.137971	
TC165048	2.137789	
TC160424	2.136576	Homo sapiens E-1 enzyme (MASA), mRNA
C78176	2.112627	

AU043475	2.109897	
AU024499	2.106700	
AU024601	2.104568	
TC188478	2.103129	
AU021766	2.096848	
AU022382	2.096010	
TC202511	2.088855	Mus musculus Pro-rich, PH, SH2 domain-containing signaling mediator (PSM) mRNA
AU022202	2.086047	
TC166103	2.081321	
TC202623	2.079226	
C86859	2.078406	Homo sapiens, clone hRPK.58_A_1, complete sequence
TC166162	2.067844	
EST03382	2.067519	Mus musculus transthyretin (Ttr), mRNA
TC208089	2.065965	
TC161597	2.065945	
TC205477	2.064887	Mus musculus potassium voltage-gated channel, subfamily H(eag-related), (Kcnh1)
TC186112	2.063845	
TC204141	2.062597	Rattus norvegicus mevalonate pyrophosphate decarboxylase mRNA, complete cds
TC197087	2.057604	
AU022204	2.056734	
AU022409	2.055760	
TC192594	2.053742	
EST03436	2.046538	
TC202525	2.043880	Rattus norvegicus hypertension-related calcium-regulated gene mRNA, complete cds
TC210779	2.042810	Homo sapiens KIAA0513 gene product (KIAA0513), mRNA
AU022341	2.042184	
AU022070	2.042046	
AU024727	2.041442	
AU043452	2.036570	
TC188626	2.035291	M.musculus mRNA for arachidonate epidermis-type 12(S)-lipoxygenase
EST03723	2.032456	
AU022460	2.029631	
TC160632	2.028687	Mus musculus cullin 1 (Cul1) mRNA, complete cds
Z46629.1	2.027188	Rat SOX 9
TC205634	2.024558	Mus musculus bone morphogenetic protein 15 (Bmp15), mRNA
TC201670	2.024546	Mus musculus homer-2b mRNA, complete cds
AU022330	2.024488	
TC161617	2.022511	Mus musculus beta-1,4-galactosyltransferase VI mRNA, complete cds
AU024594	2.021603	Mus musculus mRNA for cysteinyl-tRNA-synthetase (CysRS)
C81146	2.016730	
TC203654	2.008460	
TC161681	2.007609	
C87514	2.003433	
TC188237	2.002615	Mus musculus fragile X mental retardation syndrome 1 homolog (Fmr1), mRNA
TC174887	2.000214	Mus musculus solute carrier family 12, member 2 (Slc12a2), mRNA

As shown in Table 3, there are 142 genes that are upregulated in cells subjected to fluid flow shear stress as compared to the non-stressed cells in C3H mice. There are 134 genes that are downregulated in stressed vs. non-stressed cells in these mice (Table 4).

### **Comparison of gene expression profiles between B6 and C3H mice.**

Since our main objective is to find the genes involved in the mechanical signaling, we compared the gene expression profiles between B6 and C3H. A combined list of B6S/B6C and C3HS/C3HC was made to compare B6S with C3HS. A comparison of stress vs. control osteoblasts showed that 41 genes or ESTs displayed more than two-fold increase in expression (Table 5) whereas only 16 genes were found to be downregulated (Table 6).

**Table 5. List of genes in which expression level increased more than two-fold after application of shear stress in osteoblasts isolated from B6 mice as compared to osteoblasts isolated from C3H mice. The ratios for the microarray were determined by using Genespring software.**

<b>Accession #</b>	<b>Fold Change</b>	<b>Gene Name</b>
C81354	21.9628	
C80763	4.20637	
AF019048	3.61608	Mouse RANKL
E01057	3.34883	Mouse interleukin-1(IL-1) precursor
TC157862	3.08421	Homo sapiens mRNA; cDNA DKFZp586C1620 (from clone DKFZp586C1620); partial cds
J00370	3.03069	Mouse c-fos gene; cellular homolog to viral oncogene
AF075717	2.88893	Transforming growth factor beta 1-induced factor 2
AF053713	2.83105	Mouse Osteoprotegerin ligand
L12447	2.8031	Insuline-like growth factor binding protein 5 (IGFBP5)
TC188018	2.75545	
TC200632	2.75369	Homo sapiens CCR4-NOT transcription complex, subunit 8 (CNOT8), mRNA
AB009993	2.74642	Collagen A1(V)
X76401	2.54899	Tumor necrosis factor receptor 2
TC202099	2.51276	
D31942	2.47433	Mouse Oncostatin M
AF120489	2.45316	Growth hormone receptor/growth hormone-binding protein
X58636.1	2.41252	(LEF1) lymphoid enhancer binding factor 1
TC201479	2.39966	Homo sapiens MEBP-1 mRNA for MAPK-ERK binding protein-1, complete cds
J04069	2.39514	Insulin-like growth factor II (IGF-II)
V00727	2.38357	c-fos oncogene
AF068615	2.38111	Ciliary neutrophic factor receptor alpha precursor
TC162168	2.37976	Homo sapiens CGI-147 protein (LOC51651), mRNA
X56848	2.3708	Bone morphogenetic protein 4 (BMP-4)
X15848	2.34551	Retinoic acid receptor gamma
U78048	2.27706	Bone morphogenetic protein type II receptor BRK-3
AJ009862	2.27282	Transforming growth factor-beta 1
L28108	2.26984	Mouse PTH/PTHrP
U51001	2.25219	DLX-1 gene
Y15800	2.23637	Mouse mRNA for G-protein coupled receptor kinase 6-D

E03515	2.21036	Mouse interleukin 6 receptor protein
SM95800	2.20214	Mouse Myogenin gene
U64331	2.18271	Mouse Osteoprotegerin (OPG)
M29464	2.17397	Mouse platelet-derived growth factor $\alpha$ chain (PDGA)
U36384	2.16404	Mouse twist-related bHLH protein Dermo-1
AF067191	2.14363	Fibroblast growth factor 1.a gene, exon 1
NM_010703	2.09572	Lef 1
X53802	2.07883	Mouse mRNA for interleukin-6 receptor
J05265	2.07351	Interferon gamma receptor
E04743	2.03421	Mouse IL-1 alpha
X57413	2.01756	Transforming growth factor-beta 2
SU78076	2.00177	Mouse sepiaterin reductase gene

**Table 6. List of genes in which expression level decreased more than two-fold after application of shear stress in osteoblasts isolated from B6 mice as compared to osteoblasts isolated from C3H mice. The ratios for the microarray were determined by using Genespring software.**

Accession #	Fold Change	Gene Name
C86942	4.135808	
C78087	2.929459	
EST03087	2.875889	
TC178738	2.715629	
C78068	2.696100	
AU022194	2.598836	
C78157	2.374702	
TC192702	2.288848	
C79008	2.271746	
AU022331	2.262090	
AU024767	2.257646	Mus musculus mRNA for PC3B protein
TC174040	2.198529	
TC163941	2.189350	
TC161597	2.065945	
TC210779	2.042810	Homo sapiens KIAA0513 gene product (KIAA0513), mRNA
C81146	2.016730	

### **Specific Objective 9: Validation of microarray data with Real Time PCR.**

To further confirm our microarray data, we are now in the process of selecting genes for doing Real Time PCR. The selection of genes was based on: 1) confirmation of the genes known to be involved in the mechanical signaling; and 2) finding the genes or ESTs with unknown function that may be involved in the mechanical signaling. Thus, Real Time PCR was performed for a known gene (c-fos) and two ESTs (C81354 and C80763) selected from the microarray gene list. The results show that shear stress induces upregulation of c-fos and C80763 in B6 bone cells and not in C3H bone cells. These results were consistent with the data derived from the microarray analysis (Table 7). However, in case of C81354, microarray results showed a 21-

fold increase in expression in B6 mice as compared to C3H mice, whereas real time PCR showed no difference in the expression level in B6 and C3H osteoblasts. This shows a discrepancy between the microarray and real time PCR data and emphasizes the importance of confirming the microarray data with other, more authentic techniques as real time PCR.

Above results confirm that c-fos is involved in the mechanical signaling and further suggest that EST (accession # C80763) might play an important role in mechanical stress induced cell proliferation and differentiation which emphasizes the importance of studying this EST for its role in mechanical signaling.

Gene	Fold Change (Stress vs. Control)	
	Microarray	Real Time PCR
EST (accession# C80763)	4.20	4.18
EST (accession # C81354)	21.96	1.67
c-fos	3.03	2.92

**Table 7. Gene expression change after fluid flow shear stress in osteoblasts isolated from B6 mice by microarray and Real Time PCR. The fold changes were defined in relative to the expression level of osteoblasts not subjected to shear stress.**

### **Additional Progress for Technical Objective 3:**

In addition to C3H and B6 mice strains, we evaluated bone formation response to loading in 6 other inbred strains of mice (129J, BALB/cByJ, NZB/BINJ, RF/J, AKR/J, and CBA/J). These additional strains of mice were selected for the following reasons: 1) to establish the mouse strain that shows the best response to loading; and 2) to select an optimal mouse pair for studies on evaluation of candidate genes involved in mediating loading response on bone. Osteoblasts isolated from these mice strains were subjected to fluid flow shear strain and thymidine incorporation was measured after 24 hours of stress. As shown in Figure 6, CBA/J, B6, RF/J, Balbc and NZB show a significant increase in the shear stress induced cell proliferation whereas C3H, 129/J and AKR showed no significant change in the shear stress induced cell proliferation as compared to the normal cells from the respective strains of mice.

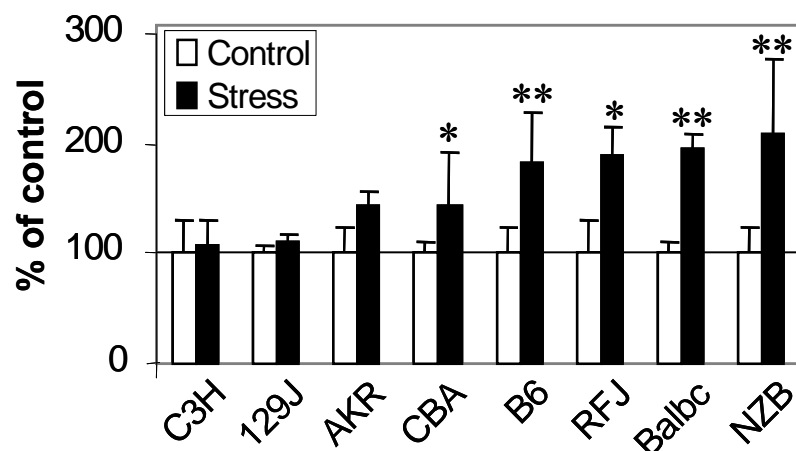


**Figure 6: Effect of fluid flow shear strain on [<sup>3</sup>H]thymidine incorporation in bone cells isolated from different strains of mice.** Cells were subjected to fluid flow for 30 min and [<sup>3</sup>H]Thymidine incorporation was measured after 24 hours of incubation. \*\*p<0.01, \*p<0.05.

Based on the response to *in vitro* mechanical loading (shear stress), the overall ranking of different mouse strains is shown in Table 8. Accordingly, C3H and 129/J seem to be poor responders whereas B6, RF/J, Balbc, and NZB seem to be good responders.

Rank	Mouse Strain	Thymidine Incorporation (% of control)	Response to Shear Stress
1	C3H	108 ± 22.69	Poor
2	129J	110 ± 08.46	Poor
3	AKR	142 ± 14.85	Medium
4	CBA	145 ± 47.06	Medium
5	B6	183 ± 46.38	Good
6	RFJ	190 ± 24.70	Good
7	Balbc	195 ± 12.93	Good
8	NZB	208 ± 70.58	Good

**Table 8. Ranking of mouse strains (Good and Poor responder) based upon the thymidine incorporation in response to fluid flow shear stress in osteoblasts isolated from different mouse strains.**

#### *Reportable Outcomes*

##### Publication:

Sonia Kapur, David J. Baylink, and K.-H. William Lau: *Fluid flow shear stress stimulates human osteoblast proliferation and differentiation through multiple interacting and competing signal transduction pathways*. Bone (2003); 32: 241-251.

##### Abstract:

Sonia Kapur, S.T Chen, D. J. Baylink, K.-H. W. Lau: *Extracellular Signal-Regulated Kinase (ERK)-1 and ERK2 Are Both Essential in the Mediation of The Flow Shear Strain-Induced Human Osteoblast Proliferation*. (2002); At 24<sup>th</sup> Annual Meeting of American Society for Bone and Mineral Research. San Antonio, Texas. September 20-24.

### Key Findings

1. We evaluated strain-induced tyrosine phosphorylation levels of key signaling proteins in C3H and B6 mice. We studied the fluid flow induced phosphorylation of MAPK and integrin expression in these cells and found that shear strain induced a significant increase in the integrin  $\beta$ 1 expression as well as the phosphorylation levels of ERK1 and ERK2 in B6 bone cells. On the contrary, no change was observed in either integrin  $\beta$ 1 expression or phosphorylation levels of ERK1 and ERK2 in C3H bone cells in response to fluid flow.
2. We also found that the protein kinase activity of both ERK1 and ERK2 are essential for the fluid flow shear stress-induced osteoblast proliferation.
3. The most intriguing finding of this study is that overexpressing of an inactive form of ERK1 or ERK2 alone is sufficient to block the actions of endogenous ERKs in response to flow shear stress in bone cell proliferation, further suggesting that both ERK1 and ERK2 are essential for shear stress-induced proliferation of bone cells.
4. The microarray analysis revealed that with over 5,000 genes explored, 109 genes show more than a two-fold increase and 139 genes show more than two-fold decrease in expression in cells subjected to fluid flow shear stress as compared to the non-stressed cells in B6 mice. In case of C3H mice, there are 142 genes that show more than two-fold increase in expression and 135 genes that are downregulated more than two-fold in cells subjected to fluid flow shear stress as compared to the non-stressed cells. A comparison of stress vs. control osteoblasts showed that only 41 genes or ESTs displayed more than two-fold increase whereas only 16 genes or ESTs showed more than two-fold decrease in expression between B6 and C3H mice.
5. Microarray and real time PCR results confirmed that c-fos is involved in the mechanical signaling and further suggested that EST (accession # C80763) might play an important role in mechanical stress induced cell proliferation. In future studies, we shall characterize C80763 and study its role in mechanical signaling.
6. In addition to B6 and C3H, bone formation response to shear stress in six different inbred strains of mice showed that RF/J, Balbc and NZB are responsive to shear stress whereas 129/J is non-responsive to shear stress. We are now in the process of determining whether some combination of these six strains would be more appropriate to the C3H and B6 for the high and low response pair.

### Conclusions

1. The *in vitro* studies show that shear stress induces an increase in the phosphorylation levels of ERK1 and ERK2 in B6 bone cells whereas no change was seen in C3H cells. Our studies further show that the protein kinase activity of both ERK1 and ERK2 are essential for the fluid flow shear stress-induced osteoblast proliferation.

2. The microarray data reveals the list of candidate genes responsible for mediating the bone formation response to mechanical loading. With over 5,000 genes explored, 41 of these genes showed more than two-fold increase in expression in B6 bone cells above C3H cells when subjected to shear stress. These genes will now be used to further evaluate the mechanical stress differential responses between these two inbred strains of mice.
3. Based on *in vitro* studies on bone formation response to shear stress in eight different strains of mice, C3H and B6 are appropriate for the poor and good response pair to mechanical loading.

**References**

1. Frangos JA, McIntire LV, Eskin SG. *Shear stress induced stimulation of mammalian cell metabolism*. Biotech Bioeng (1998); 32: 1053-60.
2. Kodama Y, Uemura Y, Nagasawa S, Beamer WG, Donahue LR, Rosen CR, Baylink DJ, Farley JR. *Exercise and mechanical loading increase periosteal bone formation and whole bone strength in C57BL/6J mice but not in C3H/HeJ mice*. Calcif Tissue Int (2000); 66(4): 298-306.

## Progress for the Period of 2004 to 2005

### Introduction:

The interstitial fluid flow through the lacunar/canalicular spaces generated by the strains exerted by mechanical loading produces strains in the mineralized matrix of bone creates a shear stress at surfaces of osteoblasts and osteocytes lining these spaces. This shear stress then generates biochemical signals that transducer to the nucleus of bone cells to exert biological effects (1). Therefore, fluid flow shear stress has been used by our laboratory as well as other laboratories as a surrogate in vitro model for mechanical loading. We have developed a Cytodyne flow chamber system for the fluid shear stress model and used to investigate the mechanism(s) whereby the shear stress transduces biochemical signals from the membrane to the nucleus is commonly referred to as the mechanotransduction mechanism (2,3).

A major objective of this work was to identify essential signaling pathways that are involved in the mechanotransduction mechanism to produce the osteogenic response. Consequently, during this reporting period, we used the Cytodyne flow chamber system to identify signaling pathways and their components that play a role in the mechanotransduction pathway.

### Body:

Our microarray analysis for differential global gene expression profiles between C57BL/6J (B6) osteoblasts and C3H/HeJ (C3H) osteoblasts suggests the involvement of at least four osteogenic signal transduction pathways in the mechanotransduction mechanism. These four pathways are the GH/IGF-I pathway, the estrogen receptor pathway, the canonical wnt pathway, and the TGF- $\beta$ /BMP pathway. Accordingly, the work for the reporting period focused on confirming the role of these pathways in the mechanotransduction pathway. The first specific objective will focus on the IGF-I pathway. For this study we used human TE85 osteosarcoma cells. The second specific objective addresses the role of each of the remaining three pathways using corresponding specific inhibitors. Osteoblasts derived from B6 mice will be used for work in specific objective #2.

### Technical Objective:

To continue *in vitro* studies to identify signaling proteins that show differential responses to mechanical loading in osteoblasts.

- 1) Identify key signaling protein/s that are regulated by tyrosine phosphorylation in osteoblasts from inbred strains of mice consistent with their response to mechanical strain.
- 2) Evaluate the role of select candidate protein/s on osteoblast cell response to mechanical strain by using a specific inhibitor of tyrosine phosphorylation of a candidate protein or by using osteoblasts from mice lacking a corresponding functional gene (i.e., knockout mice for candidate protein).

### **Specific Objective 1. To identify key signaling protein/s that are regulated by tyrosine phosphorylation in osteoblasts from inbred strains of mice consistent with their response to mechanical strain.**

We focus on the IGF-I signaling pathway first for the following two reasons: 1) bone growth factors function as autocrine and paracrine mediators of bone formation (4). We believe that the mechanism whereby mechanical stimulation of osteoblast proliferation and activity

should involve bone growth factors and corresponding signaling pathways. In this regard, IGF-I is one of the most abundant bone growth factors (4). Loading increases bone cell production of IGF-I (5, 6). The signaling pathway of IGF-I involves Erk1/2 activation, which is essential for mechanical stimulation of bone cell proliferation and activation (3). It has been suggested that

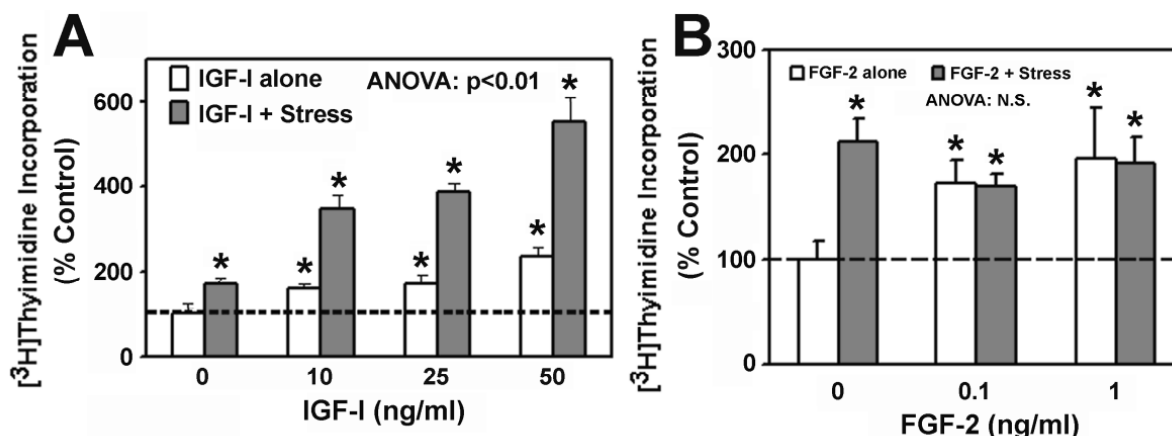


**Figure 1. Interaction between IGF-I (A) or FGF-2 (B) and fluid shear stress on the proliferation of TE85 osteosarcoma cells.** The effect of IGF-I or FGF-2 at the indicated concentrations with (filled bars) or without (open bars) a 30-min steady shear stress of 20 dynes/cm<sup>2</sup> on TE85 cell proliferation was assessed by measuring [3H]thymidine incorporation 24-hr later. Results are shown as mean  $\pm$  SD (n=6). \* $p < 0.01$  (compared to the static control).

the bone cell mitogenic response to mechanical strain is mediated by the IGF-I receptor (IGF-IR) (7). 2) There is evidence mechanical loading might have a permissive role in the IGF-I mitogenic action in bone, as skeletal unloading induces resistance to IGF-I with respect to bone formation (8). Accordingly, unloading blocked the ability of IGF-I to stimulate bone formation in the rat. IGF-I administration stimulates bone formation in the loaded bone, but not in unloaded bone (8, 9).

In these studies, human TE85 osteoblastic cells were subjected to a steady fluid shear stress of 20 dynes/cm<sup>2</sup> for 30 min followed by 24-hr incubation with osteogenic doses of IGF-I (0 to 50 ng/ml). IGF-I significantly increased the cell proliferation ( $\sim 1.5$  to 2.5 fold,  $p < 0.01$ , ANOVA) of human osteoblasts in a dose-dependent manner (Fig. 1A). The 30-minutes steady shear stress at 20 dynes/cm<sup>2</sup> alone also significantly ( $p < 0.01$ ) increased [3H]thymidine incorporation (by 70%) compared to the corresponding static control cells. The combination of shear stress and the test doses of IGF-I produced much greater than additive stimulations ( $\sim 3.5$  to 5.5 fold) of each treatment alone (Figure.1A). Two-way ANOVA indicates a highly significant interaction between the shear stress and IGF-I ( $p < 0.001$ ). These findings suggest that there is a synergistic interaction between IGF-I and fluid shear stress in the stimulation of human bone cell proliferation.

To test if the synergistic interaction between shear stress and IGF-I on human bone cell proliferation is a general feature between bone cell growth factors and shear stress, we evaluated if shear stress would also synergistically enhance the mitogenic activity of FGF-2 (another potent bone cell growth factor) in TE85 cells. Fig. 1B shows that FGF-2 alone significantly and dose dependently ( $p < 0.01$ ) stimulated the TE85 cell proliferation (by  $\sim 1.5$ -fold to 2-fold). The

combined treatment of the shear stress and FGF-2 yielded no further enhancement ( $p=N.S.$ , two-way ANOVA) than FGF-2 alone, indicating that the synergistic interaction between shear stress and IGF-I is not universal to all bone growth factors.

Because the mitogenic action of IGF-I is mediated through Erk1/2 activation, and fluid shear stress also activates Erk1/2 in osteoblasts, we investigated the effect of shear stress and/or IGF-I (or FGF-2) on Erk1/2 phosphorylation (an index of Erk1/2 activation). Fig. 2A confirms that IGF-I alone at the test doses significantly and dose dependently ( $p<0.01$ , one-way ANOVA) increased the pErk1/2 level (by ~1.2 to 5-fold) in TE85 cells. The 30-min steady shear stress alone also significantly ( $p<0.01$ ) increased the pErk1/2 level (by ~2.5-fold). The combination of shear stress and IGF-I treatment produced a synergistic ( $p<0.01$ , two-way ANOVA) enhancement (up to 12-fold) in Erk1/2 phosphorylation. Fig. 2B indicates that the mitogenic doses of FGF-2 (0.1 and 1 ng/ml) alone also markedly and significantly increased the pErk1/2 levels in TE85 cells ( $p<0.01$ , one-way ANOVA). In contrast to IGF-I, the combination treatment of shear stress and FGF-2 did not result in a further increase in the pErk1/2 level compared to the FGF-2 treatment alone ( $p=N.S.$ , two-way ANOVA). These findings further support the conclusions that the synergistic interaction between shear stress and IGF-I on bone cell proliferation is mediated through synergistic enhancement of IGF-I-dependent activation of the Erk1/2 mitogenic signaling pathway and that the synergy between shear stress and IGF-I on human bone cell proliferation is not shared by FGF-2.

To further evaluate if Erk 1/2 activation is essential for the synergy between IGF-I and

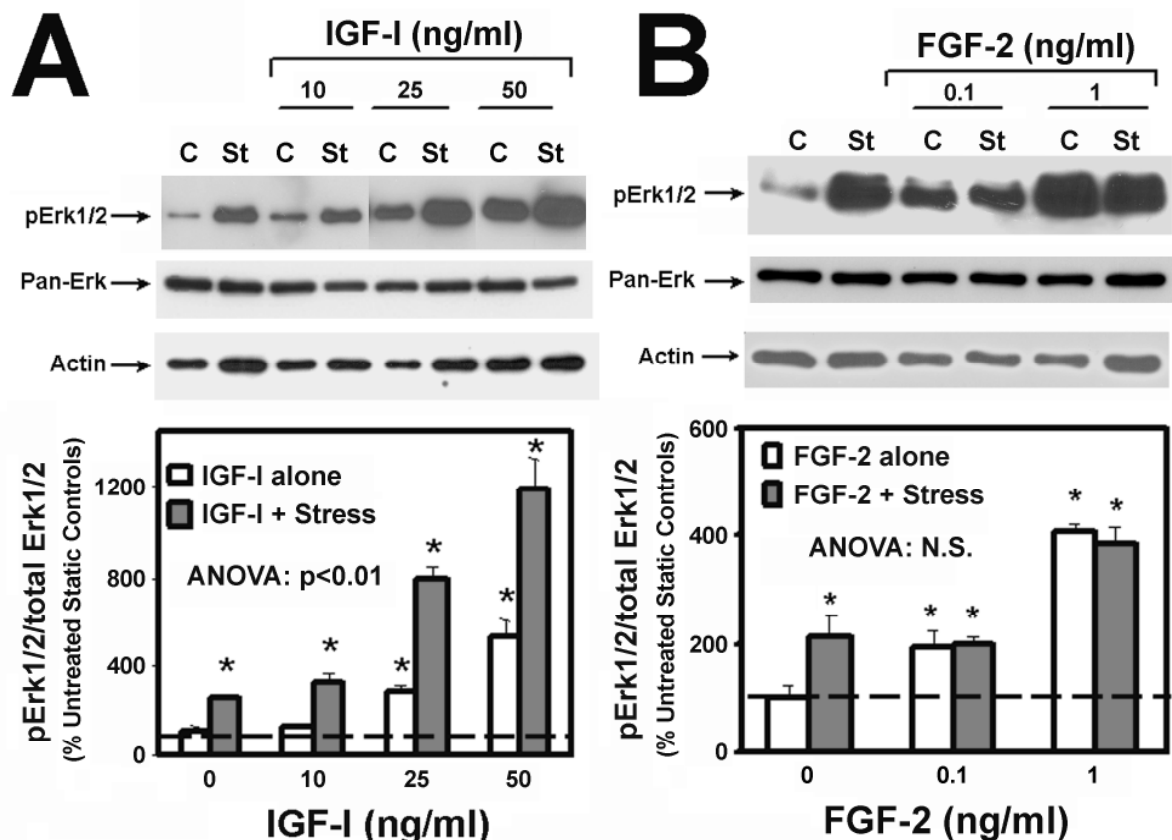


**Figure 2. Interaction between IGF-I (A) or FGF-2 (B) and fluid shear stress on Erk1/2 phosphorylation in TE85 cells.** Top panels show representative western blots of phosphorylated Erk1/2 (pErk1/2). Each blot was stripped and reblotted against anti-pan-Erk and anti-actin antibodies for loading controls. Bottom panels summarized the results of three separate repeat experiments. Results are shown as mean  $\pm$  SD. \* $p<0.01$  (compared with no addition control).

shear stress, we next determined the effect of U0126 (a specific inhibitor of MEK1) on the shear stress and/or IGF-I induced cell proliferation and Erk1/2 phosphorylation. Fig. 3A shows that

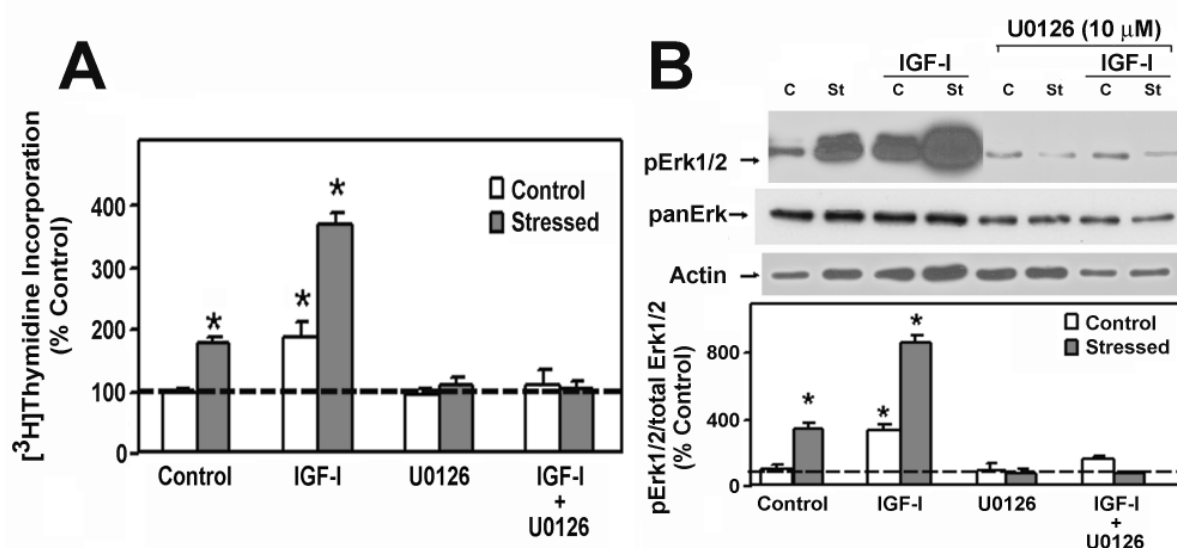


**Figure 3. Effects of U0126 (a specific inhibitor of the Erk signaling pathway) on the stimulation of cell proliferation (A) and Erk1/2 protein-tyrosine phosphorylation (B) mediated by IGF-I and/or shear stress in TE85 cells.** TE85 cells were pretreated with 10  $\mu$ M U0126 overnight before subjecting to the shear stress and/or IGF-I treatments. A shows the effects of U0126 on [3H]thymidine incorporation in response to the 30-min steady shear stress of 20 dynes/cm<sup>2</sup> and/or 10 ng/ml IGF-I. Top panel of B shows a representative western blot of pErk1/2. Each blot was stripped and reblotted against anti pan-Erk and antiactin antibodies for loading controls. Bottom panel of B summarized the results of three separate repeat experiments. Results are shown as mean  $\pm$  SD. \* $p$ <0.01 (compared with no addition control).

pretreatment with U0126 at 10  $\mu$ M completely blocked the IGF-I-mediated as well as the shear stress-induced TE85 cell proliferation. It also completely abolished the synergistic enhancement of IGF-I and shear stress. Fig. 3B shows that U0126 pretreatment completely blocked the shear stress as well as IGF-I induced phosphorylation of Erk1/2 confirming that both shear stress and IGF-I effects on cell proliferation are mediated by Erk 1/2 pathway and that the synergy between IGF-I and shear stress involve Erk 1/2 activation. These findings also indicate that the synergy between shear stress and IGF-I led to activation of bone cell proliferation occurs upstream to the Erk1/2 activation.

We next tested whether the synergy between IGF-I and shear stress occurs prior to or after the phosphorylation of IGF-IR receptor. Figure 4 shows that IGF-I significantly and dose dependently increased the phosphorylation levels of IGF-IR ( $\sim$  2 to 3.5 fold  $p$ <0.01) in the human osteoblasts *in vitro*. Shear stress alone also increased the phosphorylation levels of IGF-IR ( $\sim$  2.5 fold,  $p$ <0.01). Again the combination of IGF-I and shear stress led to a synergistic enhancement in the IGF-IR phosphorylation ( $\sim$  8 fold,  $p$ <0.01).

Because shear stress synergistically enhanced IGF-IR phosphorylation, which is initiated by the binding of IGF-I to IGF-IR, we next assessed whether the synergistic enhancement between IGF-I and shear stress was due to an increase in IGF-I binding to IGF-IR. Figure 5 shows that 30-min steady 20 dynes/cm<sup>2</sup> shear stress slightly but significantly ( $p$ <0.05) enhanced the binding of IGF-I to IGF-IR. However, this effect was too small to explain for the large

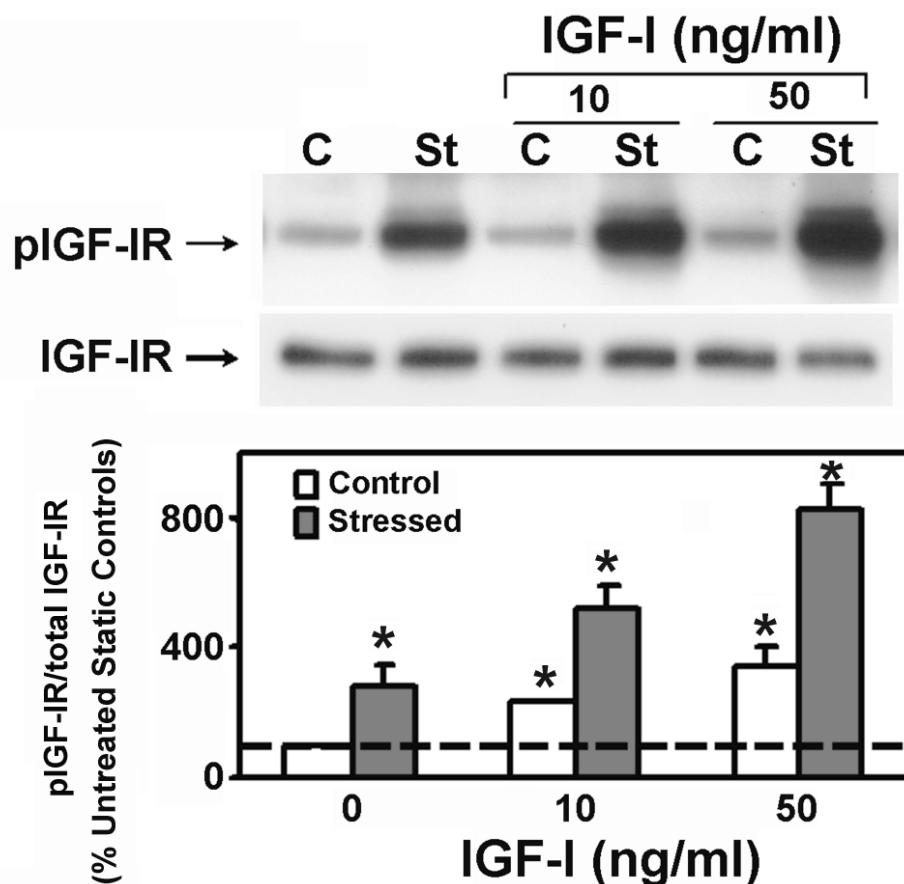


**Figure 4. Interaction between IGF-I and fluid shear stress on IGF-I receptor (IGF-IR) phosphorylation in TE85 cells.** Top panel shows a representative western blot of phosphorylated IGF-IR (pIGF-IR). The blot was stripped and reblotted against an anti-IGF-IR antibody for loading controls. Bottom panels summarized the results of three separate repeat experiments. Results are shown as mean  $\pm$  SD. \* $p < 0.01$  (compared with no addition control).

synergic interaction between IGF-I and shear stress on IGF-IR phosphorylation, Erk1/2 activation, and/or cell proliferation.

Because shear stress activates the integrin pathway, we evaluated whether integrin activation is involved in the synergy by measuring the effect of echistatin (integrin receptor antagonist) on [ $^3$ H]thymidine incorporation and IGF-IR phosphorylation in response to shear stress with or without IGF-I in human osteoblasts. As shown in figure 6A, echistatin reduced basal cell proliferation by 60%, but slightly but not significantly reduced the mitogenic response to shear stress as compared to the control. However, echistatin completely abolished the mitogenic effect of the IGF-I and also that of the combination treatment of shear stress and IGF-I. Similarly, echistatin also completely abolished the basal, shear-stress, or IGF-I-induced IGF-IR phosphorylation (Fig. 6B). These findings suggest that the synergy between IGF-I and shear stress on the proliferation and that on IGF-IR phosphorylation level may involve integrin activation.

Recent studies suggest that IGF-IR activation in response to IGF-I binding led to recruitment of SHP2 to the IGF-IR. SHP2 would then dephosphorylate IGF-IR, terminating the

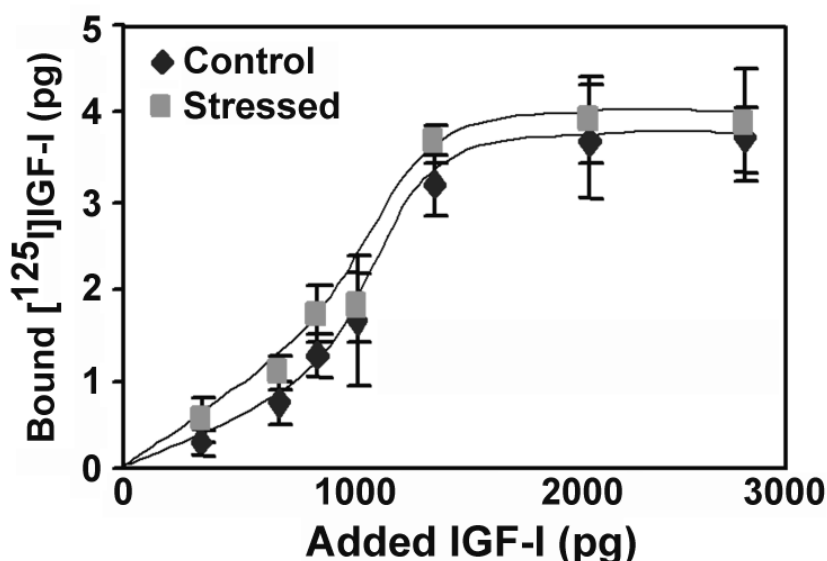


**Figure 5. Effects of fluid shear stress on specific binding of IGF-I to IGF-IR in TE85 cells.** The binding of IGF-I to surface IGF-IR of TE85 cells was performed by measuring the receptor bound [ $^{125}$ I]IGF-I. Total and non-specific IGF-I binding was determined in the absence and presence of 100 X non-radioactive “cold” IGF-I, respectively. Specific binding of IGF-I to IGF-IR was calculated by subtracting the nonspecific binding from the total binding. Only specific binding is shown in this figure. The filled squares were cells receiving the shear stress; whereas the filled diamonds were the corresponding static controls.

could also involve integrin dependent recruitment of the related SHP-1 away from the IGF-IR. Figure 8 shows that fluid shear stress, IGF-I, and the combination treatment each also significantly enhanced the recruitment of SHP-1 to integrin  $\beta$ 3 and away from the IGF-IR. However, the effects of fluid shear stress on the recruitment of SHP-2 away from the IGF-IR appeared to be bigger than those on the SHP-1 recruitment. These findings suggest that the synergy between IGF-I and shear stress at least in part involves the integrin-dependent inhibition of SHP-mediated IGF-IR dephosphorylation by recruiting away the SHP-1 and SHP2 from the phosphorylated IGF-IR

These results demonstrated for the first time that a 30-min steady fluid shear stress of 20 dynes/cm<sup>2</sup> in human osteoblastic cells enhanced synergistically the mitogenic action of IGF-I through an up-regulation of the Erk1/2-mediated IGF-I mitogenic signaling pathway. Accordingly, these findings substantiated the results of our preliminary microarray studies indicating that the mechanotransduction pathway might involve the IGF-I signaling pathway. Consequently, it appears that mechanical loading not only plays a permissive role in the osteogenic actions of IGF-I, but also interacts synergistically with the IGF-I signaling pathway to promote bone formation. More importantly, our findings that the disintegrin echistatin completely abolished the synergy on IGF-IR and bone cell proliferation and the previous finding that unloading-related resistance to IGF-I is mediated through down-regulation of integrin

activation of IGF-I signaling pathway. However, activation of the integrin pathway results in recruitment of SHP2 away from the IGF-IR complex, leading to the sustained IGF-IR phosphorylation and activation of IGF-I pathway (10). Consequently, we next evaluated the effect of IGF-I and/or shear stress on the relative amounts of SHP-2 associated with integrin  $\beta$ 3 or with IGF-IR. Figure 7 shows that shear stress, IGF-I, and the combination each significantly enhanced the recruitment of SHP-1 to integrin  $\beta$ 3 and away from IGF-IR.

We also determined whether the synergistic interaction

expression (9) together raise the strong possibility that the synergy between shear stress and IGF-I on bone cell proliferation involves integrin activation.

Our findings that shear stress, IGF-I, and the combination treatment increased the relative amount of SHP-2 that was associated with integrin  $\beta 3$  and that each also reduced the relative amount of SHP-2 co-immunoprecipitated with IGF-IR are consistent with the hypothesis that the shear stress-mediated recruitment of SHP-2 to activated integrins and away from IGF-IR may be

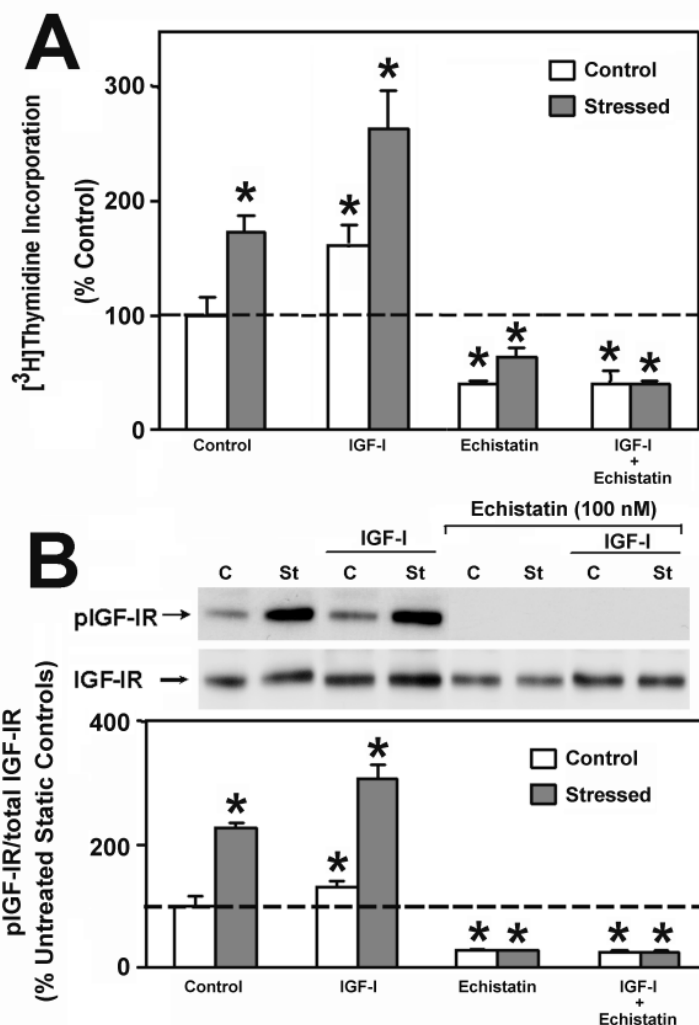


**Figure 6. Effect of echistatin on the synergy between IGF-I and shear stress with respect to cell proliferation (A) and IGF-IR phosphorylation (B).** TE85 cells were pretreated with 100 nM echistatin overnight prior to the 30-min shear stress and/or the IGF-I treatment. In A, cell proliferation was measured by [<sup>3</sup>H]thymidine incorporation. In B, the IGFIR phosphorylation level was determined by Western analysis. Top panel shows a representative western blot of pIGF-IR. The blot was stripped and reblotted against an anti-IGF-IR antibody. Bottom panels summarized the results of three separate repeat experiments. Results are shown as mean  $\pm$  SD. \* $p < 0.01$  (compared with no addition control).

osteoblasts and because SHP-2 recruitment to integrins is essential for IGF-I signaling, it is

responsible for the synergy between shear stress and IGF-IR to promote bone cell proliferation. We also found that shear stress, IGF-I, and the combination treatment also increased the relative amount of the integrin  $\beta 3$ -associated SHP-1 and reduced the relative amount of IGF-IR-associated SHP-1. This suggests that SHP-2 and the related SHP-1 are both involved in the IGF-I signaling mechanism as well as in the synergy between shear stress and IGF-I in enhancing the overall IGF-IR phosphorylation and activation.

The effect of unloading on recruitment of SHP-2 and/or SHP-1 to integrins has not been assessed previously. Thus, it is unclear at this time whether or not the unloading-induced resistance to IGF-I may also involve a reduction of SHP-2 and/or SHP-1 recruitment to integrins. However, because unloading down-regulated integrin expression in

likely that the reduced integrin recruitment of SHP-2 and/or SHP-1 in response to unloading-mediated down-regulation of the integrin pathway could also play a pivotal role in the permissive effect of mechanical loading on the IGF-I anabolic action in bone.

**Specific Objective 2: To evaluate the role of select candidate protein/s on osteoblast cell response to mechanical strain by using a specific inhibitor of tyrosine phosphorylation of a candidate protein or by using osteoblasts from mice lacking a corresponding functional gene.**

Work in the first specific objective has clearly demonstrated the involvement of the IGF-I signaling pathway in the mechanotransduction mechanism. Thus, the aim of this specific objective was to assess the potential involvement of the other three pathways, namely the canonical wnt pathway, the estrogen receptor pathway, and the TGF- $\beta$ /BMP pathway in the

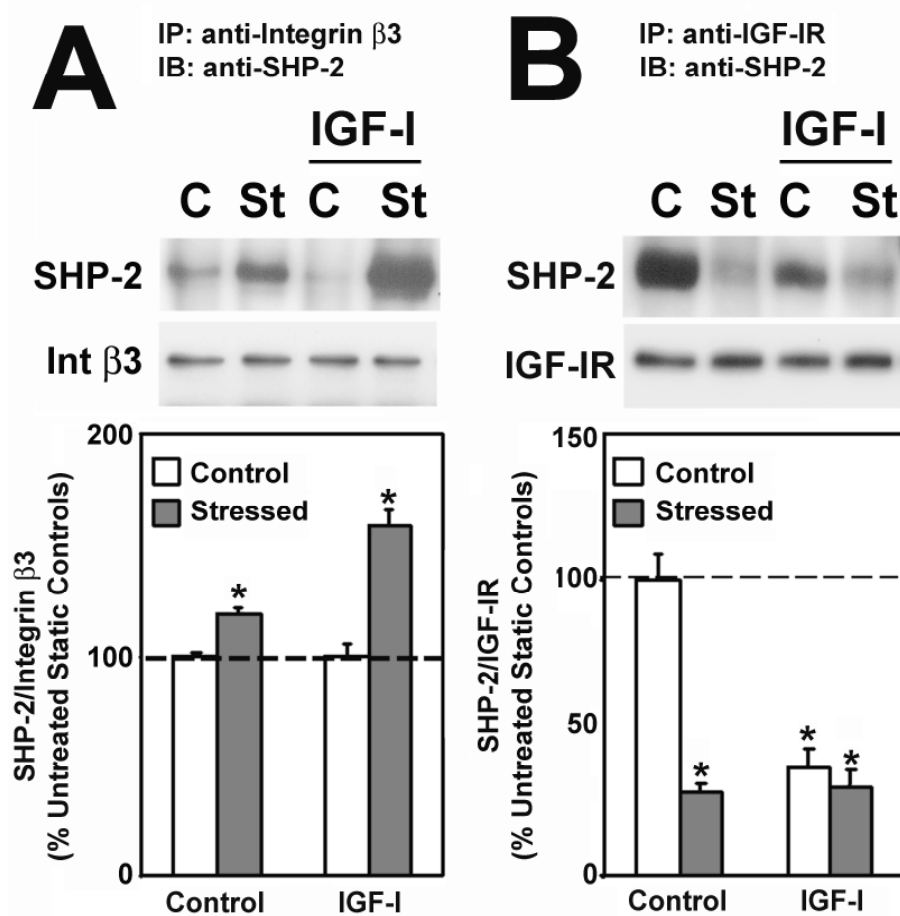


**Figure 7. Effect of IGF-I or shear stress on recruitment of SHP-2 to integrin  $\beta$ 3 or to IGF-IR.** The recruitment of SHP-2 to integrin  $\beta$ 3 and away from IGF-IR was assessed by measuring the relative amounts of SHP-2 co-immunoprecipitated with integrin  $\beta$ 3 (A) or with IGF-IR (B). The amounts of immunoprecipitated SHP-2 were normalized against the corresponding levels of immunoprecipitated integrin  $\beta$ 3 and IGF-IR, respectively. Top panels show representative Western immunoblots against SHP-2 or integrin  $\beta$ 3 and IGF-IR, respectively. Bottom panels summarize the results as percentage of respective untreated control (mean  $\pm$  SD) of 4 replicate experiments. \* $p$ <0.01.

mechanotransduction on mechanism. The approach used in this work was to evaluate the effect of a specific inhibitor of each of these three pathways on the shear stress-induced osteoblast proliferation. Since all of these signaling pathways in B6 osteoblasts appear to be responsive to fluid shear stress, B6 osteoblasts were used in these studies.

To study if the canonical Wnt/ $\beta$ -catenin pathway is involved in the mechanical signaling, we evaluated if endostatin (a specific inhibitor of the canonical Wnt pathway) would inhibit the

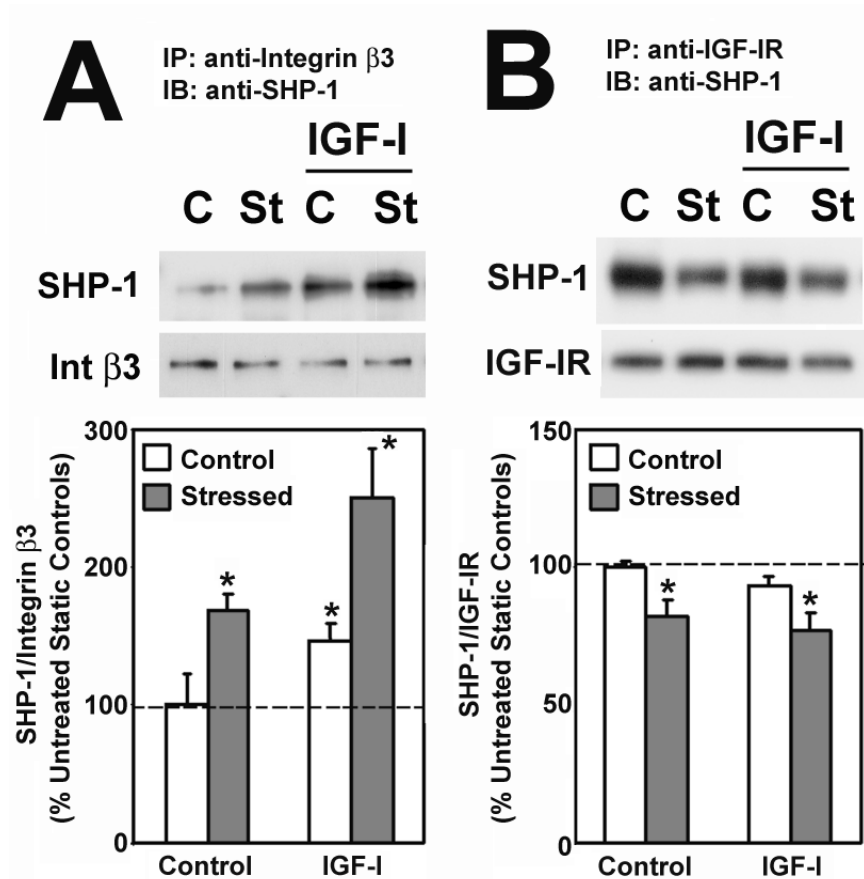


**Figure 8. Effect of IGF-I or shear stress on recruitment of SHP-1 to integrin  $\beta 3$  or to IGF-IR.** The recruitment of SHP-1 to integrin  $\beta 3$  and away from IGF-IR was assessed by measuring the relative amounts of SHP-1 co-immunoprecipitated with integrin  $\beta 3$  (A) or with IGF-IR (B). The amounts of immunoprecipitated SHP-1 were normalized against the corresponding levels of immunoprecipitated integrin  $\beta 3$  and IGF-IR, respectively. Top panels show representative Western immunoblots against SHP-1 or integrin  $\beta 3$  and IGF-IR, respectively. Bottom panels summarize the results as percentage of respective untreated control (mean  $\pm$  SD) of 4 replicate experiments. \* $p < 0.01$ .

shear stress-induced  $\beta$ -catenin expression and if endostatin would also abolish the shear stress induced cell proliferation of B6 osteoblasts. The effect of endostatin on the shear stress-induced  $\beta$ -catenin gene expression was assessed by real-time PCR. As shown in Table 1, the fluid shear stress-induced gene expression of  $\beta$ -catenin was completely blocked by treatment of 10  $\mu\text{g/ml}$  endostatin. When the effect of endostatin on the shear stress-induced [ $^3\text{H}$ ]thymidine incorporation (an index of cell proliferation) was assessed, endostatin only partially but significantly ( $p < 0.002$ ) blocked the fluid flow-induced increase in [ $^3\text{H}$ ]thymidine incorporation (Figure 9).

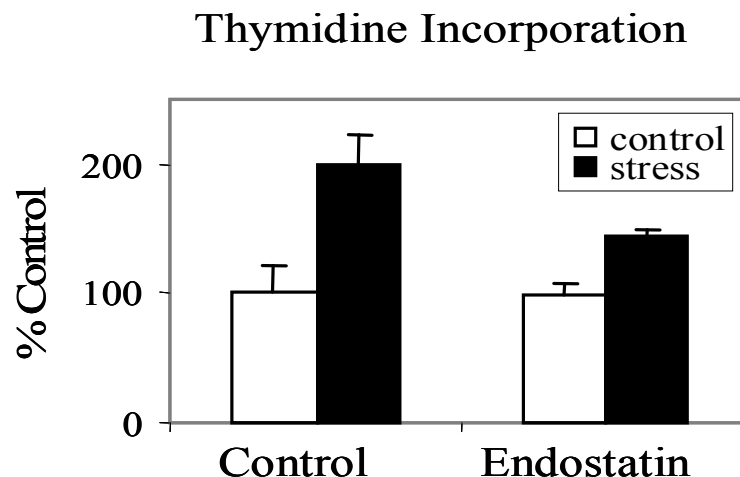


**Figure 9: Effect of endostatin pretreatment on shear strain induced cell proliferation in osteoblasts isolated from B6 mice.** Cells were pretreated with 10  $\mu\text{g/ml}$  endostatin for 24 hours and subjected to shear strain of 20 dynes/cm<sup>2</sup> for 30 minutes. [<sup>3</sup>H]thymidine incorporation was measured after 24 hours.

**Table 1. Effect of endostatin pretreatment on shear strain induced  $\beta$ -catenin expression in B6 osteoblasts.** Cells isolated from B6 mice were pretreated with 10 $\mu\text{g/ml}$  endostatin for 24 hours and subjected to shear strain of 20 dynes/cm<sup>2</sup> for 30 minutes. RNA was extracted 4 hours later and Real Time PCR was performed for  $\beta$ -catenin levels. The fold changes were defined in relative to the expression level of osteoblasts not subjected to shear strain.

Gene	Fold Change (Strain vs. Control)	
	Without ES	With ES
$\beta$ -Catenin	2.96	0.06

Since our previously studies have demonstrated that Erk1/2 activation is essential for the mechanotransduction mechanism (3), we next evaluated the effect of endostatin pretreatment on Erk1/2 activation in B6 osteoblasts to further test whether the canonical wnt pathway is important for the osteogenic response to mechanical loading. As shown in figure 10, similar to that in shear stress-induced cell proliferation, endostatin partially but significantly abolished the fluid flow-induced increase in the phosphorylation of Erk1/2.

These preliminary inhibitor findings provide strong circumstantial evidence that the canonical wnt pathway is at least in part involved in the mechanotransduction mechanism. Our results also suggest that the wnt pathway is upstream to the Erk1/2 activation. However, an intriguing and potential important observation is that endostatin at 15  $\mu\text{g/ml}$ , while it completely abolished the shear stress-induced  $\beta$ -catenin

gene expression, was only partially inhibited the shear stress-mediated activation of Erk1/2 and bone cell proliferation. The significance of this observation remains to be determined. However, it raises the strong possibility that the wnt pathway is not absolutely essential for the shear stress-mediated bone cell proliferation.

We next tested whether the estrogen receptor (ER) signaling pathway is involved in the mechanotransduction mechanism of osteoblasts. Previously studies by Lanyon and his co-workers have clearly established the important role of estrogen receptor in the mediation of mechanical stimulation of bone cell proliferation and bone formation (7). Our approach to assess the role of the estrogen receptor signaling pathway was to evaluate the effects of a specific inhibitor of estrogen receptor (ICI182780) in B6 osteoblasts on the shear stress-induced bone cell proliferation (i.e., [ $^3$ H]thymidine incorporation). In these studies, primary B6 osteoblasts were pretreated with 200 nM of ICI182780 for 24 hours prior to the 30-min shear stress of 20 dynes/cm<sup>2</sup>. The effect of ICI182780 pretreatment on [ $^3$ H]thymidine incorporation was then evaluated.

As shown in Figure 11, ICI182780 completely abolished the shear stress-induced cell proliferation in B6 osteoblasts. Further, when the effect of ICI182780 on the phosphorylation levels of Erk1/2 was studied, we found that similar to cell proliferation, ICI182780 completely abolished the shear stress-induced Erk1/2 activation as well in B6 osteoblasts (Figure 12), indicating that the ER signaling pathway is involved in the mechanotransduction mechanism in B6 osteoblasts.

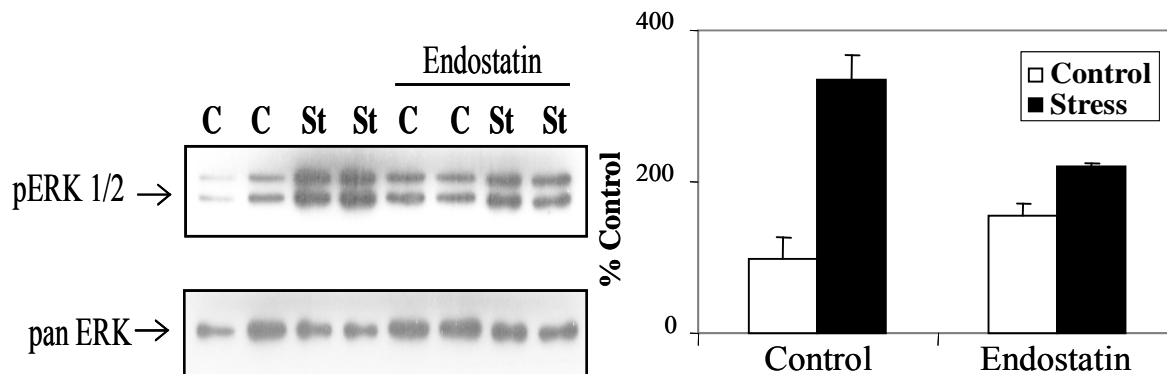


**Figure 10. Effect of endostatin on shear stress induced phosphorylation levels of ERK 1/2 in osteoblasts isolated from B6 mice.** Cells were pretreated with 10 $\mu$ g/ml endostatin for 24 hours and subjected to shear strain of 20 dynes/cm<sup>2</sup> for 30 minutes. (Left): Cell lysates were then prepared and immunoblotted with a phospho-specific anti-pan ERK antibodies. The blot was stripped and reblotted with anti-pan ERK to normalize the protein loading. (Right): The graph represents the densitometric measurements of pERK 1/2 levels from western blots normalized by pan ERK.

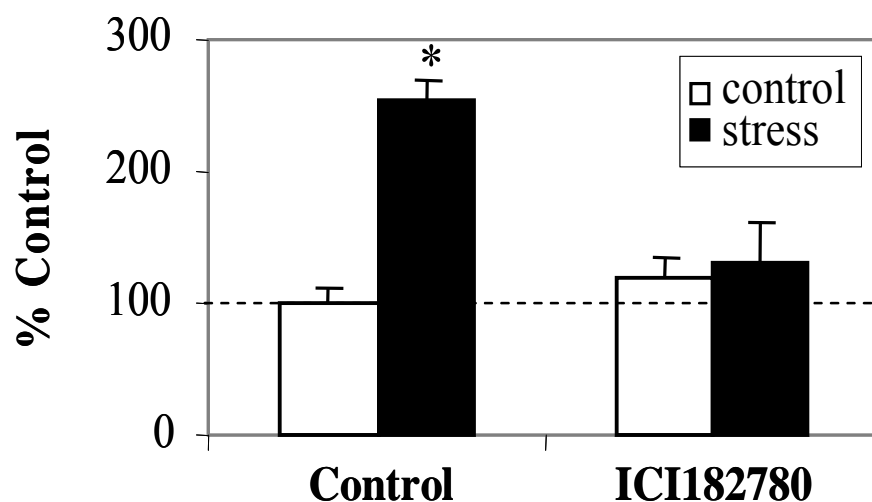


**Figure 11: Effect of ICI182780 pretreatment on shear strain induced cell proliferation in osteoblasts isolated from B6 mice.** Cells were pretreated with 200nM ICI182780 for 24 hours and subjected to shear strain of 20 dynes/cm<sup>2</sup> for 30 minutes. [<sup>3</sup>H]thymidine incorporation was measured after 24 hours. \*p<0.001.

Our preliminary findings based on the inhibitor of ER signaling pathway strongly support the work of Lanyon and co-workers that ER signaling pathway is essential for the mediation of the mechanical stimulation of bone cell proliferation, since blocking the activation of the ER signaling pathway by ICI182780 completely abolished the shear stress-mediated Erk1/2 activation and bone cell

proliferation. These findings also suggest that the ER pathway is also upstream to the Erk1/2 activation.

Finally, to test whether the BMP signaling pathway is involved in the mechanotransduction mechanisms in B6 osteoblasts, we pre-treated B6 osteoblasts with 300 ng/ml of noggin (a specific inhibitor of the BMP pathway) for 24 hrs prior to the 30-min shear stress at 20 dynes/cm<sup>2</sup>. The effects of noggin pretreatment on the shear stress-induced stimulation of [<sup>3</sup>H]thymidine incorporation (Figure 13) and Erk1/2 activation (Figure 14) were then evaluated. As shown in Figure 13, the noggin treatment completely inhibited the shear stress induced increase in the cell proliferation in B6 osteoblasts.

Similarly, the noggin treatment completely blocked the fluid shear stress-induced increase in the phosphorylation levels of Erk1/2. These results strongly indicate that the BMP signaling pathway is involved in the mechanotransduction mechanism in B6 osteoblasts.

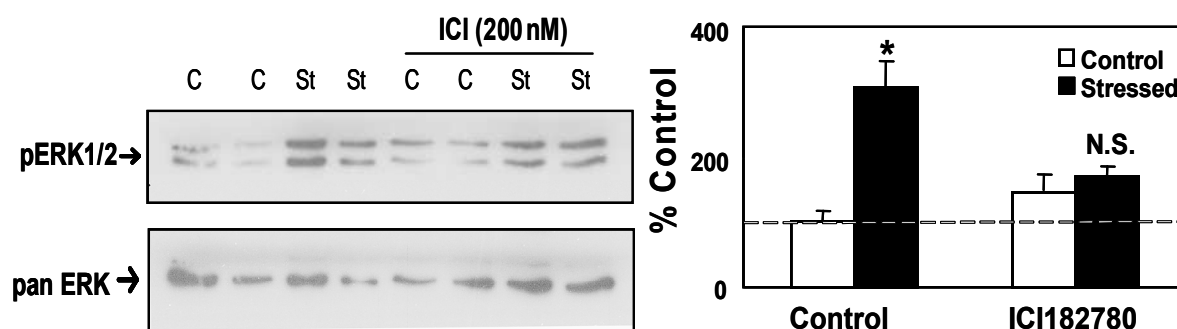


**Figure 12. Effect of ICI182780 on shear stress induced phosphorylation levels of ERK 1/2 in osteoblasts isolated from B6 mice.** Cells were pretreated with 200nM ICI182780 for 24 hours and subjected to shear strain of 20 dynes/cm<sup>2</sup> for 30 minutes. (Left): Cell lysates were then prepared and immunoblotted with a phospho-specific anti-pan ERK antibodies. The blot was stripped and reblotted with anti-pan ERK to normalize the protein loading. (Right): The graph represents the densitometric measurements of pERK 1/2 levels from western blots normalized by pan ERK. \*p<0.001

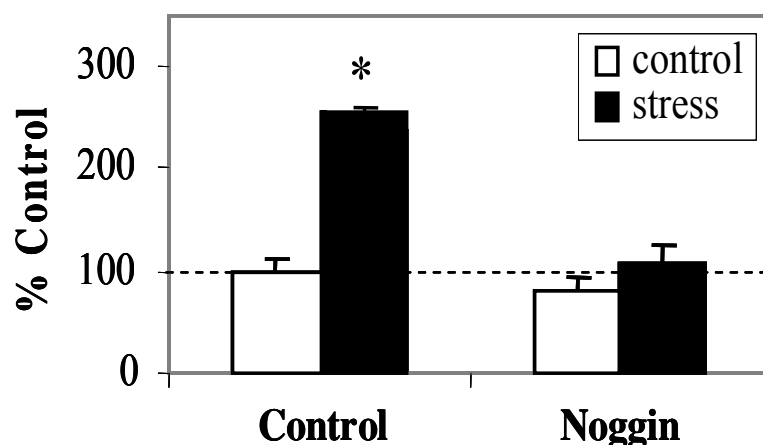


**Figure 13: Effect of Noggin pretreatment on shear strain induced cell proliferation in osteoblasts isolated from B6 mice.** Cells were pretreated with 300 ng/ml of noggin for 24 hours and subjected to shear strain of 20 dynes/cm<sup>2</sup> for 30 minutes. [<sup>3</sup>H]thymidine incorporation was measured after 24 hours. \*p<0.001.

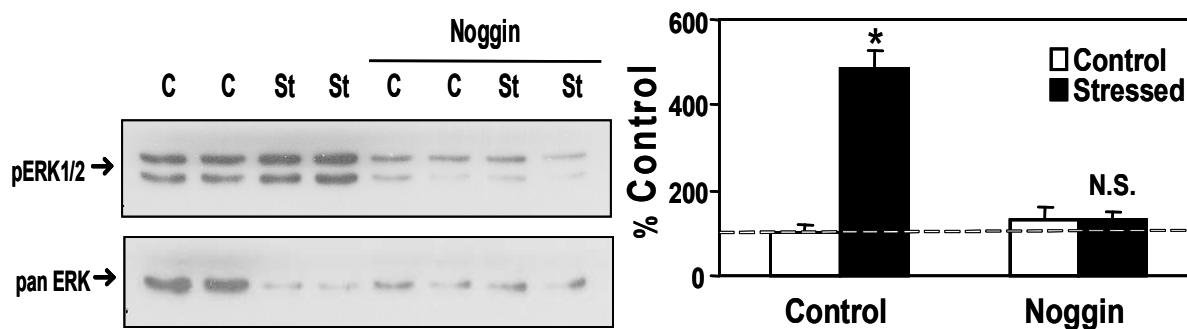


**Figure 14. Effect of Noggin on shear stress induced phosphorylation levels of ERK 1/2 in osteoblasts isolated from B6 mice.** Cells were pretreated with 300ng/ml of noggin for 24 hours and subjected to shear strain of 20 dynes/cm<sup>2</sup> for 30 minutes. (Left): Cell lysates were then prepared and immunoblotted with a phospho-specific anti-pan ERK antibodies. The blot was stripped and reblotted with anti-pan ERK to normalize the protein loading. (Right): The graph represents the densitometric measurements of pERK 1/2 levels from western blots normalized by pan ERK. \*p<0.001.

#### Key Research Accomplishments:

1. We have provided the first evidence for a synergistic interaction between shear stress and IGF-I in stimulation of osteoblastic proliferation.
2. This study also provides strong evidence that the synergy involves the integrin-dependent upregulation of IGF-IR phosphorylation through an inhibition of SHP-mediated IGF-IR dephosphorylation.
3. Studies with specific inhibitors of respective signaling pathways confirm the potential role of the canonical Wnt pathway, the BMP pathway, and the estrogen receptor pathway in the mechanotransduction mechanism.

#### Reportable Outcomes:

1. Sonia Kapur, Subburaman Mohan, David J. Baylink, and K.-H. William Lau (2005) Fluid shear stress synergizes with IGF-I on osteoblast proliferation through integrin-dependent activation of IGF-I mitogenic signaling pathway. *J Biol Chem.* 280, 20163-20170
2. K.-H. William Lau, Sonia Kapur, and David J. Baylink.(2004) Fluid shear stress synergizes with IGF-I on osteoblast proliferation through integrin-dependent activation of IGF-I receptor. *J Bone Miner Res* 19 (Suppl 1), S151, abstract # SA263, at 26<sup>th</sup> Annual Meeting of American Society for Bone and Mineral Research. Seattle, Washington.
3. Lau K-HW, Kapur S, Mohan S, and Baylink DJ (2005) Fluid shear stress synergizes with IGF-I on osteoblast proliferation through integrin-dependent upregulation of IGF-I receptor phosphorylation levels. *Transactions to the 51<sup>st</sup> Annual meeting of Orthopaed Res Soc* abstract # 845, at the 51<sup>st</sup> Annual meeting of Orthopaedic Research Society, Washington, DC..

### Conclusions:

1. These studies have confirmed our previous conclusion that the mechanotransduction mechanism is complex and is consisted of multiple anabolic signal transduction pathways. Most importantly, this work has identified at least two previously unknown pathways, namely the canonical Wnt pathway and the BMP pathway.
2. Our studies with the IGF-I signaling pathway have clearly demonstrated that not only the mechanotransduction mechanism is comprised of multiple anabolic signaling pathways, these anabolic pathways could interact synergistically with each other to promote bone cell proliferation and bone formation.
3. We have dissected the mechanism of interaction between two such pathways, namely the IGF-I and integrin pathway, and shown that the interaction between these two pathways involved recruitment of SHP-2 and/or SHP-1 to the IGF-IR. However, the nature of interaction between other pathways remains to be determined.

### References:

1. Hillsley MV, and Frangos, JA (1994) Bone tissue engineering: the role of interstitial fluid flow. *Biotech Bioeng* 43:573-581.
2. Kapur S, Baylink DJ, and Lau K-HW (2003) Fluid flow shear stress stimulates human osteoblast proliferation and differentiation through multiple interacting and competing signal transduction pathways. *Bone* 32:241-251.
3. Kapur S, Chen S-T, Baylink DJ, and Lau K-HW (2004) Extracellular signal-regulated kinase-1 and -2 are both essential for the shear stress-induced human osteoblast proliferation. *Bone* 35:535-534.
4. Mohan S, and Baylink DJ (1991) Bone growth factors. *Clin Orthop Relat Res* 263:30-48.
5. Lean JM, Jagger CJ, Chambers TJ, and Chow JW (1995) Increased insulin-like growth factor I mRNA expression in rat osteocytes in response to mechanical stimulation. *Am J Physiol* 268:E318-E327.
6. Mikuni-Takagaki Y, Suzuki Y, Kawase T, and Saito S (1996) Distinct responses of different populations of bone cells to mechanical stress. *Endocrinology* 137:2028-2035.
7. Cheng MZ, Rawlinson SC, Pitsillides AA, Zaman G, Mohan S, Baylink DJ, and Lanyon LE (2002) Human osteoblasts' proliferative responses to strain and 17  $\beta$ -estradiol are mediated by the estrogen receptor and the receptor for insulin-like growth factor I. *J Bone Miner Res* 17:593-602.

8. Sakata T, Halloran BP, Elalieh HZ, Munson SJ, Rudner L, Venton L, Ginzinger D, Rosen CJ, and Bikle DD (2003) Skeletal unloading induces resistance to insulin-like growth factor I on bone formation. *Bone* 32:669-680.
9. Sakata T, Wang Y, Halloran BP, Elalieh HZ, Cao J, and Bikle DD (2004) Skeletal unloading induces resistance to insulin-like growth factor-I (IGF-I) by inhibiting activation of the IGF-I signaling pathways. *J Bone Miner Res* 19:436-446.
10. Clemmons DR, and Maile LA (2005) Interaction between insulin-like growth factor-I receptor and  $\alpha V\beta 3$  integrin linked signaling pathways: cellular responses to changes in multiple signaling inputs. *Mol Endocrinol* 19:1-11.

## Progress for the Period of 2005 to 2007

### Introduction:

This portion of the report summarizes our progress made during years 2005-2007 on the identification of mechanosensitivity genes and the mechanotransduction mechanism(s) involved in mediating the anabolic skeletal response to mechanical stimulation, using an *in vitro* fluid shear stress model generated by the Cytodyne flow chamber system.

A major focus of this work was to address the potential role of a candidate mechanosensitivity modulating genes and its mechanotransduction, leptin receptor.

### Body:

In our original experimental approach, we plan to identify potential candidate genes from our microarray data and to determine the effect of suppression of expression of the candidate gene in osteoblasts by the siRNA technology on their anabolic response to fluid shear stress. However, because the siRNA approach is time-consuming and technically labor-intensive, we intentionally delayed the siRNA studies until we have more information about the identity potential candidate mechanosensitivity genes through a more systematic analysis, instead of arbitrarily choosing one or more novel genes whose expression was altered by the fluid shear stress. We believe that this alternative approach would be more productive. Accordingly, during the past year, we focused on two modified Technical Objectives: 1) to identify a candidate mechanosensitivity gene that may contribute at least in part the differential anabolic response to fluid shear stress between osteoblasts of C57BL/6J (B6) and those of C3H/HeJ (C3H) inbred mouse strains, and 2) to determine the molecular mechanism (i.e., mechanotransduction) whereby the candidate gene acts to regulate the anabolic response in osteoblasts.

**Technical Objectives:** The original specific objectives for the *in vitro* studies during the past year of this grant are as follows:

1. To optimize the *in vitro* siRNA techniques for the application to mouse osteoblasts in conjunction with our shear stress technology.
2. To select one or more ESTs (or known genes) for further study from our microarray data.
3. To apply the siRNA technique to suppress the candidate EST expression or known gene and then evaluate the functional role of this EST or known gene in osteoblast proliferation, differentiation, and apoptosis.
4. To continue to advance our protein-tyrosine phosphorylation studies in order to identify signaling proteins that show differences in protein-tyrosine phosphorylation levels in response to mechanical strain in bone cells isolated from those mouse strains which exhibit differential responses to the *in vitro* mouse strains. Changes in protein-tyrosine phosphorylation levels will be compared to *in vitro* parameters of osteoblast proliferation, differentiation, and apoptosis.

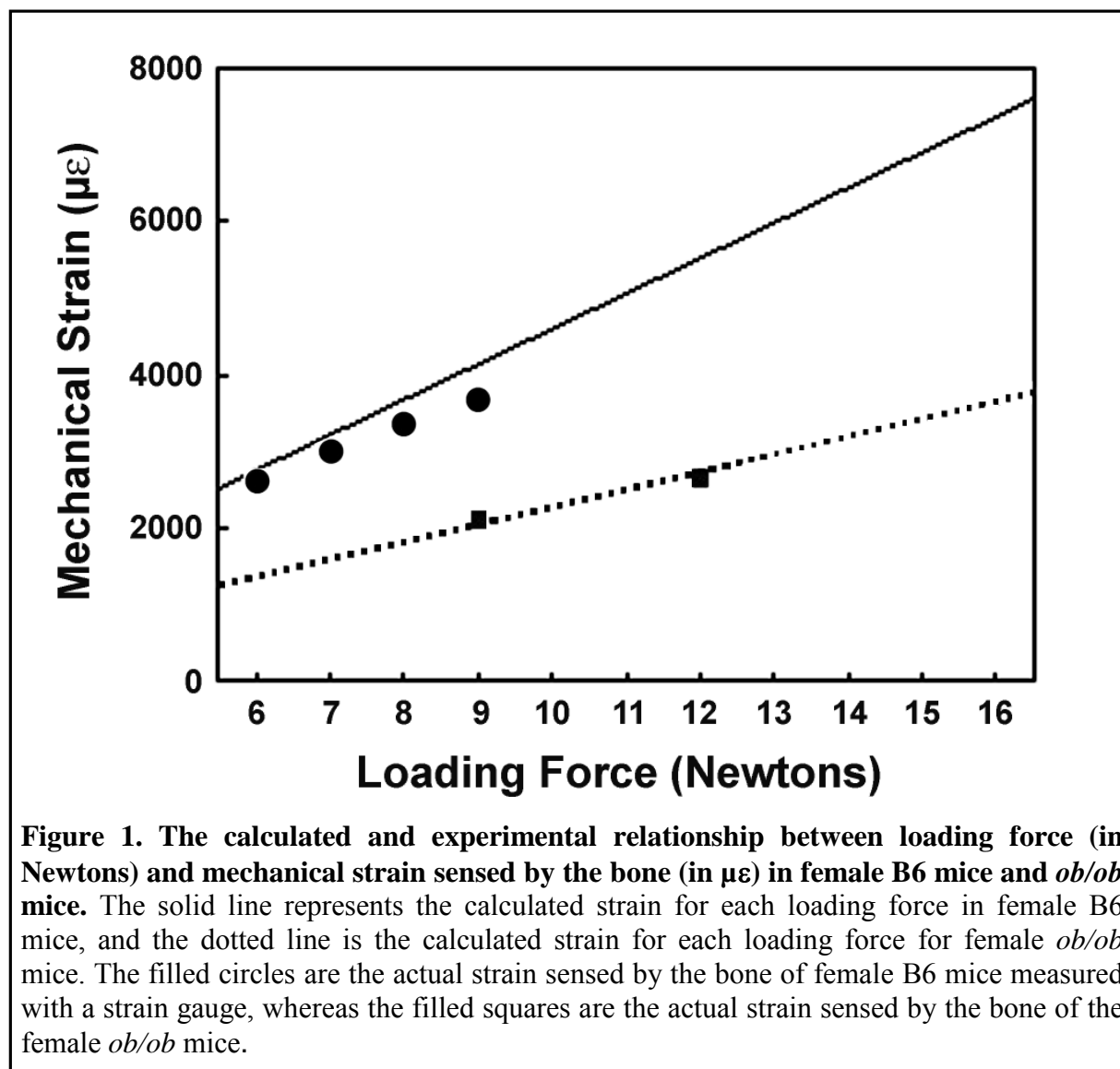
**Specific Objective #1. To identify candidate mechanosensitivity genes in osteoblasts.** B6 mice respond to mechanical stimulation with an increase in bone formation and C3H mice did not. Similarly, osteoblasts of B6 mice respond to fluid shear with an increase in cell proliferation and ALP activity *in vitro*, but the same fluid shear did not produce anabolic effects in C3H osteoblasts. Thus, we believe that comparison of the differential gene expression in osteoblasts

of these two inbred mouse strains would give important insights into the identity of potential candidate mechanosensitivity genes and the mechanotransduction involved in the anabolic response to the fluid shear stress. Accordingly, we had performed an in-house microarray analysis on B6 and C3H osteoblasts. As reported in our previous progress report, the fluid shear stress differentially upregulated the expression of a number of genes associated with at least 4 anabolic pathways [the canonical Wnt, IGF-I, estrogen receptor (ER), and BMP/TGF $\beta$  pathways] in B6 but not in C3H osteoblasts (1). We also confirmed that *in vivo* loading to the tibia also led to upregulation of the expression of these genes in B6 but not in C3H mice (1). Thus, we conclude that the “mechanosensitivity” genes contributing to the good and poor bone formation response in B6 and C3H mice, respectively, are upstream to these four pathways. We also showed that the mechanism leading to the fluid shear-induced upregulation of these 4 pathways involved two early mechanoresponsive genes, integrin  $\beta$ 1 and cyclooxygenase (Cox)-2 and that the “mechanosensitivity” genes are upstream to these two genes (1). Thus, these studies indicate that the “mechanosensitivity” genes responsible for the differential mechanical response in this pair of mouse strains are upstream even to these early mechanoresponsive genes.

Several genetic approaches have been attempted to identify genetic loci of “mechanosensitivity” genes in the C3H/B6 pair of mouse strains. A study with the B6.C3H-4T mouse strain, which was genetically identical to B6 except that it carried a segment of C3H chromosome 4 (between 40 and 80 cM), showed that these congenic mice were more responsive to mechanical stimulation in periosteal bone formation than B6 mice (2), suggesting that this C3H chromosome 4 region contains one or more genetic loci that would enhance bone mechanosensitivity in B6 mice. While these findings are exciting, it is also puzzling as to why the transfer of a DNA fragment from the nonresponsive C3H mice into B6 mice would increase their bone formation response. The mechanistic reason(s) for this seemingly contradictory finding is unclear. We interpret these findings as that there must be interactions among various “mechanosensitivity” modulating genes located at various loci, such that the interaction between genes of this C3H chromosome 4 locus with other mechanosensitivity genes in the C3H background yielded a negative response, while that in the B6 background produced an enhanced response. Nevertheless, our initial work to identify candidate mechanosensitivity gene focused on upstream signaling genes located within the 40-80 cM locus of mouse chromosome 4, since this DNA segment is currently the only genetic locus that has demonstrated ability to modulate mechanosensitivity in this pair of mouse strains. This locus is large and contains several hundreds of genes. Because the mechanosensitivity of the rat skeleton has been shown to be markedly reduced after a long period of sustained loading (3) and the loss of responsiveness after sustained activation is a hallmark characteristic of desensitization of receptor-mediated events, we were particularly interested in receptor genes or receptor-associated upstream genes.

Some of the receptor and upstream genes located in this locus are: *Lepr*, *Tie1*, *Il22ra1*, *Ptafr*, *Oprd1*, *Htr6*, *Htr1d*, *Ephb2*, *Epha2*, *Tnfrsf6*, *Tnfrsf1b*, *Tnfrsf4*, *Tnfrsf8*, *Agtrap*, *Sh3gl2*, *Tek*, *Plaa*, *Jun*, *Foxd3*, *Jak1*, *Pde4b*, *Ak2*, *Ak3*, *Ror1*, *Ppap2b*, *Inpp5b*, *Guca2a*, *Guca2b*, *Gjb3*, *Lck*, *Ptpu*, *Fdpsl2*, *Rap1ga1*, *Pla2g5*, *Pla2g2a*, *Pla2g2c*, *Frap1*, and *Gnb1*. Of these potential receptor or receptor-associated upstream genes, we were particularly interested in the *Lepr* gene as a candidate “mechanosensitivity” modulating gene. In this regard, a recent preliminary genome-wide screen study in the rat (4) has suggested that the *Lepr* gene (located within a bone-strength QTL of rat chromosome 5) was associated strongly with bone architecture and strength.

Although the leptin signaling is an important regulator of bone formation, its effects can be stimulatory or inhibitory, depending on whether the administration is peripheral or central in



nature. Leptin may stimulate bone formation through direct angiogenic and chondro-osteogenic effects (5), but it may also exert negative effects on bone formation through a hypothalamic pathway mediated downstream by the sympathetic nervous system (6). Accordingly, leptin exerts dual effects depending on bone tissue, skeletal maturity, or signaling pathway. Because of this unique dual action of the *Lepr* signaling pathway on bone formation, it has been suggested that the *Lepr* pathway may have a critical role in the “Mechanostat” theory in the overall regulation of bone mass and integrity (7).

To test whether *Lepr* may be a candidate mechanosensitivity gene, we evaluated the effects of mechanical loading on bone formation in leptin-deficient *ob/ob* mice. We reasoned that if *Lepr* or its signaling pathway indeed plays a role in determination of bone cell mechanosensitivity, the bone formation response in bone of *ob/ob* mice would be significantly

altered. Our investigation of the bone phenotype of *ob/ob* mice revealed a previously undisclosed, but very interesting, observation (8). In this regard, androgen functions produce sex-related differences in several tissues, including bones, leading to the greater periosteal expansion in the males, but these sex-related differences in bone parameters were surprisingly absent in the femur of male *ob/ob* mice. Accordingly, pQCT measurements of the periosteal circumference revealed that the significant differences between male and female B6 mice were not seen between male *ob/ob* and female *ob/ob* mice. The same was true of the endosteal circumference in B6 male and female mice ( $3.6$  vs  $3.3$  mm<sup>2</sup>,  $p < 0.0002$ ); male and female *ob/ob* mice showed no significant differences ( $3.4$  vs  $3.3$  mm<sup>2</sup>). The difference in the trabecular area of the male and female B6 mice ( $0.73$  vs  $0.56$  mm<sup>2</sup>,  $p < 0.0002$ ) was not significant in the male and female *ob/ob* mice ( $0.64$  vs  $0.61$  mm<sup>2</sup>). There were no differences in the bone parameters between B6 and *ob/ob* females. The loss of androgen effects in male *ob/ob* mice could not be explained by a decrease in free serum testosterone or estrogen levels, since it was higher in male *ob/ob* mice ( $313$  vs  $693$  pg/ml,  $p < 0.005$ ) than in B6 mice and since serum estradiol was also increased in female *ob/ob* mice relative to B6 mice ( $67$  vs  $100$  pg/ml,  $p < 0.0001$ ). It is also not due to the loss of *Lepr*, since *Lepr* mRNA levels in bones of *ob/ob* mice (by real-time PCR) were not different from those in bones of B6 mice. Preliminary real-time PCR measurements of bone expression of several androgen responsive genes suggested that their levels were lower in male *ob/ob* bones than in male B6 bones (data not shown). Although these data need to be confirmed, our results suggest that the lost of androgen-specific effects on bone in male *ob/ob* mice may be due to a defect in the androgen signaling.

Because the *ob/ob* males appear to have a defective androgen signaling in the bones, we used only female *ob/ob* and B6 mice to determine the bone response (by pQCT) to a 2-week four-point bending exercise regimen. We chose the four-point bending exercise model as the *in vivo* loading model because this model provides: 1) a controlled external loading of an intact long bone; and 2) the contralateral limb can be used as the control to determine the loading response. This loading regimen also caused a massive increase in cancellous bone formation at the periosteum of the loaded tibia of B6 mice, but not in the loaded tibia of C3H mice (1).

The bone formation response is determined by mechanical strain sensed by the bone rather than the loading force *per se* and the strain created by a given load is influenced by the bone size. Because the size of tibia of adult female *ob/ob* mice is significantly bigger than that of B6 mice (periosteal circumference:  $5.66 \pm 0.21$  vs.  $4.94 \pm 0.21$  mm,  $p < 0.0001$ ), we measured the actual strain sensed by the loaded bones of 10-week-old female *ob/ob* mice as opposed to female B6 mice at a given load with a strain gauge. The predicted strain at various loading forces on each mouse strain based on their bone size was also calculated for comparison. As shown in Figure 1, the bones of B6 mice would experience a significantly higher strain at any given load than bones of *ob/ob* mice. Hence, the loading force needed to be adjusted to ensure that a similar strain is applied to B6 and *ob/ob* mice. Accordingly, a load of 9N produced  $\sim 2100$   $\mu\epsilon$  in female adult *ob/ob* mice, which was in a similar range as that ( $\sim 2500$   $\mu\epsilon$ ) produced by a 6N load in adult female B6 mice. Therefore, we used a 9 N load for *ob/ob* mice and a 6 N load for B6 mice.

In our experiments, the Instron four-point bending device consisted of two upper vertically movable points covered with rubber pads (4-mm apart), and two 12-mm lower non-movable points covered with rubber pads. During the bending exercise, the two upper pads touched the lateral surface of the tibia through overlaying muscle and soft tissue, while the lower pads touched the medial surface of the proximal and distal parts of the tibia. The loading protocol

consisted of a 9-N load (for *ob/ob* mice) or a 6-N load (for B6 mice) at a frequency of 2 Hz for 36 cycles and the exercise was performed once daily. The right tibia was subjected to the loading exercise, while the left tibia was used as an internal unloaded control. Upon anesthesia, the ankle of the tibia was positioned on the second lower immobile points of the Instron equipment, such that the region of tibia loaded did not vary from mouse to mouse. The loading was applied for 6 days/week with a day rest for 2-weeks. Mice were sacrificed 48 hrs after the final loading and tibias were collected for pQCT measurements. As shown in Figure 2, this dosage of strain had no stimulatory effect on any of the pQCT bone parameters in B6 mice. This is not surprising, since our previous data indicated that the 6N force is insufficient to produce a bone formation response in adult B6 mice (not shown). In contrast, this mechanical strain significantly increased total bone mineral content, cortical area, cortical content, cortical thickness, mBMD and vBMD at the site of loading in *ob/ob* mice. These findings indicate that female *ob/ob* mice showed an enhanced sensitivity to mechanical stimuli in tibia compared to female B6 mice.

To further test if deficiency of leptin expression would lead to an enhanced osteogenic response to mechanical stimuli, we examined the effects of a steady fluid shear on [ $^3$ H]thymidine

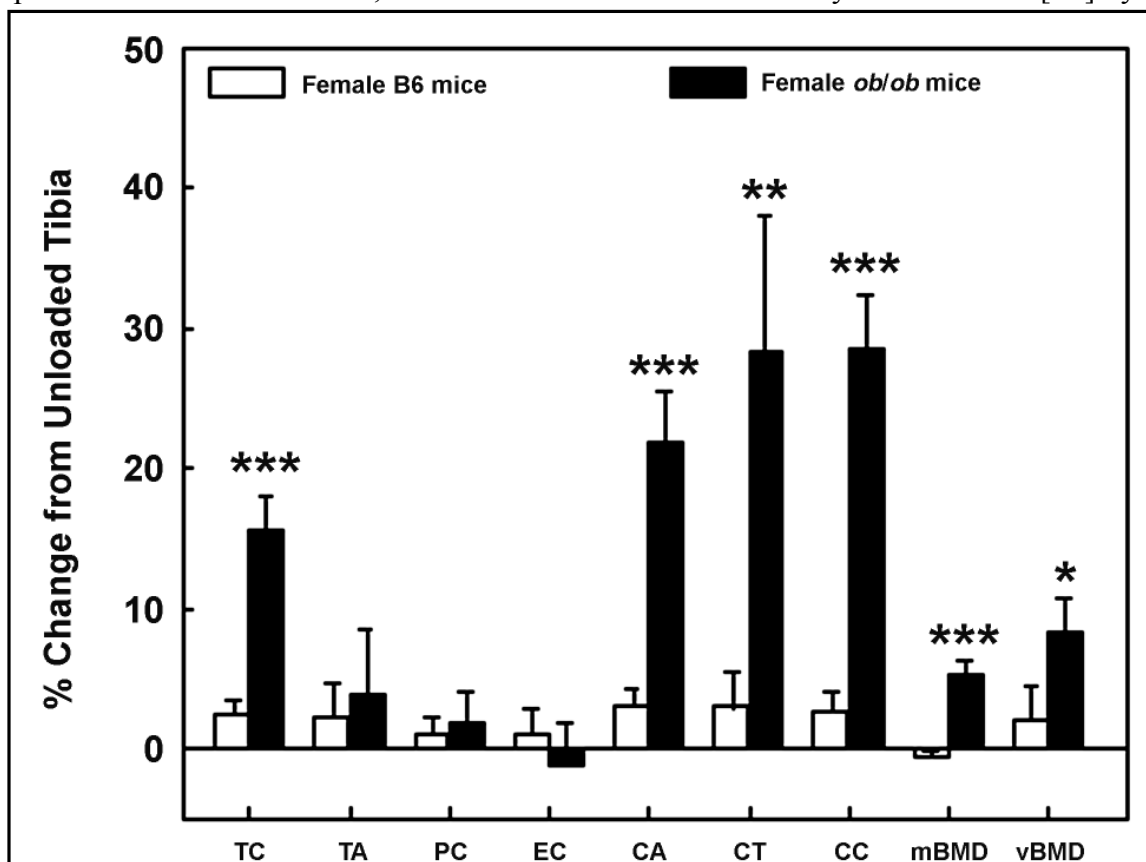


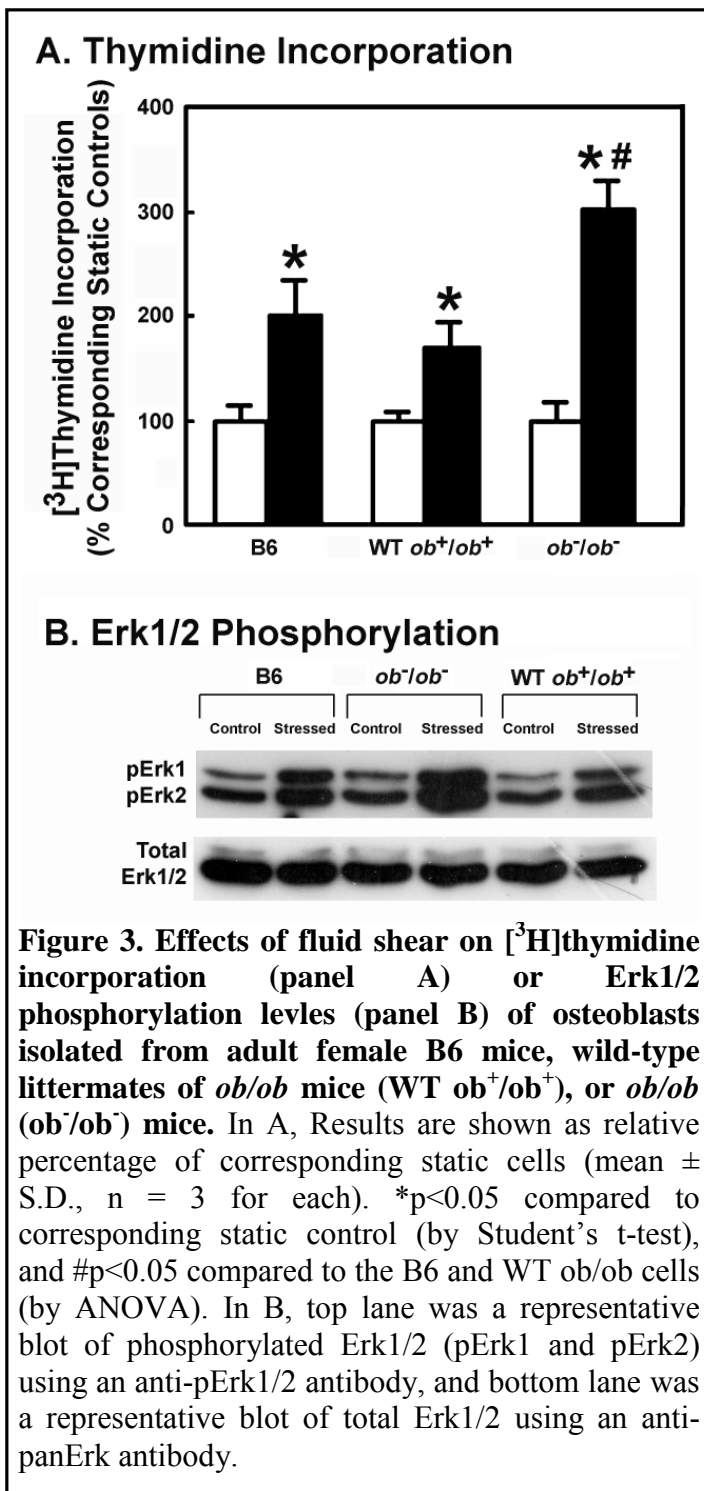
**Figure 2.** The bone responses in the tibia (determined by pQCT) of adult female *ob/ob* mice (filled bars) after a 2-week four-point bending exercise as opposed to those in the tibia of adult female B6 mice (open bars). The bending exercise was performed in 6 *ob/ob* mice and 12 B6 mice. The results are shown as relative percent change from the unloaded tibia of each individual mouse (mean  $\pm$  SEM). TC = total bone mineral content; TA = total area; PC = periosteal circumference; EC = endosteal circumference; CA = cortical area; CT = cortical thickness; CC = cortical content; mBMD = material bone mineral density; vBMD = volumetric BMD. \* $p < 0.05$ ; \*\* $p < 0.01$ ; and \*\*\* $p < 0.001$ .

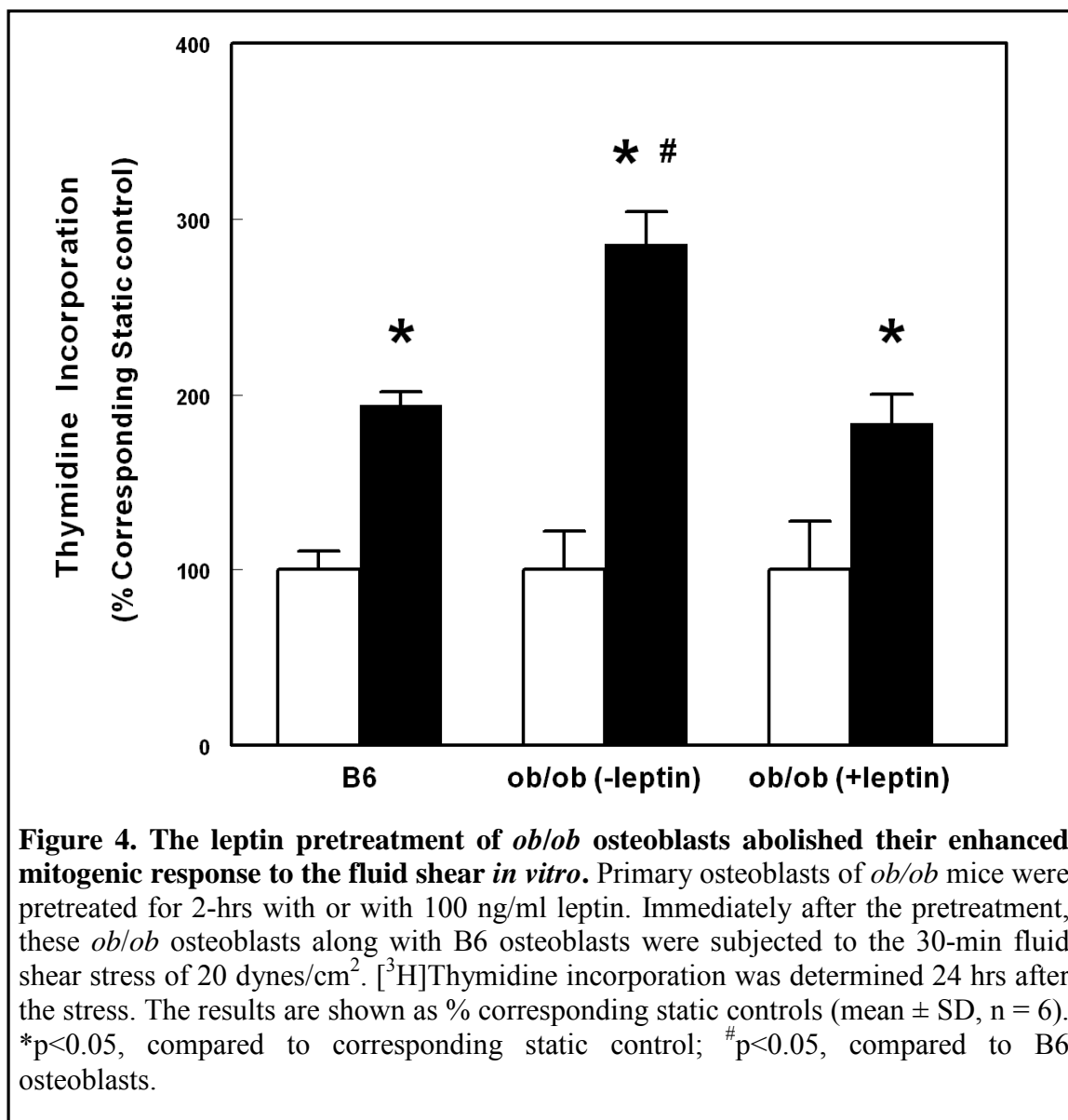
incorporation and Erk1/2 phosphorylation in osteoblasts isolated from adult female *ob/ob* mice as opposed to those in adult female B6 osteoblasts *in vitro*. Osteoblasts were isolated as previously described (1) and pooled cells were used. For comparison, osteoblasts of the WT littermates of *ob/ob* mice (*ob<sup>+</sup>/ob<sup>+</sup>*) were included. Figure 3 confirms that a 30-min steady fluid shear of 20 dynes/cm<sup>2</sup> significantly stimulated [<sup>3</sup>H]thymidine incorporation and Erk1/2 phosphorylation in female B6 osteoblasts. The same shear stress produced significantly greater increases in [<sup>3</sup>H]thymidine incorporation and Erk1/2 phosphorylation in *ob<sup>-</sup>/ob<sup>-</sup>* osteoblasts than those in B6 osteoblasts and osteoblasts of WT *ob<sup>+</sup>/ob<sup>+</sup>* littermates. The shear stress-induced [<sup>3</sup>H]thymidine incorporation and Erk1/2 phosphorylation in WT *ob<sup>+</sup>/ob<sup>+</sup>* osteoblasts were not

different from those in B6 osteoblasts. These results are highly reproducible and were seen in every repeat experiment. While these preliminary findings are exciting and support our overall hypothesis, it is also somewhat puzzling to observe an enhanced mitogenic response in the isolated *ob/ob* osteoblasts to the fluid shear, since as shown in **Fig. 5** below, these osteoblasts were deficient only in leptin production but not in the *Lepr* expression.

A potential explanation for this observation is that primary B6 mouse osteoblasts, especially after exposure of the fluid shear, may produce sufficient amounts of leptin to suppress the *Lepr* signaling. The lack of the leptin production in *ob/ob* osteoblasts may thus alleviate the suppressive effects of the endogenous leptin, resulting in an enhanced mitogenic response to mechanical stimulation. Leptin is primarily synthesized by adipose tissues. We are currently test the hypothesis that primary mouse osteoblasts may produce significant amounts of leptin, especially after the fluid shear. These *in vitro* data are consistent with the *in vivo* loading data that deficiency of leptin expression or *Lepr* signaling enhanced the osteogenic response to mechanical stimulation.

If the observed enhanced mitogenic response of *ob/ob* osteoblasts to fluid shear was indeed due to the deficiency





in the *Lepr* signaling, we reason that pretreatment of *ob/ob* osteoblasts with an effective dose of leptin prior to the fluid shear would block the enhanced response. Thus, we assessed the effects of a 2-hr pretreatment with 100 ng/ml of leptin prior to the 30-min steady shear stress of 20 dynes/cm<sup>2</sup> on [<sup>3</sup>H]thymidine incorporation in osteoblasts of *ob/ob* mice. Figure 4 shows that *ob/ob* osteoblasts without the leptin pretreatment, again, showed a significantly greater response to the shear stress than B6 osteoblasts. The mitogenic response of *ob/ob* osteoblasts to the same shear stress was markedly reduced by the leptin treatment and was now no longer different from that of B6 osteoblasts, indicating that the enhanced mitogenic response to fluid shear in *ob/ob* osteoblasts was completely obliterated by the leptin pretreatment. These preliminary data suggest that the *Lepr* signaling has a negative regulatory role in the context of mechanotransduction.

A corollary to our hypothesis that the mechanosensitivity genes contributing to the good and poor bone formation response, respectively, in B6 and C3H mice are upstream to the 4 anabolic pathways-of-interest is that the ability to upregulate these 4 pathways in response to mechanical

stimulation may be used as a screening test for candidate mechanosensitivity modulating genes. Thus, if *Lepr* is indeed a “mechanosensitivity” modulating gene in these mouse strains, it follows that the enhanced mitogenic response to fluid shear in *ob/ob* osteoblasts should be accompanied by an enhanced response in the upregulation of expression of genes associated with the four

**Table 1: Effect of the 30-min fluid shear of 20 dynes/cm<sup>2</sup> on the expression of genes of the IGF-I, BMP/TGF $\beta$ , ER, and Wnt signaling pathways in B6 osteoblasts and *ob/ob* osteoblasts measured by real-time PCR 4 hrs after the stress (n = 3 for each).**

Gene	B6 osteoblasts (Stressed/Static Control, Fold changes, mean $\pm$ SD)	<i>ob/ob</i> osteoblasts (Stressed/Static Control, Fold changes, mean $\pm$ SD)
<i>Era</i>	2.04 $\pm$ 0.30*	3.31 $\pm$ 0.20*. <sup>#</sup>
<i>Igf1r</i>	2.38 $\pm$ 0.32*	4.49 $\pm$ 0.71*. <sup>#</sup>
<i>Dlx1</i>	2.09 $\pm$ 0.42*	3.23 $\pm$ 0.65*. <sup>#</sup>
<i>Ncoal</i>	1.90 $\pm$ 0.78*	3.74 $\pm$ 0.88*. <sup>#</sup>
<i>c-fos</i>	1.95 $\pm$ 0.42*	2.56 $\pm$ 0.29*. <sup>#</sup>
<i>Ctnnb1</i>	2.71 $\pm$ 0.95*	3.80 $\pm$ 0.62*. <sup>#</sup>
<i>Wnt1</i>	2.16 $\pm$ 0.22*	3.65 $\pm$ 0.52*. <sup>#</sup>
<i>Wnt3a</i>	2.04 $\pm$ 0.22*	3.00 $\pm$ 0.62*. <sup>#</sup>

\*p<0.05, compared to the corresponding static control.

<sup>#</sup>p<0.05, compared to B6 osteoblasts.

anabolic signaling pathways-of-interest. Thus, we next compared levels of upregulation in expression of several genes associated with the IGF-I (*Igf1r*, *c-fos*), ER (*Era*, *Ncoal*), BMP/TGF $\beta$  (*Dlx1*), and canonical Wnt (*Ctnnb1*, *Wnt1*, *Wnt3a*) pathways 4 hr after the fluid shear (by real-time PCR). Table 1 shows that, while the 30-min steady fluid shear significantly upregulated

the expression of the test genes in B6 and *ob/ob* osteoblasts, the upregulation of each test gene in *ob/ob* osteoblasts was significantly greater than that in B6 osteoblasts. These results are consistent with our hypothesis that the lack of the leptin gene or the *Lepr* signaling in osteoblasts would enhance the upregulation of expression of genes associated with the 4 pathways-of-interest in response to mechanical stimulation and that these four pathways are downstream to the *Lepr* signaling.

If the *Lepr* signaling has a negative regulatory role on the mechanosensitivity in osteoblasts, then activation of the *Lepr* signaling should blunt the effect of shear stress on the upregulation of expression of genes associated with these 4 pathways-of-interest. Thus, we evaluated the effect of the overnight pretreatment of B6 osteoblasts with 100 ng/ml leptin on the expression of the test genes 4 hrs after the stress. Table 2 shows that the 2-hr pretreatment with 100 ng/ml leptin drastically suppressed the shear stress-induced upregulation of expression of the test genes. Along with our findings in Figures 3-4, we conclude that the *Lepr* signaling functions as a negative regulatory pathway in the context of mechanotransduction in osteoblasts.

If our hypothesis that the differential bone formation response to mechanical stimuli between B6 and C3H mice is in part due to a “defective” *Lepr* signaling in C3H osteoblasts has merit, we would expect a difference in either the expression of *Lepr* gene or the effectiveness of the *Lepr*

pathway between B6 and C3H osteoblasts. Thus, we evaluated if there were a difference in the basal and/or fluid shear-induced expression of *Lepr* between B6 and C3H osteoblasts. To quantitatively measure the *Lepr* mRNA levels in B6 and C3H osteoblasts, real-time PCR was

**Table 2: Effect of the overnight pretreatment with 100 ng/ml leptin on the shear stress-induced expression of genes of the IGF-I, BMP/TGF $\beta$ , ER, and Wnt signaling pathways in B6 osteoblasts by real-time PCR 4 hrs after the fluid shear (n=3 for each).**

Gene	Stressed/Static Control (No leptin pretreatment, Fold changes, mean $\pm$ SD)	Stressed/Static Control (+ leptin pretreatment, Fold changes, mean $\pm$ SD)
<i>Era</i>	2.40 $\pm$ 0.75*	1.39 $\pm$ 0.25 <sup>#</sup>
<i>Igf1r</i>	3.30 $\pm$ 0.36*	1.55 $\pm$ 0.29 <sup>#</sup>
<i>Dlx1</i>	1.68 $\pm$ 0.48*	0.75 $\pm$ 0.10 <sup>#</sup>
<i>Ncoa1</i>	2.89 $\pm$ 0.11*	1.34 $\pm$ 0.60 <sup>#</sup>
<i>c-fos</i>	3.06 $\pm$ 0.68*	1.25 $\pm$ 0.22 <sup>#</sup>
<i>Ctnnb1</i>	2.62 $\pm$ 0.54*	0.90 $\pm$ 0.30 <sup>#</sup>
<i>Wnt1</i>	2.71 $\pm$ 0.74*	0.93 $\pm$ 0.09 <sup>#</sup>
<i>Wnt3a</i>	2.56 $\pm$ 0.75*	1.66 $\pm$ 0.25 <sup>#</sup>

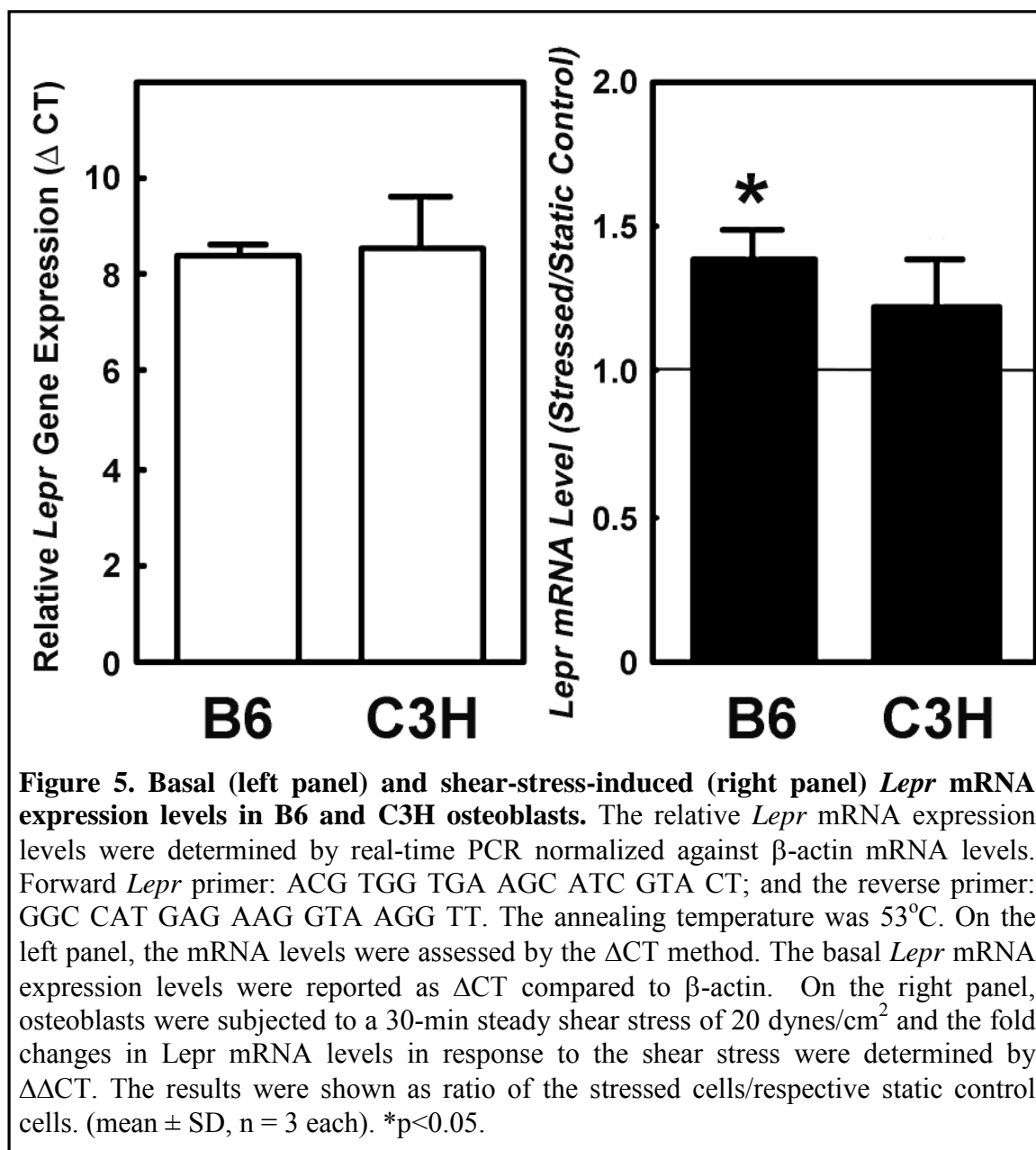
\*p<0.05, compared to the corresponding static control.

<sup>#</sup>p<0.05, compared to those without the leptin pretreatment.

performed using the following primer set for *Lepr* mRNA [forward primer: 5'-ACG TGG TGA AGC ATC GTA CT-3' and reverse primer: 5'-GGC CAT GAG AAG GTA AGG TT-3'] with an annealing temperature of 53°C. There was no difference in basal *Lepr* mRNA expression levels [reported as  $\Delta C_T$  (the difference between the threshold cycle ( $C_T$ ) of *Lepr* and that of  $\beta$ -actin)] between the two osteoblasts (left panel of **Fig. 5**). The shear stress slightly increased the *Lepr* mRNA levels by ~40% in B6 osteoblasts and ~25% in C3H osteoblasts. The increase in C3H osteoblasts approached, but did not reach, the significant level (right panel). Thus, the basal and the shear stress-induced *Lepr* mRNA expression levels in C3H and B6 osteoblasts were not significantly different.

We next assessed the possibility that polymorphisms might exist in the coding region of the *Lepr* gene between C3H and B6 mice. We cloned the full-length *Lepr* mRNA from both C3H and B6 osteoblasts by long-PCR and the DNA sequence of the entire open reading frame (ORF) of both strands of the *Lepr* gene of both C3H and B6 osteoblasts were determined and compared (Figure 6). We found that there were three single nucleotide differences in the *Lepr* ORF between B6 and C3H osteoblasts. The differences in these single nucleotides were not due to mutations introduced by the long PCR amplification, and the same variations also existed in some of the *Lepr* ORF sequences in the PubMed database. Thus, we conclude that these are SNPs: 1) G→A SNP at nucleotide 594; 2) T→C SNP at nucleotide 1041, and 3) A→G SNP at nucleotide 1075. [The nucleotide numbering system referred to that of the ORF]. Two of the SNPs are silent and are located at the wobble base, but the A→G SNP at nucleotide 1075 yielded an Ile→Val substitution at amino acid residue 359. Although the physiological significance of this substitution is unclear, we postulate that this substitution may affect the ligand binding and,

thus, the *Lepr* signaling, since the substitution is located within the ligand binding domain. Although it is beyond the scope of this proposal, it would be interesting to see if osteoblasts of other mouse strains that do not respond anabotically to the fluid shear, such as 129J and AKR (reported previously), would also exhibit this same A→G SNP at nucleotide 1075 of the *Lepr*. Our future work will address this possibility.



**Specific Aim #2: Determination of the molecular mechanism whereby the candidate gene (i.e., *Lepr*) acts to regulate the anabolic response in osteoblasts.** The mechanism(s) whereby the *Lepr* signaling pathway negatively regulates mechanotransduction in osteoblasts is unknown. Because fluid shear only slightly increased *Lepr* mRNA expression in both B6 and C3H

***SNP1: G→A at nucleotide 594***

B6 osteoblasts :	571 cgg ggt tgt gaa tgt cat gtg cc <b>g</b> gta ccc aga gcc aaa ctc 612
	R G C E C H V P V P R A K L
C3H osteoblasts:	571 cgg ggt tgt gaa tgt cat gtg cc <b>a</b> gta ccc aga gcc aaa ctc 612
	R G C E C H V P V P R A K L

***SNP2: T→C at nucleotide 1041***

B6 osteoblasts :	1009 aaa att ctg act agt gtt gga tgc aat gct t <b>ct</b> ttt cat tgc atc tac 1
	K I L T S V G S N A S F H C I Y
C3H osteoblasts:	1009 aaa att ctg act agt gtt gga tgc aat gct t <b>c</b> ttt cat tgc atc tac 1
	K I L T S V G S N A S F H C I Y

***SNP3: A→G at nucleotide 1075***

B6 osteoblasts :	1057 aaa aac gaa aac cag att <b>atc</b> tcc tca aaa cag ata gtt tgg tgg 1
	K N E N Q I <b>I</b> S S K Q I V W W
C3H osteoblasts:	1057 aaa aac gaa aac cag att <b>gtc</b> tcc tca aaa cag ata gtt tgg tgg 1
	K N E N Q I <b>V</b> S S K Q I V W W

**Figure 6. Existence of three single nucleotide polymorphisms (SNP) in *Lepr* open reading frame between B6 and C3H osteoblasts.** The bold letters in the nucleotide sequences indicate the location of SNPs. Single letter symbols are used to represent amino acid sequence. The bold and italic letter illustrates the Ile→Val substitution in the amino acid sequence.

osteoblasts (Figure 5), we conclude that the inhibitory effect of fluid shear on the *Lepr* signaling is not mediated by suppression of the *Lepr* expression. *Lepr* is a member of the class I cytokine receptor family (9) and uses Janus kinase (JAK)2-signal transducers and activators of transcription (STAT) 3 as the primary signaling (10). As schematically shown in Figure 7, the binding of leptin to *Lepr* results in transphosphorylation and activation of JAK2 and the subsequent phosphorylation of tyrosine residues in the cytoplasmic part of *Lepr*, which provide docking sites for SH2-containing signaling proteins, including STAT3, SHP2, suppressor of cytokine signaling 3 (SOCS3), and PTP1B. Recruitment of STAT3 to the phosphorylated tyr(pY)-1138 residue leads to its rapid phosphorylation, dimerization, and translocation to the nucleus to activate transcription of STAT3-inducible genes, including SOCS3. The pY-985

residue recruits either SHP2 or SOCS3. Binding of SOCS3 attenuates leptin signaling by inhibiting the receptor-associated JAKs. Recruitment of SHP2 can have both positive and negative effects on the *Lepr* signaling. On the one hand, the SHP2 binding results in binding of Grb2 to SHP2 and subsequent activation of the Ras/Raf/Erk signaling pathway, leading to, among others, the expression of c-fos. On the other hand, SHP2 dephosphorylates and inactivates JAK2, leading to termination of the *Lepr* signaling. PTP1B is a critical downstream negative regulator of the *Lepr* pathway. Deletion of PTP1B gene enhanced leptin sensitivity in mice (11). PTP1B decreased JAK2 phosphorylation and blocked leptin-induced transcription of SOCS3 and c-fos (12). The *Lepr* signaling pathway also regulates other key anabolic pathways through crosstalks, including the integrin, IGF-I, ER, BMP/TGF $\beta$ , and canonical Wnt signaling pathways. Figure 7 shows some of the interactions between the *Lepr* and the integrin signaling pathways. Specifically, the recruitment of SHP2 and/or PTP1B to integrin is essential for the integrin signaling (13,14). Recruitment of these PTPs would lead to c-Src activation (by dephosphorylating its inhibitory pY-527 residue), which in turn activates the Grb2/Ras/RAF/Erk signaling. We surmise that there is a competition between integrins and *Lepr* for recruitment of SHP2 and/or PTP1B (indicated by the thick arrows in Figure 7), and that the *Lepr* pathway inhibits the mechanical stimulation of bone formation in part through sequestering SHP2 and/or PTP-1B from binding to integrins. We further postulate that the mechanism(s) leading to the preferential recruitment of SHP2 and PTP-1B to integrins in response to mechanical stimuli is defective in C3H osteoblasts.

As a preliminary test of our model, we determined and compared the basal and shear stress-induced levels of leptin-dependent activation of JAK2/STAT3 in C3H osteoblasts and B6 osteoblasts. We reasoned that if the I359V substitution alters the efficiency of the *Lepr* signaling in C3H osteoblasts, the basal and/or shear stress-induced leptin-mediated activation of the *Lepr* signaling in the two osteoblasts should be different. As a preliminary test for this hypothesis, we measured the relative levels of total and the tyrosine phosphorylated JAK2 and total and tyrosine phosphorylated STAT3 in C3H and B6 osteoblasts with or without the 30-min steady fluid shear. We also included osteoblasts of *ob/ob* mice for comparison. Figure 8 shows that the basal leptin-mediated increases in p-JAK2 and p-STAT3 levels in the C3H were higher than those in the B6 and *ob/ob* osteoblasts. While this finding needs to be confirmed, it is entirely consistent with our premise that the I359V substitution in *Lepr* in C3H osteoblasts leads to an enhanced basal leptin-mediated activation of the *Lepr* signaling pathway. It is also interesting to note that the basal total JAK2 and STAT3 levels appeared to be several fold higher in C3H osteoblasts than in B6 and *ob/ob* osteoblasts. It raises the possibility that other genetic differences between B6 and C3H mice might cause the greater levels of JAK2 and STAT3 in C3H osteoblasts, which might in part be responsible for the differential osteogenic response to mechanical stimulation in the two mouse strains. Because there does not appear to be a significant difference in the *Lepr* mRNA expression level between the two mouse osteoblasts (Figure 5), the enhanced *Lepr* signaling seen with the C3H osteoblasts is probably related to an enhanced ligand binding affinity and/or a more efficient transduction of signals in C3H osteoblasts compared to B6 osteoblasts. The 30-min steady shear stress markedly suppressed the leptin-mediated increases in the p-JAK2 and p-STAT3 levels in all three test osteoblasts. The shear stress-mediated suppression appeared to be bigger in *ob/ob* osteoblasts compared to that in B6 and C3H osteoblasts. Although the fluid shear suppressed the leptin-mediated p-JAK2 and p-STAT3 levels in C3H osteoblasts, the resulting p-JAK2 and p-STAT3 levels were still several folds higher than the basal levels of these proteins in B6 and *ob/ob* osteoblasts. It may be speculated that the shear stress produced by physiologically

relevant levels of loading might not be sufficient to reduce the *Lepr* signaling to a level that would yield an anabolic response. The past findings that high levels of mechanical strains were able to elicit an osteogenic response in C3H mice (15) are consistent with this possibility. Moreover, because the shear stress increased the *Lepr* mRNA levels in these osteoblasts (Figure 5), the suppression of p-JAK2/p-STAT3 phosphorylation levels is not due to a reduction in the number of *Lepr*, but may be due to an inhibition of the *Lepr* signaling. While these findings need to be confirmed, these results suggest that the leptin signaling pathway is a negative pathway in the context of mechanotransduction and that mechanical stimulation activates the mechanotransduction in part by suppressing this negative pathway.

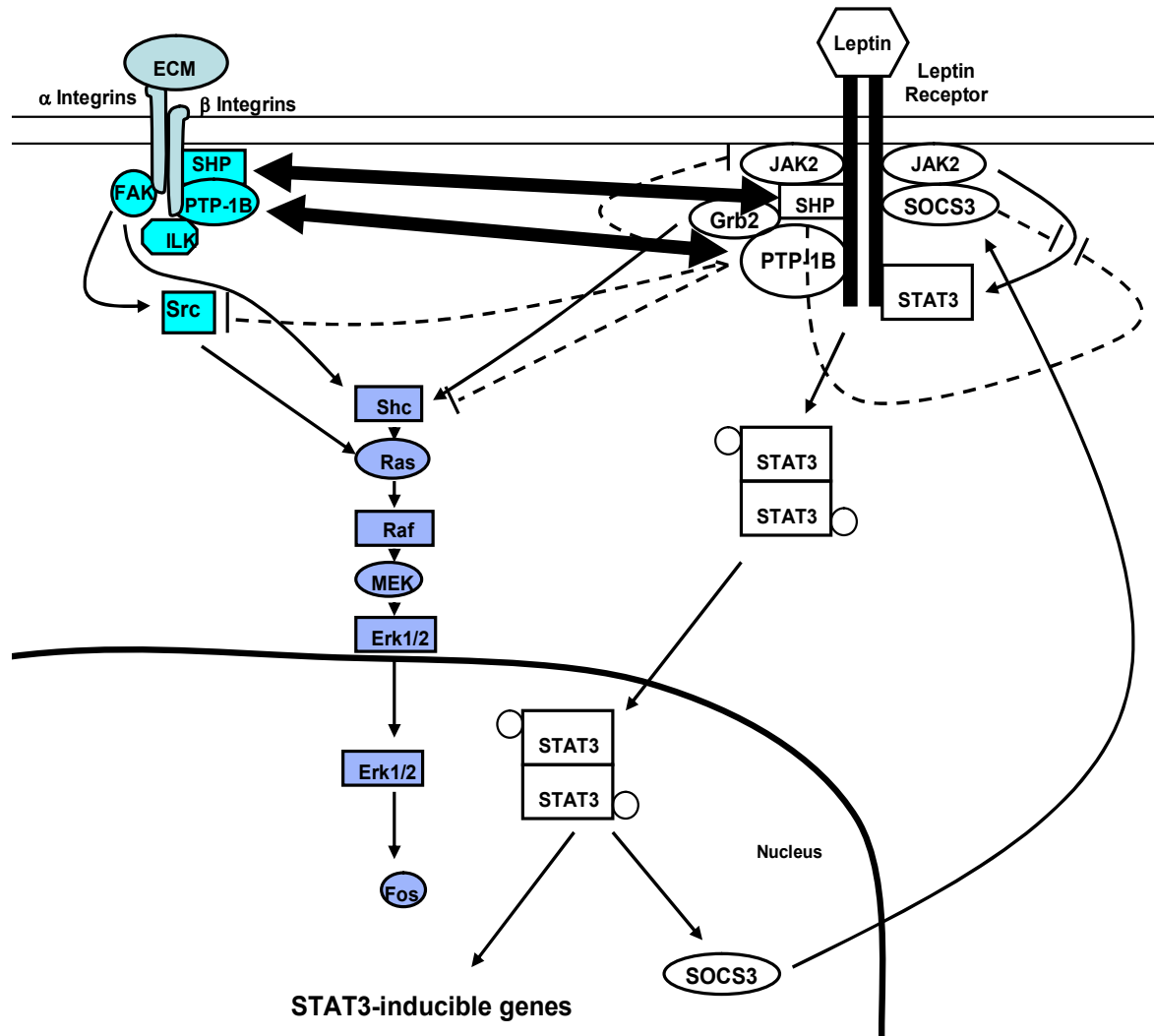
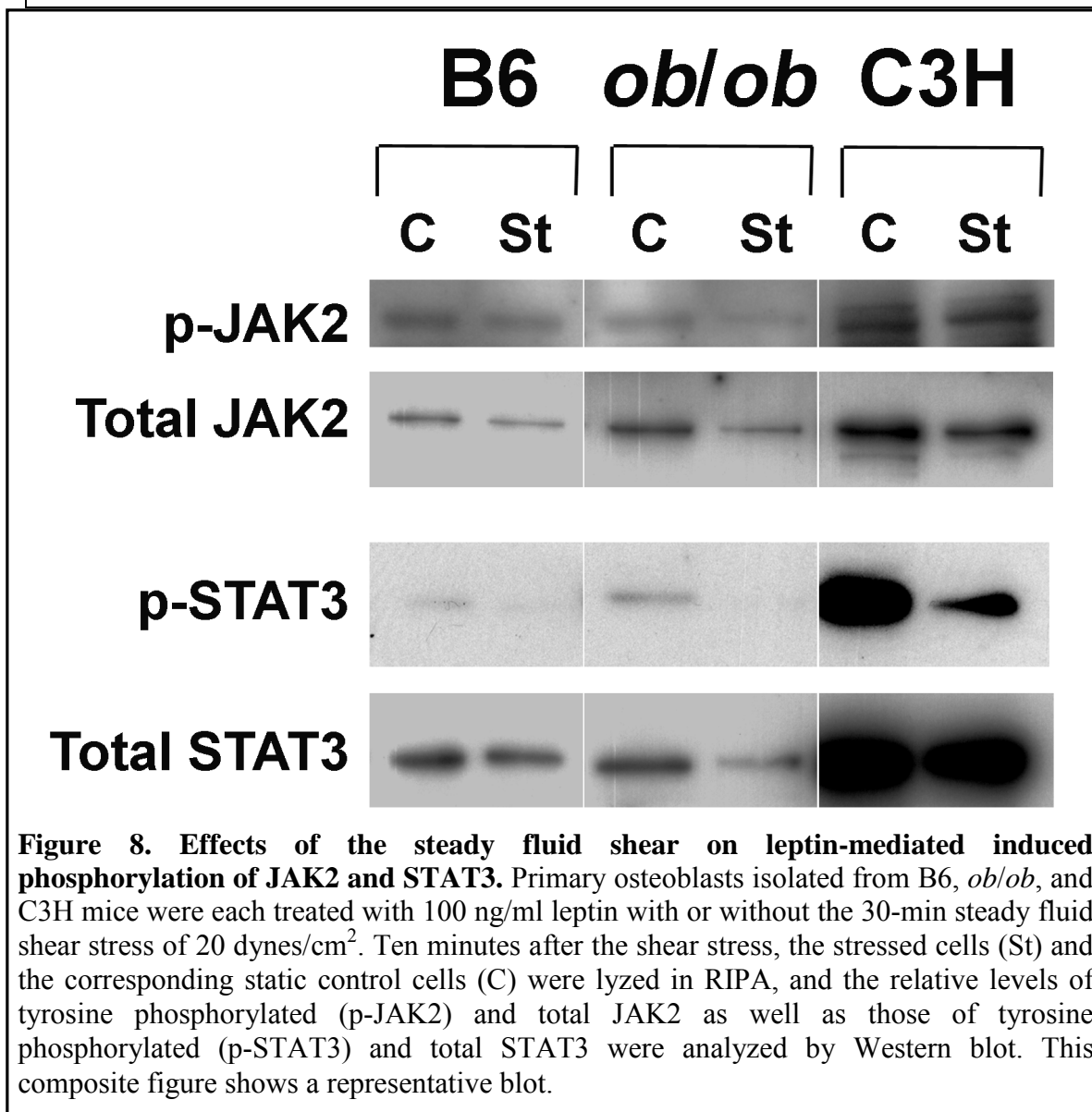


**Figure 7. Molecular mechanism of the leptin receptor signaling pathway and its potential interactions with the integrin signaling pathway.** Please refer to text for a detailed description. The solid lines represent upregulation; while the dashed lines indicate negative regulation. The thick arrows indicates shuffling of SHP2 and/or PTP1B between *Lepr* and integrins.



#### Key Research Accomplishments:

1. We have obtained strong circumstantial evidence that the *Lepr* signaling pathway is a negative regulator of mechanical stimulation of bone formation.

2. We have shown that there are three SNPs in the coding region of *Lepr* between B6 and C3H mice, and that one of the SNPs resulted in the change of the amino acid sequence of the *Lepr* protein.
3. We have obtained preliminary evidence that leads to our hypothesis that the *Lepr* signaling pathway in osteoblasts negatively regulate the anabolic response to mechanical stimuli through sequestering SHP2 and/or PTP-1B from binding to integrins.

### Reportable Outcomes:

1. Lau K-HW, Kapur S, Kesavan C, and Baylink DJ (2006) Upregulation of the wnt, estrogen receptor, insulin-like growth factor-I and bone morphogenetic protein pathways in C57BL/6J osteoblasts as opposed to C3H/HeJ osteoblasts in part contributes to the differential anabolic response to fluid shear. *J Biol Chem* 281(14), 9576-9588.
2. Kapur S, Baylink DJ, and Lau K-HW (2005) The canonical Wnt pathway is downstream to the BMP signaling pathway in mediating fluid shear stress-induced osteoblast proliferation. *J Bone Miner Res* 20 (Suppl 1), S240, abstract # SU219.

### Conclusions:

In summary, these data provide strong supports for our conclusions that 1) the *Lepr* and its signaling pathway acts as a negative regulator of mechanosensitivity, 2) the *Lepr* in osteoblasts of B6 and C3H mice might have different functional activity due to a SNP in the coding region, and the different functional activity of *Lepr* in osteoblasts of these two mouse strains may in part be responsible for the differential anabolic response to mechanical stimuli in these two mouse strains, and 3) the *Lepr* signaling pathway in osteoblasts negatively regulate the anabolic response to mechanical stimuli through sequestering SHP2 and/or PTP-1B from binding to integrins. We are now in position to apply the siRNA technology to definitively evaluate whether *Lepr* or its signaling mechanism is involved in the regulation of the osteogenic response to mechanical stimulation.

### References:

1. Lau K-HW, Kapur S, Kesavan C, and Baylink DJ (2006) Upregulation of the Wnt, estrogen receptor, insulin-like growth factor-I, and bone morphogenetic protein pathways in C57BL/6J osteoblasts as opposed to C3H/HeJ osteoblasts in part contributes to the differential anabolic response to fluid shear. *J Biol Chem* **281**, 9576-9588.
2. Robling AG, Li J, Shultz KL, Beamer WG, and Turner CH (2003) Evidence for a skeletal mechanosensitivity gene on mouse chromosome 4. *FASEB J* **17**, 324-326.
3. Saxon LK, Robling AG, Alam I, Turner CH (2005) Mechanosensitivity of the rat skeleton decreases after a long period of loading, but is improved with time off. *Bone* **36**, 454-464.
4. Turner CH, Alam I, Sun O, Li J, Fuchs RK, Edenberg HJ, Koller DL, Foroud T, Econs MJ (2005) The leptin receptor strongly influences bone structure and strength: results from a genome-wide screen in rats. *J Bone Miner Res* 20 (Suppl 1), S28, abstract 1108.

5. Thomas T (2004) The complex effects of leptin on bone metabolism through multiple pathways. *Curr Opin Pharmacol* **4**, 295-300.
6. Ducey P, Amling M, Takeda S, Priemel M, Schilling AF, Beil FT, Shen J, Vinson C, Rueger NM, Karsenty G (2000) Leptin inhibits bone formation through a hypothalamic relay: a central control of bone mass. *Cell* **100**, 197-207.
7. Gordeladze JO, Reseland JE (2003) A unified model for the action of leptin on bone turnover. *J Cell Biochem* **88**, 706-712.
8. Rundle CH, Wang X, Wergedal JE, Srivastava AK, Davis EI, Lau K-HW, Mohan S, Baylink DJ (2006) Loss of sex-specific differences in bone size in leptin-deficient (*ob/ob*) mice. *Transactions to the 52<sup>nd</sup> Annual meeting of Orthopaed Res Soc* abstract # 188.
9. Tartaglia LA, Dembski M, Weng X, Deng N, Culpepper J, Devos R, Richards GJ, Campfield LA, Clark FT, Deeds J (1995) Identification and expression cloning of a leptin receptor, OB-R. *Cell* **83**, 1263-1271.
10. Hekerman P, Zeidler J, Bamberg-Lemper S, Knobelspies H, Lavens D, Tavernier J, Joost H-G, Becker W (2005) Pleiotropy of leptin receptor receptor signaling is defined by distinct roles of the intracellular tyrosines. *FEBS J* **272**, 109-119.
11. Zabolotny JM, Bence-Hanulee KK, Stricker-Krongrad A, Haj F, Wang Y, Minokoshi Y, Kim YB, Elmquist JK, Tartaglia LA, Kahn BB, Neel BG (2002) PTP1B regulates leptin signal transduction in vivo. *Dev Cell* **2**, 489-495.
12. Zabeau L, Lavens D, Peelman F, Eyckerman S, Vandekerckhove J, Tavernier J (2003) The ins and outs of leptin receptor activation. *FEBS Lett* **546**, 45-50.
13. Oh E-S, Gu H, Saxton TM, Timms JF, Hausdorff S, Frevert EU, Kahn BB, Pawson T, Neel BG, Thomas SM (1999) Regulation of early events in integrin signaling by protein tyrosine phosphatase SHP-2. *Mol Cell Biol* **19**, 3205-3215.
14. Arias-Salgado EG, Haj F, Dubois C, Moran B, Kasirer-Friede A, Furie BC, Furie B, Neel BG, Shattil SJ (2005) PTP-1B is an essential positive regulator of platelet integrin signaling. *J Cell Biol* **170**, 837-845.
15. Pedersen EA, Akhter MP, Cullen DM, Kimmel DB, Recker RR (1999) Bone response to in vivo mechanical loading in C3H/HeJ mice. *Calcif Tissue Int* **65**, 41-46.

## Progress for the period of 2007-2008

### A. Introduction:

This portion of the report summarizes our progress made during year 2007-2008 on the *in vitro* investigation into the molecular mechanism that mediates mechanical stimulation of osteoblast proliferation and differentiation, using primary mouse osteoblasts as the cell model and fluid shear stress as a surrogate of mechanical stimulus.

**B. Technical Objectives:** The original specific objectives for the *in vitro* studies during the past year of this grant are as follows:

1. To optimize the *in vitro* siRNA techniques for the application to mouse osteoblasts in conjunction with our shear stress technology.
2. To select one or more ESTs (or known genes) for further study from our microarray data.
3. To apply the siRNA technique to suppress the candidate EST expression or known gene and then evaluate the functional role of this EST or known gene in osteoblast proliferation, differentiation, and apoptosis.
4. To continue to advance our protein-tyrosine phosphorylation studies in order to identify signaling proteins that show differences in protein-tyrosine phosphorylation levels in response to mechanical strain in bone cells isolated from those mouse strains which exhibit differential responses to the *in vitro* mouse strains. Changes in protein-tyrosine phosphorylation levels will be compared to *in vitro* parameters of osteoblast proliferation, differentiation, and apoptosis.

### C. Body:

In our original experimental approach, we plan to identify potential candidate genes from our microarray data and to determine the effect of suppression of expression of the candidate gene in osteoblasts by the siRNA technology on their anabolic response to fluid shear stress. From our microarray and subsequent studies, which have been included in the previous report, we have compelling evidence that four anabolic signaling pathways, i.e., the IGF-I, estrogen receptor, Wnt, and BMP/TGF $\beta$  signaling pathways are downstream to the “mechanosensitivity” genes contributing to the good and poor bone formation response in B6 and C3H mice, respectively (1), and that the leptin receptor gene may be one of the “mechanosensitivity” modulating gene located with the chromosome 4 QTL region that contributes in part to the differential anabolic response to mechanical loading in C57BL/6J (B6) and C3H/HeJ (C3H) mice. During the previous year of our investigation, we have accumulated a large body of compelling *in vivo* and *in vitro* evidence that the leptin receptor (Lepr) signaling mechanism may function as a negative regulator of mechanotransduction. Most of our *in vitro* evidence has been summarized in the previous progress report. Therefore, this report will focus on our *in vivo* evidence supporting a negative regulatory role for the leptin-Lepr signaling. Inasmuch as our data strongly implicating an important negative regulatory function of the Lepr signaling on mechanical stimulation of bone formation, there are two concerns about our experimental designs. First, our conclusion that the Lepr signaling is an essential regulatory mechanism of mechanical stimulation of bone formation *in vivo* was based entirely on studies with leptin-deficient (ob/ob) mice rather than

Lepr-deficient mice. Second, our *in vitro* work used a steady fluid shear stress as the mechanical stimulus. It is now generally assumed that pulsatile shear stress rather than steady shear stress is physiologically relevant. Therefore, it is necessary to confirm our *in vitro* studies with the pulsatile flow. Consequently, work of past year has been largely focused on two revised objectives:

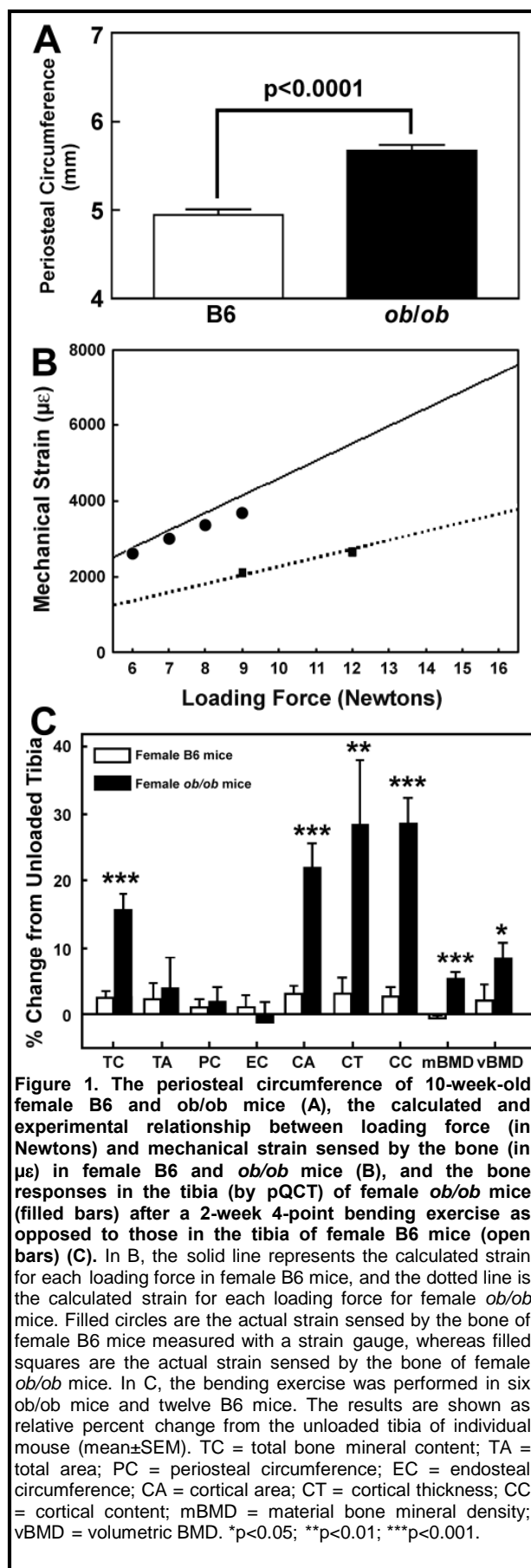
1. To generate a colony of Lepr-deficient mice for investigation.
2. To develop a pulsatile fluid flow system for subsequent confirmation studies.

The following section summarizes our progress towards some of the original objectives as well as the revised objectives:

**Specific Objective #1. To demonstrate if the leptin/Lepr signaling plays a negative mechanosensitivity modulating function in mechanical stimulation of bone formation in mice *in vivo*.**

Our previous progress report summarized our strong *in vitro* evidence that the Lepr signaling may function as a negative mechanosensitivity modulating pathway. To demonstrate that the Lepr signaling has a physiological regulatory role in mechanical stimulation of bone formation, we evaluated whether leptin-deficiency would alter bone mechanosensitivity *in vivo*. Leptin-deficient *ob<sup>-/-</sup>ob<sup>-/-</sup>* mice rather than the *Lepr*-deficient *db<sup>-/-</sup>db<sup>-/-</sup>* mice were used in this study, simply because of convenience, as we have already established a breeding colony of *ob<sup>-/-</sup>ob<sup>-/-</sup>* mice in our laboratory, and we have previously characterized the bone phenotype of these *ob<sup>-/-</sup>ob<sup>-/-</sup>* mice (2). Heterozygous male and female leptin-deficient (*ob<sup>-/-</sup>ob<sup>-/-</sup>*) breeder mice (B6.v-Lep<sup>ob</sup>/J) were obtained from the Jackson Laboratories (Bar Harbor, ME) and maintained at the J. L. Pettis Memorial V. A. Medical Center. Leptin-deficient mice were bred, and the homozygous leptin-deficient genotype was confirmed by reverse-transcriptase polymerase chain reaction (RT-PCR) as previously described (3). Our previous investigation of the bone phenotype of *ob<sup>-/-</sup>ob<sup>-/-</sup>* mice revealed that adult male *ob<sup>-/-</sup>ob<sup>-/-</sup>* mice lacked the sex-related differences in the greater periosteal expansion and that the loss of sex-related bone size differences in male *ob<sup>-/-</sup>ob<sup>-/-</sup>* mice appeared to be due to a defective androgen signaling in male *ob<sup>-/-</sup>ob<sup>-/-</sup>* mice (2). To avoid potential sex-related effects, this study used only adult (10-week-old) female leptin-deficient *ob<sup>-/-</sup>ob<sup>-/-</sup>* mice. Age-matched female B6 mice (also from the Jackson Laboratories) were included as the background strain control for comparison.

The osteogenic response to loading (in the form of 2-week four-point bending exercise) on tibia of adult female leptin-deficient *ob<sup>-/-</sup>ob<sup>-/-</sup>* mice was compared with that on tibia of age-matched female C57BL/6J (B6) background genetic strain control mice. However, Fig. 1A shows that the size (i.e., periosteal circumference) of tibia of *ob<sup>-/-</sup>ob<sup>-/-</sup>* mice was significantly bigger (by ~14%) than that of age-matched female B6 tibia. Because the bone formation response is determined by mechanical strain sensed by the bone rather than the loading force *per se*, we measured, with a strain gauge, the actual strain sensed by the loaded tibias of adult female *ob<sup>-/-</sup>ob<sup>-/-</sup>* mice as opposed to age-matched female B6 tibia at various loads. Fig. 1B shows that: 1) the determined strain sensed by the bones compared well with the calculated strain at various loading forces on each mouse strain based on respective bone size, and 2) the tibia of B6 mice with a larger bone size had indeed experienced a much higher strain at any given load than tibias



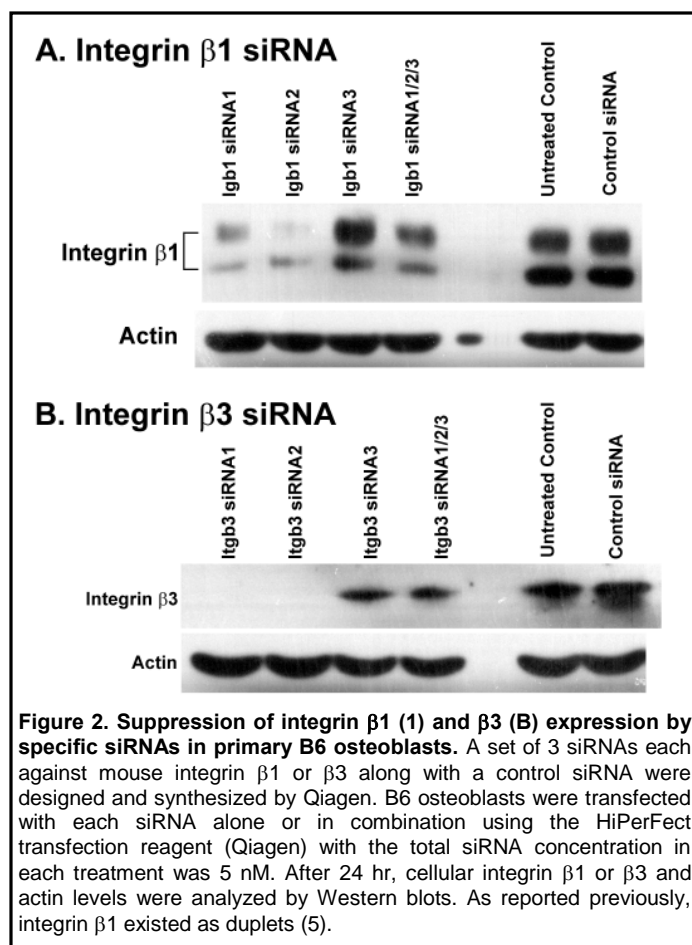
of *ob/ob* mice. Hence, the loading force for each mouse strain must be adjusted to ensure that similar mechanical strain was applied to tibia of each mouse strain. Our past studies in B6 mice used 9-N (4,5). If a 9-N load were to be used in B6 mice, a loading force of ~16-N would be needed for *ob/ob* mice. Loading forces of >12-N would break these bones. Thus, we used a 9-N load (~2,100  $\mu\epsilon$ ) for female *ob/ob* mice and a 6-N load (~2,500  $\mu\epsilon$ ) for female B6 mice.

Consistent with the previous dose-dependent studies which showed that the 6-N force is insufficient to produce a bone formation response in adult B6 mice (4,5), this dosage of strain had no effect on any of the pQCT parameters in adult female B6 mice (Fig. 1C). Conversely, this strain increased significantly total bone mineral content, cortical area, cortical content, cortical thickness, and material and volumetric bone mineral densities at the site of loading in *ob/ob* mice, indicating that *ob/ob* mice had an enhanced mechanosensitivity compared to B6 mice.

### Specific Objective 2. To optimize the *in vitro* siRNA techniques for the application to mouse osteoblasts in conjunction with our shear stress technology.

One of our original Technical Objectives was to apply the *in vitro* siRNA techniques for functional testing of candidate genes in mechanotransduction. Consequently, we have also initiated work to develop effective protocols for the *in vitro* siRNA techniques for the application to primary mouse osteoblasts.

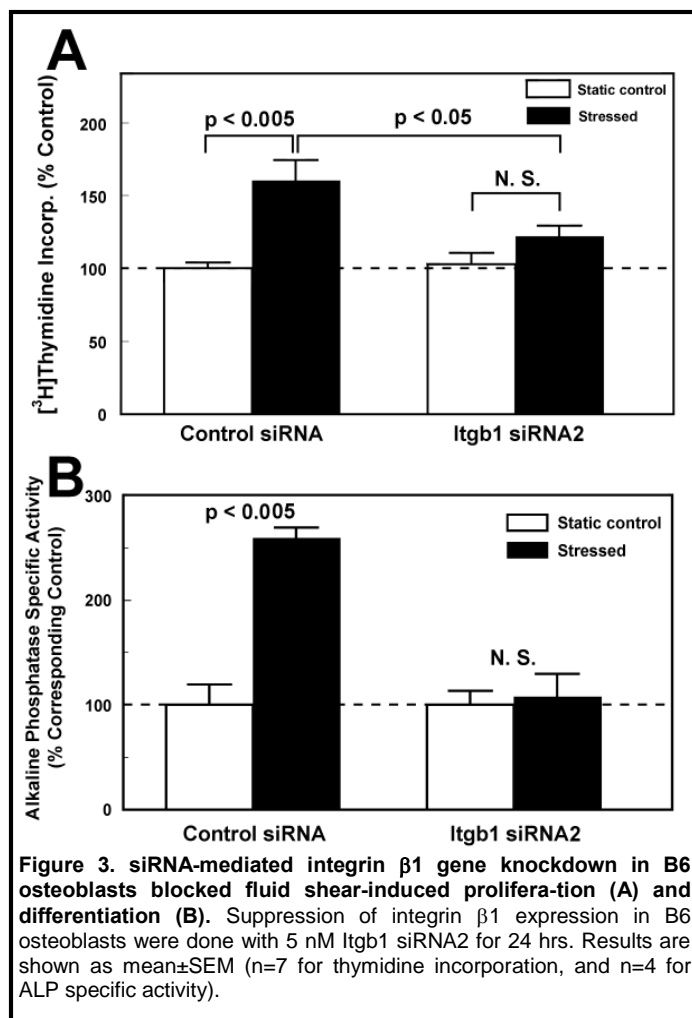
Because integrin signaling has been demonstrated to be important for mechanotransduction, we sought to develop an *in vitro* siRNA protocol using integrin  $\beta 1$  as the target gene for testing in primary mouse osteoblasts. For this work, the siRNAs were



mouse osteoblasts [with *Itgb3* siRNA1 (target sequence: CCG CTT CAA TGA AGA AGT GAA) and *Itgb3* siRNA 2 (target sequence: CAG AGG ATT GTC CTT CGA CTA), but not *Itgb3* siRNA3 (target sequence: CGC CGT GAA TTG TAC CTA CAA)] in B6 osteoblasts (Fig. 2B).

We next evaluated whether knocking down *Lepr* expression in B6 osteoblasts by specific siRNAs would affect the fluid shear-induced Erk1/2 phosphorylation. For this work, a set of three small-interfering RNA duplex (siRNA) specific for mouse *Lepr* [i.e., *Lepr* siRNA1 (target sequence: CCC GAG CAA ATT AGA AAC AAA), *Lepr* siRNA2 (target sequence: ATC GAT GTC AAT ATC AAT ATA), and *Lepr* siRNA3 (target sequence: TTG AAG CTA AAT TTA ATT CAA)] and a non-silencing control siRNA without any homology to known mammalian genes were designed and synthesized by Qiagen. For the siRNA experiment, primary B6 or C3H/HeJ (C3H) mouse osteoblasts were seeded at 60,000 cells in 24-well plate for 24 hr. The cells were transfected with the test siRNAs using the HiPerFect Transfection reagent (Qiagen). Briefly, 3  $\mu$ l of HiPerFect Transfection Reagent was added to 100  $\mu$ l of DMEM containing 75 ng of *Lepr* or negative control siRNA duplex. The reaction mixture was incubated for 10 min at room temp and was then added to each cell culture well containing 500  $\mu$ l of fresh DMEM and 10% FBS. After 16 hr of incubation at 37°C, the medium was replaced by fresh DMEM containing FBS. The effectiveness of *Lepr* suppression was assessed by Western immunoblot

pre-designed by Qiagen based on the proprietary HiPerformance siRNA Design Algorithm. A set of three siRNAs were obtained: *Igfb1* siRNA1 (target sequence: CTG CTA ATA AAT GTC CAA ATA), *Igfb1* siRNA2 (target sequence: CTG GTC CAT GTC TAG CGT CAA), and *Igfb1* siRNA3 (target sequence: CCA GCT AAT CAT CGA TGC CTA). Two of the test siRNAs (i.e., *Igfb1* siRNA1 and 2) were effective in suppressing integrin  $\beta$ 1 expression. The 24-hr pretreatment with *Igfb1* siRNA2 suppressed integrin  $\beta$ 1 expression by >90% (Fig. 2A) and blocked the fluid shear-induced proliferation, and differentiation (Fig. 3). Therefore, these findings indicate that our *in vitro* siRNA strategy can be used to effectively knock down integrin  $\beta$ 1 gene expression in primary osteoblasts, and also provide compelling evidence that integrin  $\beta$ 1 is essential in mechanotransduction. To further test our protocol, we also applied the same strategy to successfully knock down integrin  $\beta$ 3 expression in primary



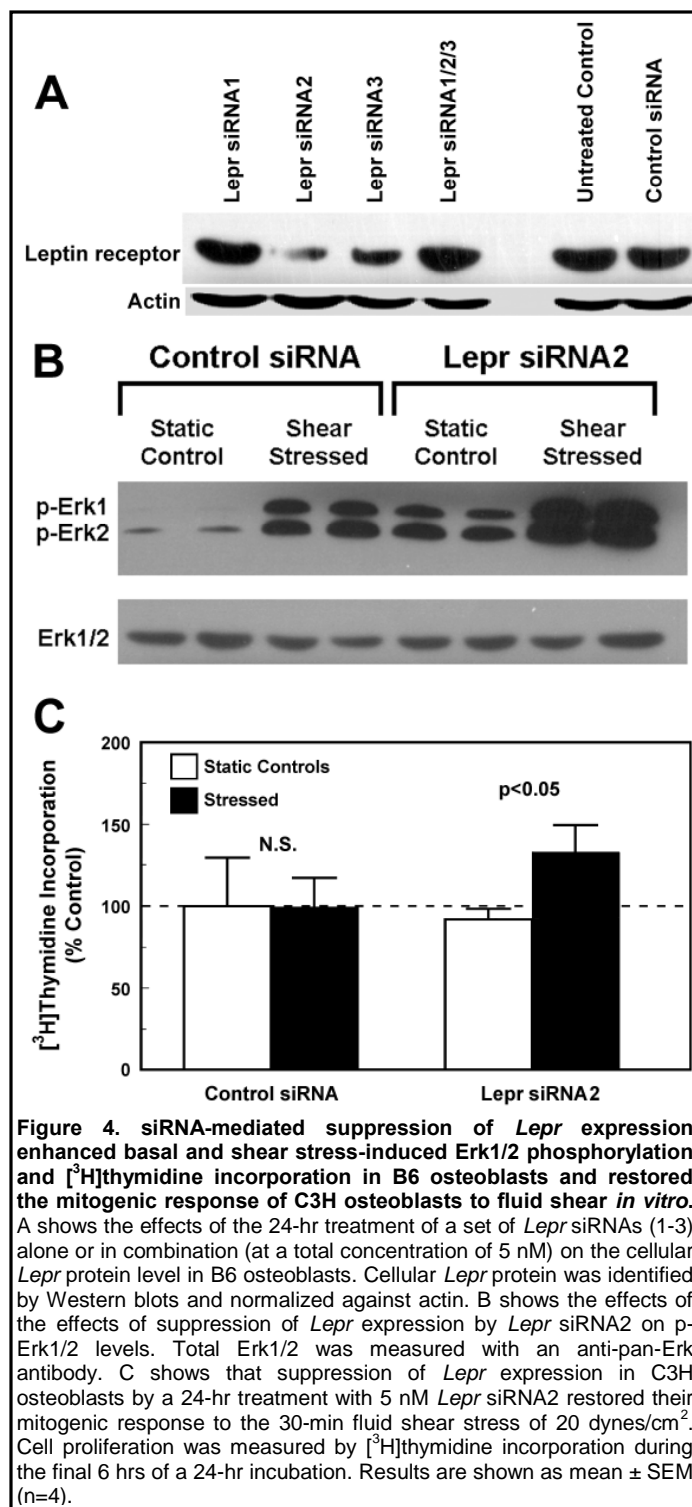
using an anti-Lepr antibody after an additional 24-48 hrs of incubation at 37°C. The protein loading was normalized against the cellular actin level using a specific anti-actin antibody.

Figure 4A shows that the 24-hr treatment with *Lepr* siRNA2 reduced cellular leptin receptor protein level in B6 osteoblasts by >70%. Down-regulation of *Lepr* expression in B6 osteoblasts by *Lepr* siRNA2 enhanced both basal (i.e., static control) and fluid shear-induced Erk1/2 phosphorylation much further in B6 osteoblasts (Fig. 4B). In addition, the siRNA-mediated knockdown of *Lepr* expression in C3H osteoblasts also led to restoration of their mitogenic responsiveness to the shear stress (Fig. 4C). These data support our contention that Lepr or its signaling is a negative regulatory mechanism in the context of mechanotransduction.

### Specific Objective #3. To generate a colony of *Lepr*-deficient mice for investigation.

In order to ensure that the observation seen with leptin-deficient mice was due to the lack of Lepr signaling and not indirectly through leptin deficiency, we sought to determine the effect (or the lack of an effect) of mechanical loading on periosteal bone formation in *Lepr*-deficient mice. For this work, we need to establish a *Lepr* KO mouse colony in our laboratory for investigation. Accordingly, we have purchased a breeding pair of heterozygous *Lepr* KO mice (B6.Cg-mLpr<sup>db</sup>/+ +/J) from the Jackson Laboratories. Homozygous *Lepr* KO mice are infertile and cannot be used in the breeding purpose. Because *Lepr*<sup>db</sup> homozygotes are functionally sterile, the coat color marker misty (*m*) has been incorporated into stocks for maintenance of the diabetes (*db*) mutation. This repulsion double heterozygote (*m* +/+ *Lepr*<sup>db</sup>) would facilitate identification of heterozygotes for breeding, while the coupling double heterozygote, (*m Lepr*<sup>db</sup>/+ +, this strain) allows identification of homozygotes before the onset of clinical symptoms. The recessive misty mutation causes a mild dilution of coat color.

The breeding program has been initiated approximately 3 months ago. The breeding pair produced a litter approximately 1 and a half month ago. Unfortunately, the mother cannibalized all pups. The breeding pair has recently produced another litter of six pups. We will genotype the



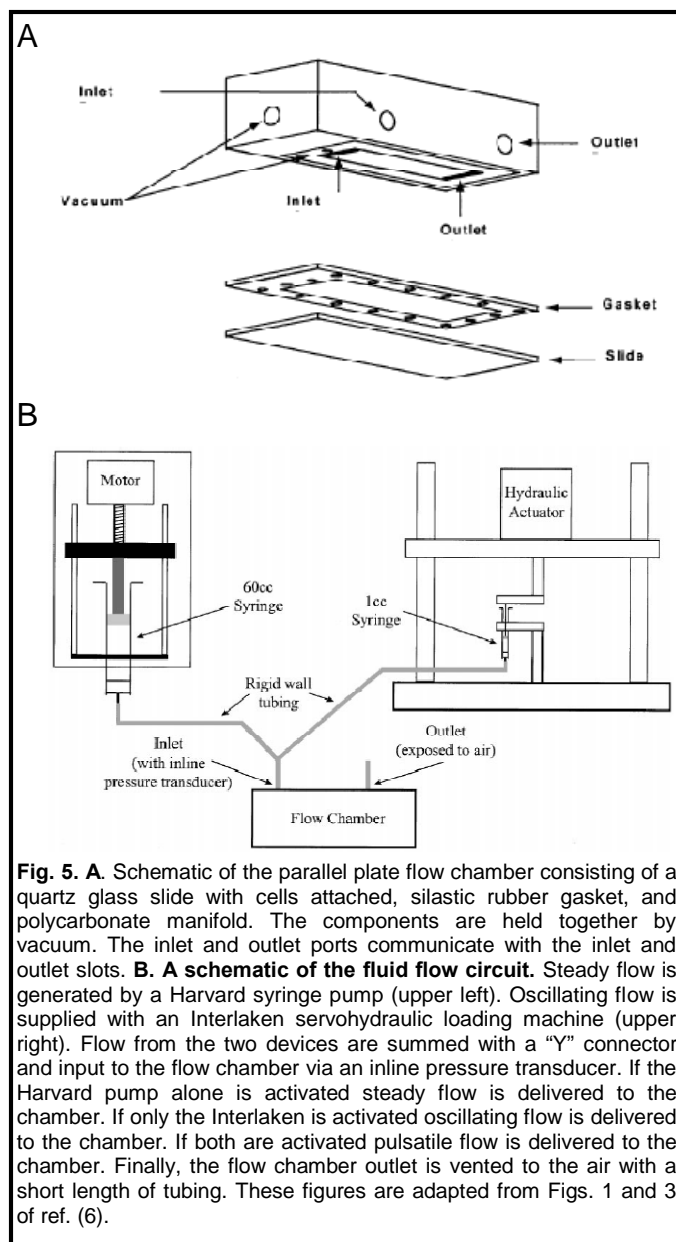
pups after weanling, and heterozygous mice will be used in further breeding to establish a colony. Homozygous pups will be used for subsequent *in vivo* and *in vitro* studies.

**Specific Objective # 4. To develop a pulsatile or oscillatory fluid flow system for subsequent confirmation studies.**

There is a concern about the physiological relevance about findings of steady shear stress as a surrogate model of mechanical loading. Although we have obtained significant important information about the mechanical signaling process with *in vitro* cell culture model employing steady fluid shear stress in the past, we feel that it would be essential to confirm our findings with a pulsatile or oscillatory flow cell culture model. A number of pulsatile or oscillatory flow cell culture models have been used by other laboratories. We chose to adapt the system developed by Jacobs *et al.* (6), because this system requires only minor modifications from our currently employed steady flow cell culture system to be converted into an oscillating or pulsatile flow cell culture system. In this model (Fig. 5), an inline pressure transducer is attached to the flow chamber inlet. The static component of flow is provided with a Harvard syringe pump. The dynamic component of flow (that yields an oscillating or pulsatile flow) is provided by a 1 ml syringe mounted in a servohydraulic loading machine. Computer generated

displacement commands are followed by the servohydraulic actuator to within 50  $\mu$ m resulting in delivery of a flow profile accurate to within 1  $\mu$ l at any point in time. Thick rigid walled plastic tubing is used throughout the flow delivery system to minimize dynamic compliance. The static and dynamic components of flow are summed with a Y connector and delivered to the flow

chamber (Figure 5A). A schematic of the fluid flow circuit is shown in Fig. 5B.



We are currently setting up this system and working on standardization of the flow system. Once this flow system is validated, we will use this flow system to confirm our key findings that were obtained from our past studies using the steady fluid flow system.

#### D. Key Research Accomplishments:

1. We have showed that leptin-deficient mice showed a significantly greater response to mechanical loading created by a four-point-bending exercise regimen, supporting our contention that the leptin-Lepr signaling acts as a negative regulatory mechanism for mechanical stimulation of bone formation.

2. We have established an effective siRNA protocol to suppress gene expression in primary mouse osteoblasts. This protocol can be used for functional testing of candidate mechanosensitivity genes.

3. We are in the process of generating a colony of Lepr deficient mice for *in vivo* and *in vitro* investigations of the regulatory role of Lepr in mechanical stimulation of bone formation.

4. We are in the process of setting up an oscillating or pulsatile fluid flow cell culture system for use in our future *in vitro* investigations.

#### E. Reportable Outcomes:

There are none during this reporting period.

#### F. Conclusions:

In summary, with the use of leptin-deficient mice *in vivo* and their osteoblasts *in vitro* using a steady flow shear system, we have now compelling *in vivo* and *in vitro* evidence that the leptin-Lepr signaling mechanism may play key regulatory role in determining the mechanosensitivity of osteoblasts. We have also established a reliable *in vitro* siRNA strategy for the application to mouse osteoblasts in conjunction with our fluid shear stress technology as a functional test for their role in mechanotransduction.

#### G. References:

1. Lau K-HW, Kapur S, Kesavan C, and Baylink DJ (2006) Upregulation of the Wnt, estrogen receptor, insulin-like growth factor-I, and bone morphogenetic protein pathways in C57BL/6J osteoblasts as opposed to C3H/HeJ osteoblasts in part contributes to the differential anabolic response to fluid shear. *J Biol Chem* **281**, 9576-9588.
2. Wang X, Rundle CH, Wergedal JE, Srivastava AK, Mohan S, Lau K-HW (2007) Loss of Sex-Specific Difference in Femoral Bone Parameters in Male Leptin Knockout Mice. *Calcif Tissue Int* **80**, 374-382.
3. Nanae M, Mori Y, Yasuda K, Kadowaki T, Kanazawa Y, Komeda K (1998) New method for genotyping the mouse Lep(ob) mutation, using a polymerase chain reaction assay. *Lab Anim Sci* **48**, 103-104.
4. Kesavan C, Mohan S, Oberholtzer S, Wergedal JE, Baylink DJ (2005) Mechanical loading induced gene expression and BMD changes are different in two inbred mouse strains. *J Appl Physiol* **99**, 1951-1957.
5. Kesavan C, Baylink DJ, Kapoor S, Mohan S (2007) Novel loci regulating bone anabolic response to loading: Expression QTL analysis in C57BL/6JXC3H/HeJ mice cross. *Bone* **41**, 223-230.
6. Jacobs CR, Yellowley CE, Davis BR, Zhou Z, Cimbala JM, Donahue HJ (1998) Differential effect of steady versus oscillating flow on bone cells. *J Biomech* **31**, 969-976.

#### Progress for the period of 2008-2010

Progress report for in vitro studies are integrated with the in vivo results and presented in the in section A dealing with in vivo studies (part A).

Molecular Genetic Studies of Bone Mechanical Strain and of Pedigrees with Very High Bone Density - DAMD17-01-1-0744

**REPORTABLE OUTCOMES:**

**A. Manuscripts:**

- 1) Umemura Y, Baylink DJ, Wergedal JE, Mohan S, and Srivastava AK: A time course of bone response to jump exercise in C57BL/6J mice. *J Bone Miner Res* 20(4):209-215, 2002.
- 2) Xing W, Baylink DJ, Kesavan C, Chadwick R, Hu Y and Mohan S Global Gene Expression Analysis in the Bones Reveals Involvement of Several Novel Genes and Pathways in Mediating an Anabolic Response of Mechanical Strain in Mice. *J Cell Biochem.* 96: 1049-1060, 2005.
- 3) Kesavan C, Mohan S, Oberholtzer S and Baylink DJ. Mechanical loading induced gene expression and BMD changes are different in two inbred mouse strains. *J Appl Physiol.* 99(5):1951-7, 2005.
- 4) Kapur S, Mohan S, Baylink DJ, and Lau K.-H. Fluid shear stress synergizes with IGF-I on osteoblast proliferation through integrin-dependent activation of IGF-I mitogenic signaling pathway. *J Biol Chem.* 280, 20163-20170, 2005.
- 5) Kesavan C, Mohan S, Srivastava AK, Kapoor S, Wergedal JE, Yu H, Baylink DJ. Identification of genetic loci that regulate bone adaptive response to mechanical loading in C57BL/6J and C3H/HeJ mice intercross. *Bone.* 39:634-643, 2006.
- 6) Lau KH, Kapur S, Kesavan C, Baylink DJ. Up-regulation of the Wnt, estrogen receptor, insulin-like growth factor-I, and bone morphogenetic protein pathways in C57BL/6J osteoblasts as opposed to C3H/HeJ osteoblasts in part contributes to the differential anabolic response to fluid shear. *J Biol Chem.* 281:9576-88, 2006.
- 7) Kesavan C, Baylink DJ, Kapoor S, and Mohan S. Novel Loci Regulating Bone Anabolic Response to Loading: Expression QTL Analysis in C57BL/6JXC3H/HeJ Mice Cross, *Bone*, 41: 223-230, 2007.
- 8) Kesavan C and Mohan S. Lack of anabolic response to skeletal loading in mice with targeted disruption of pleiotrophin gene. *BMC Research Notes:* 1:124, 2008.
- 9) Kapur, S; Amoui, M; Kesavan, C; Xiaoguang W; Mohan, S; Baylink, DJ. Leptin receptor (LEPR) is a negative modulator of bone mechanosensitivity and genetic

variations in LEPR may contribute to the differential osteogenic response to mechanical stimulation in the C57BL/6J and C3H/HeJ pair of mouse strains. J Biol Chem 285. 37607-37618.

- 10) Kesavan C and Mohan S. Bone mass gained in response to external loading is lost following cessation of loading in 10 week C57BL/6J mice. Accepted and in print with J Musculoskeletal Neuronal Interactions.
- 11) Kesavan C, Wergedal J, KHW. Lau and Mohan S. Conditional disruption of IGF-I gene in osteoblasts demonstrates obligatory and non-redundant role of IGF-I in skeletal anabolic response to mechanical loading. J Biol Chem (In preparation).
- 12) Kesavan C, Mohan S. Mechanical strain response in bone size mutant mice. Bone (In preparation)

#### **B. Abstracts:**

- 1) Kesavan C, Mohan S, Oberholtzer S, and Baylink DJ. Evidence That BMD Response To Mechanical Loading (ML) In Vivo Is Caused By Acute Up-Regulation Of Both Bone Formation (BF) Genes And Down Regulation Of Bone Resorption (BR) Genes. 26th Annual Meeting American Society of Bone and Mineral Research, Seattle, Washington, October 1-5, 2004.
- 2) Kesavan C, Mohan S, Wergedal J, and Baylink DJ. Bone anabolic response to a mechanical load is a complex trait and involves bone size, material bone density (mBMD) and volumetric bone density (vBMD) phenotypes. 26th Annual Meeting American Society of Bone and Mineral Research, Seattle, Washington, October 1-5, 2004.
- 3) Xing W, Baylink DJ, Kesavan C, Yu H, Chadwick R, Hu Y, Rajkumar R and Mohan S. Global Analysis of 22,000 Genes in the Bones Reveals Involvement of Several Novel Genes/ESTs and Pathways in Mediating the Anabolic Response of Mechanical Strain in Mice In Vivo. 26th Annual Meeting American Society of Bone and Mineral Research, Seattle, Washington, October 1-5, 2004.
- 4) Kesavan C, Baylink DJ, Wergedal JE and Mohan S. Inbred Mouse Strains Dependent Variations in the Skeletal Adaptive Responses to 4-Point Bending: Evidence for Involvement of Different Genetic Mechanisms. 26th Annual Meeting American Society of Bone and Mineral Research, Seattle, Washington, October 1-5, 2004.
- 5) Kesavan C, Mohan S, Yu H, Oberholtzer S, Wergedal JE, Baylink DJ. Novel Mechanoresponsive BMD and Bone Size QTL Identified in a Genome Wide Linkage

- Study Involving C57BL/6J-C3H/HeJ Intercross 27th Annual Meeting American Society of Bone and Mineral Research, Nashville, Tennessee, USA, September 23-27, 2005.
- 6) Lau K-HW, Kapur S, Mohan S, and Baylink DJ. Fluid shear stress synergizes with IGF-I on osteoblast proliferation through integrin-dependent upregulation of IGF-I receptor phosphorylation levels. Transactions to the 51st Annual meeting of Orthopaed Res Soc abstract # 845, 2005.
  - 7) Kesavan C, Baylink DJ, Kapoor S, Wergedal JE, Hongrun Yu and Mohan S. Quantitative Trait loci for Tibia Periosteal Circumference in the C57BL/6J-C3H/HeJ mice intercross. 28<sup>th</sup> Annual Meeting American Society for Bone and Mineral Research. September 15-19, Philadelphia, PA, 2006.
  - 8) Kesavan C, Baylink DJ, Kapoor S and Mohan S. Identifying Mechanical Loading QTL by Gene Expression Changes for Alkaline Phosphatase and Bone Sialoprotein in C57BL/6J (B6) X C3H/HeJ (C3H) Intercross. 29<sup>th</sup> Annual Meeting of the American Society for Bone and Mineral Research, September 16 – 19, Hawaii, 2007,
  - 9) Lau KHW, Kapur S, Amoui M, Wang X, Kesavan C, Mohan S, Baylink DJ. Leptin deficient (ob/ob) mice exhibit increased bone mechanosensitivity and corresponding osteoblasts show increased anabolic shear stress responses in vitro. 29<sup>th</sup> Annual Meeting of the American Society for Bone and Mineral Research, September 16 – 19, Hawaii, 2007.
  - 10) Kesavan C, Baylink DJ, Gifford P, Mohan S. The increased vBMD and bone area due to mechanical loading gradually decreased following cessation of loading. 29<sup>th</sup> Annual Meeting of the American Society for Bone and Mineral Research, September 16 – 19, Hawaii, 2007.
  - 11) Kesavan C & Mohan S. Anabolic response to skeletal loading in mice with targeted disruption of pleiotrophin gene. 30<sup>th</sup> Annual Meeting American society for Bone and Mineral Research, Montreal, Canada September 11-16, 2008.
  - 12) Kesavan C, Wergedal J, & Mohan S. Conditional disruption of IGF-I gene in osteoblasts demonstrates obligatory and non-redundant role of IGF-I in skeletal anabolic response to mechanical loading. 31<sup>st</sup> Annual Meeting of the American Society for Bone and Mineral Research, Denver, CO, September 11-15, 2009.

**List of Personnel:**

Mohan, Subburaman	Principal Investigator
Alva, E	Admin
Baez, I	Res. Tech
Baggett, L	Admin
Belcher, S	Admin
Blanco, T	Admin
Bu, L	Res. Tech
Chadwick, R	Investigator
Chen, ST	Investigator
Davidson, H	Res. Tech
Dixon, C	Res. Tech
Edderkaoui, B	Investigator
Felt, J	Res. Tech
Gifford, P.	Res. Tech
Govoni, K.	Res. Tech
Gysin, R.	Investigator
Hall, S	Investigator
Hargrave, C	Res. Tech
Hu, Y	Res. Tech
Kadmiel, M.	Res Tech
Joshi, V	Res Tech
Kapoor, A	Res. Tech
Kapur, S	Res. Tech
Klamut, H.	Investigator
Lau, W	Investigator
Levtzow, S	Admin
Lowen, N	Res. Tech
Oberholtzer, S	Res. Tech
Popa, C	Res. Aid
Popa, N	Res. Tech
Porte, R	Res. Tech
Raynor, C	Res. Tech
Rundle, C	Investigator
Rung-Aroon, J	Res. Tech
Sheng, M	Res. Scientist
Smallwood, J	Res. Tech
Srivastava, A	Investigator
Stivers, C	Res. Tech
Sumagaysay, J	Res. Tech
Tan, Q	Res. Tech
Strong, Donna D	Investigator
Wang, X	Post Doc

Xing, W	Investigator
Zhu, Y	Res. Tech
Yu, H	Research Scientist

## A time course of bone response to jump exercise in C57BL/6J mice

YOSHIHISA UMEMURA<sup>1</sup>, DAVID J. BAYLINK<sup>2</sup>, JON E. WERGEDAL<sup>2</sup>, SUBBURAMAN MOHAN<sup>2</sup>, and APURVA K. SRIVASTAVA<sup>2</sup>

<sup>1</sup>School of Health and Sport Sciences, Chukyo University, Toyota, Japan

<sup>2</sup>Musculoskeletal Disease Center, Jerry L. Pettis Memorial Veterans Medical Center, 11201 Benton St., Loma Linda, CA 92357, USA

**Abstract** Exercise, by way of mechanical loading, provides a physiological stimulus to which bone tissue adapts by increased bone formation. The mechanical stimulus due to physical activity depends on both the magnitude and the duration of the exercise. Earlier studies have demonstrated that jump training for 4 weeks produces a significant bone formation response in C57BL/6J mice. An early time point with significant increase in bone formation response would be helpful in: (1) designing genetic quantitative trait loci (QTL) studies to investigate genes regulating the bone adaptive response to mechanical stimulus; and (2) mechanistic studies to investigate early stimulus to bone tissue. Consequently, we investigated the bone structural response after 2, 3, and 4 weeks of exercise with a loading cycle of ten jumps a day. We used biochemical markers and peripheral quantitative computed tomography (pQCT) of excised femur to measure bone density, bone mineral content (BMC), and area. Four-week-old mice were separated into control ( $n = 6$ ) and jump groups ( $n = 6$ ), and the latter groups of mice were subjected to jump exercise of 2-week, 3-week, and 4-week duration. Data (pQCT) from a mid-diaphyseal slice were used to compare bone formation parameters between exercise and control groups, and between different time points. There was no statistically significant change in bone response after 2 weeks of jump exercise as compared with the age-matched controls. After 3 weeks of jump exercise, the periosteal circumference, which is the most efficient means of measuring adaptation to exercise, was increased by 3% ( $P < 0.05$ ), and total and cortical area were increased by 6% ( $P < 0.05$ ) and 11% ( $P < 0.01$ ), respectively. Total bone mineral density (BMD) increased by 11% ( $P < 0.01$ ). The biggest changes were observed in cortical and total BMC, with the increase in total BMC being 12% ( $P < 0.01$ ). Interestingly, the increase in BMC was observed throughout the length of the femur and was not confined to the mid-diaphysis. Consistent with earlier studies, mid-femur bone mass and area remained significantly elevated in the 4-week exercise group when compared with the control group

of mice. The levels of the biochemical markers osteocalcin, skeletal alkaline phosphatase, and C-telopeptide were not significantly different between the exercise and control groups, indicating the absence of any systemic response due to the exercise. We conclude that a shorter exercise regimen, of 3 weeks, induced a bone response that was greater than or equal to that of 4 weeks of jump exercise reported earlier.

**Key words** mechanical loading · bone remodeling · inbred C57BL · time course · bone density · jump exercise · femur

### Introduction

Physical activity or mechanical loading plays an important role in determining peak bone density. Physical activity creates loads on bone that have the potential to initiate bone formation and increase bone density [1–7]. Conversely, lack of mechanical loads results in rapid bone loss, as seen in immobilization studies [8–10]. A minimum effective strain (MES) [11–14], which is above average daily levels, is required to generate signals that are communicated to cells in bone tissue for adaptive bone formation through modeling. Physical activity levels above this MES can stimulate adaptive bone formation. Animal studies of bone adaptation have shown that mechanical regulation of bone due to physical activity is dependent on a combination of factors, including: (1) strain distribution; (2) strain magnitude; (3) number of repetitions; and (4) frequency [11–14].

We have previously reported [1] that mechanical loading, in the form of jump exercise, increases periosteal bone formation and bone strength in C57BL/6J mice, but not in C3H/HeJ mice. We used jump training as a model of exercise instead of treadmill exercise because jump exercise was found to be more effective in increasing limb bone mass in rodents [15]. In a previous study, 20 jumps/day for 4 weeks, which produced a bending strain of 176 N/mm<sup>2</sup> [1], was effective in gener-

Offprint requests to: A.K. Srivastava

Received: October 1, 2001 / Accepted: January 18, 2002

ating the signal for adaptive bone response through modeling. The main aim of this study was to explore changes in femoral structural parameters after 2, 3, and 4 weeks of jump exercise. Data on the earliest bone response could provide useful information for mechanistic studies at the cellular level to investigate the initial stimulus to which bone tissue adapts by increased bone formation. In addition, an earlier time point than 4-week loading, if such elicited a significant bone formation response, would save time and effort in our genetic quantitative trait loci (QTL) studies to investigate genes regulating the bone adaptive response to mechanical stimulus. The secondary objective of this study was to evaluate the response to jump exercise by: (1) using peripheral quantitative computed tomography (pQCT) to measure changes in bone density, mass, and area; and (2) using biochemical markers to study systemic changes in bone metabolism. The pQCT would offer a less cumbersome and more precise tool to study bone response to loading as compared with bone histomorphometric measurements, which were used in an earlier study (1).

## Materials and methods

### *Animals and treatment*

All animal protocols used in this study had prior approval of the Animal Subjects Committee at the Chukyo University Graduate School of Health and Sport Sciences.

Four-week old C57BL/6J mice were obtained from Japan SLC (Hamamatsu, Japan) and acclimatized for 1 week on a 12-h light/dark cycle, with food (standard chow) and water available ad libitum. Mice were randomly assigned to either the jump-exercise or the non-exercised control groups ( $n = 6$ – $7$  mice/group). Details of the jump-exercise protocol have been described in the previous report [1]. In brief, each mouse in the jump groups was placed at the bottom of a special cage, 10cm wide, 10cm deep, and 25cm high. The jumping exercise was initiated by applying an electrical current (80volts) to the wire floor of the cage. Each mouse was housed individually and jumped from the floor of the cage to catch the top edge of the cage with its forepaws. The mouse was returned to the floor of the cage to repeat the procedure. The electrical current we used had an automatic turn-on phase and turn-off phase. We placed the mice on the stimulus plate at the turn-off phase and, after the first 3 days, most of the mice could jump before the turn-on phase. Each mouse in the three jump groups jumped ten times per day, 5 days a week, for 2, 3, and 4 weeks. The control mice were largely unstressed.

At the end of the experiment, blood was collected and femurs were dissected from both hind limbs. Serum

was separated and kept at  $-70^{\circ}\text{C}$  until analyzed for biochemical markers. Femurs were kept moist and frozen at  $-70^{\circ}\text{C}$ . Frozen serum and femurs were analyzed at the J.L. Pettis Memorial Veterans Medical Center for biochemical analysis and bone density measurements, using peripheral quantitative tomography (pQCT).

### *Peripheral quantitative computed tomography (pQCT)*

Bone density, mass, and area data were obtained from excised femurs ( $n = 6$ ), and values were expressed as means  $\pm$  SD. Two different thresholds were used to analyze the pQCT scans. The high threshold analysis gives the most accurate area results. The low threshold gives the most accurate mineral content analysis. The bones were scanned nine times, covering the entire length of the femur with each slice separated by 11% of the femur length. Slice 5, which is the mid-shaft slice, was used for all calculations and comparisons. Data from individual slices were used to plot total and cortical bone mineral content (BMC) (Fig. 1). Data from individual slices were compared between jump and control groups of mice by analysis of variance (ANOVA) and post-hoc test. The precision of the repeated pQCT measurement at the mid-diaphyseal femur showed a coefficient of variation (CV) of less than 3% for all the parameters studied in this investigation.

### *Measurements of biochemical markers of bone turnover*

#### *Mouse C-telopeptide enzyme-linked immunosorbent assay (ELISA)*

The C-telopeptide measurements were performed with a mouse C-telopeptide ELISA, described earlier [16]. The sensitivity of the ELISA was 0.3ng/ml. The average within-assay CV was less than 7%; the average between-assay CV was less than 14%.

#### *Mouse osteocalcin radioimmunoassay (RIA)*

The osteocalcin measurements were performed with a mouse osteocalcin radioimmunoassay (RIA), described earlier [17]. The sensitivity of the RIA was 15ng/ml. The average within-assay CV was less than 10%; the average between-assay CV was less than 15%.

#### *Skeletal alkaline phosphatase assay*

Alkaline phosphatase was measured in serum by a kinetic method [7], using *p*-nitro-phenylphosphate (PNPP) as substrate and 15mM L-phenylalanine to inhibit intestinal alkaline phosphatase. The L-phenylalanine inhibition assay exhibited intraassay ( $n = 10$ ) and interassay ( $n = 8$ ) CVs of 1.9% and 3.8%, respectively. The assay can detect less than 10mU/ml of alkaline phosphatase in mouse serum.

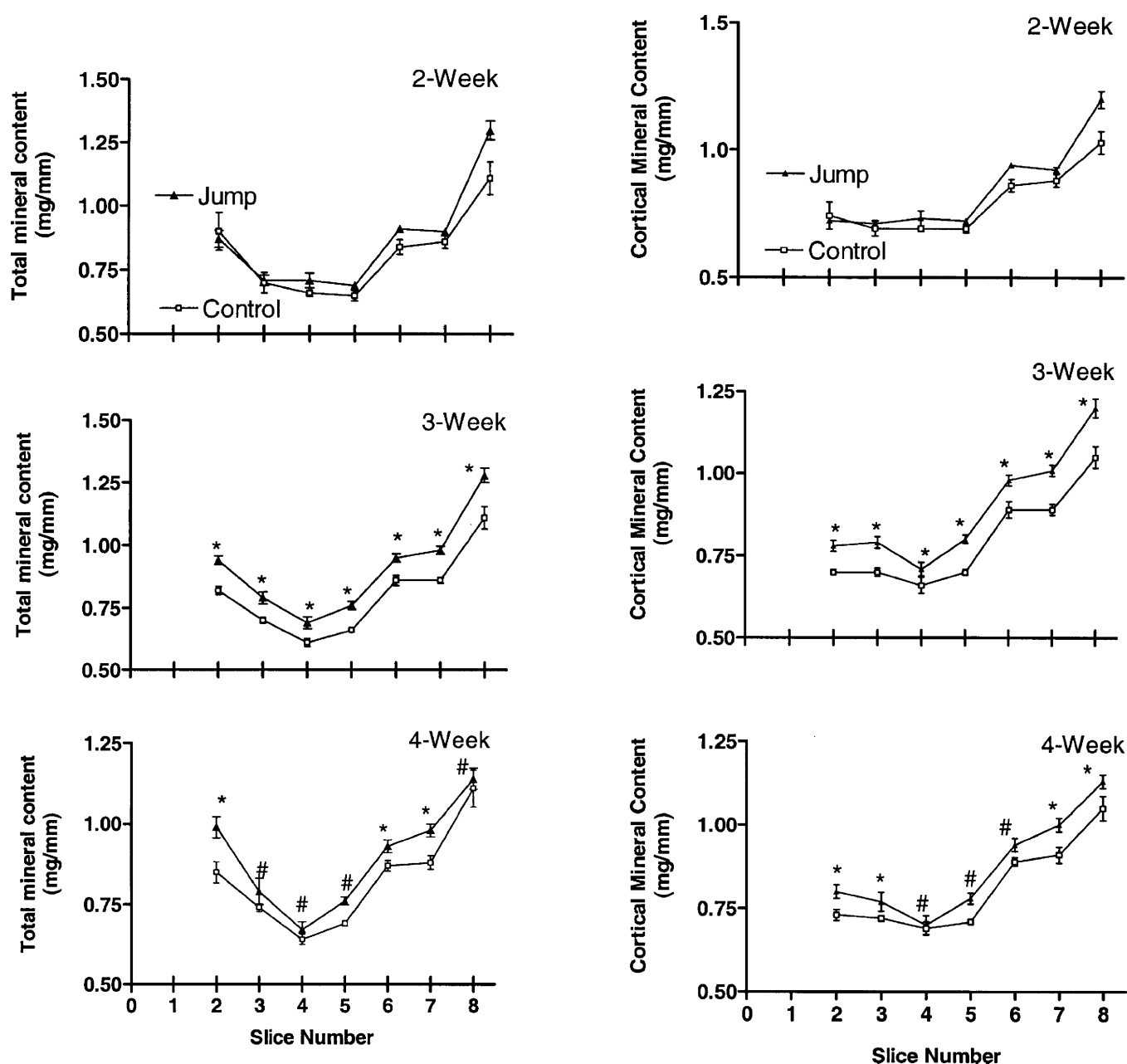


**Fig. 1.** Effects of 2, 3, and 4 weeks of jump exercise on cortical and total bone mineral content measured by peripheral quantitative computed tomography (pQCT) at nine different slices of the femur. Each slice was separated by 11% of the femur length, with slice 1 starting at the distal end. The data show (slices 1 and 9 were omitted due to large variation) that the increase in bone mineral content occurred throughout the

length of the femur. Each data point represents the mean  $\pm$  SEM ( $n = 6$ ). The  $P$  value for both cortical and total bone mineral content of control vs jump group was  $<0.0001$  by analysis of variance (ANOVA) for the 3-week and 4-week jump-exercise groups. The  $P$  values for comparison of individual slices in control and jump groups of mice by post-hoc tests are  $^{\#}P > 0.05$  and  $*P < 0.05$ .

### Statistical analysis

Comparison of biochemical markers of bone metabolism between different groups was performed by the Mann-Whitney test (with a two-tailed  $P$ -value of  $<0.05$  accepted as significant difference), because biochemical markers do not show normal distribution. All comparisons of pQCT femur structural data were performed

on slice 5 by analysis of variance (ANOVA). ANOVA was used to reveal the differences among the control and the three jump-exercise groups. Post-hoc comparisons were performed by the Neuman-Keuls method and were used to determine the differences between specific means. All data are reported as means and standard deviations.

## Results

As compared with the control group of mice, mice in the jump-exercise groups after 2, 3, and 4 weeks of exercise had no significant differences in body weight or longitudinal growth (length) of the femur, which was consistent with our previous findings [1]. The body weights were: 2-week control,  $16.9 \pm 1.1$  g; 2-week jump group,  $16.6 \pm 0.7$  g; 3-week control,  $17.9 \pm 1.1$  g; 3-week jump group,  $18.2 \pm 0.5$  g; 4-week control,  $17.9 \pm 1.0$  g; and 4-week jump group,  $17.5 \pm 0.9$  g. The femur lengths were: 2-week control,  $13.7 \pm 0.75$  mm; 2-week jump group,  $14.1 \pm 0.18$  mm; 3-week control,  $14.4 \pm 0.41$  mm; 3-week jump group,  $14.3 \pm 0.19$  mm; 4-week control,  $14.0 \pm 0.61$ ; and 4-week jump group,  $14.0 \pm 0.20$  mm.

Changes in mid-femur periosteal expansion and cross-sectional parameters are shown in Table 1. Periosteal circumference was increased by 3% ( $P < 0.05$ ) after 3 weeks of exercise and remained higher in the 4-week exercise group (Table 1). Cortical area was increased by 11% ( $P < 0.001$ ) after 3 weeks of exercise and was 8.4% higher than that in the controls in the 4-week exercise group ( $P < 0.01$ ). Total area also increased, by 6.2% ( $P < 0.01$ ), after 3 weeks of exercise, and remained elevated after 4 weeks. Cortical thickness

was elevated by 8% ( $P < 0.01$ ) and 5% ( $P$ , not significant) in the 3-week and 4-week exercise group, respectively. Although there was a time-related increase in endosteal circumference, the  $P$  values did not reach statistically significant levels.

Changes in total bone mineral density (BMD) and total and cortical bone mineral content (BMC) in the control and jump exercise groups are shown in Table 2. Changes for total and cortical BMC and total BMD between control and exercise groups did not reach significance for the 2-week exercise period. Maximum increases in total BMD and both total and cortical BMC were observed in the 3-week exercise group. Total BMD and total BMC were increased by 11.2% ( $P < 0.01$ ) and 12.5% ( $P < 0.01$ ), respectively, in the 3-week exercise group compared with the control group. Total BMC and total BMD values remained significantly elevated in the 4-week exercise group, and were 11% ( $P < 0.01$ ) and 5% ( $P < 0.05$ ), respectively, higher as compared with the control group. ANOVA values for the increase in total BMD and total BMC for treatment and weeks of exercise are shown in Table 3.

Figure 1 shows the plots for individual slices of total and cortical bone mineral content. The cortical and total BMC were significantly increased in the 3-week and

**Table 1.** Cross-sectional parameters and area of mid-shaft femur

Parameters	2-Week		3-Week		4-Week	
	Control	Jump	Control	Jump	Control	Jump
Periosteal circumference (mm)	$4.23 \pm 0.08$	$4.24 \pm 0.052$	$4.22 \pm 0.08$	$4.35 \pm 0.083^*$	$4.19 \pm 0.04$	$4.33 \pm 0.11^*$
Endosteal circumference (mm)	$3.27 \pm 0.06$	$3.23 \pm 0.08$	$3.22 \pm 0.06$	$3.27 \pm 0.10$	$3.17 \pm 0.06$	$3.25 \pm 0.103$
Cortical thickness (mm)	$0.15 \pm 0.01$	$0.16 \pm 0.006$	$0.16 \pm 0.003$	$0.17 \pm 0.007^{**}$	$0.16 \pm 0.01$	$0.17 \pm 0.005^a$
Total area (mm <sup>2</sup> )	$1.43 \pm 0.05$	$1.43 \pm 0.033$	$1.42 \pm 0.05$	$1.50 \pm 0.059^{**}$	$1.40 \pm 0.03$	$1.48 \pm 0.075^{**}$
Cortical area (mm <sup>2</sup> )	$0.53 \pm 0.03$	$0.60 \pm 0.019$	$0.59 \pm 0.013$	$0.66 \pm 0.026^{**}$	$0.59 \pm 0.03$	$0.64 \pm 0.028^{**}$

\*  $P < 0.05$ ; \*\*  $P < 0.01$

Values are means  $\pm$  SD

<sup>a</sup>NS, Not significant

**Table 2.** Bone mineral content and bone density parameters of mid-shaft femur

Parameters	2-Week		3-Week		4-Week	
	Control	Jump	Control	Jump	Control	Jump
Cortical mineral content (mg/mm)	$0.69 \pm 0.04$	$0.72 \pm 0.02$	$0.71 \pm 0.03$	$0.80 \pm 0.02^{**}$	$0.71 \pm 0.014$	$0.78 \pm 0.04^*$
Total mineral content (mg/mm)	$0.65 \pm 0.05$	$0.69 \pm 0.03$	$0.68 \pm 0.04$	$0.76 \pm 0.04^{**}$	$0.69 \pm 0.02$	$0.76 \pm 0.03^{**}$
Total bone mineral density (mg/cc)	$409 \pm 30$	$434 \pm 6$	$425 \pm 19$	$461 \pm 8^{**}$	$445 \pm 13$	$465 \pm 17^*$

\*  $P < 0.05$ ; \*\*  $P < 0.01$

Values are means  $\pm$  SD

**Table 3.** *P* values for analysis of variance (ANOVA) and Newman-Keuls post-hoc tests

	ANOVA Treatment	ANOVA Weeks	Post-hoc; week 2 vs week 3 or week 4	Post-hoc; week 3 vs week 4
Periosteal circumference at mid-femur (mm)	<i>P</i> = 0.046	NS	NS	NS
Total bone mineral content (mg/mm)	<i>P</i> = 0.03	<i>P</i> = 0.01	<i>P</i> < 0.014	NS
Total bone mineral density (mg/cc)	<i>P</i> = 0.004	<i>P</i> = 0.03	<i>P</i> < 0.03	NS

**Table 4.** Biochemical parameters in jump-exercise groups compared with control groups of mice

Parameters	2-Week		3-Week		4-Week	
	Control	Jump	Control	Jump	Control	Jump
Skeletal ALP (U/l)	152 ± 12	141 ± 34	175 ± 15	191 ± 24	164 ± 23	166 ± 23
Osteocalcin (ng/ml)	166 ± 32	168 ± 46	237 ± 60	200 ± 23	170 ± 58	141 ± 20
C-telopeptide (ng/ml)	4.4 ± 1.4	5.9 ± 1.8	5.2 ± 1.4	6.0 ± 1.7	6.2 ± 1.2	6.1 ± 1.8

Differences between control and jump groups were not significant

Values are means ± SD

ALP, Alkaline phosphatase

4-week jump groups, by ANOVA ( $P < 0.0001$ ), as compared with the respective control groups of mice. The increases in cortical and total BMC in the 3-week jump group were statistically significant (by post-hoc test) for slices 2–8, as compared with the 3-week control group. Differences between the 4-week control and exercise groups for total BMC were not significant (by post-hoc test) for slices 3–5 and 8; similarly, differences in cortical BMC for slices 4–6 were not significant.

Although some parameters, such as cortical BMC and total BMC showed a tendency to be lower in the 4-week exercise group as compared with the 3-week exercise group, these changes were not significant by ANOVA (Table 3).

Serum levels of skeletal alkaline phosphatase, osteocalcin, and C-telopeptide are shown in Table 4. None of the biochemical markers showed any significant differences between control and jump groups of mice at any time point. Data on the 4-week group were consistent with our earlier findings [1] showing that no systemic markers were elevated after 4 weeks of jump exercise.

## Discussion

The bone formation response to a mechanical loading cycle of 20jumps/day for 4 weeks in the C57BL/6J mouse model has been well documented [1]. The elevated mid-femur bone mass and area after 4 weeks of

jump exercise seen in the present study is consistent with earlier findings showing a similar response to jump exercise. However, we used a lower loading cycle, of 10jumps per day, compared with the previous study that used a loading cycle of 20jumps/day. We made this change because it has been recently reported that, in rats, a substantial bone formation response could be obtained in loading cycles of 10jumps/day, and the higher loading cycles resulted in only a marginal increase in bone response [15]. The lower loading cycle used in this study will also suit the QTL studies where large-scale screening may be required.

Our results indicate that there were slight increases in cortical area and bone mineral content (BMC) after 2 weeks of exercise, as compared with the control group of mice. However, these changes did not reach statistical significance. It could be assumed that the bone mass and area in response to jump exercise of 2 weeks duration were below the detection limits of the methods (pQCT) used in this study.

After 3 weeks of jump training, periosteal circumference, which is the most efficient means of measuring adaptation to exercise, clearly showed a significant increase in mid-femur structural parameters assessed by pQCT. Changes in bone mass and area after 3-week exercise were either greater than or comparable to those in the 4-week exercise group. However, periosteal circumference, bone density, and total and cortical BMC remained elevated in the 4-week jump group when compared with the 4-week control group of mice. The 3% increase in periosteal circumference in the

4-week jump exercise group was consistent with our previous study [1], which showed about 2.2% higher periosteal perimeter after 4 weeks of jump exercise by histomorphometric analysis. Similarly, increases in cortical (8%) and total area (6%) after 4 weeks of exercise were consistent with the earlier findings observed at 4 weeks of exercise, which showed about 8% and 4% increases in cortical and total area, by histomorphometric analysis. Notably, we did not see any increase in bone mass and area after 4 weeks of jump exercise as compared with the 3-week jump-exercise group. It may be speculated that increases in bone density, mass, and area reached maximum levels after 3 weeks of loading and then the values plateaued, showing no more changes on further loading. However, in the absence of data on longer loading duration, this assumption needs confirmation.

A significant finding of this study was that the effect of jump exercise was most evident in the increase in total and cortical BMC measured by pQCT. Similar to other parameters, the highest increases in both cortical and total BMC were observed after 3 weeks of jump exercise. Our data on the cortical as well as the total BMC of nine slices (Fig. 1) indicate that the increase in BMC occurred throughout the entire length of the femur, and was not confined to the mid-shaft region of the femur. Comparisons of individual slices showed that the increases in total and cortical BMC were significant for the 3-week exercise group. In the 4-week exercise group, these differences did not reach the significance level for slices 3–6, mainly due to the larger variation in BMC in the jump group, and also because the post-hoc test used to test statistical significance involved several variables, thus increasing the stringency of the test. A less conservative test indicated that the total and cortical BMC in most of the slices were both significantly higher in the jump groups as compared with the controls. This increase in the BMC of the entire length of the femur was particularly interesting, because earlier studies explored only a small area at a specific bone site [1–3]; thus, it was not clear whether the increase in bone mass was localized in the mid-shaft region or whether was spread throughout the length of the femur. Data presented in this study (Fig. 1) amply illustrate that the relative amount of bone mineral comprising the middle 10–12 mm of the diaphysis was consistently 9%–10% higher in the jump groups of mice as compared with the control mice.

Consistent with our earlier study [1], the endosteal circumference did not change significantly at any time point, including the 4 weeks of jump exercise. In addition, we did not observe any systemic response in bone turnover markers. Therefore, biochemical markers may not be useful in detecting early bone response to mechanical loading.

In conclusion, the present investigation showed that a significant increase in bone mass and area at our sampling site occurred after 3 weeks of jump exercise, and, as expected, these parameters remained elevated after 4 weeks of jump exercise. The results of this study show that a relatively small number of jumps/day and a short duration of jump exercise can achieve a detectable bone response; therefore, longer periods of exercise may not be necessary for bone hypertrophy to develop in mice. In addition, the data presented in this study indicate that pQCT measurements can be, effectively used to quantitatively determine changes in bone mass and area in response to the mechanical loading induced by jump exercise.

**Acknowledgments.** This work was supported by Assistance Award No DAMD17-99-1-9571. The U.S. Army Medical Research Acquisition Activity, 820 Chander Street, Fort Detrick, MD 21702-5014, is the awarding and administering acquisition office. The information contained in this publication does not necessarily reflect the position or the policy of the Government, and no official endorsement should be inferred.

## References

1. Kodama Y, Umemura Y, Nagasawa S, Beamer WG, Donahue LR, Rosen CR, Baylink DJ, Farley JR (2000) Exercise and mechanical loading increase periosteal bone formation and whole bone strength in C57BL/6J mice but not in C3H/HeJ mice. *Calcif Tissue Int* 66:298–306
2. Akhter MP, Cullen DM, Pedersen EA, Kimmel DB, Recker RR (1998) Bone response to in vivo mechanical loading in two breeds of mice. *Calcif Tissue Int* 63:442–449
3. Pedersen EA, Akhter MP, Cullen DM, Kimmel DB, Recker RR (1999) Bone response to in vivo mechanical loading in C3H/HeJ mice. *Calcif Tissue Int* 65:41–46
4. Hoshi A, Watanabe H, Chiba M, Inaba Y (1998) Bone density and mechanical properties in femoral bone of swim loaded aged mice. *Biomed Environ Sci* 11:243–250
5. Hoshi A, Watanabe H, Chiba M, Inaba Y (1998) Effects of exercise at different ages on bone density and mechanical properties of femoral bone of aged mice. *Tohoku J Exp Med* 185:15–24
6. Silbermann M, Bar Shira Maymon B, Coleman R, Reznick A, Weisman Y, Steinhagen Thiessen E, von der Mark H, von der Mark K (1990) Long-term physical exercise retards trabecular bone loss in lumbar vertebrae of aging female mice. *Calcif Tissue Int* 46:80–93
7. Jamsa T, Tuukkanen J, Jalovaara P (1998) Femoral neck strength of mouse in two loading configurations: method of evaluation and fracture characteristics. *J Biomech* 31:723–729
8. Kodama Y, Dimai HP, Wergedal J, Sheng M, Malpe R, Kutilek S, Beamer W, Donahue LR, Rosen C, Baylink DJ, Farley J (1999) Cortical tibial bone volume in two strains of mice: effects of sciatic neurectomy and genetic regulation of bone response to mechanical loading. *Bone* 25:183–190
9. Van Loon JJ, Bervoets DJ, Burger EH, Dieudonne SC, Hagen JW, Semeins CM, Doulabi BZ, Veldhuijzen JP (1995) Decreased mineralization and increased calcium release in isolated fetal mouse long bones under near weightlessness. *J Bone Miner Res* 10:550–557

10. Jamsa T, Koivukangas A, Ryhanen J, Jalovaara P, Tuukkanen J (1999) Femoral neck is a sensitive indicator of bone loss in immobilized hind limb of mouse. *J Bone Miner Res* 14:1708–1713
11. Turner CH, Forwood MR, Rho JY, Yoshikawa T (1994) Mechanical loading thresholds for lamellar and woven bone formation. *J Bone Miner Res* 9:87–97
12. Rubin CT, Lanyon LE (1984) Regulation of bone formation by applied dynamic loads. *J Bone Joint Surg Am* 66:397–402
13. Rubin CT, Lanyon LE (1985) Regulation of bone mass by mechanical strain magnitude. *Calcif Tissue Int* 37:411–417
14. Umemura Y, Ishiko T, Tsujimoto H, Miura H, Mokushi N, Suzuki H (1995) Effects of jump training on bone hypertrophy in young and old rats. *Int J Sports Med* 16:364–367
15. Umemura Y, Ishiko T, Yamauchi T, Kurono M, Mashiko S (1997) Five jumps per day increase bone mass and breaking force in rats. *J Bone Miner Res* 12:1480–1485
16. Srivastava AK, Bhattacharyya S, Castillo G, Miyakoshi N, Mohan S, Baylink DJ (2000) Development and evaluation of C-telopeptide ELISA for measurement of bone resorption in mouse serum. *Bone* 27:529–533
17. Srivastava AK, Castillo G, Wergedal JE, Mohan S, Baylink DJ (2000) Development and application of a synthetic peptide based osteocalcin assay for the measurement of bone formation in mouse serum. *Calcif Tissue Int* 67:255–259

# Global Gene Expression Analysis in the Bones Reveals Involvement of Several Novel Genes and Pathways in Mediating an Anabolic Response of Mechanical Loading in Mice

Weirong Xing,<sup>1</sup> David Baylink,<sup>1,2</sup> Chandrasekhar Kesavan,<sup>1</sup> Yan Hu,<sup>1</sup> Susanna Kapoor,<sup>1</sup> Robert B. Chadwick,<sup>1</sup> and Subburaman Mohan<sup>1,2,3,4\*</sup>

<sup>1</sup>Musculoskeletal Disease Center, JL Pettis Memorial Veterans Administration Medical Center, Loma Linda, California 92357

<sup>2</sup>Department of Medicine, Loma Linda University, Loma Linda, California

<sup>3</sup>Department of Biochemistry, Loma Linda University, Loma Linda, California

<sup>4</sup>Department of Physiology, Loma Linda University, Loma Linda, California

**Abstract** To identify the genes and signal pathways responsible for mechanical loading-induced bone formation, we evaluated differential gene expression on a global basis in the tibias of C57BL/6J (B6) mice after four days of four-point bending. We applied mechanical loads to the right tibias of the B6 mice at 9 N, 2 Hz for 36 cycles per day, with the left tibias used as unloaded controls. RNA from the tibias was harvested 24 h after last stimulation and subjected to microarray. Of the 20,280 transcripts hybridized to the array, 346 were differentially expressed in the loaded bones compared to the controls. The validity of the microarray data was established with the increased expression of bone-related genes such as pleiotrophin, osteoglycin, and legumain upon four-point bending and confirmation of increased expression of selected genes by real-time PCR. The list of differentially expressed genes includes genes involved in cell growth, differentiation, adhesion, proteolysis, as well as signaling molecules of receptors for growth factors, integrin, Ephrin B2, endothelin, and adhesion G protein coupled receptor. Pathway analyses suggested that 28 out of the 346 genes exhibited a direct biological association. Among the biological network, fibronectin and pleiotrophin function as important signaling molecules in regulating periosteal bone formation and resorption in response to four-point bending. Furthermore, some expressed sequence tags (ESTs) with no prior known function have been identified as potential mediators of mechanotransduction signaling pathways. Further studies on these previously unknown genes will improve our understanding of the molecular pathways and mechanisms involved in bone's response to mechanical stress. *J. Cell. Biochem.* 96: 1049–1060, 2005. © 2005 Wiley-Liss, Inc.

**Key words:** osteogenesis; microarray; mechanical loading; bone; gene expression

Abbreviations used: AHR, aryl-hydrocarbon receptor;  $\alpha 5\beta 3$  integrin,  $\alpha 5\beta 3$  integrin; ANXA2, annexin A2; AP-1, activating protein 1;  $\beta 2M$ ,  $\beta 2$  microglobulin; COL18A1, Collagen type XVIII alpha 1; Csrp2, cysteine and glycine-rich protein 2; CTSD, cathepsin D; EGF, epidermal growth factor; EGFR, EGF receptor; Emp1, epithelial membrane protein 1; ENPP1, ectonucleotide pyrophosphatase/phosphodiesterase 1; Ephb2, ephrin receptor B2; EPS8, EGFR pathway substrate 8; ERK, extracellular signal-regulated kinases; EST, expressed sequence tag; FCGR1A, Fc receptor IgG high affinity I; FGF7, fibroblast growth factor 7; FGFR1, FGF receptor 1; FN, fibronectin receptor; HIF-1A, hypoxia-induced factor1alpha; IER3, immediate early response gene 3; IGF, insulin-like growth factor; IGFBP5, IGF binding protein 5; IGFR, IGF receptor; Itm2a, integral membrane protein 2; Lgmn, legumain; LRR, leucine-rich repeats; MAF, musculoaponeurotic fibrosarcoma oncogene; MAPK, mitogen-activated protein kinase; MMP, matrix metalloproteinase; Npdc1, neural proliferation, differentiation

and control gene 1; Ogn, osteoglycin; PCR, polymerase chain reaction; PDGF, platelet derived growth factor; PDGFA, PDGF alpha; PDGFRA, PDGFR alpha; PDGFRB, PDGF receptor beta; Ptn, pleiotrophin; QTL, quantitative trait loci; RGDS, Ral GDP dissociation stimulator; TEPI, telomerase associated protein 1; TIM, tissue inhibitor of metalloproteinase; TNC, Tenascin C; VEGF, vascular endothelial growth factor.

Grant sponsor: U.S. Army Medical Research Acquisition Activity; Grant number: DAMD17-01-1-0744.

\*Correspondence to: Dr. Subburaman Mohan, Musculoskeletal Disease Center, Jerry L. Pettis Memorial Veterans Medical Center, Loma Linda, CA 92357.

E-mail: Subburaman.Mohan@med.va.gov

Received 11 July 2005; Accepted 12 July 2005

DOI 10.1002/jcb.20606

It is well established that bone adapts to mechanical loading by adjusting its density, shape, and strength during periods of growth and daily physical activities. Under normal conditions, such as exercise, mechanical loading stimulates bone formation, whereas overloading or unloading may result in unbalanced bone resorption and reduced growth rate [Frost, 1992; Sibonga et al., 2000]. However, the skeletal response to mechanical loading is widely varied in the normal human population [Devine et al., 2004; Rittweger et al., 2005]. For example, some postmenopausal women with severe osteoporosis display a poor anabolic response to mechanical stimuli loaded on their bones, while other patients respond normally to the same degree of mechanical loading [Preisinger et al., 1995; Yamazaki et al., 2004]. A similar variation in anabolic response to mechanical loading has also been observed in some animal models, such as the C57BL/6 (B6) and C3H/HeJ (C3H) mouse strains [Akhter et al., 1998; Pedersen et al., 1999]. We and others have found B6 mice to be more responsive to skeletal loading compared to C3H mice [Akhter et al., 1998; Kodama et al., 1999, 2000; Robling and Turner, 2002]. In addition, congenic mice of B6.C3H-4T containing a segment of mouse chromosome 4 from the C3H strain in the B6 genetic background were found to be more susceptible to mechanical loading than the B6 mice [Robling et al., 2003]. Together, these studies have confirmed that differential anabolic responses to mechanical loading are, in large part, genetically determined. Therefore, studies to identify the genes and signal transduction pathways involved in bone's adaptive response to mechanical loading are important for the future development of diagnostic markers and/or therapeutic targets for osteoporosis.

In the past few years, studies using *in vitro* culture systems have identified a number of genes susceptible to mechanical force. It has been found that these genes are involved in a number of signaling pathways, including calcium-regulated PI3K-Akt and protein kinase C [Danciu et al., 2003; Pines et al., 2003], growth factor activated extracellular signal-regulated kinases (ERK), prostaglandin synthesis [Kapur et al., 2003], and integrin pathway [Weyts et al., 2002]. While the data generated from these *in vitro* studies have provided important information, one major limitation has been that most of the data obtained were from homogenous

osteoblast cells in cell culture systems lacking the vital communications of multiple cell types such as osteocytes and osteoblasts. This is a constraint because bone osteocytes can receive and transmit changes in mechanical forces to other cell types involved in bone remodeling [Ehrlich et al., 2002; Noble et al., 2003; Yang et al., 2005]. In addition, multipotent progenitor cells can also respond to mechanical signals to differentiate toward osteoblast lineage [Estes et al., 2004]. Accordingly, there has been a considerable need for an *in vivo* analysis of gene expression patterns of mechanically loaded bones compared to unloaded bones that would address these considerations.

Several approaches have been used to identify candidate genes that contribute to phenotypic variation in inbred strains of mice, including quantitative trait loci (QTL), polymerase chain reaction (PCR) differential display, cDNA microarray, and high-throughput mutation screening of target region [Doerge, 2002]. Of these techniques, microarray holds a great deal of promise for identifying the genes in question because of its ability to simultaneously characterize the expression levels of many thousands of genes associated with various biological functions and processes using very small amounts of RNA. This technology has been applied to identify mechanically induced genes in osteoblast cells exposed to fluid shear stress and has revealed multiple molecular pathways regulating osteogenic gene expression [Kapur et al., 2003]. Therefore, in the present study, we used oligonucleotide microarrays containing over 20,000 probes and evaluated differential gene expression on a global basis in the tibias of female B6 mice after four days of four-point bending. We hypothesized that mechanical activation of one or more sensitive signaling pathways would contribute to the robust increase in new bone formation in response to four-point bending in the female B6 mice.

## MATERIALS AND METHODS

### Animals and Materials

Ten-week-old C57BL/6J female mice were obtained from the Jackson Laboratory and housed at the Jerry L. Pettis Memorial VA Medical Center Animal Research Facility (Loma Linda, CA) under standard approved laboratory conditions with controlled illumina-

tion (14 h light, 10 h dark), temperature (22°C) and unrestricted food and water. Studies were performed with the approval of the Animal Ethics Committee of the Jerry L Pettis Memorial VA Medical Center. Mouse development oligonucleotide microarray (22 K) slides were purchased from Agilent Technologies, Inc (Mountain View, CA). All probes on each slide were 60 base-pairs in length with sense orientation designed from the National Institute on Aging/National Institute of Health cDNA mouse clone set [Carter et al., 2003]. The designed microarray slides contain a single set of 22,575 spots, of which, 20,371 are target genes. In addition, the slides also include a total of 1,075 control spots (144 negative controls, 18 corner mark negative controls, 196 spike-in probes, 215 staggered start probes, 10 corner mark positive controls and 492 positive control grid). The remaining 1,129 spots are blanks. The Cyanine 5-CTP and Cyanine 3-CTP were obtained from PerkinElmer Life Science (Boston, MA).

#### **Mechanical Loading In Vivo and RNA Extraction**

Mice were externally loaded in vivo in a four-point bending device, as described previously [Akhter et al., 1998; Wang et al., 2000]. This model has been used extensively in a number of laboratories for studies on mechanical loading [Torrance et al., 1994; Cullen et al., 2001; Robling and Turner, 2002]. In previous studies, we found that 2 weeks of four-point bending at 9 N, 2 Hz for 36 cycles per day increased total volumetric bone mineral density by 15% in B6 mice [Kesava et al., 2004]. In this study, we used 4 days of loading to minimize the number of genes that change in response to loading-induced bone remodeling. Briefly, the right tibias of the mice were loaded for 4 days at 9 N, 2 Hz for 36 cycles per day, and the left tibias of the same mice were used as unloaded controls. Twenty-four hours after last stimulation, the mice were sacrificed and the corresponding tibias were removed. The bones were dissected free of soft tissue, flushed with PBS to remove the bone marrow cells, and stored in a solution of RNeasy lysis buffer (Qiagen, Inc. Austin, TX) at -20°C. To optimally evaluate mechanosensitive genes, only the region of bone that was subjected to four-point bending was used for RNA extraction. We pooled RNA from five loaded or unloaded bones to obtain sufficient RNA for microarray analysis and subsequent real-time

PCR work. To generate five pairs of samples, a total of 25 mice were divided into five groups with five mice each. Total RNA was extracted using Trizol (Invitrogen Corporation, Carlsbad, CA), and further cleaned up through RNeasy mini spin columns (Qiagen, Valencia, CA). RNA concentration and integrity were analyzed in an Agilent 2100 Bioanalyzer (Agilent Technologies, Inc.).

#### **Microarray Design and Hybridization**

Probe labeling was performed according to the manufacturer's instructions using Agilent low RNA input fluorescent linear amplification kits (Agilent Technologies, Inc.). Briefly, an aliquot of 2 µg of total RNA was reverse transcribed using a primer containing oligo (dT) and a T7 RNA polymerase promoter. After synthesis of the first and second strands of cDNA, the product was amplified in an in vitro transcription reaction in order to generate enough cRNA labeled targets in the presence of cyanine 3- or cyanine 5-labeled CTP. The dye-labeled cRNA was then purified through RNeasy mini spin columns to remove free nucleotides. The cRNA concentration and dye incorporation were measured using the NanoDrop spectrophotometer (NanoDrop Technologies, Rockland, NE). Hybridization was carried out according to the instructions provided in Agilent oligonucleotide microarray kit (Agilent Technologies, Inc.). Two micrograms of fragmented cyanine 3-labeled cRNA of unloaded reference sample was mixed with equal amounts of cyanine 5-labeled cRNA of loaded experimental sample, and the mixture was hybridized to a 22 K mouse development oligonucleotide microarray for 17 h at 60°C at 7 rpm. After hybridization, the slides were dried using a nitrogen-filled air gun, and subsequently scanned using GSI Scanarray 4000 (GSI Lumonics, Inc., Moorpark, CA). The images were analyzed using the ImaGene 5.6 software (Biodiscovery, Inc., El Segundo, CA). The ImaGene software flagged spots with intensities lower than that of the background or spots with aberrant shapes.

#### **Normalization and Analysis of Microarray Data**

Expression analysis of the microarray data from five slides was performed using the GeneSpring 6.2 (Silicon Genetics, Redwood City, CA). Local background-subtracted median signal intensities were used as intensity measures,

with the data normalized using per spot and per chip intensity/dependent LOWESS normalization [Workman et al., 2002]. Transcripts that passed with flag values "present" in all five replicates and a raw signal greater than the background were targeted for further analyses. In order to minimize the false-positive/negative error rate in our high-density oligonucleotide microarray, we chose a combination of fold change and significant difference to restrict a small gene list [Costigan et al., 2002; Schmalbach et al., 2004]. The transcripts were first scaled to an expression level of 1.5-fold change. The filtered genes (e.g.  $\geq 1.5$ -fold) were then further analyzed utilizing a one-sample Student's *t*-test with "Benjamini and Hochberg" Multiple Testing Correction [Hochberg and Benjamini, 1990]. Differentially-expressed genes in the loaded bones were defined as those whose normalized average data had a difference of 1.5-fold change or greater with *P* value  $< 0.01$ , compared with the unloaded reference samples.

### Identification of Signaling Pathways

We analyzed the gene list obtained from our microarray analysis using the PathwayAssist software (Stratagene, La Jolla, CA) to identify any specific signaling pathways, gene regulation networks, and protein interaction maps. The PathwayAssist program uses a natural language processor to retrieve information from databases such as PubMed in order to provide direct biological associations.

### Real-Time PCR

We used reverse transcriptase polymerase chain reaction (RT-PCR) for selected genes to confirm changes in transcription observed in our microarray analysis. Total RNA (2  $\mu$ g) was reverse-transcribed into cDNA by using a oligo(dT)<sub>12-18</sub> primer and SuperScript II RNase<sup>TM</sup> H<sup>-</sup> Reverse Transcriptase (Invitrogen). Real-time PCR was carried out in a 96 well plate using a 7700 ABI prism sequence detection system (Applied Biosystems, Foster City, CA). The PCR contained 100 ng of template cDNA, 1 $\times$  SYBR GREEN master mix (Qiagen) and 100 nM of specific forward and reverse primers in 25  $\mu$ l volume per reaction. Primers for the housekeeping gene,  $\beta$ -2 microglobulin ( $\beta$ 2M), were used to normalize the expression data for each gene. The thermal cycling conditions for real-time PCR were: 10 min at 95°C, followed by 40 cycles of 95°C for 15 s, and 60°C

for 1 min. Sequences of the primers were: pleiotrophin (Ptn) (forward 5-gaaaatttg-cagctgccttc, reverse 5'-ttcaaggcggattgaggtc); osteoglycin (Ogn) (forward 5'-tgcaacaggcaattct-gaag, reverse 5'-tcctt-ggcagtcagcttttt); legumain (Lgmn) (forward 5'-acctgggtgactggtacagc, reverse 5'-gattccttcacgtc-gttggt); immediate early response gene 3 (IER3) (forward 5'-tctggtcccgagattttcac, reverse 5'-ctccgaggtcaggttcaaag);  $\beta$ 2M (forward 5'-cgagcccaagaccgtctact; reverse 5'-gctattttcttctgcgtgcat); P37nb (forward 5'-aggaggcgttcatttacacg, reverse 5'-gggtttgtatgg-gaaacacg); neural proliferation, differentiation and control gene 1 (Npdc1) (forward 5'-taggcttcagcgagagatcc, reverse 5'-atggtcaaa-cagtgggttgc).

## RESULTS

### Genome-Wide Expression Profiles of Mechanically-Loaded Bones Versus Unloaded Bones

We examined global gene expression profiles in five different RNA pools from loaded and corresponding unloaded bones using an oligonucleotide array consisting of 20,371 target genes. We found that a total of 20,280 transcripts were hybridized to the array. After an initial filtering of the data, we arrived at an informative data set for further analysis consisting of 19,882 genes which had both passed with flag value "present" in all five replicates and a raw signal greater than the background. Comparison of the gene expression profiles of the loaded and unloaded bones revealed 346 differentially expressed sequences that differed by 1.5-fold or greater with a significance of  $P < 0.01$  after "Benjamini and Hochberg" multiple testing correction. Table I shows a list of differentially regulated genes whose expression levels were either up- or down-regulated at least two-fold and organized in different biological categories. The complete list of 346 differentially regulated genes is provided in the Supplementary Data posted on this Journal's Website.

To determine the validity of our microarray data, we performed various permutation analyses, which include comparisons of two loaded samples versus three loaded samples, two unloaded samples versus three unloaded samples, and a pool of two loaded plus two unloaded versus three loaded and three unloaded samples. In addition, we also performed sample reproducibility analysis by comparing two

TABLE I. Functional Categories of Selected Genes Differentially Expressed in Mechanically Loaded Bones

Gene	Access number	Description	Change	P value	Location
Cell growth/differentiation					
Ptn	AK011346	Pleiotrophin	4.29	0.0006	6
Ogn	AK014259	Osteoglycin	2.47	0.0040	13
Itim2a	NM_008409	Integral membrane protein 2A	2.85	0.0031	X
Emp1	BC034257	Epithelial membrane protein 1	2.56	0.0015	6
Lepre1	NM_019783	Leprecan 1	2.46	0.0012	4
Tgfb1	XM_122567	Transforming growth factor, beta induced, 68 kDa	2.26	0.0026	13
Pdgfrl	NM_026840	Platelet-derived growth factor receptor-like	2.18	0.0026	13
Morf4l2	NM_019768	Mortality factor 4 like 2	2.04	0.0057	X
Csrp2	NM_007792	Cysteine and glycine-rich protein 2	4.12	0.0013	10 D1
Akr1b7	AK002705	Aldo-keto reductase family 1, member B7	4.72	0.0018	6
Ephb2	BM231330	Eph receptor B2	2.54	0.0048	4 D3
Npdc1	NM_008721	Neural proliferation, differentiation and control gene 1	2.24	0.0093	2 A3
Cell adhesion					
Col5a1	NM_015734	Procollagen, type V, alpha 1	1.97	0.0011	2
Col6a3	BC005491	Procollagen, type VI, alpha 3	3.36	0.0030	1
Col8a1	NM_007739	Procollagen, type VIII, alpha 1	2.56	0.0018	16 C1
Col14a1	XM_127997	Procollagen, type XIV, alpha 1	2.37	0.0026	15
Col18a1	BC008227	Procollagen, type XVIII, alpha 1	3.40	0.0020	10
PCDH19	XM_033173	Protocadherin 19	2.28	0.0092	X
Lamb1-1	XM_126863	Laminin B1 subunit 1	2.69	0.0011	12
Nid1	NM_010917	Nidogen 1	1.99	0.0042	13
Nrp	AK011144	Neuropilin (an alternate receptor for VEGF-A)	2.13	0.0028	8
ESTs	NM_172399	A930038C07Rik (Fibronectin, type III domain)	2.06	0.0019	6
Fn	XM_129845	Fibronectin receptor	2.58	0.0012	1
Matn2	NM_016762	Musculus matrilin 2	2.76	0.0012	15
Loxl3	NM_013586	Lysyl oxidase-like 3	2.14	0.0021	6
Lox	NM_010728	Lysyl oxidase (hydroxylysine residues in collagens)	3.25	0.0042	18
Cell death					
Gas1	NM_008086	Growth arrest specific 1	2.26	0.0015	13
Bcl	BC030069	Bcl-2-related ovarian killer protein	2.48	0.0015	1 D
C1qmf6	NM_028331	C1q and tumor necrosis factor related protein 6	2.11	0.0015	15 E1
Proteolysis					
Mest	NM_008590	Mesoderm specific transcript	3.05	0.0011	6
Lgmn	NM_011175	Legumain	3.25	0.0030	12 E
Timpl	NM_011593	Tissue inhibitor of metalloproteinase 1	2.46	0.0032	X
Pcolec	NM_008788	Procollagen C-proteinase enhancer protein	2.15	0.0086	5
Serpipb6	NM_009254	Serine (or cysteine) proteinase inhibitor, clade B, member 6a	1.97	0.0039	13
EST	NM_028072	201004N24Rik (heparin-degrading endosulfatases)	1.95	0.0040	2
Signal transduction					
Semcap3	NM_018884	SemaF cytoplasmic domain associated protein 3	1.98	0.0023	6
Pdgfrb	NM_008809	Platelet derived growth factor receptor, beta polypeptide	1.97	0.0082	18
EPS8	BC030010	Epidermal growth factor receptor pathway substrate 8	1.98	0.0043	6
Gpr124	NM_054044	Adhesion G protein-coupled receptor 124	1.98	0.0015	8
Entpd2	NM_009849	Ectonucleoside triphosphate diphosphohydrolase 2	2.01	0.0029	2 A3
Scgn10	AK003659	Superior cervical ganglia, neural specific 10 (stathmin-like 2)	2.06	0.0023	3
Deamk1	BE824672	Double cortin and calcium/calmodulin-dependent protein kinase-like 1	3.80	0.0038	3
Ania4	NM_021584	Activity and neurotransmitter-induced early gene, similar to CaM-Kinase	2.87	0.0025	Y
Ednrb	AE014177	Endothelin receptor type B	2.91	0.0063	14

(Continued)

TABLE I. (Continued)

Gene	Access number	Description	Change	P value	Location
Nek6	NM_021606	NIMA (never in mitosis gene a)-related expressed kinase 6	2.14	0.0014	2
Calu	NM_007594	Calumenin (Calmodulin and related proteins, calcium binding)	2.05	0.0100	6
Ren	NM_009037	Reticulocalbin (Calmodulin and related proteins, calcium binding)	2.31	0.0037	2
D7Ertd671e	XM_133470	DNA segment, Chr 7, Ca2+-binding protein	2.02	0.0023	7
Fstl	NM_008047	Follistatin-like	3.10	0.0018	16
Taxlbp3	NM_029564	Tax1 (human T-cell leukemia virus type 1) binding protein 3 (PDZ domain)	1.97	0.0018	11
Il13ral	NM_133990	Interleukin 13 receptor, alpha 1	2.42	0.0060	X
Ccr5	XM_135269	Similar to C-C chemokine receptor 5, (rhodopsin family)	2.35	0.0015	9 F4
Igslf10	AK018323	Immunoglobulin superfamily, member 10	2.20	0.0020	3D
Transcription regulation					
Gsc	NM_010351	Goosecoid	2.30	0.0048	12
Ankrd1	BC037138	Ankyrin repeat domain 1 (cardiac muscle)	2.26	0.0099	19 C2
Gli5	BC021517	GLI-Kruppel family member GLI5		0.0094	16
Maged1	NM_019791	Melanoma antigen, family D, 1	2.33	0.0012	X
Mkrm1	NM_018810	Makorin, ring finger protein, 1	0.45	0.0008	6 B1
Heat shock proteins					
Hsp25	NM_013560	Heat shock protein, 25 kDa	2.15	0.0062	5
Serpinh1	NM_009825	Serine (or cysteine) proteinase inhibitor, clade H, member 1 (Hsp47)	2.72	0.0023	7 E1
Cytoskeleton movement					
Tnnt2	NM_011619	Troponin T2, cardiac	3.03	0.0006	1
Cald1	BC015839	Caldesmon 1	2.11	0.0040	7q33
ESTs	NM_023716	2410129E14Rik (tubulin, beta)	2.75	0.0026	13
Tuba1	NM_011653	Tubulin, alpha 1	2.40	0.0006	15
Acta2	NM_007392	Actin, alpha 2, smooth muscle, aorta	1.97	0.0015	19
S100a10	NM_009112	S100 calcium binding protein A10 (calpactin)	2.00	0.0050	3
ESTs	NM_026473	2310057H16Rik (tubulin)	4.69	0.0014	18 E1
Transport					
AI173274	NM_134090	<i>Mus musculus</i> expressed sequence AI173274, mRNA	2.33	0.0008	15 E1
Sec23a	AY082671	SEC23A	2.31	0.0039	12
P4hb	XM_126743	PDI, Thbp, ERp59; protein disulfide isomerase;	2.29	0.0017	11 80.0 cM
Slc35f5	NM_028787	Solute carrier family 35, member F5	2.11	0.0057	1
Pr1	BC024613	Protein distantly related to the gamma subunit family	1.97	0.0100	1
Other					
Scr59	BC023432	Spermatogenesis associated, serine-rich 2	2.03	0.0065	15 F1
Pfbbp1	BC035209	PTPRF interacting protein, binding protein 1	2.18	0.0045	6 G3
Fkbp9	NM_012056	FK506 binding protein 9	2.15	0.0015	6
Scd2	NM_009128	Stearoyl-Coenzyme A desaturase 2	2.56	0.0025	19
P37nb	XM_131917	Mus musculus 37 kDa leucine-rich repeat (LRR) protein	3.67	0.0040	5
Fer-1-like 3	XM_148914	RIKEN cDNA 2310051D19 gene, similar to myoferlin isoform b	2.64	0.0039	19
Spon2	NM_133903	Spondin 2, extracellular matrix protein	2.46	0.0012	5
Fkbp11	NM_024169	FK506 binding protein 11 (protein turnover, chaperones)	1.98	0.0080	15
Ms4a6d	NM_026835	Membrane-spanning 4-domains, subfamily A, member 6D	1.96	0.0026	19
Rhcd	AF057524	Rhesus blood group CE and D	0.49	0.0052	4
ESTs	BG071710	Mus musculus cDNA clone H3102C09 3', mRNA sequence	0.48	0.0060	9
ESTs	BG071952	Mus musculus cDNA clone H3105A09 3', mRNA sequence	0.43	0.0060	?
ESTs	BG074055	Mus musculus cDNA clone H3130C11 3', mRNA sequence	0.47	0.0047	7
Unknown	BG072471	Mus musculus cDNA clone H3110H06 3', mRNA sequence	0.49	0.0045	3

Functional categories of selected genes that show expression changes of two-fold (log value) or greater with  $P$  value  $\leq 0.01$  in loaded bones compared to unloaded bones. The genes with fold changes less than 0.5 are identified as down-regulated genes. GenBank accession numbers, chromosomal locations and statistical significance are also listed.

normalized samples to three other normalized samples in a two-color system. These analyses revealed that the genes identified in this study cannot be explained on the basis of false discovery rate.

Of the 346 differentially expressed genes/expressed sequence tags (ESTs) that we have identified, 304 were up-regulated, and 42 were down-regulated. A total of 157 (~46%) of these differentially-regulated genes encode proteins with no characterized function (Fig. 1). Interestingly, proteins encoded by some of the genes/ESTs contain functional motifs, such as fibronectin domain, heparin-degrading endosulfatases, tubulin, leucine rich repeats (LRR) and von Willebrand factor type C domain. The remaining 189 known genes encode proteins that could be functionally characterized into 12 categories as assessed by Gene Ontology (GO), including cell growth, differentiation, adhesion, cell cycle, cell death, proteolysis, signaling molecules, transcription regulation, heat shock proteins, cytoskeleton movement, and transport (Fig. 1). The majority of differentially expressed genes belonged to the signaling molecule category and included growth factor receptors, G-protein coupled receptors, integrin receptors,  $Ca^{++}$  dependent receptor, tyrosine/serine/threonine kinases, intracellular, and STAT cascade signaling molecules. The second, third, and fourth largest number of genes were found in cell growth, transport, and cell adhesion, respectively. In addition, we also observed increased expression of a number of genes in categories such as transcriptional regulation,

proteolysis, cell death, and heat shock proteins in the loaded bones compared to unloaded bones.

Notably, mechanical loading stimulated a large number of genes involved in cell growth, proliferation, and differentiation (Table I). These genes included growth factors (Ptn, Ogn), receptor tyrosine protein (Ephb2), and oncogenes (Iprecan1, Itm2a, Emp1, Csrp2 and Npdc1). In addition to the aforementioned genes, some transcription factors such as gooseoid and signaling molecules of growth factor receptor pathways, were also identified as promoters of cell growth.

### Validation of Microarray Data

To confirm the expression data from our oligonucleotide microarray studies, we selected five genes differentially expressed between the loaded and unloaded bones and one unchanged gene for quantitative RT-PCR analysis on five pairs of samples. Three of these genes (Ptn, Ogn, and Lgmn) have been shown to be involved in the regulation of bone remodeling [Madisen et al., 1990; Choi et al., 1999; Yang et al., 2003]. IER3 has been shown to be an immediate early response gene that regulates cell growth and apoptosis in response to stress [Wu, 2003]. P37nb is a member of a leucine-rich repeat protein family with a conserved role in regulation of proliferation, morphology and dynamics of the cytoskeleton, cell adhesion, and tissue development [Segev et al., 2004]. Npdc1 is known to be expressed in the brain with an expression that can be coordinated with the regulation of cellular proliferation and differentiation [Evrard et al., 2004]. Based on the above information, we considered the six genes as potential candidates for mechanical signaling pathway. We therefore chose these genes for confirmation by real-time PCR. Consistent with the microarray data, Ptn, Ogn, Lgmn, P37nb, and Npdc1 were found by real-time PCR to be expressed at significantly higher levels in the loaded bones. The expression of IER3 was no different between the loaded and unloaded bones, as expected based on our microarray data (Fig. 2).

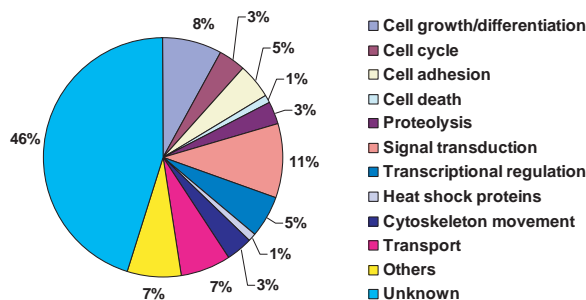


**Fig. 1.** Biological functions of the 346 genes differentially regulated between the loaded and unloaded bones. Other selections represent genes involved in protein modification, chaperoning pathways, extracellular matrix biogenesis, hemostasis, metabolism and development. A total of 157 genes/ESTs are yet to be characterized. [Color figure can be viewed in the online issue, which is available at [www.interscience.wiley.com](http://www.interscience.wiley.com).]

### Identification of Mechanosensitive Signaling Pathways Involving in Anabolic Response

To identify potential signaling pathways associated with the skeletal anabolic response to mechanical loading, we analyzed our microarray expression data using PathwayAssist

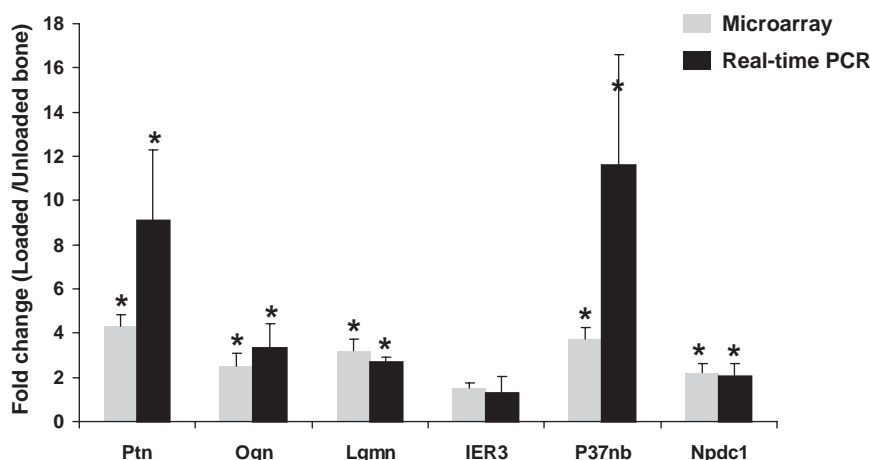


**Fig. 2.** Comparison of fold changes in expression for selected genes by microarray and real-time PCR. The results of real-time PCR were normalized to the expression of  $\beta$ -2 microglobulin ( $\beta$ 2M) in each sample, and expressed as fold change of the loaded sample over the expression level of the unloaded sample. The

data shown are means  $\pm$  SD from five replicates. Ptn: pleiotrophin; Ogn: osteoglycin; Lgmn: legumain; IER3: immediate early response gene 3; Npdc1: neural proliferation, differentiation and control gene 1. \* represents  $P < 0.01$  for loaded bones vs. unloaded bones.

[Nikitin et al., 2003]. This software comes with a built-in natural language processing module MedScan and a comprehensive database containing more than 150,000 events of regulation, interaction and modification between proteins and cell processes obtained from PubMed which allows it to generate a biological association network (BAN) of known protein–protein interactions. By importing microarray expression data into the BAN, co-expressed genes associated with specific signaling pathways can be

identified. In order to characterize signaling pathways involved in response to mechanical loading, we imported 346 differentially expressed genes into the PathwayAssist, and found that 28 of the 346 genes exhibited a direct biological association (Fig. 3). This network identified the following genes as coordinately being regulated in response to four-point bending: JUNB, MAF, TIMP1/2, MMP2,  $\alpha$ 5 $\beta$ 3 integrin, FN, TNC, Col18A1, IGFBP-5, EGFR, EPS8, ENPP1, FGF7, FGFR1, PDGFA, PDGFRA/B,

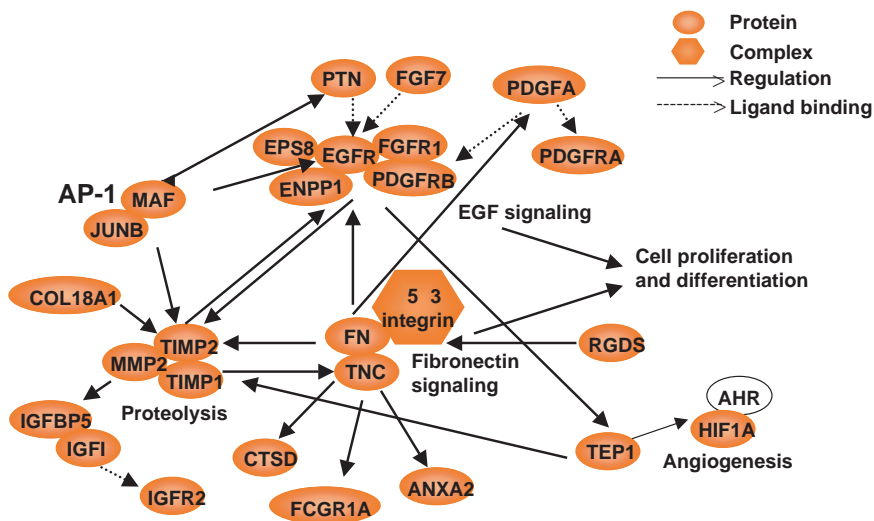


**Fig. 3.** Schematic representation of direct biological association of differentially expressed genes involved in bone remodeling. Analysis of a direct biological association of differentially expressed genes is performed using PathwayAssist 2.53 software (Stratagene, La Jolla, CA). Biologically linked proteins indicated by nodes and biological processes are shown in the diagram. An

open node represents a gene that is down-regulated in the loaded bones compared to unloaded controls. Solid nodes are genes that are up-regulated in the loaded bones compared to unloaded controls. [Color figure can be viewed in the online issue, which is available at [www.interscience.wiley.com](http://www.interscience.wiley.com).]

PTN, TEP1, CTSD, FCGR1, HIF1A, AHR, ANXA2 and RGDS. Many of these genes represent transcription factors, growth factors and growth factor receptors which have been implicated in regulating the formation and/or activity of bone cells. Some of the genes associated with the network, such as TNC, FN, TIMP1, TIMP2, MMP2, JUNB, and PDGFA, have been also shown to respond to mechanical stress in bone cells in vitro [Granet et al., 2002; Carvalho et al., 2004; Hatori et al., 2004; Ponik and Pavalko, 2004]. In addition, it has been shown that the Ptn gene, a ligand for the EGF receptor, is induced in bladder smooth muscle cells in response to mechanical strain [Park et al., 1998]. Thus, a number of genes we have identified in our four-point bending studies in bone are the same genes that have been identified as mechanosensitive genes in other cell types. Among the 28 genes in the network, fibronectin and Ptn are key signaling molecules that can activate integrin and EGF signaling pathways.

### DISCUSSION

The present study is a global microarray analysis of the mouse genome to identify differentially expressed genes in the tibias of female mice after four days of mechanical stimulation in vivo. We chose four-point bending as a loading regimen and B6 as our mouse model based on the findings that 2 weeks of four-point bending with this model caused a dramatic 15% increase in total volumetric bone mineral density, and a 40% increase in bone size [Kesavan et al., 2004]. We chose 4 days of consecutive loading based on the rationale that it leads to activation of important signaling pathways associated with rapid bone remodeling [Raab-Cullen et al., 1994b; Tanaka et al., 2003]. Consistent with the robust bone anabolic response, we identified 346 genes that were differentially expressed in the loaded bones with a 1.5 fold change or greater ( $P < 0.01$ ). Some of these genes, such as TIMP1, heat shock proteins, fibronectin, and neuropilin, have been previously implicated in bone's response to mechanical force and in mediating bone remodeling [Park et al., 1999; Swartz et al., 2001; Shay-Salit et al., 2002]. The identification of previously identified mechanosensitive genes and confirmation of microarray data by real-time PCR provided validation of our microarray results.

Previous in vivo studies of mechanical loading on rat tibias using a four point bending device revealed dynamic changes of gene expression in periosteal bone cells [Raab-Cullen et al., 1994a,b]. In those studies, it was found that transiently stimulated expression of AP-1 proteins within 2 h after loading led to increased osteoblast cell proliferation [Raab-Cullen et al., 1994b]. However, the expression of alkaline phosphatase, osteopontin, and osteocalcin, which are typically produced by mature osteoblasts, was reduced [Raab-Cullen et al., 1994b]. The transcripts of growth factors such as transforming growth factor  $\beta$  (TGF $\beta$ ) and IGF-I were increased to peak levels after 4 h of mechanical loading [Raab-Cullen et al., 1994b]. These studies suggested that acute periosteal response to external mechanical loading was associated with a change in expression of growth factors known to regulate osteoblast cell proliferation. In the present study, we found a moderate induction of AP-1 proteins (e.g. JunB and Maf), IGF-I, IGFBP-5, Ptn, EGF/FGF receptors, and other genes related to cell cycle after 4-day mechanical loading (Supplementary Data). It should be noted that all of the immediate response genes may not have been identified because the RNA used in this study was extracted 24 h after the last mechanical load. In addition, our global microarray analysis also revealed that a large number of highly expressed genes which have not been previously implicated in mechanical signaling pathways, such as Ogn, Itm2a, Emp1, leprecan 1, and Npdc1, could act as potential mediators of mechanical stress to promote cell growth.

Our microarray analysis identified 157 previously uncharacterized or unknown genes/ESTs, some containing interesting functional motifs. For example, Csrp2, located on mouse chromosome 10, has a zinc-binding domain present in Lin-11, Isl-1, and Mec-3 (LIM-domain) that can bind protein partners via tyrosine-containing motifs. These proteins have been implicated as key regulators of developmental pathways and it has been proposed that they also regulate cell proliferation and differentiation of vascular smooth muscle cells in response to injuries [Jain et al., 1996, 1998]. We also observed a novel EST (P37nb) with leucine-rich repeats (LRR), a known functional domain present in a number of proteins with diverse functions and cellular locations [Strausberg et al., 2002]. In addition, one recent study found

evidence that one of the LRR proteins, CMF608, a mechanical strain-induced bone-specific protein, is involved in promoting osteochondroprogenitor proliferation [Segev et al., 2004]. Similarly, osteoadherin is another small molecule with LRR that can promote integrin ( $\alpha 5 \beta 3$ )-mediated cell binding in bone tissue [Sommarin et al., 1998]. Our findings suggest that further studies are needed to evaluate whether these ESTs with important functional domains are involved in regulating bone cell proliferation/activity in response to mechanical loading.

In this study, we have confirmed the existence of a direct biological network consisting of the EGF receptor, fibronectin signaling, and proteolysis that are typically involved in bone formation and bone resorption [Marie et al., 1990; Anderson et al., 2004]. Our findings are supported by the fact that expression of PTN, which interacts with the EGF receptor (ErbB1/4), is also stimulated by mechanical stretch in bladder smooth muscle cells [Park et al., 1999]. In addition, it has been reported that overexpression of the PTN protein in osteoblast cells resulted in an increase in cell proliferation and periosteal bone formation [Imai et al., 1998; Tare et al., 2002]. Therefore, the issue of whether or not the elevated expression of PTN and fibronectin are major extracellular mediators of mechanical stress that activate the EGF receptor and integrin signaling pathways that are essential for bone anabolic response in response to mechanical loading requires further study.

Our study also found that several signaling molecules, including adhesion G-protein-coupled receptor 124, chemokine receptor and Eph receptor B2, were modulated by mechanical loading. Of these molecules, it has been previously established that the Eph receptor is localized within the QTL region of mouse chromosome 4 which is believed to contain mechanosensitive gene(s) [Robling et al., 2003]. In addition, the Eph receptors and their membrane-anchored ephrin ligands are important in regulating cell-cell interactions and communications [Adams et al., 2001]. Targeted disruption of the Eph receptor ligand ephrinB1 in mice has also been reported to cause abnormal cartilage segmentation and the formation of additional skeletal elements, suggesting that ephrinB1 signaling is required for normal morphogenesis of skeletal elements [Compagni et al., 2003]. Our study provides, for the first

time, evidence for increased Eph receptor B2 expression in bone cells in response to mechanical loading and establishes the groundwork for further examination of the Eph receptor signaling pathway's role in regulating bone formation.

Our experimental design involved a few waves of mechanical stimulation prior to evaluation of gene expression changes by microarray. Thus, it is possible that some of the genes altered after four days of four-point bending may be bone remodeling-related rather than mechanical responsive genes, and therefore the genes that are directly activated by mechanical stimulation cannot be discriminated. Our analysis also involved using RNA from loading region of bone that included multiple cell types (e.g. osteoblasts, stromal cells, osteocytes, and osteoclasts). Thus, we cannot conclude which cell types are contributing to changes in gene expression. Further studies are needed to address this issue.

In conclusion, we have examined the *in vivo* effect of mechanical loading on differentially expressed genes in the whole genome, and identified a number of novel genes/ESTs and pathways that may play important roles in mediating the skeletal anabolic response to mechanical force. Future studies on these unknown genes and signal molecules will provide a better understanding of the molecular pathways involved in mediating the skeleton's anabolic response to mechanical stress.

#### ACKNOWLEDGMENTS

The U.S. Army Medical Research Acquisition Activity, 820 Chandler Street, Fort Detrick MD 21702-5014, is the awarding and administering acquisition office. The information contained in this publication does not necessarily reflect the position or the policy of the Government, and no official endorsement should be inferred. All work was performed in facilities provided by the Department of Veterans Affairs. We would like to thank Mr. Sean Belcher for his editorial assistance.

#### REFERENCES

- Adams RH, Diella F, Hennig S, Helmbacher F, Deutsch U, Klein R. 2001. The cytoplasmic domain of the ligand ephrinB2 is required for vascular morphogenesis but not cranial neural crest migration. *Cell* 104:57–69.
- Akhter MP, Cullen DM, Pedersen EA, Kimmel DB, Recker RR. 1998. Bone response to *in vivo* mechanical loading in two breeds of mice. *Calcif Tissue Int* 63:442–449.

- Anderson HD, Wang F, Gardner DG. 2004. Role of the epidermal growth factor receptor in signaling strain-dependent activation of the brain natriuretic peptide gene. *J Biol Chem* 279:9287–9297.
- Carter MG, Hamatani T, Sharov AA, Carmack CE, Qian Y, Aiba K, Ko NT, Dudekula DB, Brzoska PM, Hwang SS, Ko MS. 2003. In situ-synthesized novel microarray optimized for mouse stem cell and early developmental expression profiling. *Genome Res* 13:1011–1021.
- Carvalho RS, Einhorn TA, Lehmann W, Edgar C, Al-Yamani A, Apazidis A, Pacicca D, Clemens TL, Gerstenfeld LC. 2004. The role of angiogenesis in a murine tibial model of distraction osteogenesis. *Bone* 34:849–861.
- Choi SJ, Reddy SV, Devlin RD, Mena C, Chung H, Boyce BF, Roodman GD. 1999. Identification of human asparaginyl endopeptidase (legumain) as an inhibitor of osteoclast formation and bone resorption. *J Biol Chem* 274:27747–27753.
- Compagni A, Logan M, Klein R, Adams RH. 2003. Control of skeletal patterning by ephrinB1–EphB interactions. *Dev Cell* 5:217–230.
- Costigan M, Belfort K, Karchewski L, Griffin RS, D'Urso D, Allchorne A, Sitarski J, Mannion JW, Pratt RE, Woolf CJ. 2002. Replicate high-density rat genome oligonucleotide microarrays reveal hundreds of regulated genes in the dorsal root ganglion after peripheral nerve injury. *BMC Neurosci* 3:16.
- Cullen DM, Smith RT, Akhter MP. 2001. Bone-loading response varies with strain magnitude and cycle number. *J Appl Physiol* 91:1971–1976.
- Danciu TE, Adam RM, Naruse K, Freeman MR, Hauschka PV. 2003. Calcium regulates the PI3K-Akt pathway in stretched osteoblasts. *FEBS Lett* 536:193–197.
- Devine A, Dhaliwal SS, Dick IM, Bollerslev J, Prince RL. 2004. Physical activity and calcium consumption are important determinants of lower limb bone mass in older women. *J Bone Miner Res* 19:1634–1639.
- Doerge RW. 2002. Mapping and analysis of quantitative trait loci in experimental populations. *Nat Rev Genet* 3:43–52.
- Ehrlich PJ, Noble BS, Jessop HL, Stevens HY, Mosley JR, Lanyon LE. 2002. The effect of in vivo mechanical loading on estrogen receptor alpha expression in rat ulnar osteocytes. *J Bone Miner Res* 17:1646–1655.
- Estes BT, Gimble JM, Guilak F. 2004. Mechanical signals as regulators of stem cell fate. *Curr Top Dev Biol* 60:91–126.
- Evrard C, Caron S, Rouget P. 2004. Functional analysis of the NPDC-1 gene. *Gene* 343:153–163.
- Frost HM. 1992. Perspectives: Bone's mechanical usage windows. *Bone Miner* 19:257–271.
- Granet C, Vico AG, Alexandre C, Lafage-Proust MH. 2002. MAP and src kinases control the induction of AP-1 members in response to changes in mechanical environment in osteoblastic cells. *Cell Signal* 14:679–688.
- Hatori K, Sasano Y, Takahashi I, Kamakura S, Kagayama M, Sasaki K. 2004. Osteoblasts and osteocytes express MMP2 and –8 and TIMP1, –2, and –3 along with extracellular matrix molecules during appositional bone formation. *Anat Rec A Discov Mol Cell Evol Biol* 277:262–271.
- Hochberg Y, Benjamini Y. 1990. More powerful procedures for multiple significance testing. *Stat Med* 9:811–818.
- Imai S, Kaksonen M, Raulo E, Kinnunen T, Fages C, Meng X, Lakso M, Rauvala H. 1998. Osteoblast recruitment and bone formation enhanced by cell matrix-associated heparin-binding growth-associated molecule (HB-GAM). *J Cell Biol* 143:1113–1128.
- Jain MK, Fujita KP, Hsieh CM, Endege WO, Sibinga NE, Yet SF, Kashiki S, Lee WS, Perrella MA, Haber E, Lee ME. 1996. Molecular cloning and characterization of SmLIM, a developmentally regulated LIM protein preferentially expressed in aortic smooth muscle cells. *J Biol Chem* 271:10194–10199.
- Jain MK, Kashiki S, Hsieh CM, Layne MD, Yet SF, Sibinga NE, Chin MT, Feinberg MW, Woo I, Maas RL, Haber E, Lee ME. 1998. Embryonic expression suggests an important role for CRP2/SmLIM in the developing cardiovascular system. *Circ Res* 83:980–985.
- Kapur S, Baylink DJ, Lau KH. 2003. Fluid flow shear stress stimulates human osteoblast proliferation and differentiation through multiple interacting and competing signal transduction pathways. *Bone* 32:241–251.
- Kesava CB, Baylink DJ, Wergedal JE, Mohan S. 2004. Inbred mouse strains exhibit variations in the skeletal adaptive response to 4-point bending: Evidence for involvement of different genetic mechanisms. *J Bone Miner Res* 19:S396.
- Kodama Y, Dimai HP, Wergedal J, Sheng M, Malpe R, Kutilek S, Beamer W, Donahue LR, Rosen C, Baylink DJ, Farley J. 1999. Cortical tibial bone volume in two strains of mice: Effects of sciatic neurectomy and genetic regulation of bone response to mechanical loading. *Bone* 25:183–190.
- Kodama Y, Umemura Y, Nagasawa S, Beamer WG, Donahue LR, Rosen CR, Baylink DJ, Farley JR. 2000. Exercise and mechanical loading increase periosteal bone formation and whole bone strength in C57BL/6J mice but not in C3H/HeJ mice. *Calcif Tissue Int* 66:298–306.
- Madisen L, Neubauer M, Plowman G, Rosen D, Segarini P, Dasch J, Thompson A, Ziman J, Bentz H, Purchio AF. 1990. Molecular cloning of a novel bone-forming compound: Osteoinductive factor. *DNA Cell Biol* 9:303–309.
- Marie PJ, Hott M, Perheentupa J. 1990. Effects of epidermal growth factor on bone formation and resorption in vivo. *Am J Physiol* 258:E275–E281.
- Nikitin A, Egorov S, Daraselia N, Mazo I. 2003. Pathway studio—the analysis and navigation of molecular networks. *Bioinformatics* 19:2155–2157.
- Noble BS, Peet N, Stevens HY, Brabbs A, Mosley JR, Reilly GC, Reeve J, Skerry TM, Lanyon LE. 2003. Mechanical loading: Biphasic osteocyte survival and targeting of osteoclasts for bone destruction in rat cortical bone. *Am J Physiol Cell Physiol* 284:C934–C943.
- Park JM, Borer JG, Freeman MR, Peters CA. 1998. Stretch activates heparin-binding EGF-like growth factor expression in bladder smooth muscle cells. *Am J Physiol* 275:C1247–C1254.
- Park JM, Adam RM, Peters CA, Guthrie PD, Sun Z, Klagsbrun M, Freeman MR. 1999. AP-1 mediates stretch-induced expression of HB-EGF in bladder smooth muscle cells. *Am J Physiol* 277:C294–C301.
- Pedersen EA, Akhter MP, Cullen DM, Kimmel DB, Recker RR. 1999. Bone response to in vivo mechanical loading in C3H/HeJ mice. *Calcif Tissue Int* 65:41–46.
- Pines A, Romanello M, Cesaratto L, Damante G, Moro L, D'Andrea P, Tell G. 2003. Extracellular ATP stimulates the early growth response protein 1 (Egr-1) via a protein kinase C-dependent pathway in the human osteoblastic HOBIT cell line. *Biochem J* 373:815–824.

- Ponik SM, Pavalko FM. 2004. Formation of focal adhesions on fibronectin promotes fluid shear stress induction of COX-2 and PGE2 release in MC3T3-E1 osteoblasts. *J Appl Physiol* 97:135–142.
- Preisinger E, Alacamlioglu Y, Pils K, Saradeth T, Schneider B. 1995. Therapeutic exercise in the prevention of bone loss. A controlled trial with women after menopause. *Am J Phys Med Rehabil* 74:120–123.
- Raab-Cullen DM, Akhter MP, Kimmel DB, Recker RR. 1994a. Periosteal bone formation stimulated by externally induced bending strains. *J Bone Miner Res* 9:1143–1152.
- Raab-Cullen DM, Thiede MA, Petersen DN, Kimmel DB, Recker RR. 1994b. Mechanical loading stimulates rapid changes in periosteal gene expression. *Calcif Tissue Int* 55:473–478.
- Rittweger J, Frost HM, Schiessl H, Ohshima H, Alkner B, Tesch P, Felsenberg D. 2005. Muscle atrophy and bone loss after 90 days' bed rest and the effects of flywheel resistive exercise and pamidronate: Results from the LTBR study. *Bone*.
- Robling AG, Turner CH. 2002. Mechanotransduction in bone: Genetic effects on mechanosensitivity in mice. *Bone* 31:562–569.
- Robling AG, Li J, Shultz KL, Beamer WG, Turner CH. 2003. Evidence for a skeletal mechanosensitivity gene on mouse chromosome 4. *Faseb J* 17:324–326.
- Schmalbach CE, Chepeha DB, Giordano TJ, Rubin MA, Teknos TN, Bradford CR, Wolf GT, Kuick R, Misek DE, Trask DK, Hanash S. 2004. Molecular profiling and the identification of genes associated with metastatic oral cavity/pharynx squamous cell carcinoma. *Arch Otolaryngol Head Neck Surg* 130:295–302.
- Segev O, Samach A, Faerman A, Kalinski H, Beiman M, Gelfand A, Turam H, Boguslavsky S, Moshayov A, Gottlieb H, Kazanov E, Nevo Z, Robinson D, Skaliter R, Einat P, Binderman I, Feinstein E. 2004. CMF608-a novel mechanical strain-induced bone-specific protein expressed in early osteochondroprogenitor cells. *Bone* 34:246–260.
- Shay-Salit A, Shushy M, Wolfovitz E, Yahav H, Breviaro F, Dejana E, Resnick N. 2002. VEGF receptor 2 and the adherens junction as a mechanical transducer in vascular endothelial cells. *Proc Natl Acad Sci USA* 99:9462–9467.
- Sibonga JD, Zhang M, Evans GL, Westerlind KC, Cavolina JM, Morey-Holton E, Turner RT. 2000. Effects of space-flight and simulated weightlessness on longitudinal bone growth. *Bone* 27:535–540.
- Sommarin Y, Wendel M, Shen Z, Hellman U, Heinegard D. 1998. Osteoadherin, a cell-binding keratan sulfate proteoglycan in bone, belongs to the family of leucine-rich repeat proteins of the extracellular matrix. *J Biol Chem* 273:16723–16729.
- Strausberg RL, Feingold EA, Grouse LH, Derge JG, Klausner RD, Collins FS, Wagner L, Shenmen CM, Schuler GD, Altschul SF, Zeeberg B, Buetow KH, Schaefer CF, Bhat NK, Hopkins RF, Jordan H, Moore T, Max SI, Wang J, Hsieh F, Diatchenko L, Marusina K, Farmer AA, Rubin GM, Hong L, Stapleton M, Soares MB, Bonaldo MF, Casavant TL, Scheetz TE, Brownstein MJ, Ustin TB, Toshiyuki S, Carninci P, Prange C, Raha SS, Loquellano NA, Peters GJ, Abramson RD, Mullahy SJ, Bosak SA, McEwan PJ, McKernan KJ, Malek JA, Gunaratne PH, Richards S, Worley KC, Hale S, Garcia AM, Gay LJ, Hulyk SW, Villalon DK, Muzny DM, Sodergren EJ, Lu X, Gibbs RA, Fahey J, Helton E, Kettman M, Madan A, Rodrigues S, Sanchez A, Whiting M, Young AC, Shevchenko Y, Bouffard GG, Blakesley RW, Touchman JW, Green ED, Dickson MC, Rodriguez AC, Grimwood J, Schmutz J, Myers RM, Butterfield YS, Krzywinski MI, Skalska U, Smailus DE, Schnerch A, Schein JE, Jones SJ, Marra MA. 2002. Generation and initial analysis of more than 15,000 full-length human and mouse cDNA sequences. *Proc Natl Acad Sci USA* 99:16899–16903.
- Swartz MA, Tschumperlin DJ, Kamm RD, Drazen JM. 2001. Mechanical stress is communicated between different cell types to elicit matrix remodeling. *Proc Natl Acad Sci USA* 98:6180–6185.
- Tanaka SM, Alam IM, Turner CH. 2003. Stochastic resonance in osteogenic response to mechanical loading. *Faseb J* 17:313–314.
- Tare RS, Oreffo RO, Clarke NM, Roach HI. 2002. Pleiotrophin/osteoblast-stimulating factor 1: dissecting its diverse functions in bone formation. *J Bone Miner Res* 17:2009–2020.
- Torrance AG, Mosley JR, Suswillo RF, Lanyon LE. 1994. Noninvasive loading of the rat ulna in vivo induces a strain-related modeling response uncomplicated by trauma or periosteal pressure. *Calcif Tissue Int* 54:241–247.
- Wang Y, Fraefel C, Protasi F, Moore RA, Fessenden JD, Pessah IN, DiFrancesco A, Breakefield X, Allen PD. 2000. HSV-1 amplicon vectors are a highly efficient gene delivery system for skeletal muscle myoblasts and myotubes. *Am J Physiol Cell Physiol* 278:C619–C626.
- Weyts FA, Li YS, van Leeuwen J, Weinans H, Chien S. 2002. ERK activation and alpha v beta 3 integrin signaling through Shc recruitment in response to mechanical stimulation in human osteoblasts. *J Cell Biochem* 87:85–92.
- Workman C, Jensen LJ, Jarmer H, Berka R, Gautier L, Nielser HB, Saxild HH, Nielsen C, Brunak S, Knudsen S. 2002. A new non-linear normalization method for reducing variability in DNA microarray experiments. *Genome Biol* 3:research0048.
- Wu MX. 2003. Roles of the stress-induced gene IEX-1 in regulation of cell death and oncogenesis. *Apoptosis* 8:11–18.
- Yamazaki S, Ichimura S, Iwamoto J, Takeda T, Toyama Y. 2004. Effect of walking exercise on bone metabolism in postmenopausal women with osteopenia/osteoporosis. *J Bone Miner Metab* 22:500–508.
- Yang X, Tare RS, Partridge KA, Roach HI, Clarke NM, Howdle SM, Shakesheff KM, Oreffo RO. 2003. Induction of human osteoprogenitor chemotaxis, proliferation, differentiation, and bone formation by osteoblast stimulating factor-1/pleiotrophin: Osteoconductive biomimetic scaffolds for tissue engineering. *J Bone Miner Res* 18:47–57.
- Yang W, Lu Y, Kalajzic I, Guo D, Harris MA, Gluhak-Heinrich J, Kotha S, Bonewald LF, Feng JQ, Rowe DW, Turner CH, Robling AG, Harris SE. 2005. Dentin matrix protein 1 gene *cis*-regulation: Use in osteocytes to characterize local responses to mechanical loading in vitro and In vivo. *J Biol Chem*.



# Mechanical loading-induced gene expression and BMD changes are different in two inbred mouse strains

Chandrasekhar Kesavan, Subburaman Mohan, Susanna Oberholtzer, Jon E. Wergedal and David J. Baylink

*Journal of Applied Physiology* 99:1951-1957, 2005. First published Jul 14, 2005;  
doi:10.1152/jappphysiol.00401.2005

## You might find this additional information useful...

---

This article cites 31 articles, 5 of which you can access free at:

<http://jap.physiology.org/cgi/content/full/99/5/1951#BIBL>

Updated information and services including high-resolution figures, can be found at:

<http://jap.physiology.org/cgi/content/full/99/5/1951>

Additional material and information about *Journal of Applied Physiology* can be found at:

<http://www.the-aps.org/publications/jappl>

---

This information is current as of October 28, 2005 .

# Mechanical loading-induced gene expression and BMD changes are different in two inbred mouse strains

Chandrasekhar Kesavan,<sup>1</sup> Subburaman Mohan,<sup>1,2</sup> Susanna Oberholtzer,<sup>1</sup> Jon E. Wergedal,<sup>1,2</sup> and David J. Baylink<sup>1,2</sup>

<sup>1</sup>Musculoskeletal Disease Center, Veterans Affairs Loma Linda Healthcare System, and <sup>2</sup>Department of Medicine, Loma Linda University, Loma Linda, California

Submitted 11 April 2005; accepted in final form 12 July 2005

**Kesavan, Chandrasekhar, Subburaman Mohan, Susanna Oberholtzer, Jon E. Wergedal, and David J. Baylink.** Mechanical loading-induced gene expression and BMD changes are different in two inbred mouse strains. *J Appl Physiol* 99: 1951–1957, 2005. First published July 21, 2005; doi:10.1152/jappphysiol.00401.2005.—Our goal is to evaluate skeletal anabolic response to mechanical loading in different age groups of C57B1/6J (B6) and C3H/HeJ (C3H) mice with variable loads using bone size, bone mineral density (BMD), and gene expression changes as end points. Loads of 6–9 N were applied at 2 Hz for 36 cycles for 12 days on the tibia of 10-wk-old female B6 and C3H mice. Effects of a 9-N load on 10-, 16-, and 36-wk-old C3H mice were also studied. Changes in bone parameters were measured using peripheral quantitative computed tomography, and gene expression was determined by real-time PCR. Total volumetric BMD was increased by 5 and 15%, respectively, with 8- and 9-N loads in the B6, but not the C3H, mice. Increases of 20 and 12% in periosteal circumference were reflected by dramatic 44 and 26% increases in total area in B6 and C3H mice, respectively. The bone response to bending showed no difference in the three age groups of B6 and C3H mice. At 2 days, mechanical loading resulted in significant downregulation in expression of bone resorption (BR), but not bone formation (BF) marker genes. At 4 and 8 days of loading, expression of BF marker genes (type I collagen, alkaline phosphatase, osteocalcin, and bone sialoprotein) was increased two- to threefold and expression of BR marker genes (matrix metalloproteinase-9 and thrombin receptor-activating peptide) was decreased two- to fivefold. Although expression of BF marker genes was upregulated four- to eightfold at 12 days of training, expression of BR marker genes was upregulated seven- to ninefold. Four-point bending caused significantly greater changes in expression of BF and BR marker genes in bones of the B6 than the C3H mice. We conclude that mechanical loading-induced molecular pathways are activated to a greater extent in the B6 than in the C3H mice, resulting in a higher anabolic response in the B6 mice.

bone density; mice; bone size; bone formation; bone resorption

IT IS WELL ESTABLISHED that maintenance of bone mass and development of skeletal architecture are dependent on mechanical stimulation. A number of studies have shown that mechanical loading promoted bone formation (BF) in the modeling skeleton and that removal of this stimulus resulted in a reduction in bone mass (1, 9, 13, 28, 29). In addition, recent studies have also shown that the increase in bone mass was variable in different subjects subjected to the same amount of mechanical stress, with some exhibiting a robust osteogenic response and others responding more modestly (8, 24, 26). We and others

found evidence that this variation in response to mechanical loading is, in large part, genetically determined (12, 13, 19). Accordingly, we have identified two inbred mouse strains that differ in peak bone density and exhibit considerable differences in their bone response to immobilization and mechanical loading. In our studies, we found a greater loss of bone in response to hindlimb immobilization by sciatic neurectomy in the C57B1/6J (B6) than in the C3H/HeJ (C3H) mouse strain. Furthermore, studies by Umemura et al. (28) and Kodama et al. (13), as well as four-point bending studies by Akhter et al. (1), revealed that an identical amount of mechanical force applied to both mouse models produced a greater increase in BF (i.e., periosteal and endosteal formation) parameters in B6 than in C3H mice.

In a number of in vitro studies that employed mechanical stimulation using various models in mouse and human cells, several signaling pathways, including mitogen-activated protein kinase (16, 17, 31), focal adhesive kinase (4, 18, 30), and nitric oxide (3, 11, 15, 32), were found to mediate the effects of mechanical loading in bone. However, the genetic mechanisms that contribute to any variations in anabolic response to loading remain unclear. One approach often used to identify the genetic factors or genes that contribute to differences in phenotypic variation is the quantitative trait loci (QTL) technique. In the QTL approach, two inbred mouse strains exhibiting a phenotypic difference of interest are crossed, and any genetic loci that cosegregate with the phenotype are identified. A successful QTL approach requires an optimized in vivo loading model, valid end points for measurement of difference in bone anabolic response, and an optimal age that shows the greatest difference in the phenotype in response to mechanical loading. In this study, we proposed that the magnitude of skeletal anabolic response in B6 and C3H mice is dependent on the age of the mouse and the amount of load applied, which is reflected by changes in expression levels of BF and/or bone resorption (BR) marker genes. To test this hypothesis, our initial objectives were 1) to evaluate the response of bone to different loads applied by four-point bending, 2) to determine whether any differences in the response of bone to mechanical strain between B6 and C3H mice can be accurately quantitated by peripheral quantitative computed tomography (pQCT) and/or expression levels of BF marker genes, and 3) to evaluate whether the bone response to four-point bending varies in different age groups in B6 and/or C3H mice.

Address for reprint requests and other correspondence: S. Mohan, Loma Linda Univ., Musculoskeletal Disease Center (151), Jerry L. Pettis Memorial VA Medical Center, 11201 Benton St., Loma Linda, CA 92357 (e-mail: Subburaman.Mohan@med.va.gov).

The costs of publication of this article were defrayed in part by the payment of page charges. The article must therefore be hereby marked “advertisement” in accordance with 18 U.S.C. Section 1734 solely to indicate this fact.

## MATERIALS AND METHODS

### Animals

Female B6 and C3H inbred mice of different ages (10, 16, and 36 wk) were purchased from Jackson Laboratory (Bar Harbor, ME) and housed at the Animal Research Facility, Jerry L. Pettis Memorial Veterans Affairs Medical Center (Loma Linda, CA) under appropriate conditions. Animal procedures performed in this study were approved by the Animal Studies Subcommittee of the Jerry L. Pettis Medical Center. Body weights were as follows:  $18.8 \pm 0.1$ ,  $20.7 \pm 0.3$ , and  $26.2 \pm 0.5$  g for the B6 mice and  $19.1 \pm 0.1$ ,  $20.7 \pm 0.5$ , and  $27.8 \pm 0.4$  g for the C3H mice at 10, 16, and 36 wk of age, respectively.

### In Vivo Loading Model/Regimen

We used the four-point bending method developed by Akhter et al. (1) as our in vivo loading regimen. Briefly, the four-point bending device (Instron, Canton, MA) consists of two upper vertically movable points covered with rubber pads, which are 4 mm apart, and two 12-mm lower nonmovable points covered with rubber pads. During bending, the two upper pads touch the lateral surface of the tibia through overlying muscle and soft tissue, and the lower pads touch the medial surface of the proximal and distal parts of the tibia. The loading protocol consists of a 6- to 9-N load at a frequency of 2 Hz for 36 cycles, and the training is performed once per day. The right tibia is used for the loading test and the left tibia as an internal control. After the mice were anesthetized, the ankle of the tibia was positioned on the second lower immobile points of the bending device (Instron), such that the region of the tibia that was loaded did not vary in different mice. The mice were anesthetized with 95% oxygen-5% halothane for 2–3 min, and mechanical loading was performed while the mice were anesthetized. The mice were trained for 6 days/wk with 1 day of rest for 2 wk. On the 15th day, 48 h after the last loading regimen, the mice were killed, and tibias were collected and stored at 4°C until pQCT.

### pQCT Densitometry

To determine whether there was a significant change in the geometric properties of loaded and unloaded tibias, we used the pQCT system (Stratec XCT Research, Stratec Medizintechnik, Berlin, Germany). The instrument was specifically modified for use on small bone specimens to measure bone mineral content, periosteal and endosteal circumferences, total area, and total content. Routine calibration was performed daily with a defined standard containing hydroxyapatite crystals embedded in Lucite. Scanning was performed using the manufacturer-supplied software program, which was designed to analyze the data and generate the values for the change in bone parameters. The X-ray attenuation data were analyzed on the basis of the software-defined threshold. We set up two thresholds for our analysis: 180–730 mg/cm<sup>3</sup> to measure total area, total mineral content, periosteal circumference, and endosteal circumference in the loaded vs. unloaded bones and 730–730 mg/cm<sup>3</sup> to measure cortical thickness and total volumetric and material bone mineral density (vBMD and mBMD, respectively).

To minimize the measurement errors caused by positioning of the tibia for pQCT, we used the tibia-fibular junction as the reference line. We selected four slices, 1 mm apart, beginning 3 mm proximal from the tibia-fibular junction for pQCT measurement. This region corresponds to the loading zone.

### Strain Measurement

The differences in the amount of mechanical strain ( $\mu\epsilon$ ) on the loaded region produced by different loads were measured in the B6 and C3H mice by the strain-gauge technique (2, 7, 7a). To measure the strain, we used only the loaded region of the tibia, which, according to our pQCT analysis, was the area most affected by 4-mm vertical

movable points. Briefly, a P-3500 portable strain indicator and a strain gauge of a specific range (EP-XX-015DJ-120) were used to measure the amount of mechanical strain produced by different loads. Initially, the ends of the strain gauge circuits were soldered to copper wire and glued on the medial side of the tibia, 2.09 mm from the tibia-fibular junction, to provide a consistent position on the 4-mm loading zone. The copper wires were connected to the indicator, and the amounts of strain produced by the loads on the loading zone were recorded. The strain gauge data from four individual mice were averaged for each load.

### Microcrack Detection by En Bloc Staining

The 10-wk-old B6 and C3H mice were subjected to four-point bending with a 9-N load for 10 days, and 2 days after the last load was applied, tibias were collected and stored in 10% formalin. One thick section was obtained from the loaded and unloaded bones, and both sides were measured for microcracks (bone area, mm<sup>2</sup>) by the fuchsin staining method (5).

### RNA Extraction

A lipid extraction kit (Qiagen, Valencia, CA) was used to extract RNA from bones with the following modification. After the animals were euthanized, tissues were removed and immediately transferred to liquid nitrogen and stored at –80°C until RNA extraction. A mortar and pestle with liquid nitrogen were used to grind bones into fine powder. Trizol (~1 ml) was added to each sample, and the samples were ground to a fine powder and then transferred to fresh 1.5-ml RNase-free tubes. Chloroform (200  $\mu$ l) was added to each sample, which was vortexed for 15 s and incubated at room temperature for 3 min. The samples were then centrifuged at 12,000 g for 15 min, and an aqueous layer was removed to a fresh tube after centrifugation. Ethanol (~700  $\mu$ l) was added to the fresh samples, which were then vortexed for 15 s. The samples were transferred to a spin column, and the RNA was purified according to the manufacturer's instructions. Quality and quantity of RNA were analyzed using Bio-analyzer and Nano-drop instrumentation (Agilent).

### Reverse Transcriptase Real-Time PCR

Expression of mRNA was quantitated according to the manufacturer's instructions (ABI Prism) using the SYBR green method on sequence detection systems (model 7900, Applied Biosystems). Briefly, purified total RNA (200 ng/ $\mu$ l) was used to synthesize the first-strand cDNA by reverse transcription using random hexamers and Superscript II reverse transcriptase according to the manufacturer's instructions (Invitrogen, Carlsbad, CA). This first-strand cDNA reaction (1  $\mu$ l) was subjected to real-time PCR amplification using gene-specific primers (IDT-DNA), which were designed according to the ABI Primer Express instructions using Vector NTI software. Approximately 25  $\mu$ l of reaction volume were used for the real-time PCR assay, which consisted of 1 $\times$  (12.5  $\mu$ l) Universal SYBR green PCR master mix (SYBR green dye, reaction buffers, dNTP mix, and Hot Start Taq polymerase; Applied Biosystems), each primer at 50 nM, 24  $\mu$ l of water, and 1  $\mu$ l of template. The thermal conditions consisted of an initial denaturation at 95°C for 10 min followed by 40 cycles of denaturation at 95°C for 15 s, annealing and extension at 60°C for 1 min, and a final-step melting curve of 95°C for 15 s, 60°C for 15 s, and 95°C for 15 s. All reactions were carried out in duplicate to reduce variation. The data were analyzed using SDS software (version 2.0), and the results were exported to Microsoft Excel for further analysis. The endogenous control ( $\beta$ -actin) was used to normalize the data, and the normalized values were subjected to a  $2^{-\Delta\Delta C_t}$  (where  $C_+$  is contraction threshold) formula to calculate the fold change between the control and experimental groups. The formula and its derivations were obtained from the sequence detection system user guide (ABI Prism 7900).

# Statistical Analysis

Values are means  $\pm$  SE. Regression analysis, ANOVA (Bonferroni's post hoc test), and standard *t*-test were used to compare differences from loading between the strains using the percentage obtained from loaded vs. unloaded bones. We used STATISTICA software for our analysis, and the results were considered significantly different at  $P < 0.05$ .

## RESULTS

### Bone Anabolic Response to Loading

**Total bone mineral content.** Four-point bending caused an increase in total bone mineral content in the B6 and C3H mice. The magnitude of the increase varied depending on the load between the B6 and C3H mice (Table 1). At 9 N, the percent increase in total bone mineral content in response to four-point bending was significantly greater in the B6 (48%) than in the C3H (19%) mice (Fig. 1A).

**Area.** Total area increased in response to four-point bending in the B6 and C3H mice. Dramatic increases of 44 and 26% in total area were seen after 12 days of four-point bending in the B6 and C3H mice, respectively (Table 1). The increase in total area was greater in the B6 ( $P < 0.05$ ) than in the C3H mice at 9 N, in contrast to other loads (Table 1, Fig. 1A).

**Periosteal circumference.** The periosteal circumference increased by 20 and 12% in the B6 and C3H mice, respectively, in response to four-point bending (Table 1). The B6 mice showed a greater increase in periosteal circumference than the C3H mice ( $P < 0.05$ ) at 9 N compared with other loads (Table 1, Fig. 1A).

**Total vBMD.** Four-point bending caused a dose-dependent increase in total bone density in the B6 (regression analysis,  $P < 0.01$ ), but not in the C3H mice (Table 1). The B6 mice showed 5 and 15% greater density at 8 and 9 N, respectively, after 12 days of loading, whereas the C3H mice exhibited no change (Table 1, Fig. 1B).

**Cortical density.** Cortical density increased by 4% in the B6, but not in the C3H, mice at 9 N after 12 days of four-point bending (Fig. 1A).

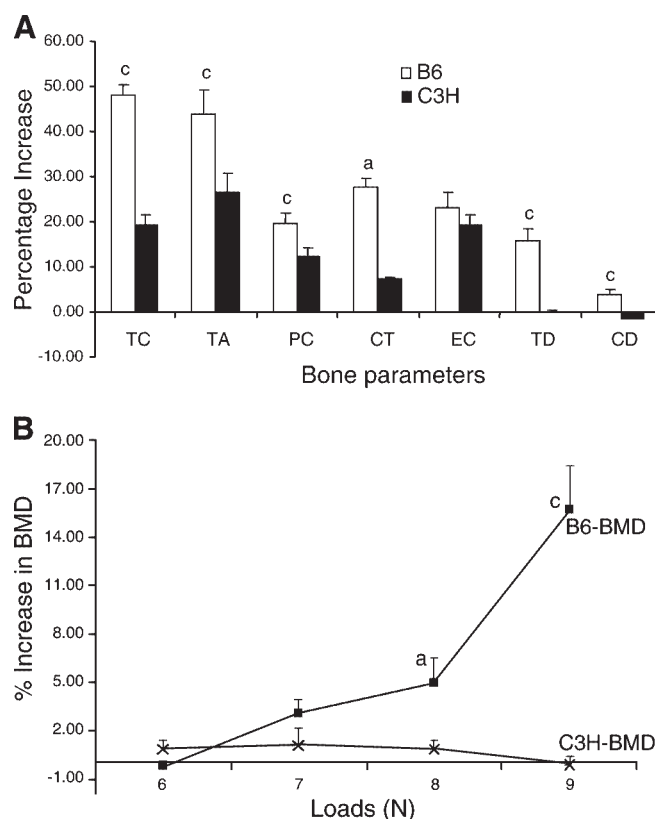


Fig. 1. A: changes in bone geometrical parameters after 12 days of 4-point bending at 9 N in 10-wk-old C57Bl/6J (B6) and C3H/HeJ (C3H) mice in vitro measured by peripheral quantitative computed tomography. TC, total content; TA, total area; PC, periosteal circumference; CT, cortical thickness; EC, endosteal circumference; TD, total density; CD, cortical density. Values are means  $\pm$  SE ( $n = 6$ ). \* $P < 0.05$ ;  $^{\circ}P < 0.001$  vs. C3H. B: changes in total volumetric bone mineral density (BMD) in response to loads applied by 4-point bending in 10-wk-old female B6 and C3H mice in vitro. Values are means  $\pm$  SE ( $n = 6$ ). \* $P < 0.05$ ;  $^{\circ}P < 0.001$  vs. corresponding unloaded bones.

Table 1. Changes in bone parameters in response to loads applied by four-point bending in 10-wk old female B6 and C3H mice

Bone Parameters	Load							
	6 N		7 N		8 N		9 N	
	Unloaded	Loaded	Unloaded	Loaded	Unloaded	Loaded	Unloaded	Loaded
<b>B6</b>								
Total area, mm <sup>2</sup>	1.42 $\pm$ 0.02	1.52 $\pm$ 0.02*	1.40 $\pm$ 0.02	1.60 $\pm$ 0.04†	1.47 $\pm$ 0.01	1.74 $\pm$ 0.01‡	1.50 $\pm$ 0.04	2.13 $\pm$ 0.04§
Total mineral content, mg/mm	0.89 $\pm$ 0.01	0.96 $\pm$ 0.02*	0.83 $\pm$ 0.02	0.96 $\pm$ 0.02*	0.89 $\pm$ 0.01	1.08 $\pm$ 0.008‡	0.87 $\pm$ 0.008	1.29 $\pm$ 0.02§
Periosteal circumference, mm	4.21 $\pm$ 0.03	4.36 $\pm$ 0.03*	4.18 $\pm$ 0.04	4.47 $\pm$ 0.05†	4.30 $\pm$ 0.02	4.67 $\pm$ 0.02‡	4.33 $\pm$ 0.05	5.17 $\pm$ 0.04§
Endosteal circumference, mm	3.12 $\pm$ 0.04	3.21 $\pm$ 0.02	3.15 $\pm$ 0.01	3.35 $\pm$ 0.04†	3.25 $\pm$ 0.02	3.46 $\pm$ 0.02‡	3.29 $\pm$ 0.06	4.02 $\pm$ 0.05§
Total density, mg/cm <sup>3</sup>	678 $\pm$ 12.94	680 $\pm$ 7.63	637 $\pm$ 12.2	655 $\pm$ 11.4	646 $\pm$ 9.83	675 $\pm$ 6.31*	626 $\pm$ 17.00	721 $\pm$ 11.9‡
Cortical density, mg/cm <sup>3</sup>	1,110.0 $\pm$ 6.96	1,114.8 $\pm$ 6.14	1,090 $\pm$ 8.60	1,095 $\pm$ 7.37	1,095 $\pm$ 5.73	1,110 $\pm$ 2.71*	1,078 $\pm$ 17.8	1,115 $\pm$ 14.3‡
<b>C3H</b>								
Total area, mm <sup>2</sup>	1.15 $\pm$ 0.01	1.2 $\pm$ 0.02	1.16 $\pm$ 0.01	1.30 $\pm$ 0.04†	1.15 $\pm$ 0.01	1.41 $\pm$ 0.03†	1.13 $\pm$ 0.03	1.42 $\pm$ 0.02§
Total mineral content, mg/mm	1.03 $\pm$ 0.01	1.07 $\pm$ 0.01*	1.04 $\pm$ 0.01	1.16 $\pm$ 0.02†	1.04 $\pm$ 0.02	1.24 $\pm$ 0.02†	1.04 $\pm$ 0.02	1.24 $\pm$ 0.01‡
Periosteal circumference, mm	3.79 $\pm$ 0.02	3.88 $\pm$ 0.04	3.81 $\pm$ 0.02	4.04 $\pm$ 0.6†	3.79 $\pm$ 0.02	4.20 $\pm$ 0.04†	3.76 $\pm$ 0.04	4.22 $\pm$ 0.03§
Endosteal circumference, mm	2.31 $\pm$ 0.01	2.38 $\pm$ 0.06	2.32 $\pm$ 0.01	2.49 $\pm$ 0.04†	2.30 $\pm$ 0.02	2.62 $\pm$ 0.06†	2.26 $\pm$ 0.04	2.70 $\pm$ 0.06‡
Total density, mg/cm <sup>3</sup>	1,001 $\pm$ 4.79	1,017 $\pm$ 10.5	1,013 $\pm$ 6.8	1,019 $\pm$ 10.1	1,021 $\pm$ 4.95	1,029 $\pm$ 4.87	1,047 $\pm$ 3.9	1,042 $\pm$ 8.07
Cortical density, mg/cm <sup>3</sup>	1,267 $\pm$ 3.56	1,264 $\pm$ 6.96	1,272 $\pm$ 5.7	1,258 $\pm$ 3.27	1,267 $\pm$ 5.32	1,256 $\pm$ 1.5	1,269 $\pm$ 14.7	1,250 $\pm$ 13.93

Values are means  $\pm$  SE ( $n = 6$ ). B6, C57Bl/6J; C3H, ChH/HeJ. \* $P < 0.05$ ; † $P < 0.01$ ; ‡ $P < 0.001$ ; § $P < 0.0001$  vs. corresponding unloaded value.

Table 2. Mechanical strain produced by load applied by four-point bending in tibia of 10-wk-old B6 and C3H mice measured by strain gauge

Load	B6	C3H
6 N	2,610±109.5	2,763±32
7 N	3,020±86.5	3,188±58
8 N	3,371±71.5	3,545±78.5
9 N	3,682±90.5	3,865±91

Values are means ± SE in  $\mu\epsilon$  ( $n = 4$ ).  $P < 0.01$ , B6 and C3H values are significantly different (2-way ANOVA).

**Cortical thickness.** Four-point bending increased cortical thickness in the B6 and C3H mice after 2 wk of mechanical loading at 9 N. The magnitude of the increase was much greater in the B6 (27%) than in the C3H (7%) mice (Fig. 1A).

**Endosteal circumference.** Endosteal circumference in response to four-point bending increased by 23 and 18% in the B6 and C3H mice (Table 1). The increase in endosteal circumference at 8 N was greater in the C3H than in the B6 mice ( $P < 0.05$ ).

#### Strain Measurement

Because the B6 and C3H mice differ in bone geometric properties, we next evaluated whether the difference in bone anabolic response to different loads in the two strains of mice could be explained on the basis of a difference in the amount of mechanical strain produced by the loads. Therefore, using the strain gauge technique, we measured the amount of mechanical strain produced by various loads applied by four-point bending on the tibia of the 10-wk-old B6 and C3H mice. The results (Table 2) revealed an increase in mechanical strain with an increase in mechanical load in the B6 and C3H mice. Mechanical strains at all loads were slightly higher in the C3H than in the B6 mice, and the differences were statistically significant ( $P < 0.01$ , ANOVA; Table 2).

#### Microcrack Detection

To rule out the possibility that the changes in bone parameters induced by a 9-N load are due to microcrack-induced healing, we measured microcracks by histological analysis. The microcrack/area was not significantly different between the loaded and unloaded bones in the B6 ( $0.82 \pm 0.05$  vs.  $0.60 \pm 0.04/\text{mm}^2$ ) or C3H ( $0.87 \pm 0.07$  vs.  $0.95 \pm 0.02/\text{mm}^2$ ) mice. Furthermore, the microcrack/area was not significantly different between the two strains in the loaded or unloaded bone.

Table 3. Changes in bone (tibia) geometric parameters in response to 12 days of four-point bending at 9 N in B6 mice at different ages

Bone Parameters	10 Weeks Old ( $n = 6$ )		16 Weeks Old ( $n = 9$ )		36 Weeks Old ( $n = 9$ )	
	Unloaded	Loaded	Unloaded	Loaded	Unloaded	Loaded
Total area, $\text{mm}^2$	1.50±0.04	2.13±0.04§	1.38±0.02	2.0±0.06§	1.47±0.04	1.91±0.06‡
Total mineral content, mg/mm	0.87±0.008	1.29±0.02§	0.95±0.01	1.36±0.02§	0.84±0.02	1.14±0.01§
Periosteal circumference, mm	4.33±0.05	5.17±0.04§	4.15±0.03	4.99±0.1§	4.30±0.06	4.90±0.07§
Endosteal circumference, mm	3.29±0.06	4.0±0.05§	2.99±0.02	3.68±0.1‡	3.40±0.06	3.80±0.10§
Total density, $\text{mg}/\text{cm}^3$	626±17.00	721±11.9‡	756±8.3	825±12.6‡	649±23.3	678±16.6
Cortical density, $\text{mg}/\text{cm}^3$	1,078±17.8	1,115±14.3‡	1,158±5.33	1,177±5*	1,086±8.00	1,131±13.3*

Values are means ± SE. \* $P < 0.05$ ; † $P < 0.01$ ; ‡ $P < 0.001$ ; § $P < 0.0001$  vs. unloaded value.

#### Mechanical Loading in the B6 and C3H Mice at Various Ages

To study the response of bone to a 9-N load as a function of age, we subjected the 10-, 16-, and 36-wk-old (retired breeder) B6 and C3H mice to four-point bending with a loading regimen similar to that described above. The results indicate that four-point bending caused significant increases in the bone parameters at 10, 16, and 36 wk of age in both strains of mice when measured by pQCT. Changes in the total mineral content, total area, periosteal circumference, and total volumetric and cortical density in all three age groups were greater in the B6 than in the C3H mice (Tables 3 and 4, Fig. 2). Using Bonferroni's post hoc test, we found no statistical difference in the bone responses between the age groups of the B6 and C3H mice.

#### Gene Expression Changes in Response to Four-Point Bending

To evaluate the involvement of osteoblast and osteoclast cell function in producing the optimal response to a given skeletal load, we used real-time PCR to measure changes in gene expression after 2, 4, 8, and 12 days of mechanical loading in the 10-wk-old female B6 mice. In the B6 mice, 2 days of four-point bending significantly decreased expression of BR genes but had no significant effect on expression of BF genes in the loaded tibia compared with the unloaded tibia (Table 5). In addition, expression of type I collagen (Col1a) and bone sialoprotein (BSP) was increased twofold and expression of matrix metalloproteinase-9 (MMP-9) and thrombin receptor-activating peptide (TRAP) was down-regulated three- and fourfold, respectively, at 4 days of loading. No change was found in expression of osteocalcin (OC) and alkaline phosphatase (ALP; Table 5). Eight days of loading caused a threefold increase in expression of Col1a, BSP, ALP, and OC and a threefold downregulation of TRAP. No change in expression of MMP-9 was found between loaded and unloaded bones after 8 days of loading (Table 5). Prolongation of loading (up to 12 days) resulted in significant changes in expression of BF (4.1-, 7.8-, 6-, and 4-fold for Col1a, BSP, ALP, and OC, respectively) and BR (7.5- and 12.2-fold for MMP-9 and TRAP, respectively) marker genes (Table 5). Expression of receptor activator of NF- $\kappa$ B ligand (RANKL) was increased fivefold after 12 days of training in loaded bone compared with unloaded bone.

Table 4. Changes in bone (tibia) geometric parameters in response to 12 days of four-point bending at 9 N in C3H mice at different ages

Bone Parameters	10 Weeks Old (n = 6)		16 Weeks Old (n = 9)		36 Week Old (n = 9)	
	Unloaded	Loaded	Unloaded	Loaded	Unloaded	Loaded
Total area, mm <sup>2</sup>	1.13±0.03	1.42±0.02§	1.15±0.03	1.51±0.02‡	1.38±0.02	1.60±0.02‡
Total mineral content, mg/mm	1.0±0.02	1.24±0.01‡	1.13±0.02	1.43±0.03‡	1.29±0.02	1.53±0.01‡
Periosteal circumference, mm	3.76±0.04	4.22±0.03§	3.80±0.05	4.34±0.04‡	4.15±0.03	4.47±0.03‡
Endosteal circumference, mm	2.26±0.04	2.70±0.06‡	2.25±0.03	2.62±0.05‡	2.57±0.04	2.70±0.05‡
Total density, mg/cm <sup>3</sup>	1,047±3.9	1,042±8.07	1,140±8.33	1,144±12.6	1,054±17.3	1,088±13
Cortical density, mg/cm <sup>3</sup>	1,269±14.7	1,250±13.93	1,343±5.66	1,311±8.33	1,344±10	1,345±7.6

Values are means ± SE. ‡P < 0.001; §P < 0.0001 vs. unloaded value.

### Difference in Expression of Genes Between the B6 and C3H Mice

Although expression levels of BF and BR marker genes were increased in both strains, the increases were significantly greater in the B6 than in the C3H mice. The most significant difference between the two mouse strains was in expression of BSP (Table 6).

### DISCUSSION

The salient features of the present study are as follows. 1) Four-point bending increased vBMD and mBMD significantly in the B6, but not in the C3H, mice. 2) Age (10–36 wk) had no effect on bone response to four-point bending. 3) Four-point

bending caused acute changes in BR and BF gene expression. 4) Four-point bending-induced changes in expression were greater in the bones of the B6 than the C3H mice.

One of the major findings of this study is a striking 15% increase in total vBMD in the tibia of the B6 mice as a result of 12 days of mechanical loading at 9 N using the four-point bending technique. vBMD was increased by 4.5% at 8 N in the B6 mice. In contrast to the response observed in the B6 mice,

Table 5. Fold change in mRNA expression of BF and BR genes in response to four-point bending in 10-wk-old female B6 mice

	n	2 <sup>-ΔΔC<sub>t</sub></sup>	Fold Change	P
<b>BF genes</b>				
2 days	5			
Type I collagen		-0.27±0.19	1.21	0.45
Bone sialoprotein		-0.05±0.48	1.03	0.29
Alkaline phosphatase		-0.41±0.37	1.3	0.66
Osteocalcin		-1.20±0.16	-2.3	0.08
4 days	5			
Type I collagen		-1.02±0.13	2.04	0.03
Bone sialoprotein		-1.03±0.16	2.04	0.006
Alkaline phosphatase		-0.53±0.17	1.45	0.18
Osteocalcin		-0.12±0.45	1.0	0.73
8 days	5			
Type I collagen		-1.93±0.11	3.84	0.001
Bone sialoprotein		-1.89±0.51	3.71	0.003
Alkaline phosphatase		-1.53±0.32	2.88	0.001
Osteocalcin		-1.45±0.43	2.72	0.01
12 days	7			
Type I collagen		-2.06±0.09	4.18	0.001
Bone sialoprotein		-3.01±0.07	7.82	0.002
Alkaline phosphatase		-2.55±0.16	5.86	0.005
Osteocalcin		-2.01±0.12	4.03	0.005
<b>BR genes</b>				
2 days	5			
TRAP		-1.88±0.35	-3.70	0.005
MMP-9		-1.61±0.39	-3.06	0.002
4 days	5			
TRAP		-1.68±0.34	-3.20	0.004
MMP-9		-1.98±0.23	-3.95	0.002
8 days	5			
TRAP		-1.61±0.44	-3.06	0.007
MMP-9		-0.28±0.21	1.21	0.2
12 days	7			
TRAP		-3.61±0.20	12.24	0.003
MMP-9		-2.91±0.13	7.54	0.008
RANKL		-2.65±0.14	5.17	0.001

Values are means ± SE. BF and BR, bone formation and resorption, respectively; TRAP, thrombin receptor-activating peptide; MMP-9, matrix metalloproteinase-9; RANKL, receptor activator of NF-κB ligand.

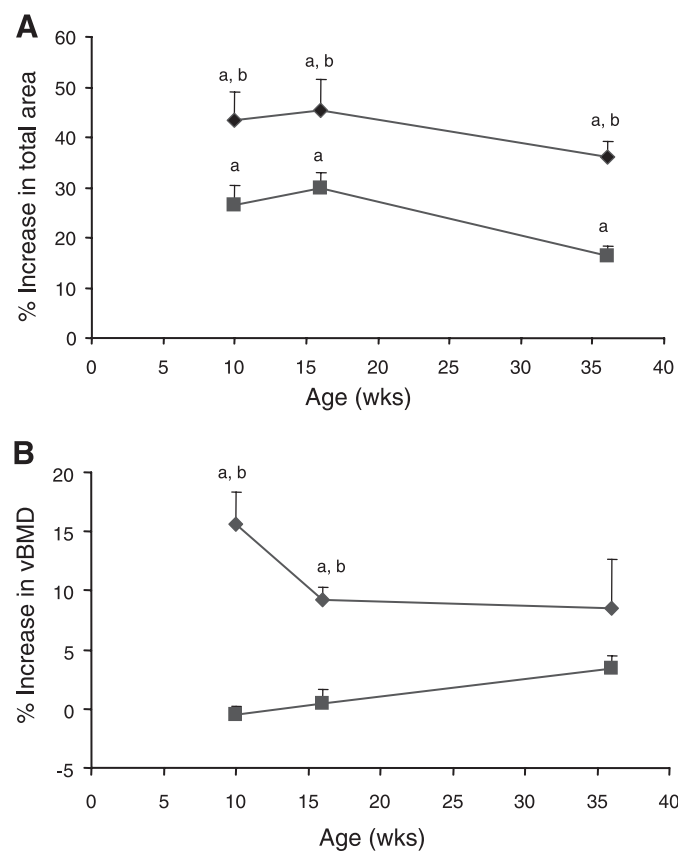


Fig. 2. Changes in total area (A) and volumetric BMD (vBMD, B) in response to 12 days of 4-point bending in 10- to 36-wk-old female B6 (◆) and C3H (■) mice in vitro. Values are means ± SE (n = 6 for 10 wk, n = 9 for 16 and 36 wk) \*P < 0.05 vs. unloaded control. bP < 0.05 vs. C3H.

Table 6. Fold change in mRNA expression of BF and BR marker genes in response to 12 days of four-point bending in 10-wk-old female B6 and C3H mice

Genes	B6	C3H	P
Type I collagen	4.23±0.28	3.19±0.29	0.02
Bone sialoprotein	7.88±0.39	2.90±0.20	0.0000
Alkaline phosphatase	6.08±1.75	3.83±0.42	0.01
Osteocalcin	4.13±0.37	2.93±0.29	0.02
TRAP	13.02±1.91	7.66±0.87	0.02
MMP-9	7.75±0.76	4.20±0.47	0.001
RANKL	5.38±0.63	3.36±0.53	0.04

Values are means ± SE (n = 7). B6 values are significantly different from C3H values.

none of the four loading regimens (i.e., 6, 7, 8, and 9 N) produced a significant increase in total vBMD in the tibia of the C3H mice. Interestingly, this lack of significant change in vBMD cannot be explained by inadequate mechanical strain, because in the tibia of the C3H mouse, a 9-N load produced a strain of 3,865  $\mu\epsilon$ , which is above the physiological range (300–3,000  $\mu\epsilon$ ) and, notably, is higher than the mechanical strain produced in the tibia of the B6 mouse. Furthermore, a mechanical load of 9 N caused a significant increase in total area and periosteal circumference in the C3H mice, suggesting that the increase in the vBMD response in the tibia of C3H mice is not caused by a lack of mechanosensitivity.

In terms of the rapid increase in total vBMD observed in the B6 mice in response to four-point bending, we found that cortical thickness was increased by 27%. Consistent with this increase in cortical thickness, bone area increased significantly as well in the response of the B6 mice to mechanical loads of 9 N. The increase in bone area and cortical thickness can be explained by the ~20% increase in periosteal circumference, which results in a ~50% increase in total area in the loaded tibia compared with the unloaded tibia after 12 days of four-point bending. In contrast to the increases observed in the B6 mice, the magnitude of increase in periosteal circumference, total area, and cortical thickness was substantially less in the C3H mice. Consistent with these data, Akhter et al. (1) found a greater increase in the periosteal BF response in B6 than in C3H mice after four-point bending. Similarly, we found a significantly greater increase in expression of BF marker genes in the loaded tibia of the B6 than the C3H mice (Table 6). On the basis of these data, we have concluded that a greater increase in periosteal bone response in the B6 mouse contributes, in part, to the observed increase in total vBMD in the tibia of loaded bones of B6 mice.

Our findings demonstrate for the first time that mechanical loading results in a significant increase in mBMD, which also contributes to an increase in total vBMD. In this regard, we consider the increase in cortical density to represent changes in mBMD, because the volume of the vascular canal, as determined by histological analysis, was too low in the loaded bones to account for the increase in cortical BMD. Therefore, we believe that a mechanical load of 9 N caused a maximum mineralization and an increase in bone maturation (age) in the tibia of the B6 mouse. Consistent with this interpretation, we found that 2 and 4 days of four-point bending caused an acute downregulation of expression of BR marker genes. Thus the loading-induced decrease in remodeling could contribute to an

increase in the rate of mineralization and, thereby, to the increase in mBMD and total vBMD in the tibia of the B6 mouse.

Our dose-response studies with different mechanical loads revealed that a significant bone anabolic response to loading was observed only at 8- and 9-N loads, which produced mechanical strains slightly above the physiological range (500–3,000  $\mu\epsilon$ ). Earlier studies (17a) demonstrated that mechanical strain produced by loads above the physiological range may lead to an accumulation of microcracks in the loaded bone. To determine whether the bone anabolic response observed after the 8- and 9-N loads was due to microcracks, we performed histological analysis on the cross-section-loaded region of the tibia of the B6 and C3H mice after 12 days of loading to identify potential microcracks. We did not observe microcracks in the B6 or C3H mice at the highest (i.e., 9-N) loads. These findings imply that differences in bone anabolic response between the C3H and B6 mice cannot be ascribed to a difference in the number of microcracks as evaluated by the method used in this study.

To include the newly formed bone, which may not have been fully mineralized, we used a threshold of 180–730 mg/cm<sup>3</sup> for evaluation of loading-induced changes in total area, total mineral content, and periosteal and endosteal circumference. Thus it is possible that the dramatic changes in mineral content and bone size after 2 wk of loading may represent woven bone in addition to mature lamellar bone. Further studies are needed to evaluate the relative contribution of woven and lamellar bone to loading-induced increases in bone size and total mineral content.

Surprisingly, we found no difference in the mechanical strain-induced bone response regardless of age in the 10-, 16-, and 36-wk-old B6 or C3H mice. In contrast to our report, other studies on rats, turkeys, and humans (10, 14, 20, 27) showed that the bone response to mechanical stimuli declines with age. There are a number of potential explanations for the discrepancy between our data and the observations of previous studies. 1) Age-related impairment in bone anabolic response may be seen in >36-wk-old mice. 2) Aging may have a greater effect on the bone response to loading in some inbred strains of mice than in others. 3) The bone response to mechanical loading may vary with age at lower, but not higher, loads.

Another interesting finding from our study was that mechanical load caused an acute inhibition of BR, as evidenced by downregulation of MMP-9 and TRAP. This finding is consistent with the previous *in vitro* study in which mechanical stress reduced the expression of RANKL, inhibiting osteoclast formation and activation (21–23). However, 12 days of prolonged loading induced expression of BR marker genes (Table 5). The increase in BR 12 days after loading may be a consequence of remodeling in response to increased BF. Accordingly, endosteal circumference is increased after 12 days of loading. Furthermore, expression of RANKL, a key regulator of BR, was increased fivefold after 12 days of loading, suggesting that any loading-induced increase in BR at the endosteum may be mediated via an increase in production of RANKL.

In this study, we compared gene expression changes between the B6 and C3H mice to test the hypothesis that the difference in the bone response between these strains in pQCT can be observed in the expression levels of BF and/or BR marker genes. As anticipated, the B6 and C3H mice showed

increased expression of BF and BR marker genes after 12 days of loading. However, the magnitude of the increases in the expression phenotypes was significantly greater in the B6 than the C3H mice (Table 6). This finding is consistent with our pQCT data, which showed a greater increase in the bone parameters in the B6 than in the C3H mice after 12 days of a 9-N load. Thus, using BMD changes and gene expression changes as end points, we have convincingly shown that the skeletal response to mechanical loading is in part genetically determined.

## ACKNOWLEDGMENTS

We thank James Dekeyser for valuable technical support in setting up the four-point bending device and strain-gauge measurement.

The information in this publication does not necessarily reflect the position or the policy of the US Government, and no official endorsement should be inferred.

## GRANTS

This work was supported by Department of Defense Assistance Award DAMD17-01-1-0074; the US Army Medical Research Acquisition Activity (Fort Detrick, MD) is the awarding and administering acquisition office. All work was performed in facilities provided by the Department of Veterans Affairs.

## REFERENCES

- Akhter MP, Cullen DM, Pedersen EA, Kimmel DB, and Recker RR. Bone response to in vivo mechanical loading in two breeds of mice. *Calcif Tissue Int* 63: 442–449, 1998.
- Akhter MP, Raab DM, Turner CH, Kimmel DB, and Recker RR. Characterization of in vivo strain in the rat tibia during external application of a four-point bending load. *J Biomech* 25: 1241–1246, 1992.
- Bacabac RG, Smit TH, Mullender MG, Dijcks SJ, Van Loon JJ, and Klein-Nulend J. Nitric oxide production by bone cells is fluid shear stress rate dependent. *Biochem Biophys Res Commun* 315: 823–829, 2004.
- Boutahar N, Guignandon A, Vico L, and Lafage-Proust MH. Mechanical strain on osteoblasts activates autophosphorylation of focal adhesion kinase and proline-rich tyrosine kinase 2 tyrosine sites involved in ERK activation. *J Biol Chem* 279: 30588–30599, 2004.
- Burr DB and Hooser M. Alterations to the en bloc basic fuchsin staining protocol for the demonstration of microdamage produced in vivo. *Bone* 17: 431–433, 1995.
- Cochran GV. Implantation of strain gauges on bone in vivo. *J Biomech* 5: 119–123, 1972.
- Cowin SC. *Bone Mechanics Handbook* (2nd ed.). Washington, DC: CRC, 2001.
- Dalsky GP, Stocke KS, Ehsani AA, Slatopolsky E, Lee WC, and Birge SJ Jr. Weight-bearing exercise training and lumbar bone mineral content in postmenopausal women. *Ann Intern Med* 108: 824–828, 1988.
- Iwamoto J, Takeda T, and Sato Y. Effect of treadmill exercise on bone mass in female rats. *Exp Anim* 54: 1–6, 2005.
- Jarvinen TL, Pajamaki I, Sievanen H, Vuohelainen T, Tuukkanen J, Jarvinen M, and Kannus P. Femoral neck response to exercise and subsequent deconditioning in young and adult rats. *J Bone Miner Res* 18: 1292–1299, 2003.
- Klein-Nulend J, Helfrich MH, Sterck JG, MacPherson H, Joldersma M, Ralston SH, Semeins CM, and Burger EH. Nitric oxide response to shear stress by human bone cell cultures is endothelial nitric oxide synthase dependent. *Biochem Biophys Res Commun* 250: 108–114, 1998.
- Kodama Y, Dimai HP, Wergedal J, Sheng M, Malpe R, Kutilek S, Beamer W, Donahue LR, Rosen C, and Baylink DJ. Cortical tibial bone volume in two strains of mice: effects of sciatic neurectomy and genetic regulation of bone response to mechanical loading. *Bone* 25: 183–190, 1999.
- Kodama Y, Umemura Y, Nagasawa S, Beamer WG, Donahue LR, Rosen CR, Baylink DJ, and Farley JR. Exercise and mechanical loading increase periosteal bone formation and whole bone strength in C57BL/6J mice but not in C3H/HeJ mice. *Calcif Tissue Int* 66: 298–306, 2000.
- Kohrt WM. Aging and the osteogenic response to mechanical loading. *Int J Sport Nutr Exerc Metab* 11, Suppl: S137–S142, 2001.
- Kunzel JG, Igarashi K, Gilbert JL, and Stern PH. Bone anabolic responses to mechanical load in vitro involve COX-2 and constitutive NOS. *Connect Tissue Res* 45: 40–49, 2004.
- Matsuda N, Morita N, Matsuda K, and Watanabe M. Proliferation and differentiation of human osteoblastic cells associated with differential activation of MAP kinases in response to epidermal growth factor, hypoxia, and mechanical stress in vitro. *Biochem Biophys Res Commun* 249: 350–354, 1998.
- Peverali FA, Basdra EK, and Papavassiliou AG. Stretch-mediated activation of selective MAPK subtypes and potentiation of AP-1 binding in human osteoblastic cells. *Mol Med* 7: 68–78, 2001.
- Reilly GC and Currey JD. Development of microcracking and failure in bone depends on the unloading mode to which it is adapted. *J Exp Biol* 202: 543–552, 1999.
- Rezzonico R, Cayatte C, Bourget-Ponzio I, Romey G, Belhacene N, Loubat A, Rocchi S, Van Obberghen E, Girault JA, Rossi B, and Schmid-Antomarchi H. Focal adhesion kinase pp125<sup>FAK</sup> interacts with the large-conductance calcium-activated *hSlo* potassium channel in human osteoblasts: potential role in mechanotransduction. *J Bone Miner Res* 18: 1863–1871, 2003.
- Robling AG and Turner CH. Mechanotransduction in bone: genetic effects on mechanosensitivity in mice. *Bone* 31: 562–569, 2002.
- Rubin CT, Bain SD, and McLeod KJ. Suppression of the osteogenic response in the aging skeleton. *Calcif Tissue Int* 50: 306–313, 1992.
- Rubin J, Fan X, Biskobing DM, Taylor WR, and Rubin CT. Osteoclastogenesis is repressed by mechanical strain in an in vitro model. *J Orthop Res* 17: 639–645, 1999.
- Rubin J, Murphy T, Nanes MS, and Fan X. Mechanical strain inhibits expression of osteoclast differentiation factor by murine stromal cells. *Am J Physiol Cell Physiol* 278: C1126–C1132, 2000.
- Rubin J, Murphy TC, Fan X, Goldschmidt M, and Taylor WR. Activation of extracellular signal-regulated kinase is involved in mechanical strain inhibition of RANKL expression in bone stromal cells. *J Bone Miner Res* 17: 1452–1460, 2002.
- Snow-Harter C, Boussein ML, Lewis BT, Carter DR, and Marcus R. Effects of resistance and endurance exercise on bone mineral status of young women: a randomized exercise intervention trial. *J Bone Miner Res* 7: 761–769, 1992.
- Tajima O, Ashizawa N, Ishii T, Amagai H, Mashimo T, Liu LJ, Saitoh S, Tokuyama K, and Suzuki M. Interaction of the effects between vitamin D receptor polymorphism and exercise training on bone metabolism. *J Appl Physiol* 88: 1271–1276, 2000.
- Turner CH, Takano Y, and Owan I. Aging changes mechanical loading thresholds for bone formation in rats. *J Bone Miner Res* 10: 1544–1549, 1995.
- Umemura Y, Baylink DJ, Wergedal JE, Mohan S, and Srivastava AK. A time course of bone response to jump exercise in C57BL/6J mice. *J Bone Miner Metab* 20: 209–215, 2002.
- Umemura Y, Ishiko T, Yamauchi T, Kurono M, and Mashiko S. Five jumps per day increase bone mass and breaking force in rats. *J Bone Miner Res* 12: 1480–1485, 1997.
- Wozniak M, Fausto A, Carron CP, Meyer DM, and Hruska KA. Mechanically strained cells of the osteoblast lineage organize their extracellular matrix through unique sites of  $\alpha_3\beta_1$ -integrin expression. *J Bone Miner Res* 15: 1731–1745, 2000.
- You J, Reilly GC, Zhen X, Yellowley CE, Chen Q, Donahue HJ, and Jacobs CR. Osteopontin gene regulation by oscillatory fluid flow via intracellular calcium mobilization and activation of mitogen-activated protein kinase in MC3T3-E1 osteoblasts. *J Biol Chem* 276: 13365–13371, 2001.
- Zaman G, Pitsillides AA, Rawlinson SC, Suswillo RF, Mosley JR, Cheng MZ, Platts LA, Hukkanen M, Polak JM, and Lanyon LE. Mechanical strain stimulates nitric oxide production by rapid activation of endothelial nitric oxide synthase in osteocytes. *J Bone Miner Res* 14: 1123–1131, 1999.

## Fluid Shear Stress Synergizes with Insulin-like Growth Factor-I (IGF-I) on Osteoblast Proliferation through Integrin-dependent Activation of IGF-I Mitogenic Signaling Pathway\*

Received for publication, February 8, 2005, and in revised form, March 14, 2005  
Published, JBC Papers in Press, March 18, 2005, DOI 10.1074/jbc.M501460200

Sonia Kapur<sup>‡§</sup>, Subburaman Mohan<sup>‡§</sup>, David J. Baylink<sup>‡§</sup>, and K.-H. William Lau<sup>‡§¶</sup>

From the <sup>‡</sup>Musculoskeletal Disease Center, Jerry L. Pettis Memorial Veterans Affairs Medical Center, and <sup>§</sup>Departments of Medicine and Biochemistry, Loma Linda University, Loma Linda, California 92357

This study tested the hypothesis that shear stress interacts with the insulin-like growth factor-I (IGF-I) pathway to stimulate osteoblast proliferation. Human TE85 osteosarcoma cells were subjected to a steady shear stress of 20 dynes/cm<sup>2</sup> for 30 min followed by 24-h incubation with IGF-I (0–50 ng/ml). IGF-I increased proliferation dose-dependently (1.5–2.5-fold). Shear stress alone increased proliferation by 70%. The combination of shear stress and IGF-I stimulated proliferation (3.5- to 5.5-fold) much greater than the additive effects of each treatment alone, indicating a synergistic interaction. IGF-I dose-dependently increased the phosphorylation level of Erk1/2 by 1.2–5.3-fold and that of IGF-I receptor (IGF-IR) by 2–4-fold. Shear stress alone increased Erk1/2 and IGF-IR phosphorylation by 2-fold each. The combination treatment also resulted in synergistic enhancements in both Erk1/2 and IGF-IR phosphorylation (up to 12- and 8-fold, respectively). Shear stress altered IGF-IR binding only slightly, suggesting that the synergy occurred primarily at the post-ligand binding level. Recent studies have implicated a role for integrin in the regulation of IGF-IR phosphorylation and IGF-I signaling. To test whether the synergy involves integrin-dependent mechanisms, the effect of echistatin (a disintegrin) on proliferation in response to shear stress  $\pm$  IGF-I was measured. Echistatin reduced basal proliferation by ~60% and the shear stress-induced mitogenic response by ~20%. It completely abolished the mitogenic effect of IGF-I and that of the combination treatment. Shear stress also significantly reduced the amounts of co-immunoprecipitated SHP-2 and -1 with IGF-IR, suggesting that the synergy between shear stress and IGF-I in osteoblast proliferation involves integrin-dependent recruitment of SHP-2 and -1 away from IGF-IR.

Mechanical loading is essential for the maintenance of skeletal architectural integrity. Loading increased bone formation and inhibited bone resorption, leading to an increase in bone mass, whereas unloading decreased bone mass through an increase in resorption and a decrease in formation (1). Although the phenomenon of increased bone formation through

an increase in osteoblast proliferation and activity in response to skeletal loading has been well described, the underlying mechanism(s) remains largely undefined. Loading produces strains in the bone that generate interstitial fluid flow through the lacunar-canalicular spaces (2). It is believed that this fluid flow exerts a shear stress at surfaces of bone cells lining the lacunar-canalicular spaces and that the shear stress generates biochemical signals in bone cells to stimulate osteoblast proliferation and activity. Shear stress stimulates bone cell proliferation and activity through multiple interacting signaling pathways (3).

Bone growth factors function as autocrine and paracrine mediators of bone formation (4, 5). The mechanism whereby mechanical loading stimulates osteoblast proliferation and activity could involve bone growth factors and corresponding signaling pathways. IGF-I<sup>1</sup> is one of the most abundant growth factors in bone (4), produced by bone cells (4–7), and an important stimulator of bone formation (4–7). Loading increases bone cell production of IGF-I *in vivo* (8) and *in vitro* (9). The signaling pathway of IGF-I involves Erk1/2 activation, which is essential for mechanical stimulation of bone cell proliferation (10). It has been reported that the bone cell mitogenic response to mechanical strain is mediated by the IGF-IR (11). In addition, recent studies suggested that loading might have a permissive role in the IGF-I mitogenic action in bone, as skeletal unloading induces resistance to IGF-I with respect to bone formation. Accordingly, unloading blocked the ability of IGF-I to stimulate bone formation in the rat (12). IGF-I administration stimulates bone formation in the loaded bone, but not in unloaded bone *in vivo* (12) and *in vitro* (12, 13). There is evidence that unloading-related resistance to IGF-I is mediated by inhibiting the activation of IGF-I pathway through down-regulation of integrin expression (13). Because unloading blocked the osteogenic action of IGF-I, we postulated that increased loading enhances the osteogenic action of IGF-I. Accordingly, it has been suggested that loading enhances the anabolic effects of IGF-I on articular cartilage formation (14) and also in nasopremaxillary growth (15).

Recent studies in smooth muscle cells (16–22) revealed that the ability of IGF-I to initiate its intracellular signals is regulated not only by its binding to its own transmembrane receptor (IGF-IR) but also by other transmembrane proteins, such as SHPS-1 and  $\alpha\beta$ 3 integrin, to recruit essential signaling pro-

\* This work was supported in part by a special appropriation to the Musculoskeletal Disease Center, Jerry L. Pettis Memorial Veterans Administration Medical Center, and by a merit review provided by the Office of Research and Development, Medical Research Service, Department of Veteran Affairs and also in part by Assistance Award DAMD17-01-1-0744.

<sup>¶</sup> To whom correspondence should be addressed: Musculoskeletal Disease Ctr. (151), Jerry L. Pettis Memorial Veterans Affairs Medical Ctr., 11201 Benton St., Loma Linda, CA 92357. Tel.: 909-825-7084 (ext. 2836); Fax: 909-796-1680; E-mail: William.Lau@med.va.gov.

<sup>1</sup> The abbreviations used are: IGF-I, insulin-like growth factor-I; IGF-IR, insulin-like growth factor-I receptor; pIGF-IR, phosphorylated IGF-IR; FGF-2, basic fibroblast growth factor; Erk1/2, extracellular regulated kinase 1/2; pErk1/2, phosphorylated Erk1/2; SHP-1, Src-homology 2 domain-containing protein-tyrosine phosphatase 1; SHP-2, Src-homology 2 domain-containing protein-tyrosine phosphatase 2; SHPS-1, SHP substrate 1; ANOVA, analysis of variance.

teins, such as SHP-2 and Shc. The integrin recruitment of SHP-2 is essential for regulation of the overall IGF-IR phosphorylation level (18) and the propagation of downstream signaling events (19). Accordingly, ligand occupancy of  $\alpha\beta$ 3 integrin results in phosphorylation of the  $\beta$ 3 integrin subunit, which leads to Downstream of tyrosine kinase I (DOKI)-mediated recruitment of SHP-2 (20). Blocking ligand occupancy of  $\alpha\beta$ 3 integrin inhibited IGF-I-dependent downstream signaling events, membrane recruitment of SHP-2, and cell migration and proliferation (21, 22). Expression of a dominant negative mutant of the  $\beta$ 3 integrin subunit in smooth muscle cells completely abolished the mitogenic activity of IGF-I (16). Thus, integrin activation may have a permissive action in the IGF-IR signaling pathway.

Integrins, which consist of a large family of heterodimers of  $\alpha$ - and  $\beta$ -subunits, function as cell surface adhesion receptors for extracellular matrices (23) and link extracellular matrix components with various intracellular signaling mechanisms (24). It is believed that mechanical strains and shear stresses are distributed to cells through extracellular matrix scaffolds that hold the cells together and that mechanical signals that propagate from the extracellular matrix converge on integrins (25). The interaction between specific bone matrix ligands and corresponding integrin receptors has been suggested to be involved in the signal transduction process linking the extracellular mechanical signals to changes in gene expression, cytoskeletal reorganization, and DNA synthesis in osteoblasts and/or osteocytes (26). Specific antibodies for several integrins blocked mechanical strain-induced cellular responses (27). The integrin- $\beta$ -catenin signal pathway has also been suggested to be involved in the cellular responses of human articular chondrocytes to mechanical stimulation (28). Thus, integrin activation has an important role in the transduction of mechanical signals. Consequently, we postulate that the integrin-dependent regulation of the IGF-I mitogenic signaling pathway could, in part, be involved in the mechanical stimulation of bone formation.

This study investigated the potential relationship between the signaling mechanism of mechanical stimulation of osteoblast proliferation and that of IGF-I-induced osteoblast proliferation by testing two hypotheses: 1) increased mechanical strain in the form of fluid shear stress could synergistically enhance the osteogenic action of IGF-I, and 2) the synergy between IGF-I and fluid shear stress involves the integrin-dependent up-regulation of IGF-IR phosphorylation through an inhibition of SHP-mediated IGF-IR dephosphorylation.

#### EXPERIMENTAL PROCEDURES

**Materials**—Tissue culture plasticware was obtained from Falcon (Oxnard, CA). Dulbecco's modified Eagle's medium was from Mediatech (Herndon, VA). Bovine calf serum was purchased from HyClone (Logan, UT). Trypsin and EDTA were products of Irvine Scientific (Santa Ana, CA). Bovine serum albumin was from United States Biochemical Corp. (Cleveland, OH). [ $^3$ H]Thymidine (48 Ci/mmol) and [ $^{125}$ I]NaI (2,215 Ci/mmol) were from ICN Biochemicals (Irvine, CA). Recombinant human IGF-I and FGF-2 were purchased from R & D Systems (Minneapolis, MN). Anti-actin, anti-IGF-IR, and anti-pErk1/2 antibodies were purchased from Santa Cruz Biotechnology (Santa Cruz, CA). Anti-pIGF-IR and anti-pan Erk antibodies were products of BIOSOURCE International (Camarillo, CA) and Transduction Labs (San Diego, CA), respectively. Other chemicals were from Fisher or Sigma.

**Fluid Shear Stress Experiments**—Human TE85 osteosarcoma cells were plated on glass slides (75  $\times$  38 mm) at  $5 \times 10^4$  cells/slide in Dulbecco's modified Eagle's medium supplemented with 10% bovine calf serum. When the cells reached ~80% confluency, the cells were serum-deprived for 24 h and subjected to a steady fluid shear stress of 20 dynes/cm $^2$  for 30 min in Cytodyne flow chambers as previously described (3). The static controls were performed on cells grown in identical conditions in Cytodyne chambers but without exposing to the shear stress.

**Cell Proliferation Assays**—Cell proliferation was assessed by [ $^3$ H]thymidine incorporation into cell DNA as described previously (29). Briefly, after 30 min of the shear stress, the treated and corresponding static control cells were incubated with the indicated dosages of IGF-I (or FGF-2) for 24 h, and [ $^3$ H]thymidine (1.5  $\mu$ Ci/ml) was added during the final 6 h of the incubation. Effects of a 2-h pretreatment with U0126 (10  $\mu$ M) or a 24-h pretreatment with a disintegrin, echistatin (100 nM), on shear stress and/or IGF-I-induced cell proliferation were also tested.

**Western Immunoblot Analyses and Immunoprecipitation**—Immediately following the 30-min shear stress and 10-min IGF-I treatments, the treated cells and corresponding controls were washed with phosphate-buffered saline and lysed in radioimmune precipitation assay buffer as described previously (3). The protein concentration of each extract was assayed with the bicinchoninic acid method. Ten  $\mu$ g of extract protein from each extract was loaded onto 10% SDS-polyacrylamide gels and transblotted to polyvinylidene difluoride membrane for Western immunoblot analysis. Erk1/2 activation was assessed by pErk1/2 level using the anti-pErk1/2 antibody normalized against the total Erk1/2 level. The pIGF-IR level was determined with an antibody against pIGF-IR, normalized against the level of total IGF-IR.

The relative level of IGF-IR-bound SHP-1 and -2 was each measured by co-immunoprecipitation followed by Western immunoblot analyses. Briefly, 1 mg of cell extract protein each from treated cells and corresponding controls was incubated with 2  $\mu$ g of anti-IGF-IR or anti-integrin  $\beta$ 3 antibodies for 2 h at 4  $^{\circ}$ C. A predetermined amount of anti-rabbit IgG beads (eBiosciences, San Diego, CA) was added for an additional 1 h at 4  $^{\circ}$ C. The bead-bound complex was washed three times with ice-cold lysis buffer (50 mM Tris-HCl, pH 8.0, 150 mM NaCl, 1% Nonidet P-40, 10 mg/ml phenylmethylsulfonyl fluoride, 10  $\mu$ g/ml aprotinin, and 1 mM sodium orthovanadate). The washed complex was then resuspended in 40  $\mu$ l of 2 $\times$  SDS sample buffer and boiled for 5 min. The relative amounts of co-immunoprecipitated SHP-1 or SHP-2 were analyzed by Western analysis using anti-SHP-1 or anti-SHP-2 antibodies, respectively.

**IGF-IR Binding Assays**—Specific IGF-I binding to IGF-IR was measured by receptor-bound [ $^{125}$ I]IGF-I in the presence of 100-fold "cold" IGF-I. Radio-iodination of IGF-I was performed by a modified chloramine T method (30). Aliquots were immediately stored at  $-70^{\circ}$ C until assay. Assays were performed within 1 week of iodination. For the IGF-IR binding assay, TE85 cells were plated on glass slides and subjected to fluid shear stress as described above. Immediately after the shear stress, the treated and corresponding static control cells were rinsed with Dulbecco's modified Eagle's medium containing 20 mM HEPES, pH 7.4, and 1 mg/ml bovine serum albumin (binding medium). Fresh binding medium was then added, and the cells were incubated with  $5 \times 10^4$  to  $2 \times 10^5$  counts/min of [ $^{125}$ I]labeled IGF-I in the absence or presence of 25–100 ng (i.e. 100-fold) of unlabeled IGF-I for total and specific binding, respectively. The cells were incubated at room temperature for 3 h, and the radioactive medium was removed and the slides rinsed five times with ice-cold binding medium. The cells were then lysed in the lysis buffer (10 mM Tris-HCl, pH 7.4, 5 mM EDTA, and 0.2% SDS). The amount of bound [ $^{125}$ I]-labeled IGF-I was then quantified by  $\gamma$  counting.

**Statistical Analyses**—Results are shown as mean  $\pm$  S.D. with at least six replicates. The statistical significance of the differences between independent groups was determined with the two-tailed Student's *t* test. The dose-dependent effects were assessed with one-way ANOVA, followed by Tukey post-hoc test. Interactions between two treatments (e.g. shear stress and IGF-I) were evaluated by two-way ANOVA. The difference was considered significant when  $p < 0.05$ .

#### RESULTS

**Effects of Fluid Shear Stress on the Bone Cell Mitogenic Action of IGF-I in TE85 Cells**—IGF-I at 10–50 ng/ml concentrations significantly and dose-dependently ( $p < 0.01$ , one-way ANOVA) increased the proliferation (i.e. [ $^3$ H]thymidine incorporation) of TE85 cells by ~1.5–2.5-fold (Fig. 1A). The 30-min steady shear stress of 20 dynes/cm $^2$  also significantly ( $p < 0.05$ ) increased [ $^3$ H]thymidine incorporation in TE85 cells by 70% compared with the corresponding static control cells. The combination of the 30-min shear stress and IGF-I treatment produced much greater than additive stimulations (3.5–5.5-fold) of each treatment alone (Fig. 1A). Two-way ANOVA indicates a highly significant ( $p < 0.01$ ) interaction between the two treatments, suggesting a synergistic interaction between shear

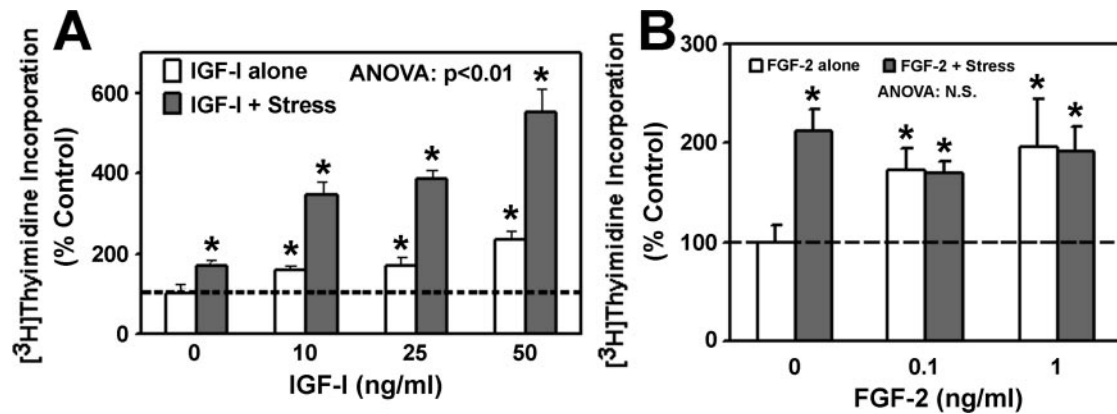


FIG. 1. **Interaction between IGF-I (A) or FGF-2 (B) and fluid shear stress on the proliferation of TE85 osteosarcoma cells.** The effect of IGF-I or FGF-2 at the indicated concentrations with (filled bars) or without (open bars) a 30-min steady shear stress of 20 dynes/cm<sup>2</sup> on TE85 cell proliferation, which was assessed by measuring [<sup>3</sup>H]thymidine incorporation 24 h later. Results are shown as mean  $\pm$  S.D. ( $n = 6$ ). \*,  $p < 0.01$  (compared with the static control). ANOVA indicates a significant ( $p < 0.01$ ) interaction between IGF-I and shear stress (A) but not between FGF-2 and shear stress (B) on [<sup>3</sup>H]thymidine incorporation. N.S., not significant ( $p > 0.05$ ).

stress and IGF-I on bone cell proliferation.

To test whether the synergistic interaction between shear stress and IGF-I on human bone cell proliferation is a general feature between bone cell growth factors and shear stress, we evaluated whether shear stress would also synergistically enhance the mitogenic activity of FGF-2 (another potent bone cell growth factor) in TE85 cells. Fig. 1B shows that FGF-2 alone significantly and dose-dependently ( $p < 0.01$ ) stimulated the TE85 cell proliferation (by  $\sim 1.5$ – $2.0$ -fold). The combined treatment of the shear stress and FGF-2 yielded no further enhancement (not significant, two-way ANOVA) than FGF-2 alone, indicating that the synergistic interaction between shear stress and IGF-I is not universal to all bone growth factors.

**Effects of Fluid Shear Stress on the IGF-I-mediated Activation of the Erk1/2 Mitogenic Signaling Pathway in Human TE85 Cells**—Because the mitogenic action of IGF-I is mediated through Erk1/2 activation and fluid shear stress also activates Erk1/2 in osteoblasts (3, 10), we investigated the effect of shear stress and/or IGF-I (or FGF-2) on Erk1/2 phosphorylation (an index of Erk1/2 activation). Fig. 2A confirms that IGF-I alone, at the test doses, significantly and dose-dependently ( $p < 0.01$ , one-way ANOVA) increased the pErk1/2 level (by  $\sim 1.2$ – $5$ -fold) in TE85 cells. The 30-min steady shear stress alone also significantly ( $p < 0.01$ ) increased the pErk1/2 level (by  $\sim 2.5$ -fold). The combination of shear stress and IGF-I treatment produced a synergistic ( $p < 0.01$ , two-way ANOVA) enhancement (up to 12-fold) in Erk1/2 phosphorylation. Fig. 2B indicates that the mitogenic doses of FGF-2 (0.1 and 1 ng/ml) alone also markedly and significantly increased the pErk1/2 levels in TE85 cells ( $p < 0.01$ , one-way ANOVA). In contrast to IGF-I, the combination treatment of shear stress and FGF-2 did not result in a further increase in the pErk1/2 level compared with the FGF-2 treatment alone (not significant, two-way ANOVA). These findings further support the conclusions that the synergistic interaction between shear stress and IGF-I on bone cell proliferation is mediated through synergistic enhancement of IGF-I-dependent activation of the Erk1/2 mitogenic signaling pathway and that the synergy between shear stress and IGF-I on human bone cell proliferation is not shared by FGF-2.

To further evaluate whether activation of the Erk1/2 mitogenic signaling pathway is essential for the synergy, we tested the effect of U0126 (a specific inhibitor of mitogen-activated protein kinase/extracellular signal-regulated kinase kinase 1) on the stimulation of cell proliferation and Erk1/2 phosphorylation induced by IGF-I with or without the shear stress. Fig. 3A shows that pretreatment with U0126 at 10  $\mu$ M completely blocked the IGF-I-mediated as well as the shear stress-induced

TE85 cell proliferation. It also completely abolished the synergistic enhancement of IGF-I and shear stress. Fig. 3B reveals that the U0126 pretreatment also completely eliminated the synergistic enhancement on Erk1/2 activation by shear stress and IGF-I. Thus, these results are consistent with the conclusion that the synergistic activation of Erk1/2 by IGF-I and shear stress is associated with the synergistic enhancement on osteoblast proliferation. These findings indicate that the synergy between shear stress and IGF-I leading to activation of bone cell proliferation occurs upstream to the Erk1/2 activation. Consistent with previous findings (3, 10), U0216 had no inhibitory effect on either basal proliferation or basal Erk1/2 activation, indicating that basal TE85 cell proliferation is mediated primarily through Erk1/2-independent pathways.

**Effect of Shear Stress on the IGF-I-mediated Phosphorylation of IGF-IR in TE85 Cells**—We next tested whether the synergy between IGF-I and shear stress occurs prior to or after the phosphorylation of IGF-IR receptor. As expected, IGF-I at the test mitogenic doses significantly increased the IGF-IR phosphorylation level in a dose-dependent manner by 2–3.5-fold (Fig. 4). The 30-min steady shear stress alone also significantly ( $p < 0.01$ ) increased the IGF-IR phosphorylation by 2.5-fold. The combination treatment of shear stress and IGF-I yielded a highly significant synergistic ( $p < 0.01$ , two-way ANOVA) enhancement in IGF-IR phosphorylation level (up to 8-fold).

**Effects of Fluid Shear Stress on the Specific Binding of IGF-I to IGF-IR in TE85 Cells**—Because shear stress synergistically enhanced IGF-IR phosphorylation, which is initiated by the binding of IGF-I to IGF-IR, we next assessed whether the synergistic enhancement between IGF-I and shear stress was because of an increase in IGF-I binding to IGF-IR. Fig. 5 shows that the application of a 30-min fluid shear stress at 20 dyne/cm<sup>2</sup> led to a relatively small, but statistically significant ( $p < 0.05$ , one-way ANOVA) enhancement in the specific binding of IGF-I to IGF-IR in TE85 cells. However, this increase appeared to be of additive nature, as the two binding curves (i.e. with or without shear stress) were parallel to each other.

**Effects of Echistatin on the IGF-I- and/or Shear Stress-induced Proliferation of TE85 Cells**—Because shear stress involves integrin activation in bone cells (3, 26, 27), we evaluated whether integrin activation is involved in the synergy between IGF-I and shear stress in TE85 cells by determining the effect of the disintegrin echistatin (a competitive integrin receptor antagonist) on IGF-I- and/or shear stress-mediated cell proliferation and IGF-IR phosphorylation. Fig. 6A shows that echistatin, not only reduced the basal (by  $\sim 60\%$ ) and shear stress-induced TE85 cell proliferation (by  $\sim 20\%$ ), but also com-

FIG. 2. **Interaction between IGF-I (A) or FGF-2 (B) and fluid shear stress on Erk1/2 phosphorylation in TE85 cells.** Top panels show representative Western blots of phosphorylated Erk1/2 (pErk1/2). Each blot was stripped and reblotted against anti-pan-Erk and anti-actin antibodies for loading controls. Bottom panels summarize the results of three separate repeat experiments. Results are shown as mean  $\pm$  S.D. \*,  $p < 0.01$  (compared with no addition control). Two-way ANOVA indicates a significant ( $p < 0.01$ ) interaction between IGF-I and shear stress but not between FGF-2 and shear stress on [ $^3$ H]thymidine incorporation. C, control; St, stressed; Pan-Erk, the anti-pan Erk antibody recognized all forms of Erks.

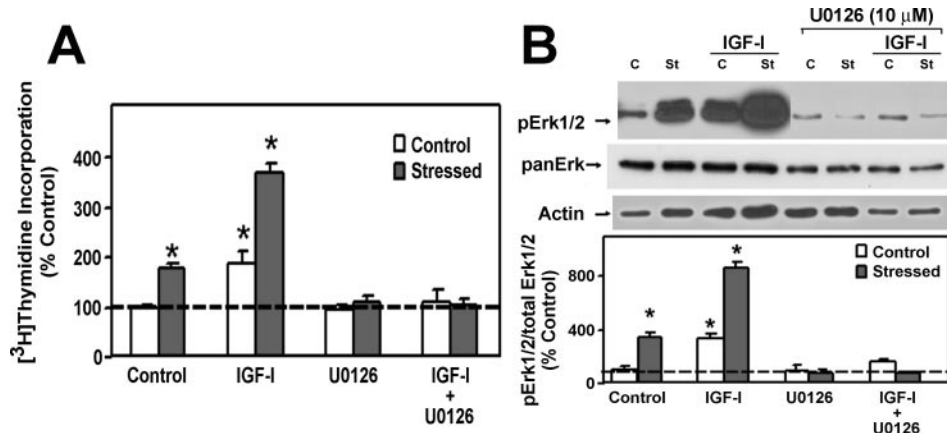
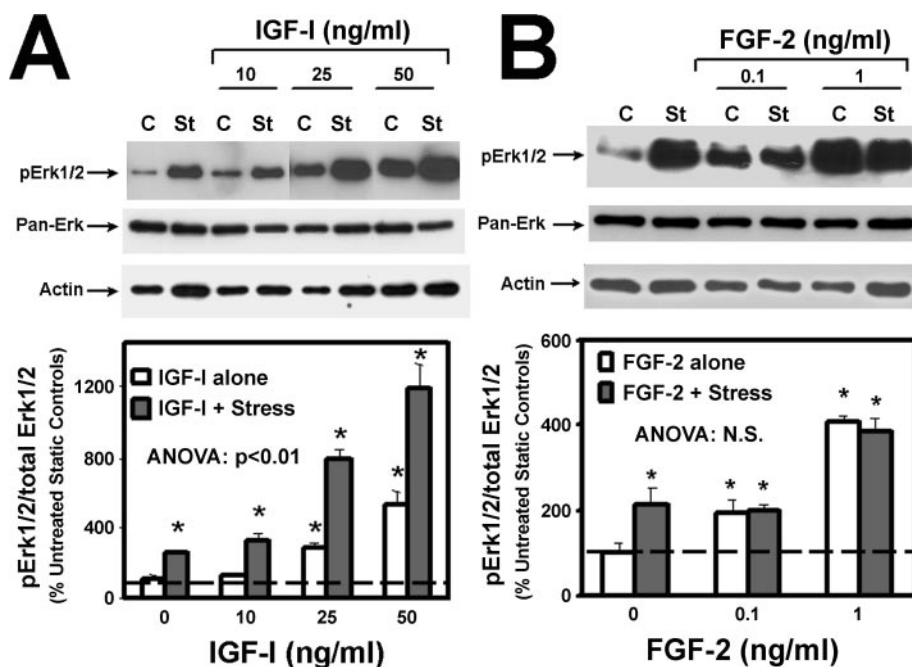


FIG. 3. **Effects of U0126 (a specific inhibitor of the Erk signaling pathway) on the stimulation of cell proliferation (A) and Erk1/2 protein-tyrosine phosphorylation (B) mediated by IGF-I and/or shear stress in TE85 cells.** TE85 cells were pretreated with 10  $\mu$ M U0126 overnight before subjecting to the shear stress and/or IGF-I treatments. A shows the effects of U0126 on [ $^3$ H]thymidine incorporation in response to the 30-min steady shear stress of 20 dynes/cm $^2$  and/or 10 ng/ml IGF-I. Top panel of B shows a representative Western blot of pErk1/2. Each blot was stripped and reblotted against anti-pan-Erk and anti-actin antibodies for loading controls. Bottom panel of B summarizes the results of three separate repeat experiments. Results are shown as mean  $\pm$  S.D. \*,  $p < 0.01$  (compared with no addition control). C, control; St, stressed; Pan-Erk, the anti-pan Erk antibody recognized all forms of Erks.

pletely abolished the increase in cell proliferation induced by IGF-I alone as well as that by the combination treatment. Similarly, echistatin also completely abolished the basal, shear-stress, or IGF-I-induced IGF-IR phosphorylation (Fig. 6B). These findings suggest that the synergy between IGF-I and shear-stress on the proliferation and that on IGF-IR phosphorylation level may involve integrin activation.

**Effects of Fluid Shear Stress on the Association of SHP-1 or -2 with IGF-IR in TE85 Cells**—To test whether integrin-dependent recruitment of SHP-2 could be involved in the synergy between IGF-I and shear stress, we determined the effect of IGF-I and/or fluid shear stress on the relative amounts of SHP-2 associated with integrin  $\beta$ 3 or with IGF-IR, determined by co-immunoprecipitation (Fig. 7, IP) followed by immunoblotting (IB). This study focused on integrin  $\beta$ 3, because this integrin subunit is one of the major subunits in osteoblasts (31) and also because integrin  $\alpha$  $\beta$ 3 has been implicated to be the essential integrin subunit in regulating the IGF-I-dependent cellular responses in smooth muscle cells (16–22). The results of Fig. 7 suggest that fluid shear stress, IGF-I, and the combina-

tion treatment each significantly enhanced the recruitment of SHP-2 to integrin  $\beta$ 3 and away from the IGF-IR. We also determined whether the synergistic interaction could also involve integrin-dependent recruitment of the related SHP-1 away from the IGF-IR. Fig. 8 shows that fluid shear stress, IGF-I, and the combination treatment each also significantly enhanced the recruitment of SHP-1 to integrin  $\beta$ 3 and away from the IGF-IR. However, the effects of fluid shear stress on the recruitment of SHP-2 away from the IGF-IR appeared to be more pronounced than those on the SHP-1 recruitment. On the other hand, treatment of IGF-I alone, although it markedly reduced the amounts of IGF-IR-bound SHP-2, did not significantly affect the amounts of SHP-2 bound to integrin  $\beta$ 3.

#### DISCUSSION

Mechanical loading is essential and required for normal bone physiology. Defective cellular responses to mechanical loading has been implicated as the etiology and progression of a number of musculoskeletal diseases, including disuse osteoporosis, senile osteoporosis, and osteoarthritis (32, 33). Appropriate

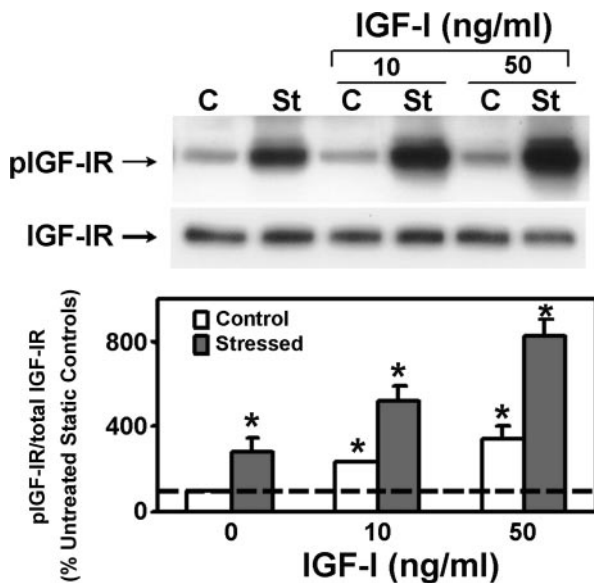


FIG. 4. Interaction between IGF-I and fluid shear stress on IGF-IR phosphorylation in TE85 cells. *Top panel* shows a representative Western blot of phosphorylated IGF-IR (pIGF-IR). The blot was stripped and reblotted against an anti-IGF-IR antibody for loading controls. *Bottom panels* summarize the results of three separate repeat experiments. Results are shown as mean  $\pm$  S.D. \*,  $p < 0.01$  (compared with no addition control). Two-way ANOVA indicates a significant ( $p < 0.01$ ) interaction between IGF-I and shear stress. C, control; St, stressed.

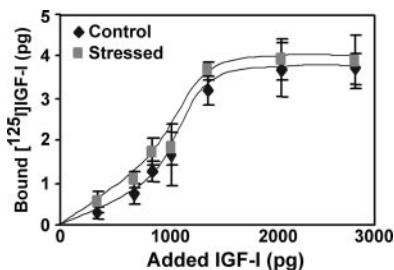


FIG. 5. Effects of fluid shear stress on specific binding of IGF-I to IGF-IR in TE85 cells. The binding of IGF-I to surface IGF-IR of TE85 cells was performed by measuring the receptor-bound [ $^{125}$ ]IGF-I. Total and nonspecific IGF-I binding was determined in the absence and presence of 100 $\times$  non-radioactive cold IGF-I, respectively. Specific binding of IGF-I to IGF-IR was calculated by subtracting the nonspecific binding from the total binding. Only specific binding is shown in this figure. The filled squares were cells receiving the shear stress, whereas the filled diamonds were the corresponding static controls.

mechanical loading is also required for fracture healing (34). Thus, it is not surprising that the molecular mechanism of this important physiological process to regulate bone formation is complex and involves multiple interacting signal transduction pathways (3, 35). Information about the nature and molecular mechanism of the interaction among these various pathways should provide, not only a better understanding of the mechanical regulation of bone formation, but also important insights into the etiology of various musculoskeletal diseases. In this regard, this investigation addresses the potential mechanism of a cross-talk between the IGF-I and integrin signaling pathways in the stimulation of bone cell proliferation in response to a steady shear stress.

In this study, we demonstrated for the first time that a 30-min steady fluid shear stress of 20 dynes/cm<sup>2</sup> in human TE85 osteosarcoma cells enhanced synergistically the mitogenic action of IGF-I through an up-regulation of the Erk1/2-mediated IGF-I mitogenic signaling pathway. Our findings that the disintegrin echistatin completely abolished the syn-

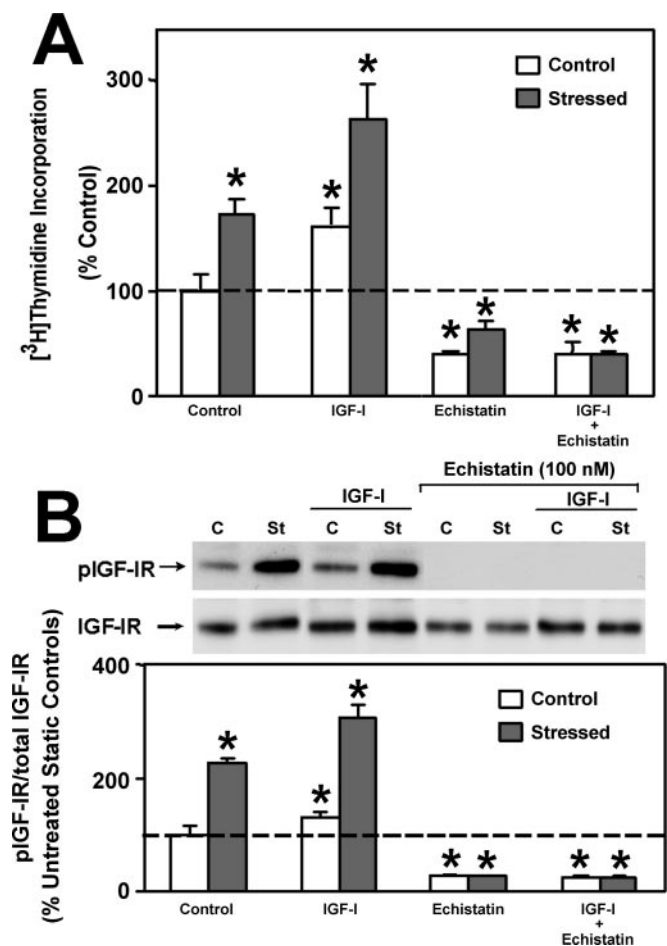
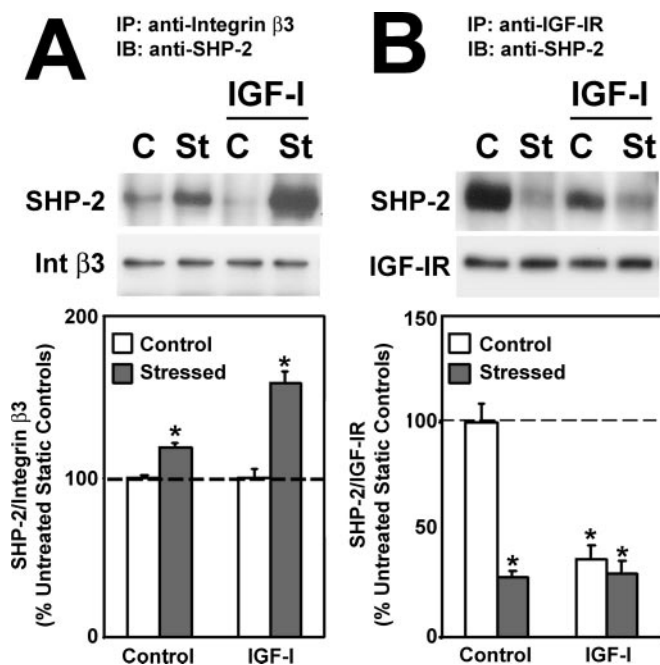
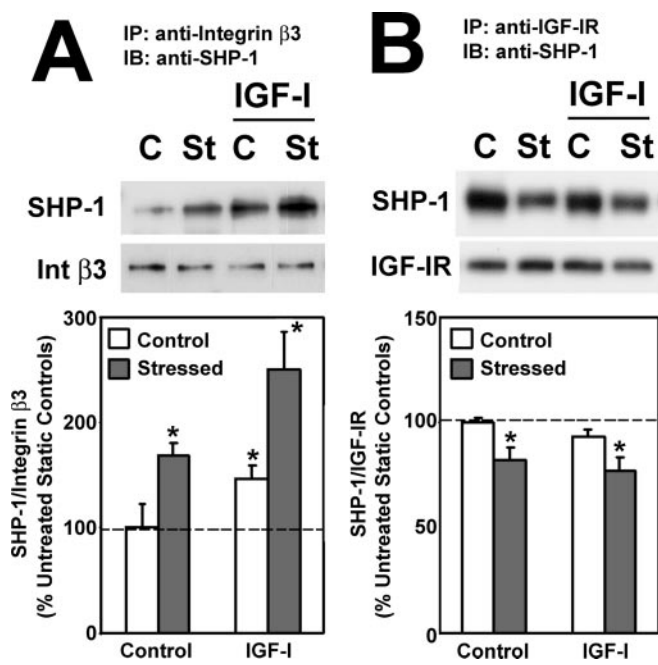


FIG. 6. Effect of echistatin on the synergy between IGF-I and shear stress with respect to cell proliferation (A) and IGF-IR phosphorylation (B). TE85 cells were pretreated with 100 nM echistatin overnight prior to the 30-min shear stress and/or the IGF-I treatment. In A, cell proliferation was measured by [ $^3$ H]thymidine incorporation as described under "Experimental Procedures." The shear stress stimulated TE85 cell proliferation by 73 and 58% in the absence or presence of the echistatin pretreatment, respectively. Thus, the echistatin pretreatment reduced the shear stress-induced proliferation by ~20%. In B, the IGF-IR phosphorylation level was determined by Western analysis as described under "Experimental Procedures." The top panel shows a representative Western blot of pIGF-IR. The blot was stripped and reblotted against an anti-IGF-IR antibody. *Bottom panels* summarize the results of three separate repeat experiments. Results are shown as mean  $\pm$  S.D. \*,  $p < 0.01$  (compared with no addition control). C, control; St, stressed.

ergy on IGF-IR and bone cell proliferation raise the strong possibility that the synergy between shear stress and IGF-I on bone cell proliferation involves integrin activation. Bikle and co-workers (12, 13) have recently reported that skeletal unloading by hind limb suspension induced a resistance to IGF-I with respect to bone formation in the rat. They also concluded that unloading-induced resistance to IGF-I was caused by inhibition of the IGF-I signaling pathway through down-regulation of the integrin pathway. This conclusion was based on the findings that 1) skeletal unloading down-regulated integrin expression and blocked the ability of IGF-I to stimulate cell proliferation in osteoblasts and 2) echistatin also blocked the IGF-I-mediated stimulation of bone cell proliferation *in vitro* (13). Consistent with the results of Bikle and co-workers, our findings demonstrated that shear stress interacts synergistically with the IGF-I signaling pathway to promote bone cell proliferation and that this interaction involves integrin  $\beta$ 3 signaling. Consequently, it appears that mechanical loading not only plays a permissive role in the osteogenic actions of IGF-I, but also



**FIG. 7. Effect of IGF-I or shear stress on recruitment of SHP-2 to integrin  $\beta 3$  or to IGF-IR.** The recruitment of SHP-2 to integrin  $\beta 3$  and away from IGF-IR was assessed by measuring the relative amounts of SHP-2 co-immunoprecipitated (IP) with integrin  $\beta 3$  (A) or with IGF-IR (B) as described under "Experimental Procedures." The amounts of immunoprecipitated SHP-2 were normalized against the corresponding levels of immunoprecipitated integrin  $\beta 3$  and IGF-IR, respectively. *Top panels* show representative Western immunoblots (IB) against SHP-2 or integrin  $\beta 3$  and IGF-IR, respectively. *Bottom panels* summarize the results as percentage of respective untreated control (mean  $\pm$  S.D.) of four replicate experiments. \*,  $p < 0.01$ ; C, control; St, stressed; Int, integrin.



**FIG. 8. Effect of IGF-I or shear stress on recruitment of SHP-1 to integrin  $\beta 3$  or to IGF-IR.** The recruitment of SHP-1 to integrin  $\beta 3$  and away from IGF-IR was assessed by measuring the relative amounts of SHP-1 co-immunoprecipitated with integrin  $\beta 3$  (A) or with IGF-IR (B) as described under "Experimental Procedures." The amounts of immunoprecipitated (IP) SHP-1 were normalized against the corresponding levels of immunoprecipitated integrin  $\beta 3$  and IGF-IR, respectively. *Top panels* show representative Western immunoblots (IB) against SHP-1 or integrin  $\beta 3$  and IGF-IR, respectively. *Bottom panels* summarize the results as percentage of respective untreated control (mean  $\pm$  S.D.) of four replicate experiments. \*,  $p < 0.01$ ; C, control; St, stressed; Int, integrin.

interacts synergistically with the IGF-I signaling pathway to promote bone formation.

The conclusion that the loading-mediated activation of integrin signaling pathways may not only allow the IGF-I signaling pathway to function (16–22) but also cross-talks with the IGF-I signaling pathway to synergistically enhance the mitogenic effects of IGF-I in bone cells is consistent with the findings of several previous studies in fibroblasts (36–39) and smooth muscle cells (16–22), showing that integrin activation has an essential regulatory role in the mediation of the signal transduction pathways and cellular responses of a number of growth factors, including platelet-derived growth factor, epidermal growth factor, FGF-2, and IGF-I. Consistent with an important role for integrin signaling pathways in mediating mechanical stimulation of bone cell proliferation and activity (23–28, 40), we found synergy between the shear stress and IGF-I on bone cell proliferation and the IGF-IR-Erk1/2 signaling pathway. In contrast to fibroblasts, which show an enhancing interaction between FGF-2 and integrin activation (36, 39), our study did not find a synergistic enhancement of shear stress on the bone cell mitogenic activity of FGF-2 and FGF-2-mediated stimulation of Erk1/2 activation in TE85 cells. This would suggest that the synergistic interaction between IGF-I and shear stress is not shared by FGF-2 in osteoblastic cells. Future work is needed to confirm whether similar synergy occurs between shear stress and platelet-derived growth factor or epidermal growth factor in bone cells to determine whether the synergy is unique to IGF-I in bone cells.

Bikle and co-workers (13) have also reported that mechanical unloading markedly diminished the ability of IGF-I to activate several members of its mitogenic signaling pathway (*i.e.* IGF-IR, Ras, Erk1/2) in osteoblasts. Accordingly, we found that

shear stress potentiates the IGF-I-mediated Erk1/2 activation. To gain insights into the molecular mechanism whereby shear stress interacts with the IGF-I signaling pathway to promote osteoblast proliferation, we examined whether synergy between shear stress and IGF-I also occurred at Erk1/2 activation and IGF-IR phosphorylation, two important steps of the IGF-I mitogenic signaling pathway. We reasoned that if the point of interaction (*i.e.* cross-talk) occurs prior to a given step in a pathway, a synergy would be evident at and after that particular step of the pathway. Conversely, if the point of interaction happens after a given step, no synergy would be expected at or prior to that given step. Accordingly, our findings that shear stress also synergized with IGF-I on Erk1/2 activation and IGF-IR phosphorylation strongly suggest that the synergy between shear stress and IGF-I to promote bone cell proliferation occurs prior to or at the step of IGF-IR phosphorylation.

Although Bikle and co-workers (13) report that skeletal unloading or the blocking of integrin activation by echistatin has no effect on the binding of IGF-I to IGF-IR in osteoblasts, our study showed that the shear stress slightly but significantly enhanced the IGF-I binding to IGF-IR. However, the increase in ligand binding was too small to explain the large synergistic enhancement of shear stress in the stimulatory action of IGF-I on IGF-IR phosphorylation (8-fold), Erk1/2 activation (12-fold), and cell proliferation (5-fold). In addition, we noted that the ligand binding curves in the absence or presence of the shear stress were parallel to each other. This would argue against a synergy between shear stress and IGF-I on IGF-IR ligand binding.

The relatively low amounts of receptor-bound IGF-I (*i.e.* <2%) compared with the total amounts of added IGF-I, presumably because of the fact that bone cells (including TE85

cells) release a large amount of IGF binding proteins (41) that compete with IGF-IR for IGF-I binding, has precluded an accurate determination of receptor number and/or binding affinity by Scatchard analysis. Thus, it is not known whether the small increase in IGF-I binding in response to shear stress was because of an increase in the number of IGF-IR or to an increase in ligand binding affinity. However, the parallel binding curves in the absence or presence of shear stress suggest that the increase in IGF-I binding could be due to a small increase in IGF-IR number. The reason for shear stress to increase the IGF-IR number is not clear, but the main point of the concept of our work is that the synergy between shear stress and IGF-I in the stimulation of bone cell proliferation occurs after the ligand binding, but prior to or at the step of IGF-IR phosphorylation, and that activation of the integrin signaling is essential for the synergy.

Recent studies from Clemmons and co-workers (16–22) in smooth muscle cells have disclosed important information about the nature of the cross-talk between the integrin signaling pathway and the IGF-I signaling pathway. Specifically, they found that activated integrin  $\beta 3$  serves to recruit SHP-2 from the cytosol and subsequently to transfer SHP-2 to SHPS-1 and IGF-IR for activating and terminating, respectively, the IGF-I signaling pathway. These findings have provided the basis that integrin activation is potentially relevant to the molecular mechanism whereby shear stress interacts with IGF-I to enhance the IGF-I signaling mechanism in bone cells. The IGF-I signaling pathway is initiated, not only by IGF-IR autophosphorylation induced by ligand binding, but also by the recruitment of activated SHP-2 to SHPS-1 from activated integrins. The transfer of activated SHP-2 to IGF-IR is responsible for the dephosphorylation of IGF-IR and the termination of the IGF-I signaling pathway (16–22). Accordingly, we postulate that mechanical strains or shear stresses, which activate the integrin signaling pathways in bone cells, enhance SHP-2 recruitment to activated integrins and also to SHPS-1. At the same time, the integrin activation in response to shear stresses inhibits the transfer of activated SHP-2 to IGF-IR, resulting in a reduction in the dephosphorylation of IGF-IR and an overall increase in IGF-IR phosphorylation level. This model would explain the synergy between shear stress and IGF-I on the IGF-IR phosphorylation level, Erk1/2 activation, and bone cell proliferation.

Our findings that shear stress, IGF-I, and the combination treatment each increased the relative amount of SHP-2 that was associated with integrin  $\beta 3$  and that each also reduced the relative amount of SHP-2 co-immunoprecipitated with IGF-IR in TE85 cells are consistent with our hypothesis that the shear stress-mediated recruitment of SHP-2 to activated integrins and away from IGF-IR may be responsible for the synergy between shear stress and IGF-IR to promote bone cell proliferation. It should be noted that the IGF-I-mediated and shear stress-induced recruitment of SHP-2 to integrin  $\beta 3$  was relatively small (*i.e.* <2-fold). However, human osteoblasts, including TE85 cells, synthesize multiple members of the integrin family (42). There is evidence that mechanical loading also up-regulated and activated other members of integrins (such as integrin  $\beta 1$ ) in bone cells, including TE85 cells (26). Therefore, it is highly possible that shear stress and/or IGF-I also increased SHP-2 recruitment to other members of the integrin family, including  $\beta 1$ , and that this may explain why the enhancement in SHP-2 recruitment to integrin  $\beta 3$  induced by IGF-I and/or shear stress was relatively low. More importantly, we found that shear stress, IGF-I, and the combination treatment each also increased the relative amount of the integrin  $\beta 3$ -associated SHP-1 and reduced the relative amount of IGF-

IR-associated SHP-1. This suggests that SHP-2 and the related SHP-1 are both involved in the IGF-I signaling mechanism as well as in the synergy between shear stress and IGF-I in enhancing the overall IGF-IR phosphorylation level.

The effect of unloading on recruitment of SHP-2 (or SHP-1) to integrins has not been assessed previously (13). Thus, it is unclear at this time whether or not the unloading-induced resistance to IGF-I may also involve a reduction of SHP-2 (and/or SHP-1) recruitment to integrins. However, because unloading down-regulated integrin expression in osteoblasts (13) and because SHP-2 recruitment to integrins is essential for IGF-I signaling (16–22), it is likely that the reduced integrin recruitment of SHP-2 and/or SHP-1 in response to unloading-mediated down-regulation of the integrin pathway could also play a pivotal role in the permissive effect of mechanical loading on the IGF-I anabolic action in bone (12, 13).

In conclusion, this study provides the first evidence for a synergistic interaction between shear stress and IGF-I in the stimulation of osteoblastic proliferation. This study also provides strong circumstantial evidence that the synergy involves an integrin-dependent up-regulation of IGF-IR phosphorylation level through an inhibition of the recruitment of SHP-1 and/or SHP-2 to IGF-IR as well as an inhibition of the SHP-1 and/or SHP-2-mediated IGF-IR dephosphorylation. These findings not only confirm that the integrin activation is essential for the IGF-I mitogenic pathway, but also provide mechanistic insights into the cross-talk between the integrin and IGF-I signaling pathways in the underlying molecular mechanisms of enhanced bone formation in response to mechanical loading.

#### REFERENCES

- Hillam, R. A., and Skerry, T. M. (1995) *J. Bone Miner. Res.* **10**, 683–689
- Hillsley, M. V., and Frangos, J. A. (1994) *Biotechnol. Bioeng.* **43**, 573–581
- Kapur, S., Baylink, D. J., and Lau, K.-H. W. (2003) *Bone* **32**, 241–251
- Mohan, S., and Baylink, D. J. (1991) *Clin. Orthop. Relat. Res.* **263**, 30–48
- Canalis, E., McCarthy, T., and Centrella, M. (1988) *J. Clin. Invest.* **81**, 277–281
- Wergedal, J. E., Mohan, S., Lundy, M., and Baylink, D. J. (1990) *J. Bone Miner. Res.* **5**, 179–186
- Hock, J. M., Centrella, M., and Canalis, E. (1988) *Endocrinology* **122**, 254–260
- Lean, J. M., Jagger, C. J., Chambers, T. J., and Chow, J. W. (1995) *Am. J. Physiol.* **268**, E318–E327
- Mikuni-Takagaki, Y., Suzuki, Y., Kawase, T., and Saito, S. (1996) *Endocrinology* **137**, 2028–2035
- Kapur, S., Chen, S.-T., Baylink, D. J., and Lau, K.-H. W. (2004) *Bone* **35**, 525–534
- Cheng, M. Z., Rawlinson, S. C., Pitsillides, A. A., Zaman, G., Mohan, S., Baylink, D. J., and Lanyon, L. E. (2002) *J. Bone Miner. Res.* **17**, 593–602
- Sakata, T., Halloran, B. P., Elalieh, H. Z., Munson, S. J., Rudner, L., Venton, L., Ginzinger, D., Rosen, C. J., and Bikle, D. D. (2003) *Bone* **32**, 669–680
- Sakata, T., Wang, Y., Halloran, B. P., Elalieh, H. Z., and Bikle, D. D. (2004) *J. Bone Miner. Res.* **19**, 436–446
- Mauck, R. L., Nicoll, S. B., Seyhan, S. L., Ateshian, G. A., and Hung, C. T. (2003) *Tissue Eng.* **9**, 597–611
- Tokimasa, C., Kawata, T., Fujita, T., Kaku, M., Kawasoko, S., Kohno, S., and Tanne, K. (2000) *Arch. Oral Biol.* **45**, 871–878
- Ling, Y., Maile, L. A., and Clemmons, D. R. (2003) *Mol. Endocrinol.* **17**, 1824–1833
- Clemmons, D. R., and Maile, L. A. (2005) *Mol. Endocrinol.* **19**, 1–11
- Maile, L. A., and Clemmons, D. R. (2002) *J. Biol. Chem.* **277**, 8955–8960
- Maile, L. A., Badley-Clarke, J., and Clemmons, D. (2003) *Mol. Biol. Cell* **14**, 3519–3528
- Ling, Y., Maile, L. A., Badley-Clarke, J., and Clemmons, D. R. (2005) *J. Biol. Chem.* **280**, 3151–3158
- Zheng, B., and Clemmons, D. R. (1998) *Proc. Natl. Acad. Sci. U. S. A.* **95**, 11217–11222
- Maile, L. A., and Clemmons, D. R. (2002) *Endocrinology* **143**, 4259–4264
- Burridge, K., and Chrzanowska-Wodnicka, M. (1996) *Annu. Rev. Cell Dev. Biol.* **12**, 463–519
- Hynes, R. O. (1999) *Trends Cell Biol.* **9**, 33–37
- Alenghat, F. J., and Ingber, D. E. (2002) *Science's STKE* [http://stke.sciencemag.org/cgi/content/full/OC\\_sigtrans;2002/119/pe6](http://stke.sciencemag.org/cgi/content/full/OC_sigtrans;2002/119/pe6)
- Carvalho, R. S., Scott, J. E., and Yen, E. H. (1995) *Arch. Oral Biol.* **40**, 257–264
- Salter, D. M., Robb, J. E., and Wright, M. O. (1997) *J. Bone Miner. Res.* **12**, 1133–1141
- Lee, H. S., Millward-Sadler, S. J., Wright, M. O., Nuki, G., and Salter, D. M. (2000) *J. Bone Miner. Res.* **15**, 1501–1509
- Lau, K.-H. W., Lee, M. Y., Linkhart, T. A., Mohan, S., Vermeiden, J., Liu, C. C., and Baylink, D. J. (1985) *Biochim. Biophys. Acta* **840**, 56–68
- Greenwood, F. C., Hunter, W. M., and Glover, J. S. (1963) *Biochem. J.* **89**,

- 114–123
31. Gronthos, S., Stewart, K., Graves, S. E., Hay, S., and Simmons, P. J. (1997) *J. Bone Miner. Res.* **12**, 1189–1197
32. Mosley, J. R. (2000) *J. Rehabil. Res. Dev.* **37**, 189–199
33. Carter, D. R., Beaupre, G. S., Wong, M., Smith, R. L., Andriacchi, T. P., Schurman, D. J., and Smith, R. L. (2004) *Clin. Orthop. Relat. Res.* **427**, (suppl.) S69–S77
34. Carter, D. R., Beaupre, G. S., Giori, N. J., and Helms, J. A. (1998) *Clin. Orthop. Relat. Res.* **355**, (suppl.) S41–S55
35. Lau, K.-H. W., Kapur, S., and Baylink, D. J. *J. Bone Miner. Res.* **19**, Suppl. 1, S79 (Abstr. F264)
36. Miyamoto, S., Teramoto, H., Gutkind, S., and Yamada, K. M. (1996) *J. Cell Biol.* **135**, 1633–1642
37. Lin, T. H., Chen, Q., Howe, A., and Juliano, R. L. (1997) *J. Biol. Chem.* **272**, 8849–8852
38. Sundberg, C., and Rubin, K. (1996) *J. Cell Biol.* **132**, 741–752
39. Howe, A., Aplin, A. E., Alahari, S. K., and Juliano, R. L. (1998) *Curr. Opin. Cell Biol.* **10**, 220–231
40. Schwartz, M. A., and Ingber, D. E. (1994) *Mol. Biol. Cell* **5**, 389–393
41. Lau, K.-H. W., Goodwin, C., Arias, M., Mohan, S., and Baylink, D. J. (2002) *Bone* **30**, 705–711
42. Clover, J., and Gowen, M. (1994) *Bone* **15**, 585–591



## Identification of genetic loci that regulate bone adaptive response to mechanical loading in C57BL/6J and C3H/HeJ mice intercross

Chandrasekhar Kesavan<sup>a</sup>, Subburaman Mohan<sup>a,b,\*</sup>, Apurva K. Srivastava<sup>a</sup>,  
Susanna Kapoor<sup>a</sup>, Jon E. Wergedal<sup>a,b</sup>, Hongrun Yu<sup>a</sup>, David J. Baylink<sup>a,b</sup>

<sup>a</sup> Musculoskeletal Disease Center, VA Loma Linda Healthcare System, Loma Linda, CA 92357, USA

<sup>b</sup> Department of Medicine, Loma Linda University, Loma Linda, CA 92357, USA

Received 17 October 2005; revised 14 March 2006; accepted 20 March 2006

### Abstract

Strain-dependent differences in bone adaptive responses to loading among inbred mouse strains suggest that genetic background contributes significantly to adaptation to exercise. To explore the genetic regulation of response to loading, we performed a genome-wide search for linkage in a cross between two strains, a good responder, C57BL/6J (B6), and a poor responder, C3H/HeJ (C3H). Using a four-point bending model, the right tibia was loaded by applying 9 N force for 36 cycles for 12 days in 10-week-old female B6×C3H F2 mice. Changes in bone density (BMD) and bone size were evaluated *in vivo* by pQCT. Measurements from non-loaded left tibia were used as an internal control to calculate loading-induced percent increase in BMD and bone size, thus excluding the possibility of identifying background QTL(s) due to natural allelic variation in mapping strains. A genome-wide scan was performed using 111 microsatellite markers in DNA samples collected from 329 F2 mice. Heritability of bone adaptive response to loading was between 70 and 80%. The mean increase, expressed as percent of unloaded tibia, was 5% for BMD, 9% for periosteal circumference (PC), and 14% for cortical thickness in F2 mice ( $n = 329$ ). All these phenotypes showed normal distributions. Absence of significant correlation between BMD response to four-point bending and body weight or bone size suggested that the bone adaptive response was independent of bone size. Interval mapping revealed that BMD response to four-point bending was influenced by three significant loci on Chrs 1 (log-of-odds ratio score (LOD) 3.4, 91.8 cM), 3 (LOD 3.6, 50.3 cM), and 8 (LOD 4.2, 60.1 cM) and one suggestive QTL on Chr 9 (LOD 2.5, 33.9 cM). Loading-induced increases in PC and Cth were influenced by four significant loci on Chrs 8 (LOD 3.0, 68.9 cM), 9 (LOD 3.0, 13.1 cM), 17 (LOD 3.0, 39.3 cM), and 18 (LOD 3.0, 0 cM) and two suggestive loci on Chr 9 (LOD 2.2, 24 cM) and 11 (LOD 2.1, 69.9 cM). Pairwise analysis showed the presence of several significant and suggestive interactions between loci on Chrs 1, 3, 8, and 13 for BMD trait. This is the first study that provides evidence for the presence of multiple genetic loci regulating bone anabolic responses to loading in the B6×C3H intercross. Knowledge of the genes underlying these loci could provide novel approaches to improve skeletal mass.

© 2006 Elsevier Inc. All rights reserved.

**Keywords:** Mechanical loading; Four-point bending; Quantitative trait loci; Mice; vBMD

### Introduction

Mechanical stimulation is one of the important factors in the development and maintenance of skeletal tissues [1–4]. Several *in vivo* studies have shown that increased mechanical stress on bone tissue changes the bone density and morphology, resulting in an increased bone mass and biomechanical strength, whereas

lack of mechanical stress leads to a rapid bone loss as evidenced by immobilization and bed rest studies [5–14]. Thus, physical exercise has been perceived as an important therapeutic strategy in humans to maintain bone mass and prevent osteoporosis. Recent studies in humans have also shown that bone anabolic response to a given mechanical load is highly variable, with some individuals exhibiting robust bone anabolic response with others responding modestly [15–18]. A similar variation has been observed among inbred strains of mice [19–21]. We [6,19] and others [21] have shown that mouse strains such as C57BL/6J (B6) respond with a much higher increase in bone density (BMD) and bone cross-sectional area as compared to the C3H/

\* Corresponding author. Loma Linda University, Musculoskeletal Disease Center (151), Jerry L. Pettis Memorial VA Medical Center, 11201 Benton Street, Loma Linda, CA 92357, USA. Fax: +1 909 796 1680.

E-mail address: Subburaman.Mohan@med.va.gov (S. Mohan).

HeJ (C3H) strain of mouse in response to a similar amount of in vivo loading. These data suggest that variations in skeletal response to mechanical loading in humans and mice are largely determined by genetic factors [12,21]. However, very little is known about the genetic regulation of mechanical loading and, so far, not a single gene has been identified that influences the skeletal response to mechanical loading [22].

One approach often used to perform genome-wide searches of genetic loci that contribute to differences in phenotypic variation is the quantitative trait loci (QTL) technique. This approach has been used in experimental animal models and in humans to study genetic regulation of bone density [23,24], bone metabolism [25], strength [26], quality, and size [27] and other traits [28]. By utilizing the QTL technique, one could (1) identify the regions within chromosomes that contain the functional genes of interest for a given phenotype; (2) estimate the influence of genetic variation on within-species phenotypic variation; and (3) evaluate QTL–QTL interactions for the effect on phenotypic variation. The limitations of the QTL approach include: (1) it is technically time-consuming and expensive; (2) initial QTL analysis does not allow high resolution mapping and further fine mapping is required to narrow down the loci containing possible candidate genes; and (3) many genes in a particular chromosomal interval may not be relevant for a specific trait. Despite the drawback that the relevance of QTL genes identified using mouse models to explain the phenotypic variation in humans remains to be established, the availability of genomic (sequences, SNPs) and animal resources (congenic lines, chromosomal substitution strains, recombinant inbred strains) facilitates the identification and functional testing of QTL of candidate genes and therefore has attracted attention among molecular geneticists to use mice for QTL studies. In this study, we used two inbred strains, C57BL/6J and C3H/HeJ, good and poor responder strains, respectively, to perform a genome-wide search for loci regulating bone adaptive response to mechanical loading.

## Materials and methods

### Mice

Female B6 and male C3H mice were obtained from the Jackson Laboratory (Bar Harbor, ME) to produce C3HB6 F1 mice, which were intercrossed to generate F2 mice. At 10 weeks of age, the mice were subjected to mechanical loading using a four-point bending model described previously [19,21]. All mice were housed under the standard conditions of 14-h light and 10-h darkness and had open access to food and water. The experimental protocols were in compliance with animal welfare regulation and approved by local IACUC.

### In vivo loading model/regimen

The four-point bending device [Instron, Canton, MA] consists of two upper movable points covered with rubber pads, which are 4 mm (millimeter) apart, and two lower non-movable points covered with rubber pads, which are 12 mm apart. After anesthetizing the mice, the ankle of the tibia was positioned on the second lower immobile points of Instron such that the region of tibia loaded did not vary in different mice. During bending, the two upper pads touch the lateral surface of the tibia through overlaying muscle and soft tissue, while the lower pads touch the medial surface of the proximal and distal parts of the tibia. One of the limitations of this model is that force applied over soft tissue may have some

local effects on blood and fluid flow. We took efforts to minimize this by changing the rubber pads frequently in the Instron mechanical tester. The loading protocol for this study consisted of a 9 N force at a frequency of 2 Hz for 36 cycles performed at the same time once a day under inhalable (5% halothane and 95% oxygen) anesthesia. The loading procedure was repeated for 6 days/week with 1 day of rest for 2 weeks. On the 15th day, in vivo pQCT measurements were performed on the loaded and non-loaded tibia of all F2 mice. Sham bending was performed as described previously [21].

### Peripheral quantitative computed tomography (pQCT) measurements

To measure loading-induced changes in the bone density and geometry in loaded and non-loaded tibias, we used pQCT (Stratec XCT 960M, Norland Medical System, Ft. Atkinson, WI) as described previously [19,29]. Calibration was performed daily with a defined standard provided by the manufacturer. Mice were anesthetized, and a two-dimensional scout view was taken first, which permits the identification of landmarks and a precise selection of the appropriate site for measurement. In order to minimize the measurement errors caused by positioning of tibia for pQCT, we used the tibia–fibular junction as the reference line. We selected two slices that start 4 mm proximal from tibia–fibular junction for pQCT measurement. This region corresponds to the loading zone. Each slice is at a 1-mm interval, and the values presented in the Results section are an average of these two slices [19]. To minimize exposure time of animals to anesthesia for in vivo pQCT measurements, we choose to scan only the loading zone in the F1 or F2 mice. Based on our previous findings [19], we used two thresholds to analyze the pQCT data: a 180–730 mg/cm<sup>3</sup> threshold was used to measure periosteal circumference (PC) and a 730–730 mg/cm<sup>3</sup> threshold was used to measure total volumetric density (vBMD), cortical volumetric bone mineral density (cortical vBMD), and cortical thickness (CTH). Cortical vBMD is defined as cortical content/cortical volume excluding the marrow cavity.

### PCR-based genetic analysis

Two days after the last loading, the mice were sacrificed and tissues such as liver and tibia were collected and stored at –80°C. Genomic DNA was extracted from the liver of each F2 mouse using a Maxi prep DNA extraction kit (Qiagen) and stored at –80°C. The quality and quantity of DNA were measured by Nano drop and Bio-analyzer (Agilent Technologies, Inc, CA). Polymerase chain reaction (PCR) primers were purchased from Applied Biosystems (ABIPRISM, Foster City, CA) to perform the genome-wide genotyping scan of the F2 population. PCR reaction conditions allowed 3–4 microsatellite markers to be multiplexed in a single electrophoretic lane. The pooled products were analyzed for fragments' size on the ABI 3100 Sequence Detection System, and Gene Scan software was used to detect size of the alleles. Allele calls and edits were performed using Genotyper software and in-house software and exported as text files for downstream analysis.

### QTL analysis

We used parametric mapping (a mapping strategy that requires the assumption of normal distribution for the quantitative trait investigation) for

Table 1  
Changes in the bone parameters in response to 12 days of sham bending at 9 N load in 10-week female B6 mice

Bone parameters	Mean ± SD		
	Non-loaded	Loaded	P value
Total area, mm <sup>2</sup>	2.01 ± 0.11	2.07 ± 0.10	0.30
Total mineral content, mg/mm	1.08 ± 0.04	1.10 ± 0.04	0.46
Periosteal circumference, mm	5.02 ± 0.14	5.10 ± 0.12	0.29
Endosteal circumference, mm	4.09 ± 0.15	4.17 ± 0.12	0.31
Total vBMD, mg/cm <sup>3</sup>	649 ± 14.64	663.7 ± 19.7	0.15
Cortical vBMD, mg/cm <sup>3</sup>	1031 ± 9.8	1038 ± 13.5	0.26

n = 7.

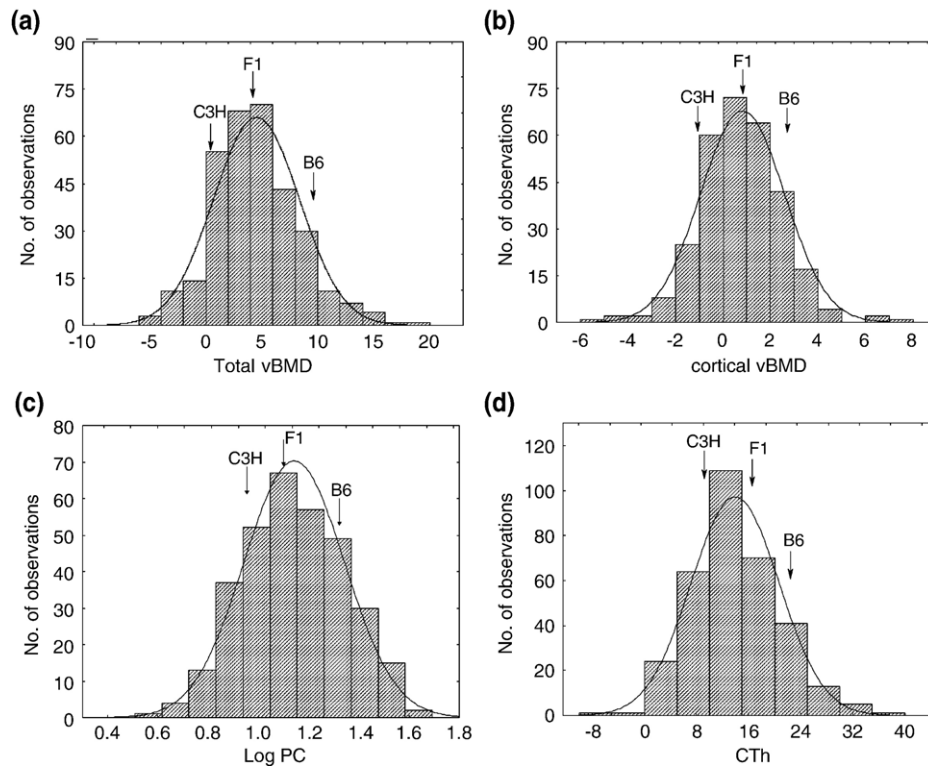


Fig. 1. Distribution of percentage changes for (a) total vBMD, (b) cortical vBMD, (c) PC, and (d) cortical thickness in the F2 population after 2 weeks of four-point bending. The  $x$  axis represents the percentage change ('-' indicates reduction), and  $y$  axis represents the number of observations (mice). Total vBMD, total volumetric bone mineral density; cortical vBMD, cortical volumetric bone mineral density; Log PC, periosteal circumference; and CTh, cortical thickness. The solid line represents theoretical normal distribution. Based on Kolmogorov–Smirnov test, total vBMD, cortical vBMD, PC, and CTh show normal distribution ( $n = 329$ ).

total vBMD, cortical vBMD, PC, and CTh in our QTL analysis. Because the distribution of the PC showed some significant skewing, analysis was also performed on log-transformed PC data. The log transformation normalized the distribution but did not alter the identification of QTL and produced only slight changes in LOD scores. The interval mapping was performed by using a MapQTL software program (Version 5.0; Wageningen, The Netherlands). The significant levels of the LOD scores used in this study were obtained by the permutation test on the studied population. By conducting a certain number of permutations (usually 1000), a threshold LOD score can be established based on the chosen probability level. As we understand, in the human genetics, the threshold LOD score is usually 3, i.e.  $P < 0.01\%$ , depending on the sample size. The permutation analysis is done by the well-established software, which has been extensively used in QTL analyses in mice and other animal models. QTLs with a genome wide error of 1%, 5%, and 32% were classified as highly significant, significant, and suggestive, respectively [30,31]. To study genome-wide interactions between QTLs, we used a Pseudomarker algorithm written for the MATLAB (Mathworks Inc., Natick, MA, USA) programming environment (obtained from [www.jax.org/research/churchill](http://www.jax.org/research/churchill)). This program analyzes the phenotypic effect of each marker taken individually (MAINSKAN run by Pseudomarker program) and also the phenotypic effects of pairs of markers or intervals (PAIRSCAN) taken jointly for their effects on the trait. In the PAIRSCAN analysis, we tested the combined (or full model) effects on a trait for a marker pair, which reflects the main the effects of both markers plus their interaction. Thresholds for significance were estimated by a 200-permutation test carried out on F2 data. The MapQTL and Pseudomarker MAINSCAN analyses gave similar results. The broad sense of heritability index of each phenotype was calculated using a formula as mentioned earlier [26].

#### Statistical analysis

Phenotypic response to mechanical loading (e.g. BMD) was calculated using the following formula: % response = [(BMD of loaded tibia – BMD of non-

loaded tibia) / BMD of non-loaded tibia  $\times 100$ ]. We used Statistica software to perform correlation analysis, phenotype distribution, and Regression analysis and two-way ANOVA. Data were analyzed using Graphpad Prism (Windows version 3.0, San Diego, CA). Correlation coefficients between phenotypes were obtained using Pearson's correlation.

Table 2

Significant and suggestive QTLs for the mechanical-load-induced phenotypes in the B6 $\times$ C3H F2 female mice

Phenotype	Chromosome	Locus	cM	LOD score	Percent variation
Total vBMD	1	D1Mit113	91.8	3.4 <sup>a</sup>	5.5
	8	D8Mit88	60.1	4.2 <sup>a</sup>	8.5
	9	D9Mit336	33.9	2.5 <sup>b</sup>	4.8
Cortical vBMD	1	D1Mit113	91.8	2.3 <sup>b</sup>	3.6
	3	D3Mit320	50.3	3.6 <sup>a</sup>	7.3
	9	D9Mit355	49.2	2.5 <sup>b</sup>	3.4
Periosteal circumference	8	D8Mit49	68.9	3.0 <sup>c</sup>	4.3
	9	D9Mit97	24	2.2 <sup>b</sup>	3.3
	11	D11Mit333	69.9	2.1 <sup>b</sup>	3.3
	18	D18Mit64	0	3.0 <sup>c</sup>	4.4
Cortical thickness	8	D8Mit88	60.1	3.6 <sup>a</sup>	5.7
	9	D9Mit2	13.1	3.0 <sup>c</sup>	3.2
	11	D11Mit333	69.9	2.5 <sup>b</sup>	4.2
	17	D17Mit93	39.3	3.0 <sup>c</sup>	4.2

Variances explained are from the peak LOD score in each phenotype.

<sup>a</sup> The threshold for the highly significant LOD score is  $P < 0.01$ .

<sup>b</sup> The threshold for the suggestive LOD score is  $P < 0.1$ .

<sup>c</sup> The threshold for the significant LOD score is  $P < 0.05$ .

## Results

### Sham bending

Previously, we reported that mechanical loading by four-point bending caused greater changes in the BMD and bone size in B6 mice after 12 days of 9 N load. In order to confirm that the increase in bone anabolic response induced by bending is not due to periosteal pad pressure, we performed sham bending in 10-week-old female B6 mice for 12 days using 9 N load at 2 Hz for 36 cycles. The results from our pQCT analysis revealed no significant changes in the BMD, periosteal circumference and other bone parameters (Table 1). This finding implies that changes in bone parameters induced by bending are not due to periosteal pad pressure as evidenced from our sham loading study.

### Bone response to mechanical loading is a heritable trait

The bone response to mechanical loading was calculated from measurements of well-established parameters, such as

total vBMD, cortical vBMD, PC, and CTh, in loaded tibia. Results for each parameter were expressed as percent change from identical measurements performed on non-loaded left tibia in each F2 mouse. The mean percent increase in response to loading in the female F1 mice ( $n = 100$ ) was 2.8% for total vBMD, 0.8% for cortical vBMD, 8.0% for PC, and 11.7% for CTh. These loading-induced increases in various skeletal parameters in F1 mice were intermediate between parent strains based on results published previously [19]. In the F2 mice ( $n = 329$ ), the mean increase in total vBMD was 5%, and that of cortical vBMD, PC, and CTh was 1.5%, 9%, and 14%, respectively (Fig. 1). The distributions of total vBMD, cortical vBMD, PC, and CTh among female F2 mice shown in Fig. 1 indicate that bone responses to mechanical loading were variable. The distributions of all four phenotypes approached normality ( $n = 329$ ), but values were predominantly positive, indicating that most mice responded to loading. These wide ranges of bone adaptive responses displayed by F2 mice are probably due to the variable genetic background of each F2 mouse. The broad sense of heritability, calculated as described earlier [26], of the loading-induced changes in the vBMD,

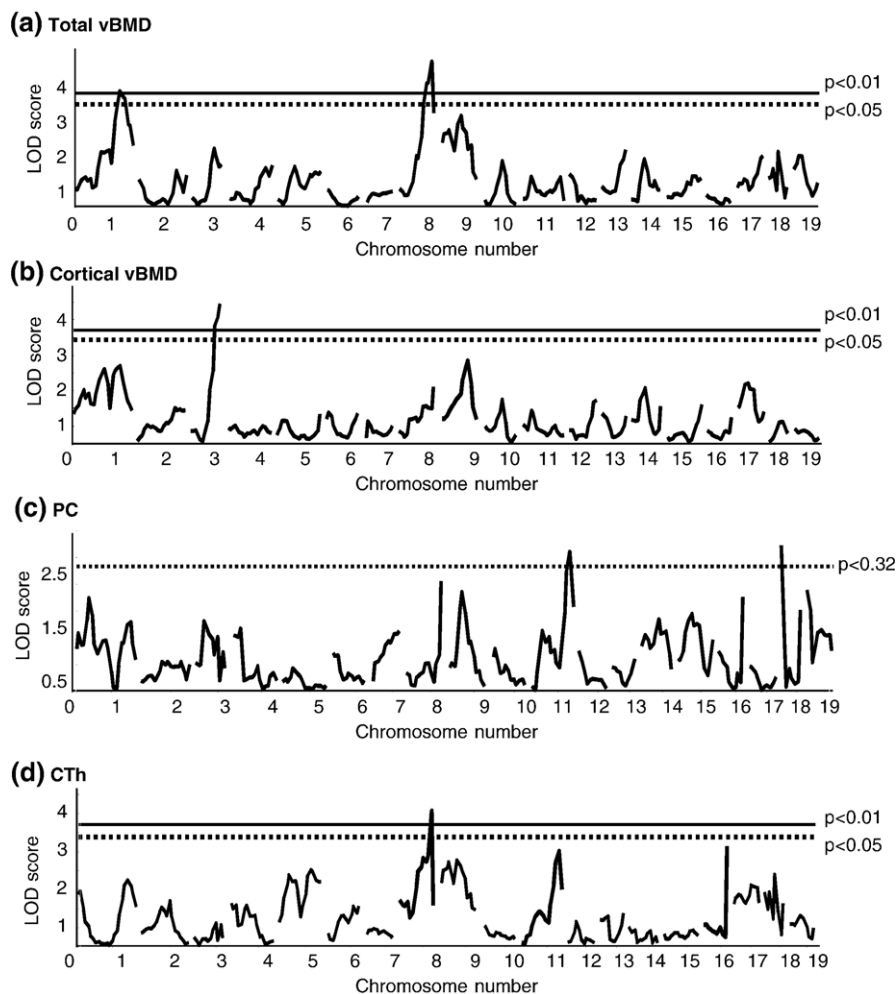


Fig. 2. Genome-wide scan for percent change in (a) total vBMD, (b) cortical vBMD and (c) PC and (d) CTh induced by mechanical loading in the F2 population of B6×C3H intercross. The y axis indicates LOD score, and x axis represents chromosomes. The solid line indicates genome-wide thresholds for significant QTL, and broken lines indicate thresholds for suggestive QTL.

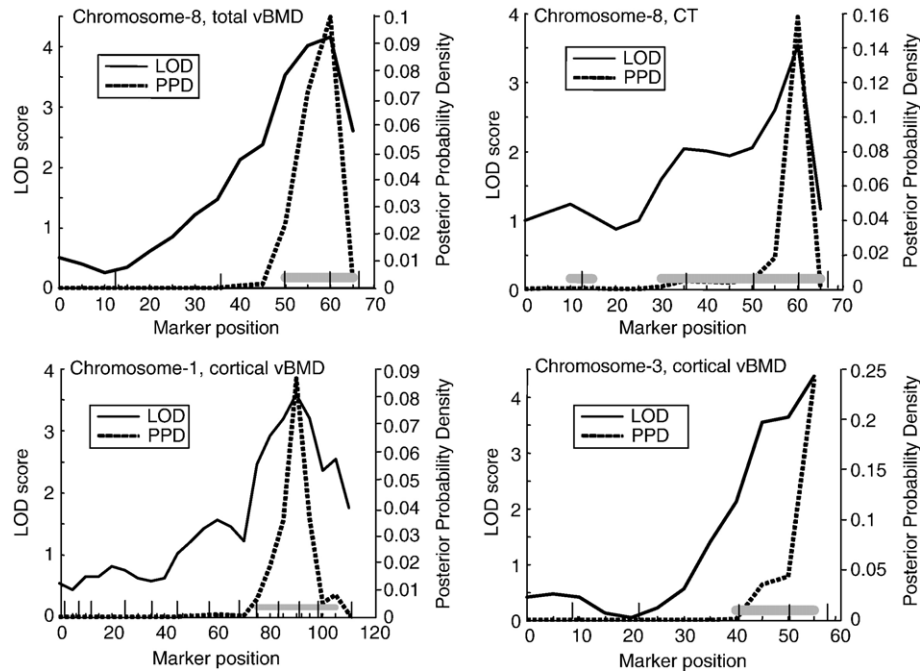


Fig. 3. Detailed map for chromosomes 8, 1, and 3 showing significant QTLs for total vBMD, cortical thickness, and cortical vBMD. LOD scores between markers were determined using Pseudomarker MAINSCAN program with a default setting of 2.5 cM between steps. The marker positions are highlighted as vertical lines in the  $x$  axis. Posterior probability density (shown on right  $y$  axis) plots allow best estimate of putative QTL position on the marker map.

cortical vBMD, PC, and CTh was 82%, 70%, 86%, and 82%, respectively.

Due to natural allelic variation in bone size between C3H and B6 strains, we expected the F2 mice to exhibit differences in

cross-sectional area. The mice with a smaller cross-sectional area receive greater mechanical strain than mice with larger cross-sectional area for the same load. In order to determine if variations in strain difference caused by difference in cross-

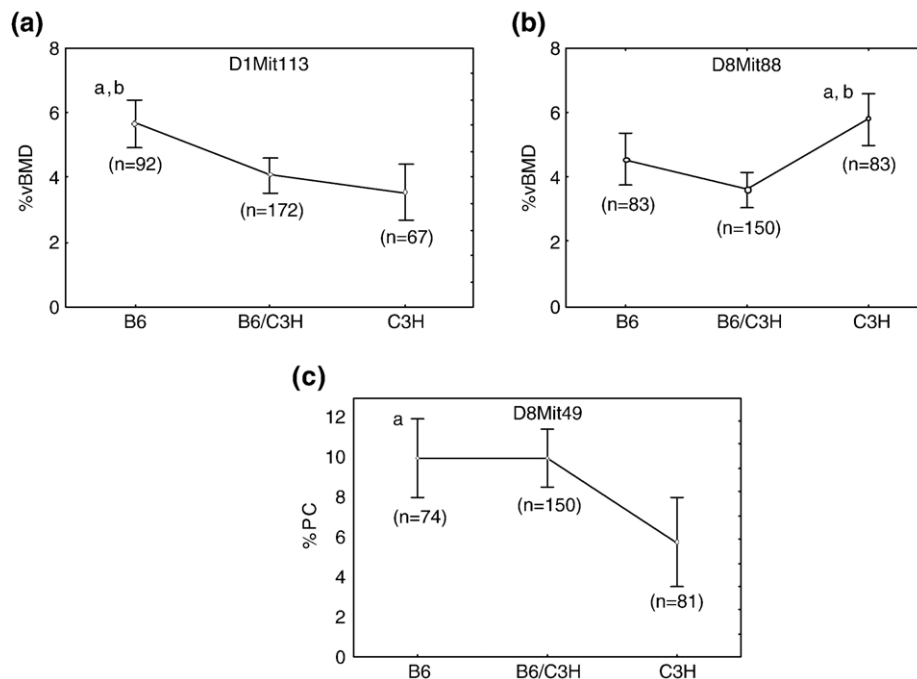


Fig. 4. Effect of B6 vs. C3H alleles at the major QTLs affecting total vBMD and bone size phenotypes on chromosomes 1 and 8. Significant differences ( $P < 0.01$ ) are indicated by the lowercase letters, where “a” indicates that the B6 or C3H allele is significantly different than mice with C3H or B6 allele and “b” indicates that the B6 or C3H allele differs from mice with B6C3H allele. The values shown here are mean  $\pm$  SD. The  $y$  axis represents percent change of vBMD and PC in the F2 population, and  $x$  axis represents mouse genotypes. The total number of mice was 329, but due to missing data, the number of genotype marker data varied.

Table 3

List of significant marker pairs showing interaction from genome-wide analysis of multiple phenotypes in B6×C3H F2 female mice

Phenotype	Chr pairs	cM1	cM2	LOD Full	LOD Int	P value (interaction)
Total	8 × 13	60	45	9.10	2.96	0.008
vBMD	1 × 13	90	45	7.57	2.65	0.01
Cortical	1 × 3	75	55	8.72	2.17	0.04
vBMD						
CT	5 × 8	80	10	7.41	4.50	0.004

For vBMD full LOD score threshold (effect of both markers in affecting the bone phenotype), significant was 7.68 ( $P < 0.05$ ), and for cortical vBMD full LOD score threshold, significant was 7.95 ( $P < 0.05$ ). Suggestive threshold was 7.32 ( $P < 0.1$ ) for vBMD and 6.83 ( $P < 0.6$ ) for CT Full LOD score effect.

sectional area contribute to a variation in BMD response, we performed a correlation analysis between periosteal circumferences of non-loaded bones versus percent BMD changes in corresponding loaded bones. The results from our study showed no significant correlation ( $r = -0.09$ ) between loading-induced percent changes in total vBMD and periosteal circumference. Furthermore, the moment of inertia of non-loaded bones did not show a significant correlation with percent changes in vBMD response. However, there could have been some difference in the shape of the bones in F2 mice whose possible effect on strain levels in affecting the BMD response to loading has not been determined in this study. Since the pQCT measurement was done in vivo, we could not evaluate if variations in strain difference caused by differences in bone shape contribute to a variation in BMD response. On the other hand, there was a slight negative correlation ( $r = -0.18$ ,  $P < 0.05$ ) between body weight and percent change in total vBMD in response to four-point bending in the F2 mice. These data suggest that variation in anabolic response to mechanical load was largely independent of body weight or bone size in female C3H×B6 F2 mice.

#### QTL for bone response to mechanical loading

The linkage map, constructed using 111 markers (average marker density: 15 cM) and loading-induced changes in total vBMD, cortical vBMD, PC, and CTh phenotypes in 329 female F2 mice, revealed evidence for the presence of several significant and suggestive loci as shown in Table 2 and Fig. 2. Loci regulating total vBMD (and cortical vBMD) were located on chromosome (Chr) 1, 3, 8, and 9, whereas loci regulating bone size, which includes periosteal circumference and cortical thickness, were located on Chrs 8, 9, 11, 17, and 18. The strongest linkage was observed on chromosome 8 for total vBMD (LOD score 4.2, 60 cM). Fig. 3 shows posterior probability density plots for QTLs located on Chrs 1, 3, and 8. The posterior probability density plot is a likelihood statistic that gives rise to the 95% confidence intervals for QTL peak indicated by a horizontal bar in the plot. The four BMD QTLs (includes total vBMD and cortical vBMD) on Chrs 1, 3, 8, and 9 accounted for 19% of the variance in response to mechanical loading. Loci on Chrs 8, 9, 11, 17, and 18 regulating bone size (includes PC and CTh) accounted for the 15% variance in the F2 mice (Table 2). Chrs 8 and 9 QTL for BMD, PC, and CTh were colocalized, whereas loci on Chrs 1 and 3 were specific for BMD and Chrs 11, 17, and 18 loci were

specific for bone size. Because there was a slight negative correlation between percent changes in BMD response in loaded bones versus body weight, we performed QTL analysis after adjusting for body weight in the F2 mice. We found that body weight adjustment yielded an additional locus (Chr 17) in addition to loci on Chrs 1, 8, and 9.

#### Allele contribution to the peak QTLs

Fig. 4 shows the contribution of alleles from B6 and C3H mice for the major QTL affecting BMD and PC. For Chr 1 BMD QTL, homozygous B6 alleles at marker *D1Mit113* showed dominant effect over C3H homozygous mice and were 5.6% (Fig. 4) higher than the homozygotes for C3H alleles. Although the response to mechanical loading was higher in the B6 strain, it is noteworthy that C3H alleles at Chr 8 increased BMD in response to mechanical loading (Fig. 4). Thus, homozygous C3H alleles at marker *D8Mit88* had 5.8% higher BMD than the homozygous B6 alleles. For this QTL, the C3H alleles best fit a recessive mode of inheritance. For PC QTL, homozygous alleles

Table 4

Significant and suggestive QTLs for the non-loaded phenotypes in the B6×C3H F2 female mice

Phenotypes	Chromosome	Locus	cM	LOD score	Percent variation
Total vBMD	1	D1Mit380	37.1	3.8 <sup>a</sup>	5.3
		D1Mit106	83.1	2.8 <sup>b</sup>	3.9
	2	D2Mit1*	14.2	2.3 <sup>b</sup>	4.6
		<b>D3Mit147</b>	<b>59.0</b>	<b>2.8<sup>b</sup></b>	<b>3.9</b>
	4	D4Mit251	66.7	3.6 <sup>a</sup>	5.4
	6	D6Mit209*	16.9	2.9 <sup>b</sup>	4.8
	<b>10</b>	<b>D10Mit233</b>	<b>63.4</b>	<b>3.8<sup>a</sup></b>	<b>5.3</b>
	12	D12Mit16*	44.5	3.3 <sup>a</sup>	5.9
	16	D16Mit60	24.0	2.9 <sup>b</sup>	4.0
	<b>17</b>	<b>D17Mit93</b>	<b>39.0</b>	<b>5.4<sup>a</sup></b>	<b>7.4</b>
Cortical vBMD	1	D1Mit380	37.2	2.7 <sup>b</sup>	3.8
	<b>3</b>	<b>D3Mit147</b>	<b>59.1</b>	<b>3.2<sup>a</sup></b>	<b>4.6</b>
	<b>10</b>	<b>D10Mit95</b>	<b>50.3</b>	<b>3.0<sup>c</sup></b>	<b>4.2</b>
	12	D12Mit16*	40.5	2.9 <sup>b</sup>	5.7
	15	D15Mit107	41.5	3.0 <sup>c</sup>	4.5
	16	D16Mit60	24.0	3.6 <sup>a</sup>	4.9
	<b>17</b>	<b>D17Mit93</b>	<b>39.3</b>	<b>5.9<sup>a</sup></b>	<b>8.0</b>
Periosteal circumference	<b>3</b>	<b>D3Mit320*</b>	<b>46.4</b>	<b>4.0<sup>a</sup></b>	<b>7.2</b>
	<b>10</b>	<b>D10Mit233*</b>	<b>57.3</b>	<b>2.4<sup>b</sup></b>	<b>3.9</b>
	<b>11</b>	<b>D11Mit285</b>	<b>49.2</b>	<b>4.3<sup>a</sup></b>	<b>6</b>
	<b>15</b>	<b>D15Mit107</b>	<b>41.5</b>	<b>3.1<sup>c</sup></b>	<b>4.7</b>
	<b>16</b>	<b>D16Mit60</b>	<b>24.0</b>	<b>3.1<sup>c</sup></b>	<b>4.3</b>
	<b>17</b>	<b>D17Mit93</b>	<b>39.3</b>	<b>5.1<sup>a</sup></b>	<b>7</b>
Cortical thickness	<b>1</b>	<b>D1Mit380</b>	<b>37.2</b>	<b>5.9<sup>a</sup></b>	<b>8</b>
		<b>D1Mit106</b>	<b>83.1</b>	<b>5.4<sup>a</sup></b>	<b>7.3</b>
	<b>3</b>	<b>D3Mit147*</b>	<b>55.3</b>	<b>2.5<sup>b</sup></b>	<b>4.2</b>
	<b>10</b>	<b>D10Mit233</b>	<b>63.4</b>	<b>3.7<sup>a</sup></b>	<b>5.1</b>
	<b>16</b>	<b>D16Mit60</b>	<b>24.0</b>	<b>3.1<sup>c</sup></b>	<b>4.2</b>
	<b>17</b>	<b>D17Mit93</b>	<b>39.3</b>	<b>4.7<sup>a</sup></b>	<b>6.5</b>
	<b>18</b>	<b>D18Mit12</b>	<b>9.8</b>	<b>2.7<sup>b</sup></b>	<b>3.8</b>
	<b>19</b>	<b>D19Mit28*</b>	<b>9.8</b>	<b>2.8<sup>b</sup></b>	<b>6</b>

Novel QTLs are highlighted in bold.

\* corresponds to marker closer to the peak LOD score.

<sup>a</sup> The threshold for the highly significant LOD score is  $P < 0.01$ .

<sup>b</sup> The threshold for the significant LOD score is  $P < 0.05$ .

<sup>c</sup> The threshold for the suggestive LOD score is  $P < 0.1$ .

from B6 mice at marker *D8Mit49* showed 10% higher PC values than the mice with homozygous C3H alleles. The Chr 8 loci regulating PC inherited in dominant mode.

#### QTL–QTL interactions

Two loci show interaction when the genotype of one locus affects the effect of other locus. PAIRSCAN analysis revealed four significant interactions (Table 3) involving loci on Chrs 8 (60 cM), 13 (45 cM), 1 (90 cM), and 13 (45 cM) and one suggestive interaction involving loci on Chrs 5 (80 cM) and 8 (10 cM). These four interactions combined together accounted for approximately 11% of the variance in loading-induced changes in BMD (includes total vBMD and cortical vBMD) and CTh (calculated by Pseudomarker FITQTL algorithm).

#### QTL analyses for bone density and size parameters using non-loaded bone

In addition to loci regulating response to loading, we used data from non-loaded tibia to identify linkage to BMD and bone size parameters. All four traits (total vBMD, cortical vBMD, PC, and CTh) showed normal distribution. Since there was a significant positive correlation ( $r$  value range from 0.13 to 0.55,  $P < 0.05$ )

between the body weight and PC, and body weight and BMD, we performed QTL analyses after adjustment for body weight. We identified 13 chromosomes that regulate changes in BMD and bone size including Chrs 1, 2, 3, 4, 6, 10, 11, 12, 15, 16, 17, 18, and 19 (Table 4, Fig. 5). Table 4 provides a list of QTLs that showed significant and suggestive linkages, the closest markers on peak QTL, and the percent variance explained by each QTL for different phenotypes. Some of the QTLs observed for the non-loaded phenotypes that include BMD and bone size are similar to the previously published QTLs [24,32–34]. In addition, we identified novel QTL for BMD on Chr 3 (LOD score 2.8, 59.0 cM), 10 (LOD score 3.8, 63.4 cM), and 17 (LOD score 5.4, 39.0 cM) and PC QTL on Chrs 3 (LOD score 4.0, 46.4 cM), 10 (LOD score 2.4, 57.3 cM), 11 (LOD score 4.3, 49.2 cM), 15 (LOD score 3.1, 41.5 cM), 16 (LOD score 3.1, 24.0 cM), and 17 (LOD score 5.1, 39.3 cM), and CTh QTL on Chrs 1, 3, 10, 16, 17, 18, and 19 (Table 4).

#### Discussion

Despite the fact that mechanical loading is an important regulator of bone mass, very little is known about the loci that contribute to the variation in bone anabolic response. Past research towards understanding the genetic variation in bone

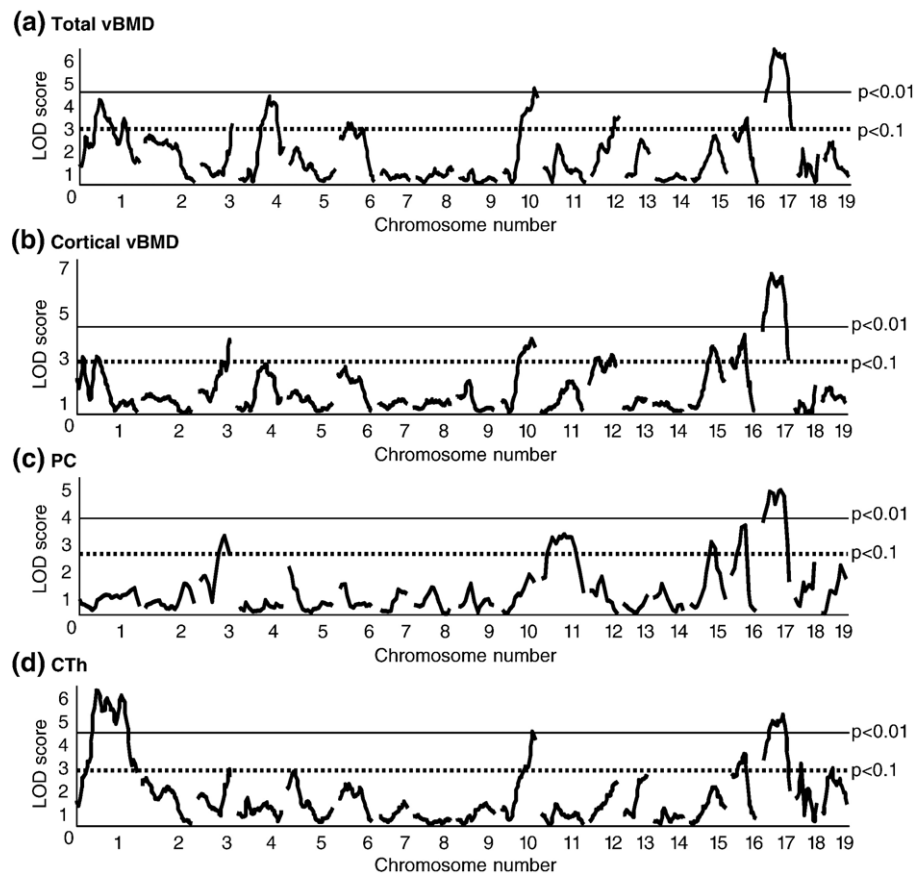


Fig. 5. Genome-wide scan associated with non-loaded (a) total vBMD, (b) cortical vBMD, (c) PC, and (d) CTh in the F2 population of B6×C3H intercross. The y axis indicates LOD score, and x axis represents chromosomes. The solid line indicates genome-wide threshold for significant QTL, and broken lines indicate thresholds for suggestive QTL.

response to mechanical loading has been mainly focused on hypotheses concerning known candidate genes. To our knowledge, this is the first genome-wide search for loci that regulate bone's anabolic response to mechanical loading. To evaluate loading-induced changes in bone adaptive response, our study design employed several selective criteria. Rationales for each of these criteria were based on evidence accumulated in previous studies [19]. The four-point bending model was used as a surrogate for other *in vivo* loading models, such as wheel running or jump training, because this model provided: (1) an extremely controlled external loading of an intact long bone; and (2) a contralateral control limb from each of the F2 mouse that can be used as a baseline to determine the loading response in the loaded limb. A criticism of using four-point bending is that it increases periosteal bone formation through pressure applied by pads as tested by sham loading rather than due to bending in mice and rats [21,35]. However, subsequent studies in mice comparing periosteal bone response in sham-loaded vs. loaded bones revealed that the magnitude of increase in bone formation was much greater in tibia subjected to four-point bending compared to sham loading. Raab-Cullen et al. reported a similar finding, using a four-point bending device in the rat model [36,37]. In this study, we have also provided evidence by performing sham bending in B6 mice. These studies are consistent with the possibility that loading-induced strain but not periosteal pressure contributed mainly to increase in periosteal bone formation in response to four-point bending. We have therefore used four-point bending as a loading model in our QTL study.

Several phenotypic end points have been used in the literature to measure the efficacy of loading-induced changes in bone parameters [6,10,19,21,38]. Based on the results of previous studies, including our recent study, we selected four parameters (total vBMD, cortical vBMD, PC, and CTh) to define the bone adaptive response. Analysis of percent change from non-loaded bone was based on the rationale that variable genetic background in each F2 mouse would affect the bone morphology (such as cross-sectional area) and influence the skeletal response independently of genetic regulation of loading. In addition, there are naturally segregating allelic variations between C3H and B6 mice that could affect BMD and bone size traits. Therefore, the use of absolute changes in BMD or periosteal circumference phenotype to study linkage would identify common, rather than specific, genetic components relevant for response to loading.

As observed with skeletal traits, response to four-point bending had a high index of heritability (70–80%). These heritability estimates were in agreement with those reported recently by Massett et al. [39] for various traits in mouse strains. Our results also agree with the 40–80% heritability estimates in humans [40] determined for physical activity. Thus, variance in bone response to mechanical loading in mice is strongly influenced by genetic factors.

The genome-wide search for associations between marker genotypes and the quantitative phenotypes of bone anabolic response to loading resulted in the localization of several QTLs in C3H×B6 F2 mice. The primary mechanism by which mechanical loading induces increases in BMD is believed to

involve periosteal modeling [19], leading to increased cortical thickness and an eventual increase in volumetric BMD. Based on this hypothesis, the QTLs identified in this study can be grouped into three categories: (1) QTLs that affect both BMD and bone size response to mechanical loading; (2) QTLs that affect only BMD response to mechanical loading; and (3) QTLs that only influence bone size response to mechanical loading.

Our findings that genetic loci in Chrs 8 and 9 show significant linkage with multiple measures of skeletal response to loading (total vBMD, PC, and CTh), even though our analysis eliminated effects of confounding factors such as bone size, suggest that these loci may contain genes that play a key role in mediating bone cell response to loading by regulating both BMD and bone size. Consistent with this idea, previous studies have shown that Chrs 8 and 9 contain genetic loci that regulate biomechanical and femur breaking strength in the multiple inbred mouse strain crosses including B6×C3H (Chr 8, 30–90 cM) [23], B6×D2 F2 mice (Chr 8, 30–57 cM) [41,42], and MRL×SJL (30–60cM) [26,43]. Taken together, these data may suggest that genes in these regions regulate biomechanical strength possibly with consequence of superior (or more favorable) response to exercise.

In addition to the mechanical loading QTL that regulated both BMD and bone size, Chr 1 (91.8 cM) and Chr 3 (50.3 cM) QTL specifically affected BMD but not bone size. Mechanical loading QTL in Chr 1 (91.8 cM) colocalizes with a major QTL identified earlier for total vBMD and other structural properties [23,44] in the congenic and B6×C3H F2 mice. Accordingly, QTL analysis of the BMD phenotype for non-loaded bones in the present study revealed a major QTL on Chr 1 at 83.1 cM, which is closer to the previous published BMD QTL. While the B6 alleles in Chr 1 contributed to higher BMD response to four-point bending (Fig. 5), C3H alleles contributed to higher BMD in non-loaded bone (data not shown). Thus, Chr 1 QTL may contain genes: (1) that contribute to natural variation in BMD between B6 and C3H strains; and (2) that respond to mechanical loading by increasing the vBMD. Our linkage analysis also identified loci on Chr 11 (69.9 cM), Chr 17 (39.3 cM), and Chr 18 (0 cM) that only influence bone size in response to mechanical loading. Furthermore, several novel loci regulating bone size on Chrs 3, 10, 11, 15, 16, 17, 18, and 19 were discovered using data from non-loaded bones. Based on these findings, it can be concluded that complex genetic mechanisms regulate variations in BMD and bone size in non-loaded and loaded bones. Another finding that provides substantial support for this concept of complex regulation of BMD and bone size is appearance of novel QTLs (Chr 5 and Chr 13) in the interaction study but not in the MAINSCAN.

It is noteworthy that a previous study reported that a congenic strain in which a small fragment of C3H Chr 4 (40–80 cM) was introgressed in a B6 background showed increased mechanosensitivity to loading. Our study, however, did not identify any QTL on Chr 4 for BMD and bone size. There are several possible explanations for why we did not find a QTL in chromosome 4: (1) the two models of loading used to study the bone anabolic responses are different; (2) the number of F2 mice used may not be adequate to identify all of the mechanical

loading QTL; and (3) while many of the mechanical loading QTLs may regulate anabolic response to four-point bending at multiple skeletal sites, there may be some QTL that are site-specific, i.e. regulate anabolic response in some but not other skeletal sites. In this regard, it is known that there are common BMD QTL that regulate BMD at multiple skeletal sites and site-specific BMD QTL that regulate BMD at some sites but not at others [24]. Consistent with the previous study, we did observe that the BMD response to mechanical loading was higher for C3H alleles on Chr 8 QTL as compared to B6 alleles. Since C3H mice demonstrate poor adaptation to mechanical loading [22] as compared to the B6 mice, these findings of high response alleles in C3H were unexpected. It is possible that C3H alleles at these loci are phenotypically silent in the context of the C3H genome but increase BMD in response to four-point bending in the presence of one or more B6 alleles.

Although this first genome-wide research for mechanical loading QTL using C3H and B6 strains of mice has revealed evidence for the presence of multiple genetic loci regulating the skeletal response to loading, our findings should be viewed in the context of the following limitations. The use of growing mice rather than mature mice may have confounded the response. In this regard, we have recently found that four-point bending significantly increased bone density in B6 mice compared to C3H mice at 10, 16, and 36 weeks [19], regardless of age. In addition, the non-loaded contralateral bone was used to control for growth effects. Second, in our recent study, we observed that the amount of strain in C3H and B6 mice was similar at 9 N force. However, the variable genetic background in each F2 mouse resulted in mice with variable cross-sectional area of tibia. With a fixed amount of force (9 N), the amount of strain experienced by each mouse will depend on cross-sectional area (moment of inertia), suggesting that a mouse with a large cross-sectional area will experience lower strain and vice versa. This would generate a variable response to loading independent of genetic response to loading. However, absence of any significant correlation between skeletal response to loading and periosteal circumference of corresponding non-loaded bone suggests that variation in loading strains was less important than variation in response due to genetics. Third, in the phenotype distribution, we found that some of the F2 mice showed negative BMD response to mechanical loading. It remains unknown whether the negative BMD response is due to loading-induced changes in architecture/shape or due to rapid increase in poorly mineralized bone at the periosteum. Fourth, our study used a relatively low number of F2 mice ( $n = 329$ ) to perform the QTL analysis. This was mainly due to practical difficulties in performing four-point-bending-based loading in a large number of mice. Therefore, the power to detect QTL was less than studies with 600–1000 animals. Thus, there are likely additional chromosomal regions that affect the bone response to loading which were undetected in this study. This was further evident by the loci interactions that showed only 11% variance. Finally, hormonal status is shown to significantly influence the response to loading, therefore the QTLs identified in this study could be specific to female mice. In this regard, mapping of each loci in the male mice will provide more definitive proof as to whether the same loci or closely

linked loci underlie the QTLs mapped to overlapping chromosomal regions using only females.

In conclusion, mechanical loading has long been identified as a means to regulate bone architecture; however, the benefits of loading depend on genetic background. The results of this study provide an important first step in identifying the genetic factors that regulate the bone adaptive response to mechanical loading. Our results confirm that response to mechanical loading has a strong genetic component, with several loci regulating loading-induced bone modeling. The future discovery of genes at these loci could provide a basis for the observed variability in bone mass accretion and maintenance due to exercise in normal healthy individuals.

### Acknowledgments

This work was supported by the Army Assistance Award No. DAMD17-01-1-0074. The US Army Medical Research Acquisition Activity (Fort Detrick, MD) 21702-5014 is the awarding and administering acquisition office for the DAMD award. The information contained in this publication does not necessarily reflect the position or the policy of the Government, and no official endorsement should be inferred. All work was performed in facilities provided by the Department of Veterans Affairs. We would like to thank Mr. Jay Javier and Mr. Alex Cortez for their contribution in this project and Mr. Sean Belcher for his editorial assistance.

### References

- [1] Turner CH, Robling AG. Exercise as an anabolic stimulus for bone. *Curr Pharm Des* 2004;10:2629–41.
- [2] Bailey DA, McCulloch RG. Bone tissue and physical activity. *Can J Sport Sci* 1990;15:229–39.
- [3] Warden SJ, Fuchs RK, Turner CH. Steps for targeting exercise towards the skeleton to increase bone strength. *Eur Medicophys* 2004;40:223–32.
- [4] Borer KT. Physical activity in the prevention and amelioration of osteoporosis in women: interaction of mechanical, hormonal and dietary factors. *Sports Med* 2005;35:779–830.
- [5] Gross TS, Srinivasan S, Liu CC, Clemens TL, Brain SD. Noninvasive loading of the murine tibia: an in vivo model for the study of mechanotransduction. *J Bone Miner Res* 2002;17:493–501.
- [6] Kodama Y, Umemura Y, Nagasawa S, Beamer WG, Donahue LR, Rosen CR, et al. Exercise and mechanical loading increase periosteal bone formation and whole bone strength in C57BL/6J mice but not in C3H/HeJ mice. *Calcif Tissue Int* 2000;66:298–306.
- [7] Mori T, Okimoto N, Sakai A, Okazaki Y, Nakura N, Notomi T, et al. Climbing exercise increases bone mass and trabecular bone turnover through transient regulation of marrow osteogenic and osteoclastogenic potentials in mice. *J Bone Miner Res* 2003;18:2002–9.
- [8] Bikle DD, Halloran BP. The response of bone to unloading. *J Bone Miner Metab* 1999;17:233–44.
- [9] Bikle DD, Sakata T, Halloran BP. The impact of skeletal unloading on bone formation. *Gravit Space Biol Bull* 2003;16:45–54.
- [10] Umemura Y, Baylink DJ, Wergedal JE, Mohan S, Srivastava AK. A time course of bone response to jump exercise in C57BL/6J mice. *J Bone Miner Metab* 2002;20:209–15.
- [11] Rubin CT, Lanyon LE. Regulation of bone formation by applied dynamic loads. *J Bone Jt Surg Am Vol* 1984;66:397–402.
- [12] Kodama Y, Dimai HP, Wergedal J, Sheng M, Malpe R, Kutilek S, et al. Cortical tibial bone volume in two strains of mice: effects of sciatic neurectomy and genetic regulation of bone response to mechanical loading. *Bone* 1999;25:183–90.

- [13] Lecoq B, Potrel-Burgot C, Granier P, Sabatier JP, Marcelli C. Comparison of bone loss induced in female rats by hindlimb unloading, ovariectomy, or both. *Jt Bone Spine* 2006;73(2):189–95.
- [14] Suzuki Y, Akima H, Igawa S, Fukunaga T, Kawakub K, Goto S, et al. Decrease of bone mineral density and muscle and/or strength in the leg during 20 days horizontal bed rest. *J Gravit Physiol* 1996;3:42–3.
- [15] Dalsky GP, Stocke KS, Ehsani AA, Slatopolsky E, Lee WC, Birge Jr SJ. Weight-bearing exercise training and lumbar bone mineral content in postmenopausal women. *Ann Intern Med* 1988;108:824–8.
- [16] Snow-Harter C, Bouxsein ML, Lewis BT, Carter DR, Marcus R. Effects of resistance and endurance exercise on bone mineral status of young women: a randomized exercise intervention trial. *J Bone Miner Res* 1992;7:761–9.
- [17] Tajima O, Ashizawa N, Ishii T, Amagai H, Mashimo T, Liu LJ, et al. Interaction of the effects between vitamin D receptor polymorphism and exercise training on bone metabolism. *J Appl Physiol* 2000;88:1271–6.
- [18] Dhamrait SS, James L, Brull DJ, Myerson S, Hawe E, Pennell DJ, et al. Cortical bone resorption during exercise is interleukin-6 genotype-dependent. *Eur J Appl Physiol* 2003;89:21–5.
- [19] Kesavan C, Mohan S, Oberholtzer S, Wergedal JE, Baylink DJ. Mechanical loading induced gene expression and BMD changes are different in two inbred mouse strains. *J Appl Physiol* 2005;99(5):1951–7.
- [20] Pedersen EA, Akhter MP, Cullen DM, Kimmel DB, Recker RR. Bone response to in vivo mechanical loading in C3H/HeJ mice. *Calcif Tissue Int* 1999;65:41–6.
- [21] Akhter MP, Cullen DM, Pedersen EA, Kimmel DB, Recker RR. Bone response to in vivo mechanical loading in two breeds of mice. *Calcif Tissue Int* 1998;63:442–9.
- [22] Robling AG, Li J, Shultz KL, Beamer WG, Turner CH. Evidence for a skeletal mechanosensitivity gene on mouse chromosome 4. *FASEB J* 2003;17:324–6.
- [23] Koller DL, Schrieffer J, Sun Q, Shultz KL, Donahue LR, Rosen CJ, et al. Genetic effects for femoral biomechanics, structure, and density in C57BL/6J and C3H/HeJ inbred mouse strains. *J Bone Miner Res* 2003;18:1758–65.
- [24] Beamer WG, Shultz KL, Donahue LR, Churchill GA, Sen S, Wergedal JR, et al. Quantitative trait loci for femoral and lumbar vertebral bone mineral density in C57BL/6J and C3H/HeJ inbred strains of mice. *J Bone Miner Res* 2001;16:1195–206.
- [25] Srivastava AK, Masinde G, Yu H, Baylink DJ, Mohan S. Mapping quantitative trait loci that influence blood levels of alkaline phosphatase in MRL/MpJ and SJL/J mice. *Bone* 2004;35:1086–94.
- [26] Li X, Masinde G, Gu W, Wergedal J, Mohan S, Baylink DJ. Genetic dissection of femur breaking strength in a large population (MRL/MpJ×SJL/J) of F2 mice: single QTL effects, epistasis, and pleiotropy. *Genomics* 2002;79:734–40.
- [27] Masinde GL, Wergedal J, Davidson H, Mohan S, Li R, Li X, et al. Quantitative trait loci for periosteal circumference (PC): identification of single loci and epistatic effects in F2 MRL/SJL mice. *Bone* 2003;32:554–60.
- [28] Lumeng L, Crabb DW. Genetic aspects and risk factors in alcoholism and alcoholic liver disease. *Gastroenterology* 1994;107:572–8.
- [29] Wergedal JE, Sheng MH, Ackert-Bicknell CL, Beamer WG, Baylink DJ. Genetic variation in femur extrinsic strength in 29 different inbred strains of mice is dependent on variations in femur cross-sectional geometry and bone density. *Bone* 2005;36:111–22.
- [30] Churchill GA, Doerge RW. Empirical threshold values for quantitative trait mapping. *Genetics* 1994;138:963–71.
- [31] Sen S, Churchill GA. A statistical framework for quantitative trait mapping. *Genetics* 2001;159:371–87.
- [32] Turner CH, Sun Q, Schrieffer J, Pitner N, Price R, Bouxsein ML, et al. Congenic mice reveal sex-specific genetic regulation of femoral structure and strength. *Calcif Tissue Int* 2003;73:297–303.
- [33] Shultz KL, Donahue LR, Bouxsein ML, Baylink DJ, Rosen CJ, Beamer WG. Congenic strains of mice for verification and genetic decomposition of quantitative trait loci for femoral bone mineral density. *J Bone Miner Res* 2003;18:175–85.
- [34] Bouxsein ML, Uchiyama T, Rosen CJ, Shultz KL, Donahue LR, Turner CH, et al. Mapping quantitative trait loci for vertebral trabecular bone volume fraction and microarchitecture in mice. *J Bone Miner Res* 2004;19:587–99.
- [35] Turner CH, Forwood MR, Rho JY, Yoshikawa T. Mechanical loading thresholds for lamellar and woven bone formation. *J Bone Miner Res* 1994;9:87–97.
- [36] Raab-Cullen DM, Akhter MP, Kimmel DB, Recker RR. Bone response to alternate-day mechanical loading of the rat tibia. *J Bone Miner Res* 1994;9:203–11.
- [37] Turner CH, Akhter MP, Raab DM, Kimmel DB, Recker RR. A noninvasive, in vivo model for studying strain adaptive bone modeling. *Bone* 1991;12:73–9.
- [38] Specker B, Binkley T, Fahrenwald N. Increased periosteal circumference remains present 12 months after an exercise intervention in preschool children. *Bone* 2004;35:1383–8.
- [39] Massett MP, Berk BC. Strain-dependent differences in responses to exercise training in inbred and hybrid mice. *Am J Physiol Regul Integr Comp Physiol* 2005;288:R1006–13.
- [40] Simonen R, Levalahti E, Kaprio J, Videman T, Battie MC. Multivariate genetic analysis of lifetime exercise and environmental factors. *Med Sci Sports Exerc* 2004;36:1559–66.
- [41] Volkman SK, Galecki AT, Burke DT, Miller RA, Goldstein SA. Quantitative trait loci that modulate femoral mechanical properties in a genetically heterogeneous mouse population. *J Bone Miner Res* 2004;19:1497–505.
- [42] Lang DH, Sharkey NA, Mack HA, Vogler GP, Vandenberg DJ, Blizard DA, et al. Quantitative trait loci analysis of structural and material skeletal phenotypes in C57BL/6J and DBA/2 second-generation and recombinant inbred mice. *J Bone Miner Res* 2005;20:88–99.
- [43] Li X, Masinde G, Gu W, Wergedal J, Hamilton-Ulland M, Xu S, et al. Chromosomal regions harboring genes for the work to femur failure in mice. *Funct Integr Genomics* 2002;1:367–74.
- [44] Yershov Y, Baldini TH, Villagomez S, Young T, Martin ML, Bockman RS, et al. Bone strength and related traits in HcB/Dem recombinant congenic mice. *J Bone Miner Res* 2001;16:992–1003.

# Up-regulation of the Wnt, Estrogen Receptor, Insulin-like Growth Factor-I, and Bone Morphogenetic Protein Pathways in C57BL/6J Osteoblasts as Opposed to C3H/HeJ Osteoblasts in Part Contributes to the Differential Anabolic Response to Fluid Shear<sup>\*S</sup>

Received for publication, August 22, 2005, and in revised form, January 13, 2006 Published, JBC Papers in Press, February 3, 2006, DOI 10.1074/jbc.M509205200

Kin-Hing William Lau<sup>1</sup>, Sonia Kapur, Chandrasekhar Kesavan, and David J. Baylink

From the Musculoskeletal Disease Center, Jerry L. Pettis Memorial Veterans Affairs Medical Center, and the Department of Medicine, Loma Linda University, Loma Linda, California 92357

C57BL/6J (B6), but not C3H/HeJ (C3H), mice responded to mechanical loading with an increase in bone formation. A 30-min steady fluid shear of 20 dynes/cm<sup>2</sup> increased [<sup>3</sup>H]thymidine incorporation and alkaline phosphatase activity and up-regulated the expression of early mechanoresponsive genes (integrin  $\beta 1$  (*Igtb1*) and cyclooxygenase-2 (*Cox-2*)) in B6 but not C3H osteoblasts, indicating that the differential mechanosensitivity was intrinsic to osteoblasts. In-house microarray analysis with 5,500 gene fragments revealed that the expression of 669 genes in B6 osteoblasts and 474 genes in C3H osteoblasts was altered 4 h after the fluid shear. Several genes associated with the insulin-like growth factor (IGF)-I, the estrogen receptor (ER), the bone morphogenetic protein (BMP)/transforming growth factor- $\beta$ , and Wnt pathways were differentially up-regulated in B6 osteoblasts. *In vitro* mechanical loading also led to up-regulation of these genes in the bones of B6 but not C3H mice. Pretreatment of B6 osteoblasts with inhibitors of the Wnt pathway (endostatin), the BMP pathway (Noggin), or the ER pathway (ICI182780) blocked the fluid shear-induced proliferation. Inhibition of integrin and Cox-2 activation by echistatin and indomethacin, respectively, each blocked the fluid shear-induced up-regulation of genes associated with these four pathways. In summary, up-regulation of the IGF-I, ER, BMP, and Wnt pathways is involved in mechanotransduction. These four pathways are downstream to the early mechanoresponsive genes, *i.e.* *Igtb1* and *Cox-2*. In conclusion, differential up-regulation of these anabolic pathways may in part contribute to the good and poor response, respectively, in the B6 and C3H mice to mechanical loading.

Mechanical loading is essential for maintenance of skeletal architectural integrity. Loading stimulates bone formation and suppresses bone resorption, leading to an overall increase in bone mass (1), whereas

unloading results in an overall decrease in bone mass, because of an inhibition of formation along with an increase in resorption (2). Loading produces strains in the mineralized matrix of bone, which generates interstitial fluid flow through lacunar/canalicular spaces (3). This fluid flow exerts a shear stress at surfaces of osteoblasts and osteocytes lining these spaces, which generates biochemical signals to produce biological effects. Multiple interacting signaling pathways are involved in translating the fluid shear signals into biological effects in bone cells (4), and these pathways are collectively referred to as the mechanotransduction mechanism. Mechanical loading is a key regulatory process for bone mass and strength (5). Knowledge of the mechanotransduction mechanism would not only yield information about the mechanical stimulation of bone formation but would also provide insights into the pathophysiology of osteoporosis and other bone-wasting diseases.

There is increasing evidence that genetics play a major part in determining the bone response to mechanical loading. Studies from our group (6, 7) and others (8, 9) demonstrate that C57BL/6J (B6)<sup>2</sup> inbred mice responded to *in vivo* mechanical loading with an increased bone formation, but C3H/HeJ (C3H) mice showed no such response. We postulate that the differential osteogenic response to mechanical stress in B6 and C3H inbred strains of mice is intrinsic to bone cells and that comparative global gene expression profiling studies in osteoblasts derived from this pair of inbred mouse strains in response to fluid shear could provide information concerning potential signaling pathways involved in the mechanical stimulation of bone formation. This would also yield important information about the identity of mechanosensitivity genes that determine the good and poor mechanical response in bone formation, respectively, in B6 and C3H mice.

The objectives of this study were 4-fold and are as follows: 1) to confirm that the differential anabolic response to mechanical loading in B6 and C3H strains of mice is intrinsic to osteoblasts, using an *in vitro* fluid flow shear stress model as a surrogate of mechanical loading (4); 2) to perform in-house microarray analyses in isolated B6 and C3H osteoblasts to identify potential signaling pathways that in part contribute to the differential osteogenic response; 3) to confirm that the pathways-of-interest are essential for fluid shear-induced cell proliferation; and 4) to determine the relationship between the pathways-of-interest and the early mechanoresponsive gene products, such as integrins and cyclooxygenase-2 (*Cox-2*).

<sup>2</sup> The abbreviations used are: B6, C57BL/6J inbred mice; ALP, alkaline phosphatase; BMP, bone morphogenetic protein; C3H, C3H/HeJ inbred mice; Cox-2, cyclooxygenase-2; ER, estrogen receptor; Erk1/2, extracellular signal-regulated kinases 1/2; pErk1/2, phosphorylated Erk1/2; EST, expressed sequence tag; IGF-I, insulin-like growth factor-I; TGF- $\beta$ , transforming growth factor- $\beta$ ; Wnt, wingless- and int-related protein.

<sup>\*</sup> This work was supported in part by a special appropriation to the Jerry L. Pettis Memorial Veterans Affairs Medical Center, Musculoskeletal Disease Center, and by a Merit Review provided by the Office of Research and Development, Medical Research Service, Department of Veteran Affairs, and in part by Assistance Award DAMD17-01-1-0744 provided by The United States Army Medical Research Acquisition Activity (Fort Detrick MD 21702-5014). The costs of publication of this article were defrayed in part by the payment of page charges. This article must therefore be hereby marked "advertisement" in accordance with 18 U.S.C. Section 1734 solely to indicate this fact.

<sup>S</sup> The on-line version of this article (available at <http://www.jbc.org>) contains supplemental Tables 1–3.

<sup>1</sup> To whom correspondence should be addressed: Musculoskeletal Disease Center (151), Jerry L. Pettis Memorial Veterans Affairs Medical Center, 11201 Benton St., Loma Linda, CA 92357. Tel.: 909-825-7084 (ext. 2836); Fax: 909-796-1680; E-mail: William.Lau@med.va.gov.

## EXPERIMENTAL PROCEDURES

**Materials**—Tissue culture plasticware was obtained from Falcon (Oxnard, CA). Dulbecco's modified Eagle's medium was from Mediatech, Inc. (Herndon, VA). Bovine calf serum was from HyClone (Logan, UT). Trypsin and EDTA were products of Irvine Scientific (Santa Ana, CA). [<sup>3</sup>H]Thymidine (48 Ci/mmol) was obtained from Research Products International (Mount Prospect, IL). Anti-pErk1/2, anti-pan-Erk1/2, anti- $\beta$ -catenin, anti-integrin  $\beta$ 1, anti-Cox-2, and anti-actin antibodies were from Santa Cruz Biotechnology (Santa Cruz, CA), Upstate Biotechnology, Inc. (Lake Placid, NY), or BD Transduction Laboratories. Echistatin, endostatin, and indomethacin were products of Sigma. ICI182780 was purchased from Tocris (Ellisville, MO), and Noggin was obtained from R&D Systems (Minneapolis, MN). Other chemicals were of molecular biology grade and were from Fisher or Sigma.

**Cell Culture and Fluid Shear Stress Experiments**—Osteoblasts, isolated from calvarias or long bones of 8-week-old B6 and C3H mice by collagenase digestion as described previously for neonatal calvarial osteoblasts (10), were maintained in Dulbecco's modified Eagle's medium supplemented with 10% bovine calf serum. Pilot studies indicated that cell passage, up to passage 7, had no significant effects on the responsiveness of primary B6 mouse osteoblasts to fluid shear stress with respect to [<sup>3</sup>H]thymidine incorporation, alkaline phosphatase (ALP) specific activity, and Erk1/2 phosphorylation. Accordingly, cells of passages 3–6 were used in this study.

50,000 cells were plated on each glass slide. At ~80% confluency, the cells were serum-deprived for 24 h and subjected to a steady fluid shear stress of 20 dynes/cm<sup>2</sup> for 30 min in the Cytodyne flow chamber as described previously (4). This dosage of fluid shear stress is believed to be within the physiologically relevant range of laminar shear stress produced by the circulation (11). Replicate glass slides of cells were placed in a parallel flow chamber but without the fluid shear stress as static controls in each experiment.

To test the potential involvement of a given signaling pathway-of-interest, cells were pretreated with a specific inhibitor of the pathway-of-interest (*i.e.* ICI182780 for the estrogen receptor (ER) pathway, endostatin for the canonical wntless- and int-related protein (Wnt) pathway, and Noggin for the bone morphogenetic protein (BMP) pathway), for 24 h prior to the fluid shear stress. To assess the role of integrin activation and Cox-2 on the up-regulation of these pathways, cells were pretreated with echistatin or indomethacin, respectively, for 2 h prior to the fluid shear stress.

**[<sup>3</sup>H]Thymidine Incorporation Assay**—Cell proliferation was assessed by [<sup>3</sup>H]thymidine incorporation during the final 6 h of the 24-h post-exposure to fluid shear as described previously (4, 12).

**Cellular ALP Specific Activity Assay**—Osteoblast differentiation was measured by the increase in the specific activity of ALP 24 h post-exposure to the shear stress as described previously (4, 13). The ALP-specific activity (*i.e.* normalized against cellular protein content) was reported to adjust for the difference in the cell number because of the increase in cell proliferation in response to fluid shear.

**Western Immunoblot Assays**—Cellular integrin  $\beta$ 1, Cox-2, and  $\beta$ -catenin were determined by Western immunoblot assays were performed as described previously (4) using respective commercial polyclonal antibodies and normalized against each corresponding cellular actin level. The relative cellular phosphorylated Erk1/2 (pErk1/2) level (an index of Erk1/2 activation) was determined with the phospho-specific antibody against pErk1/2 and normalized against corresponding total Erk1/2 level, determined with anti-pan-Erk1/2 polyclonal antibody.

**RNA Purification**—Total RNA of cells on each slide was extracted with Qiagen mini RNA kit (Qiagen, Valencia, CA). The purity and integ-

egrity of each RNA sample was confirmed with Bio-analyzer (Agilent, Palo Alto, CA). Only undegraded RNA samples were used in this study.

**In-house Microarray Hybridization and Data Analysis**—For the preparation of our in-house microarray chips, cDNA inserts of 5,500 cDNA clones of mouse, rat, human, or monkey genes or ESTs (largely mouse and human genes) were isolated, purified, and evaluated with agarose gel electrophoresis. The microarrays were printed on aminosilane-coated microscope slides (Corning, NY) with a GMS 417 Arrayer (Genetic Microsystems, Santa Clara, CA). Six replicates of each clone were printed on each slide. DNA was fixed to the slides by baking at 80 °C for 2 h.

The experimental strategy and analyses of the microarray experiment are described briefly as follows. Primary osteoblasts isolated from B6 or C3H inbred strain of mice were plated on glass slides and subjected to a 30-min steady shear stress as described above. Replicate plates of B6 or C3H osteoblasts were placed in the flow chamber without the fluid shear as the static control. Four hours after the fluid shear, total RNA was isolated. cDNA synthesized from 1  $\mu$ g of total RNA of cells received the fluid shear, and corresponding static control cells were each fluorescently labeled with Cy5 and Cy3, respectively, as previously described (14). The microarray hybridization was performed as described previously (14). The slide was scanned using a ScanArray 4000 scanner (GSI Lumonics, San Jose, CA). The fluorescent images were acquired using ScanArray software (version 2.1; GSI Lumonics), and data were analyzed using GeneSpring Image Analysis program (Silicon Genetics, San Jose, CA). Each array spot was individually inspected using the GeneSpring Image Analysis program. The microarray analysis was repeated in osteoblasts of four pairs of B6/C3H mice. Statistically significant differences in gene expression between each pair of stressed and corresponding static control samples was analyzed using Lowess Normalization and paired *t* test. Differences of *p* < 0.05 were considered significant. Only known mouse genes were analyzed further. Because the gene annotation or accession numbers of many of the known mouse genes on our array were missing, the computer-based gene ontology and pathway analyses were not performed. Tentative classification of gene functions was determined manually based on information available on the PubMed data base.

**Real Time PCR Analyses**—Real time PCR was carried out with the SYBR Green method on the MJ Research DNA Engine Opticon® 2 System (Waltham, MA). The purified total RNA was used to synthesize cDNA by reverse transcription using random hexamer primers and Superscript II reverse transcriptase (Invitrogen). The cDNA was then subjected to real time PCR amplification using the gene-specific primers listed in Table 1. The primers were designed with the IDT Vector NTI software (Coralville, IA). An aliquot (25  $\mu$ l) of reaction volume (consisted of 2 $\times$  (12.5  $\mu$ l) QuantiTect SYBR Green PCR master mix, which contained the Hot Start *Taq* polymerase (Qiagen), 0.5  $\mu$ M of primers, and 1–5  $\mu$ l of cDNA template) was used in each assay. The PCR conditions consisted of an initial 10-min hot start at 95 °C, followed by 40 cycles of denaturation at 95 °C for 30 s, annealing, and extension at appropriate temperature (50–72 °C) (see Table 1) for 30 s, and a final step of melting curve analysis from 60 to 95 °C. Each reaction was performed in triplicate. The data were analyzed using Opticon® Monitor Software 2.0. Data normalization was performed against  $\beta$ -actin, and the normalized values were used to calculate the relative fold change between the control and the experiment groups by the threshold cycle method.

**In Vivo Mechanical Loading Model**—We adapted the four-point bending exercise regimen, originally developed by Akhter *et al.* (15) on rat tibia, as the *in vivo* mechanical loading model for mouse tibia as

**TABLE 1**

List of primer sets used in the real-time PCR amplification reactions

Gene	Primer sequences	Annealing temperature	Extension temperature
		°C	
$\beta$ -Actin	Forward primer, 5'-CAG GCA TTG CTG ACA GGA TG-3'	56	72
	Reverse primer, 5'-TGC TGA TCC ACA TCT GCT GG-3'		
<i>Tgfb1</i>	Forward primer, 5'-CGG CAG CTG TAC ATT GAC TT-3'	53	72
	Reverse primer, 5'-TGT GTT GGT TGT AGA GGG CA-3'		
<i>Ctnnb1</i>	Forward primer, 5'-GAC TCA CGC AGT GAA GAA TG-3'	50	72
	Reverse primer, 5'-GCT GTA GCA GGT TCA CTA GA-3'		
<i>Bmpr1</i>	Forward primer, 5'-GCT TAT TCT GCT GCT TGT GGG-3'	53	72
	Reverse primer, 5'-ATT TAA CAG CTA GGC CCA GG-3'		
<i>Igf1r</i>	Forward primer, 5'-GCC AAC AAG TTC GTC CAC AG-3'	56	72
	Reverse primer, 5'-CCG AAG GAC CAG ACA TCA GA-3'		
<i>Wnt1</i>	Forward primer, 5'-GGT GTT GCG GTT CCT GAT GT-3'	54	72
	Reverse primer, 5'-TCC GAG GCA GAG ACA AGG AG-3'		
<i>Wnt3a</i>	Forward primer, 5'-ATA GCC TGC ATC CGC TCT GA-3'	54	72
	Reverse primer, 5'-TGG TGA CCA TTG CCT CAA CA-3'		
<i>Wnt5a</i>	Forward primer, 5'-AAC TGC AGC ACA GTG GAC AA-3'	54	72
	Reverse primer, 5'-TAG TCG ATG TTG TCT CCG CA-3'		
<i>Axin</i>	Forward primer, 5'-TCT GGA TAC CTG CCC ACT TT-3'	54	72
	Reverse primer, 5'-TGC CTT CGT TGT ACC GTC TA-3'		
<i>Lef1</i>	Forward primer, 5'-ACG GAC AGT GAC CTA ATG CA-3'	54	72
	Reverse primer, 5'-TCT CCT TTA GCG TGC ACT CA-3'		
<i>Lrp5</i>	Forward primer, 5'-ACA CTA TAT CCG CCG ATC CT-3'	53	72
	Reverse primer, 5'-GAC TGG TGC TGT AGT CAC TG-3'		
<i>Esr1</i>	Forward primer, 5'-ATG TGC AGG AGG CAG ACA TT-3'	56	72
	Reverse primer, 5'-TGG AGC CTG CTT GGA GTT AT-3'		
<i>Ncoa1</i>	Forward primer, 5'-GCA CAG CCA GGA GTG TAC AA-3'	56	72
	Reverse primer, 5'-GAC GAG AGC TGG TTG CAG TA-3'		
<i>Dlx1</i>	Forward primer, 5'-GGA CCG GAC CAG ACT CTC AT-3'	56	72
	Reverse primer, 5'-GTG GCT CAG ACC TGG TGA CT-3'		
<i>c-Fos</i>	Forward primer, 5'-CCT GAG GTC TTT CGA CAT GTG GAA-3'	56	72
	Reverse primer, 5'-AAG AGA GCA AGA AGG TGG TCG CAT-3'		

described previously (16). Briefly, the four-point bending device (Instron, Canton, MA) consisted of two upper vertically movable points covered with rubber pads (4-mm apart), and two 12-mm lower non-movable points covered with rubber pads. During the bending exercise, the two upper pads touched the lateral surface of the tibia through overlying muscle and soft tissue, whereas the lower pads touched the medial surface of the proximal and distal parts of the tibia. The loading protocol consisted of a 9-newton load at a frequency of 2 Hz for 36 cycles, and the exercise was performed once daily. The right tibia was subjected to the loading exercise, and the left tibia was used as an internal unloaded control. Upon anesthesia with halothane, the ankle of the tibia was positioned on the second lower immobile points of the Instron equipment, such that the region of the tibia loaded did not vary from mouse to mouse. The loading was applied for 6 days/week with 1 day of rest for 2 weeks. Forty eight h after the final loading, mice were sacrificed. The marrow-flushed tibias were stored at  $-80^{\circ}\text{C}$  until RNA extraction. The animal protocol was approved by the Institutional Animal Care and Use Committee of the J. L. Pettis Memorial Veterans Affairs Medical Center.

One of the potential limitations of this model is that force applied over the soft tissues may have local bruising effects that could result in inflammation. Accordingly, extra efforts were taken to minimize the bruising effect of loading on soft and hard tissues by changing the rubber pads frequently. We also looked for histological evidence for inflammation (*i.e.* presence of inflammatory cells and/or blood clots) in the loaded muscles and bones after the loading regimen in several mice in preliminary experiments, and we found no evidence for the presence of lymphocytes or other inflammatory cells in the muscle and bone tissues at the loading sites in all samples examined. We also found no evidence of blood clotting at the loading limb.

**RNA Extraction from Bones**—Briefly, bones were pulverized in liquid nitrogen. Total RNA was purified with Trizol reagent (Invitrogen), followed by RNeasy columns (Qiagen). The quality and quantity of RNA

were analyzed using Bio-analyzer and Nano-drop instrumentation, respectively. Only good quality RNAs were used for subsequent real time PCR analyses.

**Bone Histomorphometry**—Both the loaded and unloaded (control) tibiae of B6 and C3H mice were removed, after euthanasia, and fixed with 10% cold neutral buffered formalin on ice. The fixed bones were then rinsed free of formalin, defleshed, and embedded in methyl methacrylate (17). Thick (0.5 mm) cross-sections were cut from the mid-diaphysis of the tibia with a wire saw (Delaware Diamond Knives), lightly ground, and stained with Goldner's trichrome stain for mineralized bone. The stained bone slices were mounted in Fluoromount-G (Fisher) and examined under an Olympus BH-2 fluorescence/bright field microscope.

**Statistical Analysis**—Results are shown as mean  $\pm$  S.D. with 3–6 replicates or repeat measurements. Statistical significance was determined with two-tailed Student's *t* test, and the difference was significant at  $p < 0.05$ .

## RESULTS

**Effects of Fluid Shear Stress on the Proliferation, Differentiation, and Expression of Early Mechanoresponsive Genes in Primary Osteoblasts of B6 and C3H Inbred Strains of Mice**—The 30-min steady fluid shear stress of 20 dynes/cm<sup>2</sup> significantly increased ( $\sim$ 2-fold each) the [<sup>3</sup>H]thymidine incorporation (Fig. 1A) (an index of cell proliferation) and ALP-specific activity (Fig. 1B) (a marker of osteoblast differentiation) of B6 osteoblasts. No such response was seen in C3H osteoblasts.

Mechanical stimulation, including fluid shear stress, has been shown to up-regulate several early mechanoresponsive genes, such as integrins and Cox-2, within minutes in bone cells (18). Thus, we evaluated whether there was also a differential response to fluid shear in the expression of integrin  $\beta$ 1 (*Igtb1*) and Cox-2 in C3H and B6 osteoblasts. Fig. 1C shows that while the 30-min steady fluid shear stress significantly increased the cellular integrin  $\beta$ 1 protein level in B6 osteoblasts

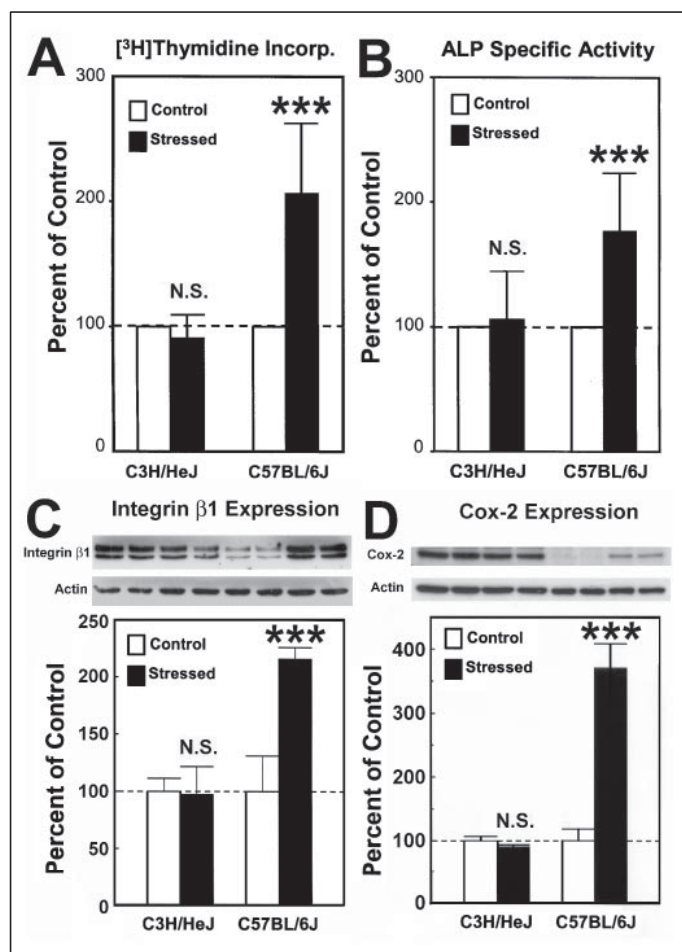


**FIGURE 1. Effects of fluid shear on cell proliferation, differentiation, and early mechanoresponsive gene expression of B6 and C3H osteoblasts.** A, cell proliferation was measured by [ $^3$ H]thymidine incorporation 24 h after a 30-min steady fluid shear at 20 dynes/cm $^2$ . B, osteoblast differentiation was monitored by an increase in the specific activity of ALP 48 h after the fluid shear. C and D, cellular integrin  $\beta 1$  protein level (C) and Cox-2 protein level (D), normalized against each cellular actin protein level, was determined by Western immunoblot assay. Results are shown as mean  $\pm$  S.D. (n = 6). \*\*\*,  $p < 0.001$ . N.S., not significant.

by  $\sim 2$ -fold 10 min after the stress, the same stress had no effect in C3H osteoblasts. Similarly, the fluid shear significantly increased Cox-2 protein expression by  $>2$ -fold in B6 osteoblasts but not in C3H osteoblasts (Fig. 1D). Fig. 1, C and D, also shows that the basal cellular integrin  $\beta 1$  and Cox-2 protein levels in C3H osteoblasts were severalfold higher than those in B6 osteoblasts. The significance of the higher basal expression of these two early mechanoresponsive genes in C3H osteoblasts is unclear. Nevertheless, these results clearly indicate that the osteogenic response to mechanical loading in this pair of inbred strains of mice is intrinsic to osteoblasts.

**In-house Microarray Analysis of Shear Stress-mediated Changes in Gene Expression in Primary Osteoblasts of B6 and C3H Mice**—Microarray analysis was performed with RNAs isolated from primary B6 or C3H osteoblasts 4 h after the 30-min fluid shear, using the in-house chips, which contained 5,500 genes or ESTs of mouse, human, and several other species. As schematically summarized in Fig. 2, of the 5,500 genes or ESTs on the microarray chip, the expression of 669 genes or ESTs in B6 osteoblasts (360 up-regulated and 309 down-regulated) and that of 474 genes or ESTs in C3H osteoblasts (212 up-regulated and 262 down-regulated) was significantly ( $p < 0.05$ ) affected by the shear stress. Among the affected gene fragments, 286 were up-regulated and 228 down-regulated in B6 osteoblasts only, and 138 of them were up-regu-

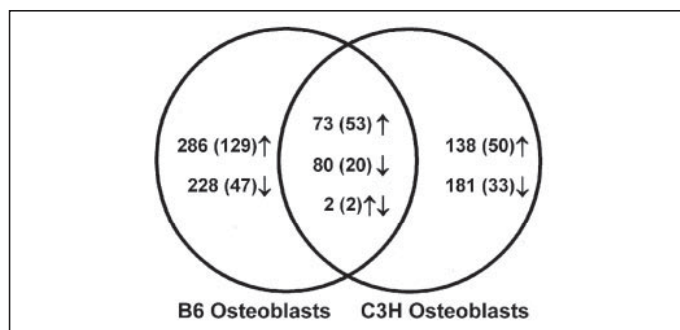


**FIGURE 2. Schematic summary of the number of genes whose expression was altered at 4 h after the 30-min steady fluid shear at 20 dynes/cm $^2$  in osteoblasts derived from B6 or C3H inbred strain of mice.** The up arrows represent up-regulated genes, and the down arrows represent down-regulated genes. The numbers indicate the total number of all genes and ESTs. The numbers within parentheses are the number of known mouse genes.

lated and 181 were down-regulated in C3H osteoblasts only. Seventy three genes or ESTs were up-regulated and 80 were down-regulated in both B6 and C3H osteoblasts. The fibronectin (*Fn1*) gene was up-regulated in B6 osteoblasts but down-regulated in C3H osteoblasts. Conversely, the solute carrier family 34 (sodium phosphate), member 2 (*Slc34a2*) gene was down-regulated in B6 osteoblasts but up-regulated in C3H osteoblasts. Although the relative changes in the expression level of these genes were mostly  $<3$ -fold, all of the changes were statistically significant ( $p < 0.05$ ).

Because we sought to identify potential signaling pathways that might contribute to the differential osteogenic response in this pair of mouse strains, subsequent analyses were focused on the known mouse genes whose expression was affected differentially in B6 osteoblasts, with an emphasis on the up-regulating genes. Accordingly, 53 known mouse genes were up-regulated and 20 known genes were down-regulated in both B6 and C3H osteoblasts (supplemental Table 1). The up-regulated genes included a number of key regulator genes of cell proliferation and differentiation in both B6 and C3H osteoblasts, including several growth factor genes (i.e. *Tgfb1*, *Vegf*, *Igf2*, *Pdgfa*, *Fgf1*, and *Op2/Bmp8b*), receptor genes (*Thr*, *Bmpr1a*, *Pthr*, *Esr2*, *Rarg*, *Fnr*, *Osmr*, *Ifngr*, and *Tnfr*), vitamin D metabolism genes (i.e. *Cyp27b1*), small G-protein genes (i.e. *Ran* and *Era1*), and several inhibitory transcription factor genes of osteoblast differentiation (i.e. *M-twist*, *Id-2*, and *Dermo-1*). Because these genes were up-regulated in both C3H and B6 osteoblasts, these mechanoresponsive genes were likely to be upstream to the mechanosensitivity genes responsible for the differential anabolic response to fluid shear between B6 and C3H osteoblasts.

The expression of 88 known mouse genes (50 up-regulated and 33 down-regulated) was altered only in C3H osteoblasts (supplemental Table 2). Some of the up-regulated genes were growth factor and receptor genes (*Csf1*, *Tgfb1*, *Igf2*, and *Fgf1*), transcription factor genes (*Hox8.1/Msx2*, and *c-Myc*), signal transduction genes (*Pld*, *Hic5*, *Itgb4bp*, and *Emk2*), and intracellular transport and trafficking genes (*Gs15*, *Cacnb3*, *Snx3*, and *Atp6d*). The shear stress also up-regulated *Pges* and *Bcl* genes in C3H osteoblasts but not in B6 osteoblasts. Because C3H osteoblasts did not respond anabolically to fluid shear, these genes were not analyzed further.

The expression of 129 known mouse genes was up-regulated in B6 osteoblasts only (supplemental Table 3). Consistent with an anabolic response to the fluid shear in B6 osteoblasts and not C3H osteoblasts, the fluid shear differentially up-regulated in B6 osteoblasts a number of genes associated with osteoblast proliferation and differentiation. These genes include, but are not limited to, bone growth factor, receptor, and associated genes (i.e. *Tgfb2*, *Bmp4*, *Fgf6*, *Kgf/Fgf7*, *Pdgfc*, *Igf1r*, *Ghr*,

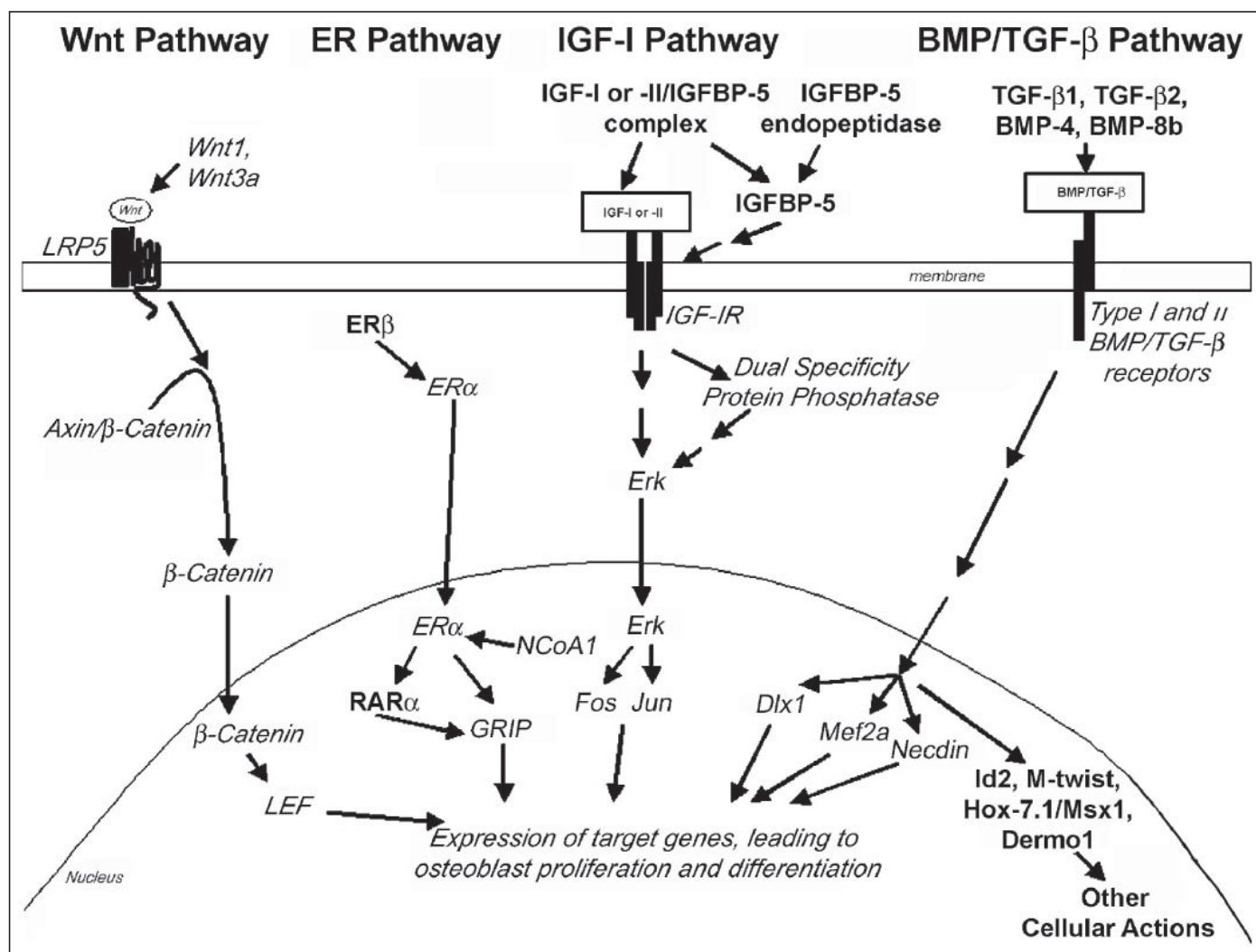


FIGURE 3. Schematic summary of the genes associated with the Wnt, the ER, the IGF-I, and the BMP/TGF- $\beta$  pathways, whose expression was up-regulated 4 h after the 30-min steady fluid shear stress of 20 dynes/cm<sup>2</sup>. Genes whose expression was up-regulated in both C3H and B6 osteoblasts are shown in **boldface letters**, and genes whose expression was up-regulated in B6 osteoblasts only are shown in *italic letters*.

*Bmpr2*, *Igf1p5*, and *Wnt5a*), cytokines, and receptor genes (*i.e.* *Osm*, *Il4*, *Il6*, *Il8*, and *Il6r*), *Esr1*, genes involved in protein and RNA synthesis, DNA synthesis, as well as cell proliferation. A number of energy and cell metabolism genes, intracellular transport and trafficking genes, as well as oxidative stress-responsive genes, such as *Hsc70*, *Osp94*, and *p47<sup>phox</sup>*, were also up-regulated in B6 but not C3H osteoblasts. Similarly, a large number of transcription factors and signal transduction molecules were differentially up-regulated in B6 osteoblasts.

**Up-regulation of the Expression of Genes of Four Anabolic Signal Transduction Pathways in B6 Osteoblasts in Response to the Fluid Shear**—A manual pathway analysis of the known mouse genes whose expression was up-regulated in B6 osteoblasts revealed that a number of genes associated with four anabolic signaling transduction pathways were differentially up-regulated in response to the fluid shear (Fig. 3). These pathways are as follows: the Wnt pathway, the BMP/transforming growth factor(TGF)- $\beta$  pathway, the ER pathway, and the growth hormone/insulin-like growth factor(IGF)-I pathway. However, some of the upstream effector genes of these signaling pathways (with the exception of the Wnt pathway) and several downstream negative regulatory transcription factor genes of osteoblast differentiation of the BMP/TGF- $\beta$  pathway (*i.e.* *Id-2*, *Dermo-1*, and *Hox-7.1/Msx1*) were also up-regulated in C3H osteoblasts, suggesting that these genes are unrelated to the mechanosensitivity genes responsible for

the differential osteogenic response to mechanical stimulation in this pair of inbred strains of mice.

To confirm the microarray data, real time PCR analyses were performed on the expression levels of several genes of each of these four signaling pathways in B6 and C3H osteoblasts 4 h after the 30-min steady fluid shear. Because the in-house microarray chips contained only a limited number of known mouse genes, particularly those of the canonical Wnt signaling pathway, additional genes of the canonical Wnt pathway (*i.e.* *Wnt1*, *Wnt3a*, and *Lrp5*) were included in the real time PCR analysis. Table 2, which summarizes and compares the real time PCR and microarray results, confirms that the expression of several key genes of the Wnt signaling pathway (*i.e.* *Wnt1*, *Wnt3a*, *Wnt5a*, *Lrp5*, *Ctnnb1*, *Lef1*, and *Axin*), IGF-I pathway (*i.e.* *Igf1* and *c-Fos*), ER pathway (*i.e.* *Esr1* and *Ncoa1*), BMP/TGF- $\beta$  pathway (*i.e.* *Tgfb1* and *Bmpr1*) were differentially up-regulated by the fluid shear in B6 osteoblasts and not in C3H osteoblasts.

**Evidence That in Vivo Mechanical Loading Up-regulated Genes Associated with the Wnt, IGF-I, ER, and BMP/TGF- $\beta$  Signaling Pathways**—To determine whether up-regulation of genes of these four anabolic signaling pathways in response to loading also occurred in bone *in vivo*, we determined the effects of this 2-week loading regimen in the form of a four-point bending exercise on the expression of genes associated

TABLE 2

Microarray and real time PCR analyses of gene expression of the Wnt, BMP/TGF- $\beta$ , IGF-I, and ER signaling pathways in response to the fluid shear in B6 osteoblasts as opposed to that in C3H osteoblasts

Gene	B6 osteoblasts		C3H osteoblasts	
	Microarray, fold changes, mean $\pm$ S.D. ( $n = 4$ )	Real time PCR, fold changes, mean $\pm$ S.D. ( $n = 6$ )	Microarray, fold changes, mean $\pm$ S.D. ( $n = 4$ )	Real time PCR, fold changes, mean $\pm$ S.D. ( $n = 6$ )
<b>The Wnt signaling pathway genes</b>				
<i>Wnt1</i>	NP <sup>a</sup>	2.32 $\pm$ 0.15 <sup>b</sup>	NP	0.85 $\pm$ 0.12
<i>Wnt3a</i>	NP	3.28 $\pm$ 0.86 <sup>b</sup>	NP	0.92 $\pm$ 0.15
<i>Wnt5a</i>	1.86 $\pm$ 0.49 <sup>b</sup>	1.85 $\pm$ 0.02 <sup>b</sup>	1.72 $\pm$ 1.23	0.14 $\pm$ 0.06
<i>Lrp5</i>	NP	3.23 $\pm$ 1.42 <sup>b</sup>	NP	0.67 $\pm$ 0.45
<i>Ctnnb1</i>	2.35 $\pm$ 0.35 <sup>b</sup>	3.36 $\pm$ 0.59 <sup>b</sup>	1.33 $\pm$ 0.22	0.84 $\pm$ 0.56
<i>Axin</i>	1.70 $\pm$ 0.51 <sup>b</sup>	3.48 $\pm$ 0.82 <sup>b</sup>	1.26 $\pm$ 0.22	0.22 $\pm$ 0.10
<i>Lef1</i>	1.63 $\pm$ 0.44 <sup>b</sup>	2.79 $\pm$ 0.49 <sup>b</sup>	1.52 $\pm$ 0.91	0.49 $\pm$ 0.15
<b>The BMP/TGF-<math>\beta</math> signaling pathway genes</b>				
<i>Tgfb1</i>	1.99 $\pm$ 0.54 <sup>b</sup>	2.44 $\pm$ 0.71 <sup>b</sup>	1.99 $\pm$ 0.86 <sup>b</sup>	0.95 $\pm$ 0.10
<i>Bmp8b</i>	1.83 $\pm$ 0.22 <sup>b</sup>	ND <sup>c</sup>	2.19 $\pm$ 0.61 <sup>b</sup>	ND
<i>Tgfb2</i>	1.71 $\pm$ 0.52 <sup>b</sup>	ND	1.88 $\pm$ 0.85	ND
<i>Bmp4</i>	1.67 $\pm$ 0.49 <sup>b</sup>	ND	1.58 $\pm$ 0.61	ND
<i>Bmpr1</i>	1.92 $\pm$ 0.55 <sup>b</sup>	3.64 $\pm$ 0.41 <sup>b</sup>	2.24 $\pm$ 1.01 <sup>b</sup>	0.81 $\pm$ 0.27
<i>Bmpr2</i>	1.62 $\pm$ 0.38 <sup>b</sup>	ND	1.78 $\pm$ 0.76	ND
<i>Id2</i>	2.06 $\pm$ 0.53 <sup>b</sup>	ND	2.64 $\pm$ 1.12 <sup>b</sup>	ND
<i>M-twist</i>	1.97 $\pm$ 0.21 <sup>b</sup>	ND	2.67 $\pm$ 0.94 <sup>b</sup>	ND
<i>Hox-7.1/Msx1</i>	1.74 $\pm$ 0.61 <sup>b</sup>	ND	1.76 $\pm$ 0.83	ND
<i>Dermo-1</i>	1.70 $\pm$ 0.56 <sup>b</sup>	ND	1.90 $\pm$ 0.53 <sup>b</sup>	ND
<i>Dlx1</i>	1.56 $\pm$ 0.36 <sup>b</sup>	1.70 $\pm$ 0.38 <sup>b</sup>	1.29 $\pm$ 0.52	1.05 $\pm$ 0.36
<i>Necdin</i>	1.37 $\pm$ 0.19 <sup>b</sup>	ND	1.18 $\pm$ 0.29	ND
<i>Mef2a</i>	1.22 $\pm$ 0.12 <sup>b</sup>	ND	0.98 $\pm$ 0.13	ND
<b>The IGF-I signaling pathway genes</b>				
<i>Igf2</i>	1.64 $\pm$ 0.27 <sup>b</sup>	ND	1.69 $\pm$ 0.53 <sup>b</sup>	ND
<i>Htra1</i>	1.93 $\pm$ 0.43 <sup>b</sup>	ND	2.25 $\pm$ 0.94 <sup>b</sup>	ND
<i>Igfbp5</i>	2.55 $\pm$ 1.59 <sup>b</sup>	ND	1.28 $\pm$ 1.37	ND
<i>Igflr</i>	1.77 $\pm$ 0.35 <sup>b</sup>	2.28 $\pm$ 0.39 <sup>b</sup>	2.24 $\pm$ 1.42	1.15 $\pm$ 0.30
<i>Mapk7</i>	1.76 $\pm$ 0.61 <sup>b</sup>	ND	2.04 $\pm$ 1.29	ND
<i>Dusp10</i>	1.49 $\pm$ 0.29 <sup>b</sup>	ND	0.61 $\pm$ 1.41	ND
<i>c-Fos</i>	2.09 $\pm$ 0.57 <sup>b</sup>	ND	1.75 $\pm$ 0.81	ND
<i>c-Jun</i>	1.34 $\pm$ 0.22 <sup>b</sup>	ND	1.39 $\pm$ 0.48	ND
<b>The ER signaling pathway genes</b>				
<i>Esr2</i>	1.93 $\pm$ 0.49 <sup>b</sup>	ND	1.64 $\pm$ 0.33 <sup>b</sup>	ND
<i>Esr1</i>	2.04 $\pm$ 0.60 <sup>b</sup>	2.24 $\pm$ 0.57 <sup>b</sup>	1.82 $\pm$ 1.21	1.14 $\pm$ 0.05
<i>Ncoa1</i>	1.60 $\pm$ 0.25 <sup>b</sup>	2.76 $\pm$ 0.81 <sup>b</sup>	1.09 $\pm$ 0.57	1.25 $\pm$ 0.38
<i>Rarg</i>	2.15 $\pm$ 0.95 <sup>b</sup>	ND	1.75 $\pm$ 0.16 <sup>b</sup>	ND
<i>Grip</i>	1.73 $\pm$ 0.56 <sup>b</sup>	ND	1.87 $\pm$ 0.83	ND

<sup>a</sup> NP indicates not present in the array chip.

<sup>b</sup>  $p < 0.05$ .

<sup>c</sup> ND indicates not determined.

with these four pathways in the loaded tibia of B6 and C3H mice by real time PCR. We have shown previously with peripheral quantitative computed tomography, serum biochemical markers, and gene expression evidence that the 2-week four-point bending loading regimen significantly increased bone formation and bone mass in B6 mice but not in C3H mice *in vivo* (18). In this study, we showed that this 2-week loading regimen also caused massive increase in cancellous bone formation (stained in blue by the Goldner's stain) at the periosteum of the loaded tibia of B6 mice, but not in the loaded tibia of C3H mice (Fig. 4), confirming that *in vivo* mechanical loading increased periosteal bone formation in B6 but not C3H mice (8, 9). Table 3 shows that the 2-week four-point bending exercise regimen significantly enhanced the expression of genes associated with the four anabolic signaling pathways-of-interest in the loaded tibia of B6 mice, but not in loaded tibia of C3H mice, confirming that *in vivo* mechanical loading also led to differential up-regulation of genes associated with these four anabolic pathways in bones of B6 and not of C3H mice.

**Involvement of the ER Signaling Pathway in the Fluid Shear-induced Bone Cell Proliferation**—To confirm the involvement of the ER signaling pathway in the fluid shear-induced osteoblast proliferation, B6 osteoblasts were pretreated with 200 nM of ICI182780, a pure antagonist of ER (19), for 24 h prior to the 30-min fluid shear, and the effect of this inhibitor on the fluid shear-induced proliferation in B6 osteoblasts was then determined. Because Erk1/2 activation is required for the fluid

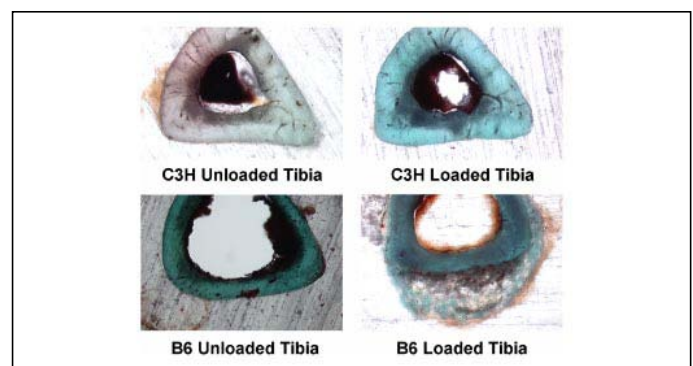


**FIGURE 4. Evidence that the 2-week four-point bending exercise regimen stimulates periosteal bone formation of the loaded tibia of 10-week female B6 mice but not of 10-week female C3H mice.** This figure shows the cross-sectional area of the nonloaded tibia (left photomicrographs) and the loaded tibia (right photomicrographs) of 10-week female C3H (the top photomicrographs) and B6 (bottom photomicrographs) mice. The sections were each stained with the Goldner's stain, which would stain bone tissues in blue color. This figure shows that the loading regimen caused a massive increase in cancellous bone formation at the periosteum of the loaded tibia of B6 mice but not of C3H mice.

shear-induced bone cell proliferation (20), the effect of the inhibitor on Erk1/2 activation (assessed by Erk1/2 phosphorylation) was also evaluated. The ICI182780 pretreatment slightly, but not significantly, enhanced basal [<sup>3</sup>H]thymidine incorporation (Fig. 5A) and Erk1/2 phos-

phorylation (Fig. 5B). However, this pretreatment completely abolished the fluid shear-induced cell proliferation and Erk1/2 activation, confirming that the ER pathway is essential for the bone cell mitogenic action of fluid shear.

**Involvement of the Canonical Wnt Signaling Pathway in the Fluid Shear-induced Bone Cell Proliferation**—There are two major Wnt signaling pathways as follows: the canonical pathway that involves  $\beta$ -catenin stabilization and activation, and the noncanonical pathway that involves G-protein-dependent intracellular  $\text{Ca}^{2+}$  release (21). We focused on the canonical pathway because this pathway plays an important role in osteoblast functions and bone formation (22). Because activation of the canonical Wnt pathway blocks the glycogen synthase kinase-3 $\beta$ -mediated  $\beta$ -catenin phosphorylation, which then prevents the subsequent ubiquitination and degradation of hyperphosphorylated  $\beta$ -catenin, the increase in cellular  $\beta$ -catenin protein can be an index of activation of the canonical Wnt pathway. In this regard, the 30-min steady fluid shear yielded a significant 2-fold increase in total  $\beta$ -catenin protein levels in B6 osteoblasts, although it had no significant effect in

C3H osteoblasts (Fig. 6), supporting the premise that fluid shear up-regulated the canonical Wnt pathway in B6 osteoblasts but not in C3H osteoblasts. Because the degradation (or “destabilization”) of  $\beta$ -catenin is mediated by phosphorylation, we had also attempted to measure the cellular levels of phosphorylated  $\beta$ -catenin in this study. Unfortunately, we were unable to detect any significant levels of phosphorylated  $\beta$ -catenin in the stressed or control osteoblasts with any of the currently commercial phospho-specific polyclonal antibodies against  $\beta$ -catenin (Santa Cruz Biotechnologies).

To determine the role of the canonical Wnt pathway in the fluid shear-induced osteoblast proliferation, B6 osteoblasts were pretreated with 10  $\mu\text{g}/\text{ml}$  of endostatin, a potent inhibitor of the canonical Wnt pathway (23), for 24 h prior to the 30-min fluid shear, and the effect of this inhibitor on fluid shear-induced cell proliferation and Erk1/2 activation was then determined. Although the endostatin pretreatment had no effect on basal [ $^3\text{H}$ ]thymidine incorporation and Erk1/2 phosphorylation, this pretreatment partially, but significantly, reduced the fluid shear-induced cell proliferation (Fig. 7A) and Erk1/2 activation (Fig. 7B). Although the primary inhibitory action of endostatin on the canonical Wnt pathway is mediated through an increase in  $\beta$ -catenin degradation, there is also evidence that endostatin suppressed  $\beta$ -catenin (*Ctnnb1*) gene expression (23). Thus, measurements of  $\beta$ -catenin mRNA transcript level may be used to assess the effect of endostatin on  $\beta$ -catenin activation. Accordingly, our findings that this dose of endostatin completely blocked the fluid shear-induced up-regulation of  $\beta$ -catenin mRNA (Fig. 7C) and protein levels (Fig. 7D) in B6 osteoblasts suggest that the partial inhibition of fluid shear-mediated cell proliferation was not due to an insufficient amount of endostatin.

**Involvement of the BMP Signaling Pathway in the Fluid Shear-induced Bone Cell Proliferation**—To assess whether the BMP signaling pathway has an essential role in the fluid shear-induced osteoblast proliferation, B6 osteoblasts were pretreated with 300 ng/ml of Noggin, an inhibitor of the BMP signaling pathway (24), for 24 h prior to the fluid shear. The Noggin pretreatment did not affect the basal cell proliferation and Erk1/2 activation but completely abolished the fluid shear-induced cell proliferation (Fig. 8A) and Erk1/2 activation (Fig. 8B) in B6 osteoblasts.

The role of the IGF-I signaling pathway in fluid shear-induced osteoblast proliferation was not evaluated in this study, because we and others have previously provided compelling evidence for the involvement

TABLE 3

Real time PCR analyses of in vivo gene expression of the Wnt, BMP/TGF- $\beta$ , IGF-I, and ER signaling pathways in response to the four-point bending exercise regimen in tibia of B6 inbred strain of mice as opposed to that of C3H inbred strain of mice (mean  $\pm$  S.D.,  $n = 6$  for each mouse strain)

None of the changes in the expression of the test genes in C3H mice was statistically significant.

Gene	B6 mice, fold changes	C3H mice, fold changes
<b>The canonical Wnt signaling pathway genes</b>		
<i>Wnt1</i>	1.81 $\pm$ 0.68 <sup>a</sup>	0.74 $\pm$ 0.45
<i>Wnt3a</i>	4.25 $\pm$ 2.12 <sup>b</sup>	3.10 $\pm$ 2.26
<i>Lrp5</i>	9.08 $\pm$ 2.76 <sup>b</sup>	3.22 $\pm$ 1.59
<i>Ctnnb1</i>	5.51 $\pm$ 2.62 <sup>b</sup>	1.29 $\pm$ 0.37
<b>The BMP/TGF-<math>\beta</math> signaling pathway genes</b>		
<i>Tgfb1</i>	2.10 $\pm$ 0.80 <sup>b</sup>	0.53 $\pm$ 0.34
<i>Bmpr1</i>	3.23 $\pm$ 0.96 <sup>b</sup>	1.64 $\pm$ 0.78
<i>Dlx1</i>	3.06 $\pm$ 1.21 <sup>a</sup>	Not detectable
<b>The IGF-I signaling pathway genes</b>		
<i>Igfr1</i>	2.74 $\pm$ 1.22 <sup>a</sup>	1.51 $\pm$ 1.08
<i>c-Fos</i>	3.73 $\pm$ 1.65 <sup>b</sup>	0.98 $\pm$ 0.65
<b>The ER signaling pathway genes</b>		
<i>Esr1</i>	3.17 $\pm$ 1.27 <sup>b</sup>	1.55 $\pm$ 0.53
<i>Ncoa1</i>	2.05 $\pm$ 0.61 <sup>b</sup>	1.56 $\pm$ 0.85

<sup>a</sup>  $p < 0.05$ .

<sup>b</sup>  $p < 0.01$ .

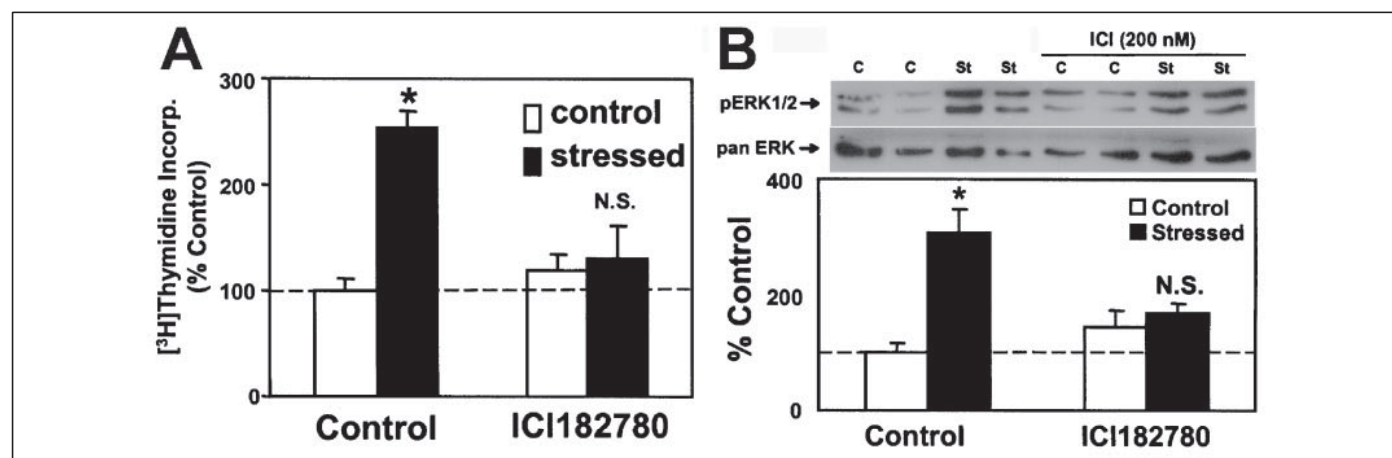
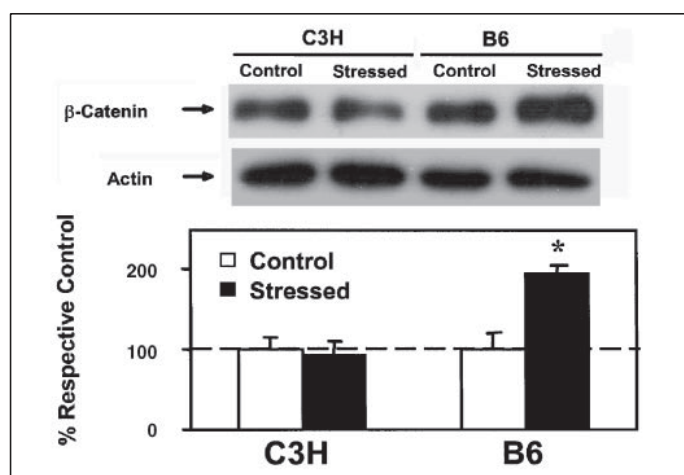


FIGURE 5. Effects of ICI182780 pretreatment on the fluid shear-induced proliferation and Erk1/2 activation in B6 osteoblasts. B6 osteoblasts were pretreated with 200 nM ICI182780 for 24 h prior to the fluid shear stress. Cell proliferation was measured by [ $^3\text{H}$ ]thymidine incorporation, and Erk1/2 activation was assessed by the pErk1/2 level. A shows the results on [ $^3\text{H}$ ]thymidine incorporation. Results are shown as mean  $\pm$  S.D. of six replicate each. B shows the representative Western blots of pErk1/2 and the pan-Erk bands and the summarized results of three separate experiments on the relative levels of pErk1/2 normalized against the total Erk1/2 (pan-Erk) protein level. The results are shown as percentage of the corresponding static control. The dashed lines represent 100% of the corresponding static control value. \*,  $p < 0.05$ . N.S., not significant.



**FIGURE 6. Effects of fluid shear on the cellular  $\beta$ -catenin protein level in C3H and B6 osteoblasts.** Top panel shows the representative Western blots of  $\beta$ -catenin and actin protein bands. Bottom panel summarizes the results of three separate experiments on the relative levels of  $\beta$ -catenin normalized against the actin level. The results are shown as percentage of the corresponding static control. The dashed lines represent 100% of the corresponding static control value. \*,  $p < 0.05$ .

of the IGF-1 signaling pathway in mechanotransduction in osteoblasts (25–28).

**Evidence that the Four Signaling Pathways-of-Interest Were Downstream to Integrin Activation and Cox-2 Expression**—To evaluate the relationship between the early mechanoresponsive events (*i.e.* integrin and/or Cox-2 activation) and up-regulation of gene expression associated with the four anabolic pathways-of-interest, we examined the effects of the inhibition of integrin activation and Cox-2 expression with a 2-h pretreatment of B6 osteoblasts with 100 nM echistatin and 1  $\mu$ M indomethacin, respectively, prior to the 30-min fluid shear stress. Gene expression associated with the four pathways-of-interest was then measured at 4 h after the shear stress by real time PCR. The test dosage of these inhibitors has each been shown to completely abolish the fluid shear-induced bone cell proliferation (4, 28). Table 4 shows that the 2-h echistatin or indomethacin pretreatment each blocked the shear stress-induced up-regulation of expression of genes associated with the four pathways-of-interest in B6 osteoblasts, indicating that the up-regulation of gene expression associated with these pathways-of-interest are downstream to integrin activation and Cox-2 expression.

## DISCUSSION

Previous studies in the B6-C3H pair of inbred strain of mice have demonstrated that genetics is an important determining factor of the bone formation response to mechanical loading (6–9, 16). In this regard, recent genetic studies with the quantitative trait linkage (29) and *N*-ethylnitrosourea mutagenesis (30) approaches on this pair of inbred mice have identified one or more quantitative trait loci on mouse chromosome 4 that are associated with mechanosensitivity in bone. However, the identity of the mechanosensitivity gene(s) or its underlying mechanism remains unknown. In this study, we showed that although primary osteoblasts isolated from B6 mice responded to a 30-min steady fluid shear stress of 20 dynes/cm<sup>2</sup> with an increase in cell proliferation and ALP activity *in vitro*, the same fluid shear did not produce similar anabolic effects in primary osteoblasts of C3H mice. Thus, it appears that the genetic component determining the mechanosensitivity of bone (at least in term of response to fluid shear) in this pair of inbred strain of mice is intrinsic to osteoblasts. Therefore, we conclude that primary osteoblasts of this pair of mouse strains can be used *in vitro* to investigate the identity and the underlying mechanism of the mechanosensitivity genes.

Global gene expression profiling by microarray analysis is a useful and complementary approach to genetic studies in the identification of genes and corresponding pathways contributing to a given phenotype (31). In this study, we have performed a microarray analysis with our in-house microarray chips on B6 osteoblasts that show good response to mechanical stimulation and C3H osteoblasts that show poor response. However, the relatively limited number of mouse gene fragments on our microarray chips precluded an extensive genome-wide assessment of the gene expression profile, and the incomplete annotation number of the gene fragments also did not permit computer-based analyses of the data. On the other hand, in contrast to previous microarray studies in chondrosarcoma cells (32) and in early osteochondroprogenitor cells (33), our study is unique in that we determined and compared a gene expression profile of B6 osteoblasts with that of C3H osteoblasts after a 30-min steady fluid shear stress. Because B6 osteoblasts, and not C3H osteoblasts, responded to fluid shear with an increase in cell proliferation and differentiation, an analysis of the genes whose expression is differentially regulated in B6 osteoblasts in response to the fluid shear could yield information about potential signal transduction pathways in the mechanotransduction mechanism, and this may help to identify potential candidate mechanosensitivity genes. Accordingly, the objective of this microarray study was not to obtain global gene expression profiling information but, rather, was to evaluate differential gene expression in B6 osteoblasts as opposed to C3H osteoblasts in response to the fluid shear to identify potential signaling pathways involved in the fluid shear-induced osteoblast proliferation. We hope to use this information to gain insights into the identity of mechanosensitivity genes that are responsible for the different bone formation response to loading in B6 and C3H mice.

Three observations of our microarray data were noteworthy. First, our study reveals that the expression of ~12% (*i.e.* 669 of 5,500) of the gene fragments on our in-house microarray chip was significantly affected (with more than half of them up-regulated) 4 h after the 30-min fluid shear in B6 osteoblasts. This relatively large number of mechanoresponsive genes in the good responding B6 osteoblasts underscores the complexity of mechanical stimulation in osteoblasts (4, 34). Of the 669 gene fragments whose expression was significantly altered by fluid shear, 514 (or 77%) were regulated differentially in B6 osteoblasts. This led us to postulate that the mechanosensitivity genes contributing to the different bone formation response in B6 and C3H mice may act on an upstream event of the mechanotransduction mechanism, leading to the subsequent changes in expression of up to 77% of the mechanoresponsive genes in B6 osteoblasts. Because there was also a differential up-regulation of at least two early mechanoresponsive genes, *i.e.* *Igf1* and *Cox-2*, in B6 osteoblasts as opposed to C3H osteoblasts, the mechanosensitivity genes in this pair of inbred mice are also upstream to these two early mechanoresponsive genes.

The second noteworthy observation is that a large number of the known mouse genes that were up-regulated differentially in B6 osteoblasts are associated with various anabolic cellular processes, such as cell proliferation, protein and RNA syntheses, energy metabolism, and intracellular transport and trafficking mechanisms. These findings support an anabolic action of the fluid shear in B6 osteoblasts but not in C3H osteoblasts. Also consistent with the previous findings that mechanical loading (or fluid shear) stimulated the local production of bone growth factors, such as IGF-I (35), IGF-II (36), and TGF- $\beta$ 1 (37, 38), we found that the fluid shear significantly up-regulated the expression of these growth factor genes as well as several other bone growth factor genes, such as *Pdgf*, *Fgf*, and *Bmp*, in mouse osteoblasts. The fact

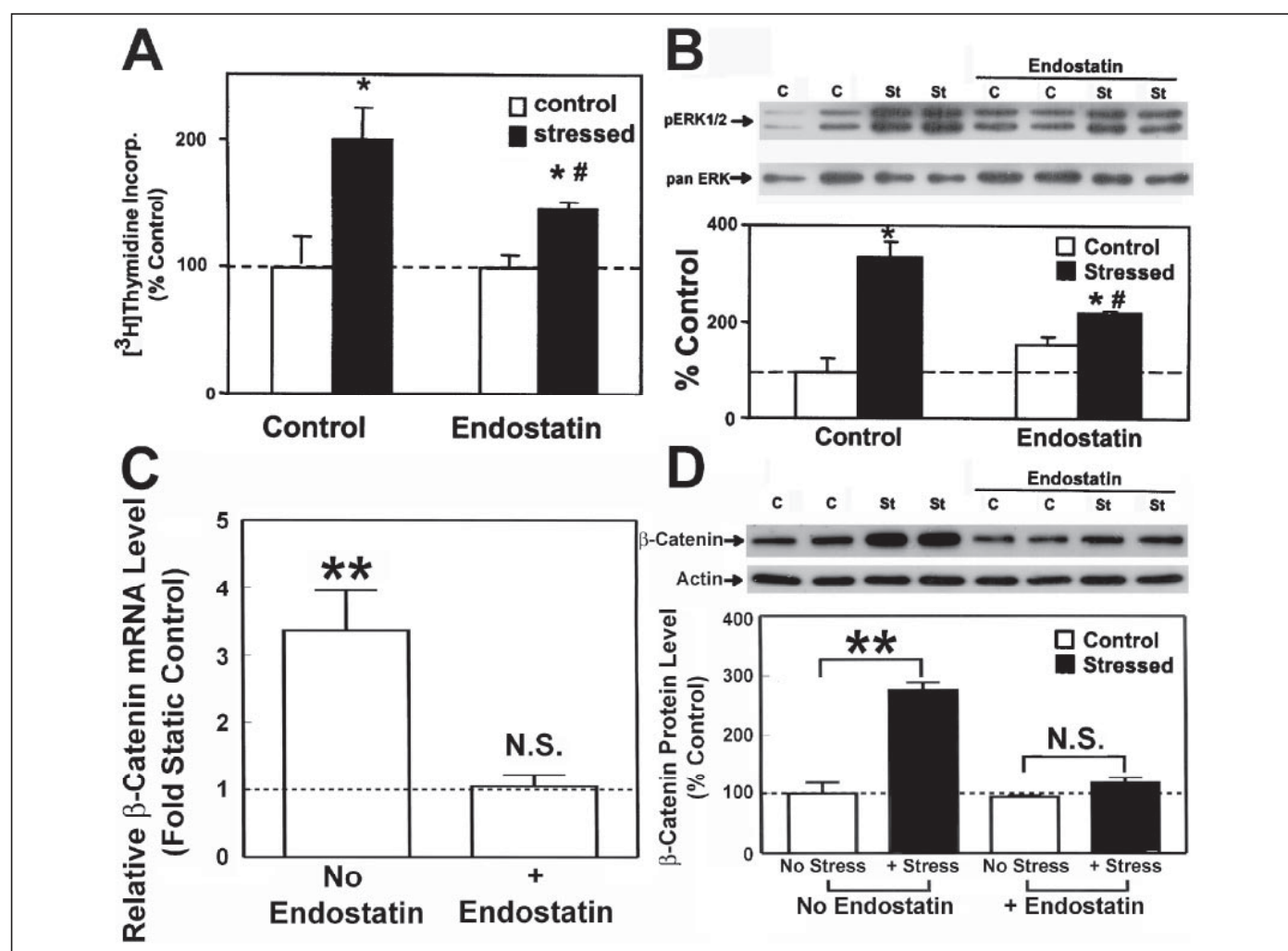


**FIGURE 7. Effects of endostatin pretreatment on the fluid shear-induced proliferation, Erk1/2, and  $\beta$ -catenin expression in B6 osteoblasts.** B6 osteoblasts were pretreated with 10  $\mu$ g/ml endostatin for 24 h prior to the fluid shear stress. Cell proliferation was measured by [ $^3$ H]thymidine incorporation, and Erk1/2 activation was assessed by the pErk1/2 level. A shows the results on [ $^3$ H]thymidine incorporation. Results are shown as mean  $\pm$  S.D. of six replicate each. B shows the representative Western blots of pErk1/2 and the pan-Erk bands and the summarized results of three separate experiments on the relative levels of pErk1/2 normalized against the total Erk1/2 (pan-Erk) protein level. The results are shown as percentage of the corresponding static control. The dashed lines represent 100% of the corresponding static control value. #,  $p < 0.05$  compared to corresponding static controls with the endostatin treatment; \*,  $p < 0.05$  compared to corresponding static controls without endostatin. C, the relative  $\beta$ -catenin mRNA level at 4 h after the fluid shear stress was determined with real time PCR. Results are shown as relative fold of static control (mean  $\pm$  S.D. of three replicate measurements). \*\*,  $p < 0.01$ . D shows the effects of the endostatin pretreatment on the  $\beta$ -catenin protein level at 4 h after the fluid shear. Top panel shows the representative Western blots of  $\beta$ -catenin and actin protein bands. Bottom panel summarizes the results of three separate experiments on the relative levels of  $\beta$ -catenin normalized against the actin level. The results are shown as percentage of the corresponding static control. The dashed lines represent 100% of the corresponding static control value. \*\*,  $p < 0.01$ . N.S., not significant; C, control; St, stressed cells.

that fluid shear stress also up-regulated several bone growth factor receptor genes (*i.e.* *Igfr1*, *Pthr1*, and *Bmpr1*) suggests that the molecular mechanism whereby mechanical loading (or fluid shear) stimulates osteoblast proliferation may in part involve paracrine/autocrine actions of bone growth factors. On the other hand, because several of these growth factor (*Igf2*, *Pdgfa*, *Vegfd*, *Fgf1*, *Tgfb1*, and *Bmp8b/Op2*) and receptor (*Bmpr1* and *Pthr1*) genes were also up-regulated in C3H osteoblasts in response to fluid shear, these growth factor and receptor genes are either unrelated to or upstream to the mechanosensitivity genes in the overall mechanotransduction mechanism in osteoblasts. We favor the latter possibility because there is strong circumstantial evidence that at least IGF-II (36) and TGF- $\beta$ 1 (39–41) are involved in the mechanical stimulation of bone formation.

The third and the more important observation of our microarray analysis is the finding that a number of genes associated with the four anabolic signaling pathways, namely the IGF-I, the ER, the canonical Wnt, and the BMP/TGF- $\beta$  signaling pathways, were up-regulated in B6 osteoblasts and not in C3H osteoblasts in response to the fluid

shear stress. The differential up-regulation of gene expression of these four signaling pathways in B6 osteoblasts was confirmed by real time PCR analyses. These findings raise the following interesting possibilities: (a) up-regulation of these four anabolic pathways is involved in the fluid shear-induced osteoblast proliferation; (b) these four signaling pathways are downstream to the mechanosensitivity genes in the overall mechanotransduction mechanism in osteoblasts. The latter possibility is consistent with our observation that the mechanosensitivity genes contributing to the different bone formation response in B6 and C3H mice may act on an upstream event of the mechanotransduction mechanism, leading to the subsequent changes of a large number of downstream mechanoresponsive genes, including genes associated with these four anabolic signaling pathways. Although our supporting data for the conclusion that each of these four pathways plays an essential role in the fluid shear-induced osteoblast proliferation were based on RNA expression data and not protein production data (with the exception of  $\beta$ -catenin), this conclusion was supported by the findings that a specific inhibitor of the

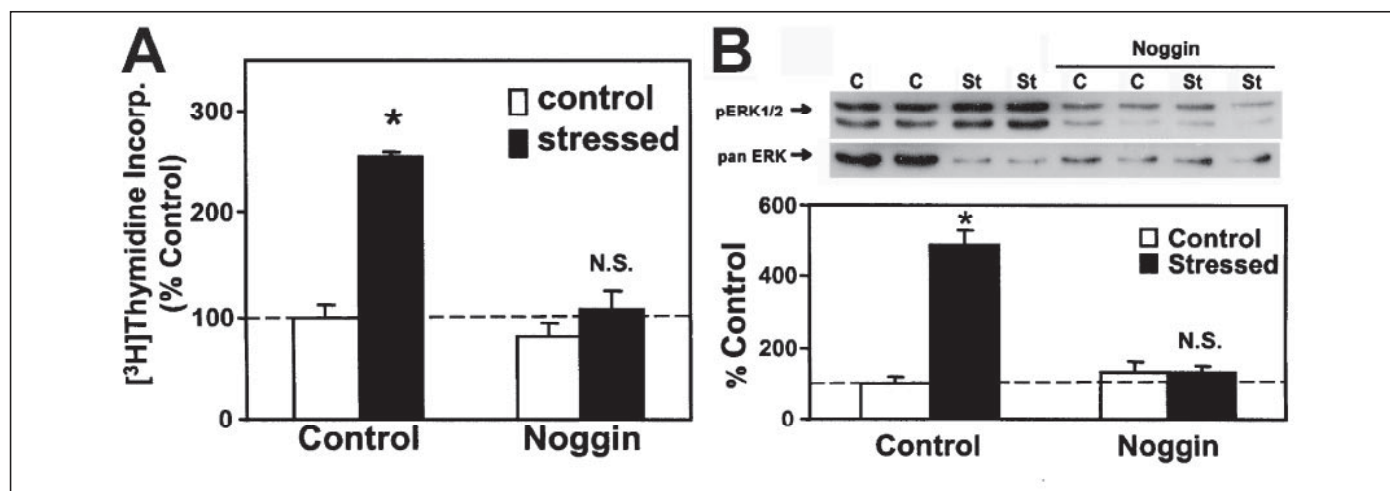


**FIGURE 8. Effects of Noggin pretreatment on the fluid shear-induced proliferation and Erk1/2 activation in B6 osteoblasts.** B6 osteoblasts were pretreated with 300 ng/ml Noggin for 24 h prior to the fluid shear stress. Cell proliferation was measured by [<sup>3</sup>H]thymidine incorporation, and Erk1/2 activation was assessed by the pErk1/2 level. **A** shows the results on [<sup>3</sup>H]thymidine incorporation. Results are shown as mean ± S.D. of six replicates each. **B** shows the representative Western blots of pErk1/2 and the pan-Erk bands and the summarized results of three separate experiments on the relative levels of pErk1/2 normalized against the total Erk1/2 (pan-Erk) protein level. The results are shown as percentage of the corresponding static control. The dashed lines represent 100% of the corresponding static control value. \*,  $p < 0.05$ . N.S., not significant; C, control; St, stressed cells.

**TABLE 4**

**Effects of inhibition of integrin activation and/or Cox-2 activity on the fluid shear-mediated up-regulation of gene expression of genes associated with the Wnt, BMP/TGF- $\beta$ , IGF-I, and ER signaling pathways in B6 osteoblasts (mean ± S.D.,  $n = 6$ )**

Up-regulation of gene expression was determined by real time PCR.

Gene	Inhibition of integrin activation (fold changes)		Inhibition of Cox-2 activity (fold changes)	
	No echistatin	+100 nM echistatin	No indomethacin	+1 $\mu$ M indomethacin
<b>The Wnt signaling pathway genes</b>				
<i>Wnt1</i>	2.51 ± 0.87 <sup>a</sup>	0.87 ± 0.15	2.59 ± 0.87 <sup>a</sup>	0.95 ± 0.35
<i>Wnt3a</i>	3.18 ± 0.68 <sup>b</sup>	1.19 ± 0.49	2.97 ± 1.00 <sup>a</sup>	1.35 ± 0.23
<i>Ctnnb1</i>	2.26 ± 0.53 <sup>a</sup>	1.27 ± 0.94	3.68 ± 1.13 <sup>a</sup>	0.76 ± 0.26
<b>The BMP/TGF-<math>\beta</math> signaling pathway genes</b>				
<i>Tgfb1</i>	2.99 ± 1.31 <sup>a</sup>	1.28 ± 0.63	2.47 ± 0.50 <sup>b</sup>	0.71 ± 0.09 <sup>b</sup>
<i>Bmpr1</i>	3.68 ± 1.49 <sup>a</sup>	0.94 ± 0.55	3.01 ± 0.17 <sup>b</sup>	0.73 ± 0.26
<i>Dlx1</i>	2.41 ± 0.63 <sup>a</sup>	0.93 ± 0.48	2.77 ± 0.95 <sup>a</sup>	1.04 ± 0.35
<b>The IGF-I signaling pathway genes</b>				
<i>Igf1r</i>	4.33 ± 1.98 <sup>a</sup>	0.77 ± 0.38	3.38 ± 1.16 <sup>a</sup>	0.97 ± 0.01 <sup>a</sup>
<i>c-Fos</i>	ND <sup>c</sup>	ND	2.83 ± 0.89 <sup>a</sup>	1.43 ± 0.49
<b>The ER signaling pathway genes</b>				
<i>Esr1</i>	3.74 ± 0.64 <sup>b</sup>	0.97 ± 0.60	3.69 ± 0.97 <sup>b</sup>	1.39 ± 0.44
<i>Ncoa1</i>	4.25 ± 2.03 <sup>a</sup>	0.79 ± 0.45	3.01 ± 0.39 <sup>b</sup>	0.92 ± 0.26

<sup>a</sup>  $p < 0.05$ .

<sup>b</sup>  $p < 0.01$ .

<sup>c</sup> ND indicates not determined.

ER signaling pathway (ICI182780), the canonical Wnt signaling pathway (endostatin), and the BMP signaling pathway (Noggin) each either completely abolished or markedly suppressed the fluid shear-induced cell proliferation in B6 osteoblasts.

We should emphasize that the *in vivo* application of mechanical loading through the 2-week four-point bending exercise regimen also led to up-regulation of expression of genes associated with the IGF-I, the ER, the canonical Wnt, and the BMP/TGF- $\beta$  signaling pathways in the loaded tibia of B6 mice. Accordingly, inasmuch as there is a general belief that osteocytes, and not osteoblasts, are most likely the primary sensors of mechanical loading in bone (42), we conclude that our *in vitro* findings with the primary mouse osteoblasts are probably physiologically relevant, even though the issue as to whether osteoblasts indeed have a functional role in translating the mechanical signal into biochemical signals in bone remains controversial.

There is compelling evidence for the involvement of the IGF-I, ER, and canonical Wnt signaling pathways in mechanotransduction in bone. With respect to the IGF-I signaling pathway, it has been reported that the bone cell mitogenic response to mechanical strain is mediated

through activation of the IGF-I receptor (25). We recently showed that fluid shear stress synergizes with IGF-I to stimulate Erk1/2 activation and osteoblast proliferation through integrin-dependent activation of the IGF-I signaling pathway (28), confirming a functional role of the IGF-I signaling pathway in the mechanical stimulation of osteoblast proliferation. Bikle and co-workers (26, 27) have also demonstrated that skeletal unloading induces resistance to IGF-I to induce bone formation, which is caused by inhibition of the IGF-I signaling pathway through down-regulation of the integrin pathway. Regarding the ER signaling pathway, Lanyon and co-workers (25, 43–46) have provided compelling evidence that ER, especially ER $\alpha$ , is essential for mechanical stimulation of bone formation. Specifically, they showed that knocking out the ER $\alpha$  (*Esr1*) expression in mice completely abolished the osteogenic response to mechanical loading *in vivo* (45) and *in vitro* (46). Their recent data suggested that ER $\beta$  may also have a certain role in mediating the mechanical signal to stimulate bone formation, because knocking out ER $\beta$  (*Esr2*) expression in female mice also blocked the mechanical stimulation of bone formation (47). In support of a role of the canonical Wnt pathway in mechanotransduction, it has been reported recently

that activation of the canonical Wnt signaling pathway by the G171V mutation of the low density LRP5 led to an enhanced response in the mechanical stimulation of bone formation (48) and that mechanical loading activated the canonical Wnt signaling pathway in TOPGAL mice, which are transgenic mice expressing a  $\beta$ -galactosidase reporter gene driven by a T cell factor  $\beta$ -catenin-responsive promoter (49). There is also evidence for a role of the TGF- $\beta$  signaling pathway in mechanotransduction in bone, although the evidence is less compelling. Accordingly, mechanical loading or fluid shear significantly up-regulated the expression and secretion of TGF- $\beta$ 1 in bone cells, whereas mechanical unloading markedly suppressed *Tgfb1* expression in bone (37–41). Consequently, our findings that the IGF-I, the ER, the canonical Wnt, and even the TGF- $\beta$  signaling pathways are involved in the mechanotransduction mechanism in B6 osteoblasts are not entirely surprising.

What was surprising to us is the finding that blocking the BMP signaling pathway in B6 osteoblasts by Noggin led to the complete abolition of the fluid shear-induced osteoblast proliferation. In this regard, although it is well known that BMPs are potent osteoblast differentiation agents, which stimulated bone formation primarily through its ability to promote osteoblast differentiation (50), there has been little evidence that BMPs can directly stimulate osteoblast proliferation. Consequently, the mechanism whereby inhibition of the BMP signaling pathway by Noggin blocked the fluid shear-induced cell proliferation and Erk1/2 activation in B6 osteoblasts is unclear. However, it has been demonstrated that there are significant cross-talks among the various signaling pathways involved in mechanotransduction (4, 34). Specifically, there is evidence in other cell types that the BMP signaling pathway can cross-talk with other signaling pathways, including the canonical and noncanonical Wnt pathways (51), and the ER pathway (52). Because we have recent preliminary data that inhibition of the BMP pathway with Noggin could completely block the fluid shear-induced up-regulation of the expression of genes associated with the canonical Wnt pathway in B6 osteoblasts (53), we tentatively conclude that the canonical Wnt pathway is downstream to the BMP signaling pathway in fluid shear stress-induced osteoblast proliferation. Accordingly, we suggest that the mechanism whereby the BMP signaling pathway mediates the fluid shear-induced osteoblast proliferation involves the subsequent activation of the canonical Wnt signaling pathway.

It is also foreseeable that there would be cross-talks among these four anabolic pathways, as there is evidence that the BMP signaling pathway can cross-talk with the ER pathway in other cell types (52) and that the IGF-I signaling pathway interacts with the ER pathway in the proliferative response of osteoblasts to mechanical strain (25). Consequently, it may be speculated that these potential cross-talks may explain why inhibition of a single signaling pathway (e.g. the ER or the BMP pathway) could lead to complete abrogation of the fluid shear-induced cell proliferation and Erk1/2 activation in B6 osteoblasts.

It is also intriguing to note that endostatin was only able to partially block the fluid shear-induced Erk1/2 activation and cell proliferation, suggesting that the canonical Wnt signaling pathway is only partially involved in mechanotransduction in osteoblasts. On the other hand, fluid shear stress appeared to also up-regulate the noncanonical Wnt signaling pathway, as the expression of *Wnt5a* was also up-regulated in response to the fluid shear stress in B6 osteoblasts. Thus, it is possible that the mechanical stimulation of osteoblast proliferation may involve up-regulation of both canonical and noncanonical Wnt pathways. Thus, blocking the canonical Wnt pathway alone is insufficient to block completely the fluid shear-induced osteoblast proliferation.

The exact molecular mechanism as to how each of these four anabolic signaling pathways mediate the fluid shear-induced osteoblast prolifer-

ation remains to be defined. However, we (20) and others (54) have demonstrated that Erk1/2 activation is required and essential for the mechanical stimulation of osteoblast proliferation. Accordingly, because blocking each of these pathways by a specific inhibitor completely blocked the fluid shear-induced cell proliferation and Erk1/2 activation in osteoblasts (this study and see Ref. 28), we believe that the molecular mechanism whereby each of these four anabolic signaling pathways mediates the mechanical stimulation of osteoblast proliferation involves Erk1/2 activation or converges to steps leading to Erk1/2 activation.

The role of early mechanoresponsive genes, such as integrins and *Cox-2*, in the mechanical stimulation of osteoblast proliferation has been documented (4, 18, 34). This study confirms that the fluid shear up-regulated the expression of at least two early mechanoresponsive genes, i.e. *Igtb1* and *Cox-2*, in B6 osteoblasts. This study also demonstrates for the first time that the up-regulation of these early mechanoresponsive genes was seen only in B6 osteoblasts and not in C3H osteoblasts, indicating that these two early mechanoresponsive genes are downstream effectors to the mechanosensitivity genes contributing to the differential osteogenic responses to mechanical loading in C3H-B6 pair of mice. More importantly, this study shows that blocking the fluid shear-induced stimulation of integrins (with echistatin) and *Cox-2* (with indomethacin) each prevented the up-regulation of gene expression associated with the four signaling pathways (i.e. the IGF-I, ER, BMP/TGF- $\beta$ , and canonical Wnt pathways) in B6 osteoblasts. Consequently, we conclude that these four signaling pathways are downstream to these two early mechanoresponsive genes in the mechanotransduction mechanism.

On the basis of our findings, we have advanced a model for the molecular mechanism of mechanotransduction in osteoblasts (Fig. 9). In this model, we postulate that the fluid shear (or mechanical strain or stress) on osteoblasts would lead to up-regulation of the expression of integrins and their signaling pathways through the putative mechanosensors and yet-to-be-defined mechanisms. Up-regulation of the integrin signaling pathway would result in the induction of *Cox-2* expression (55) as well as other early mechanoresponsive genes, such as *c-Fos* (18). One of the consequences of the activation of these early mechanoresponsive genes is the up-regulation of local growth factor production, such as IGF-I, BMPs, and TGF- $\beta$ s as well as ERs. The increased production of these growth factors would act as paracrine/autocrine effectors to activate their respective signaling pathways. We further postulate that the activation of the BMP/TGF- $\beta$  pathway would lead to up-regulation of local production of Wnts, which then activate both the canonical and non-canonical Wnt signaling pathways. Activation of each of these four pathways would each lead to Erk1/2 activation, which then subsequently would result in stimulation of osteoblast proliferation and/or differentiation. Because there is strong evidence that the integrin signaling pathway could cross-talk with the IGF-I signaling pathway through recruitment of Src homology protein phosphatase-1 (SHP-1) between integrins and IGF-I receptor (28, 56), the ER signaling pathway through activation of c-Src (57), the Wnt signaling pathway through activation of integrin-linked kinase (58), and the BMP/TGF- $\beta$  pathway (59), presumably also through c-Src activation (60), we further postulate that the cross-talks between the integrin signaling pathway and the four other pathways-of-interest further enhance up-regulation of these signaling pathways. This model is the current focus of investigations in our laboratory.

Finally, perhaps the most important information derived from this study is the finding that the mechanosensitivity genes contributing to the good and poor bone formation response, respectively, in B6 and

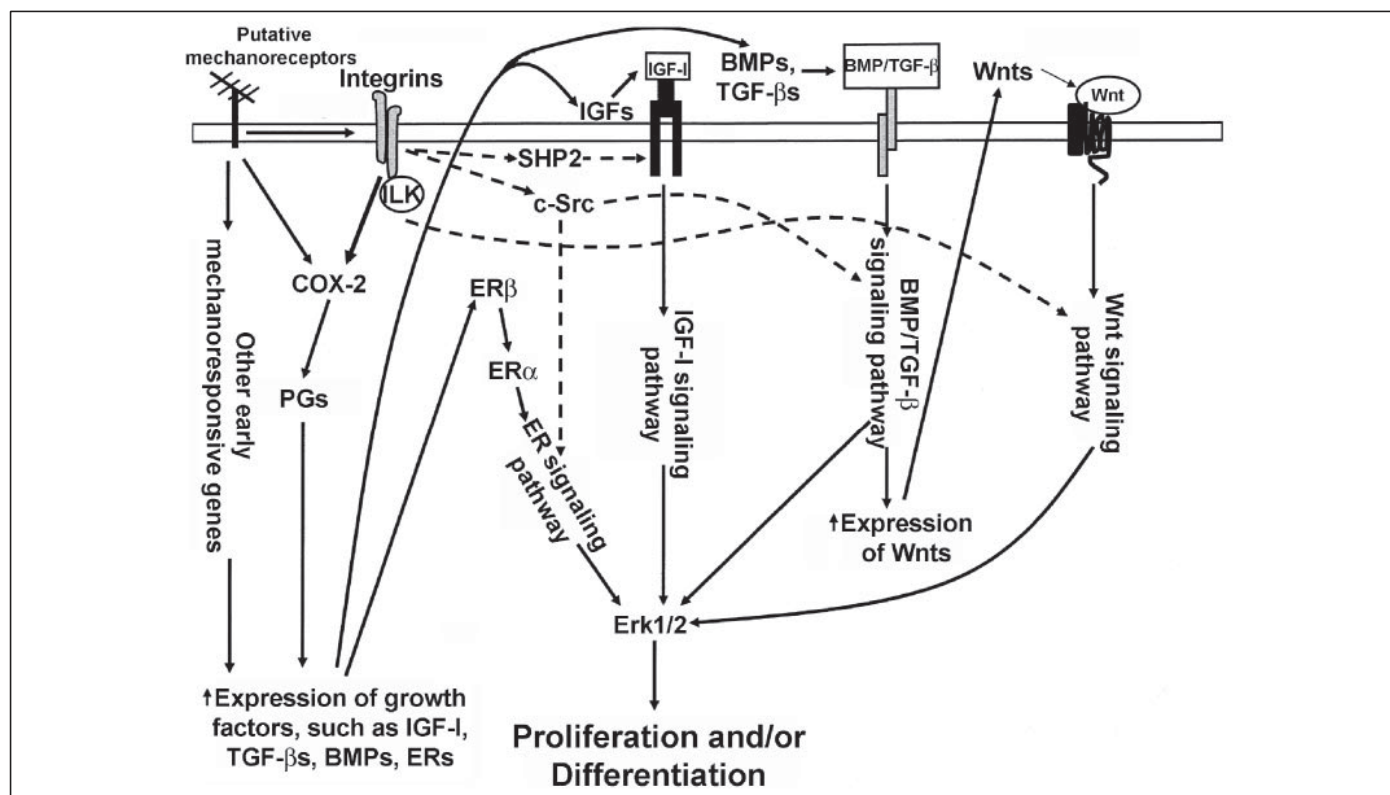


FIGURE 9. A proposed model of the molecular mechanism whereby mechanical stimulation up-regulates expression of genes associated with the IGF-I, the ER, the BMP/TGF- $\beta$ , and the Wnt pathways. Please see "Discussion" for detailed description of the model.

C3H inbred strain of mice are upstream to the IGF-I, the ER, the Wnt, and the BMP/TGF- $\beta$  signaling pathways. In this regard, we believe that the mechanosensitivity may act on an upstream event between the putative mechanosensors and the activation of integrin signaling pathway (Fig. 9). This information should be very useful in our continuing efforts to search for the identity and underlying mechanism of the mechanosensitivity genes that are responsible for the different bone formation response in this pair of inbred mice. Accordingly, we believe that the ability of a candidate gene to up-regulate the expression of genes associated with all of these four signaling pathways in response to mechanical stimulation can be a useful functional screen assay for candidate genes of mechanosensitivity. Moreover, because the mechanosensitivity genes appear to be upstream regulators, this information may allow us to narrow our search of candidate genes to upstream regulators. In this regard, the quantitative trait locus for mechanosensitivity in mouse chromosome 4 identified by Robling *et al.* (29) is a large 40–80-centimorgan region and contains several hundreds of genes, including a number of upstream signal transduction regulator genes. These include receptor genes (such as *Lepr*, *Il22ra1*, *Ptafr*, *Oprd1*, *Htr1D*, and *Htr6*, *Epha1*, and *Ephb2*, and *Tnfr*), several receptor tyrosine kinases, *Ptpu*, ion channel genes (*Gjb3*), and several other candidate genes. In order for any of these or other candidate genes to be the mechanosensitivity gene, the candidate gene must be able to up-regulate these four aforementioned anabolic signaling pathways in response to mechanical stimulation. Two genes (*Bmp8/Op2* and *Jun*) whose expression was up-regulated by the fluid shear in osteoblasts were located within this quantitative trait locus. However, because the expression of *Bmp8/Op2* was up-regulated by fluid shear in both B6 and C3H osteoblasts, and because *Jun* is a downstream effector of the signaling pathways-of-interest, neither of these two genes would likely be the mechanosensitivity gene(s) that contributes to the different bone

formation response to mechanical loading in B6 and C3H inbred strain of mice.

In conclusion, we have demonstrated that fluid shear induced an anabolic response in B6 osteoblasts but not in C3H osteoblasts, indicating that the differential osteogenic response to mechanical stimulation in this pair of inbred strain of mice is intrinsic to osteoblasts. More importantly, we showed for the first time that fluid shear differentially up-regulated the expression of genes associated with four anabolic signaling pathways (*i.e.* the IGF-I, the ER, the Wnt, and the BMP/TGF- $\beta$  pathways) in the good responder, B6 osteoblasts, and not in the poor responder, C3H osteoblasts. An important implication of these findings is that the mechanosensitivity genes contributing to the different bone formation response in B6 and C3H inbred strain of mice are upstream to these four anabolic signaling pathways. This information should be very helpful in our search of the identity and/or the underlying mechanism of mechanosensitivity genes.

## REFERENCES

- Hillam, R. A., and Skerry, T. M. (1995) *J. Bone Miner. Res.* **10**, 683–689
- Bikle, D. D., and Halloran, B. P. (1999) *J. Bone Miner. Metab.* **17**, 233–244
- Hillsley, M. V., and Frangos, J. A. (1994) *Biotechnol. Bioeng.* **43**, 573–581
- Kapur, S., Baylink, D. J., and Lau, K.-H. W. (2003) *Bone (NY)* **32**, 241–251
- Frost, H. M. (1982) *Metab. Bone Dis. and Relat. Res.* **4**, 217–229
- Kodama, Y., Umemura, Y., Nagasawa, S., Beamer, W. G., Donahue, L. R., Rosen, C. R., Baylink, D. J., and Farley, J. R. (2000) *Calcif. Tissue Int.* **66**, 298–306
- Kodama, Y., Dimai, H. P., Wergedal, J., Sheng, M., Malpe, R., Kutilek, S., Beamer, W., Donahue, L. R., Rosen, C., Baylink, D. J., and Farley, J. (1999) *Bone (NY)* **25**, 183–190
- Akhter, M. P., Cullen, D. M., Pedersen, E. A., Kimmel, D. B., and Recker, R. R. (1998) *Calcif. Tissue Int.* **63**, 442–449
- Robling, A. G., and Turner, C. H. (2002) *Bone (NY)* **31**, 562–569
- Sheng, M. H.-C., Lau, K.-H. W., Beamer, W. G., Baylink, D. J., and Wergedal, J. E. (2004) *Bone (NY)* **35**, 711–719
- He, X., Ku, D. N., and Moore, J. E., Jr. (1993) *Annu. Biomed. Eng.* **21**, 45–49
- Lau, K.-H. W., Lee, M. Y., Linkhart, T. A., Mohan, S., Vermeiden, J., Liu, C. C., and

- Baylink, D. J. (1985) *Biochim. Biophys. Acta* **840**, 56–68
13. Farley, J. R., and Jorch, U. M. (1983) *Arch. Biochem. Biophys.* **221**, 477–488
14. Li, X., Mohan, S., Gu, W., and Baylink, D. J. (2001) *Mamm. Genome* **12**, 52–59
15. Akhter, M. P., Raab, D. M., Turner, C. H., Kimmel, D. B., and Recker, R. R. (1992) *J. Biomech.* **25**, 1241–1246
16. Kesavan, C., Mohan, S., Oberholzer, S., Wergedal, J. E., and Baylink, D. J. (2005) *J. Appl. Physiol.* **99**, 1951–1957
17. Sheng, M. H.-C., Baylink, D. J., Beamer, W. G., Donahue, L. R., Lau, K.-H. W., and Wergedal, J. E. (2002) *Bone (NY)* **30**, 486–491
18. Pavalko, F. M., Chen, N. X., Turner, C. H., Burr, D. B., Atkinson, S., Hsieh, Y. F., Qiu, J., and Duncan, R. L. (1998) *Am. J. Physiol.* **275**, C1591–C1601
19. DeFriend, D. J., Anderson, E., Bell, J., Wilks, D. P., West, C. M., Mansel, R. E., and Howell, A. (1994) *Br. J. Cancer* **70**, 204–211
20. Kapur, S., Chen, S.-T., Baylink, D. J., and Lau, K.-H. W. (2004) *Bone (NY)* **35**, 534–535
21. Wang, H. Y., and Malbon, C. C. (2004) *Cell. Mol. Life Sci.* **61**, 69–75
22. Westendorf, J. J., Kahler, R. A., and Schroeder, T. M. (2004) *Gene (Amst.)* **341**, 19–39
23. Hanai, J., Gloy, J., Karumanchi, S. A., Kale, S., Tang, J., Hu, G., Chan, B., Ramchandran, R., Jha, V., Sukhatme, V. P., and Sokol, S. (2002) *J. Cell Biol.* **158**, 529–539
24. Warren, S. M., Brunet, L. J., Harland, R. M., Economides, A. N., and Longaker, M. T. (2003) *Nature* **422**, 625–629
25. Cheng, M., Zaman, G., Rawlinson, S. C., Mohan, S., Baylink, D. J., and Lanyon, L. E. (1999) *J. Bone Miner. Res.* **14**, 1742–1750
26. Sakata, T., Halloran, B. P., Elalieh, H. Z., Munson, S. J., Rudner, L., Venton, L., Ginzinger, D., Rosen, C. J., and Bikle, D. D. (2003) *Bone (NY)* **32**, 669–680
27. Sakata, T., Wang, Y., Halloran, B. P., Elalieh, H. Z., Cao, J., and Bikle, D. D. (2004) *J. Bone Miner. Res.* **19**, 436–446
28. Kapur, S., Mohan, S., Baylink, D. J., and Lau, K.-H. W. (2005) *J. Biol. Chem.* **280**, 20163–20170
29. Robling, A. G., Li, J., Shultz, K. L., Beamer, W. G., and Turner, C. H. (2003) *FASEB J.* **17**, 324–326
30. Srivastava, A. K., Kapur, S., Mohan, S., Yu, H., Kapur, S., Wergedal, J., and Baylink, D. J. (2005) *J. Bone Miner. Res.* **20**, 1041–1050
31. Gu, W.-K., Li, X.-M., Roe, B. A., Lau, K.-H. W., Edderkaoui, B., Mohan, S., and Baylink, D. J. (2003) *Curr. Genomics* **4**, 75–102
32. Karjalainen, H. M., Sironen, R. K., Elo, M. A., Kaarniranta, K., Takigawa, M., Helminen, H. J., and Lamm, M. J. (2003) *Biorheology* **40**, 93–100
33. Segey, O., Samach, A., Faerman, A., Kalinski, H., Beiman, M., Gelfand, A., Turam, H., Boguslavsky, S., Moshayov, A., Gottlieb, H., Kazanov, E., Nevo, S., Robinson, D., Skaliter, R., Einat, P., Binderman, I., and Feinstein, E. (2004) *Bone (NY)* **34**, 246–260
34. Hughes-Fulford, M. (2004) *Sci. STKE* **2004**, RE12
35. Lean, J. M., Jagger, C. J., Chambers, T. J., and Chow, J. W. (1995) *Am. J. Physiol.* **268**, E318–E327
36. Rawlinson, S. C., Mohan, S., Baylink, D. J., and Lanyon, L. E. (1993) *Calcif. Tissue Int.* **53**, 324–329
37. Klein-Nulend, J., Roelofs, J., Sterck, J. G., Semeins, C. M., and Burger, E. H. (1995) *J. Cell. Physiol.* **163**, 115–119
38. Liegibel, U. M., Sommer, U., Bundschuh, B., Schweizer, B., Hilscher, U., Lieder, A., Nawroth, P., and Kasperk, C. (2004) *Exp. Clin. Endocrinol. Diabetes* **112**, 356–363
39. Tanaka, S. M., Sun, H. B., Roeder, R. K., Burr, D. B., Turner, C. H., and Yokota, H. (2005) *Calcif. Tissue Int.* **76**, 261–271
40. Sakai, K., Mohtai, M., and Iwamoto, Y. (1998) *Calcif. Tissue Int.* **63**, 515–520
41. Raab-Cullen, D. M., Thiede, M. A., Petersen, D. N., Kimmel, D. B., and Recker, R. R. (1994) *Calcif. Tissue Int.* **55**, 473–478
42. Bonewald, L. F. (2002) *J. Musculoskelet. Neuronal Interact.* **2**, 239–241
43. Damien, E., Price, J. S., and Lanyon, L. E. (2002) *J. Bone Miner. Res.* **15**, 2169–2177
44. Jessop, H. L., Sjöberg, M., Cheng, M. Z., Zaman, G., Wheeler-Jones, C. P., and Lanyon, L. E. (2001) *J. Bone Miner. Res.* **16**, 1045–1055
45. Lee, K., Jessop, H., Suswillo, R., Zaman, G., and Lanyon, L. (2003) *Nature* **424**, 389
46. Jessop, H. L., Suswillo, R. F., Rawlinson, S. C., Zaman, G., Lee, K., Das-Gupta, V., Pitsillides, A. A., and Lanyon, L. E. (2004) *J. Bone Miner. Res.* **19**, 938–946
47. Lee, K. C., Jessop, H., Suswillo, R., Zaman, G., and Lanyon, L. E. (2004) *J. Endocrinol.* **182**, 193–201
48. Johnson, M. L. (2004) *J. Musculoskelet. Neuronal Interact.* **4**, 135–138
49. Hens, J. R., Wilson, K. M., Dann, P., Chen, X., Horowitz, M. C., and Wysolmerski, J. J. (2005) *J. Bone Miner. Res.* **20**, 1103–1113
50. Canalis, E., Economides, A. N., and Gazzerro, E. (2003) *Endocr. Rev.* **24**, 218–235
51. von Bubnoff, A., and Cho, K. W. Y. (2001) *Dev. Biol.* **239**, 1–14
52. Paez-Pereda, M., Giacomini, D., Refojo, D., Nagashima, A. C., Hopfner, U., Grubler, Y., Chervin, A., Goldberg, V., Goya, R., Hentges, S. T., Low, M. J., Holsboer, F., Stalla, G. K., and Arzt, E. (2003) *Proc. Natl. Acad. Sci. U. S. A.* **100**, 1034–1039
53. Kapur, S., Baylink, D. J., and Lau, K.-H. W. (2005) *J. Bone Miner. Res.* **20**, Suppl. 1, S240 (Abstr. SU219)
54. Lai, C.-F., Chaudhary, L., Fausto, A., Halstead, L. R., Ory, D. S., Avioli, L. V., and Cheng, S. L. (2001) *J. Biol. Chem.* **276**, 14443–14450
55. Ponik, S. M., and Pavalko, F. M. (2004) *J. Appl. Physiol.* **97**, 135–142
56. Clemmons, D. R., and Maile, L. A. (2005) *Mol. Endocrinol.* **19**, 1–11
57. Kim, H., Laing, M., and Muller, W. (2005) *Oncogene* **24**, 5629–5636
58. Novak, A., Hsu, S. C., Leung-Hagsteejn, C., Radeva, G., Papkoff, J., Montesano, R., Roskelley, C., Grosschedl, R., and Dedhar, S. (1998) *Proc. Natl. Acad. Sci. U. S. A.* **95**, 4374–4379
59. Lai, C. F., and Cheng, S. L. (2005) *J. Bone Miner. Res.* **20**, 330–340
60. Rhee, S. T., and Buchman, S. R. (2005) *Ann. Plast. Surg.* **55**, 207–215

## Novel loci regulating bone anabolic response to loading: Expression QTL analysis in C57BL/6JXC3H/HeJ mice cross

Chandrasekhar Kesavan<sup>a</sup>, David J. Baylink<sup>b</sup>, Susanna Kapoor<sup>a</sup>, Subburaman Mohan<sup>a,b,\*</sup>

<sup>a</sup> Musculoskeletal Disease Center, Jerry L. Pettis VA Medical Center 11201 Benton Street, Loma Linda, CA 92357, USA

<sup>b</sup> Department of Medicine, Loma Linda University, 11234 Anderson Street, Loma Linda, CA 92354, USA

Received 15 February 2007; revised 30 March 2007; accepted 17 April 2007

Available online 27 April 2007

### Abstract

Variations in the expression levels of bone marker genes among the inbred strains of mice in response to mechanical loading (ML) are largely determined by genetic factors. To explore this, we performed four-point bending on tibiae of 10-week female F2 mice of B6XC3H cross using 9N at 2 Hz, 36 cycles, once per day for 12 days. We collected tibiae from these mice for RNA extraction. We then measured the expression changes of bone marker genes, bone sialoprotein (BSP), alkaline phosphatase (ALP) and housekeeping genes,  $\beta$ -actin and peptidylprolyl isomerase A (PPIA), by using real-time PCR in both the loaded and the non-loaded tibiae of F2 mice ( $n=241$ ). A genome-wide scan was performed using 111 micro satellite markers in DNA sample collected from these mice. Mean increase in gene expression, expressed as fold change, ranges from 2.8 to 3.0 for BSP and 2.7 to 2.8 for ALP. Both showed a skewed distribution with a heritability response of 87 to 91%. Absence of significant correlation between the increased gene expression vs. body weight (BW) and bone size (BS) suggests that bone response to loading is independent of BS or BW. Non-parametric mapping (MapQTL program 5) revealed that BSP and ALP expression in response to bending was regulated by several significant and suggestive QTL: Loci regulating both BSP and ALP were located on Chr 8 (60.1 cM), 16 (45.9 cM), 17 (14.2 cM), 18 (38.0 cM) and Chr 19 (3.3 cM); Loci specific to BSP were found on Chrs 1 (LOD score 10.4 at 91.8 cM), 5 (5.2 at 73.2 cM) and 9 (7.0 at 13.1 cM); Loci regulating only ALP were found on Chrs 1 (7.6 at 46 and 75.4 cM), 3 (8.3 at 47 cM) and 4 (5.6 at 54.6 cM). QTLs on Chrs 1, 3, 8, 9, 17 and 18 correspond to QTLs we previously reported by pQCT measurements, thus validating these findings. In addition, we found that the QTL associated with non-loaded tibiae for BSP and ALP on Chrs 4, 16 and 18 was identical to the QTLs associated with ML. This finding suggests that regions on these chromosomes are responsible for natural variation in expression of BSP and ALP as well as for ML. This is the first expression study to provide evidence for the presence of multiple genetic loci regulating bone anabolic response to loading in the B6XC3H intercross and will lead to a better understanding of how exercise improves the skeletal mass.

© 2007 Elsevier Inc. All rights reserved.

**Keywords:** Expression QTL; Mechanical loading; Inbred strains; Bone markers; Four-point bending

### Introduction

Mechanical loading (ML) plays an important role in the maintenance of bone mass and strength. Several reports have provided evidence that mechanical loading stimulates bone formation and that immobilization or a loss of mechanical stimulation, such as bed rest or space flight, leads to a de-

crease in bone formation and an increase in bone loss [1,10,13,14,18,24,30,31,3,4,11,17,26,36]. Recent studies in humans have demonstrated that bone anabolic response varies widely among individuals when subjected to the same degree of mechanical load ranging from good to moderate response [7,9,27,29]. Analogously, experimental animals, particularly inbred strains of mice, have also shown variability with respect to mechanical loading. Studies have shown that there are greater fold changes in bone marker genes in C57BL/6J (B6) mice as compared with C3H/HeJ (C3H) mice when subjected to a same loading regimen [11]. It is likely that these variations in the bone anabolic response, in both human and mouse models, are due to

\* Corresponding author. Musculoskeletal Disease Center (151), Jerry L. Pettis Memorial VA Medical Center, 11201 Benton Street, Loma Linda, CA 92357, USA. Fax: +1 909 796 1680.

E-mail address: Subburaman.Mohan@med.va.gov (S. Mohan).

differences in the transcription levels of genes, i.e., they are genetically controlled.

One of the approaches often used to study the genetic regulation of an observed phenotype is QTL mapping. This approach has been well-established in both human and mouse models and has revealed hundreds of chromosomal regions containing genes affecting bone phenotypes such as BMD, bone size and bone strength [2,15,22,23]. Previously, using this traditional or “classical” quantitative trait loci analysis (cQTL), we have identified several loci that regulate BMD and bone size in response to mechanical loading in the B6XC3H cross [12]. In order to validate these findings and to discover additional QTLs, we have used expression QTL mapping (eQTL) in the same inbred strain cross.

Recently, a number of studies in humans and animal models have provided evidence that expression levels of genes are amenable for genetic analysis in search of loci for the phenotypic variation [8,20,25,28,32,34,35]. This eQTL approach has several advantages: (1) it can map a QTL to the gene itself, indicating whether *cis* changes or *trans* factors are responsible for the different expression levels, (2) it allows one to identify genetic regions that directly control the expression levels of genes and (3) it validates that the chromosomal region identified from cQTL analysis and determines that these regions are responsible for the difference in transcription levels of genes whether responsible for the difference in bone response to loading between the two strains of mice. In the present study, we have treated expression levels of bone markers genes as quantitative traits for two inbred strains, C57BL/6J and C3H/HeJ, a good and poor responder, respectively, in order to perform a genome-wide search of loci regulating bone anabolic response to mechanical loading.

## Materials and methods

### Mice

Female B6 and male C3H mice were obtained from the Jackson Laboratory (Bar Harbor, ME) to produce C3HB6 F1 mice, which were intercrossed to generate F2 mice. All mice were housed under the standard conditions of 14-h light and 10-h darkness, and had open access to food and water. The experimental protocols were in compliance with animal welfare regulation and approved by local IACUC.

### In-vivo loading model/regimen

Mechanical loading was performed using a four-point bending device (Instron, Canton, MA) on 10-week female F2 mice, following a previously reported protocol [11,12]. The mice were loaded using a 9 Newton (N) force at a frequency of 2 Hz for 36 cycles, once a day under inhaleable (5% halothane and 95% oxygen) anesthesia. The loading procedure was repeated for 6 days with 1 day of rest for 2 weeks. On the 15th day, mice were sacrificed and tibiae [loaded (bended bones) and non-external loaded (non-bended bones)] of the F2 mice were collected and stored in RNA later at  $-80^{\circ}\text{C}$  for further study.

### RNA extraction

A Qiagen lipid extraction kit [Qiagen, Valencia, CA] was used to extract RNA from F2 bones with the following modification. After euthanization, tissues were removed from test mice, immediately transferred into liquid nitrogen and then stored at  $-80^{\circ}\text{C}$  until RNA extraction. Bones were ground into fine powder using mortar and pestle with liquid nitrogen. Approximately

1 ml of Trizol was added to each sample and ground until it became a fine powder. This fine bone powder was transferred to fresh 1.5 ml RNase free tubes. Chloroform (200  $\mu\text{l}$ ) was added to each sample, each sample was vortexed for 15 seconds (s) and incubated at room temperature for 3 min. The samples were then centrifuged at  $12,000\times g$  for 15 min and the aqueous layer was removed to a fresh tube after centrifugation. Approximately 700  $\mu\text{l}$  of ethanol was added to the fresh samples and vortexed for 15 s. The samples were then transferred to a spin column and the RNA was purified according to the manufacturer's instructions. Quality and quantity of RNA were analyzed using Bio-analyzer and Nano-drop instrumentation (Agilent, CA, USA).

### Reverse transcriptase–real-time PCR

Quantitation of messenger Ribonucleic Acid (mRNA) expression was carried out according to the manufacturer's instructions (ABIPRISM, Foster City, CA) using the SYBR Green method on 7900 Sequence Detection systems from Applied Biosystems. Briefly, purified total RNA (200  $\mu\text{g}/\mu\text{l}$ ) was used to synthesize the first strand cDNA by reverse transcription according to the manufacturer's instructions (Bio-Rad, CA). Five microliters of the five times diluted first strand cDNA reaction, was subjected to real-time PCR amplification using gene specific primers as described earlier [11]. The data were analyzed using SDS software, version 2.0, and the results were exported to Microsoft Excel for further analysis. Data normalization was accomplished using the endogenous control ( $\beta$ -actin, PPIA) to correct for variation in the RNA quality among samples. The normalized Ct values were subjected to a  $2^{-\Delta\Delta\text{Ct}}$  formula to calculate the fold change between the non-loaded and loaded groups. The formula and its derivations were obtained from the instrument user guide.

### Genotyping

Genomic DNA extraction was extracted from the liver of each F2 mouse using a Maxi prep DNA extraction kit (Qiagen) and stored at  $-80^{\circ}\text{C}$ . Genotyping of these samples was performed as previously described [12].

### QTL analysis

The broad sense of heritability index of each phenotype was calculated and a genome-wide analysis of the F2 population of B6XC3H cross was performed as previously described [12].

### Statistical analysis

We used Statistica software (StatSoft, Inc version 7.1, 2005) to perform correlation analysis, phenotype distribution, regression analysis and two-way ANOVA. Significance levels were based on  $p < 0.05$ .

## Results

### Expression levels of bone genes induced by loading are heritable

The bone anabolic response induced by mechanical loading in the F2 mice was measured by using two bone formation markers, bone sialoprotein (BSP) and alkaline phosphatase (ALP). Expression levels from each of the markers were measured as fold change by comparing the difference between loaded tibiae vs. non-loaded tibiae. The mean fold increases in BSP and ALP, in the parents, female F1 and F2 mice, normalized by  $\beta$ -actin and by PPIA are shown in Table 1. The fold change data for the BSP and ALP marker genes in the female F2 mice, obtained after normalizing with  $\beta$ -actin and PPIA, show skewed distribution (Fig. 1). The skewed distribution appears to be due to the fold change calculation which amplifies the difference geometrically

Table 1  
Fold changes in the expression levels of bone marker genes in response to 12 days four-point bending on 10-week female mice

Groups	BSP	ALP	N
B6 parents	8.41±0.76	6.29±0.71	5
C3H parents	2.93±0.62	3.38±0.69	5
F1 $\beta$ -actin normalized	1.87±2.36	2.09±2.03	16
PPIA normalized	1.44±1.82	1.82±1.89	
F2 $\beta$ -actin normalized	3.0±2.59	2.82±2.52	241
PPIA normalized	2.83±2.31	2.70±2.31	

Values mentioned above are mean±SD of the fold change.

( $2^{-\Delta\Delta CT}$ ). Thus, by adjusting the data with natural log, the distribution became normal. The broad sense of heritability, calculated as described previously, for the loading-induced fold changes in the BSP and ALP, after normalizing with  $\beta$ -actin was 87% and 91%, respectively, and after normalizing with PPIA was 88% and 91%, respectively, in the F2 population.

We next determined whether the mRNA levels of bone formation marker genes (fold change), measured by real-time PCR, correlate with the changes in BMD and log PC measured by pQCT. The results show a significant positive correlation between fold changes and BMD ( $r=0.25$  to  $0.30$ ), and bone size ( $r=0.27$  to  $0.36$ ). These findings suggest that these two bone formation markers are responsible, in part, for the increase in BMD and PC in response to loading in the F2 mice.

Since B6 and C3H mice exhibit difference in bone size due to their genetic background, we expect a variation in the cross-sectional area among F2 mice. Due to this variation, mice with smaller cross-sectional areas are predicted to receive a higher mechanical strain, while mice with larger cross-sectional areas to receive less mechanical strain to the same load. In order to determine if this variation in strain affected the expression levels of these markers, we performed a correlation analysis between the fold changes in BSP and ALP, normalized with  $\beta$ -actin and PPIA, and non-loaded PC measurements of each F2 mouse. These results showed no correlation ( $r=-0.003$  to  $0.03$ ). Similarly, we found no correlation between body-weight and fold change data for BSP and ALP. These data suggest that variation in the increase in mRNA levels of BSP and ALP genes induced by mechanical loading is largely independent of bone size and body weight in the B6XC3H intercross.

#### Expression QTL for bone formation response induced by loading

Using 111 micro-satellite markers and loading-induced fold change data of BSP and ALP marker genes of F2 female mice ( $n=241$ ), a genome-wide analysis revealed the presence of significant and suggestive genetic loci affecting bone anabolic response (Table 2). Loci regulating both the expression of BSP and ALP, normalized with  $\beta$ -actin and PPIA, were located on

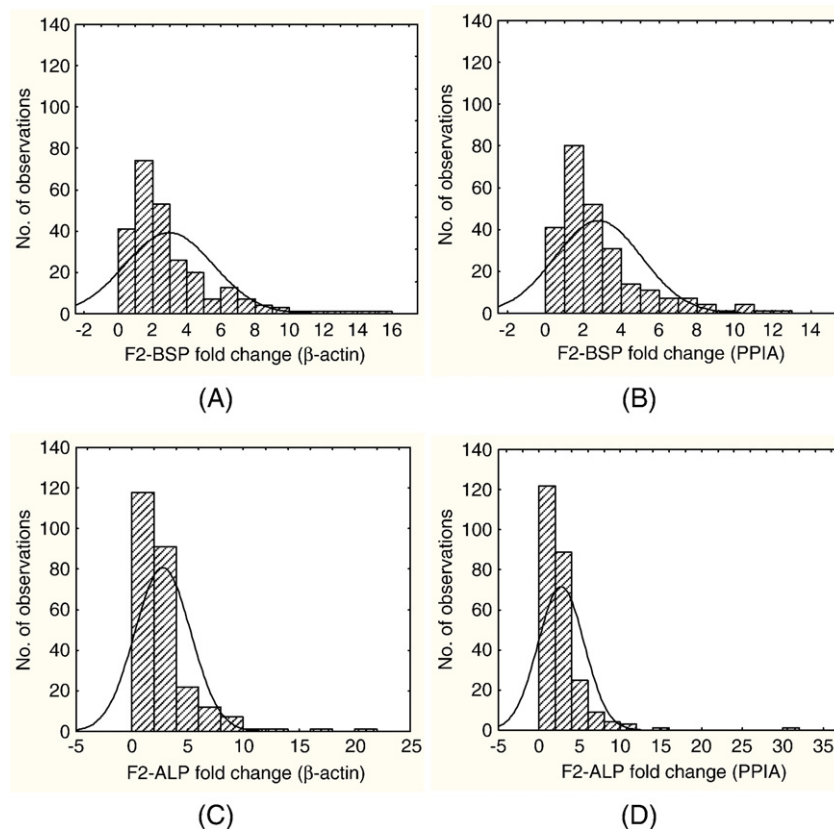


Fig. 1. Distribution of fold changes for (A) BSP normalized with  $\beta$ -actin, (B) BSP normalized with PPIA, (C) ALP normalized with  $\beta$ -actin and (D) ALP normalized with PPIA in the F2 population after 2 weeks of four-point bending. The x-axis represents the fold change and y-axis represents the number of observations (mice). BSP, Bone sialoprotein; ALP, Alkaline phosphatase;  $\beta$ -actin, Beta actin and PPIA, Peptidyl-prolyl *cis-trans* isomerase A. The solid line represents theoretical skewed distribution. Based on Kolmogorov–Smirnov test, both BSP and ALP fold change data show skewed distribution ( $n=241$ ).

Table 2

Significant and suggestive QTL identified using fold change data for the mechanical loading-induced phenotypes in the B6XC3H F2 mice

Phenotypes	Chr	Locus	cM	Actin normalization	PPIA normalization
				LOD score	LOD score
Bone sialoprotein	1	D1Mit113	91.8	–	10.4 <sup>a</sup>
	5	D5Mit143	73.2	–	5.2 <sup>c</sup>
	8	D8Mit88	60.1	7.5 <sup>b</sup>	8.8 <sup>b</sup>
	9	D9Mit2	13.1	7.0 <sup>b</sup>	4.8 <sup>c</sup>
	9	D9Mit151	69.9	7.1 <sup>b</sup>	5.0 <sup>c</sup>
	16	D16Mit153	45.9	6.7 <sup>b</sup>	7.0 <sup>b</sup>
	17	D17Mit51	14.2	9.2 <sup>a</sup>	12.3 <sup>a</sup>
	18	D18Mit144	38	8.0 <sup>b</sup>	–
	19	D19Mit68	3.3	7.2 <sup>b</sup>	10.7 <sup>a</sup>
	19	D19Mit68	3.3	–	6.9 <sup>b</sup>
Alkaline phosphatase	1	D1Mit215	47	5.0 <sup>c</sup>	7.5 <sup>b</sup>
	1	D1Mit102	75.4	6.3 <sup>b</sup>	7.6 <sup>b</sup>
	3	D2Mit147	59	7.7 <sup>b</sup>	8.3 <sup>b</sup>
	4	D4Mit308	54.6	5.5 <sup>c</sup>	5.6 <sup>b</sup>
	4	D4Mit256	82	5.6 <sup>c</sup>	5.0 <sup>c</sup>
	8	D8Mit88	60.1	10.5 <sup>a</sup>	12.3 <sup>a</sup>
	9	D9Mit151	69.9	7.4 <sup>b</sup>	–
	16	D16Mit153	45.9	5.1 <sup>c</sup>	5.9 <sup>c</sup>
	17	D17Mit51	14.2	9.3 <sup>a</sup>	9.0 <sup>b</sup>
	18	D18Mit144	38	12.6 <sup>a</sup>	5.8 <sup>c</sup>

<sup>a</sup>The threshold for the highly significant LOD score is  $p < 0.01$ .<sup>b</sup>The threshold for the significant LOD score is  $p < 0.05$ .<sup>c</sup>The threshold for the suggestive LOD score is  $p < 0.1$ .

–Corresponds to no QTL.

Chromosomes 8, 9, 16, 17, 18 and 19. Loci regulating only BSP were located on Chrs 1, 5 and 9, whereas loci regulating only ALP were located on Chrs 1, 3 and 4. For BSP, highly significant LOD scores were observed on Chr 1 (LOD score 10.4 at 91.8), Chr 17 (LOD score 12.3 at 14.2 cM) and Chr 19 (LOD score 10.7 at 3.3 cM). For ALP, highly significant LOD scores were observed on Chr 8 (LOD score 12.3, at 60 cM), Chr 17 (LOD score 9.3, at 14.2) and Chr 18 (LOD score 12.6 at 38 cM).

#### Expression QTL for housekeeping genes

To assure that the QTLs identified for BSP and ALP fold change in response to mechanical loading are not due to changes in the housekeeping genes, we calculated fold change of  $\beta$ -actin normalized by PPIA and PPIA fold change normalized by  $\beta$ -actin. We found that the mean fold difference

Table 3

Interval mapping for the fold change in  $\beta$ -actin (normalized by PPIA) and PPIA (normalized by  $\beta$ -actin) in response to mechanical loading in the B6XC3H F2 mice

Phenotypes	Chr	Locus	cM	LOD score	Variance
$\beta$ -actin	1	D1Mit430	6.6	2.0 <sup>c</sup>	3.6
	2	D2Mit66	48.1	2.8 <sup>b</sup>	5.4
	9	D9Mit151	69.9	1.9	3.6
PPIA	2	D2Mit285	72.1	*	3.3
	X	DXMit172	40.4	2.1 <sup>c</sup>	4.7

<sup>b</sup>The threshold for the significant LOD score is  $p < 0.05$ .<sup>c</sup>The threshold for the suggestive LOD score is  $p < 0.1$ .

\*QTL with very low LOD score.

Variance is explained from peak LOD score.

in  $\beta$ -actin was  $0.99 \pm 0.30$  and in PPIA was  $1.05 \pm 0.33$  in the F2 mice. Interval mapping using F2 mice ( $n = 241$ ) revealed three suggestive QTL on chromosomes 1, 9 and X and one significant QTL on Chr 2 (Table 3). We found that one of the loci on Chr 9 (69.9 cM) identified for the  $\beta$ -actin fold change data corresponds to one of the loci identified for both BSP and ALP fold change data. This finding leads us to suspect that the QTL identified for ALP and BSP on Chr 9 could be due to expression changes in the house keeping gene rather than due solely to expression changes in the marker genes.

#### QTL for BSP and ALP in non-external loaded tibia

In addition to the mechanical loading QTL, we identified QTLs that regulate the basal expression of BSP and ALP in the non-loaded tibiae, by using Ct values from real-time PCR, after normalization with  $\beta$ -actin and PPIA. Both BSP and ALP showed normal distribution in the F2 population (Fig. 2). We found that the BSP and ALP data showed no correlation with body weight suggesting that the basal expression of these two bone formation marker genes is independent of the body weight. Interval mapping was then performed using F2 female mice ( $n = 241$ ), which revealed four chromosomes, Chrs 4, 10, 16, and 18, that regulate the basal expression of BSP and ALP in the non-loaded tibiae (Table 4).

#### Discussion

The salient features of the present study are: (1) Fold change measurements in bone marker expression led to the identification of several QTLs which regulate bone adaptive response to

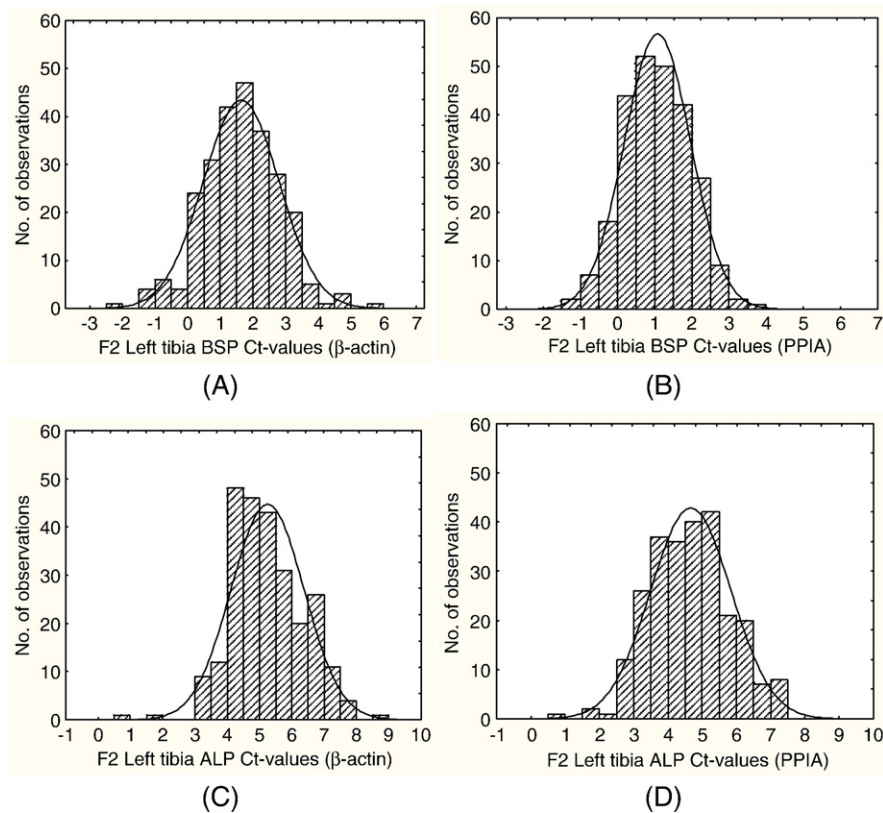


Fig. 2. Distribution of Ct values of non-external loaded tibia for (A) BSP normalized with  $\beta$ -actin, (B) BSP normalized with PPIA, (C) ALP normalized with  $\beta$ -actin and (D) ALP normalized with PPIA in the F2 population after 2 weeks of four-point bending. The x-axis represents the fold change and y-axis represents the number of observations (mice). BSP, Bone sialoprotein; ALP, Alkaline phosphatase;  $\beta$ -actin, Beta actin and PPIA, Peptidyl-prolyl *cis-trans* isomerase A. The solid line represents theoretical normal distribution. Based on Kolmogorov–Smirnov test, both BSP and ALP show normal distribution ( $n=241$ ).

loading. (2) We found QTLs common to both ALP and BSP as well as QTLs specific to ALP but not BSP or vice versa. (3) We found that some of the expression QTLs matched the classical QTL we previously identified for BMD and bone size validating our findings.

We undertook a number of precautions to ensure that the QTLs we identified are real and not due to technical or design artifacts: (1) We chose two markers, BSP and ALP, that showed significant positive correlation in bone anabolic response to loading in a previous study [11]. (2) We used fold changes rather than Ct

values to study linkages so that we would identify specific genetic changes rather than general changes. (3) We used two housekeeping genes, rather than one, to normalize the expression data in order to avoid identification of QTLs stemming from variations in RNA quality among samples. For example, loci on Chrs 9 and 18 show significant linkage with ALP and BSP, respectively, using  $\beta$ -actin, but not PPIA as an internal control. Thus, the validity of Chr 9 and 18 QTL remains to be established.

Our linkage analysis revealed several QTLs that are responsible for the increased expression levels of BSP and ALP,

Table 4  
Significant and suggestive QTL identified using Ct values for the non-externally loaded phenotypes in the B6XC3H F2 female mice

Phenotypes	Chr	Locus	cM	LOD score	Variance	LOD score	Variance
				Actin normalization		PPIA normalization	
Bone sialoprotein	4	D4Mit42	76.5	2.7 <sup>b</sup>	5.2	2.4 <sup>c</sup>	4.5
	18	D18Mit64	0	2.4 <sup>c</sup>	4.6	*	2.3
Alkaline phosphatase	4	D4Mit42	76.5	2.8 <sup>b</sup>	5.2	*	3.3
	10	D10Mit213	6.6	2.3 <sup>c</sup>	4.3		
	16	D16Mit153	45.9	1.9	3.6	2.3 <sup>c</sup>	4.2
	18	D18Mit144	38.3	2.4 <sup>c</sup>	6.7	*	2.3

<sup>b</sup> The threshold for the significant LOD score is  $p < 0.05$ .

<sup>c</sup> The threshold for the suggestive LOD score is  $p < 0.1$ .

\* QTL with very low LOD score.

Variance is explained from peak LOD score.

induced by mechanical loading in the F2 mice. If changes in BSP and ALP markers reflect skeletal changes to mechanical loading, one would expect QTLs which are common to both markers. Accordingly, we found co-localized loci on Chrs 8, 16, 17, 18 and 19 for both BSP and ALP, suggesting that both markers are responding to the same upstream signaling.

Our findings also revealed four loci on Chrs 3, 8, 17 and 18 which are identical to QTLs we previously found for BMD and/or bone size parameters [12]. This is consistent with other studies which have shown that Chrs 8 (30–90 cM), 17 (6.6 cM) and 18 (32–46 cM) contain a loci which regulate biomechanical properties in several inbred mouse strain crosses [15,16,21,22]. The fact that we found QTLs at the same loci using both bone parameters and bone formation markers, indicate that these loci do, in fact, contain genes that are not only involved in increasing bone formation in response to loading, but also involved in regulating mechanical properties of the bone, in part, through ALP and BSP expression. While the expression QTLs found on Chr 17 and 18 were contained within the region identified for the BMD and bone size, the broad QTL regions in these chromosomes raise the possibility that more than one gene could be responsible for the phenotypic changes. Fine mapping will narrow down the size of the QTL and allow us to identify it as the same QTL as identified for BMD or as a different QTL.

Surprisingly, we identified additional QTLs for BSP and/or ALP which do not correspond with any QTLs reported for bone parameters. This could be explained by: (1) changes in gene expression might be more sensitive to external loading than net change in the bone parameters (measured by pQCT) and (2) these regions may be involved in regulating the expression of BSP or ALP, but have no measured effect on bone formation.

The QTLs identified in this study common to both BSP and ALP are more than 10 cM in length, and thus, contain hundreds of genes and ESTs. Some of the known candidate genes located in these QTL regions are shown in Table 5. We have previously reported that the expression of some of these genes increases with mechanical loading using a genome-wide microarray analysis [33]. Others using various approaches have shown that many of these genes are involved in skeletal development. This confirms our present QTL findings. Although QTL analysis leads to a precise mapping of the genetic loci which contribute to our phenotype of interest, these regions are broad and contain many possible significant genes. The next phase of our study, therefore, lies in identifying which specific genes within our identified QTL regions are associated with mechanical loading.

Some of the limitations of this study are: (1) we used a relatively small number of F2 mice to perform the eQTL analysis ( $n=241$ ) relative to the cQTL analysis ( $n=329$ ). This is due to fact

Table 5

List of potential candidate genes located in the QTL region identified for skeletal anabolic response to mechanical loading

Chrs	cM	Genes	Predicted functions in bone
8	38–69	Ptger1	Prostaglandin E2 stimulates fibronectin through ptger1
		Junb	Involved in osteoblast cell proliferation
		Mt1, 2	Regulate early stage of mesenchymal stem cells differentiation
		Cdh11	Knock out (KO) mice show reduced bone density
		Hsd11b2	Regulate glucocorticoid signaling
		Cdh1	Important in embryonic limb buds development
		Cbfb	Required for the function of Runx1 and Runx2 in skeletal development
		Hsd17b2	Involved in regulation of estrogen action
		Il17c	Involved in osteoclastogenesis
		Col8a1	Increased in bone in response to mechanical loading
16	30–46	EphA3	Involved in tooth development
		Pit1	Mediates bone formation by regulating the expression of BSP
17	0–25	Map3k4	Involved in normal skeletal patterning
		Cln7	Critical for osteoclast resorption
		Thbs2	KO mice show increased bone density and cortical thickness
		Traf7	Involved in MEKK3 signaling and apoptosis
		Tnf	Important in osteoclastogenesis
		Notch3	Involved in tooth development
		Vegfa	Involved in angiogenesis of bone
		Runx2	Involved in skeletal development
		Lox	Play a key role in the collagen deposition by osteoblast
		Pdgfrb	Involved in bone remodeling phase
18	15–40	Adrb2	Produces anabolic effects on bone
		Mc4r	KO mice show decreased bone resorption and high bone mass
		Mapk4	Intracellular mediator of growth factor
		Nfatc1	Important in osteoclastogenesis
		Galr1	Important for bone healing
		Gal	Involved in bone healing
		Lrp5	Regulates osteoblast function
19	0–24	Esrra	Important in bone metabolism
		Lpxn	Involved in podosomal signaling complex in osteoclast
		Ostf1	Stimulates osteoclast formation
		Jak2	Involved in osteoblast signaling

that we encountered problems with quality and quantity in the RNA extracted from 6 mm, marrow-flushed tibiae. This relatively small sample size may account for the reduced LOD score for some of the QTLs identified in our study. (2) The QTLs identified in this study for bone formation response induced by mechanical loading were obtained from female mice. To date, studies have shown that hormones enhance the effects of mechanically induced bone formation [5,6,19]. Further studies with male mice may not only reveal whether any of the QTLs we found are female specific but may also lead to the identification of male specific QTLs involved in bone response to mechanical loading. (4) It has been predicted that some of the skeletal changes in the F2 mice could be due to periosteal pressure caused by four-point bending. Our previous findings that sham loading neither increased periosteal bone formation nor caused changes in expression levels of bone formation marker genes (data not shown) argue against this possibility [12].

## Conclusion

We provide evidence that bone formation response varies among individuals and is strongly regulated by genetic factors, as is evident from both our previous cQTL and our present eQTL analysis. From both the QTL analyses, we show that Chr 8 contains genes involved in increasing bone formation induced by mechanical loading and for biomechanical properties of the bone. Further study, with congenic and gene KO mice may help to understand the role of specific genes at the loci we have found and could provide a basis for understanding the observed variability in bone mass accretion and maintenance, resulting from exercise, in normal healthy individuals.

## Acknowledgments

This work was supported by the Army Assistance Award No. DAMD17-01-1-0074. The US Army Medical Research Acquisition Activity (Fort Detrick, MD) 21702-5014 is the awarding and administering acquisition office for the DAMD award. The information contained in this publication does not necessarily reflect the position or the policy of the Government, and no official endorsement should be inferred. All work was performed in facilities provided by the Department of Veterans Affairs. We would like to thank Mr. Peter Gifford, Mr. Jay Javier and Mr. Alex Cortez for their contribution in this project and James Dekeyser for valuable technical support in four-point bending instrument.

## References

- [1] Akhter MP, Cullen DM, Pedersen EA, Kimmel DB, Recker RR. Bone response to in vivo mechanical loading in two breeds of mice. *Calcif Tissue Int* 1998;63:442–9.
- [2] Beamer WG, Shultz KL, Donahue LR, Churchill GA, Sen S, Wergedal JR, et al. Quantitative trait loci for femoral and lumbar vertebral bone mineral density in C57BL/6J and C3H/HeJ inbred strains of mice. *J Bone Miner Res* 2001;16:1195–206.
- [3] Bikle DD, Halloran BP. The response of bone to unloading. *J Bone Miner Metab* 1999;17:233–44.
- [4] Bikle DD, Sakata T, Halloran BP. The impact of skeletal unloading on bone formation. *Gravit Space Biol Bull* 2003;16:45–54.
- [5] Borer KT. Physical activity in the prevention and amelioration of osteoporosis in women: interaction of mechanical, hormonal and dietary factors. *Sports Med* 2005;35:779–830.
- [6] Caiozzo VJ, Haddad F. Thyroid hormone: modulation of muscle structure, function, and adaptive responses to mechanical loading. *Exerc Sport Sci Rev* 1996;24:321–61.
- [7] Dalsky GP, Stocke KS, Ehsani AA, Slatopolsky E, Lee WC, Birge Jr SJ. Weight-bearing exercise training and lumbar bone mineral content in postmenopausal women. *Ann Intern Med* 1988;108:824–8.
- [8] Deutsch S, Lyle R, Dermitzakis ET, Attar H, Subrahmanyam L, Gehrig C, et al. Gene expression variation and expression quantitative trait mapping of human chromosome 21 genes. *Hum Mol Genet* 2005;14:3741–9.
- [9] Dhamrait SS, James L, Brull DJ, Myerson S, Hawe E, Pennell DJ, et al. Cortical bone resorption during exercise is interleukin-6 genotype-dependent. *Eur J Appl Physiol* 2003;89:21–5.
- [10] Gross TS, Srinivasan S, Liu CC, Clemens TL, Bain SD. Noninvasive loading of the murine tibia: an in vivo model for the study of mechanotransduction. *J Bone Miner Res* 2002;17:493–501.
- [11] Kesavan C, Mohan S, Oberholtzer S, Wergedal JE, Baylink DJ. Mechanical loading-induced gene expression and BMD changes are different in two inbred mouse strains. *J Appl Physiol* 2005;99:1951–7.
- [12] Kesavan C, Mohan S, Srivastava AK, Kapoor S, Wergedal JE, Yu H, et al. Identification of genetic loci that regulate bone adaptive response to mechanical loading in C57BL/6J and C3H/HeJ mice intercross. *Bone* 2006;39:634–43.
- [13] Kodama Y, Dimai HP, Wergedal J, Sheng M, Malpe R, Kutilek S, et al. Cortical tibial bone volume in two strains of mice: effects of sciatic neurectomy and genetic regulation of bone response to mechanical loading. *Bone* 1999;25:183–90.
- [14] Kodama Y, Umemura Y, Nagasawa S, Beamer WG, Donahue LR, Rosen CR, et al. Exercise and mechanical loading increase periosteal bone formation and whole bone strength in C57BL/6J mice but not in C3H/HeJ mice. *Calcif Tissue Int* 2000;66:298–306.
- [15] Koller DL, Schrieffer J, Sun Q, Shultz KL, Donahue LR, Rosen CJ, et al. Genetic effects for femoral biomechanics, structure, and density in C57BL/6J and C3H/HeJ inbred mouse strains. *J Bone Miner Res* 2003;18:1758–65.
- [16] Lang DH, Sharkey NA, Mack HA, Vogler GP, Vandenbergh DJ, Blizard DA, et al. Quantitative trait loci analysis of structural and material skeletal phenotypes in C57BL/6J and DBA/2 second-generation and recombinant inbred mice. *J Bone Miner Res* 2005;20:88–99.
- [17] Lang TF, Leblanc AD, Evans HJ, Lu Y. Adaptation of the proximal femur to skeletal reloading after long-duration spaceflight. *J Bone Miner Res* 2006;21:1224–30.
- [18] Lanyon LE. Using functional loading to influence bone mass and architecture: objectives, mechanisms, and relationship with estrogen of the mechanically adaptive process in bone. *Bone* 1996;18:37S–43S.
- [19] Lee KC, Jessop H, Suswillo R, Zaman G, Lanyon LE. The adaptive response of bone to mechanical loading in female transgenic mice is deficient in the absence of oestrogen receptor-alpha and -beta. *J Endocrinol* 2004;182:193–201.
- [20] Li J, Burmeister M. Genetical genomics: combining genetics with gene expression analysis. *Hum Mol Genet* 2005;14(Spec No 2):R163–9.
- [21] Li X, Masinde G, Gu W, Wergedal J, Hamilton-Ulland M, Xu S, et al. Chromosomal regions harboring genes for the work to femur failure in mice. *Funct Integr Genomics* 2002;1:367–74.
- [22] Li X, Masinde G, Gu W, Wergedal J, Mohan S, Baylink DJ. Genetic dissection of femur breaking strength in a large population (MRL/MpJ x SJL/J) of F2 Mice: single QTL effects, epistasis, and pleiotropy. *Genomics* 2002;79:734–40.
- [23] Masinde GL, Wergedal J, Davidson H, Mohan S, Li R, Li X, et al. Quantitative trait loci for periosteal circumference (PC): identification of single loci and epistatic effects in F2 MRL/SJL mice. *Bone* 2003;32:554–60.
- [24] Mori T, Okimoto N, Sakai A, Okazaki Y, Nakura N, Notomi T, et al. Climbing exercise increases bone mass and trabecular bone turnover through transient regulation of marrow osteogenic and osteoclastogenic potentials in mice. *J Bone Miner Res* 2003;18:2002–9.

- [25] Nettleton D, Wang D. Selective transcriptional profiling for trait-based eQTL mapping. *Anim Genet* 2006;37(Suppl 1):13–7.
- [26] Notomi T, Okazaki Y, Okimoto N, Tanaka Y, Nakamura T, Suzuki M. Effects of tower climbing exercise on bone mass, strength, and turnover in orchidectomized growing rats. *J Appl Physiol* 2002;93:1152–8.
- [27] Snow-Harter C, Bouxsein ML, Lewis BT, Carter DR, Marcus R. Effects of resistance and endurance exercise on bone mineral status of young women: a randomized exercise intervention trial. *J Bone Miner Res* 1992;7:761–9.
- [28] Spence J, Liang T, Foroud T, Lo D, Carr L. Expression profiling and QTL analysis: a powerful complementary strategy in drug abuse research. *Addict Biol* 2005;10:47–51.
- [29] Tajima O, Ashizawa N, Ishii T, Amagai H, Mashimo T, Liu LJ, et al. Interaction of the effects between vitamin D receptor polymorphism and exercise training on bone metabolism. *J Appl Physiol* 2000;88: 1271–6.
- [30] Turner CH. Bone strength: current concepts. *Ann N Y Acad Sci* 2006;1068:429–46.
- [31] Umemura Y, Baylink DJ, Wergedal JE, Mohan S, Srivastava AK. A time course of bone response to jump exercise in C57BL/6J mice. *J Bone Miner Metab* 2002;20:209–15.
- [32] Wang D, Nettleton D. Identifying genes associated with a quantitative trait or quantitative trait locus via selective transcriptional profiling. *Biometrics* 2006;62:504–14.
- [33] Xing W, Baylink D, Kesavan C, Hu Y, Kapoor S, Chadwick RB, et al. Global gene expression analysis in the bones reveals involvement of several novel genes and pathways in mediating an anabolic response of mechanical loading in mice. *J Cell Biochem* 2005;96:1049–60.
- [34] Yaguchi H, Togawa K, Moritani M, Itakura M. Identification of candidate genes in the type 2 diabetes modifier locus using expression QTL. *Genomics* 2005;85:591–9.
- [35] Yamashita S, Wakazono K, Nomoto T, Tsujino Y, Kuramoto T, Ushijima T. Expression quantitative trait loci analysis of 13 genes in the rat prostate. *Genetics* 2005;171:1231–8.
- [36] Ziambaras K, Civitelli R, Papavasiliou SS. Weightlessness and skeleton homeostasis. *Hormones (Athens)* 2005;4:18–27.

## Short Report

## Open Access

# Lack of anabolic response to skeletal loading in mice with targeted disruption of the pleiotrophin gene

Chandrasekhar Kesavan<sup>1</sup> and Subburaman Mohan\*<sup>1,2</sup>

Address: <sup>1</sup>Musculoskeletal Disease Center, VA Loma Linda Healthcare System, Loma Linda, CA 92357, USA and <sup>2</sup>Department of Medicine, Loma Linda University, Loma Linda, CA 92357, USA

Email: Chandrasekhar Kesavan - [chandrasekhar.kesavan@med.va.gov](mailto:chandrasekhar.kesavan@med.va.gov); Subburaman Mohan\* - [subburaman.mohan@va.gov](mailto:subburaman.mohan@va.gov)

\* Corresponding author

Published: 1 December 2008

Received: 27 June 2008

BMC Research Notes 2008, 1:124 doi:10.1186/1756-0500-1-124

Accepted: 1 December 2008

This article is available from: <http://www.biomedcentral.com/1756-0500/1/124>

© 2008 Mohan et al; licensee BioMed Central Ltd.

This is an Open Access article distributed under the terms of the Creative Commons Attribution License (<http://creativecommons.org/licenses/by/2.0>), which permits unrestricted use, distribution, and reproduction in any medium, provided the original work is properly cited.

## Abstract

**Background:** In a previous study we showed, using the whole genome microarray approach, that pleiotrophin (PTN) expression was increased by 4-fold in response to mechanical loading (ML) in a good responder C57BL/6J (B6) mice. To address PTN role in mediating ML effects on bone formation, we first evaluated time course effects of ML on expression levels of PTN gene using real time RT-PCR in 10 week female B6 mice. A 9 N load was applied using a four-point bending device at 2 Hz frequency for 36 cycles, once per day for 2, 4 and 12 days on the right tibia and the left tibia was used as internal control.

**Findings:** Four-point bending caused an acute increase in PTN expression (2-fold) within 2 days of loading and further increased (3–6 fold) with continued loading. This increase was also seen in 16 and 36-week old mice. Based on these findings, we next used PTN knockout (KO) mice to evaluate the cause and effect relationship. Quantitative analysis showed that two weeks of ML induced changes in vBMD and bone size in the PTN KO mice (8% and 6% vs. non-loaded bones) were not significantly different from control mice (11% and 8% in vBMD and bone size vs. non-loaded bones).

**Conclusion:** Our results imply that PTN is not a key upstream mediator of the anabolic effects of ML on the skeleton.

## Findings

### Background

Mechanical loading is now recognized as an important stimulator of bone formation. Numerous studies in animal and humans, using various loading models have demonstrated that loading increases bone mass while unloading decreases bone mass [1-6]. To date, reports have shown that several growth factors and signaling pathways are known to be activated by ML [7-11]. However, the relative contribution of each of these pathways to ML induced bone formation is not known. We previously,

using genome-wide microarray approach have reported that mechanical loading by four-point bending caused a 4-fold increase in Heparin binding growth factor, otherwise known as PTN, in a good responder B6 mouse [7]. PTN, a 36 amino acid bone growth factor rich in lysine and cysteine residues, is also known as Osteoblast Specific Factor 1. PTN is involved in diverse functions, which includes: cell recruitment, cell attachment and proliferation, differentiation, angiogenesis, and neurogenesis [12-14]. *In vitro* studies have demonstrated that PTN has the ability to promote adhesion, migration, expansion and

differentiation of human osteoprogenitor and MC3T3-E1 cells [15-17]. *In vivo* studies using transgenic approach have shown that ovariectomy induced bone loss, due to estrogen deficiency, were protected by an increase in the expression of the PTN gene [18]. Another transgenic study, with overexpression of the human PTN gene showed an increase in cortical thickness, bone volume and cancellous bone volume [15]. In addition, immunocytochemistry studies has provided visual evidence for PTN at the site of new bone formation [15,16]. Based on the above findings and our data that PTN expression is increased in response to ML, we hypothesize that PTN play a role in mediating anabolic effects of ML on bone formation. To test this hypothesis, we performed ML using four-point bending device on mice with disruption of PTN gene and control mice with intact PTN gene.

## Methods

### Mice

Female C57BL/6J (B6) mice were purchased from Jackson laboratory (Bar Harbor, ME). PTN gene knock out (KO) mice (PTN-129 in B6 background) were generated by Dr. Thomas F. Vogt and the breeding pairs were kindly provided by Princeton University, NJ, USA, for our studies. PTN KO mice were crossed with wild type B6 mice to generate the heterozygotes. These were crossed with each other to generate 25% homozygous PTN KO mice, 50% heterozygous and 25% littermate wild type mice. The body weight of PTN KO and control mice used for this study are  $18.20 \pm 0.95$  g and  $19.0 \pm 1.39$  g, respectively. The differences in body weight were not statistically significant ( $p = 0.20$ ). All mice were housed under the standard conditions of 14-hour light and 10-hour darkness, and had free access to food and water. The experimental protocols were in compliance with animal welfare regulations and approved by local IACUC.

### Genotyping

At 3-weeks (wks) of age, DNA was extracted from tail of female mice, using a PUREGENE DNA purification kit (Gentra System, Inc., Minneapolis, MN) according to the manufacturer's protocol. Polymerase chain reaction (PCR) was performed to identify PTN KO mice from wild type or heterozygous mice. Primers specific for neomycin gene (forward 5' CTT GCT CCT GCC GAG AAA GTA T 3' and reverse 5' AGC AAT ATC ACG GGT AGC CAA C 3' with a PCR product of 369 bp). Primers specific for PTN gene (forward 5' TCT GAC TGT GGQA GAA TGG CAG T 3' and reverse 5' CTT CTT CCA GTT GCA AGG GAT C 3' with a PCR product of 147 bp) were used for genotyping. The following conditions were used to perform the PCR reaction: 95°C for 2 minutes; 35 cycles at 95°C for 40 sec, 57°C for 40 sec, 72°C for 40 sec; 70°C for 40 sec. The PCR products were run on a 1.5% agarose gel and the image

taken with a Chemilmager 4400 (Alpha Innotech Corp., San Leandro, CA).

### In vivo loading model/regimen

ML was performed using a four-point bending device [Instron, Canton, MA], as previously reported [1]. The mice were loaded using a  $9.0 \pm 0.2$  Newton (N) force at a frequency of 2 Hz for 36 cycles, once a day under inhalable anesthesia (5% Isoflurane and 95% oxygen). The right tibia was used for loading and the left tibia as internal non-loaded control.

For the time course study, the loading was performed at 2-, 4- and 12-days on 10-week female B6 mice. After 24 hours of the last loading, mice were euthanized and tibiae were collected for RNA extraction.

For varying age groups of female B6 mice, female PTN KO and control mice, the loading was performed for 12 days. After 48 hours of the last loading, following *in vivo* bone measurement, mice were euthanized; tibiae (loaded and non-loaded) were collected and stored at -80°C for further experiments.

### Peripheral quantitative computed tomography (pQCT) measurements

To measure four-point bending induced changes in the bone parameters in loaded and non-loaded tibiae, we used pQCT (Stratec XCT 960 M, Norland Medical System, Ft. Atkinson, WI) as described previously [1].

### RNA extraction

RNA was extracted from the loaded and non-loaded bones using qiagen lipid extraction kit [Qiagen, Valencia, CA], as previously described [1]. Quality and quantity of RNA were analyzed using the 2100 Bio-analyzer (Agilent, Palo Alto, CA, USA) and Nano-drop (Wilmington, DE).

### Reverse Transcriptase – Real time PCR

Using 200 ng purified total RNA, first strand cDNA was synthesized by iScript cDNA synthesis kit (BIO-RAD, CA, USA), according to the manufacturer's protocol. Quantitative real time PCR was performed, as previously described, in order to analyze the expression levels of PTN and PPIA ((peptidyl)prolyl isomerase A), an endogenous control [1]. The data were analyzed using SDS software, version 2.0, and the results were exported to Microsoft Excel for further analysis. Data normalization was accomplished using the endogenous control (PPIA) to correct for variation in the RNA quality among samples. The normalized Ct values were subjected to a  $2^{-\Delta\Delta Ct}$  formula to calculate the fold change between the loaded and non-loaded groups. The formula and its derivations were obtained from the instrument user guide.

### Statistical Analysis

Values are given as mean  $\pm$  SD. ANOVA (Bonferroni's post-hoc test) and standard t-test were used to compare the difference between load and non-loaded bones at various time-points, ages and strains using the fold change and percentage data. We used Statistica software (StatSoft, Inc version 7.1, 2005) to perform the analysis and the results were considered significant at  $p < 0.05$ .

### Results and discussion

In the previous study using whole genome microarray analysis, we reported that ML caused a significant increase in PTN expression in the good responder female B6 mouse [7]. In order to confirm this finding, we evaluated temporal changes in PTN expression during 2 weeks of four-point bending. We found that ML caused a 2-fold increase in PTN expression as early as 2 days that was sustained during the entire 2 weeks of mechanical loading (Figure 1). Furthermore, ML effects on PTN expression was seen in three different age groups of mice, 10-, 16- and 36-weeks (Figure 2). These data demonstrate that PTN is a mechanoresponsive gene in the bones of mice. In contrast to this *in vivo* finding, an *in vitro* study using cultured human osteoblast cells have shown that PTN expression decreases in response to mechanical stimulation [19]. Although we cannot fully explain this discrepancy between our data and the *in vitro* study, possible explanations include: 1) Osteoblast responsiveness to mechanical

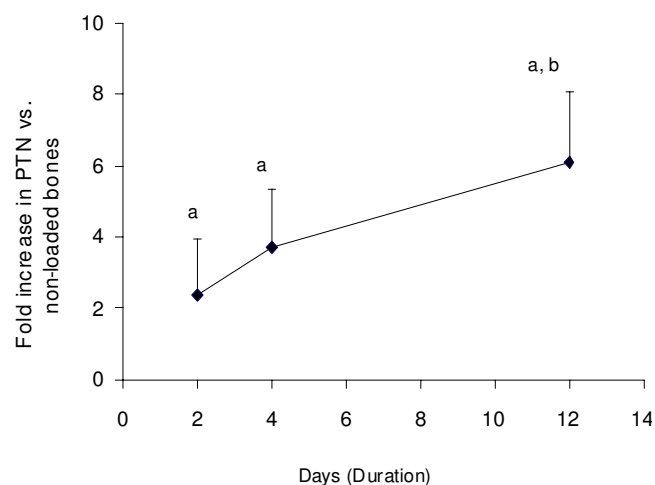


**Figure 1**

**Expression levels of PTN gene as a function of duration of loading.** The y-axis represents fold increase in the PTN gene in response to four-point bending on tibia and the x-axis represents duration of loading on 10-week female B6 mice. Values are mentioned as mean  $\pm$  SD, <sup>a</sup> $p < 0.01$  vs. non-loaded tibiae, <sup>b</sup> $p < 0.05$  vs. 2-days (Post Hoc test, ANOVA),  $N = 5$ .

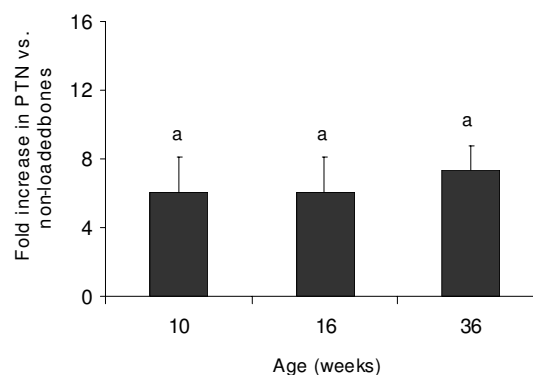


**Figure 2**

**Expression levels of PTN gene as a function of age.**

The y-axis represents fold increase in the PTN gene in response to 12 days of four-point bending on tibia and the x-axis represents varying age groups of female B6 mice. Values are mentioned as mean  $\pm$  SD. <sup>a</sup> $p < 0.05$  vs. non-loaded bones,  $N = 5$ .

loading may differ *in vivo* vs. *in vitro*. 2) Type of mechanical loading and the amount of strain utilized were different between the two studies.

It is well established that the amount of mechanical strain exerted by a given load is largely dependent on the cross sectional area (moment of inertia) such that a mouse with a large cross sectional area will experience lower mechanical strain and vice versa [1,20]. In order to assure that the difference in the bone responsiveness to loading between PTN KO mice and controls is not due to difference in the mechanical strain, we measured the bone size by pQCT at tibia mid diaphysis and calculated the mechanical strain using a mathematical model (Stephen C. Cowin: Bone Mechanics Hand book, 2nd edition, 2001, chapter: Techniques from mechanics and imaging) for both sets of mice before the loading. We found that there is no significant difference in the bone size (4.55 mm vs. 4.69 mm,  $p = 0.50$ ) as well as in the mechanical strain for 9 N (6310  $\mu\epsilon$  vs. 6351  $\mu\epsilon$ ,  $p = 0.91$ ) between the PTN KO mice and controls. Thus, the applied load was the same for both sets of mice.

To determine if ML induced increase in PTN expression contributes to anabolic effects of ML, we performed four-point bending using a load (9 N) that has been shown to exert significant changes in BMD [1]. If PTN is an important mediator of skeletal anabolic response to loading, we anticipated PTN KO mice to show reduced anabolic effects of ML on bone. We found that there was, indeed, a small reduction in ML response in the PTN KO mice (Figure 3, see additional file 1); however, these changes were

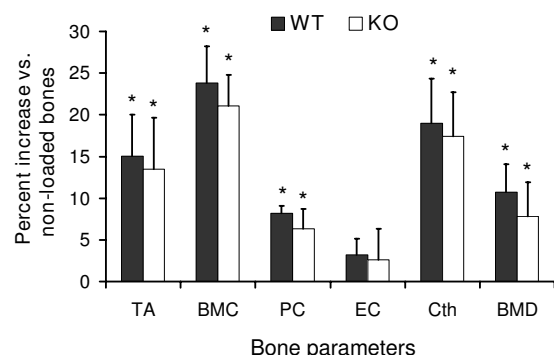


**Figure 3**  
**Changes in bone parameters in response to ML on 10-wk female PTN KO and control mice.** Values are mentioned as mean  $\pm$  SD. The y-axis represents percent increase in bone parameters in response to four-point bending on tibia and x-axis represent skeletal parameters. TA, Total area; BMC, bone mineral content; PC, periosteal circumference; EC, endosteal circumference; Cth, cortical thickness and BMD, bone mineral density. \* $p < 0.05$  vs. corresponding non-externally loaded tibiae,  $N = 7$ .

not statistically significant (Since there was no difference in the response, we did not proceed any further with histomorphometric analysis). A potential explanation for the lack of significant differences between the control and KO mice is that PTN disruption could lead to increased expression of other molecules which share similar functional properties to compensate for the loss of PTN. For example, midkine belong to the family of HB-GAM as PTN that has been shown to have similar functional properties. Mice with midkine or PTN deficiency have been reported to have normal low auditory response while mice with both gene deficits showed impaired auditory response [21]. A similar observation has been also reported with regard to fertility. Mice with disruption of both genes were infertile while mice with deficiency in either midkine or PTN gene were able to produce similar number of offspring's [22]. Another study has shown that mouse with absence of PTN gene resulted in normal skeletal growth and this is likely due to an increase in midkine expression as evident from their microarray data [23]. Overall, these findings suggest that factors of the same family are exhibiting overlapping function and thus, interfering with the activity of one factor may not necessarily lead to disruption of physiological activities such as bone formation response to loading. The issue of whether disruption of both PTN and midkine will exert a greater deficit in the skeletal anabolic response to ML compared to individual knock out requires further study.

## Competing interests

The authors declare that they have no competing interests.

## Authors' contributions

All experimental procedures, data analysis and study coordination were carried out by CK. SM contributed to the design, data interpretation and manuscript preparation. All authors read and approved the final manuscript.

## Additional material

### Additional file 1

*pQCT measurement of bone parameters. The data in this file shows absolute changes in bone parameters in response to loading between PTNKO and control mice.*

Click here for file

[<http://www.biomedcentral.com/content/supplementary/1756-0500-1-124-S1.doc>]

## Acknowledgements

This work was supported by the Army Assistance Award No. DAMD17-01-1-0074. The US Army Medical Research Acquisition Activity (Fort Detrick, MD) 21702-5014 is the awarding and administering acquisition office for the DAMD award. The information contained in this publication does not necessarily reflect the position or the policy of the Government, and no official endorsement should be inferred. All work was performed in facilities provided by the Department of Veterans Affairs. We would like to thank Mr. Peter Gifford and Anil Kapoor for their animal work in this project and James Dekeyser for his technical support in four-point bending instrument.

## References

1. Kesavan C, Mohan S, Oberholtzer S, Wergedal JE, Baylink DJ: **Mechanical loading-induced gene expression and BMD changes are different in two inbred mouse strains.** *J Appl Physiol* 2005, **99**(5):1951-1957.
2. Akhter MP, Cullen DM, Pedersen EA, Kimmel DB, Recker RR: **Bone response to in vivo mechanical loading in two breeds of mice.** *Calcif Tissue Int* 1998, **63**(5):442-449.
3. Kodama Y, Dimai HP, Wergedal J, Sheng M, Malpe R, Kutilek S, Beamer W, Donahue LR, Rosen C, Baylink DJ, et al.: **Cortical tibial bone volume in two strains of mice: effects of sciatic neurectomy and genetic regulation of bone response to mechanical loading.** *Bone* 1999, **25**(2):183-190.
4. Snow-Harter C, Bouxsein ML, Lewis BT, Carter DR, Marcus R: **Effects of resistance and endurance exercise on bone mineral status of young women: a randomized exercise intervention trial.** *J Bone Miner Res* 1992, **7**(7):761-769.
5. Umemura Y, Ishiko T, Yamauchi T, Kuroki M, Mashiko S: **Five jumps per day increase bone mass and breaking force in rats.** *J Bone Miner Res* 1997, **12**(9):1480-1485.
6. Bikle DD, Sakata T, Halloran BP: **The impact of skeletal unloading on bone formation.** *Gravit Space Biol Bull* 2003, **16**(2):45-54.
7. Xing W, Baylink D, Kesavan C, Hu Y, Kapoor S, Chadwick RB, Mohan S: **Global gene expression analysis in the bones reveals involvement of several novel genes and pathways in mediating an anabolic response of mechanical loading in mice.** *J Cell Biochem* 2005, **96**(5):1049-1060.
8. Lau KH, Kapur S, Kesavan C, Baylink DJ: **Up-regulation of the Wnt, estrogen receptor, insulin-like growth factor-I, and bone morphogenetic protein pathways in C57BL/6J osteoblasts as opposed to C3H/HeJ osteoblasts in part contributes to the differential anabolic response to fluid shear.** *J Biol Chem* 2006, **281**(14):9576-9588.

9. Triplett JW, O'Riley R, Tekulve K, Norvell SM, Pavalko FM: **Mechanical loading by fluid shear stress enhances IGF-I receptor signaling in osteoblasts in a PKCzeta-dependent manner.** *Mol Cell Biomech* 2007, **4(1)**:13-25.
10. Boutahar N, Guignandon A, Vico L, Lafage-Proust MH: **Mechanical strain on osteoblasts activates autophosphorylation of focal adhesion kinase and proline-rich tyrosine kinase 2 tyrosine sites involved in ERK activation.** *J Biol Chem* 2004, **279(29)**:30588-30599.
11. Bacabac RG, Smit TH, Mullender MG, Dijcks SJ, van Loon JJ, Klein-Nulend J: **Nitric oxide production by bone cells is fluid shear stress rate dependent.** *Biochem Biophys Res Commun* 2004, **315(4)**:823-829.
12. Gieffers C, Engelhardt W, Brenzel G, Matsuishi T, Frey J: **Receptor binding of osteoblast-specific factor I (OSF-I/HB-GAM) to human osteosarcoma cells promotes cell attachment.** *Eur J Cell Biol* 1993, **62(2)**:352-361.
13. Petersen W, Rafii M: **Immunolocalization of the angiogenic factor pleiotrophin (PTN) in the growth plate of mice.** *Arch Orthop Trauma Surg* 2001, **121(7)**:414-416.
14. Amet LE, Lauri SE, Hienola A, Croll SD, Lu Y, Levorse JM, Prabhakaran B, Taira T, Rauvala H, Vogt TF: **Enhanced hippocampal long-term potentiation in mice lacking heparin-binding growth-associated molecule.** *Mol Cell Neurosci* 2001, **17(6)**:1014-1024.
15. Imai S, Kaksonen M, Raulo E, Kinnunen T, Fages C, Meng X, Lakso M, Rauvala H: **Osteoblast recruitment and bone formation enhanced by cell matrix-associated heparin-binding growth-associated molecule (HB-GAM).** *J Cell Biol* 1998, **143(4)**:1113-1128.
16. Yang X, Tare RS, Partridge KA, Roach HI, Clarke NM, Howdle SM, Shakesheff KM, Oreffo RO: **Induction of human osteoprogenitor chemotaxis, proliferation, differentiation, and bone formation by osteoblast stimulating factor-1/pleiotrophin: osteoconductive biomimetic scaffolds for tissue engineering.** *J Bone Miner Res* 2003, **18(1)**:47-57.
17. Tare RS, Oreffo RO, Clarke NM, Roach HI: **Pleiotrophin/Osteoblast-stimulating factor I: dissecting its diverse functions in bone formation.** *J Bone Miner Res* 2002, **17(11)**:2009-2020.
18. Masuda H, Tsujimura A, Yoshioka M, Arai Y, Kuboki Y, Mukai T, Nakamura T, Tsuji H, Nakagawa M, Hashimoto-Gotoh T: **Bone mass loss due to estrogen deficiency is compensated in transgenic mice overexpressing human osteoblast stimulating factor-1.** *Biochem Biophys Res Commun* 1997, **238(2)**:528-533.
19. Liedert A, Augat P, Ignatius A, Hausser HJ, Claes L: **Mechanical regulation of HB-GAM expression in bone cells.** *Biochem Biophys Res Commun* 2004, **319(3)**:951-958.
20. Kesavan C, Mohan S, Srivastava AK, Kapoor S, Wergedal JE, Yu H, Baylink DJ: **Identification of genetic loci that regulate bone adaptive response to mechanical loading in C57BL/6J and C3H/HeJ mice intercross.** *Bone* 2006, **39(3)**:634-643.
21. Zou P, Muramatsu H, Sone M, Hayashi H, Nakashima T, Muramatsu T: **Mice doubly deficient in the midkine and pleiotrophin genes exhibit deficits in the expression of beta-tectorin gene and in auditory response.** *Lab Invest* 2006, **86(7)**:645-653.
22. Muramatsu H, Zou P, Kurosawa N, Ichihara-Tanaka K, Maruyama K, Inoh K, Sakai T, Chen L, Sato M, Muramatsu T: **Female infertility in mice deficient in midkine and pleiotrophin, which form a distinct family of growth factors.** *Genes Cells* 2006, **11(12)**:1405-1417.
23. Lehmann W, Schinke T, Schilling AF, Catala-Lehnen P, Gebauer M, Pogoda P, Gerstenfeld LC, Rueger JM, Einhorn TA, Amling M: **Absence of mouse pleiotrophin does not affect bone formation in vivo.** *Bone* 2004, **35(6)**:1247-1255.

Publish with **BioMed Central** and every scientist can read your work free of charge

"BioMed Central will be the most significant development for disseminating the results of biomedical research in our lifetime."

Sir Paul Nurse, Cancer Research UK

Your research papers will be:

- available free of charge to the entire biomedical community
- peer reviewed and published immediately upon acceptance
- cited in PubMed and archived on PubMed Central
- yours — you keep the copyright

Submit your manuscript here:  
[http://www.biomedcentral.com/info/publishing\\_adv.asp](http://www.biomedcentral.com/info/publishing_adv.asp)



**LEPTIN RECEPTOR (*LEPR*) IS A NEGATIVE MODULATOR OF BONE MECHANOSENSITIVITY AND GENETIC VARIATIONS IN *LEPR* MAY CONTRIBUTE TO THE DIFFERENTIAL OSTEOGENIC RESPONSE TO MECHANICAL STIMULATION IN THE C57BL/6J AND C3H/HeJ PAIR OF MOUSE STRAINS\***

**Sonia Kapur<sup>1</sup>, Mehran Amoui<sup>1</sup>, Chandrasekhar Kesavan<sup>1</sup>, Xiaoguang Wang<sup>1</sup>, Subburaman Mohan<sup>1,2,3,4</sup>, David J. Baylink<sup>2</sup>, and K.-H. William Lau<sup>1,2,3</sup>.**

<sup>1</sup>Musculoskeletal Disease Center, Jerry L. Pettis Memorial VA Medical Center, Loma Linda, and Departments of <sup>2</sup>Medicine, <sup>3</sup>Biochemistry, and <sup>4</sup>Physiology, Loma Linda University School of Medicine, Loma Linda, California, U. S. A.

Running Title: *Lepr* is a negative bone mechanosensitivity gene.

Address correspondence to: K.-H. William Lau, Ph.D., Musculoskeletal Disease Center (151), Jerry L. Pettis Memorial VA Medical Center, 11201 Benton Street, Loma Linda, CA 92357. Fax: (909) 796-1680, E-mail: [William.Lau@med.va.gov](mailto:William.Lau@med.va.gov)

This study investigated the role of leptin receptor (*Lepr*) signaling in determining the bone mechanosensitivity and also evaluated whether differences in the *Lepr* signaling may contribute to the differential osteogenic response of the C57BL/6J (B6) and C3H/HeJ (C3H) pair of mouse strains to mechanical stimuli. This study shows that a loading strain of ~2,500  $\mu\epsilon$ , which was insufficient to produce a bone formation response in B6 mice, increased significantly bone formation parameters in leptin-deficient *ob<sup>-/-</sup>* mice, and that a loading strain of ~3,000  $\mu\epsilon$  also yielded greater osteogenic responses in *Lepr*-deficient *db<sup>-/-</sup>* mice than in wild-type littermates. *In vitro*, a 30-min steady shear stress increased [<sup>3</sup>H]thymidine incorporation and Erk1/2 phosphorylation in *ob<sup>-/-</sup>* osteoblasts and *db<sup>-/-</sup>* osteoblasts much greater than those in corresponding wild-type osteoblasts. The siRNA-mediated suppression of *Lepr* expression in B6 osteoblasts enhanced, but in osteoblasts of C3H [the mouse strain with poor bone mechanosensitivity] restored, their anabolic responses to shear stress. The *Lepr* signaling (leptin-induced Jak2/Stat3 phosphorylation) in C3H osteoblasts was higher than that in B6 osteoblasts. One of the three single nucleotide polymorphisms in the C3H *Lepr* coding region yielded an I359V substitution near the leptin binding region, suggesting that genetic variation of *Lepr* may contribute to a dysfunctional *Lepr* signaling in C3H osteoblasts. In conclusion, *Lepr* signaling is a negative modulator of bone mechanosensitivity. Genetic variations in *Lepr*, which results in a dysfunctional *Lepr* signaling in C3H mice, may

contribute to the poor osteogenic response to loading in C3H mice.

Genetics play a key role in determining the bone response to mechanical loading. Accordingly, C57BL/6J (B6)<sup>1</sup> inbred strain of mice respond to *in vivo* loading with an increase in bone formation, but C3H/HeJ (C3H) inbred strain of mice show no such response (1-4). Quantitative trait locus (QTL) mapping studies of the C3H/B6 pair of mouse strains revealed that the bone mechanosensitivity is regulated by genes located in multiple QTLs on a number of chromosomes (5, 6) and that significant interactions exist among these QTLs (6). Thus, the genetic component contributing to the differential bone response to loading in the B6/C3H pair of mouse strains is complex and involves multiple genes. Studies of the identity of and interactions among these mechanosensitivity modulating genes would yield not only information about mechanical stimulation of bone formation but also insights into the pathophysiology of various bone-wasting diseases, e.g., osteoporosis.

Our previous studies, using primary osteoblasts of the C3H/B6 pair of mouse strains as an *in vitro* model system and fluid shear stress as an *in vitro* surrogate of mechanical strain (7), have disclosed two pieces of relevant information: 1) some of the genetic components determining bone mechanosensitivity in the C3H/B6 pair of mouse strains are intrinsic to osteoblasts, and 2) some of the “mechanosensitivity” genes contributing to the good and poor bone formation response in B6 and C3H mice, respectively, are upstream to four anabolic pathways [the wingless- and int-related protein (Wnt), IGF-I, estrogen receptor (ER), and

bone morphogenetic protein (BMP)/transforming growth factor  $\beta$  (TGF $\beta$ ) pathways].

Our search for candidate mechanosensitivity genes has focused initially on mouse chromosome 4, because functional genetic studies indicated that at least one region in mouse chromosome 4 harbors mechanosensitivity modulating genes. Specifically, the B6.C3H-4T congenic mouse strain, which is genetically identical to B6 except that it carried a segment of C3H chromosome 4 (between 40 and 80 cM), was more responsive to mechanical stimulation in periosteal bone formation than B6 mice (8). A N-ethylnitrosourea mutagenesis study in B6 mice identified a mutant exhibiting reduced bone mechanosensitivity and the mutation was mapped to chromosome 4 (9). Because the chromosome 4 congenic locus is currently the only clearly defined chromosomal region that has demonstrated functional ability to modulate mechanosensitivity (8), we focused on candidate genes on this region.

The possibility that at least some of the mechanosensitivity genes in the B6/C3H pair of mouse strains are upstream to the four aforementioned anabolic pathways (7) led to our decision of narrowing our initial search to candidate genes that may function as upstream signaling genes. It has been reported that the mechanosensitivity of the rat skeleton was markedly reduced after a long period of sustained loading (10). Loss of responsiveness after sustained activation is a hallmark characteristic of desensitization of receptor-mediated events. Thus, we decided to focus on receptor or receptor-associated genes. Although there are more than fifty receptor or receptor-associated genes located in this chromosome 4 congenic locus, we were interested in the leptin receptor (*Lepr*) gene for the following reasons: 1) It is located in this chromosomal 4 congenic region (8); 2) because *Lepr* is the cell surface receptor for leptin, *Lepr* is considered an upstream gene in the context of the leptin signaling pathway; 3) leptin deficiency had contrasting effects on weight-bearing (long bones) versus less weight-bearing (vertebrae) bones in mice (11); and 4) a preliminary genome-wide screen study in the rat suggested that *Lepr* was associated with bone architecture and strength (12), both of which are key determining factors of mechanical responsiveness. The osteogenic effects of leptin can be stimulatory or inhibitory,

depending on whether the route of administration is peripheral (13) or central (14). Because of this unique dual action on bone formation, it has been suggested that the leptin/*Lepr* signaling has a critical role in the "Mechanostat" theory of mechanical regulation of bone mass (15).

The objectives of the present study were two-fold: the first objective was to test the hypothesis that *Lepr* and/or its signaling plays a modulating role in bone mechanosensitivity. Our *in vivo* approach to test this hypothesis was to compare the bone formation response of leptin-deficient *ob<sup>-/-</sup>/ob<sup>-/-</sup>* mice and also that of *Lepr*-deficient *db<sup>-/-</sup>/db<sup>-/-</sup>* mice to a two-week four-point bending loading regimen with that of the background strain, B6, mice, or wild-type (WT) littermates, respectively. Our *in vitro* approach, which used primary osteoblasts as an *in vitro* model system and fluid shear stress as an *in vitro* surrogate of mechanical loading, was to compare the anabolic response of *ob<sup>-/-</sup>/ob<sup>-/-</sup>* and *db<sup>-/-</sup>/db<sup>-/-</sup>* osteoblasts to fluid shear with that of osteoblasts of corresponding WT littermates to demonstrate modulating functions of the leptin/*Lepr* signaling in bone cell mechanosensitivity. The second objective sought to determine if a dysfunction leptin/*Lepr* signaling in C3H osteoblasts may in part contribute to the contrasting osteogenic response to fluid shear stress between B6 and C3H osteoblasts. Leptin-deficient *ob<sup>-/-</sup>/ob<sup>-/-</sup>* mice were included in these experiments, because 1) we have previously shown that *ob<sup>-/-</sup>/ob<sup>-/-</sup>* mice lacked the sex-related differences in the greater periosteal expansion (16), which suggests a dysfunctional periosteal bone formation response to loading; and 2) rescue experiments with direct pretreatment with leptin protein can be performed in cells of *ob<sup>-/-</sup>/ob<sup>-/-</sup>* mice to confirm functional role of leptin (or *Lepr* signaling) on mechanosensitivity *in vitro*. Such straightforward rescue experiments would not be feasible with cells of *Lepr*-deficient *db<sup>-/-</sup>/db<sup>-/-</sup>* mice.

## EXPERIMENTAL PROCEDURES

**Materials** - Tissue culture plasticware was obtained from Falcon (Oxnard, CA). Dulbecco's modified Eagle's medium (DMEM) was from Mediatech, Inc. (Herndon, VA). Fetal bovine serum (FBS) was purchased from HyClone (Logan, UT). [ $^3$ H]Thymidine (48 Ci/mmol) was a product of Research Products International (Mount

Prospect, IL). Anti-pErk1/2, anti-pan-Erk1/2, anti-actin, anti-Lepr, anti-Jak2, anti-Stat3 antibodies were obtained from Santa Cruz Biotechnology (Santa Cruz, CA), Upstate Biotechnology (Lake Placid, NY), or BD Transduction Laboratories (La Jolla, CA). Other chemicals were from Fisher (Los Angeles, CA) or Sigma (St. Louis, MO).

*Animals* - Heterozygous male and female leptin-deficient ( $ob^{+}/ob^{-}$ ) breeder mice (B6.v-Lepr<sup>ob</sup>/J) as well as heterozygous male and female Lepr-deficient ( $db^{+}/db^{-}$ ) mice (B6.BKS-Lepr<sup>db</sup>) were obtained from the Jackson Laboratories (Bar Harbor, ME). A colony of each knockout mouse strain was generated and maintained at the J. L. Pettis Memorial V. A. Medical Center. Homozygous leptin-deficient genotype in  $ob^{-}/ob^{-}$  mice was confirmed by reverse-transcriptase polymerase chain reaction (RT-PCR) as previously described (17), and homozygous Lepr-deficient  $db^{-}/db^{-}$  genotype was also confirmed by a PCR-based end-point analysis genotyping assay recommended by the Jackson Labs. Our previous investigation of the bone phenotype of  $ob^{-}/ob^{-}$  mice revealed that young adult male  $ob^{-}/ob^{-}$  mice lacked the sex-related differences in the greater periosteal expansion and that the loss of sex-related bone size differences in young adult male  $ob^{-}/ob^{-}$  mice appeared to be due to a defective androgen signaling (16). To avoid potential sex-related effects, this study used only 10 weeks-old female leptin-deficient  $ob^{-}/ob^{-}$  mice and 12 weeks-old female  $db^{-}/db^{-}$  mice as well as corresponding age-matched WT littermates. Age-matched female B6 mice (also from Jackson Laboratories) were included in this study as the background strain control for  $ob^{-}/ob^{-}$  mice.

*In vivo mechanical loading model* - Our rationale for choosing the two-week four-point bending regimen as the *in vivo* loading model and the description of the model has been described in details previously (7). The loading was applied for 6 days/week with 1 day of rest for 2 weeks. Forty-eight h after the final loading, bone parameters of the loaded and contralateral unloaded tibiae (internal controls) were determined with peripheral quantitative computed tomography (pQCT). The animal protocol was reviewed and approved by the Institutional Animal Care and Use Committee of the J. L. Pettis Memorial V.A. Medical Center.

*Strain gauge measurements* - The amount of mechanical strain on the loaded region of the tibia produced by each indicated load was measured by the strain-gauge technique using a P-3500 portable strain indicator and a strain gauge of a specific range (EP-XX-015DJ-120) (4). Briefly, the ends of the strain gauge circuits were soldered to copper wire and glued on the medial side of the exposed tibia, 2.09 mm from the tibia-fibular junction, to provide a consistent position on the 4-mm loading zone. The copper wires were connected to the indicator, and the amounts of strain produced by the loads on the loading zone were recorded. The strain gauge data from four mice from each mouse strain were averaged for each test load.

*Bone parameter measurements* - Bone parameters (total bone mineral content, total tissue area, periosteal circumference, endosteal circumference, cortical area, cortical thickness, cortical content, material bone mineral density, and volumetric bone mineral density) were determined by pQCT (Stratec XCT 960M, Norland Medical Systems, Ft. Atkinson, WI) with the analysis threshold settings of 730-730 for cortical bone and 180-730 for cancellous bone.

*Cell cultures* - Osteoblasts, isolated from calvarias of 8 weeks-old B6 and C3H mice by collagenase digestion as described previously (7, 18), were maintained in DMEM supplemented with 10% FBS. Osteoblasts were also isolated from calvarias of 10 weeks-old female  $ob^{-}/ob^{-}$  mice, 12 weeks-old female  $db^{-}/db^{-}$  mice, and corresponding age-matched WT littermates. Cell passage, up to passage 7, had no significant effects on the responsiveness of primary B6 osteoblasts to fluid shear stress with respect to [<sup>3</sup>H]thymidine incorporation, alkaline phosphatase activity, and Erk1/2 phosphorylation (data not shown). Thus, cells of passages 3–6 were used in this study.

*Shear stress experiments* - Fifty thousand cells were plated on each glass slide. At ~80% confluency, the cells were serum-deprived for 24 h and subjected to a steady fluid shear stress of 20 dynes/cm<sup>2</sup> for 30 min in the Cytodyne flow chamber as described previously (19). This dosage of shear stress is considered within the physiologically relevant range of laminar shear stress produced by the circulation (20). Replicate glass slides of cells were placed in parallel flow chambers but without the shear stress as static controls for comparison.

*[<sup>3</sup>H]Thymidine incorporation assay* - Cell proliferation was assessed by [<sup>3</sup>H]thymidine incorporation during final 6 h of the 24-h post-exposure to shear stress (7, 19).

*Western immunoblot assays* - The relative cellular phosphorylated extracellular regulated kinase 1/2 (pErk1/2) level was determined with the antibody against pErk1/2 and normalized against corresponding the total Erk1/2 level (determined with the anti-panErk1/2 antibody) as previously described (7, 19).

For measurements of leptin-induced activation of Janus kinase (Jak)2/signal transducers and activators of transcription (Stat)3 signaling, primary osteoblasts isolated from B6, *ob/ob*, or C3H mice were treated with 100 ng/ml leptin for 24 h and were then subjected to the 30-min steady shear stress. Ten minutes after the shear stress, the stressed and static control cells were lysed in radioimmunoprecipitation assay buffer, and the relative levels of tyrosyl-phosphorylated Jak2 (pY-Jak2), total Jak2, pY-Stat3, and total Stat3 were analyzed by Western immunoblots using respective specific antibodies.

*Lepr co-immunoprecipitation assay* - Ten minutes after the shear stress, the stressed and static control cells from 3 slides each were pooled and lysed in radioimmunoprecipitation assay buffer and cell extract protein (0.5 µg) of the stressed and static control B6 osteoblasts was immunoprecipitated with the anti-Lepr antibody. The immune complex was resolved on 10% SDS-PAGE, and the co-immunoprecipitated Jak2 was identified with an anti-Jak2 antibody. The stripped blot was reblotted against an anti-Stat3 antibody to identify the co-immunoprecipitated Stat3.

*Real-time RT-PCR analyses* - Real-time PCR was carried out with the SYBR Green method on the MJ Research DNA Engine Opticon® 2 System (Waltham, MA). Briefly, total RNA was extracted with Qiagen mini RNA kit (Qiagen, Valencia, CA). The purified total RNA was used as template for synthesizing cDNA by reverse transcription using random hexamer primers and Superscript II reverse transcriptase (Invitrogen, Carlsbad, CA). An aliquot of the cDNA was subjected to real-time PCR amplification using gene-specific primer sets listed in Supplemental Table S1. An aliquot (25 µl) of reaction mixture [consisted of 2X (12.5 µl) QuantiTect SYBR Green PCR master mix, which contained the Hot Start *Taq* polymerase (Qiagen),

0.5 µM of primers, and 1–5 µg of cDNA template] was used in each assay. The PCR amplification condition was consisted of an initial 10-min hot start at 95 °C, followed by 40 cycles of denaturation at 95 °C for 30 s, annealing, extension for 30 s at an appropriate temperature (50–72 °C) (see Supplemental Table S1), and a final step of melting curve analysis from 60 to 95 °C. The data were analyzed using Opticon® Monitor Software 2.0. Data normalization was performed against β-actin mRNA, and the normalized values were used to calculate relative fold change by the threshold cycle (ΔC<sub>T</sub>) method.

*Leptin protein enzyme immunoassay (EIA)* - Secretion of leptin protein from primary B6 and C3H osteoblasts were determined by measuring the amounts of leptin protein in 24-h conditioned media (CM). Briefly, 24-h CM (7 ml each) of replicate cultures (4 slides each) of primary B6 and C3H osteoblasts without (i.e., basal) or with the 30-min shear stress were collected separately, lyophilized, and resuspended in 0.7 ml of deionized water. The amount of leptin protein in each resuspended CM was determined with a commercial mouse leptin EIA (mouse Leptin TiterZyme® EIA, Cat. # 900-019; Assay Designs, Ann Arbor, MI), and reported as pg leptin per mg cellular protein per 24 h.

*Lepr siRNA experiments* - A set of three small-interfering RNA duplex (siRNA) specific for mouse *Lepr* [i.e., *Lepr* siRNA1 (target sequence: CCC GAG CAA ATT AGA AAC AAA), *Lepr* siRNA2 (target sequence: ATC GAT GTC AAT ATC AAT ATA), and *Lepr* siRNA3 (target sequence: TTG AAG CTA AAT TTA ATT CAA)] and a non-silencing control siRNA without any homology to known mammalian genes were designed and synthesized by Qiagen. For the siRNA experiment, primary B6 or C3H osteoblasts were seeded at 60,000 cells in 24-well plate for 24 h. The cells were transfected with the test siRNAs using the HiPerFect Transfection reagent (Qiagen). Briefly, three µl of HiPerFect Transfection Reagent was added to 100 µl of DMEM containing 75 ng of *Lepr* (or control) siRNA duplex. The reaction mixture was incubated for 10 min at room temp and was added to each cell culture well containing 500 µl of fresh DMEM and 10% FBS. After 16 h of incubation at 37°C, the medium was replaced by fresh DMEM

containing FBS. The effectiveness of *Lepr* suppression after an additional 24-48 h of incubation at 37°C was assessed by Western immunoblot using an anti-*Lepr* antibody. The protein loading was normalized against the cellular actin level using a specific anti-actin antibody.

*Cloning of full-length Lepr cDNA from B6 and C3H osteoblasts* – The full-length cDNA of the signal-transducing long form of *Lepr* (LRb) was cloned from both C3H and B6 osteoblasts by a RT-PCR-based cloning approach. Briefly, total RNA was purified from C3H and B6 osteoblasts with the RNeasy kit (Qiagen). Two µg of total RNA of C3H or B6 osteoblasts was each reverse transcribed into first-strand cDNA using oligo(dT) primer with the RNase H–reverse transcriptase (Superscript II Invitrogen Life Technologies) in the presence of the deoxynucleotides. The full-length *Lepr* cDNA was produced by PCR using the following primer set (forward primer: 5'-AAA AGG ATC CAG ATG ATG TGT CAG AAA TTC-3' and reverse primer: 5'-AAA AAA GCT TTC AAA GAG TGT CCG TTC TCT-3'). To facilitate cloning, *Bam*HI and *Hind*III restriction sites (underlined), respectively, were added to the forward and reverse primer. The PCR amplification was performed with native pfu DNA polymerase (Stratagene, La Jolla, CA) with the condition consisting: a 1-min hot start at 95°C, 35 cycles of 45-s denaturation at 95°C, 45-s annealing at 63 °C, 1-min extension at 72 °C, and a final 10-min extension at 72 °C. The 2,615-bp *Lepr* PCR product of C3H and B6 osteoblasts was gel-purified, digested with *Bam*HI and *Hind*III restriction enzymes, and cloned into pcDNA3.1 at these two restriction sites. The entire coding region of B6 and C3H *Lepr* gene was each determined by sequencing both strands of cDNA.

*Statistical analysis* - Statistical significance was determined with two-tailed Student's *t*-test, and the difference was significant at  $p < 0.05$ .

## RESULTS

*Bone formation response to mechanical loading in tibias of female leptin-deficient ob/ob and Lepr-deficient db/db mice* – To test whether leptin/*Lepr* signaling has modulating functions on bone mechanosensitivity, we first compared the osteogenic response to a 2-week four-point bending loading regimen on tibias of young adult

female leptin-deficient *ob/ob* mice with that on tibias of age-matched female B6 (background genetic strain control) mice. The size (periosteal circumference) of tibia of young adult female *ob/ob* mice was significantly bigger (by ~14%) than that of age-matched female B6 tibia (Fig. 1A). Because the bone formation response is determined by mechanical strain sensed by the bone rather than the loading force *per se*, and because the amount of strain generated by a given load is largely determined by the size of bone, we measured, with a strain gauge, the actual strain sensed by the loaded tibias of young adult female *ob/ob* mice as opposed to age-matched female B6 tibia at various loads (Fig. 1B). The determined strain sensed by the bones compared well with the calculated strain (based on respective bone size) at various loading forces for the two mouse strains. The tibia of B6 mice with a smaller bone size had indeed experienced a much higher strain at any given load than tibias of *ob/ob* mice. Accordingly, we adjusted the loading force for each mouse strain to ensure that similar mechanical strain was applied to tibia of each mouse strain. Our past studies in B6 mice used 9-N, which showed a substantial bone formation response (4-6, 8, 9). If a 9-N load were to be used in B6 mice, a loading force of ~16-N is needed for *ob/ob* mice for similar mechanical strain. However, because the magnitude of bone formation response differences between the two strains at higher loads may not be as large, and because the lower strain is physiologically more relevant than the higher strain, we decided to use a 9-N load (~2,100 µε) for young adult female *ob/ob* mice but only a 6-N load (~2,500 µε) for young adult female B6 mice.

To adjust for the small difference in the actual mechanical strain sensed by the B6 tibia as opposed to the *ob/ob* tibia, the pQCT bone parameters were reported as % change from corresponding unloaded tibia per 1,000 µε (Fig. 1C). Consistent with the previous finding that a 6-N load is insufficient to produce a bone formation response in young adult B6 mice (4), the mechanical strain of ~2,500 µε (6-N force) had no significant effect on any of the pQCT parameters in young adult female B6 mice. In contrast, this mechanical strain increased significantly total bone mineral content, cortical area, cortical

content, cortical thickness, and material and volumetric bone mineral densities at the loading site in *ob<sup>-</sup>/ob<sup>-</sup>* mice, indicating that *ob<sup>-</sup>/ob<sup>-</sup>* mice had an enhanced mechanosensitivity compared to B6 mice.

*Anabolic response of ob<sup>-</sup>/ob<sup>-</sup> osteoblasts to fluid shear stress* - To determine whether leptin deficiency would also lead to an enhanced anabolic response to mechanical stimuli in osteoblasts *in vitro*, we assessed the effects of a 30-min steady fluid shear of 20 dynes/cm<sup>2</sup> on [<sup>3</sup>H]thymidine incorporation and Erk1/2 phosphorylation in osteoblasts of young adult female *ob<sup>-</sup>/ob<sup>-</sup>* mice as opposed to those in osteoblasts of age-matched female B6 mice and WT littermates (*ob<sup>+</sup>/ob<sup>+</sup>*). Fig. 2 confirms that the shear stress stimulated [<sup>3</sup>H]thymidine incorporation and Erk1/2 phosphorylation in B6 osteoblasts. However, the same stress produced significantly greater increases in [<sup>3</sup>H]thymidine incorporation and Erk1/2 phosphorylation in *ob<sup>-</sup>/ob<sup>-</sup>* osteoblasts than in B6 or WT osteoblasts.

If the enhanced mitogenic response of *ob<sup>-</sup>/ob<sup>-</sup>* osteoblasts to fluid shear was due to a deficiency in leptin expression, pretreatment with an effective dose of leptin should block the enhanced response in *ob<sup>-</sup>/ob<sup>-</sup>* osteoblasts. Consistent with this speculation, the mitogenic response to shear stress in *ob<sup>-</sup>/ob<sup>-</sup>* osteoblasts was reduced markedly by a 2-h pretreatment with 100 ng/ml leptin and in fact it was returned to a level that was no longer different from that seen in B6 osteoblasts (Fig. 3).

*Effects of leptin deficiency on the fluid shear-induced upregulation of genes associated with four anabolic pathways in mouse osteoblasts* - Our previous studies revealed that fluid shear stress differentially upregulated in B6, but not C3H, osteoblasts, the expression of a number of genes associated with four anabolic pathways [the Wnt, IGF-I, ER, and BMP/TGF $\beta$  pathways] (7). To test whether the enhanced mitogenic response in leptin-deficient *ob<sup>-</sup>/ob<sup>-</sup>* osteoblasts is accompanied by an enhanced response in upregulation of genes associated with these four anabolic pathways, relative expression levels of several genes associated with the IGF-I (*Igf1r*, *c-fos*), ER (*Era*, *Ncoa1*), BMP (*Dlx1*), and Wnt (*Ctnnb1*, *Wnt1*, *Wnt3a*) pathways 4 h after the fluid shear were measured by real-time RT-PCR (Supplemental Table S2). While the shear stress significantly upregulated the expression of each test gene in B6

and *ob<sup>-</sup>/ob<sup>-</sup>* osteoblasts, the upregulation was significantly and consistently greater in *ob<sup>-</sup>/ob<sup>-</sup>* osteoblasts than in B6 osteoblasts. The shear stress-induced upregulation of expression of these test genes in B6 osteoblasts as well as in *ob<sup>-</sup>/ob<sup>-</sup>* osteoblasts was blocked by the overnight leptin pretreatment (Table 1), indicating that the leptin signaling is likely acting upstream to these four anabolic pathways.

*Enhanced osteogenic response to mechanical loading in tibias of female Lepr-deficient db<sup>-</sup>/db<sup>-</sup> mice* - We next sought to confirm that enhanced mechanosensitivity can also be seen in *Lepr*-deficient *db<sup>-</sup>/db<sup>-</sup>* mice by comparing the periosteal bone formation response to a 2-week four-point bending loading regimen on tibia of young adult female *Lepr*-deficient *db<sup>-</sup>/db<sup>-</sup>* mice with that on tibia of age-matched female WT littermates. Like *ob<sup>-</sup>/ob<sup>-</sup>* mice, the periosteal circumference of tibia of 12 weeks-old female *db<sup>-</sup>/db<sup>-</sup>* mice was also bigger (by 5.6%,  $p < 0.001$ ) than that of age-matched female WT littermates (Fig. 4A). Thus, we used a loading force of 9 N on *db<sup>-</sup>/db<sup>-</sup>* tibias (which produced a strain of  $\sim 3,100 \mu\epsilon$ ) and a loading force of 6.5-7.5 N on tibias of WT littermates (which yielded a strain of  $\sim 3,000 \mu\epsilon$ ) to ensure that a similar mechanical strain was applied to the tibia of both mouse strain. Although this mechanical strain produced significant bone formation responses (e.g., mBMC and vBMD) in both *db<sup>-</sup>/db<sup>-</sup>* mice and WT littermates (Fig. 4B), the response in *db<sup>-</sup>/db<sup>-</sup>* tibias was significantly ( $p < 0.01$  for each) greater than that in tibias of WT littermates, confirming that mice deficient in *Lepr* expression indeed exhibited enhanced bone formation response to loading.

*Enhanced anabolic response of db<sup>-</sup>/db<sup>-</sup> osteoblasts to fluid shear stress* - Fig. 5 confirms that while the 30-min steady fluid shear at 20 dynes/cm<sup>2</sup> enhanced [<sup>3</sup>H]thymidine incorporation and Erk1/2 phosphorylation in both *db<sup>-</sup>/db<sup>-</sup>* osteoblasts and WT osteoblasts, the increases were also significantly ( $p < 0.05$ ) larger in *db<sup>-</sup>/db<sup>-</sup>* osteoblasts than in WT osteoblasts. Thus, osteoblasts of *Lepr*-deficient mice also have an enhanced anabolic response to mechanical stimulation.

*Functional role of Lepr in the anabolic response to the fluid shear stress in mouse osteoblasts* - To confirm a functional role of *Lepr* in determining the anabolic response to

mechanical stimuli in B6 osteoblasts, the effects of siRNA-mediated knockdown of *Lepr* expression on the mitogenic action of fluid shear stress in B6 osteoblasts were investigated. The effects of three *Lepr* siRNAs alone or in combination on *Lepr* expression in B6 were examined. The treatment with *Lepr* siRNA2 reduced cellular *Lepr* protein level by >70% (Fig. 6A). Down-regulation of *Lepr* expression in B6 osteoblasts by *Lepr* siRNA2 enhanced both basal (i.e., static control) and fluid shear-induced Erk1/2 phosphorylation much further in B6 osteoblasts (Fig. 6B). These findings together indicate that leptin/*Lepr* signaling has a negative modulating role in the anabolic response to mechanical stimuli in these mouse osteoblasts.

*Role of Lepr in the lack of an anabolic response in C3H osteoblasts to fluid shear stress* - We next tested whether the lack of a significant anabolic effect in C3H osteoblasts to shear stress is related to dysfunctional *Lepr* or *Lepr* signaling. Accordingly, if the lack of a mitogenic response to fluid shear stress in C3H osteoblasts (7) is due to a dysfunctional *Lepr*, suppression of expression or activity of *Lepr* in C3H osteoblasts should restore the responsiveness of these cells to shear stress with an increase in cell proliferation. Consistent with this prediction, the siRNA-mediated suppression of *Lepr* expression in C3H osteoblasts restored their mitogenic responsiveness to fluid shear stress (Fig. 7). Thus, the lack of an anabolic response to shear stress in C3H osteoblasts could be due to a dysfunctional *Lepr*.

*Basal and shear stress-induced secretion of leptin and Lepr gene expression levels in C3H and B6 osteoblasts* - Human osteoblasts have been shown to produce and secrete leptin protein (21). To investigate the possibility that the good and poor anabolic response to shear stress of B6 and C3H osteoblasts, respectively, might be due to secretion of different amounts of leptin protein by B6 and C3H osteoblasts, we measured the amounts of leptin protein in the 24-h CM of B6 and C3H osteoblasts with or without the 30-min fluid shear (Fig. 8A). The amount of leptin in CM of each static control culture was low but detectable (~2 pg/mg cellular protein/24 h). The shear stress increased the CM leptin concentration by ~3-fold in either osteoblast culture. However, there was no significant difference in basal or shear stress-induced leptin secretion levels between the B6 and C3 osteoblasts, indicating that

the differential anabolic response to shear stress between B6 and C3H osteoblasts was probably not due to differences in leptin secretion.

We next investigated whether the differential anabolic response was due to differences in *Lepr* expression levels between B6 and C3H osteoblasts by measuring the relative mRNA levels of the signal-transducing (long) form of *Lepr* in primary osteoblasts of these two mouse strains by real-time RT-PCR (Fig. 8B). There was no significant difference in basal *Lepr* mRNA levels (reported as  $\Delta C_T$ ) (left panel). Although the shear stress increased the *Lepr* mRNA levels slightly by ~40% in B6 osteoblasts and ~25% in C3H osteoblasts (right panel), the difference between the two was not statistically significant. Thus, the difference in anabolic response to shear stress between the two mouse osteoblasts was also unlikely due to different expression levels of the functional form of *Lepr*.

*Comparison of leptin-dependent activation of Jak2/Stat3 signaling in C3H and B6 osteoblasts* - We next tested the alternative possibility that the different anabolic response to fluid shear stress of B6 and C3H osteoblasts might be due to different abilities of *Lepr* to trigger its signaling activity in the two mouse osteoblasts. *Lepr* is a member of the class I cytokine receptor family and uses the Jak2/Stat3 pathway as its primary signaling mechanism (22-24). Thus, we measured the relative ratios of pY-Jak2/total Jak2 and pY-Stat3/total Stat3, as indices of activation of the *Lepr* signaling, without (basal) or with the fluid shear in C3H and B6 osteoblasts. Osteoblasts of *ob<sup>-/-</sup>* mice were included for comparison. To ensure full activation of the *Lepr* signaling, the cells were pre-treated with 100 ng/ml leptin for 24 h prior to the shear stress. The basal leptin-dependent increases in pY-Jak2 (Fig. 9A) and in pY-Stat3 (Fig. 9B) levels were two-fold higher in C3H osteoblasts than those in B6 and *ob<sup>-/-</sup>* osteoblasts, suggesting that C3H osteoblasts might have a functionally more active *Lepr* signaling. The shear stress markedly reduced the relative levels of pY-Jak2 (Fig. 9A) and pY-Stat3 (Fig. 9B) in B6, *ob<sup>-/-</sup>*, as well as C3H osteoblasts. However, the shear stress-related reduction in the levels of these pY-proteins was also comparatively smaller in C3H osteoblasts than in B6 osteoblasts.

It is interesting that the total Jak2 and Stat3 levels were two- to threefold higher in C3H

osteoblasts than in B6 or *ob<sup>-/-</sup>* osteoblasts. Thus, it may be argued that while fluid shear suppressed the leptin-mediated pY-Jak2 and pY-Stat3 levels in C3H osteoblasts, the remaining pY-Jak2 and pY-Stat3 levels in C3H osteoblasts were still several-fold higher than basal pY-Jak2 and pY-Stat3 levels in B6 and *ob<sup>-/-</sup>* osteoblasts, simply because of the much higher basal total levels of these proteins in C3H osteoblasts.

Other members of the class I cytokine receptor family could also activate the Jak2/Stat3 signaling. To ensure that the fluid shear-mediated reduction in the Jak2/Stat3 activation was related to the *Lepr* signaling, we performed co-immunoprecipitation experiment to assess the relative amounts of *Lepr*-associated Jak2/Stat3 in B6 osteoblasts (Fig. 9C). The fluid shear reduced markedly the amounts of *Lepr*-bound Jak2 and Stat3; a finding consistent with the interpretation that the reduced Jak2/Stat3 activation was in large part related to the shear stress-mediated reduction in the *Lepr* signaling.

*Single nucleotide polymorphisms (SNPs) in Lepr coding region* - A large number of SNPs have been identified in the coding and noncoding regions of human *Lepr* (25), and the three nonsynonymous SNPs (i.e., K109R, Q223R, and K665N SNPs) in human *Lepr* are associated strongly with adiposity, body composition, BMD, fracture risk, and leptin response (26, 27). Because SNPs in noncoding regions are usually involved in regulation of gene expression but not gene functions, and because Fig. 8B indicates that the *Lepr* gene expression in C3H and B6 osteoblasts was not different, we focused on SNPs in the coding region. Comparison of coding region of the *Lepr* cDNA sequence of C3H and B6 osteoblasts revealed three single nucleotide differences (Fig. 10). These differences were not PCR-introduced mutations, since the same variations existed in some of the *Lepr* coding region sequences in the PubMed database. Thus, there are three SNPs in the coding sequence of *Lepr* between the B6 and C3H mouse strains: 1) G→A SNP at nucleotide 594; 2) T→C SNP at 1041, and 3) A→G SNP at 1075. Two of the SNPs are located at the wobble base and are silent (i.e., synonymous), but the A→G SNP at 1075 is nonsynonymous and results in the I359V substitution.

## DISCUSSION

Mechanical loading is a key physiological regulatory mechanism for periosteal bone formation and is essential for the maintenance of skeletal architectural integrity and bone strength. It is now clear that determination of the overall osteogenic response to mechanical loading has a large genetic component. However, despite several genetic linkage and association studies that have identified a number of genetic loci harboring mechanosensitivity modulating genes on various chromosomes (1-10, 28), little information about the identity of these mechanosensitivity genes is available. In this study, we provide several lines of strong *in vivo* and *in vitro* evidence that *Lepr* or its signaling may function as a negative modulator of bone mechanosensitivity in the mouse. Accordingly, we showed that young adult female leptin-deficient *ob<sup>-/-</sup>* mice exhibited an enhanced bone formation response to loading compared to young adult female B6 control mice *in vivo* and that the *in vitro* anabolic response of osteoblasts of *ob<sup>-/-</sup>* mice to a steady fluid shear stress was consistently and significantly greater than that in osteoblasts derived from WT littermates or B6 control mice. More importantly, we demonstrate that loading on tibias of young adult *Lepr*-deficient *db<sup>-/-</sup>* mice produced significantly greater periosteal bone formation response than that on tibias of age-matched WT littermates and that osteoblasts derived from *db<sup>-/-</sup>* mice also exhibited enhanced anabolic response to the fluid shear *in vitro*. These findings together lead us to conclude that the *Lepr* or its signaling has a negative modulating role in the osteogenic response to mechanical stimulation. The facts that shear stress reduced the leptin-dependent, *Lepr*-mediated phosphorylation of Jak2 and Stat3 along with the amounts of total Jak2 and Stat3 in *ob<sup>-/-</sup>* and also B6 osteoblasts further allow us to postulate that mechanical stimulation of the osteoblast activity and bone formation is in part mediated through suppression of the *Lepr* signaling in osteoblasts.

It is a general belief that osteocytes are the primary sensory cells of loading-induced fluid shear within the bone that transmit biological signals to osteoblasts at the bone surfaces (29, 30), because osteocytes are well situated within the bone to detect the fluid shear stress (29), have the ability to communicate with other bone cells through an extensive network of cellular processes

connected at gap junctions (31), and respond to mechanical stimuli (32, 33). However, because primary osteocytes are difficult to isolate, we did not determine the effects of shear stress on the anabolic response of osteocytes of *ob<sup>-/-</sup>* and *db<sup>-/-</sup>* mice in this study. On the other hand, there is evidence that osteoblasts also sensed and responded to mechanical signals, and that the gene expression response and/or mechanotransduction mechanism in osteocytes and osteoblasts appear mostly similar (34). Therefore, we speculate that fluid shear stress would produce similar enhanced osteogenic responses in osteocytes of *ob<sup>-/-</sup>* and *db<sup>-/-</sup>* mice in response to fluid shear stress as those seen in osteoblasts of these mice, such that *Lepr* or its signaling would play a similar negative modulating role in the overall mechanosensitivity of osteocytes.

The molecular mechanism by which *Lepr* (or *Lepr* signaling) acts to negatively modulate the anabolic response of osteoblasts to mechanical stimulation remains to be determined. However, because the fluid shear stress-induced upregulation of expression of genes of the four anabolic signal transduction pathways (i.e., Wnt, IGF-I, ER, and BMP/TGF $\beta$ ) was significantly enhanced in leptin-deficient *ob<sup>-/-</sup>* osteoblasts compared to B6 mice, and because this enhanced expression of these genes of the four anabolic pathways was abolished by the leptin pretreatment, we conclude that leptin (or its signaling) acts upstream to these four anabolic pathways to negatively modulate the anabolic response to mechanical stimulation in these osteoblasts. Consistent with the possibility that *Lepr* signaling is upstream to at least some of these anabolic pathways is the finding that ablation of ER $\alpha$  [which is essential for mechanotransduction (35)] blocked the leptin-mediated upregulation of proopiomelanocortin in hypothalamus (36). In addition, mice deficient in ER $\alpha$  (36) or IGF-I (37) exhibited elevated serum leptin levels. This is consistent with a feedback upregulation of leptin expression in ER $\alpha$  or IGF-I KO mice.

The mechanism by which leptin/*Lepr* signaling acts to negatively regulate these four anabolic pathways remains to be determined. In this regard, the activated *Lepr* recruited a number of signaling proteins, including SHP2 and PTP1B, through its phosphorylated tyrosine residues (22-

24). There is circumstantial evidence that the *Lepr* signaling interacts and regulates other key signaling pathways, including the integrin, IGF-I, ER, BMP/TGF $\beta$ , and Wnt signaling pathways, through SHP2 or PTP1B (38-40). It is conceivable that the *Lepr* signaling may negatively modulate the anabolic response to mechanical stimulation in part by suppressing these four anabolic pathways through crosstalk involving signaling proteins, such as SHP2 and PTP1B, in osteoblasts.

Our findings that the leptin/*Lepr* signaling functions as a negative modulator of bone mechanosensitivity in mouse osteoblasts may have physiological implications in humans, in that it may play a role in the only recently recognized strong intra-regulatory relationship between fat and bone (41). Thus, it is not surprising that leptin or *Lepr* signaling [the key negative regulatory hormone for body fat (42)] also play a negative regulatory role in bone responsiveness to mechanical loading. More importantly, the findings that 1) the increase in obesity in postmenopausal women was associated with an increase in the circulating leptin level (43), 2) estrogen replacement in postmenopausal women decreased serum leptin levels (44), and 3) the *PvuII* and *XbaI* polymorphisms of ER $\alpha$  significantly influence the association between the Q223R polymorphism of human *Lepr* and peak bone mineral density (45) raise the interesting possibility that the suppressive action of leptin or *Lepr* signaling on bone mechanosensitivity might also have a role in the reduction in bone formation in postmenopausal osteoporotic patients. Our future studies will address these very interesting possibilities.

A major objective of this study is to evaluate whether genetic variations in *Lepr* may contribute in part the contrasting osteogenic response to mechanical stimulation between the C3H and B6 pair of inbred mouse strains (1-4,7). In this respect, this study, in addition to presenting compelling evidence that the *Lepr* signaling functions as a negative modulator in bone mechanosensitivity, also offers strong evidence to support our contention that there are significant differences in *Lepr* or its signaling between B6 and C3H osteoblasts and that these differences may in part contribute to the good and poor osteogenic response to mechanical loading in B6 and C3H mice, respectively (1-4,7). Accordingly,

we showed that downregulation of *Lepr* expression by siRNA in C3H osteoblasts restored the anabolic response to the shear stress stimulation. It is also interesting to note that the basal levels of Jak2 and Stat3 levels in C3H was two- to three-fold higher than that in B6 and *ob/ob* osteoblasts. The leptin-induced pY-Jak2 and pY-Stat3 levels in C3H osteoblasts was also two- to three-fold greater than that in B6 and *ob/ob* osteoblasts, suggesting that the basal *Lepr* signaling was significantly greater in C3H osteoblasts than B6 osteoblasts. Since there were no apparent differences in the basal expression levels of *Lepr* or basal secretion rates of leptin protein between C3H and B6 osteoblasts *in vitro*, we conclude that the basal *Lepr* signaling activity in C3H osteoblasts is “hyperactive” compared to that in B6 osteoblasts. The reason for elevated basal levels of Jak2 and Stat3 in C3H osteoblasts is unclear. One possible explanation is that the elevated basal levels of Jak2 and Stat3 in C3H osteoblasts could be a result of the physiological feedback upregulation of their biosynthesis of Jak2 and Stat3 in response to a “hyperactive” *Lepr* or *Lepr* signaling. We cannot, however, rule out the possibility that other genetic differences existed between B6 and C3H inbred strains of mice might be responsible for the elevated basal expression levels of Jak2 and Stat3 in C3H osteoblasts. Moreover, the increases in pY-Jak2 and pY-Stat3 levels in C3H osteoblasts could merely be the consequence of the high basal Jak2 and Stat3 levels in these cells. Future work is needed to determine the mechanistic reasons for the elevated Jak2/Stat3 and pY-Jak2/pY-Stat3 in C3H osteoblasts compared to B6 osteoblasts.

Regardless of the reason, the higher basal Jak/Stat levels and the greater *Lepr* signaling in C3H osteoblasts could provide a potential explanation for the lack of an anabolic response to mechanical stimulation in these osteoblasts. Accordingly, although the shear stress also reduced the leptin-mediated pY-Jak2 and pY-Stat3 levels in C3H osteoblasts, the resulting pY-Jak2 and pY-Stat3 levels in the stressed C3H osteoblasts were still high compared to those in B6 osteoblasts. Thus, it is conceivable that the shear stress produced by physiologically relevant levels of loading might not be sufficient to suppress the *Lepr* signaling in C3H mice to a level that would be low enough to allow for an anabolic response in

C3H mice. Congruent with this possibility and our contention that a significantly higher loading stress would be needed to reduce the *Lepr* signaling in C3H osteoblasts to levels that allow for an anabolic response, past findings that higher than physiological levels of mechanical strain were able to elicit an osteogenic response in C3H mice (46).

This study also disclosed an important piece of information that might be relevant to the potential mechanism leading to the “hyperactive” *Lepr* signaling in C3H osteoblasts. Accordingly, we found three SNPs existed in the coding region of the *Lepr* gene between C3H and B6 mice. One of these SNPs is a nonsynonymous SNP that results in an I359V substitution in the *Lepr* protein in C3H osteoblasts. This amino acid residue is located within the Ig-like C2-type domain of the extracellular region of the protein (47). This hydrophobic, Ig-like C2-type domain is believed to be involved in the leptin binding (47). Because the leptin binding domain has been mapped to residues 323-640 (48), this I359 residue may be involved in the leptin binding and/or the conformational change needed for activation of the *Lepr* signaling. In this regard, there is strong evidence that activation of *Lepr* signaling was induced by ligand-dependent or -independent receptor dimerization (49, 50) or conformational change (50, 51). There is evidence that fluid shear induces conformational change in membrane receptors (52) and in membrane-associated proteins (53). Thus, it is possible that fluid shear stress alters dimerization and/or conformation of *Lepr*, which could then affect ligand binding affinity and/or its efficiency to activate intracellular signals. Thus, although the physiological significance of this substitution is unclear, we postulate that this I359V substitution in C3H *Lepr* may either increase leptin binding affinity and/or may favor the conformation that would yield a more functionally active (i.e., “hyperactive”) *Lepr* in C3H osteoblasts. However, we cannot completely ignore the other two “silent” SNPs, since it is recently reported that a “silent” SNP in the *MDR1* gene altered the substrate specificity of its gene product, P-glycoprotein (54). This “silent” SNP in *MDR1* altered the kinetics of protein translation, affecting the timing of co-translational folding and insertion of the gene product into the membrane, and thereby changed the structure of the effectors and substrate

binding sites.

In summary, we have demonstrated that the *Lepr* signaling in mouse osteoblasts functions as a negative modulator of the anabolic response to mechanical stimulation *in vivo* and *in vitro*. We also presented strong *in vitro* evidence supporting the possibility that mechanical stimuli, such as fluid shear stress, exert anabolic effects in part through suppression of the *Lepr* signaling in

mouse osteoblasts. Finally, this study offers strong circumstantial evidence that the good and poor osteogenic response of B6 and C3H mice, respectively, to mechanical stimulation were in part due to a dysfunctional *Lepr* signaling in C3H mice, which is the result of a key genetic variation in the coding region of the *Lepr* between the B6 and C3H mice.

## REFERENCES

1. Akhter, M. P., Cullen, D. M., Pedersen, E. A., Kimmel, D. B., and Recker, R. R. (1998) *Calcif. Tissue Int.* **63**, 442-449.
2. Kodama, Y., Umemura, Y., Nagasawa, S., Beamer, W. G., Donahue, L. R., Rosen, C. R., Baylink, D. J., and Farley, J. R. (2000) *Calcif. Tissue Int.* **66**, 298-306.
3. Robling, A. G., and Turner, C. H. (2002) *Bone* **31**, 562-569.
4. Kesavan, C., Mohan, S., Oberholtzer, S., Wergedal, J. E., and Baylink, D. J. (2005) *J. Appl. Physiol.* **99**, 1951-1957.
5. Kesavan, C., Mohan, S., Srivastava, A. K., Kapoor, S., Wergedal, J. E., Yu, H., and Baylink, D. J. (2006) *Bone* **39**, 634-643.
6. Kesavan, C., Baylink, D. J., Kapoor, S., and Mohan, S. (2007) *Bone* **41**, 223-230.
7. Lau, K.-H. W., Kapur, S., Kesavan, C., and Baylink, D. J. (2006) *J. Biol. Chem.* **281**, 9576-9588.
8. Robling, A. G., Li, J., Shultz, K. L., Beamer, W. G., and Turner, C. H. (2003) *FASEB J.* **17**, 324-326.
9. Srivastava, A. K., Kapur, S., Mohan, S., Yu, H., Kapur, S., Wergedal, J., and Baylink, D. J. (2005) *J. Bone Miner. Res.* **20**, 1041-1050.
10. Saxon, L. K., Robling, A. G., Alam, I., and Turner, C. H. (2005) *Bone* **36**, 454-464.
11. Hamrick, M. W., Pennington, C., Newton, D., Xie, D., and Isaacs, C. (2004) *Bone* **34**, 376-383.
12. Turner, C. H., Alam, I., Sun, O., Li, J., Fuchs, R. K., Edenberg, H. J., Koller, D. L., Foroud, T., and Econs, M. J. (2005) *J. Bone Miner. Res.* **20** (Suppl 1), S28, abstract 1108.
13. Thomas, T. (2004) *Curr. Opin. Pharmacol.* **4**, 295-300.
14. Ducy, P., Amling, M., Takeda, S., Priemel, M., Schilling, A. F., Beil, F. T., Shen, J., Vinson, C., Rueger, N. M., and Karsenty, G. (2000) *Cell* **100**, 197-207.
15. Gordeladze, J. O., and Reseland, J. E. (2003) *J. Cell. Biochem.* **88**, 706-712.
16. Wang, X., Rundle, C. H., Wergedal, J. E., Srivastava, A. K., Mohan, S., and Lau, K.-H. W. (2007) *Calcif. Tissue Int.* **80**, 374-382.
17. Namae, M., Mori, Y., Yasuda, K., Kadowaki, T., Kanazawa, Y., and Komeda, K. (1998) *Lab. Anim. Sci.* **48**, 103-104.
18. Sheng, M. H.-C., Lau, K.-H. W., Beamer, W. G., Baylink, D. J., and Wergedal, J. E. (2004) *Bone* **35**, 711-719.
19. Kapur, S., Baylink, D. J., and Lau, K.-H. W. (2003) *Bone* **32**, 241-251.
20. Hillsley, M. V., and Frangos, J. A. (1994) *Biotechnol. Bioeng.* **43**, 573-581.
21. Reseland, J. E., Syversen, U., Bakke, I., Qvigstad, G., Eide, L. G., Hjertner, O., Gordeladze, J. O., and Drevon, C. A. (2001) *J. Bone Miner. Res.* **16**, 1426-1433.
22. Frühbeck, G. (2006) *Biochem. J.* **393**, 7-20.
23. Tartaglia, L. A. (1997) *J. Biol. Chem.* **272**, 6093-6096.
24. Ghilardi, N., and Skoda, R. C. (1997) *Mol. Endocrinol.* **11**, 393-369.
25. Thompson, D. B., Ravussin, E., Bennett, P. H., and Bogardus, C. (1997) *Hum. Mol. Genetics* **6**, 675-679.
26. de Luis Roman, D., de la Fuente, R. A., Sagrado, M. G., Izaola, O., and Vicente, R. C. (2006) *Arch. Med. Res.* **37**, 854-859.

27. Fairbrother, U. L., Tanko, L. B., Walley, A. J., Christiansen, C., Froguel, P., and Blakemore, A. I. (2007) *J. Bone Miner. Res.* **22**, 544-550.
28. Robling, A. G., Warden, S. J., Shultz, K. L., Beamer, W. G., and Turner, C. H. (2007) *J. Bone Miner. Res.* **22**, 984-991.
29. Aarden, E. M., Burger, E. H., and Nijweide, P. J. (1994) *J. Cell. Biochem.* **55**, 287-299.
30. Lanyon, L. E. (1993) *Calcif. Tissue Int.* **53**(Suppl 1), S102-S017.
31. Jones, S. J., Gray, C., Sakamaki, H., Arora, M., Boyde, A., Gourdie, R., and Green, C. (1993) *Anat. Embryol* **187**, 343-352.
32. Dodds, R. A., Ali, N., Pead, M. J., and Lanyon, L. E. (1993) *J Bone Miner Res* **8**, 261-267.
33. Cheng, B., Zhao, S., Luo, J., Sprague, E., Bonewald, L. F., and Jiang, J. X. (2001) *J. Bone Miner. Res.* **16**, 249-259.
34. Iqbal, J., and Zaidi, M. (2005) *Biochem. Biophys. Res. Commun.* **328**, 751-755.
35. Jessop, H. L., Suswillo, R. F., Rawlinson, S. C., Zaman, G., Lee, K., Das-Gupta, V., Pitsillides, A. A., and Lanyon, L. E. (2004) *J. Bone Miner. Res.* **19**, 938-946.
36. Hirose, M., Minata, M., Harada, K. H., Hitomi, T., Krust, A., and Koizumi, A. (2008) *Biochem. Biophys. Res. Commun.* doi:10.1016/j.bbrc.2008.04.073 [Epub ahead of print, 2008 Apr 23].
37. Fernandez-Moreno, C., Pichel, J. G., Chesnokova, V., and De Pablo, F. (2004) *FEBS Lett.* **557**, 64-68.
38. Lund, I. K., Hansen, J. A., Andersen, H. S., Moller, N. P. H., and Billestrup, N. (2005) *J. Mol. Endocrinol.* **34**, 339-351.
39. Oh, E.-S., Gu, H., Saxton, T. M., Timms, J. F., Hausdorff, S., Frevert, E. U., Kahn, B. B., Pawson, T., Neel, B. G., and Thomas, S. M. (1999) *Mol. Cell Biol.* **19**, 3205-3215.
40. Arias-Salgado, E. G., Haj, F., Dubois, C., Moran, B., Kasirer-Friede, A., Furie, B. C., Furie, B., Neel, B. G., and Shattil, S. J. (2005) *J. Cell Biol.* **170**, 837-845.
41. Reid, I. R. (2008) *Osteoporos. Int.* **19**, 595-606.
42. Zhang, Y., Proenca, R., Maffei, M., Barone, M., Leopold, L., and Friedman, J.M. (1994) *Nature* **372**, 425-432.
43. Hong, S. C., Yoo, S. W., Cho, G. J., Kim, T., Hur, J. Y., Park, Y. K., Lee, K. W., and Kim, S. H. (2007) *Menopause* **14**, 835-840.
44. Lambrinoudaki, I. V., Chrostodoulakos, G. E., Economou, E. V., Vlachou, S. A., Panoulis, C. P., Alexandrou, A. P., Kouskouni, E. E., and Creatsas, G. C. (2008) *Maturitas* **59**, 62-71.
45. Koh, J.-M., Kim, D. J., Hong, J. S., Park, J. Y., Lee, K.-U., Kim, S.-Y., and Kim, G. S. (2002) *Eur. J. Endocrinol.* **147**, 777-783.
46. Pedersen, E. A., Akhter, M. P., Cullen, D. M., Kimmel, D. B., and Recker, R. R. (1999) *Calcif Tissue Int* **65**, 41-46.
47. Niv-Spector, L., Gonen-Berger, D., Gourdou, I., Biener, E., Gussakovsky, E. E., Benomar, Y., Ramanujan, K. V., Taouis, M., Herman, B., Callebaut, I., Djiane, J., and Gertler, A. (2005) *Biochem. J.* **391**, 221-230.
48. Fong, T. M., Huang, R. R., Tota, M. R., Mao, C., Smith, T., Varnerin, J., Karpitsky, V. V., Krause, J. E., and Van der Ploeg, L. H. (1998) *Mol. Pharmacol.* **53**, 234-240.
49. Devos, R., Guisez, Y., van der Heyden, J., White, D. W., Kalai, M., Fountoulakis, M., and Plaetinck, G. (1997) *J. Biol. Chem.* **272**, 18304-18310.
50. Biener, E., Charlier, M., Ramanujan, V. K., Daniel, N., Eisenberg, A., Bjorbaek, C., Herman, B., Gertier, A., and Djiane, J. (2005) *Biol. Cell* **97**, 905-919.
51. Couturier, C., and Jockers, R. (2003) *J. Biol. Chem.* **278**, 26604-26611.
52. Chachisvillis, M., Zhang, Y. L., and Frangos, J. A. (2006) *Proc. Natl. Acad. Sci. USA* **103**, 15463-15468.
53. Fleming, I., Bauersachs, J., Fisslthaler, B., and Busse, R. (1998) *Cir. Res.* **82**, 686-695.
54. Kimchi-Sarfaty, C., Oh, J. M., Kim, I.-W., Sauna, Z. E., Calcagno, A. M., Ambudkar, S. V., Gottesman, M. M. (2007) *Science* **315**, 525-528.

## FOOTNOTES

\*This work was supported in part by the United States Army Medical Research Acquisition Activity Assistance Award (DAMD17-01-1-0744). The United States Army Medical Research Acquisition Activity, 820 Chandler Street, Fort Detrick MD 21702-5014, is the awarding and administering acquisition office. The information contained in this publication does not necessarily reflect the position or the policy of the government, and no official endorsement should be inferred. This work was also supported in part by a Merit Review provided by the Office of Research and Development, Medical Research Service, Department of Veteran Affairs. All work was performed in facilities provided by the Department of Veterans Affairs. Preliminary results were presented at the American Society of Bone and Mineral Research, Honolulu, HI, September 2007 (abstract # 1081).

## ABBREVIATIONS

<sup>1</sup>The abbreviations used are: B6, C57BL/6J inbred strain of mice; BMP, bone morphogenetic protein; C3H, C3H/HeJ inbred strain of mice; CM, conditioned medium; C<sub>T</sub>, cycle threshold; DMEM, Dulbecco's modified Eagle's medium; EIA, enzyme immunometric assay; ER, estrogen receptor; Erk1/2, extracellular regulated kinases 1/2; FBS, fetal bovine serum; Jak, Janus kinase; Lepr, leptin receptor; pErk1/2, phosphorylated Erk1/2; pQCT, peripheral quantitative computed tomography; pY, tyrosyl-phosphorylated; QTL, quantitative trait locus; RT-PCR, reverse-transcriptase polymerase chain reaction; S.D., standard deviation; S.E.M., standard error of the mean; siRNA, small-interfering RNA; SNP, single nucleotide polymorphism; Stat, signal transducers and activators of transcription; TGFβ, transforming growth factor; Wnt, the wingless- and int-related protein; WT, wild-type.

Table 1: Effect of an overnight pretreatment with 100 ng/ml leptin on the shear stress-induced expression of genes of the IGF-I, BMP/TGF $\beta$ , ER, and Wnt signaling pathways in B6 osteoblasts and *ob/ob* osteoblasts by real-time PCR 4 h after the fluid shear (n = 6 for each).

Gene	B6 osteoblasts		<i>ob/ob</i> osteoblasts	
	Stressed/Static Control (No leptin, Fold changes, mean $\pm$ S.D.)	Stressed/Static Control (+ leptin, Fold changes, mean $\pm$ S.D.)	Stressed/Static Control (No leptin, Fold changes, mean $\pm$ S.D.)	Stressed/Static Control (+ leptin, Fold changes, mean $\pm$ S.D.)
<i>Era</i>	2.40 $\pm$ 0.75*	1.39 $\pm$ 0.25 <sup>#</sup>	3.31 $\pm$ 0.20*	1.18 $\pm$ 0.24 <sup>#</sup>
<i>Igf1r</i>	3.30 $\pm$ 0.36*	1.55 $\pm$ 0.29 <sup>#</sup>	4.49 $\pm$ 0.71*	1.78 $\pm$ 0.38 <sup>#</sup>
<i>Dlx1</i>	1.68 $\pm$ 0.48*	0.75 $\pm$ 0.10 <sup>#</sup>	3.23 $\pm$ 0.65*	1.12 $\pm$ 0.21 <sup>#</sup>
<i>Ncoa1</i>	2.89 $\pm$ 0.11*	1.34 $\pm$ 0.60 <sup>#</sup>	3.74 $\pm$ 0.88*	0.98 $\pm$ 0.17 <sup>#</sup>
<i>c-fos</i>	3.06 $\pm$ 0.68*	1.25 $\pm$ 0.22 <sup>#</sup>	2.56 $\pm$ 0.29*	1.32 $\pm$ 0.08 <sup>#</sup>
<i>Ctnnb1</i>	2.62 $\pm$ 0.54*	0.90 $\pm$ 0.30 <sup>#</sup>	3.80 $\pm$ 0.62*	1.08 $\pm$ 0.28 <sup>#</sup>
<i>Wnt1</i>	2.71 $\pm$ 0.74*	0.93 $\pm$ 0.09 <sup>#</sup>	3.65 $\pm$ 0.52*	1.68 $\pm$ 0.34 <sup>#</sup>
<i>Wnt3a</i>	2.56 $\pm$ 0.75*	1.66 $\pm$ 0.25 <sup>#</sup>	3.00 $\pm$ 0.62*	1.52 $\pm$ 0.18 <sup>#</sup>

\*p<0.05, compared to the corresponding static control.

<sup>#</sup>p<0.05, compared to those without the leptin pretreatment.

## FIGURE LEGENDS

Figure 1. The periosteal circumference of 10-week-old female B6 and *ob<sup>-</sup>/ob<sup>-</sup>* mice (A), the relationship between loading force (in Newtons) and mechanical strain sensed by the bone (in  $\mu\epsilon$ ) in female B6 and *ob<sup>-</sup>/ob<sup>-</sup>* mice (B), and the mechanical strain-adjusted bone responses in the tibia (by pQCT) of female *ob<sup>-</sup>/ob<sup>-</sup>* mice (filled bars) after a 2-weeks 4-point bending loading compared to those in the tibia of female B6 mice (open bars) (C). In B, the solid line represents the calculated strain for each loading force in female B6 mice, and the dotted line is the calculated strain for each loading force for female *ob<sup>-</sup>/ob<sup>-</sup>* mice. Filled circles are the actual strain sensed by the bone of female B6 mice measured with a strain gauge, whereas filled squares are the actual strain sensed by the bone of female *ob<sup>-</sup>/ob<sup>-</sup>* mice. In C, the bending exercise was performed in six *ob<sup>-</sup>/ob<sup>-</sup>* mice and twelve B6 mice. The results are shown as relative percent change from the unloaded tibia of individual mouse per 1,000  $\mu\epsilon$  [mean  $\pm$  standard error of the mean (S.E.M.)]. TC = total bone mineral content; TA = total area; PC = periosteal circumference; EC = endosteal circumference; CA = cortical area; CT = cortical thickness; CC = cortical content; mBMD = material bone mineral density; vBMD = volumetric BMD. \* $p < 0.05$ ; \*\* $p < 0.01$ ; \*\*\* $p < 0.001$ , compared to B6 mice.

Figure 2. Effects of fluid shear on [ $^3$ H]thymidine incorporation (A) and Erk1/2 phosphorylation (B) of osteoblasts of young adult female B6 mice, wild-type littermates of *ob<sup>-</sup>/ob<sup>-</sup>* mice (WT *ob<sup>+</sup>/ob<sup>+</sup>*), or leptin-deficient (*ob<sup>-</sup>/ob<sup>-</sup>*) mice. In A, results are shown as the % of respective static cells [mean  $\pm$  standard deviation (S.D.),  $n = 4$ ]. \* $p < 0.05$  vs. static control, and # $p < 0.05$  vs. the B6 and WT cells. In B, top was a representative blot of pErk1 and pErk2 (using an anti-pErk1/2 antibody) and total Erk1/2 (identified by an anti-panErk antibody). Bottom summarizes the relative amounts of pErk1/2 normalized against total Erk and results are shown as percentage of respective static control (mean  $\pm$  S.D.,  $n = 4$ ). \* $p < 0.05$ , compared to static control; # $p < 0.05$ , compared to B6 osteoblasts or WT osteoblasts.

Figure 3. The leptin pretreatment of *ob<sup>-</sup>/ob<sup>-</sup>* osteoblasts abolished their enhanced mitogenic response to the fluid shear *in vitro*. Osteoblasts of *ob<sup>-</sup>/ob<sup>-</sup>* mice were pretreated for 2-h with or without 100 ng/ml leptin. Immediately after the pretreatment, these *ob<sup>-</sup>/ob<sup>-</sup>* osteoblasts along with B6 osteoblasts were subjected to the 30-min fluid shear stress of 20 dynes/cm $^2$ . [ $^3$ H]Thymidine incorporation was determined as described before (5). Results are shown as % of corresponding static controls (mean  $\pm$  S.D.,  $n = 6$ ). \* $p < 0.05$ , compared to static control; # $p < 0.05$ , compared to B6 osteoblasts.

Figure 4. The periosteal circumference of 12-week-old female B6 and *db<sup>-</sup>/db<sup>-</sup>* mice (A) and the mechanical strain-adjusted bone responses in the tibia (by pQCT) of female *db<sup>-</sup>/db<sup>-</sup>* mice (filled bars) after a 2-weeks 4-point bending loading compared to those in the tibia of female B6 mice (open bars) with a 9-N load and a 6.5- to 7.5-N load, respectively (B). The 9-N load on the tibia of *db<sup>-</sup>/db<sup>-</sup>* mice yielded an average mechanical strain of  $\sim 3,100 \mu\epsilon$ ; while the 6.5- to 7.5-N load on the tibia of WT littermates produced an average strain of  $\sim 3,000 \mu\epsilon$ . The bending exercise was performed in six 12-week-old female *db<sup>-</sup>/db<sup>-</sup>* mice and six age- and sex-matched WT littermates. The results are shown as relative percent change from the unloaded tibia of individual mouse per 1,000  $\mu\epsilon$  [mean  $\pm$  standard error of the mean (S.E.M.)]. TA = total area; PC = periosteal circumference; mBMD = material bone mineral density; vBMD = volumetric BMD. \* $p < 0.05$ , compared to respective unloaded contralateral tibia; and # $p < 0.05$ , compared to WT-littermates.

Figure 5. Effects of fluid shear on [ $^3$ H]thymidine incorporation (A) and Erk1/2 phosphorylation (B) of osteoblasts of 12-week-old female *Lepr*-deficient *db<sup>-</sup>/db<sup>-</sup>* mice and of osteoblasts of age- and sex-matched littermates. In A, results are shown as the % of respective static cells [mean  $\pm$  standard deviation (S.D.),  $n = 6$ ]. \* $p < 0.05$  vs. static control, and # $p < 0.05$  vs. the WT littermates. In B, top was a representative blot of pErk1 and pErk2 (using an anti-pErk1/2 antibody) and total Erk1/2 (identified by an anti-panErk antibody). Bottom summarizes the relative amounts of pErk1/2 normalized against total Erk and results

are shown as percentage of respective static control (mean  $\pm$  S.D., n = 4-6). \*p<0.05, compared to static control; #p<0.05, compared to osteoblasts of WT littermates.

Figure 6. siRNA-mediated suppression of *Lepr* expression enhanced basal and shear stress-induced Erk1/2 phosphorylation in B6 osteoblasts *in vitro*. A shows the effects of the 24-h treatment of a set of *Lepr* siRNAs (1-3) alone or in combination (at a total concentration of 5 nM) on the cellular *Lepr* protein level in B6 osteoblasts. Cellular *Lepr* protein was identified by Western blots and normalized against actin. B shows the effects of suppression of *Lepr* expression by *Lepr* siRNA2 on pErk1/2 levels. Total Erk1/2 was measured with an anti-pan-Erk antibody. The relative amounts of pErk1/2 normalized against total Erk and results are shown as percentage of the control siRNA-treated static control cells (mean  $\pm$  S.D., n = 4-6). \*p<0.05, compared to control siRNA-treated static control cells; #p<0.05, compared to stressed control siRNA-treated cells.

Figure 7. Suppression of *Lepr* expression in C3H osteoblasts by a 24-h treatment with 5 nM *Lepr* siRNA2 restored their mitogenic response to fluid shear stress. Primary osteoblasts isolated from 10-week-old female C3H mice were treated for 24 h with 5 nM *Lepr* siRNA2 (right bars) or the control siRNA (left bars). After the respective siRNA treatment, the cells were placed in the flow chamber with (dark bars) or without (open bars) subjection to a 30-min shear stress of 20 dynes/cm<sup>2</sup>. Cell proliferation was measured by [<sup>3</sup>H]thymidine incorporation during the final 6 h of a 24-hr incubation. Results are shown as mean  $\pm$  S.E.M. (n=4).

Figure 8. Comparison of basal and shear-stress-induced secretion levels of leptin into conditioned media (CM) by B6 and C3H osteoblasts *in vitro* (A), and basal and shear-stress-induced *Lepr* mRNA expression levels in B6 and C3H osteoblasts (B). In A, the 24-h CM of B6 (left) or C3H osteoblasts (right) with or without the 30-min fluid shear were concentrated 7-fold, and the amounts of leptin in each concentrated CM was assayed with the mouse leptin EIA kit (Assay Designs, Inc.) and normalized against cellular protein content. Results are shown as mean  $\pm$  S.D. (n = 4 each). In B, the relative *Lepr* mRNA expression levels were determined by real-time RT-PCR. Left: the mRNA levels were assessed by the  $\Delta$ CT method and basal *Lepr* mRNA expression was reported as  $\Delta$ CT compared to  $\beta$ -actin. Right: cells were subjected to a 30-min steady shear stress of 20 dynes/cm<sup>2</sup>. The fold change in *Lepr* mRNA levels in response to the shear stress was determined by  $\Delta\Delta$ CT, and the results were shown as ratio of the stressed cells/static control cells (mean  $\pm$  S.D., n = 3 each). \*p<0.05, compared to static control cells.

Figure 9. Effects of fluid shear stress on leptin-mediated induced phosphorylation of JAK2 and STAT3 (A) and on the amounts of co-immunoprecipitated Jak2 and Stat3 with *Lepr* in B6 osteoblasts (B). In A, primary osteoblasts isolated from B6, *ob<sup>-/-</sup>*, and C3H mice were each treated with 100 ng/ml leptin with or without the 30-min steady fluid shear stress of 20 dynes/cm<sup>2</sup>. Ten minutes after the shear stress, the stressed cells (St) and the corresponding static control cells (C) were lysed in RIPA, and the relative levels of pY-Jak2 and total Jak2 as well as those of pY-Stat3 and total Stat3 were analyzed by Western blot. In B, immediately after the 30-min shear stress, cell extracts of the stressed and static control B6 osteoblasts were immunoprecipitated (IP) with anti-*Lepr* and blotted (IB) against anti-Jak2 (left panel) or anti-Stat3 (right panel).

Figure 10. Existence of three SNPs in *Lepr* open reading frame between B6 and C3H osteoblasts. The Capital, underlined letters in the nucleotide sequences indicate the location of SNPs. Single letter symbols are used to represent amino acid sequence. The shaded and italic letter shows the location of Ile→Val substitution in the amino acid sequence.

Figure 1.

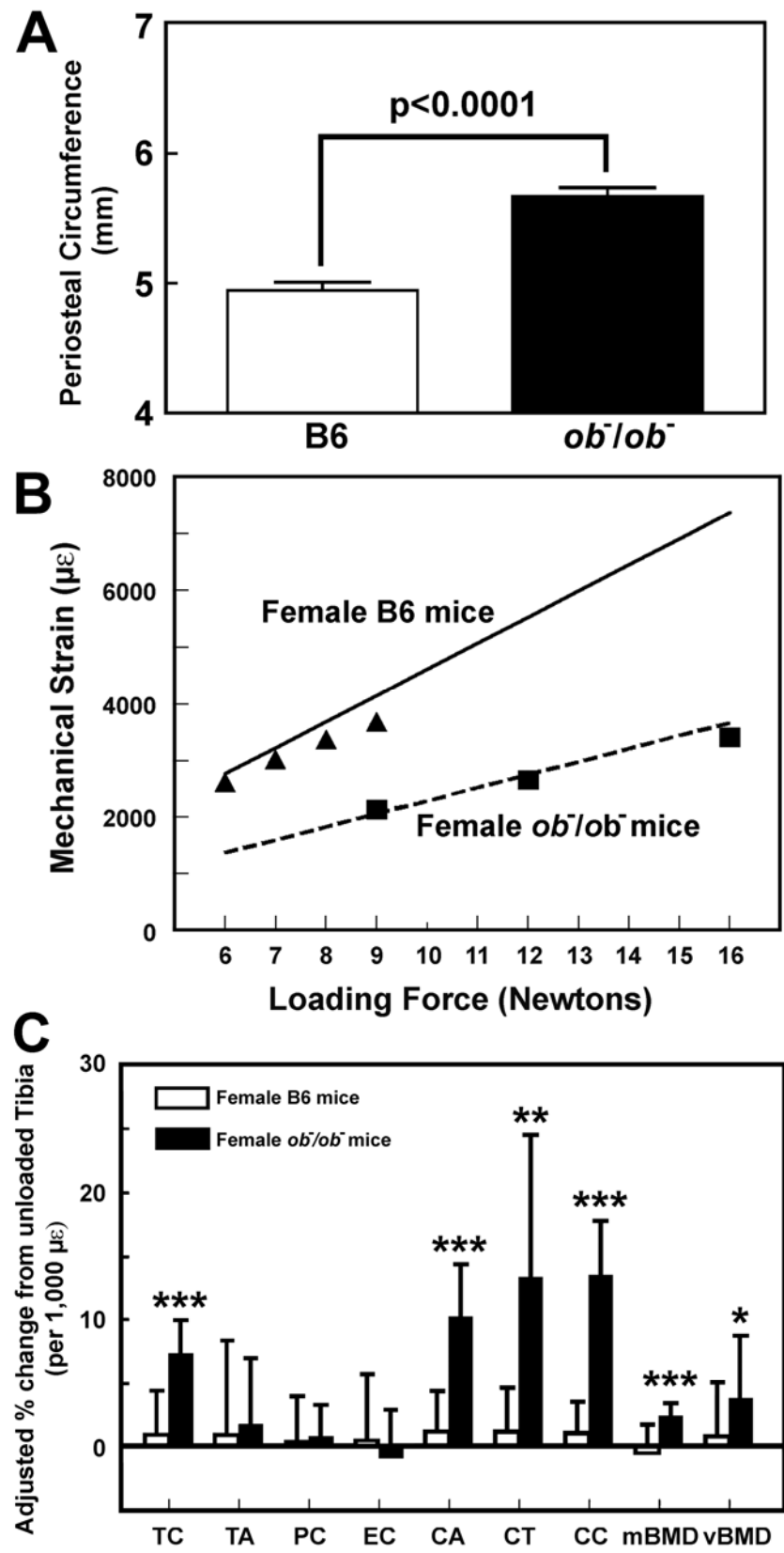
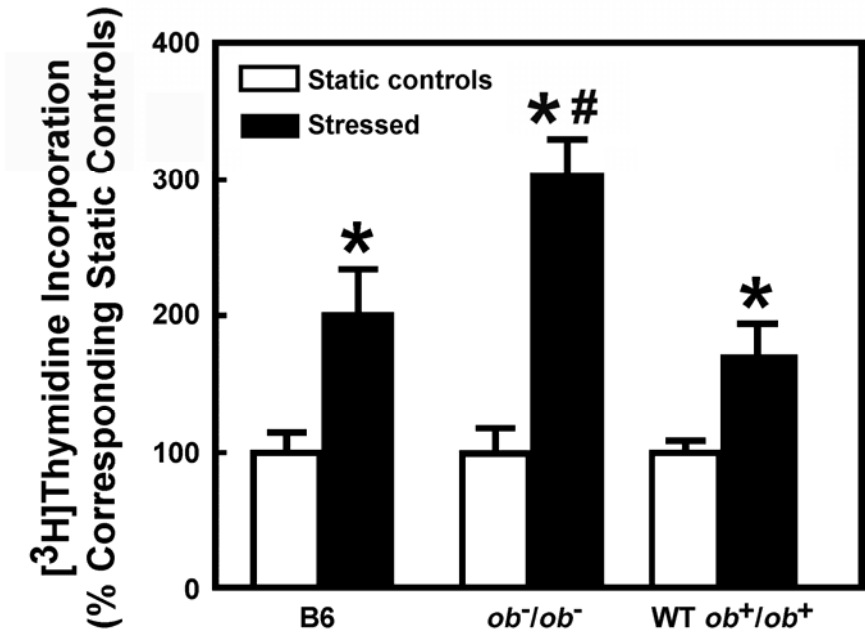


Figure 2.

A. Thymidine Incorporation



B. Erk1/2 Phosphorylation

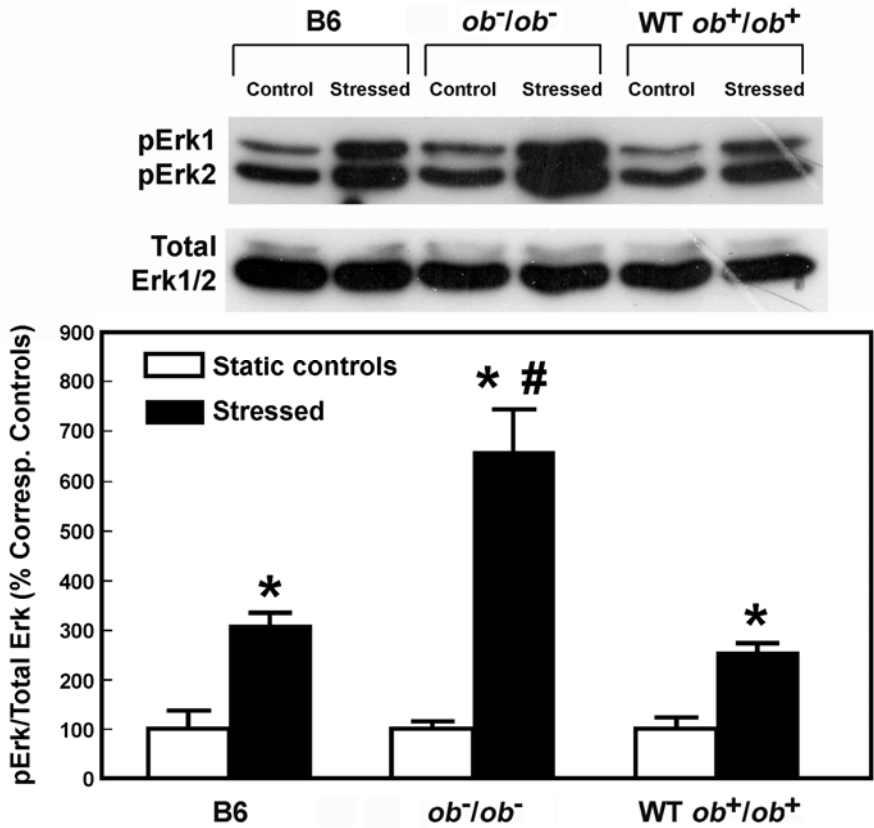


Figure 3.

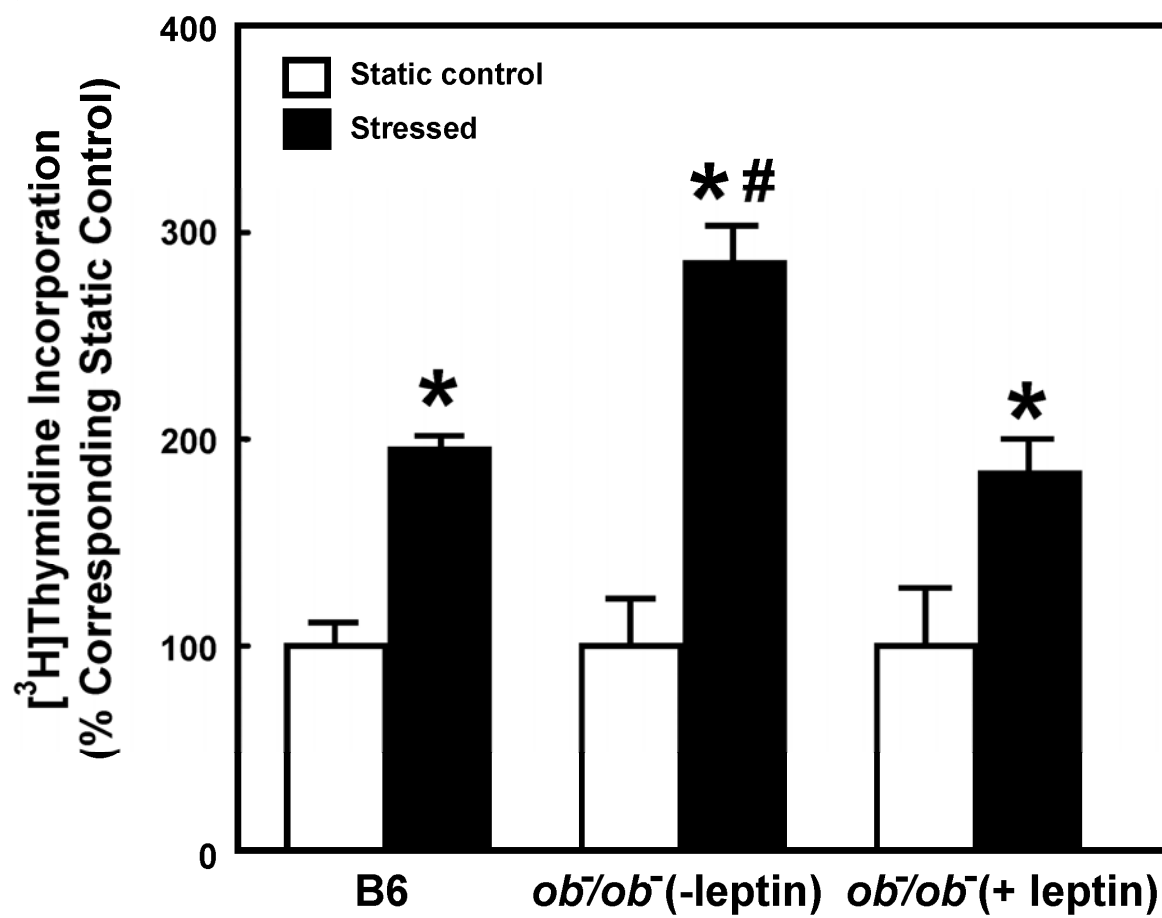


Figure 4.

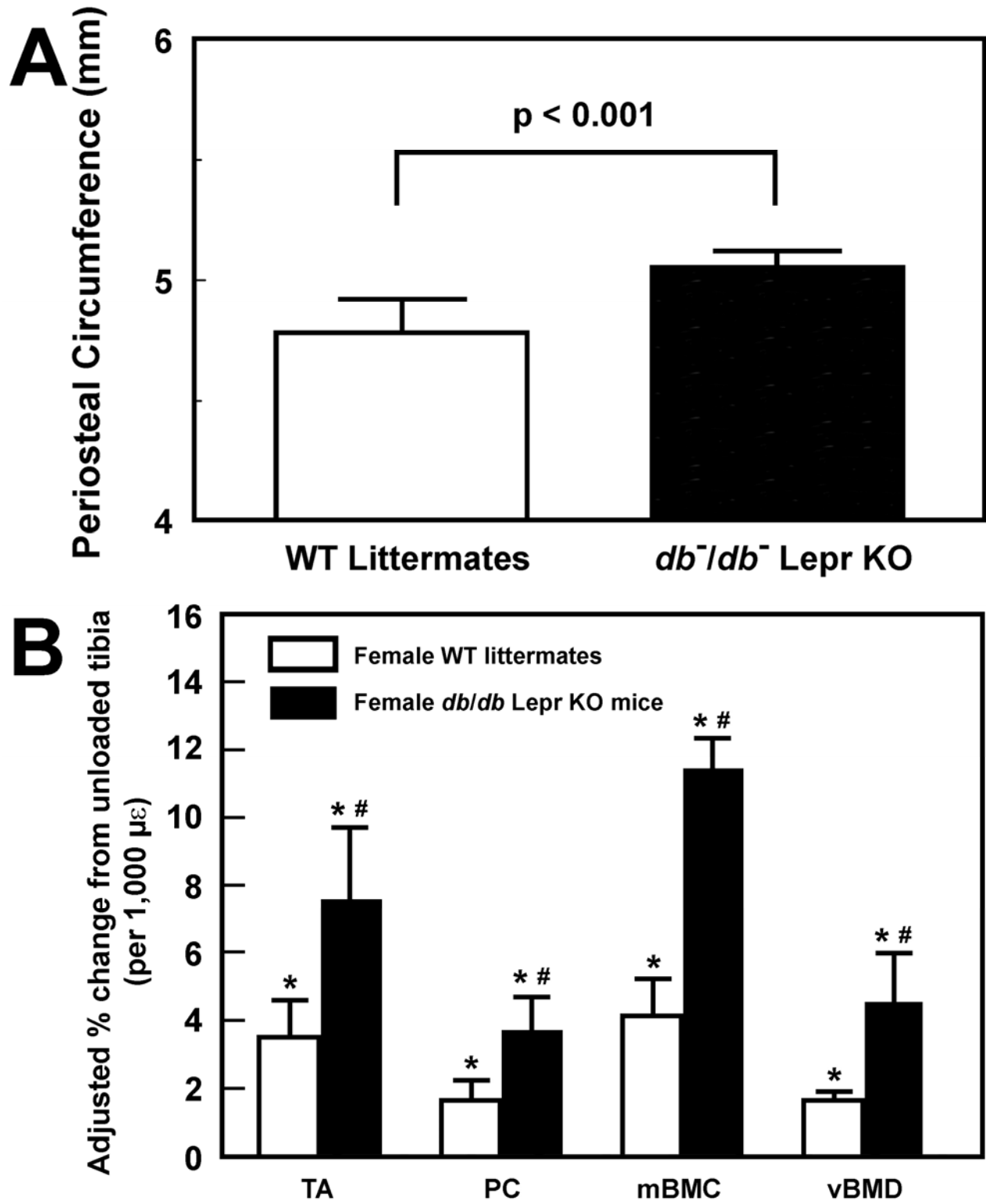


Figure 5.

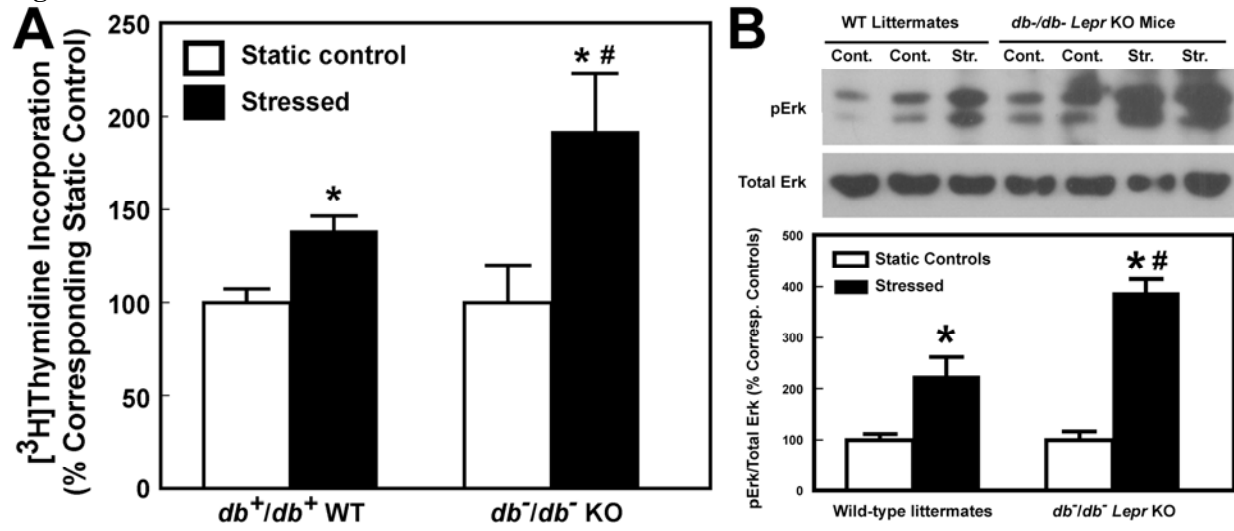


Figure 6.

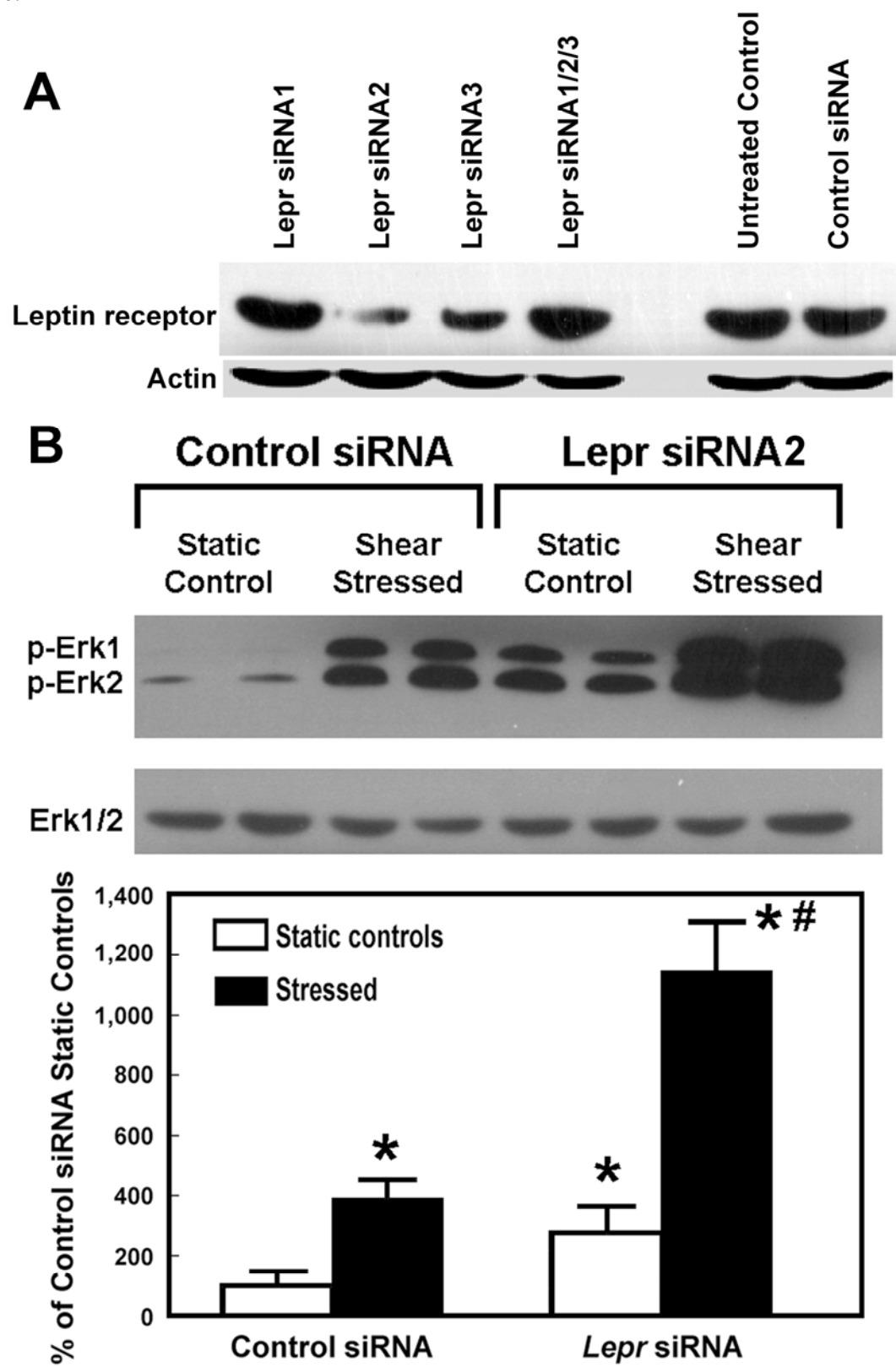


Figure 7.

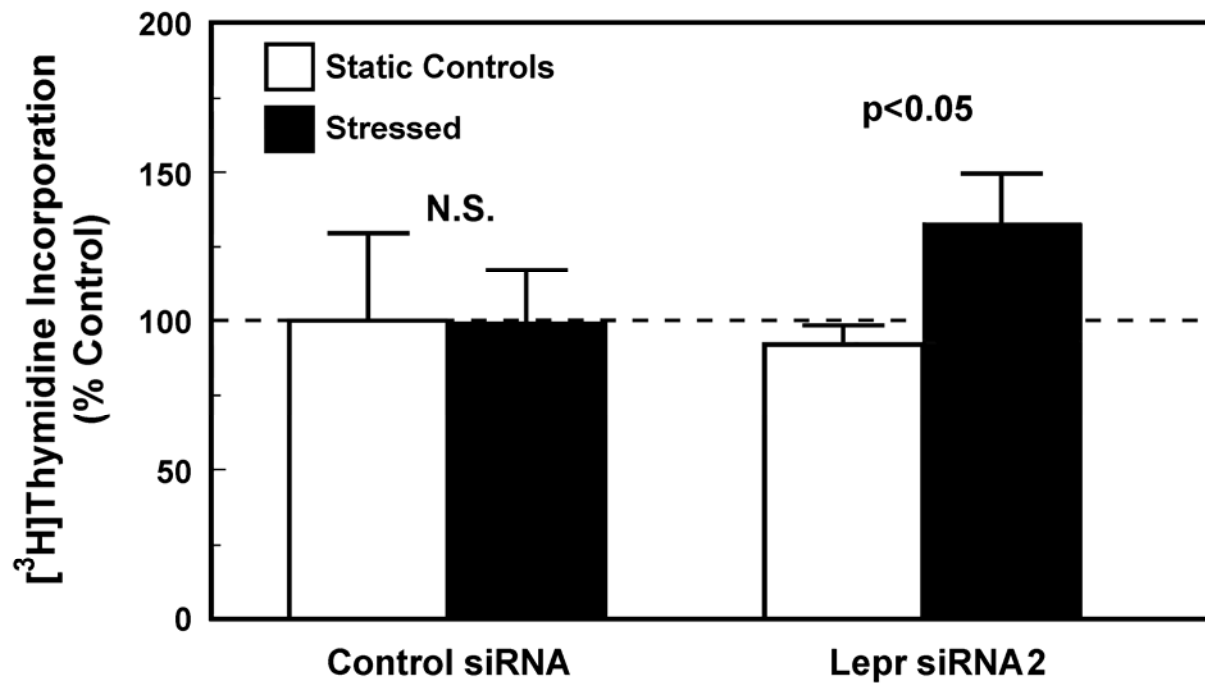
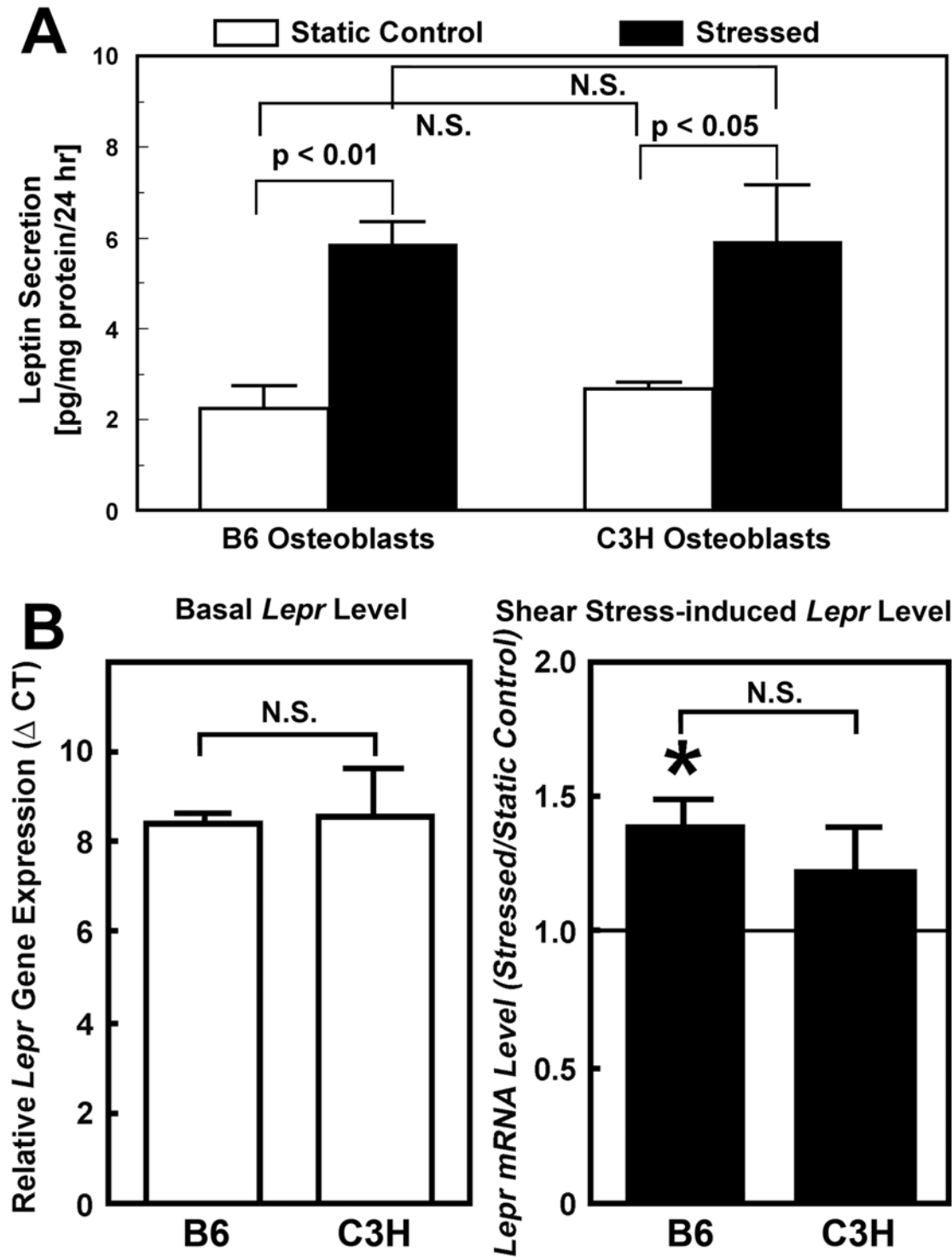


Figure 8.



**Figure 9.**

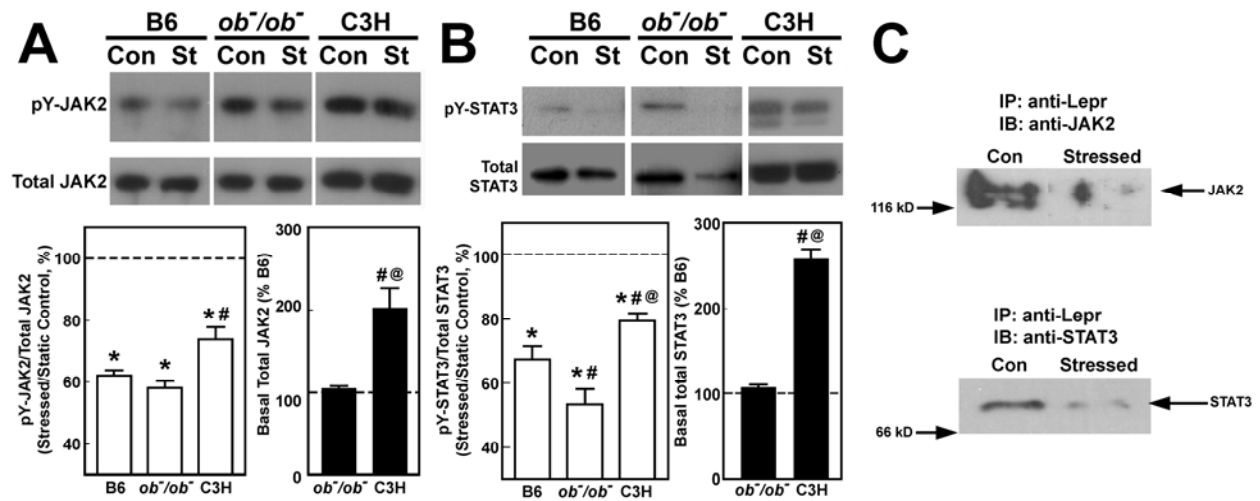


Figure 10.

**SNP1: G→A at nucleotide 594 (Silent SNP)**

B6 osteoblasts: 571 cgg ggt tgt gaa tgt cat gtg ccG gta ccc aga gcc aaa ctc 612  
R G C E C H V P V P R A K L  
C3H osteoblasts: 571 cgg ggt tgt gaa tgt cat gtg ccA gta ccc aga gcc aaa ctc 612  
R G C E C H V P V P R A K L

**SNP2: T→C at nucleotide 1041 (Silent SNP)**

B6 osteoblasts: 1009 aaa att ctg act agt gtt gga tcg aat gct tcI ttt cat tgc atc tac 1056  
K I L T S V G S N A S F H C I Y  
C3H osteoblasts: 1009 aaa att ctg act agt gtt gga tcg aat gct tcC ttt cat tgc atc tac 1056  
K I L T S V G S N A S F H C I Y

**SNP3: A→G at nucleotide 1075 (Ile→Val SNP)**

B6 osteoblasts: 1057 aaa aac gaa aac cag att Atc tcc tca aaa cag ata gtt tgg tgg 1101  
K N E N Q I I S S K Q I V W W  
C3H osteoblasts: 1057 aaa aac gaa aac cag att Gtc tcc tca aaa cag ata gtt tgg tgg 1101  
K N E N Q I V S S K Q I V W W

## Original Article

# Bone mass gained in response to external loading is preserved for several weeks following cessation of loading in 10 week C57BL/6J mice

C. Kesavan<sup>1,2</sup> and S. Mohan<sup>1,2</sup><sup>1</sup>Musculoskeletal Disease Center, VA Loma Linda Healthcare System, Loma Linda, CA 92357, USA;<sup>2</sup>Department of Medicine, Physiology and Biochemistry, Loma Linda University, Loma Linda, CA 92354, USA

## Abstract

**Objective:** Dynamic loads lead to increases in bone mass. How long these gains are maintained after cessation of loading, however, is not fully understood. **Methods:** A long term study was performed in which skeletal changes were monitored by pQCT every 2-4 weeks (wks) for a 12 wk period after application of external loading using four-point bending device on 10 wk old female C57BL/6J mice. **Results:** 2 wks of loading caused 15-40% increase in bone parameters (vBMD, cross sectional area (CSA)) and bone strength (yield load, maximum load and toughness). Positive correlations between these two parameters ( $r = 0.72$  to  $0.88$ ,  $p < 0.05$ ) suggest that the changes in bone parameters induced by loading are responsible, in part, for the increase in bone strength. Once loading is terminated the bone response did not continue. The vBMD gained by loading was significant for a period of 5 wks and returned to the levels of controls at 12 wks. The CSA though declined but was still significantly elevated at 12 wks. Bone strength showed no difference between loaded and non-loaded bones at 12 wks. **Conclusion:** Our results show that external loading increased bone mass, was maintained for several weeks after termination of last loading.

**Keywords:** Density, Bone fate, Physical Exercise, Rehabilitation, Mice

## Introduction

Mechanical loading (ML) is an effective stimulator of bone formation. Past studies using animal and human models have shown that loading increases bone formation while non-loading, such as prolonged bed rest, immobilization, and space flight, results in the increase of bone loss<sup>1-9</sup>. We, and others, using inbred strains of mice, have reported that ML causes increases in the volumetric bone mineral density (vBMD) when measured by peripheral quantitative computed tomography (pQCT)<sup>2,3</sup>. Thus, physical exercise has been used as a strategy to maintain BMD

and prevent osteoporotic fractures in men and women.

Clinical studies in young and postmenopausal women subjected to treadmill exercise have shown that exercise induced benefits, such as increases in vBMD and bone mineral content (BMC), are eventually lost if exercise is ceased completely<sup>10</sup>. Similar data was presented by Vuori et al. when reporting that unilateral leg presses done four times a week, for 12 months increased bone mass, but returned to pre-training levels with only 3 months of retirement from exercise<sup>11,12</sup>. Another study involving gymnasts also showed that bone density gained by long term loading declines followed by off season (unloading)<sup>13</sup>. Thus, data from various independent studies in humans suggests that exercise induced bone mass benefits erode over time. Animal studies using a rat model have shown that increased femoral bone density, gained through treadmill exercise, resulted in a decreased bone formation rate after deconditioning<sup>14,15</sup>. However, the issue of how deconditioning affects bone mass maintenance in mechanosensitive mouse model is not well understood.

We, and others, have previously shown that compared to all other mouse strain, C57BL/6J (B6), a low bone density mouse, responds well to ML. We have reported that 2 wks of ML by four-point bending causes a 10-15% increase in tibia vBMD

The authors have .....

Corresponding author: Subburaman Mohan, Ph.D., Musculoskeletal Disease Center (151), Jerry L. Pettis Memorial VA Medical Center, 11201 Benton Street, Loma Linda, CA 92357, USA  
E-mail: Subburaman.Mohan@va.gov

Edited by: .....

Accepted 22 September 2010

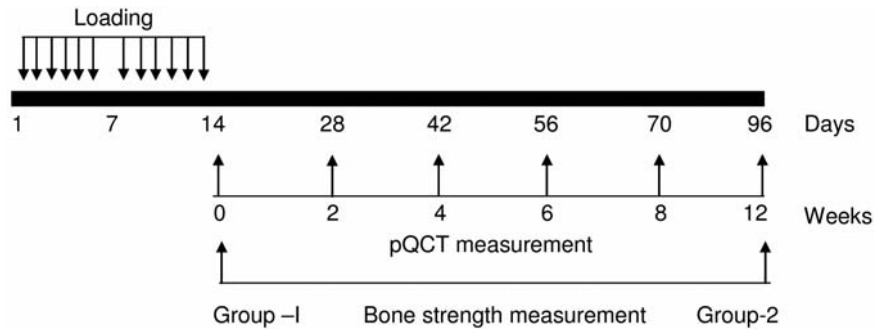


**Figure 1.** A schematic representation of the study design. (a) In group-I, mice were euthanized on day 14 after *in vivo* pQCT measurement of bone parameters, followed by tibias were collected and stored at 4°C for mechanical testing. (b) In group-II, mice were euthanized on day 96 after *in vivo* pQCT measurement of bone parameter, followed by tibias were collected to perform mechanical testing.

and a 30-40% increase in cross-sectional area in 10 week old female B6 mice<sup>3</sup>. Thus, in this mechanosensitive B6 mouse, there is a robust increase in both vBMD and bone size after 2 wks of four-point bending, but, how long this newly formed bone, induced by four-point bending is maintained after cessation of loading is still unclear. Furthermore, to our knowledge, no study has examined whether bone mass or bone strength gained by four-point bending is maintained or lost after termination of loading and hence, the present study was carried out to address the above issue.

## Materials and methods

### Mice

10 Female C57BL/6J were purchased from the Jackson Laboratory (Bar Harbor, Me). All mice were housed under standard conditions of 14-hour light and 10-hour darkness, and had free access to food and water. The body weights of these animals measured before the initial loading were  $18.32 \pm 0.79$  grams. The experimental protocols were in compliance with animal welfare regulations and approved by our local IACUC.

### *In vivo* loading model and peripheral quantitative computed tomography (pQCT) measurements

At 10 wks of age, two groups (n=5/group) of female B6 mice were subjected to ML using the four-point bending device as described previously<sup>3</sup>. The loading protocol consists of a 9.0 Newton (N) force (9N produce 3682 micro strain) at a frequency of 2 Hz for 36 cycles, performed daily under inhalable anesthesia (5% Halothane and 95% oxygen). The loading procedure was repeated for 6 days/week with 1 day of rest for 2 wks. The right tibia was used for loading and the left tibia as contralateral internal control in each mouse (From onwards in this manuscript, we will call right tibia as loaded bone and left tibia as non-loaded bone). In group-I, mice were euthanized by carbon dioxide inhalation on day 14 after *in vivo* pQCT measurement of bone parameters. Tibias were collected and stored at 4°C for mechanical testing. In group-II, mice were subjected to 2 weeks of mechanical loading followed by *in vivo* pQCT

measurement at the end of loading and at 2, 4, 6, 8 and 12 weeks after loading. Mice were euthanized at 12 week after *in vivo* pQCT measurement of bone parameter. Tibias were then collected to perform mechanical testing. A schematic representation of the study design is shown in Figure 1.

### Peripheral quantitative computed tomography (pQCT) measurements

To measure loading induced changes in bone parameters in the loaded and non-loaded bone, we used pQCT (Stratec XCT 960M, Norland Medical System, Ft. Atkinson, WI) as described previously<sup>3,16</sup>. The resolution of pQCT scan is 70 micron. *In vivo* pQCT measurements were performed at immediate (0-time point), 2, 4, 6, 8, and 12 wks after the last loading regimen.

### Mechanical properties of bone

Tibiae were stored frozen in gauze moistened with PBS and thawed in PBS at 4°C. The anterior-posterior diameter (AP.Dm) and lateral-medial diameter (LM.Dm) were measured with calipers. The tibiae were tested by three-point bending using the Instron DynaMight testing system (Model 8840; Instron, Canton, MA, USA) as previously described<sup>17</sup>. Each tibia was placed on two immovable supports which were 5 mm apart. An initial 1.0 N was applied on the tibia at a position of 2.10 mm away from the tibia-fibular junction to prevent the rotation of the bone due to the shape of the tibia and to be consistent in breaking region between the bones. Furthermore, this area corresponds to the 4 mm loading region<sup>3,16</sup>. It was then loaded from this midpoint at a constant rate (2 mm/minute) to the point of fracture. Load displacement curves were used to calculate yield load ( $P_y$ ), maximum load ( $P_{max}$ ) and toughness (Ut). Cross sectional moment of inertia was calculated from the measured anterior-posterior diameter and lateral-medial diameter and from the average cortical thickness obtained by pQCT analysis as previously described<sup>18,19</sup>. The number of mice used for this experiment is n=5 of which one mice had a technical problem in breaking the bone, and was excluded from the study. Thus, data from only 4 mice were used for this analysis.

### Statistical analysis

Data are presented as Mean±Standard error (SE). Loading induced changes in skeletal parameters were determined by calculating percent changes in the loaded versus non-loaded bones of the same animal to avoid any inherent variation between animals. One-way ANOVA (Newman-Keuls Post Hoc test) was used to evaluate the influence of time on the loaded and non-loaded bones. Correlation matrices (values for bone parameters and mechanical properties of respective mouse were used for correlation) were used to determine whether there is any association between changes in skeletal parameters and mechanical properties. Standard t-test was used to compare skeletal changes between loaded and non-loaded bone. We used STATISTICA software (StatSoft, Inc version 7.1, 2005) for our analysis and the results were considered significantly different at  $p < 0.05$ .

### Results

#### Bone anabolic response after cessation of loading

Two wks of four-point bending increased bone mineral content (BMC) by 45% in the loaded bone compared to corresponding non-loaded bone. The increased BMC was maintained (10-45%) throughout the 12 week cessation period after last loading (Figure 2a). The increased BMC in the loaded bone is caused by both bone size and vBMD changes. Bone size, as reflected by periosteal circumference (PC), was increased by 18% after two wks of ML and was significantly different from corresponding non-loaded bone throughout the entire study (Figure 2b). vBMD was increased by 14% after two wks of ML and remained high compared to non-loaded bones only until 4 wks after cessation of exercise (Figure 2c).

ANOVA analysis revealed that absolute values of non-loaded bones for PC were not different between the post loading time points while in the loaded bones, PC values of 6, 8 and 12 wks were different ( $p = 0.03$ ) from 0, 2 and 4 wks post loading time points (Figure 2b). Similarly, for vBMD, the absolute values of loaded bones showed no significant different between the post loading time points while the absolute values of non-loaded bones at 6, 8 and 12 week were significantly different ( $p < 0.05$ ) from 0, 2 and 4 week post loading time points as evident from ANOVA analysis (Figure 2c). In the case of BMC, the values of loaded bone were not different between the post loading time points while in the non-loaded bones, the values of 12 week were significantly different from 0, 2, 4, 6 and 8 wks of post loading time points (ANOVA analysis).

Figure 3 shows percent changes in loading induced increases in cross sectional area (bone size), cortical area, cortical thickness and vBMD as a function of time after cessation of last loading. Mechanical loading induced gains in all four parameters declined with time but at different rates. The vBMD and cortical thickness gained after two weeks of loading in the loaded bone was significant over non-loaded bones for a period of 5-6 weeks and then returned to the levels of control at 12 weeks. However, the gain in the CSA and cortical area after two weeks of loading though declined but still was significantly elevated at 12 weeks.

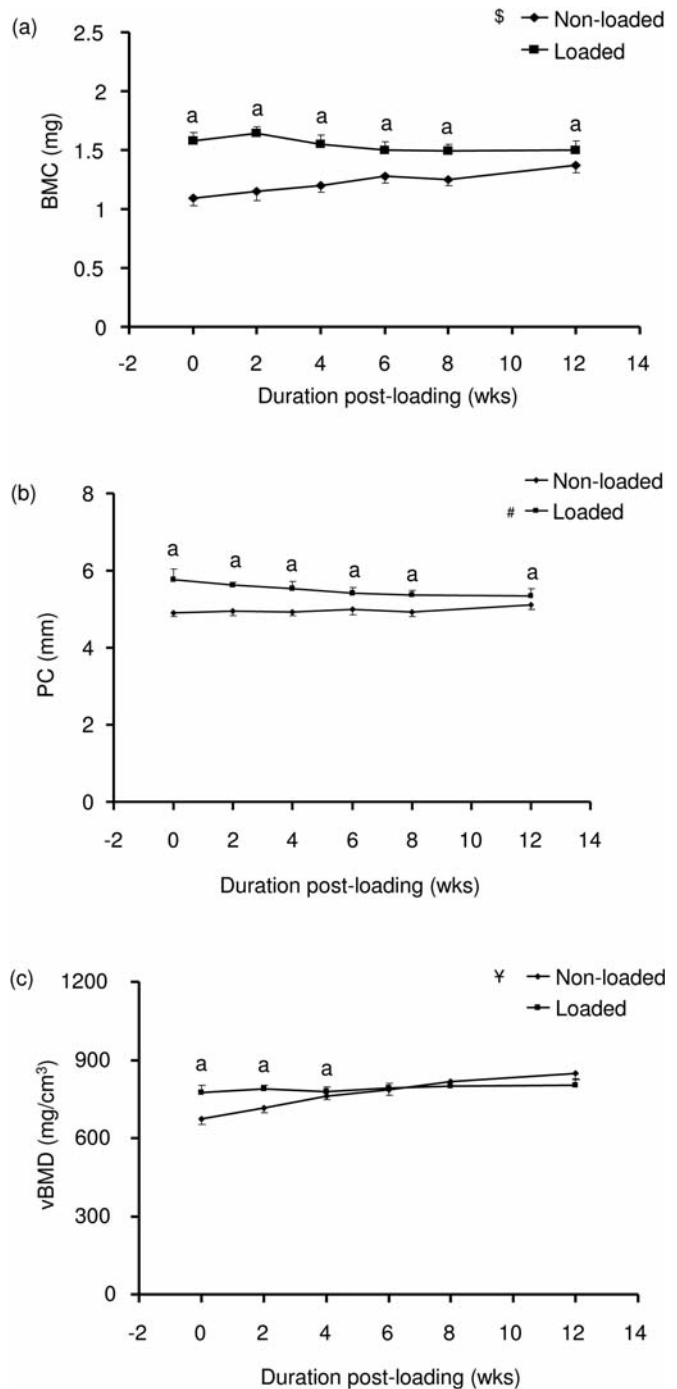


**Figure 2.** Changes in bone parameters measured at different time points after cessation of loading. The y-axis corresponds to absolute changes in bone parameters in response to 12 days four-point bending on 10 week female C57BL/6J mice. The x-axis corresponds to various time points. (a) Bone mineral content (BMC), (b) Periosteal circumference (PC) and (c) total volumetric Bone mineral Density (vBMD). Values are mean±SE, <sup>a</sup> $p < 0.05$  vs. non-loaded bone,  $N = 5$ . <sup>#</sup>PC loaded values of 6-, 8- and 12-week are different from 0-, 2-, and 4 week ( $p < 0.05$ , ANOVA, Newman-Keuls Post Hoc Test). <sup>¥</sup>vBMD non-loaded values of 6-, 8- and 12- week are different from 0-, 2-, and 4-weeks ( $p < 0.05$ , ANOVA, Newman-Keuls Post Hoc Test). <sup>\$</sup>BMC non-loaded values of 12 week are different from 0-, 2-, 4-, 6- and 8-weeks ( $p < 0.05$ , ANOVA, Newman-Keuls Post Hoc Test).

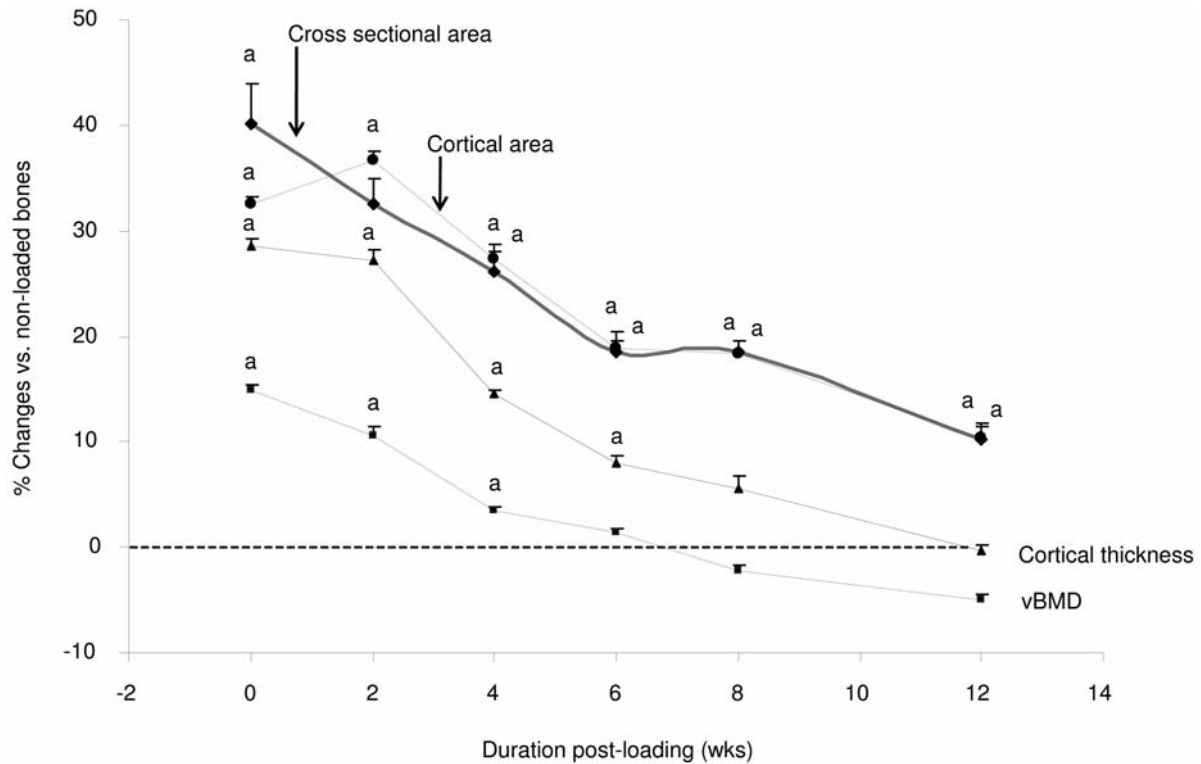


**Figure 3.** Changes in CSA and vBMD measured at different time points after cessation of loading. The y-axis corresponds to percent change and x-axis corresponds to duration post-loading (weeks). CSA, Cross sectional area and vBMD, total volumetric bone mineral density, values are mean $\pm$ SE, <sup>a</sup> $p < 0.05$  vs. non-loaded bone, N=5.

Parameters	0 week		12 week	
	Non-loaded bone	Loaded bone	Non-loaded bone	Loaded bone
Yield load (N)	14.48 $\pm$ 0.42	20.34 $\pm$ 0.84*	17.64 $\pm$ 0.72	16.44 $\pm$ 0.13
Maximum load (N)	18.54 $\pm$ 0.67	24.05 $\pm$ 0.58*	21.93 $\pm$ 0.39	21.05 $\pm$ 0.17
Toughness (N/mm <sup>2</sup> )	2.17 $\pm$ 0.03	3.30 $\pm$ 0.10*	2.03 $\pm$ 0.02	1.94 $\pm$ 0.14
Abbreviations: N, Newton				
Values are mean $\pm$ SE with four mice per group, * $p < 0.05$ vs. non-loaded bones.				
0- and 12-week mechanical parameters of loaded bones are significantly different (ANOVA, Newman-Keuls Post Hoc test).				
0- and 12-week mechanical parameters of non-loaded bones are not significantly different, $p = 0.07$ (ANOVA, Newman-Keuls Post Hoc test).				

**Table 1.** Changes in mechanical properties of bone measured at 0- and 12-weeks after the cessation of last loading.

#### Bone mechanical properties after termination of loading

In order to determine if the increase in skeletal parameters reflects an increase in bone mechanical properties, we performed a bone breaking study on the loaded and non-loaded bones of mice immediately after the loading and at 12 wks after cessation of loading. We found that immediately after 2 wks of loading, yield load, maximum load and toughness were significantly increased by 42%, 29% and 42%, respectively in the loaded bones compared to non-loaded bones (Table 1).

However, at 12 wks, there was no difference in the above parameters between loaded and non-loaded bones (Table 1). Furthermore, we also performed a correlation analysis between these mechanical properties vs. vBMD, CSA and cortical thickness to elucidate whether increase in bone mechanical properties is due to an increase in the changes in bone parameters, measured by pQCT. The results show a significant correlation between vBMD, area and cortical thickness with yield load, maximum load and toughness ( $r = 0.72$  to  $0.88$ ,  $p < 0.05$ ).

## Discussion

In this study, the choice of inbred strain of mice, the loading device and regimen used were based on previous findings<sup>3,16</sup>. Two wks of four-point bending on the right tibiae when compared to left tibiae resulted in a significant increase in bone parameters, such as BMC, CSA and vBMD, as shown in Figure 1. The magnitude of increase in skeletal parameters after 2 wks of loading is consistent with our previous study<sup>3</sup>. However, in this study, we show that this increase in CSA (40%) and vBMD (15%) gained immediately after 2 wks of loading, did not continue over time after the cessation of last external loading. The decrease in the difference in CSA between non-loaded and loaded bones over time raises a question of whether this is due to loss of bone mass acquired during loading or due to the influence of growth in the loaded or non-loaded bones. The findings from our study illustrate that the reduction in CSA difference between non-loaded and loaded bones over time was purely due to a gradual loss in gained bone and not due to growth as evident from ANOVA analysis. In the case of vBMD, we found a significant increase in vBMD with advancing age (i.e. between 12 and 22 wks) by ANOVA in the non-loaded but not in the loaded bone. It is possible that vBMD increased in the non-loaded bone is to compensate for the increased body weight during this period while in the loaded bones this did not occur as the vBMD is sufficiently increased due to the four-point bending. It remains to be determined whether the lack of vBMD difference between the loaded and non-loaded bones at 12 wks after cessation of external loading is due to a difference in bone accretion rates between non-loaded and loaded bones between 12 and 22 wks of age and/or due to partial loss of ML-induced newly formed bone after cessation of loading in the loaded tibia.

In the pQCT analysis of bone parameters using the lower threshold (180-730), we found that the magnitude of increase in periosteal circumference (PC) was  $18\% \pm 7.0$  after the last loading and was significant when compared with  $7.2\% \pm 1.7$  using the higher threshold (730-730). This is due to rapid accumulation of low mineralized bone at the periosteal surface. This is most prevalent immediately after the last day of loading, as seen by the red color using the pQCT threshold indicator (Figure 4). Consequently, we found a significant increase in CSA immediately after the last day of loading, accompanied by an increase in vBMD. Over time, we found that the periosteal circumference in the loaded tibia tends to reduce gradually. As a result, the magnitude of difference between loaded and non-loaded tibia reduced at 12 wks after cessation of loading, resulting in no difference in the periosteal circumference of loaded tibia between lower (PC,  $9.13\% \pm 3.9$ ) and higher threshold (PC,  $9.8\% \pm 1.2$ ). These findings, suggest that the newly formed bone undergoes remodeling at the periosteal site to cortical bone over time which leads to a reduction in bone size in order to accommodate the loading induced changes in the bone shape. During this remodeling process, we found that the rate of loss in gained CSA (bone size) after cessation of loading was 10% every 2 wks for 8 wks. These data, suggest that the positive effects of ML on CSA were

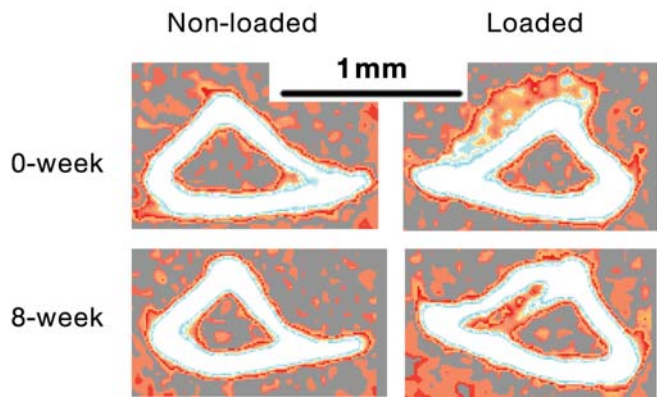


**Figure 4.** Cross sectional area of non-loaded vs. loaded bone. This figure shows the newly formed bone at the periosteal site in response to 2 weeks of loading and its fate over time after cessation of loading. The arrow corresponds to newly formed bone and the white color represents cortical bone.

maintained for several wks after the cessation of the last external loading and this is consistent with the earlier reports in rat and human model<sup>20-22</sup>.

Since in our study, we found a significant increase in bone parameters in response to loading and because earlier reports have shown that an increase in bone parameters leads to an increase in bone mechanical properties, we anticipate a measurable difference in mechanical properties between the bones immediately after loading and at 12 wks. Accordingly, the findings from our study revealed that bone strength was significantly increased by 29 to 42% immediately after 2 wks of loading (Table 1) and this increase in bone strength is in part, mediated by an increase in vBMD and CSA as evident from our correlation analysis. However, at 12 wks after the cessation of loading, we found that there was no difference in the yield load, maximum load and toughness between the loaded and non-loaded bones (Table 1). This is because; the vBMD in the non-loaded bones increased with advancing age and the CSA decreased gradually in the loaded bones, together contributing for the loss of bone strength difference between the loaded and non-loaded bones at 12 wks.

Some of the limitations of this study are as follows: 1) In the past, reports by others have predicted that some of the skeletal changes induced by four-point bending are due to periosteal pressure. In our previous QTL study, we found that sham-loading neither increased periosteal bone formation nor caused changes in expression levels of bone marker genes, demonstrating that the skeletal changes induced by bending are not due to periosteal pressure<sup>16</sup> and this is also consistent with earlier reports<sup>23</sup>. This finding also applies to the present study since we used the same loading model and regimen. 2) In this study, we used 10 wk old mice for our four-point bending experiment. Since bones continue to grow beyond 10 wks although at much lower pace this raises a question whether growth has any effect on the response to loading. In the past,

we have performed four-point bending on three ages (10-, 16- and 36 wks) and reported that there was no significant difference in the bone response between the age groups for a given load. However, it remains to be determined whether the loss rate in bone mass after cessation of loading is different in young vs. old mice. 3) It is worth mentioning that the four-point bending method of loading also adds lamellar bone initially, however, as the duration of loading becomes larger, there is an increase in accumulation of bone forming osteoblast cells at the loading site. As a result, this gives rise to a large amount of low mineralized bone, so called woven bone over the lamellar bone. Our study, however, cannot rule out the contribution of woven bone vs. lamellar bone. 4) The four-point bending loading method applied in this study produced woven bone at the periosteal surface which is remodeled subsequently. Since the site of loading is at the mid diaphysis which contains no trabecular bone, this method of loading is not applicable to evaluate the loading response on lamellar bone. Future studies using axial loading model which induces both trabecular and cortical bone formation are needed to determine if axial loading induces woven bone or lamellar bone at the trabecular site. Since exercise induces lamellar bone formation in humans, it is likely that axial loading in mice will also promote lamellar bone formation in the metaphysis of tibia. 5) In the past, we have measured micro-cracks by histological analysis to rule out the possibility whether the changes on bone parameters induced by four-point bending are due to micro-crack induced healing. We found that there was no significant difference in the micro-crack areas between loaded and non-loaded bones of B6 mice. In the present study, we have used the same loading regimen and therefore, the response induced by four-point bending cannot be attributed to damaged induced bone formation. Furthermore, we did not observe any fracture as evident from X-ray and pQCT image<sup>16</sup>.

In conclusion, our study shows that the positive effects of mechanical loading on bone were maintained for a substantial period of time after the cessation of the last external loading.

#### Acknowledgements

*This work was supported by the Army Assistance Award No. DAMD17-01-1-744. The US Army Medical Research Acquisition Activity (Fort Detrick, MD) 21702-5014 is the awarding and administering acquisition office for the DAMD award. The information contained in this publication does not necessarily reflect the position or the policy of the Government, and no official endorsement should be inferred. All work was performed in facilities provided by the Department of Veterans Affairs. We would like to thank Mr. James Dekeyser for his technical support of the four-point bending instrument and Peter Gifford for the animal work.*

#### References

1. Bailey DA, McCulloch RG. Bone tissue and physical activity. *Can J Sport Sci* 1990;15(4):229-39.
2. Akhter MP, Cullen DM, Pedersen EA, Kimmel DB, Recker RR. Bone response to *in vivo* mechanical loading

- in two breeds of mice. *Calcif Tissue Int* 1998;63(5):442-9.
3. Kesavan C, Mohan S, Oberholtzer S, Wergedal JE, Baylink DJ. Mechanical loading-induced gene expression and BMD changes are different in two inbred mouse strains. *J Appl Physiol* 2005;99(5):1951-7.
4. Kodama Y, Umemura Y, Nagasawa S, et al. Exercise and mechanical loading increase periosteal bone formation and whole bone strength in C57BL/6J mice but not in C3H/HeJ mice. *Calcif Tissue Int* 2000;66(4):298-306.
5. Lang TF, Leblanc AD, Evans HJ, Lu Y. Adaptation of the proximal femur to skeletal reloading after long-duration spaceflight. *J Bone Miner Res* 2006;21(8):1224-30.
6. Mori T, Okimoto N, Sakai A, et al. Climbing exercise increases bone mass and trabecular bone turnover through transient regulation of marrow osteogenic and osteoclastogenic potentials in mice. *J Bone Miner Res* 2003;18(11):2002-9.
7. Turner CH, Robling AG. Exercise as an anabolic stimulus for bone. *Curr Pharm Des* 2004;10(21):2629-41.
8. Bikle DD, Halloran BP. The response of bone to unloading. *J Bone Miner Metab* 1999;17(4):233-44.
9. Bikle DD, Sakata T, Halloran BP. The impact of skeletal unloading on bone formation. *Gravit Space Biol Bull* 2003;16(2):45-54.
10. Dalsky GP, Stocke KS, Ehsani AA, Slatopolsky E, Lee WC, Birge SJ, Jr. Weight-bearing exercise training and lumbar bone mineral content in postmenopausal women. *Ann Intern Med* 1988;108(6):824-8.
11. Vuori I, Heinonen A, Sievanen H, Kannus P, Pasanen M, Oja P. Effects of unilateral strength training and detraining on bone mineral density and content in young women: a study of mechanical loading and deloading on human bones. *Calcif Tissue Int* 1994;55(1):59-67.
12. Karlsson MK. The skeleton in a long-term perspective—are exercise induced benefits eroded by time? *J Musculoskelet Neuronal Interact* 2003;3(4):348-51; discussion 356.
13. Snow CM, Williams DP, LaRiviere J, Fuchs RK, Robinson TL. Bone gains and losses follow seasonal training and detraining in gymnasts. *Calcif Tissue Int* 2001;69(1):7-12.
14. Iwamoto J, Yeh JK, Aloia JF. Effect of deconditioning on cortical and cancellous bone growth in the exercise trained young rats. *J Bone Miner Res* 2000;15(9):1842-9.
15. Pajamaki I, Kannus P, Vuohelainen T, et al. The bone gain induced by exercise in puberty is not preserved through a virtually life-long deconditioning: a randomized controlled experimental study in male rats. *J Bone Miner Res* 2003;18(3):544-52.
16. Kesavan C, Mohan S, Srivastava AK, et al. Identification of genetic loci that regulate bone adaptive response to mechanical loading in C57BL/6J and C3H/HeJ mice intercross. *Bone* 2006;39(3):634-43.
17. Wergedal JE, Sheng MH, Ackert-Bicknell CL, Beamer WG, Baylink DJ. Mouse genetic model for bone strength and size phenotypes: NZB/B1NJ and RF/J inbred strains. *Bone* 2002;31(6):670-4.

18. Wergedal JE, Ackert-Bicknell CL, Tsaih SW, et al. Femur mechanical properties in the F2 progeny of an NZB/B1NJ x RF/J cross are regulated predominantly by genetic loci that regulate bone geometry. *J Bone Miner Res* 2006; 21(8):1256-66.
19. Turner CH, Roeder RK, Wiczorek A, Foroud T, Liu G, Peacock M. Variability in skeletal mass, structure, and biomechanical properties among inbred strains of rats. *J Bone Miner Res* 2001;16(8):1532-9.
20. Warden SJ, Fuchs RK, Castillo AB, Nelson IR, Turner CH. Exercise when young provides lifelong benefits to bone structure and strength. *J Bone Miner Res* 2007;22(2):251-9.
21. Fuchs RK, Snow CM. Gains in hip bone mass from high-impact training are maintained: a randomized controlled trial in children. *J Pediatr* 2002;141(3):357-62.
22. Turner CH, Woltman TA, Belongia DA. Structural changes in rat bone subjected to long-term, *in vivo* mechanical loading. *Bone* 1992;13(6):417-22.
23. Akhter MP, Cullen DM, Recker RR. Bone adaptation response to sham and bending stimuli in mice. *J Clin Densitom* 2002;5(2):207-16.

Conditional Disruption of IGF-I Gene in Osteoblasts Demonstrates Obligatory and Non-Redundant Role of IGF-I in Skeletal Anabolic Response to Mechanical Loading

Chandrasekhar Kesavan<sup>1,2</sup>, Wergedal J<sup>1</sup>, William Lau K H<sup>1, 2, 3 & 4</sup>, Subburaman Mohan<sup>1, 2, 3 & 4</sup>

**Running title:** Local IGF-I mediates bone anabolic response to loading.

<sup>1</sup>Musculoskeletal Disease Center, VA Loma Linda Healthcare System, Loma Linda, CA.

<sup>2</sup>Department of Medicine, Loma Linda University, Loma Linda, CA.

<sup>3</sup>Department of Biochemistry, Loma Linda University, Loma Linda, CA.

<sup>4</sup>Department of Physiology, Loma Linda University, Loma Linda, CA.

Address correspondence: Subburaman Mohan. Ph.D, Research Professor of Medicine, Loma Linda University, Musculoskeletal Disease Center (151), Jerry L. Pettis Memorial VA Medical Center, 11201 Benton Street, Loma Linda, CA 92357 Phone: 909-825-7084, ext. 2932, FAX: 909-796-1680, E-Mail: [Subburaman.mohan@va.gov](mailto:Subburaman.mohan@va.gov)

## Abstract

Insulin like growth factor (IGF-I) is a potent anabolic agent and an important determinant of peak bone mineral density (BMD). *In vitro* and *in vivo* studies have shown that IGF-I expression increases in cells of osteoblast lineage in response to mechanical stimulation (MS). Although, there are several lines of evidence which supports role for IGF-I in MS, direct evidence is lacking. Based on the past findings and our preliminary data, we have proposed the hypothesis that IGF-I act as a mediator of bone anabolic response to ML. To test this, we generated mice with conditional disruption of IGF-I gene in osteoblasts using cre-loxp approach. At 10 weeks, these mice were subjected to four-point bending and axial method of loading (AL). The right tibia was used for loading and left tibia as contralateral control. Due to difference in bone size between KO and wild type (WT) mice, strains were calculated and measured by mathematical and strain gauge approach, respectively. Adjusted loads were applied on tibias such that both sets of mice receive same amount of mechanical strains. 2 weeks of AL in the WT mice induced 5 to 15% increase in BMD and bone size while in the KO mice little or no change was seen in these parameters and this finding is consistent with four-point method of loading. In addition to cortical parameters, AL also induced 8 to 25% increase in secondary spongiosa of trabecular parameters (BV/TV, Tb.Th, Tb.BMD) in the WT mice while in the KO mice no such increase was seen in these parameters in response to loading. Furthermore, histomorphometric analysis revealed that axial loading increased bone formation by 60% and decreased TRAP+ OC cells by 50% in the WT. In contrast, in the KO mice, there was a decrease in TRAP+ OC cells but was not significant. Consistent with the *in vivo* findings, *in vitro* ML also revealed that blocking IGF-I action resulted in inhibition of fluid flow stress induced cell proliferation when compared to control that showed 45% increase in proliferation. One way ANOVA analysis revealed

expression levels of Ephrin B1, B2, A2, EphB2 and NR4a3 were different in the loaded bones of WT mice. In conclusion, the findings of our study demonstrate that osteoblast derived IGF-I are critical in mediating mechanical signal into anabolic signal in bone and other growth factors cannot compensate for the loss of osteoblast derived IGF-I.

### **Key words**

Axial loading, IGF-I, Micro-CT, Gene expression, Osteoid

### **Introduction**

Osteoporosis is a serious health issue, characterized by low bone mass which affects millions of elderly individuals. To some extent, this disease is both preventable and treatable. At present, physical exercise has been used as one of the strategy to maintain bone mass and prevent osteoporosis in humans. Numerous studies have shown that mechanical loading (ML) promotes bone formation and that unloading results in reduction in bone mass (1, 4, 13, 27). The molecular mechanisms mediating the effects of loading on bone, however, are less well-known. To date, a series of cellular and molecular events, particularly the intra- and intercellular signaling pathways, and the molecular components that regulate this pathway by responding to mechanical stimulation, have been investigated using *in vitro* models (5, 7, 11, 16-18). The data generated from *in vitro* models, although informative, is limited by the fact that most of the data were obtained from homogenous osteoblast cells in cell cultures. These models lack the vital communication between various types of cells, such as osteocytes, osteoblast and osteoprogenitors cells, which have been shown to respond to ML. Thus, the molecular components that respond to ML *in vivo* have not been fully understood. Once these components

have been identified, it will be able to elucidate their role in regulating bone formation. This in turn leads to a better understanding of the complex series of cellular and molecular events involved in bone formation, thus providing strategic pharmacological intervention to enhance or maximize the osteogenic effects of exercise.

In terms of potential mediators of anabolic response to ML, there is now considerable evidence that IGF-I is a strong candidate. These includes 1) Studies, to date, using several approaches such as microarray, in-situ hybridization and Real time RT-PCR have shown that loading increases IGF-I production in bone cells *in vitro* and *in vivo* (22, 26, 30); 2) Transgenic mice with elevated IGF-I expression in osteoblast exhibited increased bone formation in response to loading when compared to control mice (10) and 3) IGF-I administration induced bone formation in GH-deficient normally loaded rats but not in unloaded rats, thus suggesting that skeletal unloading induces resistance to IGF-I (23, 24). All these findings, though, provide indirect evidence for the role of IGF-I in mediating the bone anabolic response to loading, the cause and effect relationship between loading-induced increases in IGF-I expression and skeletal anabolic changes is lacking. Since mechanical loading increases IGF-I production in bone cells and because IGF-I is an important regulator of bone formation, we propose the hypothesis that “anabolic effects of mechanical loading on bone formation are mediated by osteoblast derived IGF-I. We tested this hypothesis in the present study using mice with conditional disruption of IGF-I gene in type I collagen producing osteoblast and their corresponding control mice.

## **EXPERIMENTAL PROCEDURES**

*Animals and genotyping* - Breeding pairs of transgenic mice in which Cre recombinase is driven by the procollagen, type I  $\alpha$ II gene (Col1 $\alpha$ 2-Cre) bred with transgenic mice in which exon 4 of the IGF-I gene is flanked by the loxP gene (IGF-I<sup>lox/lox</sup>) to generate Cre<sup>+</sup> loxP<sup>+/+</sup> (homozygous conditional IGF-I KO), Cre<sup>+</sup> loxP<sup>+/-</sup> (heterozygous conditional KO) and Cre negative loxP (littermate control) mice for our studies. Both the Cre and loxP mice have been backcrossed several generations with C57BL/6J mice to minimize the effect of mixed genetic background in the skeletal response to ML. The experimental procedures performed in this study were approved by the Animal Studies Subcommittee at the Jerry L. Pettis Memorial Veterans Affairs Medical Center.

*Genotyping of Cre/loxP mice* - At three weeks of age, DNA was extracted from tail tissue using a PUREGENE DNA Purification Kit (Gentra Systems, Inc., Minneapolis, MN) according to the manufacturer's protocol. As described earlier (9) PCR was performed to identify mice with Cre recombinase and/or loxP sites.

*Strain calculation* - At 9-weeks (n=5), the differences in the amount of mechanical strain produced by varying loads were calculated using mathematical approach (Stephen C. Cowin: Bone Mechanics Hand book, 2nd edition, 2001, chapter: Techniques from mechanics and imaging) on both IGF-I KO and wild type mice (WT). In addition, we also measured the amount of strain produced by loads using strain-gauge technique as described earlier (13) in both male and female IGF-I KO and WT mice.

*Four-point bending and in vivo Peripheral quantitative computed tomography (pQCT) measurement* - To evaluate cortical bone anabolic response to ML in IGF-I KO and littermate control mice (from now onwards called wild type mice), we used four-point bending method of loading. At 10 weeks, adjusted loads were applied on the tibia of both sets of mice (9N for WT and 6N for IGF-I KO mice) such that both mice receive same amount of mechanical strain. The loading was performed at 2Hz frequency, for 36 cycles, once per day for 12 days on both sets of mice. The right tibia was used for loading and the left tibia as contralateral internal control for both sets of mice. The loading were performed as described earlier (13). After 48 hours of last loading, mice were euthanized and tibias were collected and stored at 10% formalin for further analysis. Four-point bending induced changes in the bone parameters in loaded and non-externally loaded tibiae were measured by pQCT (Stratec XCT 960M, Norland Medical System, Ft. Atkinson, WI) as described previously (13).

*Tibia Axial loading* - To study the anabolic effects of exercise on trabecular area, we used tibia axial loading model which was originally developed by Dr. Charles Turner's group and subsequently adapted for tibia by Dr. Lance Lanyon's group (2, 8, 19, 25, 28). At 10 weeks of age, loading were started on both male and female of conditional IGF-I KO mice and corresponding WT mice. The apparatus and protocol for dynamically loading the mouse has been adapted from previously published studies (8, 25). The mice were positioned in a servo hydraulic mechanical testing machine as described earlier (8, 25). Adjusted axial load (Trapezoidal-shaped pulse period=0.1s [loading 0.025s, hold 0.05s and unloading 0.025s]; rest time between pulse=10 s; cycles/day=40) were applied on the right tibia of both IGF-I KO and WT mice such that both sets of mice receive same amount of mechanical strain. The left tibia

was used as contralateral internal control. The loading was performed at 3 alternate days/ week for 2 weeks. Mice were anesthetized while loading by using 4% Isoflurane and 2 liter/minute medical oxygen. On the 15<sup>th</sup> day, 48 hours after the last load, the mice were euthanized and the bones were collected and stored at -80°C for further analyses.

*μCT (Computed tomography)* - To measure microarchitectural changes of trabecular bone as well as cortical bone formation in response to axial loading, we used Micro-CT, a high resolution tomography image system (Scanco In vivo CT40, Switzerland). Routine calibration was performed once a week using a three-point calibration phantom corresponding to the density from air to cortical bone. Bones were immersed in 1X PBS to prevent them from drying and scanning was performed using 75Kv X-ray at resolution of 10.5 μm. To minimize the position error (slice positioning) and to be consistent in our sampling site from mouse to mouse, we undertook several precautionary steps, which includes 1) A scout view of the whole tibia was taken first in the micro-CT to determine landmarks and precise selections of measurement sites. 2) We used growth plate of the tibia as the reference point. 3) To measure trabecular parameters, we started our scan 30 slices away from the growth plate, which was 0.315 mm and progressing towards distal up to 0.840 mm providing a total of 50 slices (525 μm) and 3) Similarly, to measure cortical parameters, scanning was performed at 5.5 mm away from the growth plate and progressing towards distal up to 6.55 mm, providing a total of 100 slices (1050 μm). This area of scanning represents 37% positioning of whole of bone. After acquiring the radiographic data, images were reconstructed by using 2-D image software (as described by manufacturers). The area of the trabecular analysis was outlined within the trabecular compartment and similarly for the cortical bone. Every 10 sections were outlined, and the intermediate sections were

interpolated with the contouring algorithm to create a volume of interest, followed by three dimensional analysis using Scanco in vivo software. Parameters such as bone volume (BV, mm<sup>3</sup>), bone volume fraction (BV/TV, %), apparent density (mg HA/ccm), trabecular number (Tb.N, mm<sup>-1</sup>), trabecular thickness (Tb.Th, μm) and trabecular space (Tb.Sp, μm) were evaluated in the loaded and non-externally loaded bones of both sets of mice. The values in the table represent average of the above slices for each parameter. Since IGF-I KO mice are smaller in bone length compared to littermate WT mice; we adjusted for this difference in length using standard calculation such that the sampling site is same for both sets of mice.

*RNA extraction* - RNA was extracted from the loaded and non-externally loaded bones using qiagen lipid extraction kit [Qiagen, Valencia, CA], as previously described. Quality and quantity of RNA were analyzed using the 2100 Bio-analyzer (Agilent, Palo Alto, CA, USA) and Nano-drop (Wilmington, DE).

*Gene expression- Reverse Transcriptase - Real time RT-PCR* - Quantitative real time RT-PCR was used to determine the expression levels of genes as previously described. Real time RT-PCR was carried out according to the manufacturer's instructions (ABIPRISM, Foster City, CA.) using the SYBR Green method on 7900 Sequence Detection systems from Applied Biosystems. Briefly, purified total RNA [200μg/μl] was used to synthesize the first strand cDNA by reverse transcription according to the manufacturer's instructions [Bio-Rad, CA]. 5μl of the five times diluted first strand cDNA reaction, was subjected to real time PCR amplification using gene specific primers as described earlier. The data were analyzed using SDS software, version 2.0, and the results were exported to Microsoft Excel for further analysis. Data normalization was

accomplished using the endogenous control ( $\beta$ -actin, PPIA) to correct for variation in the RNA quality among samples. The normalized Ct values were subjected to a  $2^{-\Delta\Delta Ct}$  formula to calculate the fold change between the non-externally loaded and loaded groups. The formula and its derivations were obtained from the instrument user guide.

*Histomorphometric analysis* - Mice were injected with calcein according to their body weight on 1<sup>st</sup> and 10<sup>th</sup> day before the last day of the loading. After the last day of loading, mice were euthanized; tibias were collected and fixed overnight with 10% cold neutral buffered formalin. Twenty four later, bones were rinsed with 1XPBS to be free of formalin and embedded in methyl methacrylate. Thick cross-sections (0.5 mm in thickness) were cut from the mid-diaphysis of the bones with a wire saw (Delaware Diamond Kives) and this cross-section was then ground lightly. For metaphyseal sections thin longitudinal section (5 microns) were cut, stained with Goldners trichrome stain, mounted in Fluoromount-G (Fisher Scientific, Pittsburgh, PA), or left unstained and examined under a Olympus BH-2 fluorescence/bright field microscope. Histomorphometric analysis was performed on these bones as described earlier (15).

*Fluid Shear Stress (FFS)* - In vitro mechanical stress was applied on MC3T3 cells as described earlier (Ref). Four groups (n=5 replicate for each group) of MC3T3 cells were plated on a glass slides (75 × 38 mm) at  $5 \times 10^4$  cells/slide in Dulbecco's modified Eagle's medium supplemented with 10% bovine calf serum. Once, when the cells reached ~80% confluency, the cells were serum-deprived for 24 hours and according to our experiment design, groups were subjected to a steady fluid flow stress of 20 dynes/cm<sup>2</sup> for 30 min in Cytodyne flow chambers as previously described (11).

Group-I cells subjected to FFS without any BP4 and its corresponding static control (Group-II) cells kept in identical conditions in Cytodyne chamber but without exposing to the FFS. Group-III cells were incubated with BP4 (300ng) for 1 hour prior to FFS and its corresponding static control (Group-IV) also incubated with BP4 and kept in identical conditions in Cytodyne chamber but without exposing to the shear stress.

Cell proliferation assay-Cell proliferation was assessed by [<sup>3</sup>H] thymidine incorporation into cell DNA as described previously (11).

*Statistical Analysis* - Data were presented as Mean  $\pm$  SE. Regression analysis; ANOVA (Newman Keuuslus -Post Hoc Test) and standard T-test were used to compare differences from loading between the strains using the percentage obtained from loaded vs. non-externally loaded bones  $[(\text{Non-loaded} - \text{Loaded})/\text{Non-loaded} \times 100]$ . We used STATISTICA software for our analysis and the results were considered significantly different at  $p < 0.05$ .

## **RESULTS:**

*Strain calculation, four-point bending and changes in cortical parameters between wild type littermate and IGF-I KO mice*

Since bones of IGF-I KO mice have smaller circumference than WT mice, we predict that mice with smaller circumference tend to receive higher mechanical strain than mice with larger circumference. In order to assure that the difference in skeletal anabolic response to loading is due to lack of local IGF-I and not due to differences in mechanical strain, we calculated the amount of mechanical strain produced by varying loads in both sets of mice using

mathematical approach (Ref). The results from our study shows that 6N load in IGF-I KO mouse produces mechanical strain equivalent to 9N load in the WT mice. Based on this data, adjusted loads were applied on both sets of mice using four-point bending device.

Figure 1, shows that, in response to 12 days of four-point bending, the loaded bones of WT mice showed significant increase in the newly formed while no such formation was seen in the loaded bones of IGF-I KO mice (Figure 1). Accordingly, skeletal parameters, such as total area (cross sectional area), bone mineral content and bone mineral density, measured by pQCT, were significantly increased in the externally loaded bones when compared to non-externally loaded bones of WT mice (Figure 2). In contrast, in the IGF-I KO mice, if any, these parameters showed little or no change in bone response to loading. Overall, the findings of the four-point bending experiment reveal that anabolic effects of mechanical loading on bone formation is significantly lesser in mice deficient in osteoblast derived IGF-I when compared to the WT mice (Figure 2).

*Strain measurements, axial loading and changes in trabecular and cortical between wild type littermate and IGF-I KO mice*

Again, due to difference in bone size between IGF-I KO and WT mice, we measured the amount of mechanical strain produced by varying loads in both male and female IGF-I KO and WT mice by using strain-gauge approach (Ref). The results from our study show that female IGF-I KO mice produced 780  $\mu\epsilon$  for a 6N load similar to the mechanical strain produced by a 12N load (825  $\mu\epsilon$ , n=3) in the female WT mice. Similarly, male IGF-I KO mice produced 745  $\mu\epsilon$  for a 6.5N load equivalent to the mechanical strain produced by a 12N load (773  $\mu\epsilon$ , n=3) in the

male WT mice. Based on this strain data, adjusted axial load was applied such that both sets of mice received similar amount of mechanical strain.

In response to alternate days of axial loading for two weeks, we found that the WT mice showed 23% increase in BV/TV, 21% increase in trabecular density and 19% increase in trabecular thickness with very little change in trabecular number (Figure 3) but not significant. In contrast, in the IGF-I KO mice, trabecular space were increased, with decrease in other bone parameters such as TV/BV, Tb. N, and Tb. Th was observed in response to loading (Figure 3).

In addition to trabecular parameters of secondary spongiosa, we also measured cortical parameters and found that the total volume, density and cortical thickness were increased by 7 to 13% in WT mice (Figure 4). While in the IGF-I KO mice, little or no change was observed in these parameters (Figure 4).

#### *Histomorphometric analysis of skeletal parameters in response to axial loading*

To determine the impact of osteoblast derived IGF-I deficiency on bone formation response to mechanical loading, we performed histomorphometric measurements at the secondary spongiosa of trabecular bone on both loaded and non-externally loaded bones of IGF-I KO and WT mice. We found that osteoid perimeter, a measure of length of formation and trabecular thicknesses were increased by 60% approximately in the loaded bones of WT mice (Figure 5). In the IGF-I KO mice, no such increase was seen in any of these parameters in the loaded bones. In addition to the formation, we also measured TRAP-labeled surface, a marker for osteoclast activity. We found that TRAP labeled surface was significantly reduced in the loaded bones of WT mice while in the IGF-I KO mice, though, there was a decrease, but was not significant (Figure 5).

### *Gene expression analysis in response to axial loading*

In order to identify the genes that mediate mechanical signal into bone anabolic response to loading, we measured expression levels of several genes in the loaded and non-externally loaded bones of both IGF-I KO and WT mice by using real time RT-PCR. These includes dentin matrix sialoprotein, IGF-I, Tnnt2, ephrin B2, ephrin A2, ephrin A4, b-catenin, EphB2, EphB4, Nr4a3, SOST, Osterix and SDF1. The rationale for selecting these genes was based on our earlier findings in microarray and QTL study, and their relevance in bone. Among these, IGF-I, ephrin B1, B2, A2, EphB2, Nr4a3 and Tnnt2 expression were different in the loaded bones of WT mice (1.5 to 3-fold,  $p < 0.05$ ) when compared to non-externally loaded bones. In contrast, in the IGF-I KO mice, there was no change in any of these genes in the loaded bones compared to non-externally loaded bones (Table-1).

### *Effect of fluid flow stress on the cell proliferation in MC3T3 cells with and without IGF-I action*

To validate the in vivo findings, we performed in vitro fluid flow stress using MC3T3 cells with and without IGF-I blocker, BP4. 30 minutes of 20 dynes/cm<sup>2</sup> FFS on MC3T3 cells without BP4 significantly increased cell proliferation (45%) and that MC3T3 cells treated with BP4 showed 30% reduction in FFS induced cell proliferation.

## **DISCUSSION**

The key findings of this study are as follow; 1) Four-point bending increased BMD and bone size significantly in the IGF-I WT mice but not in mice disruption with osteoblast derived IGF-I; 2) Bone produced IGF-I is also important in mediating mechanical signal into anabolic effects at the trabecular site; 3) Mechanical loading increased trabecular bone in the WT mice

largely by increasing existing trabecular thickness than by number. 3) Histology data provide evidence that loss of trabecular response to loading in the IGF-I KO mice is not due to axial loading induced increase in bone resorption.

Previously, using monolayer cultures, we have shown that mechanical stimulation increase osteoblast cell proliferation in the presence of IGF-I (11, 17). Likewise, in vivo, we and others have shown that IGF-I expression is increased in response to loading and decreased in response to unloading (6, 17, 21). However, most of these reports indirectly show that IGF-I mediates bone anabolic response to loading but there is no direct evidence to show relationship between increase in IGF-I expression and skeletal changes. In this study, to test that association, we generated conditional IGF-I KO mice using Cre-loxp approach and subjected these mice to mechanical loading. Initially, we used four-point bending method of loading to evaluate the involvement of osteoblast derived IGF-I in cortical bone response. The rationales for choosing this loading model, duration of loading are based on previous reports (1, 13). Our findings demonstrate for the first time that mice deficient in osteoblast derived IGF-I show little or no change in cortical response while the mice with osteoblast derived IGF-I show significant increase in cortical response as evident from an increase in BMD. The lack of response in the IGF-I KO mice cannot be explained by inadequate mechanical strain because we applied same amount of mechanical strain based on the measured strain data on both sets of mice. The dramatic change in skeletal response in the WT mice and not in the KO mice is largely, in part, due to increase in osteoblast cell proliferation and function mediated by an increase in IGF-I action. Accordingly, in vitro, we show that MC3T3 cells subjected to mechanical stress showed 45% increase in cell proliferation whereas when IGF-I action was blocked with IGFBP4, stress

induced increase in cell proliferation was reduced by 30%. Therefore, based on these findings, we concluded that osteoblast derived IGF-I action is critical in translating the mechanical signal into anabolic effects on bone and lack of local IGF-I cause impairment in these signals leading to little or no change in skeletal parameters.

While four-point bending method of loading induces mostly periosteal bone response since the load is applied on the cortical bone area which lack trabecular bone, we next evaluate if the bone cell produced IGF-I is also involved in inducing trabecular bone formation. Furthermore, in terms of the pathogenesis of osteoporosis, it is well known that loss of trabecular bone is a major contributor to etiology of the disease. Therefore, the next goal of our study was to select an in vivo loading model that can stimulate both trabecular and periosteal bone formation. To date, a number of loading models including jump exercise, wheel running and axial loading have been used to evaluate trabecular bone formation response (12, 25, 27, 29). We have chosen axial method of loading because this model mimics exercise patterns of walking in humans and this model has been shown to induce both cortical as well as trabecular bone formation response to mechanical loading. Furthermore, studies have shown that axial loading on ulna or tibia results in robust increase in both cortical and trabecular bone formation after two weeks of mechanical loading. Based on these rationales, we next evaluated the trabecular anabolic response to axial loading in both IGF-I KO and WT mice.

In response to two weeks of axial loading, we found that mice with osteoblast derived IGF-I showed 27% increase in trabecular bone volume. This study, demonstrates for the first time that osteoblast produced IGF-I is important in mediating the anabolic effects of ML on bone

formation at the trabecular site. In terms of mechanism, we found that increase in trabecular bone in response to axial loading in the WT mice is largely, in part, mediated by an increase in trabecular thickness rather than by generating new trabeculae number. A similar type of observation has been also reported earlier in mice over expressing osteoblast produced IGF-I. They have shown that mice over expression osteoblast produced IGF-I showed increased trabecular bone volume without increased osteoblast proliferation. Taken together the finding from our study and past study illustrate that the genes and the signaling pathways activated by downstream of IGF-I are likely involved in increasing the function of existing osteoblast cells rather generating new osteoblast cells in increasing trabecular response to loading.

In contrast, in the IGF-I KO mice, when same amount of mechanical strain were applied no such increase was seen in any of trabecular parameters however, a small decrease in trabecular thickness was seen in response to loading. The decrease in trabecular response to mechanical loading in the IGF-I KO mice in our micro-CT analysis was an unexpected finding and thus, it also raises a question whether this is due to an increase in bone resorption. Therefore, to address this, we measured TRAP labeled surface on the bones (loaded and non-externally loaded tibia) of both sets of mice to determine whether axial loading induced increase in bone resorption is the causes for the trabecular bone loss in the loaded bones of IGF-I knockout mice. However, the results from our study revealed no such increase in TRAP+ positive OC cells in the loaded bones of IGF-I KO mice. In contrast, in the loaded bones of WT mice, we found a significant decrease in TRAP+ OC cells suggesting that axial loading blocks bone resorption. These findings, together demonstrate that loss of trabecular bone in the loaded bones of IGF-I KO mice is not due to increase in bone resorption, however, further study is require to provide an

explanation for the small loss of trabecular bone volume in the IGF-I KO mice in response to loading.

Now that, using both tomography and loading model, we have shown that osteoblast derived IGF-I are involved in mediating bone anabolic response to mechanical loading, the next phase of our study is to identify the molecular components that are down stream of IGF-I contributing for the increased bone anabolic response to loading using mRNA from osteoblast derived IGF-I mice. Our results revealed several genes that differentially expressed between loaded and unloaded bones. Among these, increase in IGF-I gene expression in response to loading in the WT mice provides a substantial evidence for the proposed hypothesis in this study. In addition to this, increase in other genes such as ephrin A2, B1, B2, EphB2, Nr4a3 and Tnnt2 in response to loading in the WT but not in the IGF-I KO mice suggest that these genes to some extent, in part, are, responsible for the IGF-I mediated bone anabolic response to loading. Increase in ephrin A2, EphB2 and Tnnt2 are new and there relevance with bone is yet to be determined. Reports in the past have shown that ephrin B1, B2, EphB2 and Nr4a3 are involved in osteoblast differentiation (3, 20, 31), however, our study show that they are also involved in bone response to mechanical loading. Further study utilizing various molecular approaches is necessary to determine the functional role of these genes in relation to bone adaptive response to mechanical loading.

Some of the limitations of this study are as follow; 1) In this manuscript, we would like to discuss that recent studies several have shown that osteocytes derived IGF-I are critical for bone anabolic response to mechanical loading. Thus, one could raise a question whether the skeletal

effects observed in our study in response to loading in the WT and KO mice is due to osteoblast or osteocytes derived IGF-I. In our study, we have knocked out IGF-I only in osteoblast and since most of these osteoblast becomes osteocytes, we anticipate the osteocytes also to be deficient in IGF-I. Nevertheless, at this moment, our study cannot rule out whether the effect is from osteoblast or osteocytes. Further study using osteocytes deficient IGF-I mice will delineate the contribution of osteocytes vs. osteoblast derived IGF-I in regulating bone anabolic response to loading.

2) In the past, reports by others have predicted that some of the skeletal changes induced by four-point bending are due to periosteal pressure. In our previous QTL study, we found that sham-loading neither increased periosteal bone formation nor caused changes in expression levels of bone marker genes, demonstrating that the skeletal changes induced by bending are not due to periosteal pressure (14). This finding also applies to the present study since we used the same loading model and regimen.

3) It is worth mentioning that the four-point bending method of loading also adds lamellar bone initially; however, as the duration of loading becomes larger, there is an increase in accumulation of bone forming osteoblast cells at the loading site. As a result, this gives rise to a large amount of low mineralized bone, so called woven bone over the lamellar bone. This great increase in woven bone cannot be attributed to the pathological response because in the past, we have measured micro-cracks by histological analysis to rule out the possibility whether the changes on bone parameters induced by four-point bending are due to micro-crack induced healing. We found that there was no significant difference in the micro-crack areas between loaded and unloaded bones of good responder C57BL/6J mouse (13). Furthermore, we did not observe any fracture as evident from X-ray and pQCT image.

4) In the past, we have shown that changes in skeletal anabolic response to loading were not significantly different between male and female and therefore, in the present study, we combine both male and female data together for the analysis.

In summary, Osteoblast produced IGF-I are essential for the mechanical loading induced increase in new bone formation, thus suggesting that other growth factors cannot compensate for the lack of local IGF-I to produce skeletal anabolic response to mechanical loading.

### **Acknowledgment**

This work was supported by the National Institute of Health and by Army Assistance Award No. DAMD17-01-1-744. The information contained in this publication does not necessarily reflect the position or the policy of the Government, and no official endorsement should be inferred. All work was performed in facilities provided by the Department of Veterans Affairs.

## Figure Legends

**Figure 1:** Cross sectional area of the externally loaded and non-externally loaded bones of IGF-I KO and wild type mice obtained from pQCT after 12 days of four-point bending. The arrow corresponds to the newly formed bone. The white color corresponds to cortical bone.

**Figure 2:** Changes in skeletal parameters measured by pQCT in response to 12 days of four-point bending in IGF-I KO and wild type mice. The y-axis represents percent increase and x-axis represents bone parameters. Values are mentioned as mean  $\pm$  SE. The TA, total area; BMC, bone mineral content and BMD, bone mineral density. <sup>a</sup>p<0.05 vs. corresponding non-externally loaded tibiae and <sup>b</sup>p<0.05 vs. IGF-I KO mice, N=8.

**Figure 3:** Changes in trabecular parameters of secondary spongiosa measured by micro-CT after 2 weeks of axial loading in IGF-I KO and wild type mice. The y-axis represents percent increase and x-axis represents bone parameters. Values are mentioned as mean  $\pm$  SE. The BV/TV, bone volume/total volume; Tb.N, trabecular number; Tb.Th, trabecular thickness; Tb.Sp, trabecular space and Tb.BMD, trabecular bone mineral density. <sup>a</sup>p<0.05 vs. corresponding non-externally loaded tibiae and <sup>b</sup>p<0.05 vs. IGF-I KO mice, N=10

**Figure 4:** Changes in cortical bone parameters measured by micro-CT at the diaphysis after two weeks of axial loading on 10 week IGF-I KO and wild type mice. The y-axis represents percent increase and x-axis represents bone parameters. Values are mentioned as mean  $\pm$  SE. The TV, total volume; BMD, bone mineral density and Cth, cortical thickness. <sup>a</sup>p<0.05 vs. contralateral controls and <sup>b</sup>p<0.05 vs. IGF-I KO mice, N=15.

**Figure 5:** Histomorphometric analyses of bone formation response to axial loading in IGF-I KO and wild type mice. Values are mentioned as mean  $\pm$  SE. The O.pm, osteiod perimeter; Tb.Th, trabecular thickness and TRAP, tartrate-resistance acidic phosphatase, N=9.

## Reference:

1. Akhter, M. P., Cullen, D. M., Pedersen, E. A., Kimmel, D. B., and Recker, R. R. Bone response to in vivo mechanical loading in two breeds of mice. *Calcif Tissue Int* 63:442-9; 1998.
2. Alam, I., Warden, S. J., Robling, A. G., and Turner, C. H. Mechanotransduction in bone does not require a functional cyclooxygenase-2 (COX-2) gene. *J Bone Miner Res* 20:438-46; 2005.
3. Allan, E. H., Hausler, K. D., Wei, T., Gooi, J. H., Quinn, J. M., Crimeen-Irwin, B., Pompolo, S., Sims, N. A., Gillespie, M. T., Onyia, J. E., and Martin, T. J. EphrinB2 regulation by PTH and PTHrP revealed by molecular profiling in differentiating osteoblasts. *J Bone Miner Res* 23:1170-81; 2008.
4. Bikle, D. D., Sakata, T., and Halloran, B. P. The impact of skeletal unloading on bone formation. *Gravit Space Biol Bull* 16:45-54; 2003.
5. Boutahar, N., Guignandon, A., Vico, L., and Lafage-Proust, M. H. Mechanical strain on osteoblasts activates autophosphorylation of focal adhesion kinase and proline-rich tyrosine kinase 2 tyrosine sites involved in ERK activation. *J Biol Chem* 279:30588-99; 2004.
6. Bravenboer, N., Engelbregt, M. J., Visser, N. A., Popp-Snijders, C., and Lips, P. The effect of exercise on systemic and bone concentrations of growth factors in rats. *J Orthop Res* 19:945-9; 2001.
7. Danciu, T. E., Adam, R. M., Naruse, K., Freeman, M. R., and Hauschka, P. V. Calcium regulates the PI3K-Akt pathway in stretched osteoblasts. *FEBS Lett* 536:193-7; 2003.
8. De Souza, R. L., Matsuura, M., Eckstein, F., Rawlinson, S. C., Lanyon, L. E., and Pitsillides, A. A. Non-invasive axial loading of mouse tibiae increases cortical bone formation and modifies trabecular organization: a new model to study cortical and cancellous compartments in a single loaded element. *Bone* 37:810-8; 2005.
9. Govoni, K. E., Wergedal, J. E., Florin, L., Angel, P., Baylink, D. J., and Mohan, S. Conditional deletion of insulin-like growth factor-I in collagen type 1alpha2-expressing cells results in postnatal lethality and a dramatic reduction in bone accretion. *Endocrinology* 148:5706-15; 2007.
10. Gross, T. S., Srinivasan, S., Liu, C. C., Clemens, T. L., and Bain, S. D. Noninvasive loading of the murine tibia: an in vivo model for the study of mechanotransduction. *J Bone Miner Res* 17:493-501; 2002.
11. Kapur, S., Mohan, S., Baylink, D. J., and Lau, K. H. Fluid shear stress synergizes with insulin-like growth factor-I (IGF-I) on osteoblast proliferation through integrin-dependent activation of IGF-I mitogenic signaling pathway. *J Biol Chem* 280:20163-70; 2005.
12. Kelly, S. A., Czech, P. P., Wight, J. T., Blank, K. M., and Garland, T., Jr. Experimental evolution and phenotypic plasticity of hindlimb bones in high-activity house mice. *J Morphol* 267:360-74; 2006.
13. Kesavan, C., Mohan, S., Oberholtzer, S., Wergedal, J. E., and Baylink, D. J. Mechanical loading-induced gene expression and BMD changes are different in two inbred mouse strains. *J Appl Physiol* 99:1951-7; 2005.

14. Kesavan, C., Mohan, S., Srivastava, A. K., Kapoor, S., Wergedal, J. E., Yu, H., and Baylink, D. J. Identification of genetic loci that regulate bone adaptive response to mechanical loading in C57BL/6J and C3H/HeJ mice intercross. *Bone* 39:634-43; 2006.
15. Kim, J., Xing, W., Wergedal, J., Chan, J. Y., and Mohan, S. Targeted disruption of nuclear factor erythroid-derived 2-like 1 in osteoblasts reduces bone size and bone formation in mice. *Physiol Genomics* 40:100-10. 2004.
16. Kunnel, J. G., Igarashi, K., Gilbert, J. L., and Stern, P. H. Bone anabolic responses to mechanical load in vitro involve COX-2 and constitutive NOS. *Connect Tissue Res* 45:40-9; 2004.
17. Lau, K. H., Kapur, S., Kesavan, C., and Baylink, D. J. Up-regulation of the Wnt, estrogen receptor, insulin-like growth factor-I, and bone morphogenetic protein pathways in C57BL/6J osteoblasts as opposed to C3H/HeJ osteoblasts in part contributes to the differential anabolic response to fluid shear. *J Biol Chem* 281:9576-88; 2006.
18. Liedert, A., Kaspar, D., Blakytyn, R., Claes, L., and Ignatius, A. Signal transduction pathways involved in mechanotransduction in bone cells. *Biochem Biophys Res Commun* 349:1-5; 2006.
19. Ohashi, N., Robling, A. G., Burr, D. B., and Turner, C. H. The effects of dynamic axial loading on the rat growth plate. *J Bone Miner Res* 17:284-92; 2002.
20. Pirih, F. Q., Nervina, J. M., Pham, L., Aghaloo, T., and Tetradis, S. Parathyroid hormone induces the nuclear orphan receptor NOR-1 in osteoblasts. *Biochem Biophys Res Commun* 306:144-50; 2003.
21. Raab-Cullen, D. M., Thiede, M. A., Petersen, D. N., Kimmel, D. B., and Recker, R. R. Mechanical loading stimulates rapid changes in periosteal gene expression. *Calcif Tissue Int* 55:473-8; 1994.
22. Reijnders, C. M., Bravenboer, N., Tromp, A. M., Blankenstein, M. A., and Lips, P. Effect of mechanical loading on insulin-like growth factor-I gene expression in rat tibia. *J Endocrinol* 192:131-40; 2007.
23. Sakata, T., Halloran, B. P., Elalieh, H. Z., Munson, S. J., Rudner, L., Venton, L., Ginzinger, D., Rosen, C. J., and Bikle, D. D. Skeletal unloading induces resistance to insulin-like growth factor I on bone formation. *Bone* 32:669-80; 2003.
24. Sakata, T., Wang, Y., Halloran, B. P., Elalieh, H. Z., Cao, J., and Bikle, D. D. Skeletal unloading induces resistance to insulin-like growth factor-I (IGF-I) by inhibiting activation of the IGF-I signaling pathways. *J Bone Miner Res* 19:436-46; 2004.
25. Sugiyama, T., Saxon, L. K., Zaman, G., Moustafa, A., Sunter, A., Price, J. S., and Lanyon, L. E. Mechanical loading enhances the anabolic effects of intermittent parathyroid hormone (1-34) on trabecular and cortical bone in mice. *Bone* 43:238-48; 2008.
26. Triplett, J. W., O'Riley, R., Tekulve, K., Norvell, S. M., and Pavalko, F. M. Mechanical loading by fluid shear stress enhances IGF-1 receptor signaling in osteoblasts in a PKCzeta-dependent manner. *Mol Cell Biomech* 4:13-25; 2007.
27. Umemura, Y., Baylink, D. J., Wergedal, J. E., Mohan, S., and Srivastava, A. K. A time course of bone response to jump exercise in C57BL/6J mice. *J Bone Miner Metab* 20:209-15; 2002.
28. Warden, S. J., and Turner, C. H. Mechanotransduction in the cortical bone is most efficient at loading frequencies of 5-10 Hz. *Bone* 34:261-70; 2004.

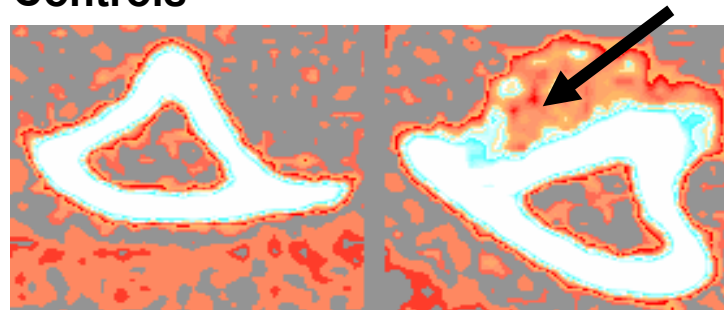
29. Westerlind, K. C., Fluckey, J. D., Gordon, S. E., Kraemer, W. J., Farrell, P. A., and Turner, R. T. Effect of resistance exercise training on cortical and cancellous bone in mature male rats. *J Appl Physiol* 84:459-64; 1998.
30. Xing, W., Baylink, D., Kesavan, C., Hu, Y., Kapoor, S., Chadwick, R. B., and Mohan, S. Global gene expression analysis in the bones reveals involvement of several novel genes and pathways in mediating an anabolic response of mechanical loading in mice. *J Cell Biochem* 96:1049-60; 2005.
31. Xing, W., Kim, J., Wergedal, J., Chen, S. T., and Mohan, S. Ephrin B1 regulates bone marrow stromal cell differentiation and bone formation by influencing TAZ transactivation via complex formation with NHERF1. *Mol Cell Biol* 30:711-21.

Table -1 Quantitative analysis of mRNA levels of genes measured by real time RT-PCR after two weeks of axial loading on 10 week IGF-I KO and wild type mice.

Genes	Fold Change	
	WT	IGF-I KO
Insulin like growth factor-1	2.34 ± 0.28 *	1.0 ± 0.16
Ephrin B1	2.23 ± 0.23*	0.55 ±0.04
Ephrin B2	2.06 ± 0.1 *	0.51 ± 0.07
Ephrin A2	1.7 ± 0.04 *	0.59 ± 0.06
EphB2	3.94 ± 0.41*	1.3 ± 0.18
Tnnt2	4.84 ± 0.6*	1.06 ± 0.10
Nr4a3	2.79 ± 0.22*	0.91 ± 0.09

\*p<0.05 vs. non-externally loaded bones, Values are Mean ± SE, N=5-6

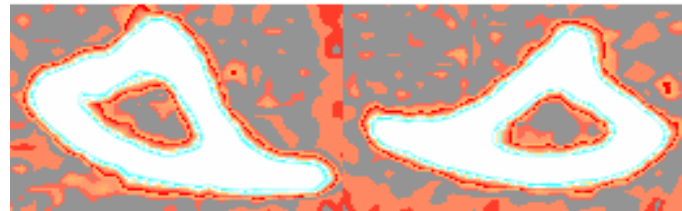
### Controls



Non-externally  
loaded

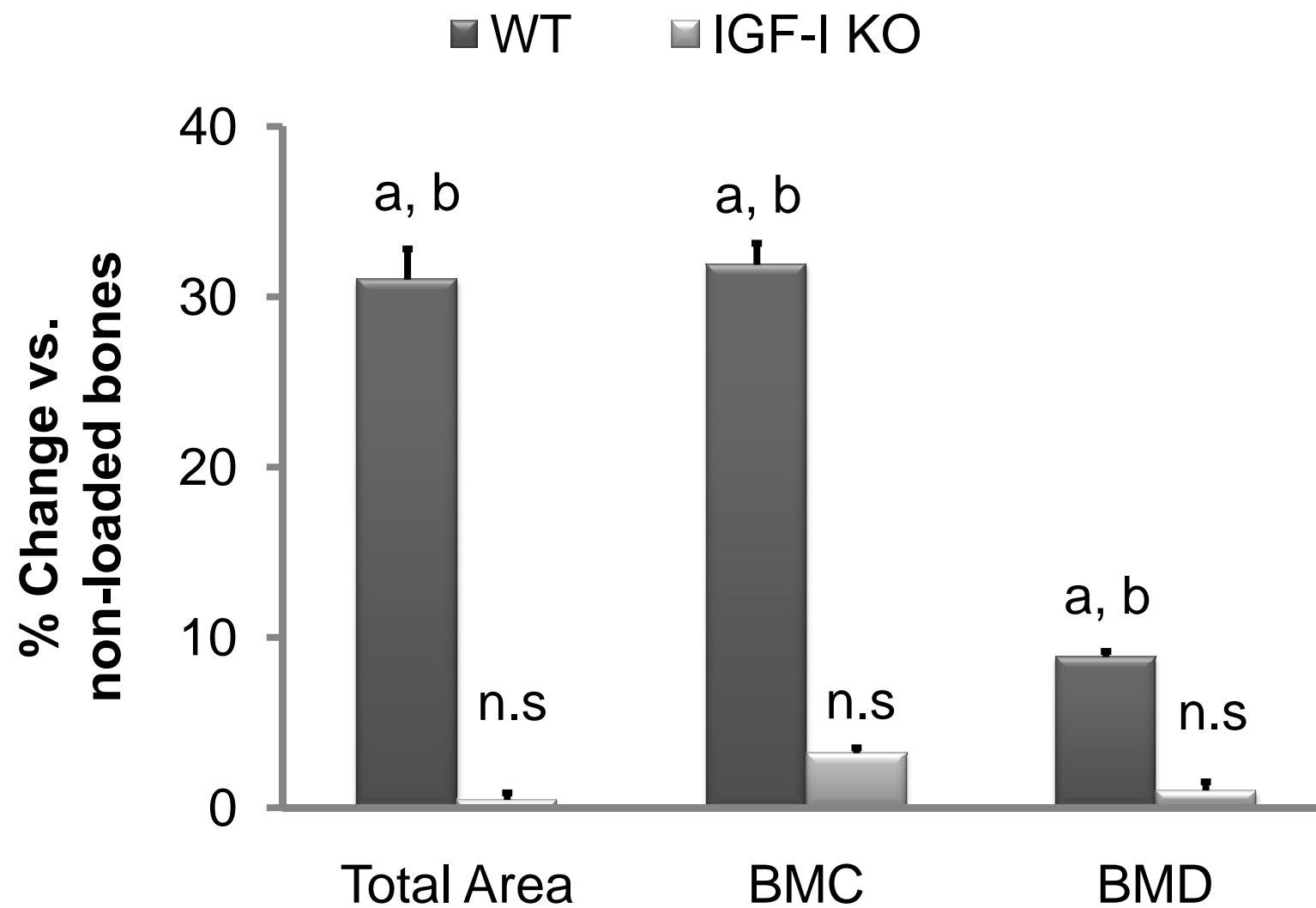
Loaded

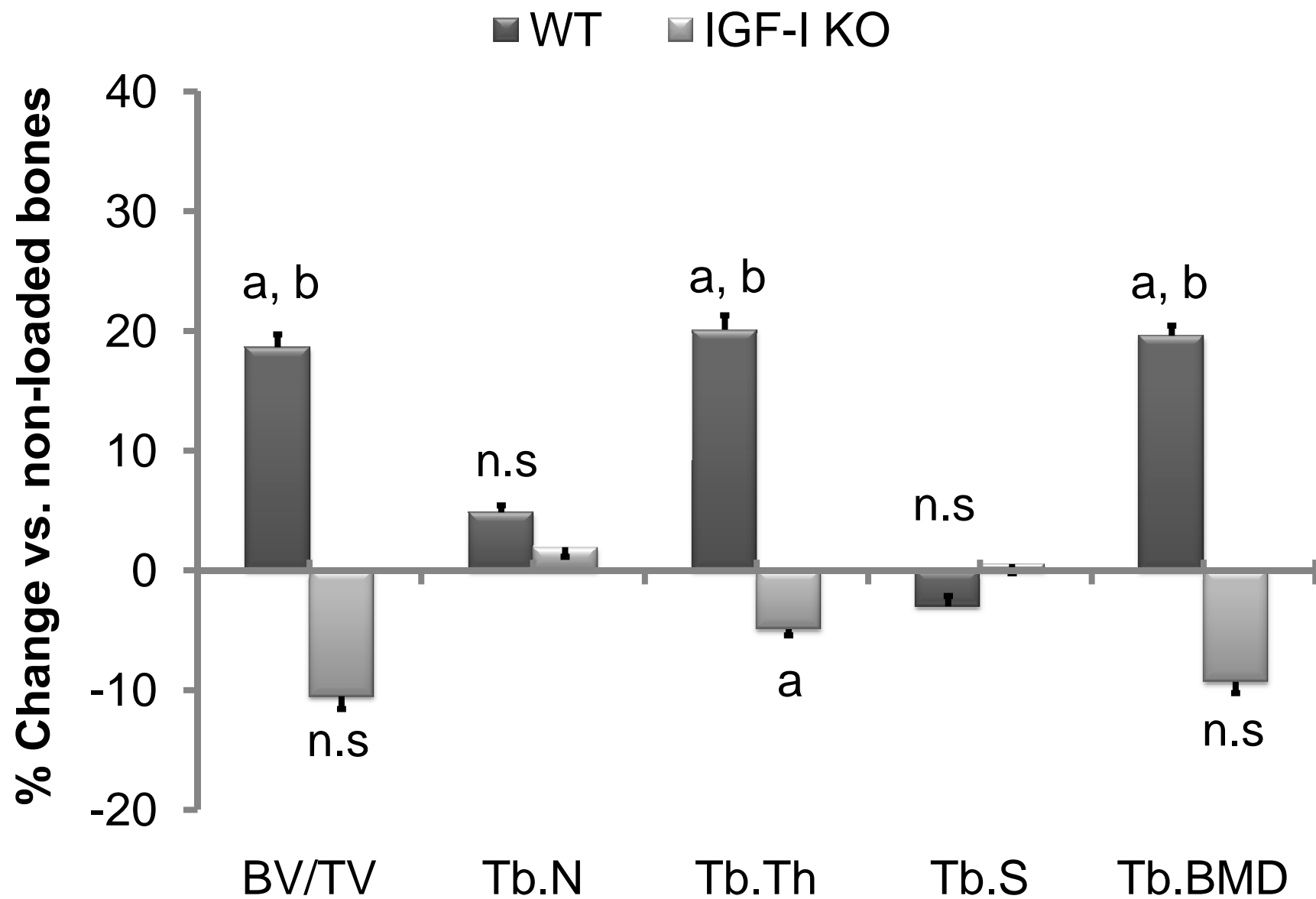
### IGF-I KO mice

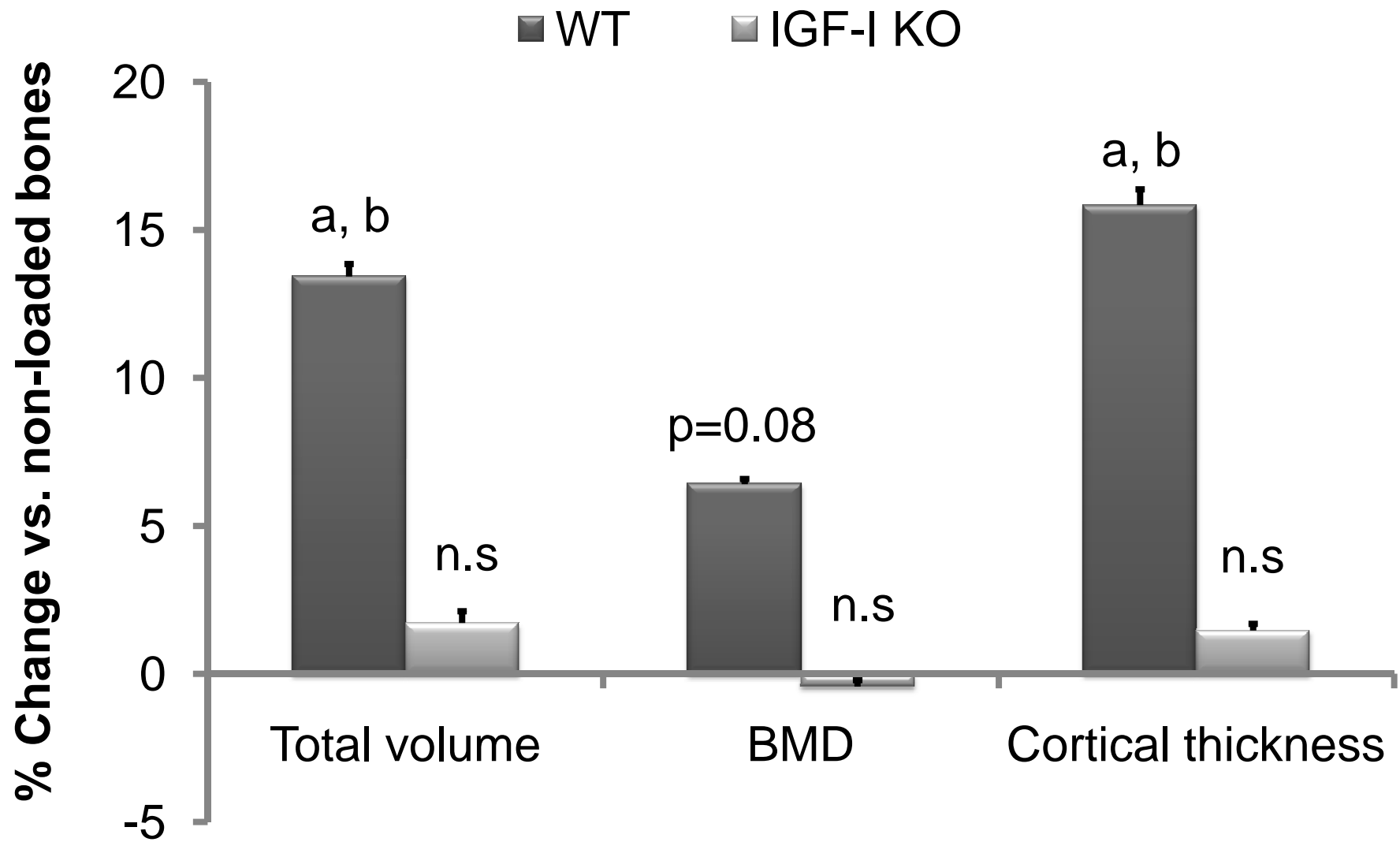


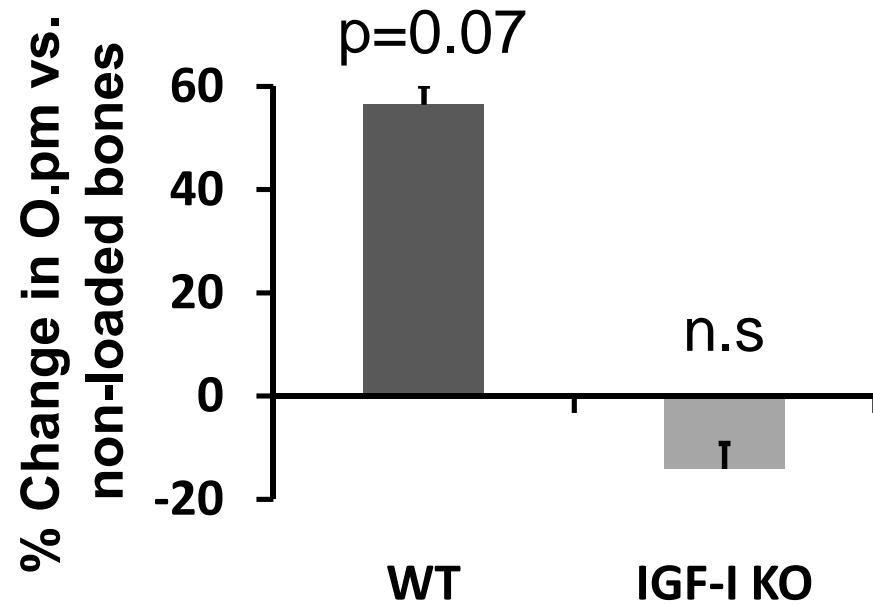
Non-externally  
loaded

Loaded

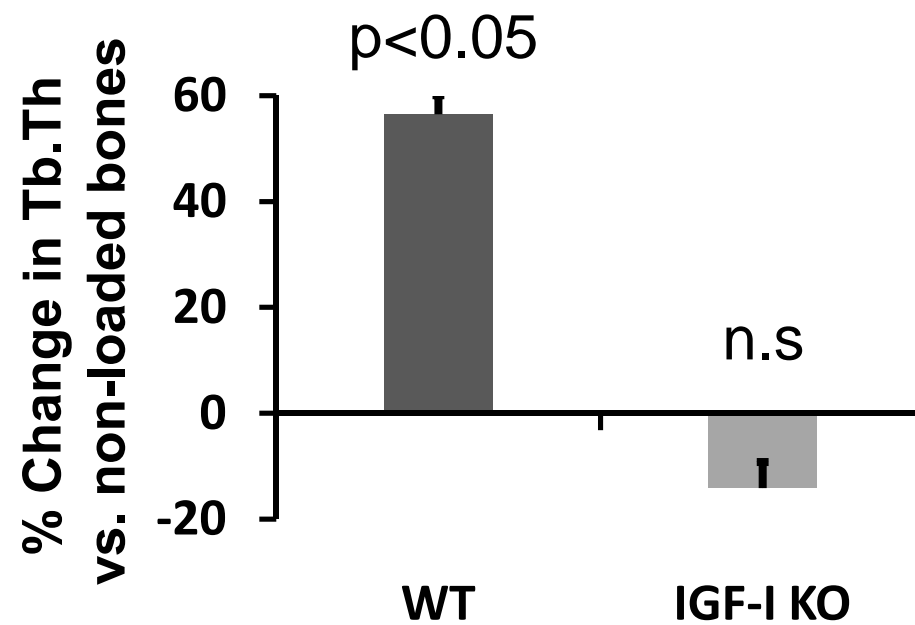




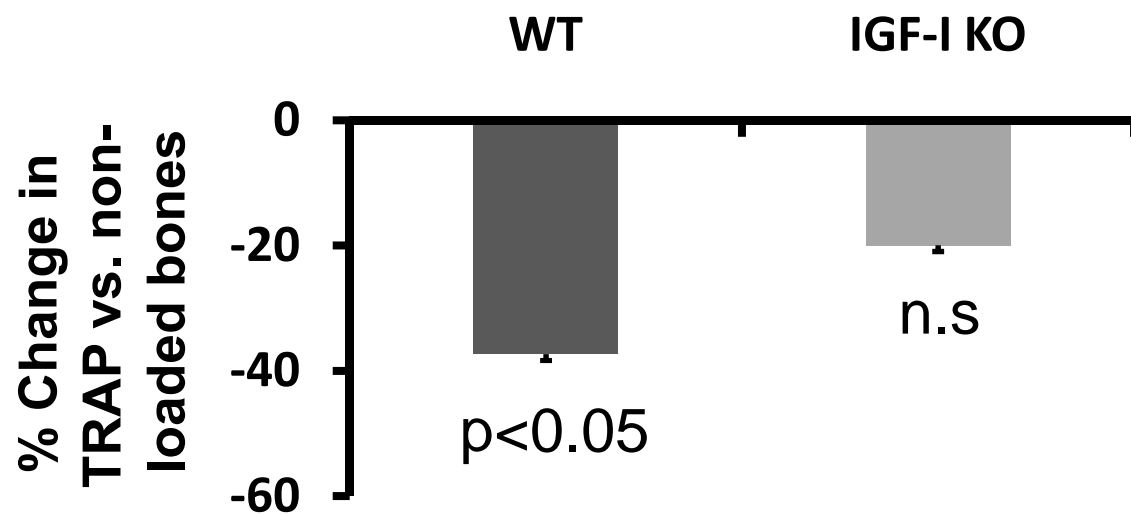




(A)



(B)



(C)

 **Print this Page for Your Records****Close Window**

## **Evidence That BMD Response To Mechanical Loading (ML) In Vivo Is Caused By Acute Up-Regulation Of Both Bone Formation (BF) Genes And Down Regulation Of Bone Resorption (BR) Genes**

C. Kesavan\*, S. Mohan, S. Oberholtzer\*, D. J. Baylink. JLP VAMC, Loma Linda, CA, USA.

**Presentation Number:** SU212

Increase in bone mass in response to skeletal loading is an important adaptive response. It is likely that regulation of both osteoblast (OB) and osteoclast cell functions are involved in producing an optimal response to a given skeletal load. To evaluate the OB and osteoclast cell response to mechanical input, we tested the hypothesis that in vivo ML by 4-point bending leads to acute reduction in the expression of BR genes and a progressive increase in the expression of BF marker genes. We measured expression changes by real time PCR in 12 genes that relate to BF and BR at d2, 4, 8 and 12 of training in 10-wk old C57Bl/6J mice. A 9N load at 2Hz (36cycles) was applied on the right tibia by a 4 point bending device and the left tibia was used as an internal control. 12 days of loading caused a highly significant ( $p<0.001$ ) increase in BMC (33%), volumetric BMD (14%) and total area (26%) as measured by pQCT in the loaded bone compared to corresponding unloaded bone. Measurement of gene expression changes by real time PCR at d2 showed significant ( $p<0.01$ ) change in the down-regulation of BR makers MMP and TRAP by 2 and 4-fold with no change in the expression of BF genes compared to control. 4-days of loading caused down regulation of BR genes MMP-9, TRAP and Sodium-potassium pump by 3, 5, and 2-fold respectively ( $p<0.0001$ ). In contrast, the expression of type-I collagen (Col 1) and bone sialoprotein (BSP) was increased by 2-fold as expected. After 8 days of loading, the expression of TRAP was decreased by 3-fold while expression of Col 1, ALP, BSP, and osteocalcin (OC) was increased by 3-fold. Surprisingly, the expression level of BR marker genes were increased after 12 days of loading (MMP-9 by 12 fold and TRAP by 7.5 fold) which may reflect loading induced increase in remodeling. In contrast, expression of Col 1, BSP, ALP and OC increased by 4.2, 8, 6 and 4 fold respectively ( $p<0.001$ ). In order to determine if gene expression change can be used as a surrogate for bone anabolic response, we determined the correlation between expression levels and BMD changes and found total BMD measured by pQCT showed significant correlation with BSP ( $r=0.54$ ,  $p<0.01$ ) and OC ( $r=0.66$ ,  $p<0.01$ ) expression. Conclusions: 1) ML by 4-point bending increased both size and volumetric BMD after 12 days; 2) The expression levels of BF genes were increased throughout the loading period; 3) This is the first report to demonstrate acute reduction in BR marker genes in response to loading. 4) The increase in expression of BR genes at day 12 may indicate loading induced remodeling of bone. 5) Our findings demonstrate the usefulness of gene expression changes as surrogate marker for bone anabolic response to ML.

**OASIS - Online Abstract Submission and Invitation System™ ©1996-2010, Coe-Truman Technologies, Inc.**

 [Print this Page for Your Records](#)[Close Window](#)

## **Bone Anabolic Response To A Mechanical Load Is A Complex Trait And Involves Bone Size, Material Bone Density (mBMD) And Volumetric Bone Density (vBMD) Phenotypes**

C. Kesavan\*, S. Mohan, J. Wergedal, D. J. Baylink. JLP VAMC / LLU, Loma Linda, CA, USA.

**Presentation Number:** SU213

Different mouse strains show large variations in BMD in response to the same mechanical load, suggesting that bone response to mechanical loading is genetically regulated. To test the hypothesis that the mechanical load response is a complex trait, we applied 4-point bending to the tibia to evaluate response in six different strains of mice in order to select the two strains with the most different response. These were C3H/HeJ (C3), the poor responder, and C57BL/6J (B6), the good responder. These two parents were used to produce 300 F2 mice. The 4-point bending method utilized a 9N load (3500 ue, upper limit of physiological strain) at 2Hz for 36 cycles and was applied for 12 days. Two days after the last load, skeletal changes were evaluated by pQCT. In these F2 mice, all three phenotypes (change in bone size, mBMD and vBMD) showed Gaussian distributions, consistent with complex traits. Heredity indexes ranged from 86-70%. The vBMD data demonstrate that some F2 mice had decreased bone density in response to the load whereas other mice gained as much as 20% in vBMD of the tibia. The other phenotypes ranged from -5 to +5% for mBMD, and -10 to +30% for bone size in the F2 mice. Cortical BMD reflects material bone mineral density (mBMD) since vascular canal volume in our sampling site is too low to alter cortical BMD (less than 1% of the bone volume). Our data on mBMD of bone formed prior to loading indicates for the first time that mechanical loading increases mBMD. We next determined if the magnitude of bone anabolic response to 4-point bending is dependent on body size. None of the three phenotypes were positively correlated with body weight. Furthermore, there was no significant difference between the bone size (unloaded bones) and the degree of change in vBMD in response to loading. These data demonstrate that a differential anabolic response cannot be explained by differences of applied mechanical strain in the F2 mice or to differences in body size. Summary: 1) Anabolic response to a standard mechanical load can be divided into at least three different phenotypes (change in bone size, vBMD and mBMD). 2) These three phenotypes show a Gaussian curve in the B6/C3H F2 mice consistent with a complex trait controlled by several genes. 3) Bone size and vBMD changes are dependent upon new bone formation, found to be exceedingly variable in our F2 mice. However, the mBMD phenotype, a measurement of mineral density in preexisting bone, implies that there is a mechanism to increase mBMD material density i.e. the bone quality can adapt to a large mechanical load. Conclusion: This study shows genetic-environmental adaptive interactions in bone of a remarkable magnitude.

**OASIS - Online Abstract Submission and Invitation System™ ©1996-2010, Coe-Truman Technologies, Inc.**

 [Print this Page for Your Records](#)
[Close Window](#)

## Global Analysis of 22,000 Genes in the Bones Reveals Involvement of Several Novel Genes/ESTs and Pathways in Mediating the Anabolic Response of Mechanical Strain in Mice *In Vivo*

W. Xing, D. J. Baylink, C. Kesavan\*, H. Yu\*, R. B. Chadwick, Y. Hu\*, R. Rajkumar\*, S. Mohan. JLP VAMC / LLU, Loma Linda, CA, USA.

**Presentation Number:** SA180

To clarify the mechanisms and identify the genes responsible for mediating the effects of mechanical loading on osteogenesis, we evaluated differential gene expression on a global basis in the tibias of 10-wk old C57BL/6J (B6) females after 4 days of 4-point bending. We chose 4 point bending as a loading regimen based on our findings that it produces a robust bone anabolic response (15% increase in BMD after 2 wks,  $P < 0.001$ ) compared to other forms of loading in B6 mice. The right tibias of the mice were loaded at 9N, 2Hz for 36 cycles per day and the left tibias of the same mice were used as unloaded controls. RNA from the tibias harvested 24 hrs after last stimulation was subjected to oligonucleotide microarray-based analysis of 22,000 mouse genes. In total, 1074 genes/ESTs were significantly up- or down-regulated ( $N=5$ , t-test:  $p < 0.05$ ), of which, 741 are known and can be characterized into 120 biological processes. As expected, genes related to biological processes such as extracellular matrix synthesis, cell growth, cell adhesion, immune response and proteolysis were increased, thus validating the microarray data. Functional annotation of known genes and unknown genes/ESTs based on functional motifs revealed several interesting and unique findings: 1) Of the known genes, 27 exhibit kinase activity (e.g., CDK2, PTK2, CDC42) and 34 exhibit receptor activity (e.g., PDGF, BMP, toll-like). These findings suggest that multiple pathways are stimulated in this large response to loading in bone. In this regard, several growth factor genes (e.g. pleiotrophin, osteoclycin, PDGF $\alpha$ , inhibin $\beta$ , IL25, nephroblastoma overexpressed gene) that have not been previously implicated in mechanical loading pathway have been identified as mediators of mechanical stress; 2) Of the 1074 significantly expressed genes, 31% express EST clones, some of which contain functional domains such as LIM, cysteine-rich protein and leucine-rich repeats, which are characteristics of motifs found in transcription factors, suggesting that future studies on these ESTs are essential for complete understanding of the molecular pathways for mechanical loading; 3) Pathway analysis revealed involvement of both well known (Integrin, Wnt, Calcium channels) and less known (Orphan GPCR, small ligand GPCR, apoptosis) pathways in mediating the effects of loading in bone. Conclusions: 1) This is the first study to examine the in vivo effect of mechanical loading on differentially expressed genes in the whole genome; 2) We have identified a number of novel genes, ESTs and pathways that have not been previously implicated to play a role in mechanical loading.

**OASIS - Online Abstract Submission and Invitation System™ ©1996-2010, Coe-Truman Technologies, Inc.**

 **Print this Page for Your Records****Close Window****Inbred Mouse Strains Exhibit Variations In The Skeletal Adaptive Response to 4-Point Bending: Evidence For Involvement Of Different Genetic Mechanisms**C. Kesavan\*, D. J. Baylink, J. E. Wergedal, S. Mohan, JLP VAMC / Loma Linda Univ Dept Med, Loma Linda, CA, USA.**Presentation Number:** M215

A fundamental feature of skeletal tissue is its adaptive response in the amount of bone tissue present and the configuration of this tissue in response to mechanical loads. The present study was undertaken to test the hypotheses that: 1) different inbred strains of mice would show variable responses to a given mechanical load; and 2) within these mouse strains, the mechanisms involved in these adaptive interactions to mechanical loads would be variable. We compared bone anabolic response to 4 point bending in four different, commonly used inbred strains of mice (C57BL/6J [B6], DBA, C3H/HeJ [C3] and Balb/c). A 9N load (except for Balb/c in which 8N was used since 9N caused fractures) at 2Hz for 36 cycles was applied for 12 days on right tibia and left tibia was used as internal control. Two days after last loading, skeletal changes were evaluated by pQCT. A dramatic 15.7% and 10.8% increase in total vBMD ( $P<0.0001$ ) was seen in C57BL and DBA mice after 12 days of loading. While vBMD increased by 3% ( $P<0.05$ ) in Balb/c, no increase in vBMD was seen in C3H mice (-0.5%) after the same duration of training. We subsequently performed dose response studies (6, 7, 8 and 9 N load) using B6 as good responder and C3H as poor responder strain. While 4 point bending caused a dose-dependent increase in BMD in B6, it did not cause a BMD increase in C3 mice at any of the four loads tested. The lack of BMD response in C3H mice cannot be explained on the basis of differential mechanical strain since strain gage measurements revealed a slightly higher mechanical strain in C3 mice compared to B6 mice at all four loads tested. 4 point bending increased endosteal circumference in a dose-dependent manner in both B6 and C3 mice in a similar manner with no difference in slopes ( $B6=y:5.891x-34.44$ ,  $C3H=y:5.859x-32.44$ ,  $p>0.05$ ). On the contrary, the increase in periosteal circumference in response to 4 point bending was greater in B6 mice compared to C3 mice ( $B6=y:5.3x-29.58$ ,  $C3H=y:2.98x-14.23$ ,  $p<0.05$ ). Conclusions: 1) the increase in BMD by 4-point bending is variable in four strains tested, from no response to 15.7% increase in BMD after 2 weeks; 2) in B6 mice, 4 point bending increased both periosteal and endosteal circumference in a dose-dependent manner; 3) in C3 mice, there was an impaired periosteal response, but the magnitude of increase at the endosteum was similar to that of the B6 mice; 4) because the C3 mice responded as well as the B6 mice to the endosteum, it follows that the impairment in responsiveness to C3 mice is not due to an overall decrease in detection of the mechanical signal and accordingly, different genetic mechanisms may regulate periosteal and endosteal responses to mechanical loading.

**OASIS - Online Abstract Submission and Invitation System™ ©1996-2010, Coe-Truman Technologies, Inc.**

 **Print this Page for Your Records**
**Close Window**

# **Novel Mechanoresponsive BMD and Bone Size QTL Identified in a Genome Wide Linkage Study Involving C57BL/6J-C3H/HeJ Intercross**

C. Kesavan, S. Mohan, H. Yu\*, S. Oberholtzer\*, J. E. Wergedal, D. J. Baylink. JLP VAMC and LLU, Loma Linda, CA, USA.

**Presentation Number:** SA183

Previously, we demonstrated that 2 wks of 4-point bending caused a dramatic 15% increase in volumetric BMD (vBMD) in the tibia of C57BL/6J (B6) but not C3H/HeJ (C3H) mice. To identify the genetic loci that contribute to variation in BMD response to mechanical loading (ML), we performed a genome wide linkage study in the B6-C3H mice intercross. The left tibiae of 329 B6-C3H F2 female mice at 10 wk age were subjected to 9 N cyclic load at 2Hz for 36 cycles daily for 2 wks while right tibia was used as unloaded control. Two days after the last loading, vBMD and bone size (periosteal circ.) were measured by pQCT. ML- induced changes ( $[(\text{loaded-unloaded/unloaded}) \times 100]$ ) in vBMD (-5 to +15%) and bone size (-5 to +20%) in the B6-C3H F2 mice showed normal distributions consistent with the complex traits controlled by several genes. % change in BMD or bone size in the F2 mice of loaded bones did not correlate with body wt, suggesting that variation in bone anabolic response to ML is independent of body size. Genome-wide search using 110 microsatellite markers with 15 cM intervals in the F2 mice revealed the following ML QTLs for BMD and bone size phenotypes (% change in loaded vs unloaded bone) using MAPQTL program ( $a=P<0.01$ ;  $b=P<0.05$ ):

Phenotype	Locus	LOD Score	% Variation
vBMD	D1Mit113	3.4 <sup>a</sup>	4.7
vBMD	D8Mit88	4.2 <sup>a</sup>	5.8
vBMD	D9Mit336	2.5 <sup>b</sup>	3.5
Bone Size	D8Mit49	3.0 <sup>b</sup>	4.1
Bone Size	D9Mit97	2.8 <sup>b</sup>	3.9
Bone Size	D11Mit333	2.6 <sup>b</sup>	3.6
Bone Size	D18Mit64	2.8 <sup>b</sup>	3.5

We found that ML BMD QTL for chr. 8 and 9 and bone size QTL for chr. 8 and 18 could not be detected using phenotype data from unloaded bones, suggesting that these QTLs are unique to ML phenotypes. Furthermore, chromosome 8 BMD QTL has not been reported for BMD in any other inbred strain crosses. Conclusions: 1) Our study provides the first demonstration of chromosomal location of genetic loci affecting variation in skeletal anabolic response to ML in the B6-C3H intercross. 2) Only 15 % of the genetic variation was accounted for by the identified ML QTL suggesting additional QTL or interactions exist. 3) Future identification of the genes responsible for the ML QTL should lead to improved understanding of molecular pathways for ML-induced skeletal anabolic response.

**OASIS - Online Abstract Submission and Invitation System™ ©1996-2010, Coe-Truman Technologies, Inc.**

## PubMed

U.S. National Library of Medicine  
National Institutes of Health



Display Settings: Abstract

J Biol Chem. 2005 May 20;280(20):20163-70. Epub 2005 Mar 18.

### **Fluid shear stress synergizes with insulin-like growth factor-I (IGF-I) on osteoblast proliferation through integrin-dependent activation of IGF-I mitogenic signaling pathway.**

Kapur S, Mohan S, Baylink DJ, Lau KH.

Musculoskeletal Disease Center, Jerry L. Pettis Memorial Veterans Affairs Medical Center, Loma Linda, California 92357, USA.

#### **Abstract**

This study tested the hypothesis that shear stress interacts with the insulin-like growth factor-I (IGF-I) pathway to stimulate osteoblast proliferation. Human TE85 osteosarcoma cells were subjected to a steady shear stress of 20 dynes/cm<sup>2</sup> for 30 min followed by 24-h incubation with IGF-I (0-50 ng/ml). IGF-I increased proliferation dose-dependently (1.5-2.5-fold). Shear stress alone increased proliferation by 70%. The combination of shear stress and IGF-I stimulated proliferation (3.5- to 5.5-fold) much greater than the additive effects of each treatment alone, indicating a synergistic interaction. IGF-I dose-dependently increased the phosphorylation level of Erk1/2 by 1.2-5.3-fold and that of IGF-I receptor (IGF-IR) by 2-4-fold. Shear stress alone increased Erk1/2 and IGF-IR phosphorylation by 2-fold each. The combination treatment also resulted in synergistic enhancements in both Erk1/2 and IGF-IR phosphorylation (up to 12- and 8-fold, respectively). Shear stress altered IGF-IR binding only slightly, suggesting that the synergy occurred primarily at the post-ligand binding level. Recent studies have implicated a role for integrin in the regulation of IGF-IR phosphorylation and IGF-I signaling. To test whether the synergy involves integrin-dependent mechanisms, the effect of echistatin (a disintegrin) on proliferation in response to shear stress +/- IGF-I was measured. Echistatin reduced basal proliferation by approximately 60% and the shear stress-induced mitogenic response by approximately 20%. It completely abolished the mitogenic effect of IGF-I and that of the combination treatment. Shear stress also significantly reduced the amounts of co-immunoprecipitated SHP-2 and -1 with IGF-IR, suggesting that the synergy between shear stress and IGF-I in osteoblast proliferation involves integrin-dependent recruitment of SHP-2 and -1 away from IGF-IR.

PMID: 15778506 [PubMed - indexed for MEDLINE] **Free Article**

Publication Types, MeSH Terms, Substances

LinkOut - more resources

 [Print this Page for Your Records](#)[Close Window](#)

**Session:** Genetics: Linkage and Heritability Studies

**Presentation Number:** SU131

**Title:** Quantitative Trait Loci for Tibia Periosteal Circumference in the C57BL/6J-C3H/HeJ Mice Intercross

**Presentation Start:** 9/17/2006 11:30:00 AM

**Presentation End:** 9/17/2006 2:30:00 PM

**Category:** L - Genetics of Bone and Mineral Disorders

**Authors/Speakers:** C. Kesavan, D. J. Baylink, S. Kapoor\*, J. E. Wergedal, H. Yu, S. Mohan. JLP VAMC and LLU, Loma Linda, CA, USA.

Bone size (BS) is an important determinant of both bone strength and the risk for osteoporotic fractures in humans. BS is highly variable and heritable, as evidenced by studies in humans. We sought to test the hypotheses that: 1) BS is a complex trait controlled by multiple genes; and 2) BS that differs in different skeletal sites is regulated by common and bone specific QTL. We performed a genome-wide linkage study using B6 and C3H inbred strains of mice with extreme differences in BS. We previously generated 329 female F2 mice from the B6-C3H intercross. We used the non-loaded left tibia to identify BS QTL. At 12-wks, *in vivo* pQCT was performed and periosteal circumference (PC) was measured. A genome-wide scan was performed using 111 micro-satellite markers in DNA samples collected from the liver of the F2s. Heritability response for PC was 73%. The range of PC was 3.93 to 6.08 mm and, adjusted with body weight (BW), was 0.19 to 0.30 mm in the F2s. There was a normal distribution of PC values in the F2s. Presence of significant correlation between BS and BW suggested that some of the QTL obtained for PC are the same for BW. After adjusting with BW, interval mapping revealed that BS was influenced by five significant loci and one suggestive loci (below).

Trait	Chr	Marker	cM	LOD	Variance %	Alleles contributed by
Bone size	3	D3Mit320*	46.4	4.0 <sup>a</sup>	7.2	C3H
	10	D10Mit233*	57.3	2.4 <sup>c</sup>	3.9	C3H
	11	D11Mit285	49.2	4.3 <sup>a</sup>	6	B6
	15	D15Mit107	41.5	3.1 <sup>b</sup>	4.7	B6
	16	D16Mit60	24.0	3.1 <sup>b</sup>	4.3	B6
	17	D17Mit93	39.3	5.1 <sup>a</sup>	7	C3H

Highly significant <sup>a</sup> LOD score ( $p < 0.01$ ), <sup>b</sup> ( $p < 0.05$ ) and <sup>c</sup> suggestive LOD score ( $p < 0.1$ ), \*Marker closest to the peak LOD score.

Chr 17 showed highest significance after adjustment with bodyweight. Pairwise analysis showed the presence of several significant interactions between loci on Chrs 1, 2, 4, 12 and 14 for the BS trait. In summary, novel Chr 3 QTL specific for tibia size regulation and known QTL (Chr 10, 11, 15, 16 & 17) have been identified for femur PC trait in B6-C3H F2 mice. The known QTL are also involved in regulating BMD, thus suggesting that the genes in these QTL may regulate multiple phenotypes. Chr 10 and Chr 11 have been identified in multiple strain crosses, suggesting the importance of this QTL in BS regulation. In conclusion, QTL identified for BS are same as QTL previously identified for femur, suggesting that same mechanisms are involved in regulation of BS in both femur and tibia.

 **Print this Page for Your Records**
**Close Window**

**Session:** Bone, Cartilage and Connective Tissue Matrix: Mechanical Stress

**Presentation Number:** T152

**Title:** Identifying Mechanical Loading QTL by Gene Expression Changes for Alkaline Phosphatase and Bone Sialoprotein in C57BL/6J (B6) X C3H/HeJ (C3H) Intercross

**Presentation Start:** 9/18/2007 11:30:00 AM

**Presentation End:** 9/18/2007 2:30:00 PM

**Category:** H - Disorders of Bone and Mineral Metabolism (genetic, basic, and translational)

**Authors/Speakers:** C. Kesavan, D. Baylink\*, S. Kapoor\*, S. Mohan. MDC, J.L. Pettis VAMC, Loma Linda, CA, USA.

Previous studies have shown that mechanical loading (ML) 1) produces a more robust skeletal anabolic response in B6 mice than C3H mice, which is largely mediated by genetic differences and 2) induces greater expression of bone formation (BF) marker genes in the bones of B6 mice compared with C3H mice. We, therefore, tested the hypothesis that the variation in skeletal anabolic response to ML in the F2 mice of B6 and C3H intercross is largely due to changes in BF response. To examine this, we measured expression changes in two BF markers, namely bone sialoprotein (BSP) and alkaline phosphatase (ALP) in the loaded and non-loaded bones of 10-week F2 female mice (n=241). Loading was performed daily on the right tibia by four-point bending using a 9 Newton at 2Hz, 36 cycles, for 12 days. The left tibiae were used as internal controls. The expression levels of ALP and BSP were quantitated after normalization with two house keeping genes, actin and PPIA. The mean increase in gene expression in the F2 mice, expressed as fold change, ranged from  $3.0 \pm 2.8$  for BSP and  $2.7 \pm 2.8$  for ALP, and showed significant correlation ( $r=0.25$  to  $0.36$ ,  $p<0.01$ ) with changes in BMD and bone size. A genome-wide search using 111 microsatellite markers with 15 cM intervals in the

Locus *	$\beta$ -actin Normalization		PPIA Normalization	
	BSP-LOD	ALP-LOD	BSP-LOD	ALP-LOD
D8Mit88	7.5 <sup>b</sup>	10.5 <sup>a</sup>	8.8 <sup>b</sup>	12.3 <sup>a</sup>
D9Mit151	7.1 <sup>b</sup>	7.4 <sup>b</sup>	5.0 <sup>c</sup>	-
D16Mit153	6.7 <sup>b</sup>	5.1 <sup>c</sup>	7.0 <sup>b</sup>	5.9 <sup>c</sup>
D17Mit51	9.2 <sup>a</sup>	9.3 <sup>a</sup>	12.3 <sup>a</sup>	9.0 <sup>b</sup>
D18Mit144	8.0 <sup>b</sup>	12.6 <sup>a</sup>	-	5.8 <sup>c</sup>
D19Mit68	7.2 <sup>b</sup>	-	10.7 <sup>a</sup>	6.9 <sup>b</sup>

\*determined using MapQTL program; <sup>a</sup> $p<0.01$ , <sup>b</sup> $p<0.05$ , <sup>c</sup> $p<0.1$

F2 mice revealed QTLs on Chrs 8, 9, 17 and 18, which corresponded to ML QTLs we previously identified using changes in BMD and bone size as end points. We identified two new ML QTLs on Chrs 16 and 19 using gene expression data. In conclusion: 1) Identification of several common QTL for BMD, BSP and ALP phenotypes suggests that the skeletal response to ML is largely mediated by increased BF; 2) Identification of genes that are involved in regulating BSP and ALP expression in response to ML will lead to improved understanding of the molecular pathways regulating the bone response to ML.

OASIS - Online Abstract Submission and Invitation System™ ©1996-2010, Coe-Truman Technologies, Inc.

 **Print this Page for Your Records****Close Window**

**Session:** Bone Biomechanics and Quality I

**Presentation Number:** 1081

**Title:** Leptin-deficient (ob/ob) Mice Exhibit Increased Bone Mechanosensitivity and Corresponding Osteoblasts Show Increased Anabolic Shear Stress Responses In Vitro

**Presentation Start:** 9/17/2007 4:30:00 PM

**Presentation End:** 9/17/2007 4:45:00 PM

**Category:** P - Bone Biomechanics and Quality

**Authors/Speakers:** K. H. W. Lau<sup>1</sup>, S. Kapur<sup>\*1</sup>, M. Amoui<sup>\*1</sup>, X. Wang<sup>\*1</sup>, C. Kesavan<sup>\*1</sup>, S. Mohan<sup>1</sup>, D. J. Baylink<sup>2</sup>. <sup>1</sup>Loma Linda VAMC, Loma Linda, CA, USA, <sup>2</sup>Loma Linda Univ., Loma Linda, CA, USA.

We sought to test the hypothesis that the leptin receptor (Lepr) pathway plays an important role in bone mechanosensitivity based on the rationales that Lepr is located within one of the mouse genetic loci that showed mechanosensitivity modulating effects and that Lepr signaling is essential for skeletal maturation and metabolism. To test this hypothesis, the osteogenic response to loading (in the form of 2-week four-point bending) in tibia of adult female ob/ob mice [in C57BL/6J (B6) background] was compared with those in adult female B6 tibia. To adjust for the 14% greater bone size in ob/ob mice, the load was adjusted to produce similar levels of mechanical strain (2129  $\mu\epsilon$  at 9N for ob/ob mice vs. 2500  $\mu\epsilon$  at 6N for B6 mice). This mechanical strain was insufficient to produce a bone anabolic response in B6 mice; whereas in ob/ob mice this strain increased total BMC (16%), cortical area (22%), content (29%), and thickness (28%), and BMD (8%) [ $p < 0.05$  for each]. To further test if leptin deficiency would enhance osteogenic response to mechanical stimuli, the effects of a 30-min fluid shear (20 dynes/cm<sup>2</sup>) on [<sup>3</sup>H]thymidine incorporation (TdR) and Erk1/2 phosphorylation in ob/ob osteoblasts were compared to those of wild-type (WT) littermates and B6 mice. While the shear stress increased TdR and Erk1/2 in osteoblasts of B6 and WT littermates (each by ~2-fold,  $p < 0.05$ ), the stimulation in ob/ob osteoblasts was greater (> 3-fold,  $p < 0.05$  vs. B6 osteoblasts). In addition, 2-hr pretreatment of ob/ob osteoblasts with 100 ng/ml of leptin completely abrogated the enhanced mitogenic response. Because it has been reported that the mechanism whereby mechanical stimuli act to stimulate proliferation involves upregulation of genes of the IGF-I, Wnt, BMP/TGF $\beta$ , and estrogen receptor pathways, we next determined whether the Lepr pathway acts upstream to these 4 pathways by assessing the effects of the fluid shear on the expression levels of representative genes of these pathways in ob/ob and B6 osteoblasts (by real-time PCR). The upregulation of each test gene of the 4 pathways in ob/ob osteoblasts was much greater ( $p < 0.05$ ) than those in B6 osteoblasts. The 2-hr leptin pretreatment also abrogated the shear stress-induced upregulation of these genes in ob/ob osteoblasts. Conclusions: 1) In vivo, the Lepr pathway inhibits the anabolic responses to mechanical loading which is consistent with increased basal values for bone size in the ob/ob mouse, 2) In vitro, the Lepr pathway also has a negative modulating role in the mechanosensitivity of mouse osteoblasts, and 3) The Lepr pathway acts upstream of 4 selected major anabolic pathways to modulate mechanosensitivity.

OASIS - Online Abstract Submission and Invitation System™ ©1996-2010, Coe-Truman Technologies, Inc.

 **Print this Page for Your Records**
**Close Window**

**Session:** Bone, Cartilage and Connective Tissue Matrix: Mechanical Stress

**Presentation Number:** T151

**Title:** The Increased vBMD and Bone Area due to Mechanical Loading Gradually Decreased Following Cessation of Loading

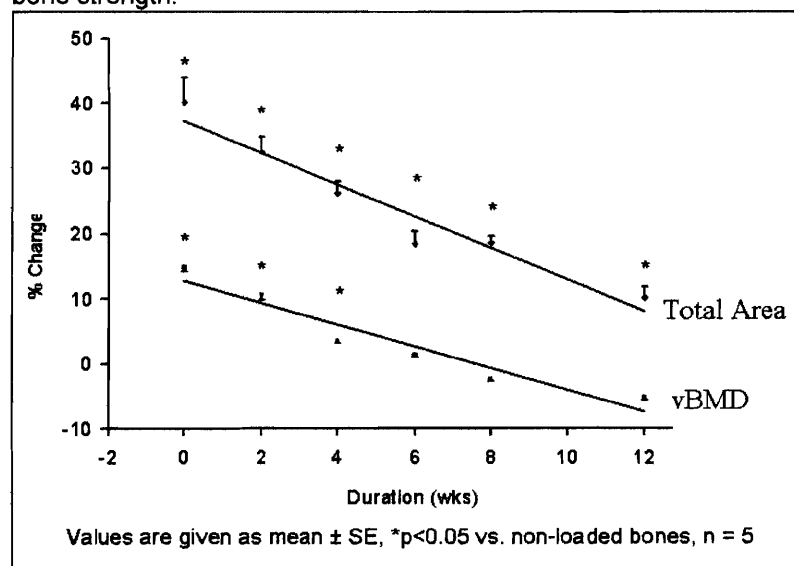
**Presentation Start:** 9/18/2007 11:30:00 AM

**Presentation End:** 9/18/2007 2:30:00 PM

**Category:** D - Bone, Cartilage and Connective Tissue Matrix

**Authors/Speakers:** C. Kesavan, D. J. Baylink\*, P. Gifford\*, S. Mohan. MDC, J.L. Pettis VAMC, Loma Linda, CA, USA.

Dynamic loads lead to increases in volumetric (v) BMD and cross sectional area. However, the issue of how long these gains are maintained after cessation of loading has not been fully understood. To address this question, we performed a long term study in which skeletal changes were monitored every 2-4 weeks for a 12 week period following cessation of external loading. A four-point loading device was used to apply external loading (9N at a frequency of 2Hz for 36 cycles once per day for 12 days) to the right tibia of 10-week old female mice. Skeletal changes were monitored by *in vivo* pQCT. The value of the left non-loaded tibia was subtracted from the value of the right loaded tibia to determine the changes associated with loading at each time point. Two-weeks of four-point loading caused a drastic 40% increase in total area (TA) and 15% increase in total vBMD. However, the increase in size due to external loading did not continue once the external loading was stopped. Furthermore, cessation of loading resulted in a continuous loss of both bone size (TA) and vBMD. The vBMD returned to normal at 12 weeks with a half life of 6 weeks. The TA declined with a half life of 8.5 weeks and was still significantly elevated at 12 weeks. Thus, the decline in elevated TA proceeded at a much slower pace than the loading induced increases in vBMD. Conclusions: 1) External loading-induced increases in bone are lost over a period of time but at a much slower pace than the induction of the increases; 2) While a single burst of external loading provides increased bone mass temporarily, periodic loading may be necessary to maintain long term bone strength.



 **Print this Page for Your Records****Close Window**

**Session:** Bone Biomechanics and Quality II  
**Presentation Number:** 1142  
**Title:** Anabolic Response to Skeletal Loading in Mice with Targeted Disruption of Pleiotrophin Gene  
**Presentation Start:** 9/14/2008 8:45:00 AM  
**Presentation End:** 9/14/2008 9:00:00 AM  
**Category:** P. Bone Biomechanics and Quality  
**Authors/Speakers:** C. Kesavan, S. Mohan, Musculoskeletal Disease Center, Jerry L Pettis VA Medical Center, Loma Linda, CA, USA.

Bone formation induced by mechanical loading (ML) results from increased recruitment, proliferation and differentiation of osteoblast lineage cells. Pleiotrophin (PTN), an extracellular matrix associated protein, implicated in diverse functions, is also involved in recruitment of the osteoblasts to the site of bone formation. In a recently published study using whole genome microarray approach to identify the genes and the signal pathways responsible for ML-induced bone formation, we found that PTN expression was increased by 4-fold in response to ML in a good responder C57BL/6J (B6) mice. Furthermore, transgenic overexpression of PTN in mice resulted in increased bone formation. Therefore, we sought to determine whether the anabolic effects of ML on bone formation are mediated by PTN. We first evaluated time course effects of ML on expression levels of PTN gene using real time RT-PCR in 10 week old female B6 mice. A 9N load was applied using a four-point bending device at 2Hz frequency for 36 cycles, once per day for 2, 4 and 12 days on the right tibia and the left tibia was used as internal control. Four-point bending caused an acute increase in PTN expression (2-fold) within 2 days of loading and further increased (3 to 6 fold) with continued loading (4 to 12 days). The increase in PTN expression in response to ML was also seen in 16 and 36-week old mice. Based on these findings, we next used mice with targeted disruption of PTN gene to evaluate the cause and effect relationship between the change in PTN expression and ML induced changes in bone response. Since the mechanical strain produced by a given load depends largely on bone size, we measured periosteal circumference in the tibia of knockout (KO) and control mice and found no differences ( $4.55 \pm 0.24$  vs  $4.69 \pm 0.21$ ,  $p=0.50$ ). We, therefore, applied 9N load for both groups of mice ( $n=6-7$ ). Quantitative analysis of ML-induced skeletal response measured by pQCT showed that two weeks of four point bending increased vBMD and bone size by 8% and 6% respectively in the PTN KO mice compared to the 11% and 8% increases seen in the littermate control mice. Although BMD and bone size response to ML were reduced by 23% ( $p=0.21$ ) and 18% ( $p=0.13$ ) respectively in PTN KO mice compared to control mice, these changes were not statistically significant. The issue of whether lack of significant difference in ML response between PTN KO and control mice is due to compensation by other members of PTN family is being pursued. In conclusion, our findings using PTN KO mice seem to suggest that PTN is not a key upstream mediator of the anabolic effects of ML on the skeleton.

**OASIS - Online Abstract Submission and Invitation System™ ©1996-2010, Coe-Truman Technologies, Inc.**



The American Society for  
Bone and Mineral Research

**Categories:**

Growth Factors, Cytokines, Immunomodulators (Basic)  
Bone, Cartilage and Connective Tissue Matrix & Development (Basic)  
Osteoblasts (Basic)

**Oral Presentations, Presentation Number: 1119**

**Session: Concurrent Oral Session 20: Growth Factors, Cytokines, Immunomodulators I:  
Anabolic Signaling**

**Sunday, September 13, 2009 3:30 PM - 3:45 PM, Colorado Convention Center, Room 205-207**

\* Chandrasekhar Kesavan, JLP VA Medical Center, USA, Jon Wergedal, Jerry L. Pettis Memorial VA Medical Center, USA, Subburaman Mohan, JL Pettis VA Memorial Medical Center, USA

Although a key role for mechanical stress (MS) in the development of skeletal architecture and in the maintenance of bone mass is well established, little is known about the genes and their signaling pathways that contribute to MS response in bone in vivo. Based on the findings that the expression of IGF-I, a key bone formation (BF) regulator, increases rapidly in response to MS in osteoblasts (OBs) in vitro and in vivo, we proposed the hypothesis that OB produced IGF-I is the key mediator of skeletal anabolic response to MS. To test the cause and effect relationship of OB produced IGF-I and skeletal anabolic response to mechanical loading (ML), we generated mice with conditional disruption of IGF-I in OBs using Cre/loxP technology. In our initial study, a 4-point bending device was used to apply daily a load to the mid diaphysis of tibia of 10-wk old mice at a frequency of 2Hz for 36 cycles for a period of 2 weeks. Because bone size was smaller in the knockout (KO) compared to wild type (WT) mice, the load was adjusted such that the applied load produced equivalent amount of strain in both KO and WT mice. Measurement of skeletal changes by pQCT revealed that two weeks of ML caused a robust 10% ( $P<0.05$ ) and 39% ( $P<0.01$ ) increases in BMD and cross sectional area (CSA), respectively, in the WT mice. However, application of the same amount of strain to KO mice did not significantly increase either BMD (3.2%) or CSA (3%). Accordingly, expression levels of BSP (2.4 fold,  $P<0.01$ ) and runx2 (2.1 fold,  $P=0.05$ ) as measured by real time RT-PCR were increased significantly in response to ML in the WT but not KO mice. To determine if OB-produced IGF-I is also necessary for ML-induced changes in trabecular bone, we next used tibial axial loading model to apply 12N in WT and 6.5 N in KO of axial load to generate 825 and 747 $\mu$  strain, respectively, in the WT and KO mice at 10 weeks of age. Micro-CT analyses of newly formed trabecular bone at secondary spongiosa, at 10.5 $\mu$  resolution, revealed 23%, 19% and 21% (all  $P<0.05$ ) increases in trabecular BV/TV, thickness and density in the loaded bones of WT mice compared to corresponding non-loaded bones. In contrast, trabecular bone parameters, if any, were decreased in the loaded bones of KO mice. We conclude that OB produced IGF-I is obligatory for the ML-induced increase in new BF, thus suggesting that other growth factors cannot compensate for lack of local IGF-I to produce skeletal anabolic response to ML.

**Disclosures:** None

\* **Presenting Author(s):** Chandrasekhar Kesavan, JLP VA Medical Center, USA